

Journal of Polymer Science

Part A-1: Polymer Chemistry

Contents

E. SAITO, C. CANNAVO, et K. HAYASHI: Etude par RPE des Radicaux Libres dans le Tétraoxane Irradié	2309
E. N. ZILBERMAN, A. E. KULIKOVA, N. M. PINCHUK, N. K. TAIKOVA, and N. A. OKLADNOV: Transformations of Chloroethylenes in the Presence of Aprotic Acids	2325
JOGINDER LAL and G. S. TRICK: Glass Transformation Temperatures of Polymers of Olefin Oxides and Olefin Sulfides	2339
V. V. KORSHAK, N. I. BEKASOVA, and L. G. KOMAROVA: Synthesis and Properties of Polyamides and Polyesters from Neocarboranedicarboxylic Dichloride	2351
P. H. VANDEWYER and G. SMETS: Photochromic Polypeptides	2361
E. N. KUMPANENKO, A. I. VARSHAVSKAYA, L. V. KARMILOVA, and N. S. ENIKOLOPYAN: Kinetics of Thermal and Acidic Degradation of Poly-1,3-dioxolane	2375
YASUSHI JOH, SEIKI KURIHARA, TOSHIO SAKURAI, and TATSUNORI TOMITA: Stereospecific Polymerization of Methacrylonitrile. VI. Effect of Esters as a Complexing Agent with Diethylmagnesium Catalyst	2383
HIDEFUMI HIRAI, KATSUMA HIRAKI, ISAMU NOGUCHI, TAKEO INOUE, and SHOJI MAKISHIMA: Electron Spin Resonance Study on Polymerization of Conjugated Dienes by Homogeneous Catalyst Derived from <i>n</i> -Butyl Titanate and Triethylaluminum	2393
HIDEFUMI HIRAI and TADASHI IKEGAMI: Polymerization of Coordinated Monomers. V. Polymerization of Methyl Methacrylate-Lewis Acid Complexes	2407
WASABURO KAWAI and SHIGERU KATSUTA: Cyclocopolymerization of <i>p</i> -Chlorostyrene with 4-Vinylcyclohexene	2421
YOSHIO IWAKURA, KEIKICHI UNO, and SHIGERU KUROSAWA: Polyhydrazides. IV. Preparation and Properties of Poly- <i>N</i> -Ethyl- and Isopropylhydrazide Oxadiazoles	2429
DANIEL W. BROWN, ROBERT E. LOWRY, and LEO A. WALL: Radiation-Induced Copolymerization of Tetrafluoroethylene and 3,3,4,4,5,5,5-Heptafluoropentene-1 Under Pressure	2441
G. MONTAUDO, F. BOTTINO, S. CACCAMESE, P. FINOCCHIARO, and G. BRUNO: Synthesis and Properties of Some Linear Oligobenzyls and Polybenzyls	2453
I. PENCZEK and ST. PENCZEK: The Role of Solvent Polarity and Cocatalyst Structure in the Cationic Polymerization of 3,3-Bis(chloromethyl)oxetane	2465
G. MONTAUDO, P. FINOCCHIARO, S. CACCAMESE, and F. BOTTINO: Polycondensation of Benzyl Chloride and its Derivatives: A Study of the Reaction at Different Temperatures	2475
ANDRZEJ BUKOWSKI and STANISLAW POREJKO: Use of Carbon Suboxide to Obtain Block and Graft Copolymers. I. Grafting of Carbon Suboxide on Polyamide 6	2491
ANDRZEJ BUKOWSKI and STANISLAW POREJKO: Use of Carbon Suboxide To Obtain Block and Graft Copolymers. II. Grafting of Carbon Suboxide on Polyethylene	2501

(continued inside)

Journal of Polymer Science **Part A-1: Polymer Chemistry**

Board of Editors: H. Mark • C. G. Overberger • T. G. Fox

Advisory Editors:

R. M. Fuoss • J. J. Hermans • H. W. Melville • G. Smets

Editor: C. G. Overberger

Associate Editor: E. M. Pearce

Advisory Board:

T. Alfrey, Jr.	E. M. Fettes	C. S. Marvel	W. H. Sharkey
W. J. Bailey	N. D. Field	F. R. Mayo	W. R. Sorenson
D. S. Ballantine	F. C. Foster	R. B. Mesrobian	V. T. Stannett
M. B. Birenbaum	H. N. Friedlander	H. Morawetz	J. K. Stille
F. A. Bovey	K. C. Frisch	M. Morton	M. Szwarc
J. W. Breitenbach	N. G. Gaylord	S. Murahashi	A. V. Tobolsky
W. J. Burlant	W. E. Gibbs	G. Natta	E. J. Vandenberg
G. B. Butler	A. R. Gilbert	K. F. O'Driscoll	L. A. Wall
S. Bywater	J. E. Guillet	S. Okamura	F. X. Werber
T. W. Campbell	H. C. Haas	P. Pino	O. Wichterle
W. L. Carrick	J. P. Kennedy	C. C. Price	F. H. Winslow
H. W. Coover, Jr.	W. Kern	B. Rånby	M. Wismer
F. Danusso	J. Lal	J. H. Saunders	E. A. Youngman
F. R. Eirich	R. W. Lenz	C. Schuerch	

Contents (continued), Vol. 8

JOHN C. SAAM and DAVID J. GORDON: Chain Transfer with Siloxanes During Free-Radical Polymerization.....	2509
H. H. G. JELLINEK and S. N. LIPOVAC: The Vacuum and Oxidative Pyrolysis of Poly- <i>p</i> -xylylene.....	2517
R. L. HARVILLE and SAMUEL F. REED, JR.: Polymerization Studies on Allylic Compounds. IV. Methallylic Compounds.....	2535
KATSUMA HIRAKI, TAKEO INOUE, and HIDEFUMI HIRAI: Electron Spin Resonance Study of Polymerization of Butadiene with Tris(acetylacetonato)titanium and Triethylaluminum.....	2543
MITSUTAKA SAITO, HIDEO TADA, and YUJIRO KOSAKA: Alkyl Chain Branching in Ethylene-Vinyl Acetate Copolymer.....	2555
FUKUJI HIGASHI, AKIRA TAI, and KAZUO ADACHI: The Reaction Between Diethyl Succinylsuccinate (1,4-Diethoxycarbonyl-2,5-dihydroxy-1,4-cyclohexadiene) and Amines and Its Application to Polymer Synthesis.....	2563

(continued on inside back cover)

The Journal of Polymer Science is published in four sections as follows: Part A-1, Polymer Chemistry, monthly; Part A-2, Polymer Physics, monthly; Part B, Polymer Letters, monthly; Part C, Polymer Symposia, irregular.

Published monthly by Interscience Publishers, a Division of John Wiley & Sons, Inc., covering one volume annually. Publication Office at 20th and Northampton Sts., Easton, Pa. 18042. Executive, Editorial, and Circulation Offices at 605 Third Avenue, New York, N. Y. 10016. Second-class postage paid at Easton, Pa. Subscription price, \$325.00 per volume (including Parts A-2, B, and C). Foreign postage \$15.00 per volume (including Parts A-2, B, and C).

Copyright © 1970 by John Wiley & Sons, Inc. All rights reserved. No part of this publication may be reproduced by any means, nor transmitted, nor translated into a machine language without the written permission of the publisher.

Etude par RPE des Radicaux Libres dans le Tétraoxane Irradié

E. SAITO, C. CANNAVO, et K. HAYASHI, *Centre d'Etudes Nucléaires de Saclay, Commissariat à l'Energie Atomique, Gif-sur-Yvette, Saclay, France*

Synopsis

The free radicals induced in tetraoxane at liquid nitrogen temperatures by ^{60}Co γ -rays have been studied by ESR. The powder spectrum as well as the spectra of the single crystal rotated around the b axis have been studied through their modifications from -196°C up to $+80^\circ\text{C}$. These spectra show that at low temperatures two radicals exist conserving the cyclic nature of the parent molecule. During the course of annealing, starting at -140°C and towards -85°C they are gradually replaced by radicals with a linear structure, this being the first step in the post-polymerization process of tetraoxane. Further increase in temperature leads to radical sites situated on the polymer chains. At low temperatures evidence has also been found for the formyl radical, radical pairs, and a photo-sensitive radical.

INTRODUCTION

Des études antérieures¹ ont montré que le tétraoxane (tétramère cyclique du formaldéhyde) se polymérise à l'état solide après irradiation lorsqu'on le soumet à un recuit. L'irradiation peut être réalisée à l'aide d'une source au ^{60}Co ou par un accélérateur d'électrons. On présume que la polymérisation est issue des radicaux créés pendant l'irradiation. Aussi il nous a paru intéressant d'utiliser la technique de la RPE pour déterminer la nature de ces radicaux et pour étudier leur comportement lorsqu'on élève la température.

Nous avons tout particulièrement centré notre étude sur le spectre que donne un cristal unique. Nous avons ainsi pu obtenir des informations plus complètes et plus faciles à interpréter que si nous nous étions limités à l'étude de la poudre.

Un cas assez proche est celui du polyoxyméthylène étiré étudié par Yoshida et Rånby.² L'étirement a orienté les chaînes $-\text{O}-\text{CH}_2-\text{O}-\text{CH}_2-$ et a permis d'obtenir des spectres avec une structure hyperfine plus prononcée pour certains angles. Les auteurs ont pu leur faire correspondre les radicaux $-\text{CH}_2-\text{O}^\cdot$, $\cdots-\dot{\text{C}}\text{H}-\cdots$, et $\cdots-\dot{\text{C}}\text{H}_2$.

PARTIE EXPERIMENTALE

Les cristaux uniques de tétraoxane ont été obtenus par évaporation lente de solutions dans l'éthanol. Ils se présentent sous forme d'aiguilles

très fines. Les monocristaux ont été triés à l'aide d'un microscope polarisant. La détermination des angles entre les faces latérales de l'aiguille au moyen d'un goniomètre optique a permis de contrôler que l'axe géométrique de l'aiguille est dirigé suivant l'axe cristallographique [010], ce qui a été aussi vérifié par une étude aux rayons X.

Les monocristaux sont placés dans des tubes de silice pure scellés sous atmosphère. Ces tubes ont une extrémité effilée pour que l'aiguille puisse s'y loger et que son axe soit maintenu au voisinage de la verticale.

L'irradiation est effectuée avec le cristal dans l'extrémité non effilée du tube lequel est plongé dans l'azote liquide. La source de ^{60}Co (CEN/Saclay SPCA) ou l'accélérateur d'électrons CIRCE (Corbeville-Orsay) ont été utilisés à cette fin. Les doses reçues ont été de l'ordre de 10 Mrad.

Après l'irradiation l'extrémité effilée du tube est chauffée au chalumeau pour éliminer les centres paramagnétiques qui y ont été créés. Le tube est ensuite refroidi entièrement et on le retourne très rapidement pour faire glisser le cristal dans l'extrémité effilée. Il est alors transféré dans un vase Dewar à azote liquide ou dans un vase Dewar tubulaire refroidi par un courant d'azote gazeux. Ces vases Dewar se trouvent dans la cavité résonante de l'appareil RPE.

L'appareil RPE est un Varian V 4502-13, modulation 100 keps, aimant de 9 pouces équipé d'un Fieldial. L'emploi d'une cavité double permettait la détermination de g , l'échantillon de référence étant le KCl-goudron 0,1%, $g = 2,0028$. Pour le recuit, nous avons utilisé l'appareil à température variable Varian E 4557.

On a commencé par étudier les variations du spectra obtenu à -196°C en faisant tourner le cristal de 10° en 10° autour de l'axe [010]. L'angle de rotation du cristal est lu à l'aide d'un rapporteur gradué en degré, concentrique au tube de silice. On a ensuite effectué à angle fixe un recuit à partir de -170°C traçant le spectra tous les 5°C . On s'est plus particulièrement attardé aux températures où le spectre présentait des changements importants. On a ainsi effectué pour le même cristal six rotations à -196 , -140 , -85 , -30 , -20 et $+40^\circ\text{C}$.

RESULTATS ET INTERPRETATIONS

Spectra de la Poudre

La poudre a été irradiée à -196°C et le spectre obtenu à cette température est donné par la Figure 1. Nous voyons qu'il est difficile d'analyser un tel spectre à cause de l'anisotropie en g et de la constante de couplage dans les structures hyperfines.

Cependant, comme on irradie une plus grande quantité de matière lorsque le tétraoxane est en poudre qu'à l'état de monocristal, le nombre de radicaux créés sous irradiation est plus grand. Il est alors possible de maintenir la poudre à des températures plus élevées tout en observant un spectra sans bruit de fond apparent. Les Figures 2 et 3 donnent l'évolution

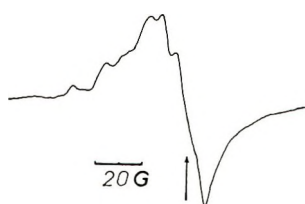


Fig. 1. Spectre du tétraoxane en poudre irradié à -196°C .

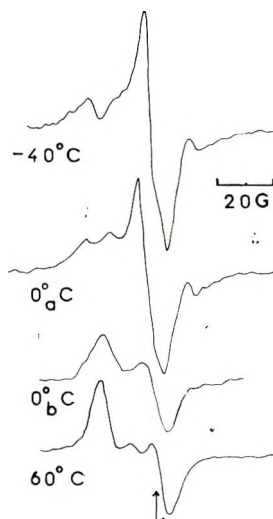


Fig. 2. Spectre du tétraoxane en poudre irradié à -196°C et recuit jusqu'à $+60^{\circ}\text{C}$ (0°_a début du recuit; 0°_b fin du recuit).

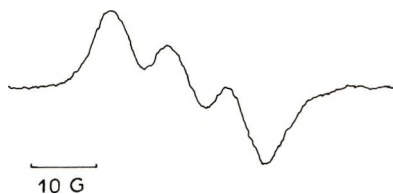


Fig. 3. Spectre du tétraoxane en poudre irradié à -196°C et recuit jusqu'à $+80^{\circ}\text{C}$.

du spectre pendant le recuit jusqu'à $+80^{\circ}\text{C}$. A -40°C nous avons un triplet.

Vers 0°C apparaît un doublet dont l'écartement entre les deux raies est de 17,2 gauss. Puis vers 60°C une nouvelle raie grandit entre les deux pics du doublet précédent jusqu'à devenir aussi intense. Vers $+80^{\circ}\text{C}$ ces pics sont devenus un triplet (Fig. 3) comme le confirme l'étude sur le cristal unique.

Dans la suite du texte, on comparera les spectres de la poudre (Figs. 1 à 3) avec ceux relatifs au cristal.

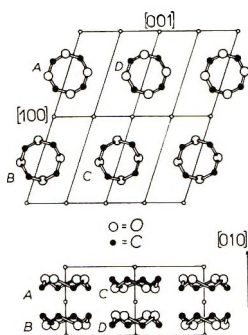


Fig. 4. Schéma de la maille cristalline du tétraoxane.³

Spectre du Monocristal

Structure cristalline. Le tétraoxane cristallise dans le système monoclinique avec quatre molécules par cellule unitaire (Fig. 4).³ Les cristaux que nous avons obtenus par sublimation sont des aiguilles fines dont l'axe est parallèle au vecteur $[010]$ (cf. ci-dessus). Nous n'avons pu faire que des rotations autour de l'axe $[010]$ car l'appareillage que nous possédons actuellement ne permet pas de réaliser des rotations autour de deux autres axes, l'ensemble des trois axes constituent un trièdre.

Rotation à -196°C . Il existe un groupe de raies intenses et de raies satellites de faible intensité de part et d'autre.

Les Raies Centrales

Résultats Experimentaux. Le Figure 5 donne l'aspect de ces raies pour trois angles de rotation différents. A 30° et à 40° il y a quatre raies distinctes que nous désignons par D_1 , S_1' et D_1' , alors qu'il n'y a que trois raies plus ou moins élargies à 90° . De part et d'autre de ces quatre raies existe encore deux raies D_2 , D_2' qui n'apparaissent qu'à certaines positions du cristal (Fig. 6). La raie à champ faible D_2 est plus distincte que celle à champ plus élevé. Elle semble être noyée dans le pic de la raie D_1' .

La position de ces raies en fonction de l'angle de rotation du cristal repéré par rapport à la direction du champ magnétique extérieur est donnée par la Figure 6.

Il existe en plus de ces raies un doublet photosensible (P, P') mise en évidence par une irradiation au ^{60}Co effectuée à l'abri de la lumière et dans un tube en spectrosil. Le cristal est maintenu dans une position telle que le spectre obtenu à -196°C possède quatre raies centrales bien distinctes (Fig. 7a).

La lumière émise par une lampe de tungstène n'a pas modifié la hauteur des pics P et P'. Par contre avec une lampe UV de longueur d'onde $>3000 \text{ \AA}$ nous avons obtenu une diminution très rapide de ces pics (Fig. 7b). Il ne subsiste que les épaulements D_2 , D_2' qu'une illumination prolongée n'a pu faire disparaître, La différence entre les spectres avant et après

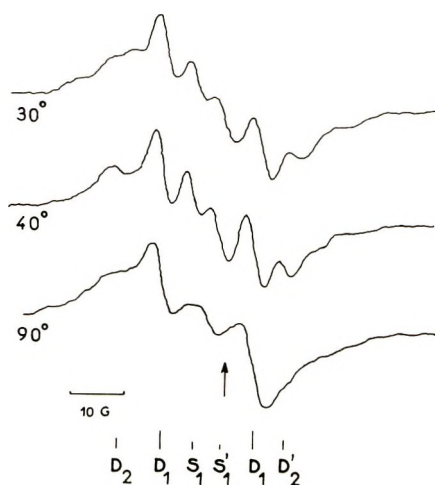


Fig. 5. Spectres du cristal de tétraoxane irradié à -196°C pour trois angles de rotation.

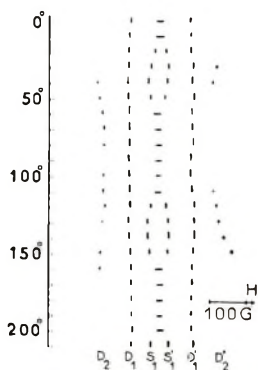


Fig. 6. Spectres du cristal de tétraoxane irradié à -196°C . Etude de la position des raies en fonction de l'angle de rotation du cristal.

illumination donne le doublet (P , P') du radical photosensible qui a un écart hyperfin de 31 gauss (Fig. 7c).

Nous n'avons pu nous assurer que le doublet (P , P') et les raies (D_2 , D_2') sont confondus bien que ces pics semblent avoir la même position dans le spectre.

Des essais qualitatifs de saturation de puissance ont montré que les raies (S_1 , S_1') s'élargissent, les raies du doublet (D_1 , D_1') un peu moins, lorsqu'on augmente la puissance des microondes. Le doublet photosensible n'a pas subi de variations de largeur de raies.

Interprétation. On peut tenter d'expliquer l'existence de radicaux $-\dot{\text{C}}\text{H}_2$ en groupant les raies de deux façons différentes: (S_1 , S_1') et (D_1 , D_1') ou (S_1 , S_1') et (D_2 , D_2').

Dans le premier cas, nous n'observons pas les rapports d'intensité 1/2/1 qui correspondent à deux protons équivalents. Les essais de saturation

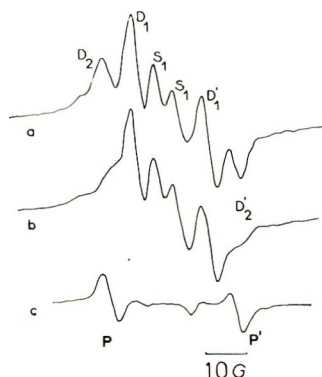


Fig. 7. Détermination du doublet photosensible: (a) spectre obtenu après irradiation à -196°C à l'abri de la lumière; (b) spectre obtenu après irradiation à -196°C , le cristal ayant été soumis à une lampe UV; (c) différence des deux spectres précédents.

de puissance montrent une certaine liaison entre ces raies. Cependant ces remarques ne sont pas convaincantes.

La constante de couplage serait de l'ordre de 8 gauss. En introduisant une anisotropie dans le couplage et comme les deux hydrogènes sont orientés différemment, on peut expliquer la présence de quatre raies. Avec un écart hyperfin de 6 gauss pour un hydrogène et de 11 gauss pour l'autre, on obtient les quatre raies qui apparaissent aux angles de 40 et 140° .

Néanmoins, nous avons des valeurs très faibles de l'écart hyperfin: 6 et 8 gauss. Les tenseurs de couplage hyperfin peuvent avoir un des axes avec la valeur minimale de 8 à 10 gauss mais les autres axes ont des valeurs nettement au-dessus: 20 et 33 gauss.⁴

Dans le deuxième cas, à certaines orientations (Figs. 5 et 6), on pourrait penser que les raies (S_1 , S_1') et (D_2 , D_2') forment un quadruplet dû à un radical $-\dot{\text{C}}\text{H}_2$ pour lequel les interactions avec deux hydrogènes ont des constantes de couplage différentes. Mais à d'autres angles, tandis que les raies (S_1 , S_1') gardent leurs intensités respectives, les raies (D_2 , D_2') disparaissent. De plus la saturation de puissance ne semble pas affecter les raies (D_2 , D_2').

L'existence des radicaux $-\dot{\text{C}}\text{H}_2$ est elle-même problématique. D'abord la présence d'un radical $-\dot{\text{C}}\text{H}_2$ suppose l'ouverture de la molécule et donc une énergie suffisante. Ensuite celle-ci implique que chaque extrémité $-\dot{\text{C}}\text{H}_2$ soit bloquée dans deux positions orthogonales. Ainsi s'expliquent la symétrie d'ordre 4 observée pour les raies (S_1 , S_1'). Enfin la suite de l'exposé montrera qu'un triplet intense qui n'a aucun rapport avec les raies précédentes existe vers -80°C .

On peut donc conclure que l'on est en présence de quatre (ou trois) couples distincts de raies: (S_1 , S_1'), (D_1 , D_1'), (D_2 , D_2') et (P , P').

De plus, les raies (S_1 , S_1') et (D_1 , D_1') reprennent le même aspect tous les 90° . Ce fait est lié à la structure des molécules de tétraoxane et à leur position dans la maille cristalline. D'après la Figure 4, les molécules se

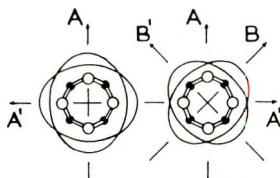


Fig. 8. Ellipses du tenseur de g du radical (A) à gauche, et du tenseur de A du doublet (D_1) à droite.

trouvent dans le plan perpendiculaire à l'axe de rotation [010]. L'axe de symétrie d'ordre 4 de la molécule et l'axe de symétrie d'ordre 2 de la maille cristalline sont parallèles à l'axe [010].

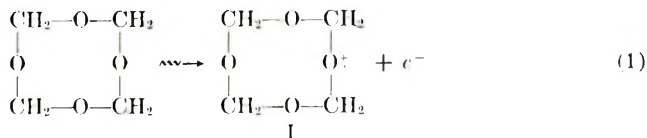
L'interprétation des couples (S_1, S_1'), (D_1, D_1') qui tient compte des écarts hyperfins et de la structure chimique des radicaux est la suivante. Cet ensemble de trois ou quatre raies est la superposition d'un doublet (D_1) avec une légère anisotropie dans l'écart hyperfin et de deux singulets (S_1) et (S_1') ayant une anisotropie en g .

Chaque singulet est attribué à un radical-ion (A), l'électron célibataire étant sur l'oxygène. Comme les quatre oxygènes ont autant de chance de porter cet électron célibataire, les directions qui correspondent à deux oxygènes symétriquement opposés dans la molécule sont équivalentes. Nous avons donc deux directions orthogonales A et A' le long desquelles un des tenseurs de g est à sa valeur maximale et l'autre à sa valeur minimale (Fig. 8: les ellipses sont déformées pour faciliter l'exposé). Quand le champ magnétique extérieur est parallèle à A ou A' les deux singulets (S_1) et (S_1') se séparent nettement.

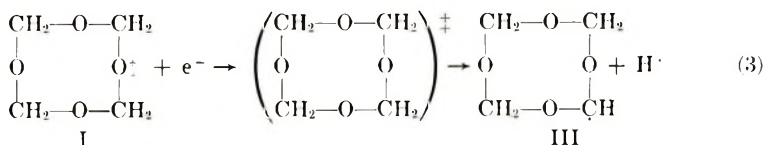
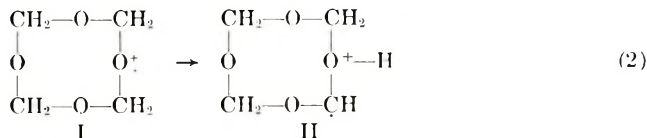
Le doublet (D_1) est dû à un radical cyclique. D'abord parce que la symétrie d'ordre quatre du singulet implique la stabilité du cycle. Ensuite parce qu'il apparaît vers -140°C un doublet très stable de symétrie d'ordre 2, de g différent, mais avec une constante de couplage analogue à (D_1) qui ne peut provenir que de l'ouverture du cycle. Le doublet (D_1) est donc attribué à la molécule ayant perdu un des hydrogènes (C). Supposons que la liaison avec l'hydrogène restant soit dirigée suivant la bissectrice de l'angle O—C—O que forment les liaisons du carbone avec les deux oxygènes. Le radical peut se trouver sur l'un quelconque des quatre carbones. Nous avons donc deux directions orthogonales B et B' pour lesquelles un des tenseurs A prend sa valeur maximale et l'autre sa valeur minimale. Si l'anisotropie n'est pas trop forte, la différence de valeurs entre les deux ellipses dans les directions B et B' est relativement faible, la résolution sera insuffisante et nous ne verrons que deux raies élargies. Par contre, dans les directions A et A' les ellipses se croisent, les raies se superposent et deviennent plus nettes. Ces directions correspondent à celles où les deux singulets sont nettement séparés (Fig. 5, angle de 40°C).

Il semble donc établi par les valeurs de g différentes de celles trouvées à des températures plus élevées ainsi que par la symétrie d'ordre 4 que ces radicaux appartiennent à un cycle fermé.

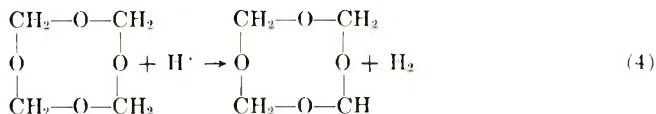
Interprétation chimique. On peut envisager la suite de réactions suivantes:



Ce radical-ion peut conduire à deux espèces différentes:



Le proton ainsi obtenu peut aussi réagir avec une molécule pour donner le radical III:



La formation d'hydrogène au cours de la polymérisation n'est pas contestable.

L'ion I correspond aux singulets (S_1) et (S_1'). Le radical III correspond au doublet (D_1) (écart hyperfin: 17 gauss), (g voisin de 2,0030). Quant au radical II nous lui attribuons provisoirement le doublet photosensible (P , P').

Nous n'avons pas trouvé d'interprétation pour les raies (D_2 , D_2'). La variation de leurs positions en fonction de l'orientation du cristal montre une symétrie d'ordre 2 ce qui indique que l'orientation du radical est plutôt liée à la structure cristalline. Cependant, les raies (P , P') et (D_2 , D_2') occupant pratiquement la même position dans le spectre, on peut aussi se demander s'il ne faut pas les attribuer au même radical. Ceci suppose que l'élimination des raies (P , P') n'est pas complète à la lumière du jour et aux rayons UV.

Les Raies Extérieures

A côté des raies principales se trouvent des raies secondaires plus faibles (quelques pour cent des raies principales). Elles comprennent en particulier (Figs. 9 et 10): Un doublet (g voisin de 2,0033). Comme l'écart entre les raies est de 132 gauss, on peut l'attribuer au radical $\text{H—}\dot{\text{C}} = \text{O}$;^{5,6} deux raies symétriques dont l'écart varie beaucoup en fonction de l'angle. Il passe de 455 gauss (écart maximum) à 270 gauss pour une rotation de

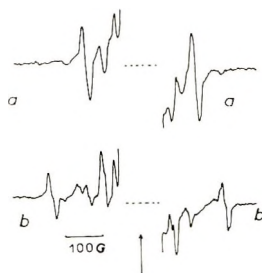


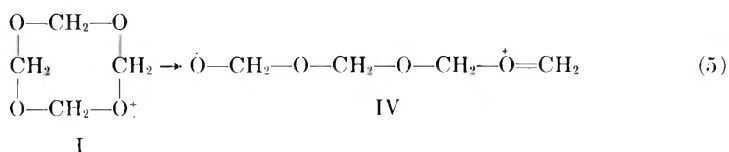
Fig. 9. Les raies extérieures du spectre du cristal de tétraoxane irradié à -196°C .

30° ; deux raies symétriques dont l'écartement varie peu en fonction de l'angle. L'écart maximum est de 288 gauss.

Les quatre dernières raies correspondent à la transition $\Delta m_s = \pm 1$ entre les trois niveaux $S = +1, 0, -1$, due à l'existence de paires de radicaux. Pour confirmer cette hypothèse nous avons cherché un signal aux alentours de 1600 gauss correspondant à la transition interdite $\Delta m_s = 2$ ($g = 4,0$). Celui-ci a une intensité si faible qu'un balayage simple ne permet pas de le détecter. Il a été nécessaire d'utiliser un accumulateur de spectres (mémoire Digitale Varian C-1024). On a obtenu une raie nette (rapport signal sur bruit d'environ 6) en sommant cent fois le signal de la région de 1600 gauss.

Avec les données actuelles nous ne pouvons pas calculer la distance entre ces paires de radicaux car nous n'avons pas fait les rotations complémentaires autour des deux autres axes.

Passage de -196°C à -85°C . Lorsque l'on élève la température, les raies extérieures citées précédemment diminuent d'intensité mais sont les seules parmi les raies secondaires à persister encore à -140°C . Par contre les raies centrales se différencient nettement (Fig. 11). Seules les raies correspondant aux singulets (S_1), (S_1') subissent un changement important. La rotation du cristal à -140°C montre que ces singulets ont perdu leur symétrie d'ordre 4 pour acquérir une symétrie d'ordre 2. Ce nouveau singulet (S_2) correspondrait d'après ce qui a été dit ci-dessus à l'ouverture du cycle donnant ainsi naissance au radical IV:



C'est cet ion radical qui initie la post-polymérisation du tétraoxane.¹

Vers -140°C apparaissent plusieurs raies dont l'intensité augmente lorsque l'on continue à élever la température. On constate alors les transformations suivantes (Fig. 11). Les doublets (D_1) et (D_2) et le singulet (S_2) disparaissent au profit des triplets (T_1) et (T_2) et d'un doublet (D_3).

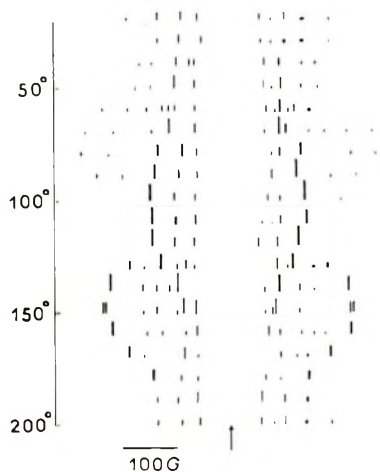


Fig. 10. Spectres du cristal de tétraoxane irradié à -196°C . Étude de la position des raies extérieures en fonction de l'angle de rotation du cristal.

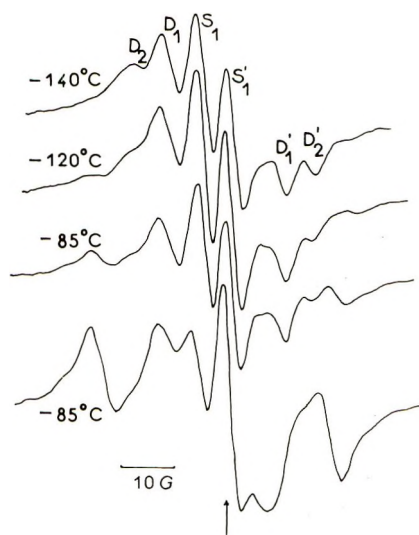


Fig. 11. Evolution du spectre du cristal de tétraoxane irradié à -196°C lorsque la température de recuit passe de -140°C à -85°C .

La rotation du cristal à -85°C (Fig. 12) a permis d'analyser les raies essentielles du spectre. C'est vers cette température que les triplets (T_1) et (T_2) prennent leur intensité maximale.

Rotation à -85°C . Pour comprendre certaines anomalies du spectre telle que la disparition d'une raie de faible intensité ou au contraire une augmentation trop importante de son intensité, il faut supposer que certaines raies se superposent exactement ou se séparent nettement. C'est ce qui arrive lorsque le cristal est à 90° et 110° (Figs. 12, 13a, et 13b).

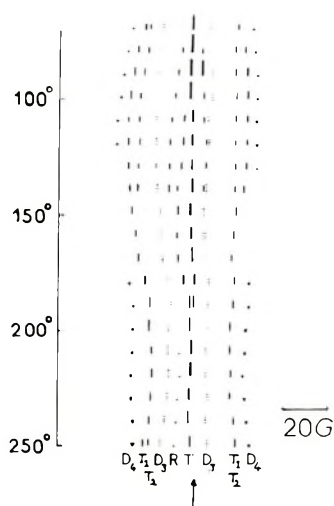


Fig. 12. Etude de la position des raies en fonction de l'angle de rotation du cristal après un recuit jusqu'à -85°C .

Avec cette hypothèse on peut décomposer le spectre en deux triplets (T_1) et (T_2) de même intensité et dont le g varie de 2,0036 à 2,0057. Ces triplets proviennent de deux radicaux $-\dot{\text{C}}\text{H}_2$ ayant chacun une orientation privilégiée dans la maille cristalline. De plus les deux hydrogènes de chaque radical ont une constante de couplage différente.

En effet, un radical $-\dot{\text{C}}\text{H}_2$ peut donner soit quatre raies d'égale intensité si les constantes de couplage sont différentes pour les deux hydrogènes, soit trois raies dont les intensités sont dans le rapport 1/2/1 si elles sont égales. Avec deux radicaux $-\dot{\text{C}}\text{H}_2$ on conçoit alors que suivant les valeurs de g et des constantes de couplage des deux hydrogènes on observe de 3 à 8 raies.

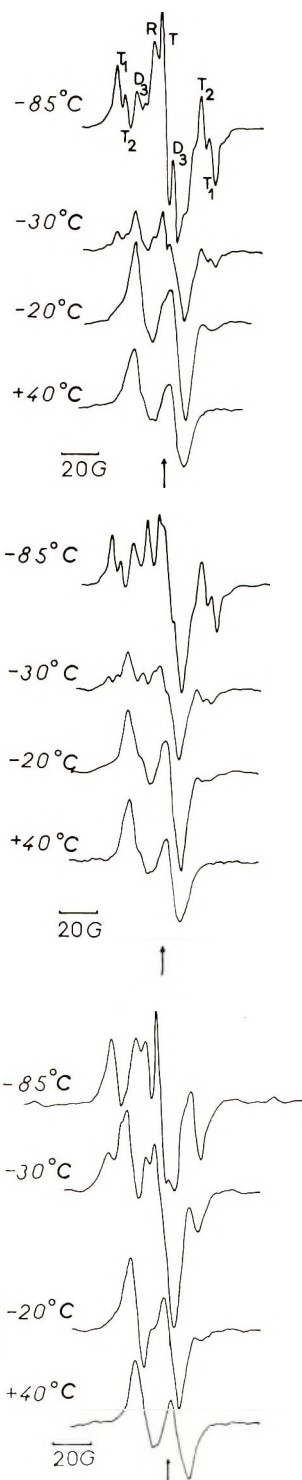
Si les valeurs de g et les constantes de couplage sont très voisines les deux triplets se confondent (Fig. 13d). Si seules les constantes de couplage diffèrent pour les deux hydrogènes d'un radical mais restent cependant voisines pour les deux radicaux, on obtient quatre raies (Fig. 13c). Enfin si les valeurs de g et des constantes de couplage diffèrent on obtient huit raies (Figs. 13a et 13b).

Avec les résultats expérimentaux actuels, on ne peut déterminer les constantes de couplage de chaque hydrogène. Notons simplement qu'elles varient de 17 à 34 gauss.

En plus des raies précédentes existent un doublet extérieur peu intense (D_1) décelable à certains angles, et une autre raie (R). Ces raies n'ont pu être analysées.

Enfin le doublet (D_3) semble avoir lui aussi une anisotropie en g et un écartement qui dépend de l'angle de rotation.

La naissance des triplets peut s'expliquer par l'ouverture due à l'agitation thermique du radical III cyclique [réaction (6)]. Cette transformation est assez lente comme le prouve l'évolution du spectre à -85°C (Fig. 11).



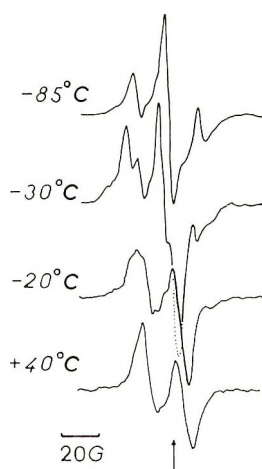
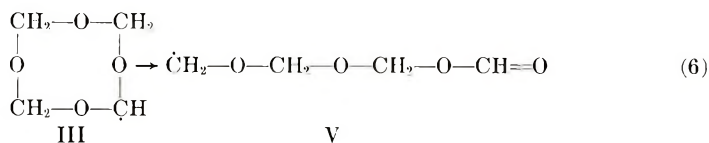


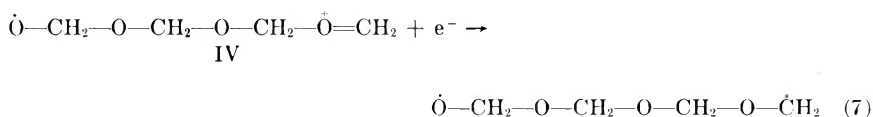
Fig. 13. Evolution du spectre du cristal de tétraoxane irradié à -196°C lorsque la température de recuit passe de -85°C à $+40^{\circ}\text{C}$. (a) à 90° ; (b) à 110° ; (c) à 170° ; (d) à 210° .



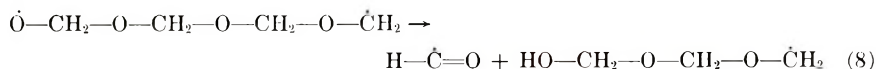
Cette hypothèse tiendrait compte de la disparition du doublet (D_1) lié à la présence du radical III ainsi que du passage de la symétrie d'ordre 4 à la symétrie d'ordre 2.

Les extrémités $-\overset{\cdot}{\text{C}}\text{H}_2$ doivent occuper deux positions privilégiées dans la maille cristalline. Ainsi pour certaines directions du champ magnétique les quatre hydrogènes ayant des constantes de couplage différentes on a le type de spectre indiqué sur les Figures 13.

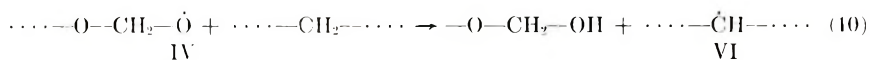
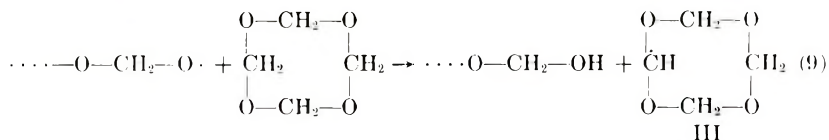
Une autre réaction possible est la suivante :



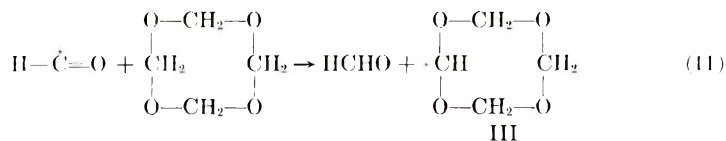
Mais elle conduit à une espèce chimique qui ne doit pas être stable. La réaction 8 expliquerait la disparition du singulet (S_2) lié au radical (D) et la présence du radical $\text{H}-\overset{\cdot}{\text{C}} = \text{O}$ (présence à -80°C d'un doublet avec un écart hyperfin de 127 gauss).



En parallèle, les réactions suivantes peuvent se produire :



Le radical $\text{H}-\dot{\text{C}}=\text{O}$ réagit aussi suivant des réactions analogues à (9) et (10) :



La disparition du singulet (S_2) et du radical $\text{H}-\dot{\text{C}}=\text{O}$ se fait non seulement au profit des triplets réactions (9) et (11) suivie par la réaction (7) mais aussi au profit du doublet (D_3) : réactions (10) et (12).

Passage de -85°C à 60°C . Lorsque l'on élève la température les triplets disparaissent au profit du doublet (D_2) (Fig. 13). Ce comportement peut s'expliquer par la réaction suivante :

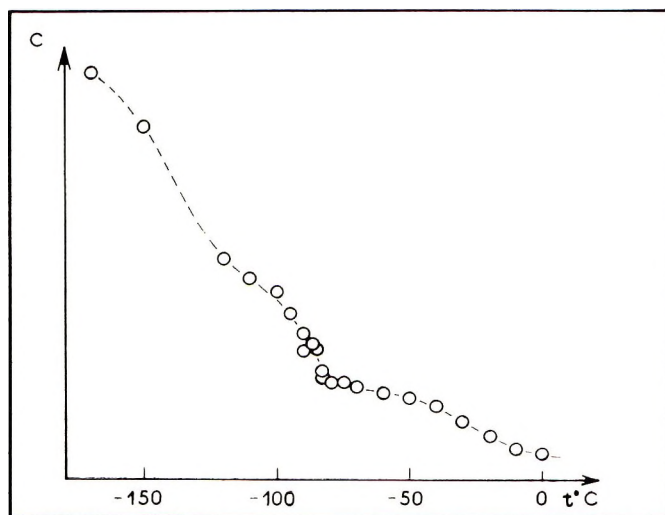
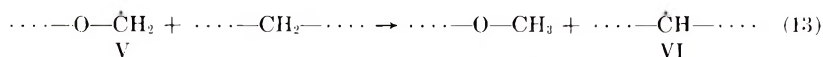


Fig. 14. Concentration relative des radicaux en fonction de la température de recuit (Ordonnée en unités arbitraires).

Entre -80°C et -50°C la transformation triplet-doublet se fait presque à concentration constante des radicaux comme le montre la Figure 14. Ceci implique que la réaction (13) est prépondérante et l'emporte sur la disparition des radicaux.

A -30°C les deux triplets existent toujours mais ils n'ont que 50% de leur intensité maximale. Le doublet (D_1) a pratiquement disparu.

Vers -20°C la résolution et l'amplification de l'appareil n'ont permis de distinguer qu'un seul triplet pratiquement isotrope. L'écart entre chaque raie est de 22 gauss. Il se peut que l'agitation thermique rende les deux triplets équivalents; alors la position des radicaux $-\dot{\text{C}}\text{H}_2$ devient isotrope. Cette hypothèse est confirmée par le fait que des mesures de second moment de la résonance nucléaire permettent de dire que la rotation des molécules commence vers -10°C .⁷

Le triplet disparaît complètement à $+5^{\circ}\text{C}$. Ces observations concordent avec celles de Sasakura et al.⁸ Ces auteurs ont noté la présence d'un triplet lorsque l'on irradie du polyoxyméthylène à 0°C , ce triplet étant instable à cette température.

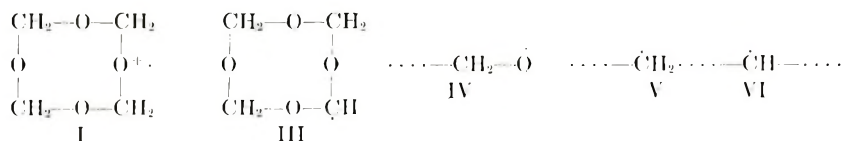
Le doublet (D_3) est isotrope comme le montre une rotation à 40°C ($g = 2,0062$, écart hyperfin 17,7 gauss). Dès 0°C ce doublet apparaît avec la poudre (écart: 17,2 gauss) (Fig. 2).

La raie (R) existe toujours ($g = 2,0104$).

Enfin une autre raie (X) apparaît au centre du doublet vers $+20^{\circ}\text{C}$ ($g = 2,0062$). Il se peut qu'elle soit due au radical $\cdots-\text{CHOO}\cdot$. Une expérience avec la poudre nous a montré qu'elle pouvait devenir aussi intense que le doublet (Fig. 3).

CONCLUSION

Cette étude nous a permis de préciser que les radicaux:



existent dans les intervalles de température suivants: I et III $< -85^{\circ}\text{C}$; IV -140 à -85°C ; (V) -120 à $+5^{\circ}\text{C}$; VI $> -30^{\circ}\text{C}$.

L'existence d'un radical photosensible a été démontrée ainsi que celle de paires de radicaux.

Il serait intéressant de préciser encore cette étude par les tenseurs de g et de A et d'interpréter les raies D_2 , D_1 et R, d'autre part, de faire d'autres études analogues à celle-ci, particulièrement sur le trioxane-trimère cyclique du formaldéhyde—afin d'en comparer les résultats avec ceux de la présente étude.

References

1. C. Cannavo et K. Hayashi, Communication privée.
2. H. Yoshida et B. Rånby, *J. Polym. Sci. A*, **3**, 2289 (1965).
3. Y. Chatani, T. Uchida, H. Tadokoro, K. Hayashi, M. Nishii, et S. Okamura, *J. Macromol. Sci. Physics*, **B-2**, 567 (1968).
4. A. Horsfield, J. R. Morton, et D. H. Whiffen, *Mol. Phys.*, **4**, 327 (1961); *Landolt-Börnstein Nouvelle serie, groupe II*, Vol. 1, H. Fischer Ed., Springer Verlag, Berlin, 1965.
5. I. L. Cochran et F. J. Adrian, Fifth International Symposium on Free Radicals, Uppsala, 1961.
6. C. Chachaty et R. Marx, *J. Chim. Phys. (Paris)*, **1962**, 792.
7. K. Hayashi, K. Hayashi, et S. Okamura, *Ann. Rept. Japan. Assoc. Rad. Res. Polym.*, **7**, 169 (1965-1966).
8. H. Sasakura, N. Takeuchi, et T. Mizuno, *J. Phys. Soc. Japan*, **17**, 572 (1962).

Received November 3, 1969

Transformations of Chloroethylenes in the Presence of Aprotic Acids*

E. N. ZILBERMAN, A. E. KULIKOVA,
 N. M. PINCHUK, N. K. TAIKOVA, and N. A. OKLADNOV,
*Research Institute of Organochlorine Compounds and Acrylics,
 Dzerzhinsk, USSR*

Synopsis

The cationic polymerization of vinyl chloride, vinylidene chloride, and *cis*- and *trans*-1,2-dichloroethylenes with the use of Lewis acid-type catalysts has been studied. Vinylidene chloride is smoothly polymerized in the presence of $ZnCl_2$ at 40°C to form the dimer, 1,1,3,3-tetrachlorobutene-1, and poly(vinylidene chloride) having somewhat increased crystallinity (45%). Vinyl chloride is polymerized very slowly in the presence of $AlCl_3$ and $TiCl_4$ to give dimeric, trimeric, tetrameric, and low molecular weight polymer products. The polymerization is followed by carbonium ion isomerization that leads to reaction products of branched structure. The *cis*- and *trans*-1,2-dichloroethylenes react in the presence of $AlCl_3$ only at 50–60°C, and their polymerization is terminated at the stage of dimer and cyclic trimer formation. A mechanism of carbonium ion-initiated polymerization of chloroethylenes is proposed, and the causes which lead to early termination of polymerization are discussed.

INTRODUCTION

Previously¹ it has been shown that cationic polymerization of vinylidene chloride (VDC) catalyzed by $AlCl_3$ is terminated at the stage of dimer (1,1,3,3-tetrachlorobutene-1) and cyclic trimer (1,1,3,3,5,5-hexachlorocyclohexane) formation. Polymerization termination at the early stages is explained by the formation of a stable complex of dimer with $AlCl_3$ that prevents from monomer molecule addition to dimer and also by the cyclic structure of the trimer. The aim of the present work was to reach higher degrees of VDC polymerization; to do this, the process was carried out in the presence of $ZnCl_2$, which does not possess such strong dehydrochlorinating and cyclizing ability and is not so strong complexing agent as $AlCl_3$. It was of interest to study the behavior of the other chloroethylenes under the influence of aprotic acids. We have investigated the possibility of the cationic polymerization of vinyl chloride (VC) and 1,2-dichloroethylene (DCE).

* Paper presented at the IUPAC Symposium on Macromolecular Chemistry, Budapest, 1969.

EXPERIMENTAL

$ZnCl_2$ and $AlCl_3$, both freshly baked, and vinylidene chloride, vinyl chloride, *cis*- and *trans*-1,2-dichloroethylenes with the constants corresponding to the literature data were used. Peroxides were absent from the monomers, as shown by iodometric determinations.

The infrared spectra were recorded on a UR-10 spectrometer. Solid samples were prepared in the form of 3% concentration pellets pressed with KBr. The liquids were used in the form of thin films between NaCl plates.

The NMR-spectra were recorded on a CLA² analytical spectrometer at a frequency of 60 MHz at room temperature with hexamethyldisiloxane as a reference. The chemical shifts were expressed by the δ scale (in parts per million relative to tetramethylsilane). A 70% solution (by weight) of 1,1,3,5-tetrachlorohexane and diastereoisomers of 1,1,2,3,4-pentachlorobutane, and a 10% solution of 1,1,5,5-tetrachloro-3-methylpentane in chlorobenzene were prepared for structure determination.

Dipole moments were determined in benzene solution at 20°C.

The differential thermal analysis was performed with a unit consisting of standard measuring and recording apparatus,³ isophthalic acid being chosen as a reference.

The degree of crystallinity was determined by a technique described in the literature.⁴

The separation of tetrachlorohexane isomers was carried out by a preparative gas-liquid chromatography technique with the Etalon apparatus of Dzerzhinsk OKBA [column temperature, 160°C; length, 3.3 m; diameter, 14 mm; sorbent, Chromosorb W (0.4-0.6 mesh) plus 20% poly(ethylene glycol adipate); evaporator temperature, 250°C; nitrogen as carrier gas, flow rate 300 ml/min].

The purity of separated fractions was examined by a Tsvet chromatograph [column temperature, 150°C; length, 1 m; diameter, 6 mm; 15% of poly(ethylene glycol adipate) on TND sorbent (0.25 mm); helium as carrier gas, flow rate 1.2 l./h].

Polymerization of Vinylidene Chloride with $ZnCl_2$

Polymerization of vinylidene chloride with the use of $ZnCl_2$ was carried out in sealed ampoules; 60 g (0.62 mole) of VDC and 8.42 g (0.062 mole) of $ZnCl_2$ were charged into the ampoule under nitrogen. To remove traces of air the contents of the ampoules were frozen three times in liquid nitrogen, evacuated, and then sealed. The ampoules were placed into a shaking thermostat and kept for 75 hr at +40°C. The polymerization was terminated by pouring the reaction mixture into a tenfold volume of ice water. The precipitated polymer was filtered, washed with methanol and water until chloride ions were absent, and dried *in vacuo*; the yield was 5.9 g (9.8%) of PVDC.

ANAL. Calcd for $(C_2H_2Cl_2)_n$: C, 24.74%; H, 2.06%; Cl, 73.20%. Found: C, 24.63; H, 2.13%; Cl, 73.52%.

The PVDC obtained is poorly soluble in boiling chlorobenzene and cyclohexanone. The aqueous filtrate obtained after removing polymer was extracted with ether. The extract was washed with water until disappearance of chloride ions in the wash, dried over anhydrous sodium sulfate, and distilled *in vacuo*: 8.35 g (13.9%) of 1,1,3,3-tetrachlorobutene-1 with the constants corresponding to the literature data¹ was separated.

Polymerization of Vinyl Chloride with $AlCl_3$

The mixture of 31.5 g (0.5 mole) of vinyl chloride and 0.67 g (0.005 mole) of $AlCl_3$ was cooled in an ampoule by a mixture of Dry Ice and acetone. Then the ampoule was placed in liquid nitrogen and after threefold freezings *in vacuo* was sealed, placed into a shaking thermostat at $+25^\circ C$, and unsealed after 120 hr. The reaction mixture from 10 similar ampoules was carefully poured into ice water. The oil layer and the solid precipitate were separated, and the aqueous layer was extracted with ether. The obtained extracts were combined with the oil layer and the solid precipitate and filtered to remove a brown product, which was extracted with ether in a Soxhlet apparatus for 10 hr, washed with water until chloride ions were absent from the wash, then dried *in vacuo*; 8.2 g (4%) of polymer P_2 were obtained.

ANAL. Found: C, 51.62%; H, 5.80%; Cl, 38.18%.

The polymer is insoluble in organic solvents as well as in sulfuric acid.

The ether solutions were washed with water until disappearance of chloride ions, dried over $CaCl_2$; then a three-fold volume of methanol was added. The amorphous yellow powder obtained was filtered off, washed with a small amount of methanol, and dried *in vacuo*. Polymer P_1 was obtained in 5.0 g (2%) yield.

ANAL. Found: C, 46.96%; H, 5.33%; Cl, 46.52%.

The molecular weight of the product was 1300 (in benzene), bromine number (in ethylene dichloride) 45. The specific viscosity of a 1% solution in ethylene dichloride for a number of samples ranged from 0.015 to 0.05.

The filtrate obtained by separation of polymer P_1 was carefully evaporated in air and an additional quantity of P_1 (0.1 g) settled, which was filtered off. Vacuum distillation of the same filtrate yielded 9.7 g of 1,1,3-trichlorobutane, [bp $88.5^\circ C/99$ mm, d_4^{20} 1.2703, n_D^{20} 1.4621; MR_D 34.96, (calcd 35.27); M 167.5 in benzene, (calcd 161.5); lit.⁵ n_D^{25} 1.3170; n_D^{25} 1.4600], 1.5 g (0.3%) of a mixture of 1,1,3,5-tetrachlorohexane and 1,1,5,5-tetrachloro-3-methylpentane, and 0.8 g (0.2%) of a tetramer [bp $102^\circ C/5$ mm, d_4^{20} 1.3326, n_D^{20} 1.4938].

ANAL. Calcd for the tetramer, $C_8H_{12}Cl_4$: C, 38.40%; H, 4.80%; Cl, 56.80%; MW, 250. Found: C, 37.81%; H, 4.73%; Cl, 56.68%; MW, 248 (in benzene).

1,1,3,5-Tetrachlorohexane separated from its mixture with 1,1,5,5-tetrachloro-3-methylpentane by preparative gas-liquid chromatography (with a retention time of 2197 sec) has n_D^{20} 1.4855.

ANAL. Calcd for $C_6H_{10}Cl_4$: C, 32.14%; H, 4.46%; Cl, 63.39%; MW, 224. Found: C, 32.15%; H, 4.46%; Cl, 63.35%; MW, 225 (in benzene).

1,1,5,5-Tetrachloro-3-methylpentane (with retention time of 2915 sec) has n_D^{20} 1.4873.

ANAL. Calcd for $C_6H_{10}Cl_4$: C, 32.14%; H, 4.46%; Cl, 63.39%; MW, 224. Found: C, 33.00%; H, 4.54%; Cl, 62.91%; MW, 226.5 (in benzene).

Polymerization of *cis*-1,2-Dichloroethylene in the Presence of $AlCl_3$

A mixture of 91.3 g (0.94 mole) *cis*-1,2-DCE and 12.6 g (0.094 mole) $AlCl_3$ was heated in a stream of dry purified nitrogen for 15 hr at 70°C, intense hydrogen chloride evolution being observed. Acetylene chloride formed was absorbed with Ilosway solution; 0.1 g of cupric chloroacetylenide with 50% copper content was isolated.

After cooling, the reaction mixture was carefully treated with 50 ml water and subjected to steam distillation. The oil layer of the distillate was separated, and the aqueous one was extracted with ether. The ether extracts were combined with the oil layer, dried over $CaCl_2$, and distilled; 5.5 g of unreacted 1,2-DCE (in which chromatographically 1.5% *trans* isomer was found), 26.5 g (21%) 1,1,2-trichloroethane (having constants corresponding to the literature data), and 15.8 g (16%) of a mixture of diastereoisomers of 1,1,2,3,4-pentachlorobutane were found. The last mixture was separated into two isomers by preparative gas-liquid chromatography. Erythro-1,1,2,3,4-pentachlorobutane has bp 80°C/5 mm, d_4^{20} 1.5626, n_D^{20} 1.5100; MR_D 45.06 (calcd 45.00).

ANAL. Calcd for $C_4H_2Cl_5$: C, 20.83%; H, 2.17%; Cl, 77.00%; MW, 230.4. Found: C, 20.77%; H, 2.15%; Cl, 76.45%; MW, 235 (in benzene).

Threo-1,1,2,3,4-pentachlorobutane has mp 48°C, bp 113°C/19 mm; d_4^{50} 1.5513; n_D^{50} 1.5100; MR_D 44.85, (calcd 45.00).

ANAL. Calcd for $C_4H_2Cl_5$: C, 20.83%; H, 2.17%; Cl, 77.00%; MW, 230.4. Found: C, 21.07%; H, 2.13%; Cl, 76.50%; MW, 232.

The infrared spectra of the two isomers are shown in Figure 1.

The residue remaining after distillation of the reaction mixture was washed with water until chloride ions were absent and extracted with methanol in a Soxhlet apparatus for 16 hr. From the methanol extract, after evaporation, a light brown product was obtained from which, after repeated precipitations with methanol, 1.4 g of α -1,2,3,4,5,6-hexachlorocyclohexane were separated, mp 150°C. The melting point of the sample was not depressed by addition of authentic α -1,2,3,4,5,6-hexachlorocyclohexane. The absorption bands at 785 and 700 cm^{-1} , characteristic of α -isomer of hexachlorocyclohexane,⁶ were observed in the infrared spectra of the compound obtained. The residue (37.5 g) obtained after extraction was a dark brown powder insoluble in common solvents. The absorption

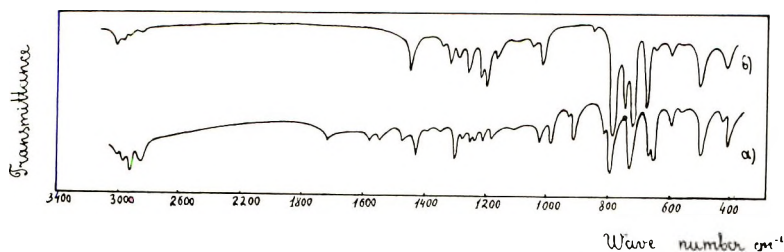


Fig. 1. Infrared spectra: (a) liquid 1,1,2,3,4-pentachlorobutane; (b) solid 1,1,2,3,4-pentachlorobutane.

bands at $1595\text{--}1580\text{ cm}^{-1}$ ($\nu_{\text{C}=\text{C}_{\text{conj.}}}$) and 1720 cm^{-1} ($\nu_{\text{C}=\text{O}}$) were found in the infrared spectra of the polymer.

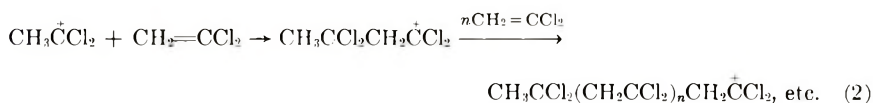
ANAL. Found: C, 43.0%; H, 1.8%; Cl, 49.0%.

RESULTS

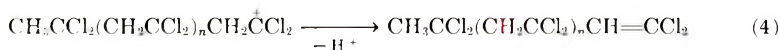
Vinylidene chloride was smoothly polymerized in the presence of ZnCl_2 at $+40^\circ\text{C}$ by a cationic mechanism with the formation of the dimer (1,1,3,3-tetrachlorobutene-1) and poly(vinylidene chloride) [see eqs. (1)–(4)]. It should be supposed that the chain initiation occurs owing to carbonium-Chain initiation:



Chain propagation:



Chain termination:



ion $\text{CH}_3\overset{+}{\text{C}}\text{Cl}_2$ formation. This ion is generated by the addition of a proton, which is present in the reaction mixture due to some catalyst moisture, to VDC. Macrocation propagation results from successive addition of monomer molecules to the $\text{CH}_3\overset{+}{\text{C}}\text{Cl}_2$ carbocation. In chain termination, the β -proton is lost, and this leads to the appearance of 1,1,3,3-tetrachlorobutene-1 and poly(vinylidene chloride) (PVDC).

According to the x-ray crystallographic studies the crystallinity of PVDC obtained is 45% while that of PVDC formed by a radical mechanism varies within the range of 38–42%.⁴ The increased crystallinity of PVDC obtained with ZnCl_2 may be related to the fact that polymers of more ordered

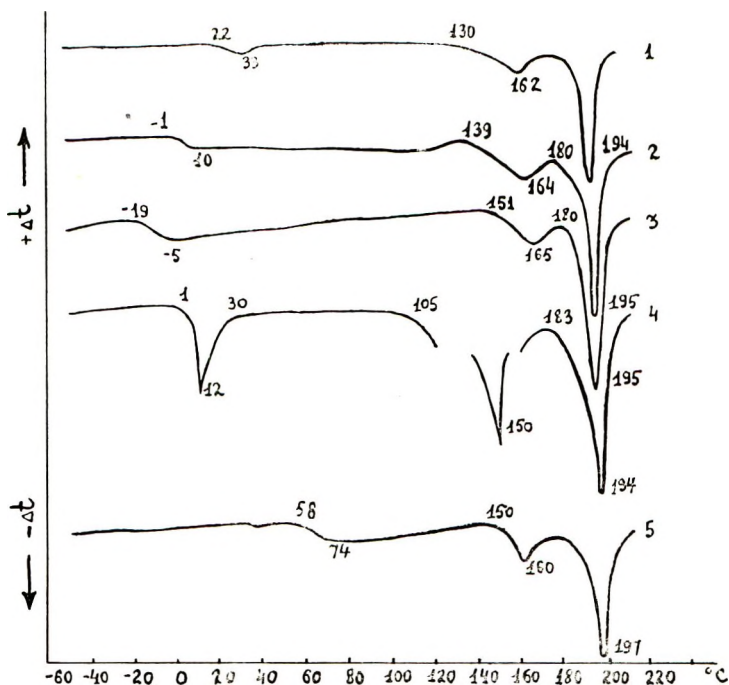


Fig. 2. Thermograms of poly(vinylidene chloride): (1) polymer obtained in the presence of AIBN by the suspension method; (2), (3), (4) polymer obtained in the presence of $ZnCl_2$ for 25, 50, and 75 hr, respectively; (5) polymer obtained by thermal polymerization (25–30°C) for 75 hours.

structure are formed with the use of ionic catalysts. It is also very likely that the higher crystallinity of PVDC obtained by us is due to its relatively low molecular weight. As a result, in formation of polymer, conformations responsible for high crystallinity are predominant. Similar conformation changes for higher molecular weight polymers are difficult.

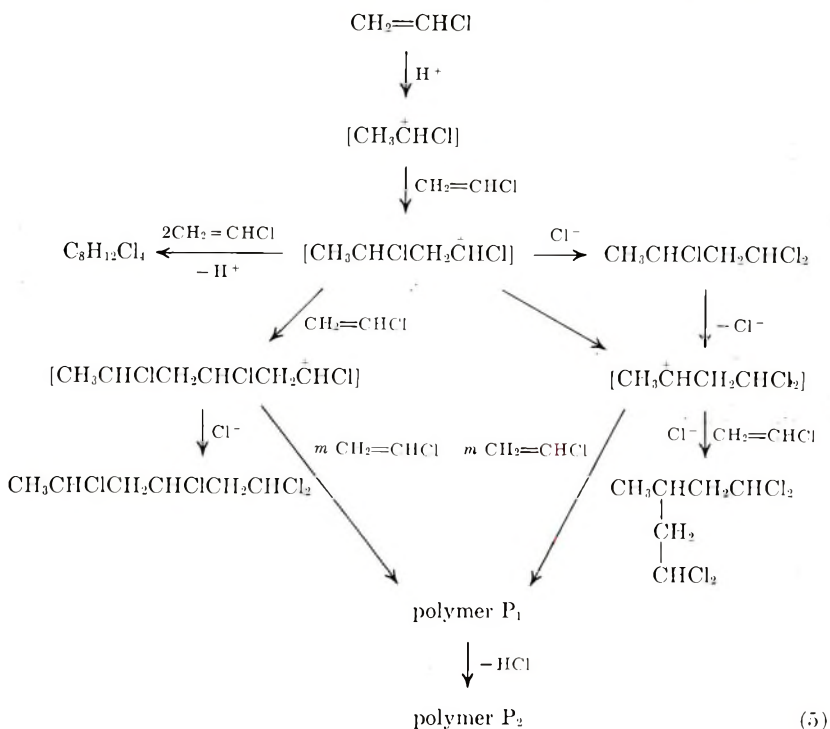
PVDC formed in the presence of $ZnCl_2$ was investigated by differential thermal analysis. The thermograms (Fig. 2) show that in the polymerization of VDC there are formed both perfect crystals melting in the temperature range of 180–200°C and less perfect ones melting at lower temperatures.

The increase of polymerization time does not influence the melting point of the main polymer fraction while endothermic premelting effect value is increased. This appears to be associated with the accumulation of low molecular weight fractions in the polymer with increasing polymerization time. The existence of an endothermic premelting effect may be also associated with different morphology of the supermolecular structure of PVDC.⁷

Vinyl chloride is polymerized by a cationic mechanism with the use of more active catalysts than $ZnCl_2$. The reaction proceeds under the effect of $AlCl_3$ and very slowly under the influence of $TiCl_4$. The polymerization

of VC is not initiated by ZnCl_2 , SnCl_4 , or FeCl_3 , even in the presence of ethyl alcohol, water, trichloroacetic acid, and *tert*-butyl chloride.

At 25°C and a 100:1 molar ratio of vinyl chloride to AlCl_3 , formation of oligomeric and polymeric compounds is observed. In this case 1,1,3-trichlorobutane,⁵ 1,1,3,5-tetrachlorohexane, and its isomer (1,1,5,5-tetrachloro-3-methylpentane), a product of empirical formula $\text{C}_8\text{H}_{12}\text{Cl}_4$, the polymer P_1 containing about $1/3$ $(-\text{CH}=\text{CH}-)$ units and the polymer P_2 with 50% of above mentioned units were obtained [eqs. (5)]. The polymerization rate increases with temperature rise. However, dehydro-



chlorination is simultaneously increased, which leads to a polymer with a higher content (up to 80%) of vinylenic units.

The structure of tetrachlorohexanes which have not been previously described was established by the NMR (Fig. 3) and infrared spectra (Fig. 4). In the NMR spectrum of one of the isomers there is a doublet at $\delta = 1.4$ ppm with 6 Hz splitting that is formed by protons of the methyl group of the CH_3-CHCl fragment. The multiplet with a center at $\delta = 1.8$ ppm belongs to protons of the methylene group in $-\text{CHClCH}_2\text{CHCl}-$ fragments; the multiplet with the center at $\delta = 2.4$ ppm is related to methylene protons of the fragment $-\text{CHClCH}_2\text{CHCl}_2$. The signals at $\delta = 4.2$ ppm are explained by the presence of protons of the CHCl group, and the signal at $\delta = 6.0$ ppm is indicative of the CHCl_2 group. The infrared spectrum shows an absorption in the region of $600-700\text{ cm}^{-1}$ typical of

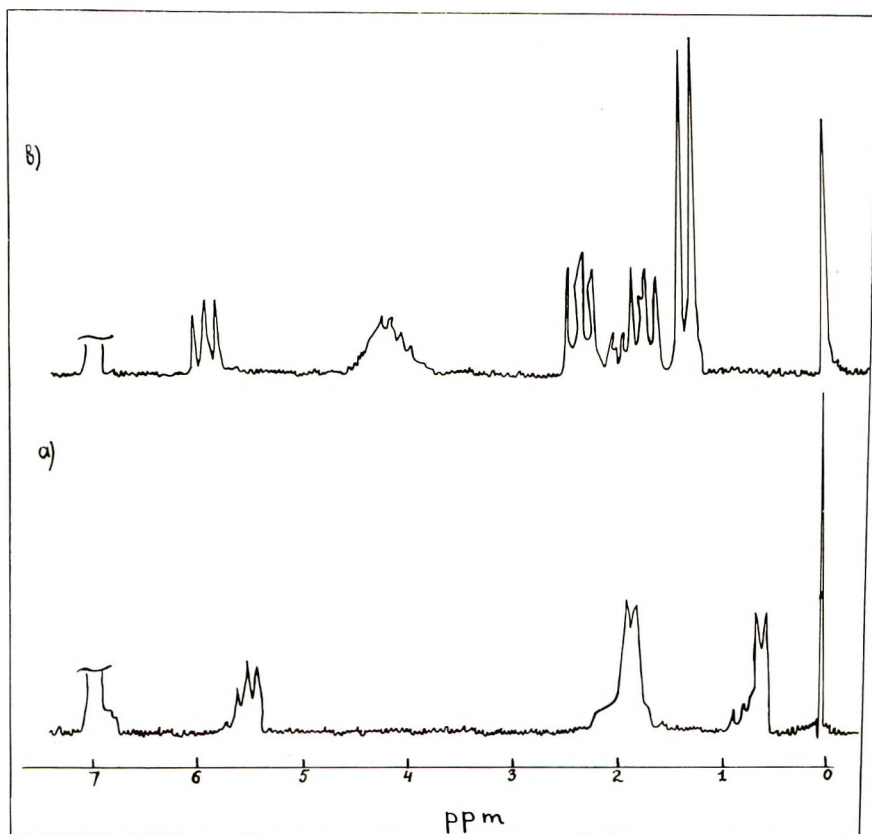


Fig. 3. NMR spectra of vinyl chloride polymerization products: (a) 1,1,5,5-tetrachloro-3-methylpentane; (b) 1,1,3,5-tetrachlorohexane.

vinyl chloride units of PVC. Thus, the given data are evidence in favor of a 1,1,3,5-tetrachlorohexane structure.

The second isomer of tetrachlorohexane contains in the NMR spectrum a signal at $\delta = 0.7$ ppm given by methyl protons of the CH_3CH fragment. The multiplet centered at $\delta = 2.0$ ppm is explained by the presence of methylene and methine protons. The signal at $\delta = 5.6$ ppm belongs to the CHCl_2 group protons. By measuring the integrated signal areas it has been determined that there are three methyl protons of the CH_3CH fragment, five methylene and methine protons, as well as two protons from the CHCl_2 group in the molecule of the isomer. Thus on the basis of the NMR spectrum, a 1,1,5,5-tetrachloro-3-methylpentane structure can be attributed to the second isomer. The infrared spectrum contains only absorption bands at 670 and 770 cm^{-1} , which are specific to the CHCl_2 group, in the range 600–800 cm^{-1} ; this confirms the structure proposed.

The vinyl chloride tetramer of $\text{C}_8\text{H}_{12}\text{Cl}_4$ formulation shows absorption in the infrared spectrum in the range of 1640 cm^{-1} ($\nu_{\text{C}=\text{C}}$), 623 cm^{-1} (charac-

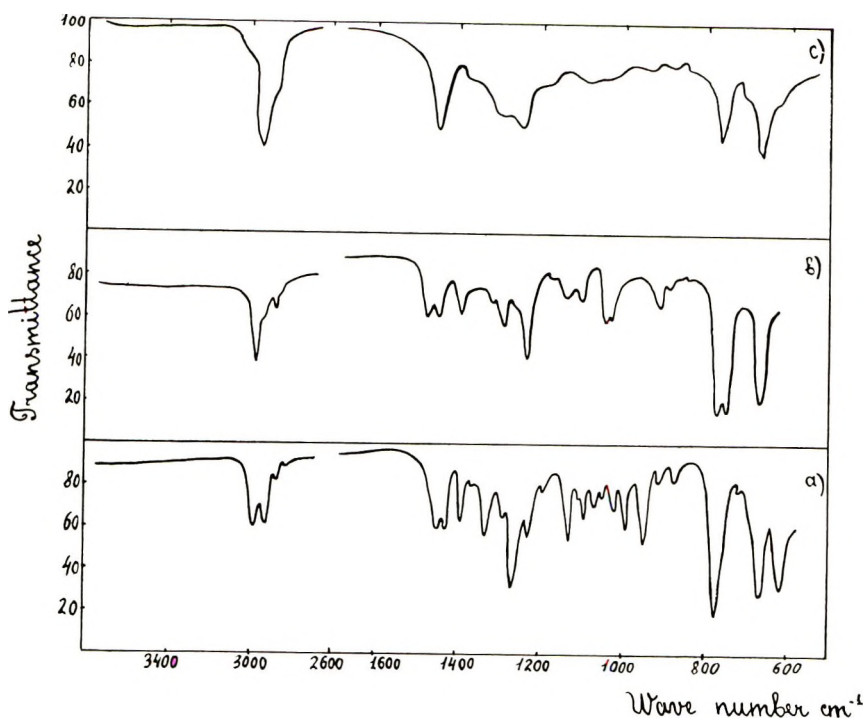


Fig. 4. Infrared spectra of oligomeric and polymeric compounds obtained from vinyl chloride: (a) 1,1,3,5-tetrachlorohexane; (b) 1,1,5,5-tetrachloro-3-methylpentane; (c) polymer P_1 .

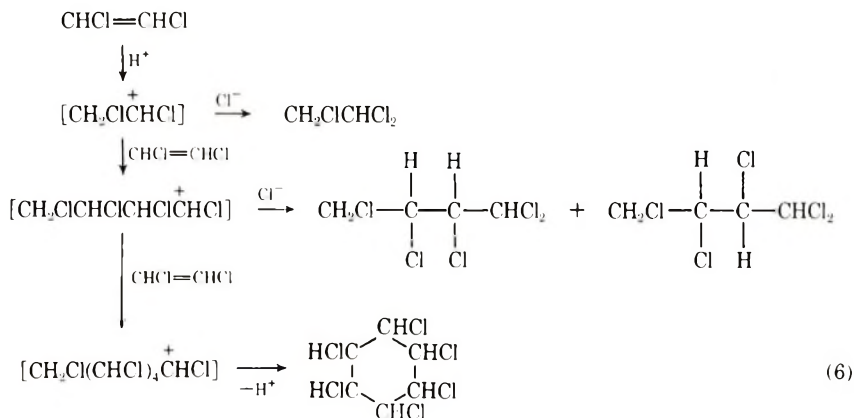
teristic of the CHCl group) and 665 and 770 cm^{-1} (typical of the CHCl_2 group). This suggests that the tetramer is mainly of a linear structure and contains $+\text{CH}_2\text{CHCl}+$, $+\text{CH}=\text{CH}+$, and $+\text{CH}_2\text{CHCl}_2$ units, the latter being at the end of molecule.

As for the structure of the polymer P_1 it was established that it is of rather low molecular weight (the degree of vinyl chloride polymerization is ~ 30) and branched structure. Since its infrared spectrum (Fig. 4) is close to that of 1,1,5,5-tetrachloro-3-methylpentane it should be considered that this polymer has branched $+\text{CH}(\text{CH}_2\text{CHCl}_2)-\text{CH}_2+$ and $+\text{CH}=\text{CH}+$ units. The weak absorption in the range of $615-620\text{ cm}^{-1}$ indicates that the polymer P_2 has small amount of vinyl chloride units. The low molecular weight of the polymer is explained by accumulation of HCl in the reaction mixture which enhances the probability of chain termination.⁸

The polymerization of vinyl chloride can be supposed to occur similarly as to that of vinylidene chloride. In this case at first carbonium ion CH_3CHCl^+ is formed due to the addition of a proton to a monomer molecule [see eqs. (5)]. Interaction of this carbonium ion with the second molecule of VC leads to formation of a new carbonium ion, $\text{CH}_3\text{CHCl}^+\text{CH}_2\text{CHCl}$. The latter can be either stabilized by addition of chloride anion, or can

give, after adding the third molecule of initial monomer, a trimeric cation $\text{CH}_3\text{CHCl}^+\text{CH}_2\text{CHClCH}_2\text{CHCl}$, rise to 1,1,3,5-tetrachlorohexane. Secondary reactions between 1,1,3-trichlorobutane and vinyl chloride in the presence of AlCl_3 leads⁹ apparently to formation of 1,1,5,5-(tetrachloro-3-methyl)pentane.

Cis- and *trans*-1,2-dichloroethylenes, under the influence of AlCl_3 , react at a marked rate only on heating to 50–60°C. In this case [eqs. (6)], 1,1,2-trichloroethane, a mixture of two diastereoisomers of 1,1,2,3,4-pentachlorobutane,¹⁰ a cyclic trimer (α -1,2,3,4,5,6-hexachlorocyclohexane) and a polymeric product of a formula close to $(\text{C}_2\text{HCl})_n$ are formed. Intramolecular dehydrochlorination of 1,2-DCE which proceeds to a negligible extent leads also to formation of monochloroacetylene.



The yields of the above-mentioned compounds are appreciably diminished with decreasing reaction temperature and only reciprocal isomerization of *cis*- and *trans*-1,2-DCE's is observed at -50 to 0°C. Below 0°C, the polymerization is not initiated even by the addition of titanium tetrachloride, ethyl alcohol, water, or *tert*-butyl chloride, which usually increase the AlCl_3 catalytic effect of AlCl_3 .

It should be noted that the yields of the reaction products formed from *trans*-1,2-DCE are much lower in comparison with *cis*-1,2-DCE. Evidently the higher reactivity of *cis*-isomer is associated with its asymmetric structure and relatively high dipole moment. It is not impossible that *trans*-1,2-DCE reacts in the presence of AlCl_3 only after its isomerization to the *cis* form.

Transformation of 1,2-DCE seems to start with formation of a carbonium ion, $\text{CH}_2\text{ClCHCl}^+$, to which monomer molecules are successively added by the reactions (6), where the stabilization of carbonium ion $\text{CH}_2\text{ClCHCl}^+$ can proceed in different directions. It is transformed to initial 1,2-DCE due to splitting off of a β -proton and to 1,1,2-trichloroethane on interacting with a chlorine anion. However, the carbonium ion initially formed in collision

with a monomer molecule may also give the dimeric ion $\text{CH}_2\text{Cl}^+\text{CHCl}^-\text{CHCl}^+\text{CH}_2\text{Cl}^-$. The dimeric ion, in turn, either adds chlorine anion converting to 1,1,2,3,4-pentachlorobutane or by interacting with a new 1,2-DCE molecule forms the trimeric cation $\text{CH}_2\text{Cl}^+(\text{CHCl})_2\text{CHCl}^+$ under the influence of AlCl_3 , cyclizing¹¹ to hexachlorocyclohexane. From all possible isomers of hexachlorocyclohexane only α -isomer was obtained. This is probably associated with its highest stability in the presence of AlCl_3 .¹²

The dimer of 1,2-DCE (1,1,2,3,4-pentachlorobutane) was separated into two isomers, liquid and solid, identical to those obtained by Prins,¹⁰ who however did not ascertain their steric configuration. By means of Stewart-Briegleb models we have established that carbon skeleton of both isomers has the same conformation, however, two diastereoisomeric forms may exist: erythro (I) and threo (II):



The dipole moments measured by us for liquid and solid isomers are 7.7 and 1.5 D, respectively. Furthermore, the threo isomer usually has a higher melting point than the erythro form¹³ due to its more rigid structure. Based on this we have concluded that the liquid isomer of 1,1,2,3,4-pentachlorobutane has the erythro structure (I) and the solid one possesses a threo structure (II).

Polymer obtained from 1,2-DCE consists of $+\text{CH}=\text{CCl}+$ and



units, approximately in equal proportions. Oxalic acid, carbon dioxide, and insoluble chlorine-containing residue were obtained by oxidation of the polymer.¹⁴ Since polymeric products are formed in the reaction mixture prior to appearance of acetylene chloride and this compound is not polymerized under the reaction conditions, polymer formation may result only from intermolecular dehydrochlorination of both 1,2-DCE and its oligomers.

DISCUSSION

Thus, we have carried out oligomerization of vinylidene chloride, vinyl chloride, and 1,2-dichloroethylene by a cationic mechanism. The reaction proceeds most easily with vinylidene chloride and with most difficulty with 1,2-dichloroethylene. It is probable that the ability of chloroethylenes to undergo cationic polymerization would depend on the ease of formation of carbonium ions which are polymerization initiators¹⁵ and upon the stability of these cations. In this case, chloroethylenes, in accordance with their ability to undergo protonation, that is to form carbonium ions, may be

placed in the order: $\text{CH}_2=\text{CCl}_2 > \text{CH}_2=\text{CHCl} > \text{cis-CHCl}=\text{CHCl} > \text{trans-CHCl}=\text{CHCl}$. The proton reacts with vinylidene chloride most readily, due to greater polarity of this monomer molecule. The stability of the carbonium ions which initiate the polymerization decreases in the following order:



The higher stability of the $\overset{+}{\text{CH}_3\text{CCl}_2}$ ion is explained by the fact that two chlorine atoms at a positively charged carbon compensate its positive charge to a greater extent than one chlorine atom¹⁶ as in the case of the $\overset{+}{\text{CH}_3\text{CHCl}}$ ion. The $\overset{+}{\text{CH}_2\text{ClCHCl}}$ carbonium ion is yet less stable due to a negative inductive effect of the neighboring CH_2Cl group, which prevents positive charge delocalization.

It has been already noted above that in the case of vinylidene chloride and 1,2-dichloroethylene the polymerization with AlCl_3 is stopped at the dimer and trimer formation stage while, with the same catalyst, polymers with a larger number of units are obtained from vinyl chloride. Termination of polymerization of the first two compounds takes place in the following ways. Firstly, their dimers (1,1,3,3-tetrachlorobuten-1 and 1,1,2,3,4-pentachlorobutane) under the reaction conditions form with AlCl_3 stable, colored complexes which do not react further with monomer molecules. Secondly, intermediate trimeric cations arising from vinylidene chloride and 1,2-dichloroethylene are stabilized in the presence of AlCl_3 to saturated cyclic compounds, which definitely stops the polymerization. In the case of vinyl chloride, cyclization does not take place and the possibility of further chain propagation remains. Thus the tendency to ring formation is enhanced with increasing the amount of chlorine atoms in the monomer molecule and therefore also in intermediate carbonium ions. It is apparently associated with the less extended molecule structure of the highly chlorinated cation and the possibility of release of more energy when unstressed six-membered rings are formed from them. Finally, a significant accumulation of hydrogen chloride in the reaction mixture as a result of the dehydrochlorination reaction products under the effect of AlCl_3 also contributes to termination of the polymer chain.

In conclusion, it should be noted that chloroethylene dimers and trimers obtained by us may be considered as model compounds for the structure of single units and groups of chlorine-containing polymers and copolymers.

We are thankful to Dr. I. Ya. Slonim and O. A. Mochalova for obtaining and interpreting the NMR spectra and to L. I. Fedorova for separation of tetrachlorohexane isomers by the preparative gas-liquid chromatography technique.

References

1. A. E. Kulikova, E. N. Zilberman, N. K. Taikova, and N. M. Pinchuk, *Zh. Org. Khim.*, **4**, 1899 (1968).
2. A. N. Lubimov, N. Z. Belitskii, I. Ya. Slonim, A. F. Varenik, and V. N. Fedorov, *Zavodsk. Lab.*, **32**, 1163 (1966).
3. N. A. Okladnov, I. N. Razinskaya, and B. P. Starkman, *Vysokomol. Soedin.*, **8**, 1190 (1966).
4. V. P. Lebedev, N. A. Okladnov, and M. N. Shlykova, *Vysokomol. Soedin.*, **9A**, 495 (1967).
5. L. Schmerling, *J. Amer. Chem. Soc.*, **68**, 1653 (1946).
6. L. W. Daasch, *Anal. Chem.*, **19**, 779 (1947).
7. D. N. Bort, I. N. Vishnevskaya, and V. A. Kargin, *Vysokomol. Soedin.*, in press.
8. A. P. Gantmacher, S. S. Medvedev, and T. E. Lipatova, *Dokl. Akad. Nauk SSSR*, **86**, 1109 (1952).
9. L. Schmerling, in *Friedel-Crafts and Related Reactions*, Vol. II, Part II, Chap. XXVI, G. Olah, Ed., Interscience, New York, 1964.
10. H. J. Prins, *Rec. Trav. Chim.*, **56**, 121, 123 (1937).
11. L. M. Kogan, *Uspekhi Khim.*, **28**, 133 (1959).
12. J. Ortowski and Z. Eckstein, *Przemysl Chem.*, **40**, 643 (1961).
13. L. I. Petron, *J. Amer. Chem. Soc.*, **89**, 2674 (1967).
14. E. N. Zilberman, A. E. Kulikova, N. K. Taikova, and A. N. Smirnov, *Dokl. Akad. Nauk SSSR*, **174**, 1094 (1967).
15. F. S. D'yachkovskii, G. A. Kazaryan, and N. S. Enikolopyan, *Vysokomol. Soedin.*, **11A**, 822 (1969).
16. R. H. Martin, F. W. Lampe, and R. W. Taft, *J. Amer. Chem. Soc.*, **88**, 1353 (1966).

Received November 26, 1969

Glass Transformation Temperatures of Polymers of Olefin Oxides and Olefin Sulfides

JOGINDER LAL and G. S. TRICK, *Research Division, The Goodyear Tire and Rubber Co., Akron, Ohio 44136*

Synopsis

A number of polymers belonging to poly(olefin oxide) and poly(olefin sulfide) series have been prepared and their glass transformation temperatures determined by dilatometry and differential thermal analysis. In the poly(olefin oxide) series, the T_g remained practically unchanged as the length of the pendent alkyl group was increased from methyl to *n*-hexyl. However, a 20°C decrease in T_g was observed when the pendent group was changed from ethoxymethyl to *n*-hexoxymethyl. In the poly(olefin sulfide) series, the T_g value decreased as the pendent alkyl group changes from methyl to ethyl. Replacement of ether oxygen in the polymer main chain by sulfide sulfur increased the T_g value. In some polymers, first-order transitions were observed, but their significance has not been assessed.

INTRODUCTION

The influence of pendent groups on the glass transformation temperature T_g of polymers has been reported¹ in the literature for several series of vinyl polymers. In these polymers, the pendent groups are located on alternate carbon atoms of the polymer chain. In contrast, the pendent groups are present on every third atom of polymer chain of poly(olefin oxides), $(-O-CH_2-CH(R)-)_n$. We have systematically varied the pendent groups in these polymers and evaluated the influence of these variations on T_g values. Similar data have also been obtained on a limited number of poly(olefin sulfides), $(-S-CH_2-CH(R)-)_n$.

EXPERIMENTAL

Materials

Olefin Oxides and Their Polymers. Most of the monomers were obtained from commercial sources (Table I).

Samples of 1,2-hexene oxide, 1,2-octene oxide, and 1,2-dodecene oxide were kindly supplied by ARCO Chemical Company and FMC Corporation. Monomers were distilled over calcium hydride under nitrogen, and their middle cuts were used for polymerization. Propylene oxide, 1,2-butene oxide, 1,2-hexene oxide, and 1,2-octene oxide had a high degree of purity

TABLE I
Boiling Points and Refractive Indices of Olefin Oxides,



Monomer	R group	Boiling point, °C/mm	Refractive index, n_D^{20}	Literature Values	
				Boiling Point, °C/mm	Refractive index, n_D^{20}
Olefin oxides					
Propylene oxide	CH ₃	34/739	1.3615	34.3 ^a 35 ^b 59 ^c 61-62 ^b	n_D^{20} 1.3657 ^a n_D^{17} 1.3681 ^b n_D^{17} 1.3857 ^b
1,2-Butene oxide	C ₂ H ₅	61/739	1.3797	117-119/750 ^a 61/15 ^d	n_D^{20} 1.4060 ^a n_D^{20} 1.4193 ^d
1,2-Hexene oxide	<i>n</i> -C ₄ H ₉	117/740	1.4024	97-98/3.5 ^d	n_D^{20} 1.4356 ^d
1,2-Octene oxide	<i>n</i> -C ₆ H ₁₃	—	1.4163	124-125/15 ^e	n_D^{22} 1.4355 ^e
1,2-Dodecene oxide	<i>n</i> -C ₁₀ H ₂₁	57/0.2	1.4328	87-88/23 ^f	n_D^{26} 1.5331 ^f
Styrene oxide	C ₆ H ₅	54/3.8, 65/8	1.5310	53-54/85 ^g 61/65 ^g 124-126 ^h	n_D^{25} 1.4012 ^g n_D^{26} 1.4046 ^g n_D^{26} 1.406 ^h
3-Methoxy-1,2-epoxypropane	CH ₃ OCH ₂	25/22	1.4010	60-70/20 ^k	n_D^{25} 1.4150 ^k
3-Ethoxy-1,2-epoxypropane	CH ₃ CH ₂ OCH ₂	—	1.4050		
3- <i>n</i> -Butoxy-1,2-epoxypropane	CH ₃ (CH ₂) ₃ OCH ₂	51/5	1.4160		

3- <i>n</i> -Hexoxy-1,2-epoxypropane	$\text{C}_6\text{H}_{13}(\text{CH}_2)_5\text{OCH}_2$	80/5	1.4252	105/20 ^g	n_D^{25} 1.4242 ^g
3-Allyloxy-1,2-epoxypropane	$\text{CH}_2=\text{CHCH}_2\text{OCH}_2$	49/7.5	1.4310	154 ⁱ	n_D^{20} 1.4324 ⁱ
Olefin sulfides					
Propylene sulfide	CH_3	74/740	1.4716	74 ^j 75-77 ^k 75-76 ^l	n_D^{20} 1.4770 ^j n_D^{19} 1.473 ^k n_D^{15} 1.4780 ^l
1,2-Butene sulfide	C_2H_5	100.5/737	1.4689	101-105 ^k	n_D^{15} 1.475 ^k
3-Allyloxy-1,2-epithio propane	$\text{CH}_2=\text{CHCH}_2\text{OCH}_2$	59/4 ⁿ	1.4894 ^m	56-57/6.5 ⁿ	n_D^{20} 1.4936 ⁿ

^a Value from catalog of Aldrich Chemical Company.²

^b Data of Moureu and Dode.³

^c Data of Emmons and Pagano.⁴

^d Data of Swern et al.⁵

^e Data of Rothstein.⁶

^f Data of Golumbic and Cottle.⁷

^g Data of Flores-Gallardo and Pollard.⁸

^h Data of Fairbourne et al.⁹

ⁱ Value from Peninsular Chemresearch Catalog.¹⁰

^j Data of Sigwalt.¹¹

^k Data of Delépine and Jaffoux.¹²

^l Data of Culvenor et al.¹³

^m Data of Lal.¹⁴

ⁿ Data of Brodoway.¹⁵

TABLE II
 Preparation and Properties of Poly(olefin Oxides) and Poly(olefin Sulfides)

Monomer	Polymerization	Inherent viscosity, dl/g	Refractive index n_D^{20}	Density, g/cc	Glass transformation temperature T_g , °C		Melting temperature T_m , °C	
					Calorimetric	Dilatometric	Calorimetric	Lit. values
Propylene oxide	$E_{1/2}Zn-H_2O(1:1)$; benzene, 50°C	A 6.7	1.457; 1.454 ^b	1.005	-67, -72 ^c	-76	-60 ^d -75 ^e	60 ^f 73 ^g 73-76 ^h
1,2-Butene oxide	$E_{1/2}Zn-S(1:4)$; bulk, 50°C	B 2.3	1.461	0.970	-68, -73 ^c	--	-60 ^d -83 ^e	None None
1,2-Butene oxide	Zinc <i>n</i> -butyl xanthate, bulk, 50°C	B 3.0	1.458	0.966	-60, -74 ^c	-70	--	--
1,2-Hexene oxide	$E_{1/2}Zn-S(1:4)$; benzene, 50°C	B --	--	0.925	-68	--	--	71
1,2-Hexene oxide	Modified zinc <i>n</i> -butyl xanthate, benzene, 50°C	B 1.1	--	0.970	-70	--	--	72
1,2-Octene oxide	$E_{1/2}Zn-S(1:4)$; bulk, 50°C	C 1.8	1.469	0.944	-67, -74 ^c	--	--	86
1,2-Octene oxide	Modified zinc <i>n</i> -butyl xanthate; bulk, 50°C	C 1.1	--	0.974	-74 ^b	--	--	87 ^c
1,2-Dodecene oxide	$E_{1/2}Zn-S(1:4)$; bulk, 50°C	C --	--	0.862	--	--	-41 ^e	40 ^f and 102
1,2-Dodecene oxide	Modified zinc <i>n</i> -butyl xanthate; bulk, 50°C	C 2.4	--	--	--	--	--	54 and 103; 103 ^b
Styrene oxide	$E_{1/2}Zn-S(1:4)$; benzene, 50°C	D 3.0	--	1.118	--	41	40 ^e	149 ^k 162, ^e 170 ^l
3-Methoxy-1,2-epoxypropane	$E_{1/2}Zn-S(1:4)$; benzene, 50°C	A 1.5	1.467; 1.480 ^b	1.095	-62	--	--	57
3-Ethoxy-1,2-epoxypropane	$E_{1/2}Zn-S(1:4)$; benzene, 50°C	A 2.0	1.465	1.025	-61	--	--	None

3- <i>n</i> -Butoxy-1,2-epoxypropane	$Et_2Zn-S(1:4)$; benzene, 50°C	B	2.4	1.45S	0.982	-79	—	27
3- <i>n</i> -Hexoxy-1,2-epoxypropane	$Et_2Zn-S(1:4)$; benzene, 50°C	B	2.8	1.459	0.966	-83, -88 ^g	—	44 ^f
3-Allyloxy-1,2-epoxypropane	$Et_2Zn-S(1:3.5)$; benzene, 50°C	A	4.6	1.47S	1.04S	-74	-78	None
Propylene sulfide	$Et_2Zn-S(1:10)$; bulk, -20°C	B	1.7	1.597	1.10	-37	—	53
Propylene sulfide	$Et_2Zn-S(1:3)$; benzene, 30°C	B	0.5	1.596	—	—	-47	—
Propylene sulfide	Cadmium isopropyl xanthate, benzene, 0°C	B	0.9	1.596	1.12	-37	—	None
1,2-Butene sulfide	$Et_2Zn-H_2O(0.9:1)$; benzene, 23°C	B	0.7	1.570	1.090	-47	—	None
1,2-Butene sulfide	Activated zinc sulfide; bulk; 25°C ^o	B	0.5	1.575	1.096	-48	-55	None
3-Allyloxy-1,2-epithiopropene	$Et_2Zn-H_2O(0.8:1)$; benzene, 30°C	B	2.2	1.553 ^p	1.123; 1.111	-58	-60	None

^a A = isooctane-insoluble fraction; B = precipitated in methanol containing phenyl 2-naphthylamine stabilizer; C = fraction insoluble in boiling acetone; D = fraction insoluble in acetone at 25°C.

^b Rapidly quenched.

^c By differential thermal analysis.

^d Data of Faucher.²⁰

^e Data of Allen et al.²¹

^f Small endotherm.

^g Data of Chu and Price.²²

^h Data of Aggarwal et al.²³

ⁱ Benzene-insoluble reaction product of zinc *n*-butyl xanthate and excess *n*-butyl alcohol. Data of Lal,¹⁹ example no. 1.

^j Not detectable, probably due to crystallinity.

^k Data of Vandenberg.²⁴

^l Data of Blanchette.²⁵

^m Data of Adamek et al.²⁶

ⁿ Data of Nevin and Pearce.²⁷

^o Water-insoluble reaction product of zinc acetate and sodium hydrosulfide (molar ratio 1:2).

^p Data of Lal.¹⁴

(>99.5% by GLC). 1,2-Dodecene oxide was 82% pure. Some physical constants of the various monomers are given in Table I.

Propylene oxide was polymerized with a diethylzinc-water catalyst¹⁶ prepared *in situ* (molar ratio diethylzinc/water = 1:1). All other monomers were polymerized with preformed diethylzinc-sulfur catalyst¹⁷ preparations which had been aged for 2 hr at room temperature (zinc/sulfur atomic ratio = 1:4). A few monomers were also polymerized with other catalysts. They were: zinc *n*-butyl xanthate¹⁸ and the benzene-insoluble reaction product¹⁹ of zinc *n*-butyl xanthate and excess *n*-butyl alcohol. Polymerizations were carried out in bulk or in benzene solution (volume ratio monomer/benzene = 0.2:1 to 3:1) with 0.6-5 weight parts catalyst per 100 weight parts monomer. Generally, monomers having longer R groups (Table I) polymerized slowly and required higher catalyst and/or lower solvent levels.

All polymerizations were carried out under nitrogen in 4-oz bottles which were tumbled in a water bath maintained at 50°C. They were allowed to proceed to 50% or greater conversion. The polymerization was stopped by chilling the bottle and adding about 20 ml methanol containing phenyl 2-naphthylamine (PBNA) as a stabilizer. The methods of isolating polymers are shown in Table II. In method A, the polymeric material was dried under aspirator vacuum for 24 hr and then under 2 torr for about 68 hr at 40°C. The dried mass was suspended in excess isooctane (200 ml/g of polymer) for 48 hr at 25°C to extract low molecular weight material, followed by drying of the isooctane-insoluble fraction. In method B, the polymeric material was precipitated in excess methanol containing PBNA. In methods C and D, the polymeric mass was precipitated as in method B, dried, and subsequently extracted with excess boiling acetone (15 min) and acetone at 25°C (24 hr), respectively.

Olefin Sulfides and Their Polymers. Propylene sulfide was obtained commercially. 1,2-Butene sulfide was synthesized from 1,2-butene oxide by reaction with potassium thiocyanate.²⁸ The preparation of 3-allyloxy-1,2-epithiopropane has been previously reported.¹⁴ Some physical constants of these monomers and conditions for their polymerization are also shown in Tables I and II. These polymers were precipitated in excess methanol containing PBNA.

Physical Properties

Inherent viscosities were determined at 30°C on 0.1% solution of the polymer in toluene or another solvent wherever indicated. These values are expressed in units of deciliters/gram. Except where noted, refractive index measurements were made on samples that had been kept at room temperature for several days.

Densities of the polymers were measured by the use of a density gradient column or by alcohol displacement. Transition temperatures were measured with a dilatometer,¹ differential thermal analyzer (Du Pont Model 900), or the calorimeter attachment to the DTA. With the latter two

measurements, T_g was taken as the point at which a change in heat capacity was first observed on the heating cycle, while T_m was taken as the temperature of the peak of the melting endotherm (Figs. 1-3). All measurements on the DTA or calorimeter attachment were made at a heating rate of 10°C/min.

The DTA and calorimetric results are usually reproducible to $\pm 1^\circ\text{C}$. The dilatometric results are subject to greater error, depending to some extent upon the amount of curvature observed in the volume-temperature plot in the transition region. The lack of a clear relation between dilatometric and calorimetric T_g values is considered to arise from errors in the dilatometric values.

DISCUSSION AND CONCLUSIONS

Glass Transformation Temperatures

In the poly(olefin oxide) series it is found that the T_g is independent of the length of the alkyl side chain. As seen in Figure 1, the transition observed for poly(octene oxide) is less well defined than those for poly(propylene oxide), poly(butene oxide), and poly(hexene oxide). However, repeated measurements on a number of different samples using both DTA and calorimetry have confirmed that the data reported are valid. In addition, there is no evidence that the presence of crystallinity is affecting our experimental results. By cooling in liquid air it was possible to quench completely a sample of poly(hexene oxide). On the heating cycle the sample showed a T_g , crystallization exotherm, and corresponding melting endotherm with the glass transformation being identical, within experimental error, with that observed on a partially crystalline material. Similar techniques were not successful for completely quenching the poly(octene oxide), but different methods of thermal treatment, leading to some variation in degree of crystallinity, produced no variation in the observed T_g . No direct check could be made on variations in stereoregularity of the polymers reported and the possible influence of such variations upon the T_g values. However, Table I shows that polymers prepared with quite different catalysts, presumably leading to differences in stereoregularity, show no differences in glass transformation behavior.

The independence of T_g on the length of the side chain is in marked contrast to our previous results on poly(vinyl alkyl ethers).¹ It appears likely that in the poly(olefin oxide) series the glass transformation temperature is largely governed by main-chain flexibility with very little contribution from the alkyl side groups. Another factor which probably makes some contribution is the reduced frequency of occurrence of the side groups in the olefin oxide series as compared to the vinyl alkyl ether series. Such an explanation would account for the marked difference in T_g of polyethylene and polypropylene, whereas poly(ethylene oxide) and poly(propylene oxide) have similar T_g values. However, it should be noted from Table II that the polymers containing alkoxyalkyl side groups do show the

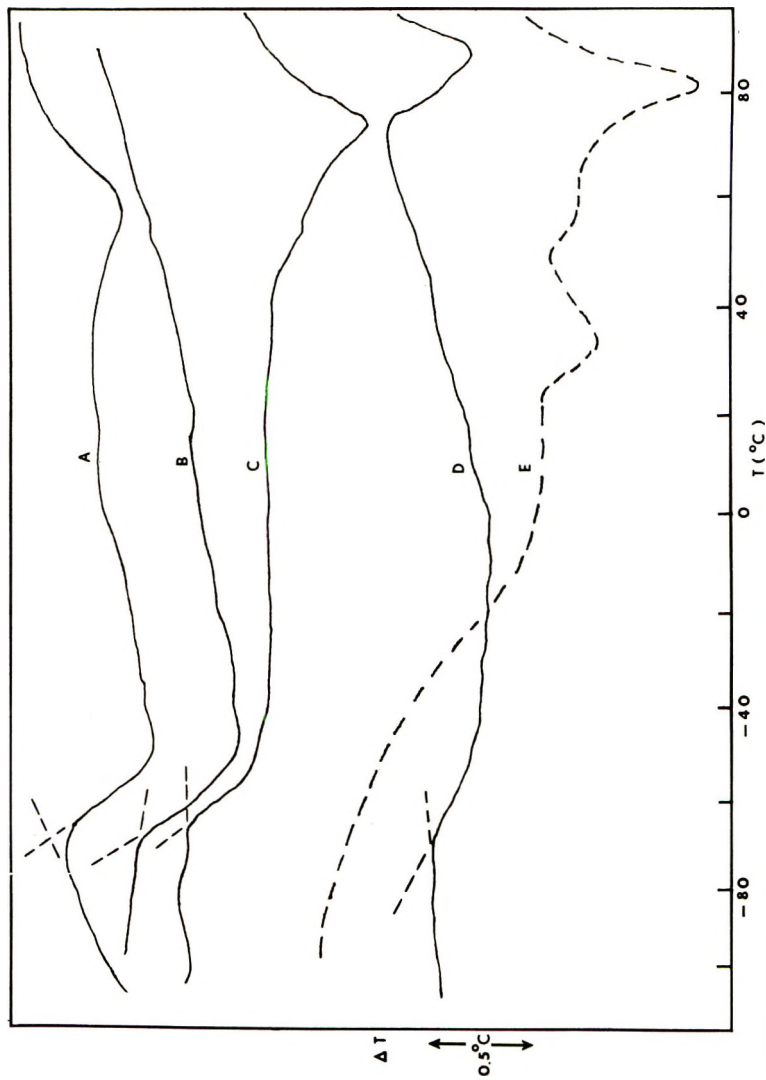


Fig. 1. Transition temperatures: (A) poly(propylene oxide); (B) poly(butene oxide); (C) poly(hexene oxide); (D) poly(octene oxide); (E) poly(dodecene oxide), add 20°C to T readings.

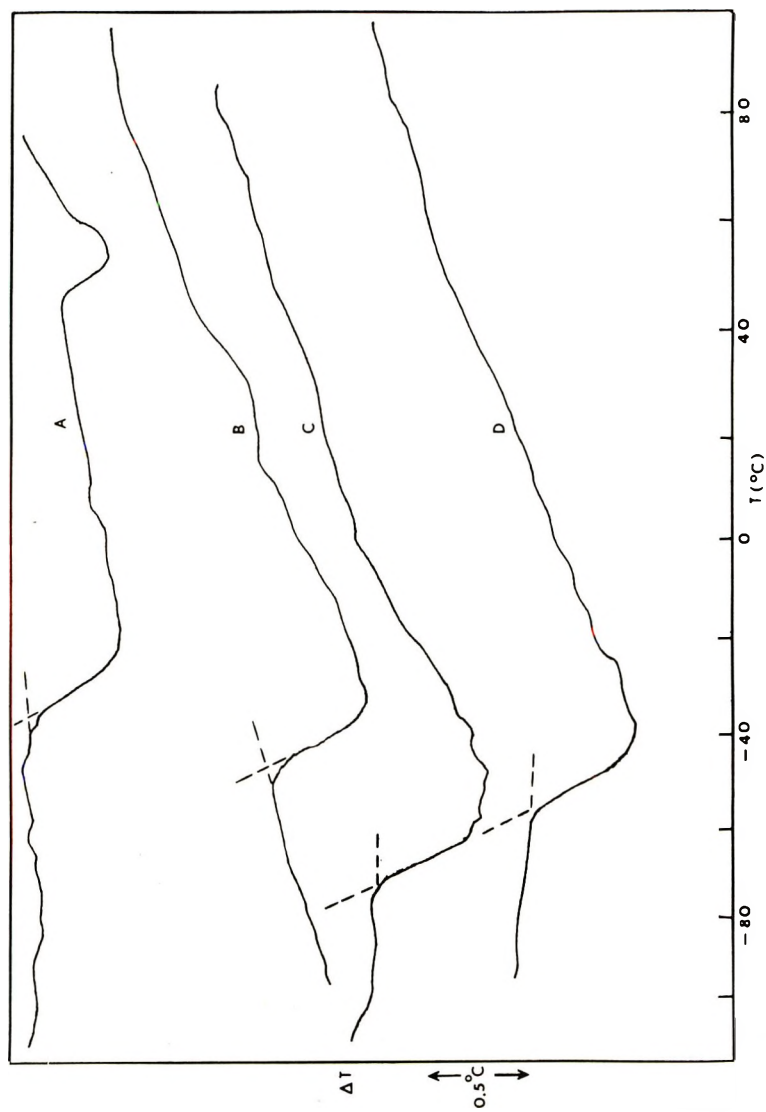


Fig. 2. Transition temperatures: (A) poly(propylene sulfide); (B) poly(butene sulfide); (C) poly(3-allyloxy-1,2-epoxypropane); (D) poly(3-allyloxy-1,2-epithiopropane).

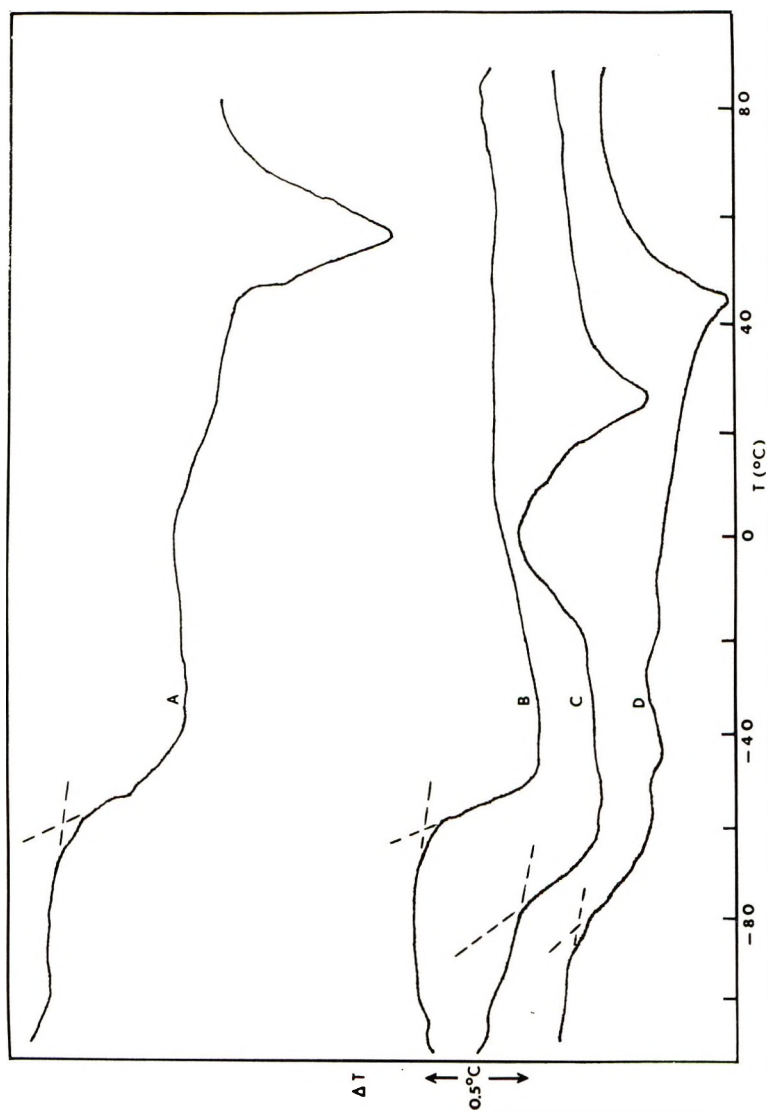


Fig. 3. Transition temperatures: (A) poly(3-methoxy-1,2-epoxypropane); (B) poly(3-ethoxy-1,2-epoxypropane); (C) poly(3-*n*-butoxy-1,2-epoxypropane); (D) poly(3-*n*-hexoxy-1,2-epoxypropane).

usual decrease in T_g with increase in length of side group. Hence, in this case, the side chain must be making a contribution to the T_g . The results in Table II also show that replacement of the ether oxygen in the main chain by sulfide sulfur increases the T_g ; this is similar to the observation¹ on polymers of vinyl alkyl ether and vinyl alkyl sulfide. Interestingly enough, the difference in T_g of poly(propylene oxide) and poly(styrene oxide) is about 110°C; this is similar to the difference in glass temperature between polypropylene and polystyrene.

Melting Temperatures

Any interpretation of the melting points of polymers of this type containing long side groups must include an appreciation that such polymers can have crystallinity arising from at least two sources: (a) that arising from crystallization of the side chains; (b) that arising from tactic sequences in the main chain and involving both the main chain and the side chain. In polymers containing short side groups, crystallization will arise from tactic sequences. However, in polymers with long side groups, it is difficult to distinguish between main-chain and side-chain crystallinity without detailed x-ray examination. Some limited x-ray examinations have been made of some of the polymers reported here. Poly(butene oxide) was amorphous in the unstretched state and could not be properly stretched to give a fiber diagram. A vulcanized copolymer of butene oxide and allyl glycidyl ether gave, on stretching to 600%, a sharp fiber diagram with a repeat distance along the stretch axis of 5.51 Å. Poly(1,2-octene oxide) was crystalline when unstretched; when stretched it gave a sharp fiber diagram with spacings along the equator of 18.3, 6.2, and 4.21 Å, suggesting a large spacing normal to the stretching direction. The repeat distance on the stretch axis was 5.50 Å, the same as for poly(butene oxide) and in marked contrast to the value of 6.92 Å reported²⁹ for poly(propylene oxide). The latter value was attributed to a twisting zig-zag backbone.

It is hoped that transition temperature measurements in progress on poly- α -olefins will assist in the interpretation of the significance of the melting temperatures reported here.

The authors wish to express their thanks to R. N. Thudium for the x-ray diffraction results and to J. M. Ryan and J. Hionides for technical assistance.

This is contribution No. 418 from the Goodyear Tire & Rubber Company, Research Division, Akron, Ohio.

References

1. J. Lal and G. S. Trick, *J. Polym. Sci. A*, **2**, 4559 (1964), and references contained therein.
2. Catalog, Aldrich Chemical Company, 1967.
3. H. Moureu and M. Dode, *Bull. Soc. Chim. France* [5], **4**, 281 (1937).
4. W. D. Emmons and A. S. Pagano, *J. Amer. Chem. Soc.*, **77**, 89 (1955).
5. D. Swern, G. N. Billen, and J. T. Scanlan, *J. Amer. Chem. Soc.*, **68**, 1504 (1946).
6. B. Rothstein, *Bull. Soc. Chim. France* [5], **2**, 1936 (1935).

7. C. Columbic and D. L. Cottle, *J. Amer. Chem. Soc.*, **61**, 996 (1939).
8. H. Flores-Gallardo and C. B. Pollard, *J. Org. Chem.*, **12**, 831 (1947).
9. A. Fairbourne, G. P. Gibson, and D. W. Stephens, *J. Chem. Soc.*, **1932**, 1965.
10. Catalog, Peninsular Chemresearch, 1967.
11. S. Boileau and P. Sigwalt, *C. R. Acad. Sci. (Paris)*, **252**, 882 (1961).
12. M. Delépine and P. Jaffeux, *C. R. Acad. Sci. (Paris)*, **172**, 158 (1921).
13. C. C. J. Culvenor, W. Davies, and K. H. Pausacker, *J. Chem. Soc.*, **1946**, 1050.
14. J. Lal, *J. Polym. Sci. B*, **3**, 969 (1965).
15. N. Brodoway, U.S. Pat. 3,222,324 (December 7, 1965).
16. R. Sakata, T. Tsuruta, T. Saegusa, and J. Furukawa, *Makromol. Chem.*, **40**, 64 (1960).
17. J. Lal, *J. Polym. Sci. A-1*, **4**, 1163 (1966).
18. J. Lal, *J. Polym. Sci. B*, **5**, 793 (1967).
19. J. Lal, U.S. Pat. 3,409,565 (November 5, 1968).
20. J. A. Faucher, *J. Polym. Sci. B*, **3**, 143 (1965).
21. G. Allen, C. Booth, and C. Price, *Polymer*, **8**, 414 (1967).
22. N. S. Chu and C. C. Price, *J. Polym. Sci. A*, **1**, 1105 (1963).
23. S. L. Aggarwal, L. Marker, W. L. Kollar, and R. Geroch, *Elastomer Stereospecific Polymerization*, (*Adv. Chem. Ser.*, **52**), American Chemical Society, Washington, D. C., 1966, p. 88.
24. E. J. Vandenberg, *J. Polym. Sci.*, **47**, 486 (1960).
25. J. A. Blanchette, U.S. Pat. 2,916,463 (December 14, 1960).
26. S. Adamek, B. B. J. Wood, and R. T. Woodhams, *Rubber Plastics Age*, **46**, 56 (1965).
27. R. S. Nevin and E. M. Pearce, *J. Polym. Sci. B*, **3**, 487 (1965).
28. K. Dachlauer and L. Jackel, German Pat. 636,708 (October 15, 1936).
29. E. Stanley and M. Litt, *J. Polym. Sci.*, **43**, 453 (1960).

Received July 10, 1969

Revised December 4, 1969

Synthesis and Properties of Polyamides and Polyesters from Neocarboranedicarboxylic Dichloride

V. V. KORSHAK, N. I. BEKASOVA, and L. G. KOMAROVA,
Institute of Organoelement Compounds, Moscow, U.S.S.R.

Synopsis

Polyamides and polyesters based on neocarboranedicarboxylic dichloride and previously not described have been prepared by low-temperature polycondensation in solution and characterized. In preparing the polyamides, the following diamines were used: benzidine, hexamethylenediamine, *m*-phenylenediamine, *p*-phenylenediamine, 4,4'-diaminodiphenyl ether, 4,4'-diaminodiphenylmethane, 4,4'-diaminodiphenyl sulfide, and hydroquinone diaminodiphenyl ester. Polyesters were obtained by using the following diols: phenolphthalein, hydroquinone, 4,4'-dihydroxydiphenylpropane, 9,9-dihydroxydiphenylfluorene, 1,6-hexanediol, and ethylene glycol. The resulting neocarborane polyesters melt and are easily soluble in tetrahydrofuran, amide solvents, and chloroform. The neocarborane polyamides described do not melt, are readily soluble in tetrahydrofuran and dimethylformamide, and form transparent films; they are thermostable in an inert atmosphere at high temperatures.

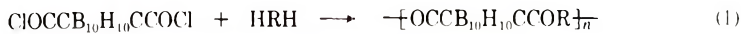
INTRODUCTION

In the last few years, papers have been published in which synthesis and some properties of polymers containing carborane nuclei¹⁻⁷ are described. It may be concluded that the incorporation of a carborane nucleus in the polymeric chain considerably increases the thermal stability of the polymers.

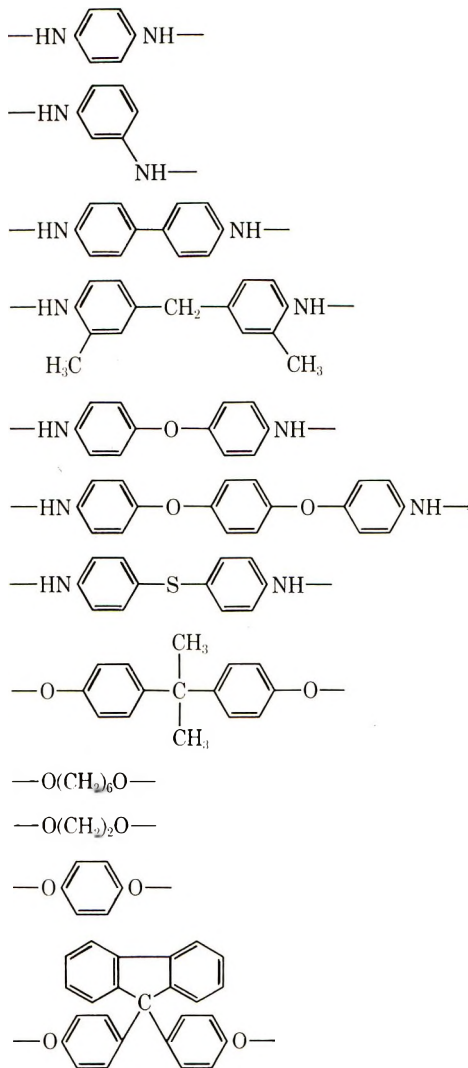
The present paper deals with the synthesis and properties of polyamides and polyesters containing neocarborane nuclei and previously not described.

RESULTS AND DISCUSSION

Neocarborane polyamides and polyesters were obtained by low temperature polycondensation of neocarboranedicarboxylic dichloride (Fig. 1) with aromatic and aliphatic diamines or diols in solution in the presence of triethylamine according to eq. (1).



where R = —NH(CH₂)₆NH—



Tetrahydrofuran, chloroform, and pyridine were used as solvents for polycondensation. Instead of these, other solvents, such as tetrachloroethane, benzene, and acetone, may be used in polyesterneocarborane synthesis. Table I shows the influence of a solvent on the molecular weight of polyamidoneocarboranes.

It was found that the best solvents for formation of polyamidoneocarboranes were tetrahydrofuran and chloroform, rather than dimethylacetamide, which is usually used in polyamide synthesis. It is probable that due to a high reactivity neocarboranedicarboxylic dichloride reacts not

TABLE I
Influence of the Solvent Used in Preparation on the Molecular Weight of
Polyamidoneocarborane

$$\left[\text{COCB}_{10}\text{H}_{10}\text{CCONH} \text{---} \text{C}_6\text{H}_4\text{---C}_6\text{H}_4\text{---NH} \right]_n$$

Solvent	η_{red} (in dimethylformamide), dl/g
Tetrahydrofuran	1.6
Chloroform	2.1
Pyridine	0.95
Dimethylacetamide	0.11

only with diamine, but also with dimethylacetamide, and that this leads to low molecular weight substances only. If neocarboranedicarboxylic dichloride and the corresponding diamine or diol are taken in an equivalent ratio, neocarborane polyamides and polyesters of the highest molecular weights are formed. As can be seen from Figure 2, variations of this ratio in either direction decreases molecular weights of the polymers. Thus, this reaction exemplifies once more the rule of the nonequivalence of functional groups.⁸⁻¹⁰

The polycondensation of neocarboranedicarboxylic dichloride with diamines proceeds at room temperature and is completed approximately 20 min after the reaction has begun (Fig. 3). Neocarboranedicarboxylic dichloride reacts with diols in the same manner. Varying the temperature from -10 to $+40^\circ\text{C}$ does not markedly affect the molecular weight of the resulting neocarborane polymers, the yield in all cases being 97–100%.

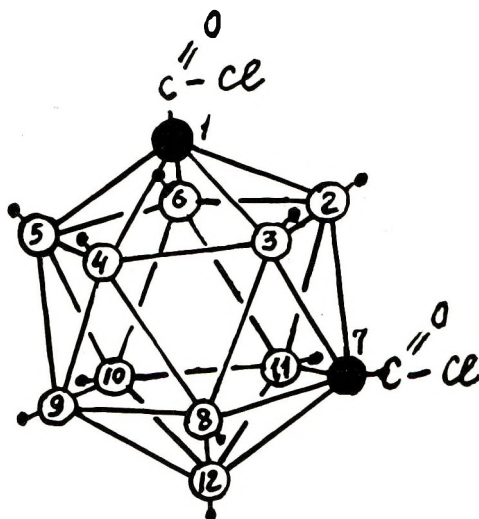
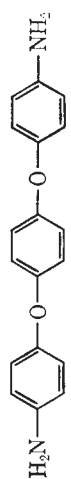
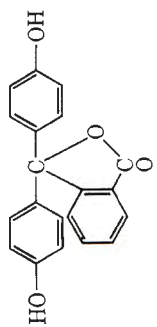
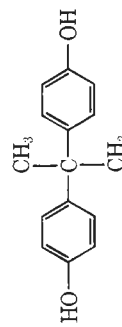
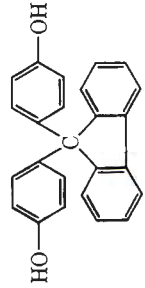


Fig. 1. Structural formula of neocarboxylic dichloride. White circles denote boron atoms; large dark circles are carbon atoms included in the carborane skeleton; small dark circles are hydrogen atoms.

TABLE II
Properties of Neocarborane Polyamides and Polyesters
 $[-OCCB_{10}H_{10}CCOR-]_n$

No.	Starting diamine or diol	$n_{D,25}^{25}$ (in scatter-DMF) in g/dl	MW (light scattering) in g THF	Softening point, °C	Appearance	Analysis							
						Found			Calcd. for a unit				
						C, %	H, %	B, %	N, %	C, %	H, %	B, %	N, %
1		2.16	53000	unmelted	White fibrous solid, amorphous	50.19	5.54	27.16	6.93	50.40	5.23	28.39	7.36
2		0.68	15000	"	"	38.47	5.93	34.60	9.68	39.45	5.23	35.53	9.21
3		0.46	—	"	White fibrous solid, crystalline	38.99	5.86	33.99	8.49	39.45	5.23	35.53	9.21
4		1.34	14500	"	White fibrous solid, amorphous	49.42	5.82	25.29	6.17	48.45	5.08	27.27	7.07
5		0.32	22400	"	"	51.69	5.89	25.67	7.09	51.74	5.62	27.42	7.11
6		0.59	35600	"	Grey fibrous solid, amorphous	46.30	5.28	25.81	6.09	46.57	4.88	26.22	6.79
7		0.25	7700	"	White fibrous solid, amorphous	53.84	6.52	24.80	6.41	53.99	6.20	25.60	6.64

S		0.38	19400	"	53.11	5.64	21.73	4.20	54.07	4.95	22.14	5.74	
9	$H_2N(CH_2)_6NH_2$	0.16	18200	70	White powder	39.51	7.93	32.59	8.75	38.43	7.74	34.61	8.97
10		0.26 ^a	—	decomp. >300	White fibrous solid, amorphous	55.49	4.43	21.00	—	56.01	4.31	21.02	—
		0.18 ^a	11100 ^a	"									
11		0.16 ^a	3000 ^a	225	White fibrous solid, crystalline	53.74	5.91	24.83	—	53.77	5.70	25.48	—
12	HO(CH ₂) ₆ OH	0.36	18900	235	"	39.22	4.95	34.52	—	39.15	4.61	35.31	—
13	HO(CH ₂) ₆ OH	0.08 ^a	—	—	Light yellow grease	38.98	7.21	33.36	—	38.19	7.05	34.40	—
14		0.16 ^a	8200	300 (dec)	White fibrous solid	64.44	5.25	18.17	—	63.71	4.79	19.79	—
15	HO(CH ₂) ₆ OH	0.09	2400	150	White powder, crystalline	28.00	5.71	40.62	—	27.89	5.46	41.88	—

^a Reduced viscosity and ebullioscopic molecular weight were determined in chloroform.

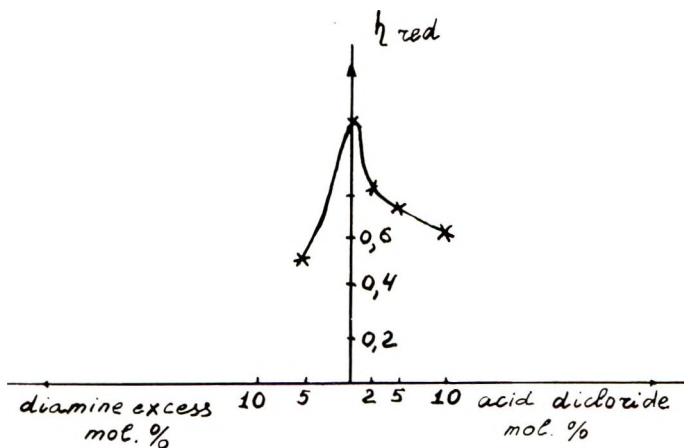


Fig. 2. Influence of the ratio of starting substances on the molecular weight of polyamidoneocarbonylboranes.

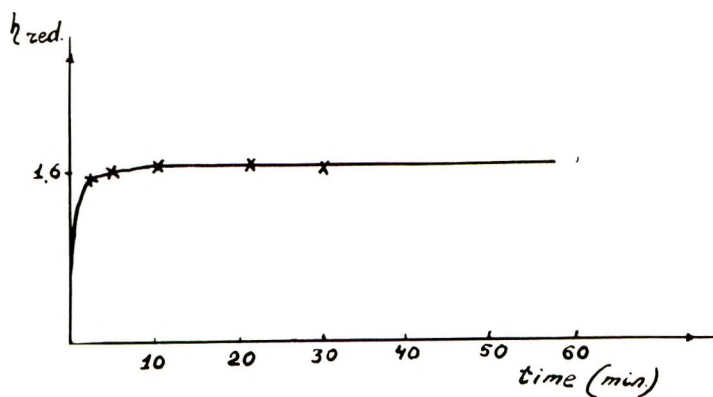


Fig. 3. Influence of the reaction time on the molecular weight of polyamidoneocarbonylboranes.

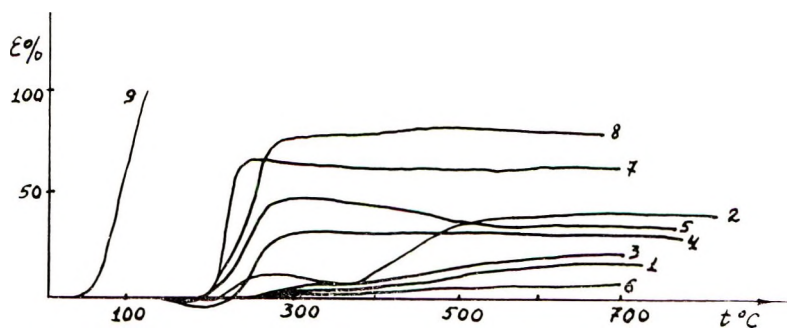


Fig. 4. Thermomechanical curves for neocarbonylborane polyamides. Numbers on curves correspond to polymer numbers in Table II.

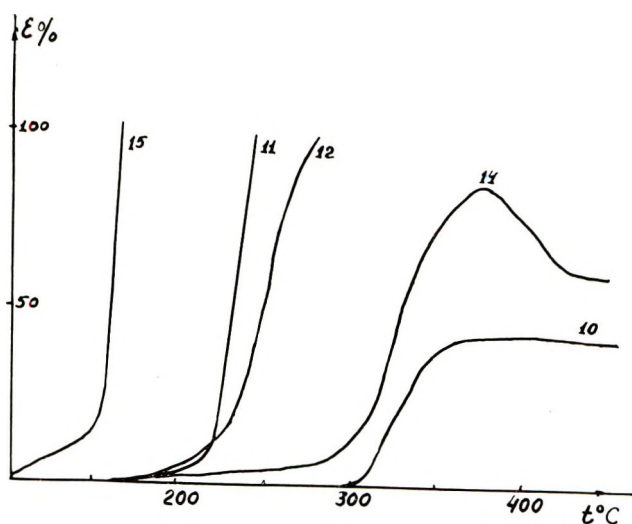


Fig. 5. Thermomechanical curves for neocarboration polyesters. Numbers on curves correspond to polymer numbers in Table II.

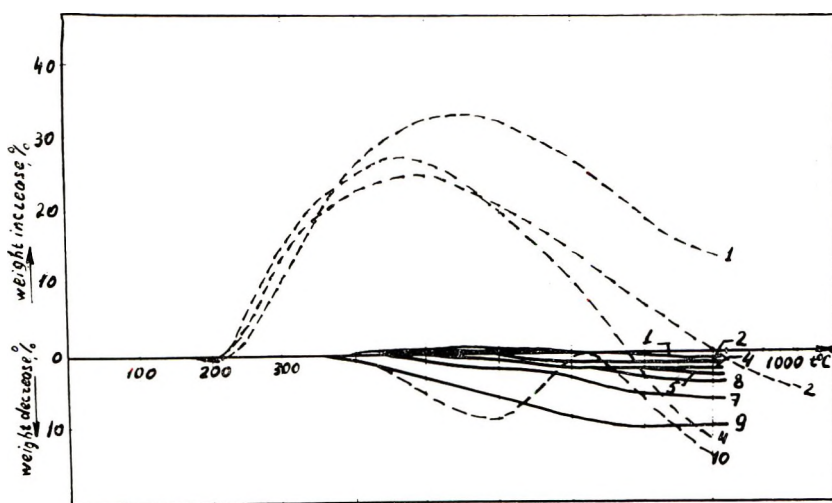


Fig. 6. Dynamic thermogravimetric analysis data for neocarboration polymers: (—) in an inert atmosphere; (---) in air. Numbers on curves correspond to polymer numbers in Table II.

Properties of the polymers are given in Table II; thermomechanical curves are shown in Figures 4 and 5.

All neocarboration polyamides and polyesters are easily soluble in tetrahydrofuran, dimethylformamide, dimethylacetamide, and cresol. Some of them are soluble in pyridine, chloroform, and acetone.

Infrared spectra of the polymers show a clearly defined absorption band at $\sim 2600\text{ cm}^{-1}$ characteristic of B—H bond vibrations of the carborane

nucleus. Furthermore, the infrared spectra of neocarborane polyamides show an absorption band at $\sim 1630\text{ cm}^{-1}$ attributed to the amide $\text{C}=\text{O}$ bond, and spectra of the neocarborane polyesters shown an absorption band at $\sim 1760\text{ cm}^{-1}$ assigned to the ester $\text{C}=\text{O}$ bond.

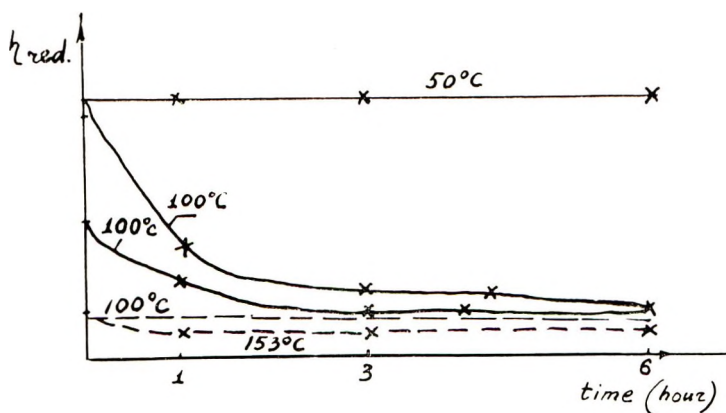


Fig. 7. Destruction of (—) poly-*p,p'*-diphenylenecarborane-dicarbonamide with initial reduced viscosities of 1.1 and 0.6 and (---) polyhexamethylenecarborane-dicarbonamide in dimethylformamide at different temperatures.

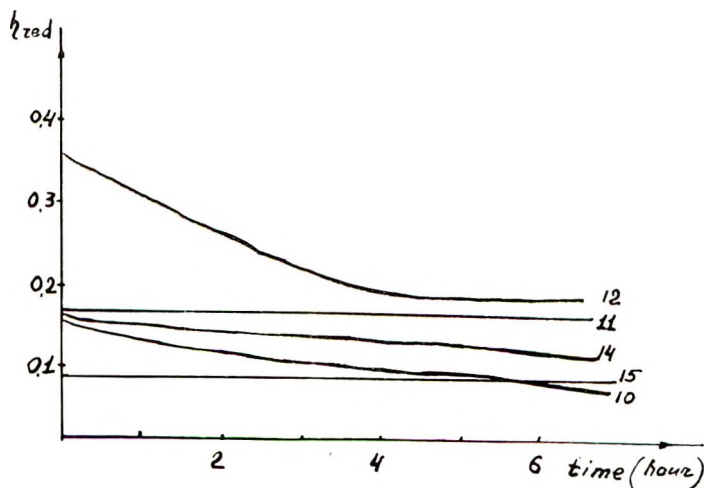


Fig. 8. Destruction of neocarborane polyesters by boiling water. Numbers on curves correspond to polymer numbers in Table II.

The resulting polyamidoneocarborane readily form amorphous films from tetrahydrofuran solution. The films have a rather high tensile strength. For instance, for polyphenylenecarboranedicarbonamide with $\eta_{red} = 1.1\text{ dl/g}$ the tensile strength is $\sim 900\text{ kg/cm}^2$, the elongation being 15%.

Thermogravimetric studies on polyamidoneocarboranes (at a heating rate of 4.5°C/min) showed that in an inert atmosphere there is practically no weight loss up to 1000°C, while in air oxidation takes place, initially apparently to boric acid, and then to boric anhydride; it begins already at 200–250°C and results in an increased weight of polymer (Fig. 6, curves 1–9). Polyamidoneocarborane films turn slightly yellow but retain their strength, molecular weight, and solubility in organic solvents after heating at 250°C for 4 hr in an inert atmosphere. The destructure of polyester-neocarborane from phenolphthalein in air starts after 300°C (Fig. 6, curve 10), a weight increase of the polyester being observed at 700°C due probably to intense oxidation of boron atoms to B₂O₃.

All the polyamidoneocarboranes proved to be stable to cold and boiling water, as well as to 5% aqueous KOH and H₂SO₄ and 40% aqueous H₂SO₄ at room and boiling temperature. Boiling in 40% aqueous KOH only brings about the destructure of polymers of high molecular weight.

Polyamidoneocarboranes are not affected by dimethylformamide either at room temperature or at 50°C. At a higher temperature polymer destruction in dimethylformamide takes place, as can be seen from Figure 7.

Polyester neocarboranes are also stable to cold water, but some of them undergo destruction in boiling water (Fig. 8).

EXPERIMENTAL

Materials

Neocarborane, C,C'-neocarboranedicarboxylic acid, and neocarboranedicarboxylic dichloride were obtained by the methods previously described.⁸

Synthesis of Poly-*p,p'*-diphenyleneneocarboranedicarbonamide in Chloroform

A 1.1-ml portion of thoroughly dried triethylamine and 1.08 ml of neocarboranedicarboxylic dichloride were added to 0.69 g of benzidine in 25 ml of chloroform stirred in an inert gas at 40°C. The mixture was stirred at this temperature for 1 hr and poured into hexane. The precipitate was a white fibrous polymer. It was thoroughly washed with water to remove triethylamine hydrochloride and dried at 90–100°C under vacuum. The yield was 1.43 g (~100%). The polymer did not melt; η_{red} was 2.2 dl/g in tetrahydrofuran; the molecular weight was 53 000 (determined by light-scattering in tetrahydrofuran).

Synthesis of Poly-*p,p*-diphenylene oxide neocarboranedicarbonamide in Tetrahydrofuran

A 1.1-ml portion of triethylamine and 0.86 g of neocarboranedicarboxylic dichloride were added to 0.64 g of *p,p'*-diaminodiphenyl oxide stirred in an inert gas in 25 ml of tetrahydrofuran at room temperature. The mix-

ture was stirred at this temperature for an hour and then poured into water. Further procedure as described above. The yield was 1.27 g ($\sim 100\%$). The polymer did not melt; η_{red} was 1.34 dl/g in tetrahydrofuran; the molecular weight (light scattering in tetrahydrofuran) was 14 000.

Other polyamidoneocarbonanes and polyesterneocarbonanes, from hydroquinone, phenolphthalein, dioxydiphenylpropane, and ethylene glycol, were obtained similarly.

Synthesis of Poly(hexamethyleneneocarbonanedicarbonate)

A 0.83-ml portion of thoroughly dried triethylamine and 0.799 g of neocarbonanedicarboxylic dichloride were added to 0.32 g of hexandiol stirred in an inert gas in 15 ml of tetrahydrofuran at room temperature. The mixture was stirred for 2 hr.

After the reaction was completed, triethylamine chloride was filtered off, tetrahydrofuran was removed by evaporation, first at room temperature and then at 40–50°C/1mm Hg.

The yield of the vaselinelike, light yellow polymer was 0.76 g ($\sim 82\%$ of theory), $\eta_{\text{red}} = 0.08$ dl/g.

References

1. J. Green, N. Mayes, and M. Cohen, *J. Polym. Sci. A*, **2**, 3113 (1964).
2. J. Green, N. Mayes, A. Kotloby, and M. Cohen, *J. Polym. Sci. A*, **2**, 3135 (1964).
3. J. Green, N. Mayes, A. Kotloby, M. Fein, E. O'Brien, and M. Cohen, *J. Polym. Sci. B*, **2**, 109 (1964).
4. S. Papetti, B. Schaeffer, A. Gray, and T. Heying, *J. Polym. Sci. A-1*, **4**, 1623 (1966).
5. J. Green and N. Mayes, *J. Macromol. Sci.*, **A1**, 135 (1967).
6. V. V. Korshak, M. W. Sobolevski, A. F. Zhigach, I. G. Sarishvili, and Z. M. Frolova, *Vysokomol. Soedin.*, **105**, **N8**, 584 (1968).
7. V. V. Korshak, I. G. Sarishvili, A. F. Zhigach, and M. V. Sobolevski, *Usp. Khim.*, **36**, 2068 (1967).
8. V. V. Korshak and S. R. Rafikov, *Dokl. Akad. Nauk SSSR*, **48**, 36 (1945).
9. V. V. Korshak, *Usp. Khim.*, **35**, 1040 (1966).
10. V. V. Korshak, *Pure Appl. Chem.*, **12**, 101 (1966).
11. D. Grafstein and J. Dvorak, *Inorg. Chem.*, **2**, 1128 (1963).

Received September 17, 1969

Revised December 5, 1969

Photochromic Polypeptides

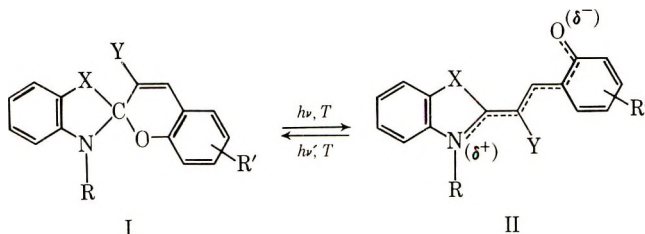
P. H. VANDEWYER and G. SMETS, *Laboratory of Macromolecular Chemistry, University of Louvain, Belgium*

Synopsis

Two photochromic polypeptides were synthesized by reaction of 1-(4-iodobutyl)-3,3-dimethylindolino-6'-nitrobenzospiropyran with poly-L-tyrosine; their molar contents on photochromic units were 27.3 and 44.7%. The spectra of the photo-induced merocyanines and their decoloration kinetics were compared with these of the monomeric model compound, obtained by reaction of the same *N*-(4-iodobutyl)-indolinospirogyran derivative with *N*-acetyltyrosine methyl ester. Different types of solvents have been examined, mainly dimethylformamide and pyridine, acetone and tetrahydrofuran, and methanol and ethylene glycol. The polypeptides showed a much less pronounced solvatochromism than their model; on the other hand, their absorption spectra presented two absorption maxima instead of one for the model. These differences in photochromic behavior were interpreted on the basis of the solvation of the polymeric chain. Inverse photochromism was observed for polypeptide P₂ as well as for the model in ethylene glycol solution; this effect is due to a higher merocyanine content at the thermal equilibrium spirogyran \rightleftharpoons merocyanine in high polar solvent.

INTRODUCTION

Of all the photochromic systems studied at this time, the spirogyrans have received most attention.¹⁻⁶ Their photochromism involves a scission reaction of the bond between the spiro carbon and the pyran oxygen atoms followed by a change of molecular configuration:



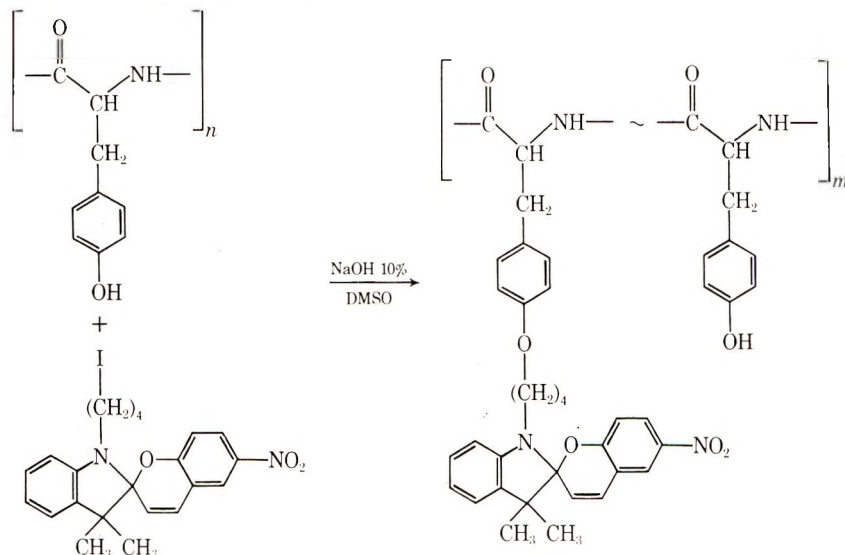
where $X = CMe_2$, $Y = H$, $h\nu =$ ultraviolet light; or $X = S$, $Y = Me$, $h\nu' =$ visible light. The merocyanines (II), formed by ultraviolet irradiation of I, are zwitterionic species and display a strong solvatochromism.⁷⁻¹⁰ The influence of the solvent is also very pronounced in their coloration and decoloration kinetics.¹¹⁻¹³ On the other hand, merocyanines are very sensitive to steric effects, especially in the case of benzothiazolinospirogyrans¹³ when compared to indolinospirogyrans.^{14, 15}

These phenomena justify the use of spiropyrans as a tool for studying polar and steric effects in polymer molecules.¹⁵⁻¹⁷ For the same reason we undertook the study of polypeptides containing spiropyran side chains.

It is now well established that many polypeptides present a helicoidal structure in the solid phase^{18,19} as well as in solutions in appropriate solvents.²⁰⁻²⁴ It was assumed that this structure could influence the behavior of spiropyrans when built into the polypeptide.

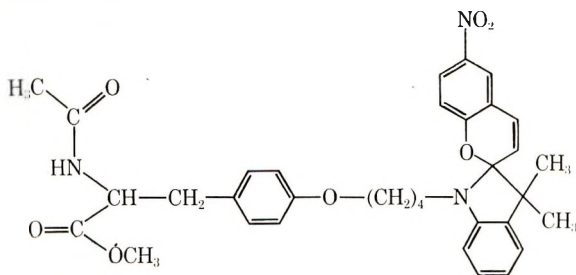
RESULTS

Poly-L-tyrosine was chosen as starting material for the synthesis of photochromic polypeptides. As the reaction of L-tyrosine with alkylhalides²⁵ is known to proceed easily, *N*-(ω -haloalkyl) indolinospirobenzopyran have been coupled with poly-L-tyrosine. Two different polymers were obtained



by this method; polymer P₁ contained 54.7 wt-% of spiran units (27.3 mole-%) and its osmotic molecular weight was 10,000 ($\bar{X}_n = 10$). Polymer P₂ contained 72.3 wt-% of spiran (44.7 mole-%) and had a molecular weight of 4000 ($5 < \bar{X}_n < 6$). By the same method, *N*-acetyltyrosine methyl ester (NATM) was transformed into its nitrobenzopyrrol-indolino-spiran derivative, which was used during this study as the reference model substance.

Model compound M



Compound

Optical Absorption Spectra

Table I summarizes the absorption maxima of polymers P₁ and P₂ and of the model compound M, as recorded immediately after ultraviolet irradiation.

Table I shows a marked difference between the solvatochromism of the model compound and that of the polymers. For the model compound a negative solvatochromism has been observed as expected, the polymers however show practically no solvatochromism; apparently no relationship exists between their λ_{\max} and the polarity E_t of the solvent; furthermore, two absorption maxima are always observed for both polymers (Fig. 1). Neither of these two absorption maxima can be attributed to salt formation resulting from the action of the free phenol groups with the open merocyanine molecule. Indeed, on addition of *N*-acetyl-L-tyrosine methyl ester (NATM) containing a free phenolic group to a solution of the model and to

TABLE I
Absorption Maxima of Photochromic Polytyrosines (P₁ and P₂) and Model Substance (M) after Ultraviolet Irradiation

Solvent	E_t^a	Absorption maxima, nm		
		M	P ₁	P ₂
Ethylene glycol	56.3	530	520, 553 ^{b,c}	Ins
Methanol	55.5	534	Ins ^d	Ins
Dimethylformamide	43.7	567	526, 560	527, 560
Acetone	42.2	578	522, 558 ^c	525, 560 ^c
Pyridine	40.2	590	530, 568	530, 568
Tetrahydrofuran	37.4	591	529, 563 ^c	529, 563 ^c

^a E_t = Dimroth's solvent polarity values.⁷

^b λ_{\max} determined on the nonirradiated solution.

^c Saturated solution, (concn < 0.1 g/l.).

^d Ins = insoluble.

TABLE II
Influence of the Addition of *N*-Acetyl-L-tyrosine Methyl Ester (NATM) on the Absorption Spectrum of the Model Compound (M) and Polymer P₁ in Acetone Solution

Photochrome	[NATM], mole l. $\times 10^3$	Optical density ^a				
		At 425 nm	At λ_{\max}	λ_{\max} , nm	At λ_{\max}	λ_{\max} nm
[M] = 2.5×10^{-4} mole/l.	0	0.322	2.406	578		
	1.92	0.355	2.317	578		
	10.9	0.580	2.200	578		
	47.5	0.580	1.69	577		
	169	0.702	1.28	563		
[P ₁] = 0.1 g/l. ^b	0	0.160	0.267	525	0.39	558
	42.2	0.318	0.267	525	0.39	558
	173	0.363	0.260	525	0.38	558

^a Optical densities determined immediately after irradiation for 90 sec ($\lambda_{\text{irr}} > 300$ nm).

^b Saturated solutions.

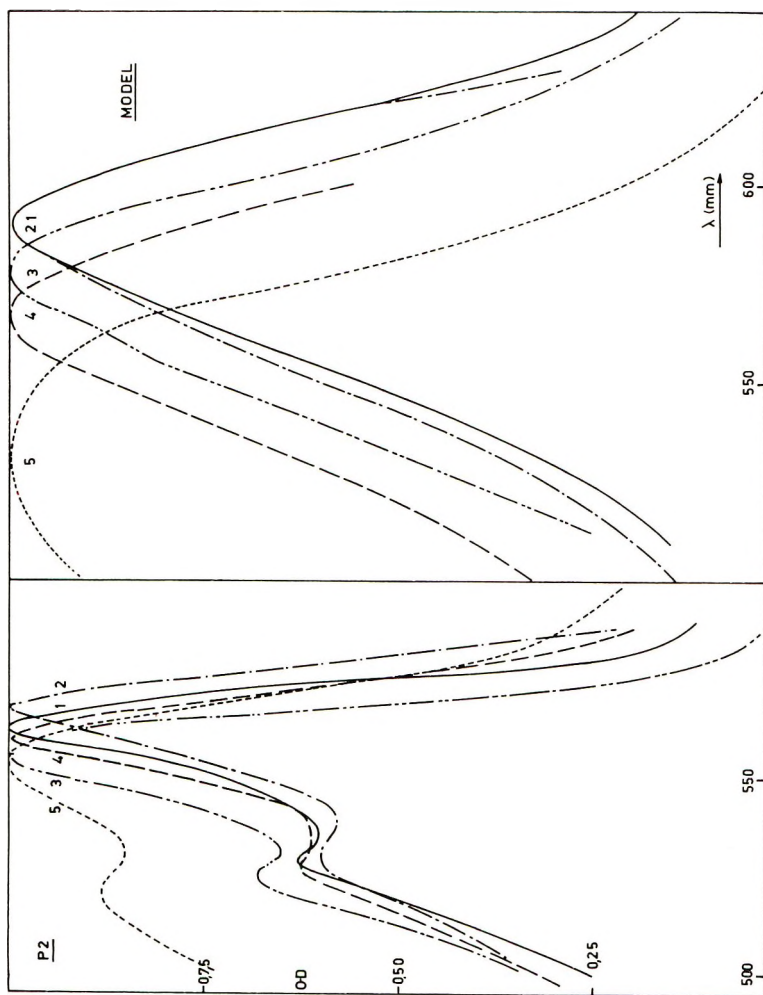


Fig. 1. Solvatochromism of polytyrosine P_2 and model compound, visible light absorption spectra, in various solvents: (1) tetrahydrofuran; (2) pyridine; (3) acetone; (4) dimethylformamide; (5) ethylene glycol.

a solution of P_1 , salt formation occurs; its absorption maximum, however, is located at 425 nm, i.e., much lower than the two maxima observed for the polymers (Table II).

The existence of the two absorption maxima characterizing P_1 and P_2 must be attributed to the presence of two isomers of the colored form. The existence of such isomers has been proved previously by several authors,^{6,16,17,26-32} usually by irradiation of spiropyrans at low temperature in the glassy state.

Decoloration Kinetics

The kinetics of the decoloration reaction was studied in various solvents; they differ markedly with the nature of the solvent used. Three groups of solvent will be considered successively.

Dimethylformamide and Pyridine. In these solvents the kinetics of decoloration obey a first-order relationship for M as well as for the two polymers (Table III).

TABLE III
Kinetics of Decoloration in Dimethylformamide and Pyridine at 20°C^a

Photochrome	$k \times 10^3, \text{min}^{-1}$	
	Dimethylformamide	Pyridine
$[M] = 3.3 \times 10^{-4} \text{ mole/l.}$	5.57 ± 0.07	28.0 ± 0.1
$[P_1] = 0.13 \text{ g/l.}$	3.62 ± 0.05	17.0 ± 0.2
$[P_2] = 0.4 \text{ g/l.}$	5.72 ± 0.07	17.2 ± 0.1

^a $\lambda_{irr} > 300 \text{ nm.}$

In dimethylformamide the rate constants for M and P_2 are practically equal. The slower rate with P_1 can be attributed to the solvent effect of free phenolic groups, which are more numerous in P_1 than in P_2 . In pyridine, the difference between P_1 and P_2 vanishes, as all the phenolic units are neutralized by the basic solvent. However, in this solvent, the model compound M discolors more rapidly than the polymers.

It should be pointed out that, in both solvents, the positions of the absorption maxima λ_{max} of M, P_1 , and P_2 remain constant. Furthermore, the ratio r of the optical densities of the two absorption peaks of P_1 and P_2 also remain unchanged during the decoloration reaction even at high degree of conversion. In dimethylformamide it is 0.68 and 0.62 and in pyridine 0.63 and 0.60 for polymers P_1 and P_2 , respectively.

Acetone and Tetrahydrofuran. In these two solvents the decoloration kinetics of the model and polymers deviate from a first-order relationship. The variation of the optical density with the time follows the relation:

$$D = ae^{-x_1t} + be^{-x_2t}$$

The experimental results are given in Table IV. From these data it can

be seen that the model compound discolors much more rapidly than P₁ and P₂. Furthermore P₁ discolors somewhat more slowly than P₂, as was also the case in DMF solutions. In the case of the model compound a strong hypochromic shift of λ_{\max} is observed during the decoloration reaction (Table V). This shift is not observed in the case of polymers P₁ and P₂, although the absorption peak (Fig. 2) intensity ratios r decrease slowly

TABLE IV
Decoloration Rate Constants X_1 and X_2 of M, P₁, and P₂ in Acetone and Tetrahydrofuran at 20°C

Photochrome	$X_1 \times 10^2, \text{min}^{-1}$		$X_2 \times 10^2, \text{min}^{-1}$	
	Acetone	Tetrahydrofuran	Acetone	Tetrahydrofuran
[M] = 3.3×10^{-4} mole/l.	89.0 ± 0.7	39.8 ± 0.4	17.36 ± 0.02	23.9 ± 0.5
P ₁ , saturated soln ^a	21.9 ± 0.7	18.9 ± 0.1	3.32 ± 0.03	5.43 ± 0.07
P ₂ , saturated soln ^a	28.6 ± 0.1	22.6 ± 0.2	4.02 ± 0.02	5.96 ± 0.06

^a In acetone, < 0.1 g/l.; in THF, ca. 0.2 g/l.

TABLE V
Influence of the Degree of Decoloration on the Absorption Spectra of the Model Compound M and Polymer P₂

Solvent	Temp, °C	λ_{irr} , nm	[M] = 6.7 × 10 ⁶ mole/l.		P ₂ , saturated soln ^a		Decoloration, %
			λ_{\max} , nm	Decoloration, %	λ_{\max} , nm	r^b	
Tetrahydrofuran	25	300	591	0	563	^c	0
			589	56	563	0.68	22
			569	78	564	0.66	40
			563	93	562	0.64	66
			561	96	563	0.64	91
						563	0.62
Acetone	22	365	578	0	555	0.72	0
			578	31	555	0.72	22
			578	49	555	0.70	56
			571	63			
			570	73	557	0.69	74
			561	85	556	0.68	79
			559	90	556	0.66	before irradiation

^a P₂ = 0.2 g/l. in THF; ≤ 0.1 g/l. in acetone.

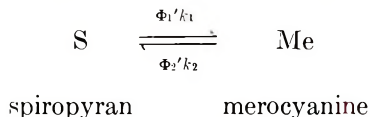
^b r indicates the ratio of the two optical densities at the two λ_{\max} absorptions.

^c First absorption peak is only a shoulder of the second peak; r is uncertain.

with the degree of conversion and tend to the initial value before irradiation.

By using monochromatic ultraviolet light (365 nm) instead of ultraviolet and visible light (300 nm), one observes a slight bathochromic influence of the wavelength of the irradiation source (1 and 3 nm in tetrahydrofuran, and 3 and 5 nm in acetone for M and P₂, respectively).

Glycol and Formamide. These two hydrogen-bonding solvents were supposed to be able to modify the peculiar structure of the polypeptides and consequently influence the photochromism of the polymers. In fact, polypeptide P₁ is only poorly soluble, while P₂ is insoluble in formamide and ethylene glycol. This fact is obviously due to the presence of spiropyran units which exert a screening effect and prevent the solvent molecules from breaking the amide hydrogen bonding. On the other hand (and surprisingly), M as well as P₁ shows an inverse photochromism on irradiation with ultraviolet light. A similar phenomenon was observed by Przystal³³ during his study of indolino-quinolino-spiropyran in benzyl alcohol. This inverse photochromism can not be attributed to traces of acid contaminating the solvents; indeed, it persists even in the presence of large amounts of pyridine in ethylene glycol solutions (up to 10 vol-%) both for the model compound M and for the polymeric polypeptide P₁. The reason for an inverse photochromism can best be understood on the basis of the equilibrium



At equilibrium:

$$K_e = \frac{k_1}{k_2} = \frac{[\text{Me}_e]}{[\text{S}_e]} = \frac{[\text{Me}_e]}{[\text{C}] - [\text{Me}_e]}$$

where [S_e] and [Me_e] are the equilibrium concentrations of colorless spiropyran and merocyanine, respectively, while [C] is the concentration of spiropyran based on initial amount dissolved before equilibration. Thus

$$[\text{Me}_e] = K_e[\text{C}]/(1 + K_e)$$

If one neglects the contribution of the relatively slow thermal reactions, one can express the rate of photochemical transformations S ⇌ Me as

$$\text{rate} = \Phi_1 I_{\text{abs}_1} [\text{S}_e] - \Phi_2 I_{\text{abs}_2} [\text{Me}_e] = \Phi_1 (I_{\text{abs}_1}/K_e) - \Phi_2 I_{\text{abs}_2} [\text{Me}_e]$$

Inverse photochromism will thus be observed when $\Phi_2 I_{\text{abs}_2} > \Phi_1 I_{\text{abs}_1}/K_e$ i.e., when [Me_e] is sufficiently high compared to [S_e]. The equilibrium constant of the reaction spiropyran ⇌ merocyanine has therefore been evaluated for the model compound in methanol ($E_t = 55.5$) and ethylene glycol ($E_t = 56.3$) and compared to that of the homologous substance the 1,3,3-trimethylindolino-6'-nitrobenzospirropyran as determined in ethanol ($E_t = 51.9$) by Flannery¹² (K_e at 25°C = $8.43 \pm 2.71 \times 10^{-3}$). Assuming a molar extinction coefficient of 3.5×10^4 in polar solvents, a value of 42.3 ± 12.5

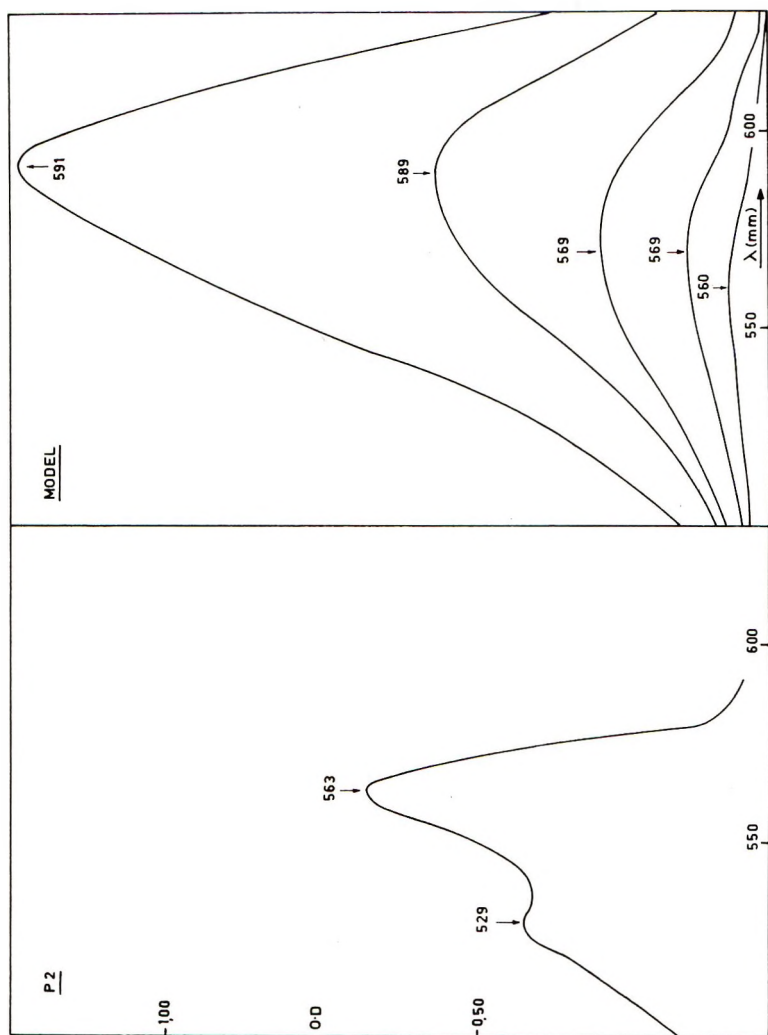


Fig. 2. Influence of the degree of decoloration on the absorption spectra of the model compound and polymer P_2 . Solvent: tetrahydrofuran.

$\times 10^{-3}$ at 30°C was found in methanol and $133 \pm 42.5 \times 10^{-3}$ at 26°C in ethylene glycol. It seems, therefore, that the high polarity of these two solvents is responsible for a higher equilibrium concentration of merocyanine $[\text{Me}_e]$ and consequently of the inverse photochromism.

The kinetics of thermal colorations of M and P_1 in ethylene glycol at 30°C (after irradiation at $>300\text{ nm}$) have also been examined. It can easily be shown that the plot of the logarithm of the optical density against time has a slope equal to the sum of both rate constants of ring opening (k_1) and ring closure (k_2), both in the case of positive and negative photochromism.¹²

This method yields a value of $(k_1 + k_2)$ of 9.4×10^{-3} for the model compound at $[\text{M}] = 3.3 \times 10^{-4}$ mole/l.; for a saturated solution of the polymer P_1 (about 0.1 g/l.), $(k_1 + k_2)$ is equal to $15.3 \times 10^{-3}\text{ min}^{-1}$.

As can be seen from these data and very surprisingly, the polypeptide P_1 has a much higher $(k_1 + k_2)$ value (about fivefold) than the model compound in ethylene glycol, contrary to the data obtained in all other solvents.

DISCUSSION

The results of our comparative study indicate strong differences in photochromic behavior.

The model compound exhibits an almost classical photochromic behavior, i.e., negative solvatochromism and decoloration rate constants which increase with decreasing polarity of the solvent. Two abnormal facts have, however, been observed. Firstly, complex kinetics and large variations in the absorption spectra (Fig. 1) are indicated in solvents of low polarity of THF and acetone; these effects are explained by assuming the existence of two isomers which coexist in solution, as was already observed by Wippler et al.³⁰⁻³⁴ although on a much more reduced time scale. Secondly, inverse photochromism is observed in solvents of high E_t polarity (glycol and formamide). It is assumed that this situation arises from the high tendency, in highly polar solvents, of the model compound to undergo thermal ring opening.

On the other hand, the polypeptides exhibit a kinetic and spectral behavior which is much less affected by the polarity of the solvent. This difference is most strikingly illustrated by Figure 3, in which the reciprocal value of the wavelength is plotted against the E_t value of the solvent. A much stronger solvent dependence is thus obviously shown by the model compound. The same behavior is shown by the kinetics of the decoloration reaction. This low solvent dependence of the photochromic behavior of the polypeptides is likely to be due to the incomplete solvation of the macromolecule. Solvents of low polarity (THF and acetone) solvate the spiro-pyran units but are repelled by the polypeptide spiral. On the other hand, hydroxylic solvents, although good solvating agents for polypeptides, are screened off from the polypeptide group by the shielding effect of the spiro-

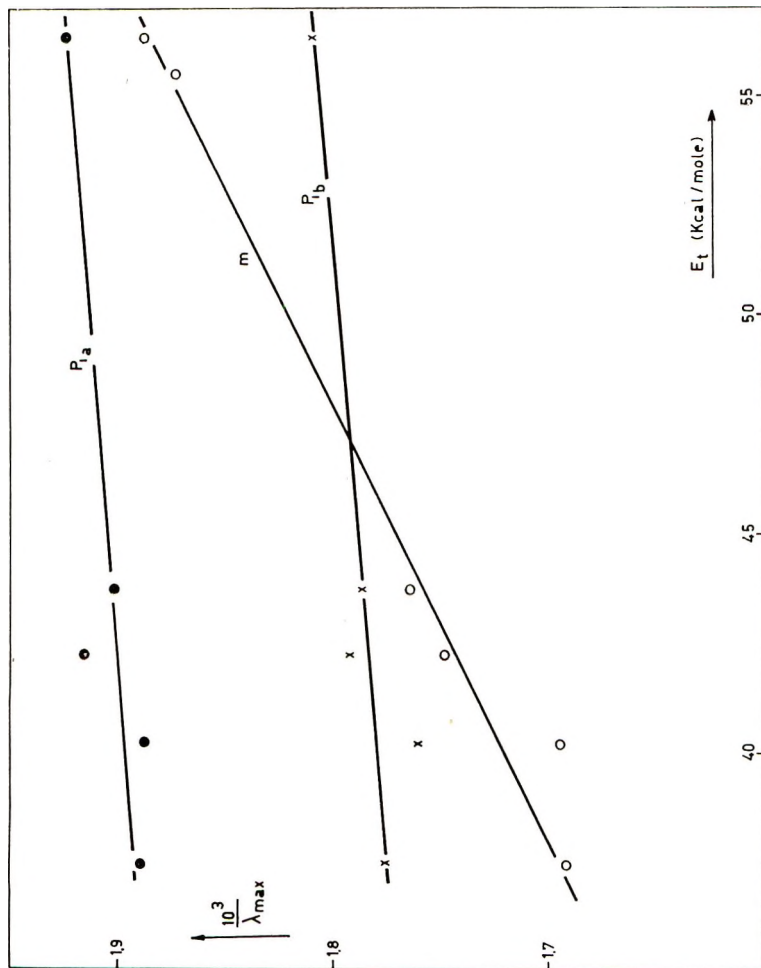


Fig. 3. Variation of $1/\lambda_{\max}$ as a function of the polarity of the solvent for the model compound and for photochromic polytyrosine P₁ at shorter (a) and high (b) wavelength λ_{\max} .

pyran units. Dimethylformamide and pyridine are able to solvate both spiropyran and polypeptide units and are therefore good solvents.

EXPERIMENTAL

Starting Materials

Diiodobutane (Fluka), L-tyrosine (Schuchardt), ethyl chloroformate (Schuchardt) and benzyl chloride (Fluka, puriss.) were used without further purification. For kinetic measurements analytical-grade solvents were used. Dimethylformamide was fractionated prior to use.

Syntheses

1-(4-Iodobutyl)-3,3-dimethylindolino-6-nitrobenzospiropyran

1-(4-Iodobutyl)-2,3,3-trimethylindolinium iodide is obtained, together with a small quantity of the double quaternary salt (10%), on heating 0.1 mole 2,3,3-trimethylindoline with 0.4 mole diiodobutane in a sealed tube for 24 hr. The solid was filtered off, thoroughly washed with acetone and ether and vacuum-dried.

A 4.7-g portion of the quaternary salt and 1.67 g 5-nitrosalicylaldehyde were suspended in 20 ml hot butanone; 1 ml piperidine was added and the mixture heated for 2–3 minutes. On cooling, part of the spiropyran precipitates; the major part was obtained after evaporation of the filtrate and extraction of the residue with a 1:1 toluene–heptane mixture. The mixture of mono- and bis-spiran is easily separated by fractional crystallization from ethanol–benzene (9:1), mp 110°C.

ANAL. Calcd for $C_{22}H_{23}IN_2O_3$: C, 53.88%; H, 4.72%; N, 5.71%. Found: C, 54.40%; H, 4.75%; N, 5.80%.

The NMR spectra showed absorptions for C-(CH₃)₂ at 8.7 (s) and 8.8 τ (s); 3'-H, 4.1 τ (d); N-CH₂-CH₂-CH₂CH₂I, 8.00–8.35 τ (m); and N-CH₂-CH₂-CH₂-CH₂I, 6.7–7.0 τ (m). Here (s) denotes single, (d) double, and (m) multiple peaks.

N-Acetyl-L-tyrosine Methyl Ester

N-acetyl-L-tyrosine was prepared by acetylation of L-tyrosine following the method of du Vigneaud;³⁴ mp 152.4°C.

N-acetyl-L-tyrosine methyl ester³⁵ was obtained by treating the acid at –5°C with a mixture of thionyl-chloride and methanol; mp 135–136°C; $[\alpha]_{546}^{28} = 34.3^\circ$ ($c = 2\%$, MeOH).

Model Compound

1-(4-Iodobutyl)-3,3-dimethylindolino-6-nitrobenzospiropyran (10 mmole) and N-acetyl-L-tyrosine methyl ester (10 mmole) dissolved in 40 ml dimethyl sulfoxide were treated with 4 ml of 10% NaOH and then stirred at 80°C for 5 hours. After cooling, the mixture was poured into ice water

and the precipitate filtered off and washed with water. It was redissolved in chloroform and the resulting solution washed twice with 10% aqueous K_2CO_3 . The chloroform solution was then dried over sodium sulfate and evaporated; residual solid was recrystallized from ethanol-benzene (9:1); mp 108°C.

ANAL. Calcd: C, 68.09%; H, 6.22%; N, 7.01%; O, 18.67%. Found: C, 68.96%; H, 6.17%; N, 7.45%; O, 17.29%.

The NMR showed $C(\underline{CH}_3)_3$, 8.72 (s) and 8.80 τ (s); $CO\underline{CH}_3$, 6.27 τ (s); $3'H$, 4.1 τ (d).

Poly-L-tyrosine

O-Benzyl-L-Tyrosine. This was prepared by benzylation of the copper complex of L-tyrosine, followed by decomposition of the resulting O-benzyl-L-tyrosine copper complex; yield, 46%; mp 238°C.

N-Carbethoxy-O-benzyl-L-tyrosine. To a cold solution of 0.1 mole O-benzyl-L-tyrosine and 0.3 mole NaOH, 0.2 mole ethyl chloroformate was added under stirring for 10 min. After being allowed to stand for 1 hr the reaction mixture was acidified with concentrated HCl in the presence of Congo Red as indicator. The N-carbethoxy-O-benzyl-L-tyrosine was extracted with ether, the ether solution dried over Na_2SO_4 , and evaporated *in vacuo*. The residue solidified on cooling and was recrystallized from carbon tetrachloride; yield 80%; mp 119–121°C.

4(4-Benzoyloxybenzyl)oxazolid-2,5-dione. A mixture of 0.1 mole N-carbethoxy-O-benzyltyrosine and 0.2 mole thionyl chloride were heated at 40°C under stirring. When the gas evolution decreased the mixture was warmed to 55°C and excess thionyl chloride vacuum-distilled off. The N-carboxy anhydride solidifies on cooling. It is crystallized from a 2:2:1 mixture of carefully dried benzene, petroleum ether and dioxane; yield 84%; mp 136–138°C (lit. mp 142°C³⁶).

The infrared spectrum showed two $C = O$ amide absorption peaks at 1850 and 1775 cm^{-1} and $N - H$ absorption at 3440 cm^{-1} .

Poly-O-benzyl-L-tyrosine. To a solution of 0.1 mole of N-carboxy anhydride in 120 ml dry dioxane 5×10^{-3} mole of Et_3N was added and the mixture refluxed for 24 hr with stirring. After evaporation of the solvent under vacuum the residue was dissolved in dichloroacetic acid. The polymer was precipitated into water and purified by two more precipitations from trifluoroacetic acid solutions. After washing with water, ethanol, and ether, it was dried *in vacuo*.

Poly-L-tyrosine. The polymer was obtained by suspending poly-O-benzyl-L-tyrosine in glacial acetic acid and stirring at 50°C for 5 hr while HBr gas was bubbled through the suspension. The resulting solution was dropped into a tenfold excess of ether; the polymer was filtered off and purified by two precipitations from its dimethylformamide solutions into water. It was finally washed and dried *in vacuo*; yield 46%; $n = 39$; $[\alpha]_{546}^{28} = 28.1^\circ$.

Photochromic Polypeptides (P_1 and P_2). Poly-L-tyrosine (0.815 g) dissolved in 10 ml of 2% NaOH was heated at 80°C; 40 ml dimethyl sulfoxide and 5 mmole of I were added. The resulting solution was stirred for 5 hours and then poured into 500 ml methanol containing 20 mmole *N*-acetyl-L-tyrosine methyl ester, which were added to neutralize remaining polymeric phenolate ions, if any. This procedure was repeated once more, and the polymer was finally purified by precipitation in pure ethanol of its DMF solution. After washing and drying *in vacuo* at 50°C, 0.9 g of a highly colored, purple solid was obtained (P_1).

Polymer P_2 was prepared similarly, but with a double quantity of the 1-(4-iodobutyl)-3,3-dimethylindolino-6-nitrobenzospiropyran. Heating was prolonged up to 16 hr.

Kinetic measurements were carried out with a Hitachi-Perkin-Elmer Model spectrophotometer.

Spectra were recorded on a Cary Model 16 U. V. spectrophotometer.

CONCLUSION

The results of this study show that photochromic polypeptides are not very sensitive to solvent effects, as compared to ordinary photochromic macromolecules.^{16,17} This situation can be explained by assuming a repulsion between the central helix of the polypeptide and most of the solvent molecules in such a way that the solvation of the spiropyran units is much less complete than in the case of the model compound.

The authors are indebted to the High Polymer Research Center (I.W.O.N.L.) and to the Centre des Hauts Polymères—Agfa-Gevaert N.V., Belgium, for supporting this research. They are very grateful to Dr. S. Toppet for interpretation of the NMR spectra.

References

1. R. Dessauer and J. Paris, *Advan. Photochem.*, **1**, 275 (1963).
2. P. Douzou and C. Wippler, *J. Chim. Phys.*, **60**, 1409 (1963).
3. W. Luck and H. Sand, *Angew. Chem. Intern. Ed.*, **3**, 570 (1964).
4. R. Exelby and R. Grinter, *Chem. Revs.*, **65**, 247 (1965).
5. E. Fischer, *Fortschr. Chem. Forsch.*, **7**, 605 (1967).
6. T. Bercovici, R. Heiligman-Rim, and E. Fischer, *Mol. Photochem.*, **1**, 23 (1969).
7. K. Dimroth, C. Reichardt, T. Siepmann, and F. Bohlmann, *Anal. Chem.*, **661**, 1 (1963).
8. L. G. S. Brooker, G. H. Keyes, and D. W. Heseltine, *J. Amer. Chem. Soc.*, **73**, 5350 (1951).
9. A. I. Kiprianov and W. J. Petrukin, *Zh. Obshch. Khim.*, **10**, 613 (1940).
10. A. I. Kiprianov and E. S. Timoshenko, *Zh. Obshch. Khim.*, **17**, 1468 (1947).
11. H. Kokelenberg, Ph.D. thesis, Louvain, 1967.
12. J. B. Flannery, Jr., *J. Amer. Chem. Soc.*, **90**, 5660 (1968).
13. P. H. Vandeweyer, J. Hoefnagels, and G. Smets, *Tetrahedron*, **25**, 3251 (1969).
14. A. Hinnen, C. Audie, and R. Gautron, *Bull. Soc. Chim. France*, **1968**, 3190.
15. J. Hoefnagels, Ph.D. thesis, Louvain, 1969.
16. P. H. Vandeweyer and G. Smets, in *Macromolecular Chemistry Brussels-Louvain 1967* (*J. Polym. Sci. C*, **22**), G. Smets, Ed., Interscience, New York, 1968, p. 231.
17. G. Smets and P. H. Vandeweyer, paper presented to American Chemical Society, Division of Polymer Chemistry, *Preprints*, **9**, 211 (1968).

18. M. L. Huggins, *Chem. Revs.*, **32**, 195 (1943).
19. L. Pauling and R. B. Corey, *Proc. Nat. Acad. Sci. U.S.*, **37**, 235 (1951).
20. P. Urnes and P. Doty, *Advan. Protein Chem.*, **16**, 401 (1961).
21. M. Goodman, C. M. Deber, and A. M. Felix, *J. Amer. Chem. Soc.*, **84**, 3773 (1962).
22. M. Goodman and J. J. Schulman, in *Perspectives in Polymer Science (J. Polym. Sci. C, 12)*, E. S. Proskauer, E. H. Immergut, and C. G. Overberger, Eds., Interscience, New York, 1966, p. 36.
23. M. Goodman, A. M. Felix, C. M. Deber, A. R. Brouse, and G. Schwartz, *Biopolymers*, **1**, 371 (1963).
24. M. Goodman and A. Kossoy, *J. Amer. Chem. Soc.*, **88**, 5010 (1966).
25. S. L. Solar and R. R. Schumaker, *J. Org. Chem.*, **31**, 1996 (1966).
26. Y. Hirshberg and E. Fischer, *J. Chem. Soc.*, **1954**, 3129.
27. R. Heiligman-Rim, Y. Hirshberg, and E. Fischer, *J. Phys. Chem.*, **66**, 2465, 2470 (1962).
28. M. W. Windsor, R. S. Moore, and J. R. Novak, *Spectrochim. Acta*, **18**, 1364 (1962).
29. G. I. Lashkov and A. V. Shablya, *Optik Spektroskopiya*, **14**, 821 (1965).
30. J. C. Metras, M. Mosse, and C. Wippler, *J. Chim. Phys.*, **61**, 660 (1964).
31. J. Arwand, C. Wippler, and F. Beaurc d'Augeres, *J. Chim. Phys.*, **64**, 1105 (1967).
32. Z. G. Gardlund, *J. Polym. Sci. B*, **6**, 57 (1968).
33. F. Przystal, T. Rudolph, and J. P. Phillips, *Anal. Chim. Acta*, **41**, 391 (1968).
34. V. du Vigneaud and C. E. Meyer, *J. Biol. Chem.*, **98**, 295 (1932).
35. H. Zahn and K. Mella, *Z. Physik. Chem. (Leipzig)*, **344**, 75 (1966).
36. J. Noguchi, T. Saito, and T. Hayakawa, *Chem. Abstr.*, **55**, 2508c (1961).
37. J. G. Calvert and J. N. Pitts, Jr., *Photochemistry*, Wiley, New York, 1966, p. 487.

Received December 18, 1969

Kinetics of Thermal and Acidic Degradation of Poly-1,3-dioxolane*

E. N. KUMPANENKO, A. I. VARSHAVSKAYA, L. V. KARMILOVA,
and N. S. ENIKOLOPYAN, *Institute of Chemical Physics, Academy of
Sciences, Moscow, U.S.S.R.*

Synopsis

The kinetics and parameters of thermal and acidic degradation of poly-1,3-dioxolane were investigated in order to elucidate the mechanism of degradation and to obtain information on the nature of active centers. Both homolytic and heterolytic breaking of a macromolecule were shown to be random and occur at the acetal bond. Thermal degradation was found to proceed in two stages, depending on temperature and involving active centers of a different nature, i.e., macroions and macroradicals. The rate-determining step of thermal degradation appears to be one involving the radical component, similarly to thermal degradation of olefin polyoxides. Acidic degradation occurs solely by the depolymerization mechanism, as in the case of polyaldehydes. It was concluded that the degradation mechanism depends not only on the chain structure and the thermodynamic properties of the system, but also on the nature of active centers.

INTRODUCTION

An important task in the investigation of the acetal degradation mechanism is to establish whether its active centers are of a radical or of an ionic nature. However, at high temperatures, direct identification is hindered by low concentrations and the lability of active centers. Study of the kinetics and products of ion- or radical-induced degradation and comparison of the results obtained with those observed for thermal degradation permit establishing both the nature of active centers and the extent of its effect on the degradation direction.

EXPERIMENTAL

The paper describes the results of comparative investigation of the kinetics and products of thermal and acidic polydioxalane (PDO) degradation in inert medium (*in vacuo*, 10^{-4} torr, dry A) over a temperature range of 140 to 310°C. The polymer was obtained by polymerization of 1,3-dioxolane in bulk in the presence of different initiators (BF_3OEt_2 , I_2 , H_2SO_4). It was freed of traces of catalyst by multiple precipitations and was dried *in vacuo*. Polymer samples $MW = 2-37 \times 10^3$ ($DP = 13-250$) of a size

* Presented at the International Symposium on Macromolecular Chemistry, Budapest, 1969.

0.02 g (2.7×10^{-4} mole DO) were used. The destruction kinetics was studied by the gravimetric technique, from variations in the molecular weight and in the composition of products. Volatile products were identified by gas-liquid chromatography (GLC); liquid and solid residues were analyzed by infrared spectroscopy for the presence of $-\text{OH}$, $-\text{C}=\text{O}$ and $-\text{C}=\text{C}-$ groups. The number of polymer chain ruptures to the moment of time t from the start of degradation were calculated by making use of the expression:

$$n = M_0 \left[\left(\frac{1 - \alpha}{P_{nt}} \right) - \left(\frac{1}{P_{n0}} \right) \right]$$

where M_0 is the polymer amount in base moles. α is the degree of degradation, P_{n0} and P_{nt} are mean numerical values of the polymerization degree for the initial and degraded polymer, respectively. Picric acid (PA), 0.1–1 wt-%, was used as the acidolysis agent.

RESULTS AND DISCUSSION

The regular variations in molecular weight with the degree of degradation (Fig. 1) are evidence that polymer chain rupture follows a random law both in acidolysis and in thermal degradation. Heterolytic rupture occurs at a temperature T lower than the ceiling temperature ($T = 140^\circ\text{C} < T_c$),¹ whereas homolytic rupture is observed only at $T > T_c$ ($\geq 250^\circ\text{C}$). The initial rate of rupture essentially depends on temperature. The effective activation energies for acidolysis and thermal degradation determined from the temperature dependence of the initial chain rupture rate $(dn/dt) - (1/T)$ are $E_a = 17 \pm 2$ kcal/mole, $E_T = 31 \pm 2$ kcal/mole, respectively (Fig. 2). The first value, E_a , is in good agreement with that obtained for low-

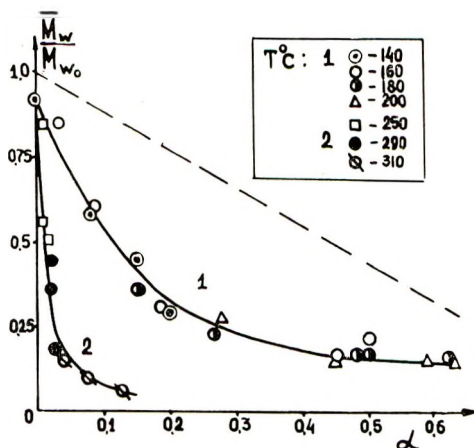


Fig. 1. Relative decrease in weight-average molecular weight (M_w/M_{w0}) of polydioxolane as a function of the degree of degradation: (1) by acidolysis, (2) by thermal degradation.

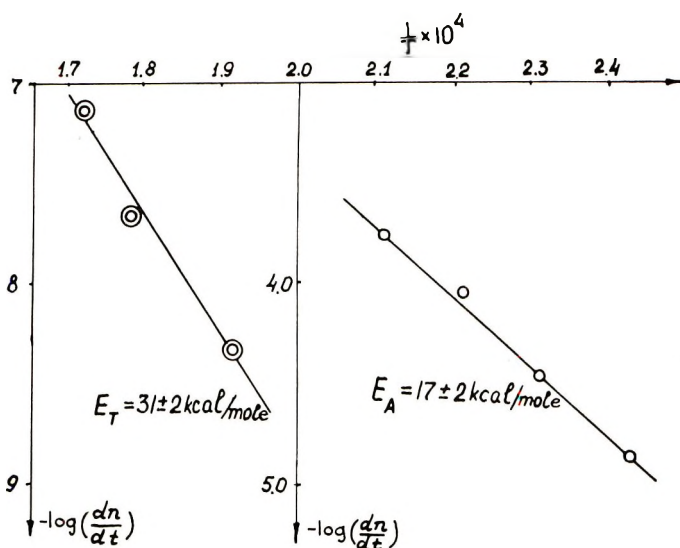


Fig. 2. Temperature dependence of the initial rate of PDO chain rupture: (1) by acidolysis; (2) by thermal degradation (Arrhenius plot).

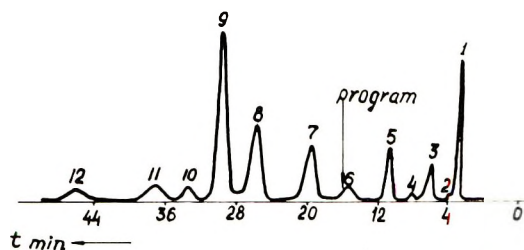


Fig. 3. Chromatogram of products of PDO degradation at 310°C: (1) light gases, (3) CH_3CHO ; (4) $\text{C}_2\text{H}_4\text{O}$; (7) CH_3OH ; (8) $\text{C}_2\text{H}_5\text{OH}$, (9) DO, (10) THF, (11) ethylal. Squalane, $T_{\text{column}} = 15\text{--}75^\circ\text{C}$ (programmed $dT/dt = 10^\circ\text{C}/\text{min}$) DIF; carrier gas-A.

temperature acidic hydrolysis of PDO² and acidolysis of polyaldehydes^{3,4} and the second, T_T , is in keeping with E_{true} for thermal degradation of polyoxymethylene with ester endgroups⁵ which is known to occur at the acetal bond. The E_{eff} value for thermal degradation of olefin polyoxides (44–46 kcal/mole) at the ester bond is considerably higher than that obtained.⁶ These facts may be considered as indirect evidence that thermal degradation occurs in preference at the acetal bond.

However, the acidolysis and thermal degradation products are essentially different. The cyclic monomer, 1,3-dioxalane, is the only light volatile product of acidic degradation at any temperature. No other products were discovered. Thermal degradation yielded numerous volatile species, such as H_2 , C_2H_6 , C_2H_4 , CO , CO_2 , $\text{C}_2\text{H}_4\text{O}$, CH_3CHO , CH_3OH , DO, ethylal THF, etc. (Fig. 3). These were found to be not secondary, but primary products of the PDO molecules dissociation, as shown by specific experi-

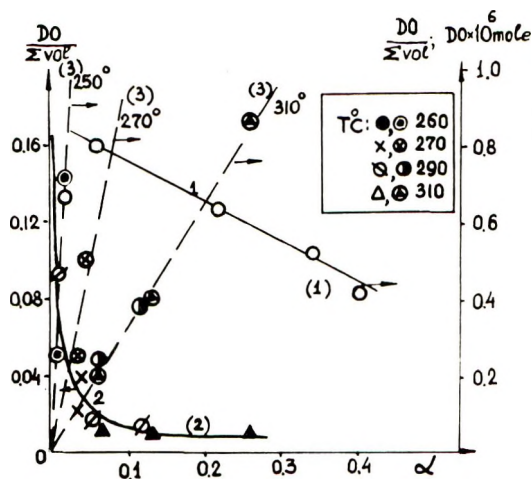


Fig. 4. Dioxolane accumulation (3) and its relative content ($[DO]/\Sigma volat$) (1,2) as a function of the degree of degradation: (1) by acidolysis ($T = 160^\circ C$); (2) by thermal degradation ($T = 250\text{--}310^\circ C$).

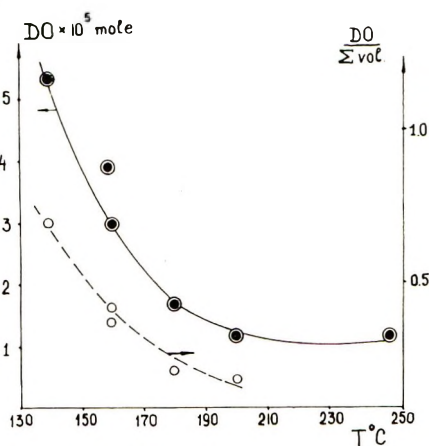


Fig. 5. Temperature dependence of the relative dioxolane yield ($[DO]/\Sigma volat$); 30 min degradation time.

ments. Both reactions yielded oligomer fragments of the polydioxalane chain that were volatile at T_d ($\overline{DP} = 5\text{--}8$ according to infrared spectroscopy⁷). Nonvolatiles solid residues represented linear fragments of the PDO chain ($\overline{DP} = 10\text{--}12$) containing OH, CHO endgroups, and —C=C— bonds. Dioxalane accumulation and its relative content ($[DO]/\Sigma volat$) markedly decreased with the degree of degradation (Fig. 4) and with temperature (Fig. 5). However, while with thermal degradation ($T \geq 250^\circ C$) the monomer content did not exceed 10% of all volatile products, with acidolysis it was no less than 50%, even at high degrees of conversion (Fig. 4). The dioxalane yield per one chain rupture was estimated by com-

TABLE I
Dioxolane Yield per Mole of Chain Rupture (ν)
during Polydioxolane Degradation

By acidolysis		By thermal degradation	
$T, ^\circ\text{C}$	$\nu = [\text{DO}]/n$ mole/mole	$T, ^\circ\text{C}$	$\nu = [\text{DO}]/n$ mole/mole
140	9.7-8.3	160	6-8
160	13.0-12.0	250	2
180	11.0-9.4	290	$2-3.5 \times 10^{-2}$
200	14.0-12.0	310	$0.5-1.4 \times 10^{-2}$

parison of the number of chain ruptures with the total dioxolane amount obtained (Table I).

These results show that depolymerization is not the predominant mechanism of PDO thermal degradation, which is different from the observation for polyaldehydes.⁸⁻¹¹ The active centers, seemingly of an ionic nature, are capable of intramolecular detachment of the monomer only at early stages of the process. The following facts are in favor of the ionic nature of the depolymerization active centers. (1) Depolymerization is the sole mechanism of acidic degradation at T close to the ceiling temperature. (2) The dioxolane fraction in thermal degradation products is greatly dependent on the extent it is washed off the catalyst, whereas the yields of other products are insensitive to it. (3) The reverse reaction, polymerization with opening of the ring, is of an ionic nature and is not initiated by radicals. Catalyst fractions remaining in the polymers even after it is washed off may account for the ionic nature of active centers. However, the polymer chain degradation is the main component of the overall PDO thermal degradation accompanied by formation of light products and oligomer fragments, the same as observed for the degradation of olefin polyoxides. The diversity of volatile products, the marked increase in their amounts with temperature, their independence of the catalyst type and of the extent to which it was washed off indicate that the active centers of PDO thermal degradation are of a radical nature. In order to verify this, the regularities of polymer chain rupture and the composition of products of thermal PDO degrada-

TABLE II
Composition of Products, Initial Rate of Polymer Chain Rupture ($dn/dt)_0$, and Dioxolane Yield ν per mole of Chain Rupture by Degradation of Polydioxolane under the Action of Different Initiators (I) at 160°C , $\alpha \leq 0.1$

I	t , min	Volatiles, %			$(dn/dt)_0$, mole/sec	$\nu = [\text{DO}]/n$, mole/mole
		Gaseous fraction	Dioxolane	Oligo- mers		
None	180	6	35	45-50	7×10^{-10}	6-8
Benzoyl peroxide	30	18.3	5	70	9×10^{-9}	0.05-0.2
Picric acid	30	None	65.5-70	30	1.8×10^{-9}	12-13

tion initiated by radicals were studied under conditions making impossible rupture of the acetal bond with formation of radicals ($T = 150\text{--}160^\circ\text{C}$).

Benzoyl and dicumyl peroxides (BP and DCP) (1 wt-%) were used as initiators. The products of low-temperature and thermal degradation appeared to be identical and markedly differed from those of acidolysis. In the presence of peroxides the rate of initial chain rupture was by an order of magnitude higher than that of spontaneous dissociation of a macromolecule, and the monomer yield per rupture was 50 to 100 times less (Table 2).

Higher concentrations of the peroxide added increased yields of all light products except dioxalane, the amount of which remained constant. This suggested that the main component of PDO degradation was of a radical nature. On the basis of the data obtained it is suggested that thermal PDO degradation is a complex process involving two types of active centers, namely, macroradicals and macroions, and that the courses of their subsequent conversions are different. Macroions degrade mostly by a depolymerization mechanism with detachment of monomer and oligomer fragments. Polymer radicals readily enter into transfer reactions accompanied by isomerization to form light products and stable linear oligomers. The ionic component fraction decreases with increasing temperature, whereas the probability and rate of the radical process increase markedly, and at $250\text{--}270^\circ\text{C}$ this process becomes predominant. The data obtained are insufficient for detailed elucidation of the PDO degradation mechanism, but it may be seen to be similar to thermal degradation of polyoxides, rather than of polyaldehydes, though both are initiated at the acetal bond. Indeed, the formation of certain products, such as CH_2O , $\text{C}_2\text{H}_4\text{O}$, C_2H_4 , C_2H_6 , CO_2 , THF, may be accounted for only by reactions involving both acetal and ester bonds of the macromolecule. The thermal PDO degradation may be assumed to develop at high temperatures through macroradicals R_{II} ($\sim\text{CH}_2\text{—O—CH}_2\text{—CH}_2\text{—}\dot{\text{O}}$) and R_{III} ($\dot{\text{C}}\text{H—CH}_2\text{—O}\sim$) that are identical in structure to the active centers of thermal PEO degradation. The primary alkyl macroradical R_1 ($\dot{\text{C}}\text{H}_2\text{—O—CH}_2\text{—CH}_2\sim$) generated by spontaneous rupture of a PDO molecule at the acetal bond and identical to the active center of POM degradation apparently readily converts to R_{III} .

The results obtained seem to warrant the conclusion that the direction and mechanism of polyacetal degradation depend not only on the structure and thermodynamic parameters, but also on the nature of active centers.

References

1. L. A. Haritonova, G. V. Rakova, A. A. Shaginyan, and N. S. Enikolopyan, *Vysokomol. Soedin.*, **A9**, 2586 (1967).
2. A. A. Berlin, M. A. Hakimdyanova, L. V. Karmilova, and N. S. Enikolopyan, *Vysokomol. Soedin.*, **A10**, 1496 (1968).
3. G. Delzenne and G. Smets, *Makromol. Chem.*, **23**, 16 (1957).
4. J. Mejzlik, *Makromol. Chem.*, **59**, 184 (1963).
5. L. A. Dudina and N. S. Enikolopyan, *Vysokomol. Soedin.*, **5**, 986 (1963).
6. S. L. Madorsky and S. Strauss, *J. Polym. Sci.*, **36**, 183 (1960).

7. E. F. Oleinik and N. S. Enikolopyan, *Vysokomol. Soedin.*, **A9**, 2609 (1967).
8. W. Kern and H. Cherdron, *Makromol. Chem.*, **40**, 101 (1960).
9. L. A. Dudina and N. S. Enikolopyan, *Vysokomol. Soedin.*, **4**, 869 (1962).
10. L. A. Dudina, L. V. Karmilova, and N. S. Enikolopyan, *Dokl. Akad. Nauk SSSR*, **150**, 309 (1963).
11. A. F. Bovey and R. C. Wands, *J. Polym. Sci.*, **14**, 113 (1954).
12. M. P. Frank, *Makromol. Chem.*, **63**, 135 (1963).

Received December 18, 1969

Stereospecific Polymerization of Methacrylonitrile. VI. Effect of Esters as a Complexing Agent with Diethylmagnesium Catalyst

YASUSHI JOH, SEIKI KURIHARA, TOSHIO SAKURAI, and
TATSUNORI TOMITA, *Research Laboratories, Mitsubishi Rayon
Co., Ltd., Miyuki-cho, Otake City, Hiroshima, 739-06, Japan*

Synopsis

The stereospecific polymerizations of methacrylonitrile with diethylmagnesium were carefully studied by using various ethers as complexing agents. The complexed ethers exhibit a beneficial effect on the stereoregularity of the resulting polymer, namely, the crystallinity increased by using ethers as a complexing agent. The polymerization rate and the molecular weight of the polymer also increased by using ether-complexed catalysts. The polymerization behavior was studied with the dioxane-diethylmagnesium complex as a typical complexed catalyst. The behavior was mostly similar to that of the diethylmagnesium alone, that is, the rate of the polymerization increased in proportion to monomer concentration, and the solubility index increased with increasing monomer concentration. Interestingly, the viscosity of the acetone-insoluble fraction increased with increasing monomer concentration, while that of the acetone-soluble fraction was independent of monomer concentration. This is explained by considering that the catalyst has at least two kinds of catalytic species, one being the species that produces the crystalline polymer by a coordinated anionic polymerization, another being the one from which an amorphous polymer is obtained by a conventional anionic mechanism. The fact that the viscosity of the polymer decreased with increasing the initiator concentration is explained in terms of chain transfer to the initiator. In case of diethylmagnesium alone, the viscosity of the polymer is independent of the initiator concentration.

INTRODUCTION

In the stereospecific polymerization of methacrylonitrile by organometallic catalysts, Natta et al.^{1,2} reported that the addition of Lewis bases having a higher basicity than that of the nitrogen of methacrylonitrile, e.g., diethyl ether, is enough to hinder stereospecific polymerization. They explained this phenomenon by considering that in order to induce the stereospecific polymerization, it is necessary that the monomer must coordinate itself with the catalyst. Therefore, it had been thought necessary to use solvents which essentially contain no electron-donor atom in the molecule in order to obtain stereoregular polymethacrylonitrile.

However, Joh et al.^{3,4} showed that strong electron-donor solvents such as tetrahydrofuran, dioxane, and anisole did not disturb the stereospecific polymerization of methacrylonitrile and that the polymers obtained in these

solvents have higher stereoregularity and higher molecular weight than those obtained in hydrocarbon solvents.

In the stereospecific polymerization of methacrylonitrile by Et_2Mg we have found that a small amount of ether, about comparable to that of the catalyst, is enough to increase the conversion and the stereoregularity of the resulting polymer.

In the present paper, the effect of ethers as complexing agents with Et_2Mg catalyst is described.

EXPERIMENTAL

Materials

Monomer. Methacrylonitrile (Vistron Corp.) has purified by successive washing with 1% sodium hydroxide aqueous solution followed by water. After being dried over CaCl_2 , it was fractionally distilled immediately before use over CaH_2 under nitrogen. This gave essentially a single peak when analyzed by vapor phase chromatography; bp 90.2°C , n_{D}^{30} 1.3943.

Solvents. Toluene was purified by the usual method, as described in the previous paper.³ Ethers used were distilled over CaH_2 under nitrogen atmosphere, then stored over molecular sieves. Trioxane was recrystallized from an *n*-heptane-ethanol (7:3) mixture and then purified by sublimation. Other solvents such as methanol, acetone, and dimethyl formamide were used without purification.

Diethylmagnesium (Et_2Mg). Diethylmagnesium was prepared according to Schlenk's procedure. Details of the procedure were given in another paper.³

Polymerization

All the operations were carried out under nitrogen atmosphere. A 300-ml three-necked flask equipped with a sealed mechanical stirrer, a reflux condenser, and a pressure-equalized dropping funnel was arranged for carrying out a reaction in an atmosphere of nitrogen by fitting into the top of the condenser a T-tube attached to a low-pressure supply of nitrogen and to a liquid paraffin bubbler.

In the flask was placed 0.004 mole of MgEt_2 and 20 ml of toluene which was freshly distilled. To this suspension, a given amount of ether was added and the mixture was boiled once for a few minutes, then the reaction vessel was placed in a water bath adjusted at 70°C and 180 ml of toluene was introduced. The polymerization was started by introducing 20 ml of purified methacrylonitrile at 70°C . It took about 12 sec to introduce all of the monomer. After adding the monomer, red polymer began to precipitate and a slight rise of temperature in the reaction medium was observed. The rise of temperature after the addition of monomer ranged from 1°C to 10°C , which was slightly higher than for the case of MgEt_2 alone. A white polymer was isolated by pouring the reaction mixture into a large excess of methanol acidified with a small amount of HCl.

Solubility Index

The polymer obtained was extracted with acetone in a Soxhlet extractor for 24 hr. The solubility index for acetone represents the per cent of the insoluble fraction of total polymer. Then, 2 g of the acetone-insoluble fraction was placed in a vessel and to this, 100 ml of dimethyl formamide was introduced. The mixture was allowed to stand at room temperature with occasional shaking for 48 hr. The extremely swollen polymer was isolated by centrifugation and precipitated by the addition of methanol. The per cent of the insoluble fraction is the solubility index for DMF.

Crystallinity Index

The crystallinity index was determined for the acetone-insoluble fractions. The measurement of the crystallinity index was given in another paper in detail^{5,6} in which the close relation between the index and stereoregularity was discussed.

Viscosity Measurement

Intrinsic viscosities were measured in Cl_2CHCOOH at 30°C for the acetone-insoluble fractions and the molecular weights were calculated by Joh's relationship⁴

$$[\eta] = 2.27 \times 10^{-4} M^{0.75}.$$

RESULTS AND DISCUSSION

Effect of the Complexed Ethers on Polymerization

In the previous papers^{3,4} it was reported that ether solvents have a beneficial effect on the stereoregularity of methacrylonitrile polymerization with organomagnesium catalysts. However, the role of the ethers has not been studied in detail. It is very interesting to determine whether small amounts of ethers would have the same effect. Thus, the effect of ethers as complexing agents with diethylmagnesium catalyst was examined.

Table I shows the effect of dioxane as complexing agent on the polymerization of methacrylonitrile by MgEt_2 . The MgEt_2 itself is insoluble in toluene and thus is a heterogeneous catalyst in this polymerization. However, the addition of dioxane brings about a change of the catalyst situation so as to increase the solubility of the catalyst in the solvent. Two-mole equivalents of dioxane are sufficient to dissolve the catalyst in toluene. Table I shows that by using dioxane as a complexing agent, the polymerization activity increased remarkably and the resulting polymers have higher molecular weights than the polymer prepared by MgEt_2 alone. It should be noted that the crystallinity of the resulting polymer increased by using the complexed catalysts.

Table II gives the results of the polymerizations with various MgEt_2 -ether complexes. The change in the solubility of the catalyst by the ad-

TABLE I
 Polymerization of Methacrylonitrile by $MgEt_2$ -Dioxane Complexes^a

Catalyst		Nature of catalyst	Temperature rise after monomer addition, °C	Conversion, %	Solubility index, %		[η], ^b dl/g	Molecular weight ^b	Crystallinity index, ^b %
Et_2Mg , mole	Dioxane, mole				for acetone	for DMF			
0.004	—	heterogeneous	1.5	46.3	73.1	69.5	2.16	1.90×10^5	36.1
0.004	0.002	partly soluble, still heterogeneous	4.0	64.2	70.0	75.5	2.82	2.7×10^5	41.8
0.004	0.004	mostly soluble, still heterogeneous	9.5	66.6	64.8	79.0	3.53	3.6×10^5	44.8
0.004	0.008	homogeneous	10.5	69.6	65.9	69.0	3.49	3.6×10^5	38.9
0.004	0.016	homogeneous	9.0	64.4	66.7	67.5	3.05	3.0×10^5	41.6
0.004	0.040	homogeneous	9.0	72.2	67.1	74.6	3.73	3.9×10^5	37.1

^a Polymerization conditions: toluene, 200 ml; monomer, 20 ml; polymerization temperature, 70°C; polymerization time, 4 hr.

^b Measured for the acetone-insoluble fractions.

TABLE II
 Polymerization of Methacrylonitrile by $MgEt_2$ -Ether Complexes^a

Ethers	Ether/ Et_2Mg mole ratio	Nature of catalyst	Tempera- ture rise after monomer addition, $^{\circ}C$	Conver- sion, %	Solubility index, %		$[\eta]$, dl/g	Molecular weight ^b	Crystal- linity index, %
					for acetone	for DMF			
1,4-Dioxane	0 1/2	heterogeneous partly soluble, still heterogeneous	1.5 4.0	46.3 64.2	73.1 70.0	69.5 75.5	2.16 2.82	1.90×10^5 2.70×10^5	36.1 41.8
1,4-Dioxane	2.0	homogeneous	10.5	69.0	65.9	69.0	3.49	3.60×10^5	38.9
Ethyl ether	1.0	heterogeneous	5.0	64.2	71.4	74.5	2.64	2.48×10^5	44.4
Isopropyl ether	1.0	heterogeneous	3.5	52.5	70.8	75.5	2.37	2.15×10^5	47.8
<i>n</i> -Butyl ether	1.0	heterogeneous	3.5	58.0	87.2	74.5	2.82	2.67×10^5	44.9
THF	1.0	homogeneous	9.0	67.9	66.9	71.3	3.36	3.40×10^5	35.2
Anisole	1.0	heterogeneous	2.0	49.4	72.8	72.5	2.47	2.26×10^5	42.1
Trioxane	1/3	heterogeneous	2.5	43.6	73.8	72.5	2.40	2.15×10^5	45.3
Trioxane	2/3	heterogeneous	2.5	48.1	74.0	72.5	2.39	2.15×10^5	45.4
Trioxane	1.0	heterogeneous	3.0	49.1	75.1	74.0	2.36	2.13×10^5	42.4
Furan	1.0	heterogeneous	1.0	44.8	74.6	70.5	2.24	2.00×10^5	42.7
Dimethoxy methane	1/2	heterogeneous	4.0	57.0	74.4	76.5	3.18	3.15×10^5	43.8
4,4-Dimethyl-1,3- dioxane	1/2	heterogeneous	5.0	59.4	74.8	75.5	3.13	3.09×10^5	42.6
1,3-Dioxane	1.0	homogeneous	8.5	62.5	75.3	78.0	3.11	3.06×10^5	43.0
1,3-Dioxane	2.0	homogeneous	8.0	59.5	72.8	69.5	3.04	2.97×10^5	41.4
1,3-Dioxolane	1.0	partly soluble, still heterogeneous	6.5	63.1	74.2	77.5	3.24	3.23×10^5	40.4
Phenyl ether	1.0	heterogeneous	2.5	46.7	73.0	68.5	2.40	2.18×10^5	47.9
Ethylene glycol dimethyl ether	1/2	homogeneous	9.0	64.0	78.1	75.6	3.45	3.52×10^5	42.3

^a Polymerization conditions: $MgEt_2$, 0.004 mole; toluene, 200 ml; monomer, 20 ml; polymerization temperature, 70 $^{\circ}C$; polymerization time, 4 hr.

^b Measured for the acetone-insoluble fractions.

dition of ethers is given in the table. It is also seen that the conversion together with the molecular weight increases by using the ether-complexed catalysts compared with the MgEt_2 alone. The crystallinity indices obviously increased by using ethers as complexing agent.

Another interesting phenomenon is that the crude reaction product with MgEt_2 was a mixture of a harsh, coarse polymer with a fine, powdery one, while the polymer obtained with the ether-complexed catalyst had little or no coarse materials. Especially the homogeneous catalysts such as the MgEt_2 -tetrahydrofuran (1:1) and MgEt_2 -dioxane (1:2, 1:4, 1:8) complexes produced very fine, powdery products with no coarse material. This would indicate that the polymerization with the ether-complexed catalyst proceeds more smoothly than that with diethylmagnesium alone.

The beneficial effect^{3,4} of the ether solvents upon the stereoregular polymerization of methacrylonitrile is not only due to the solvent effect, but also to the effect of the complexed ethers on the catalyst, since a very small amount of the ethers has a similar effect.

The increase in polymerization rate might be ascribed to the dissolution of the catalyst to increase the number of active sites compared to diethylmagnesium alone. The increase in stereoregularity might be explained in terms of a steric effect of the ethers in coordinating with the diethylmagnesium through their oxygen atoms.

Polymerization Behavior with Et_2Mg -Dioxane Complex

Using the MgEt_2 -dioxane (1:3) complex as a typical ether-complexed catalyst, further studies of the polymerization were made.

Effect of Monomer Concentration

The effect of the monomer concentrations upon the polymerization was investigated and the results are shown in Figures 1 and 2. The rate of the

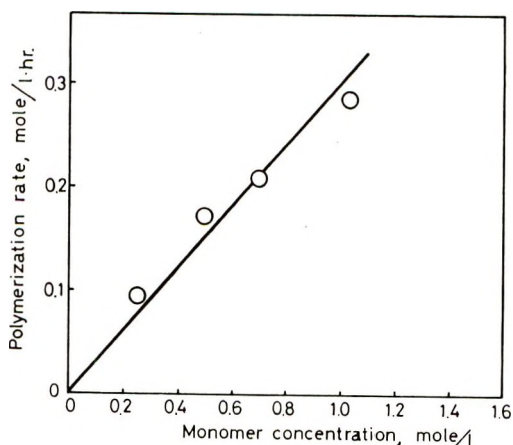


Fig. 1. Effect of monomer concentration on polymerization rate. Polymerization conditions: catalyst 1:3 MgEt_2 -dioxane complex, 0.004 mole; polymerization temperature, 70°C; in toluene.

polymerization increased in proportion to monomer concentration, and the solubility index for acetone also increased with increasing monomer concentration.

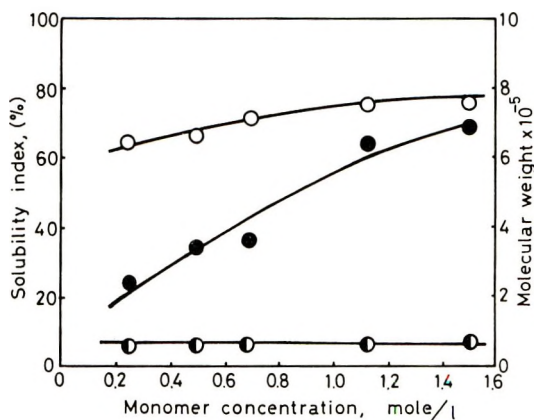


Fig. 2. Effect of monomer concentration on polymerization. Polymerization conditions: 1:3 MgEt_2 -dioxane complex, 0.004 mole; polymerization temperature, 70°C ; polymerization time, 1 hr; in toluene: (○) solubility index for acetone; (●) molecular weight of the acetone-insoluble fraction; (○) molecular weight of the acetone-soluble fraction.

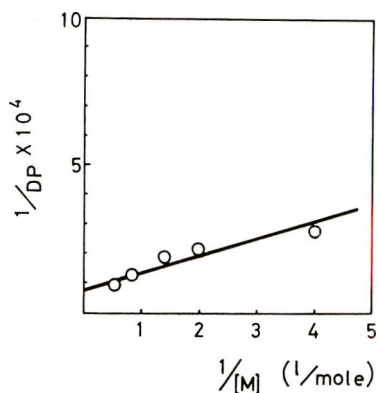


Fig. 3. Relation between $1/\overline{DP}$ and $1/[M]$ for acetone-insoluble fraction. Polymerization conditions are those given in Figure 2.

Interestingly, the viscosities of the acetone-soluble fractions, which gave an amorphous x-ray diagram, are independent of monomer and initiator concentration, while those of the acetone-insoluble fractions, which were crystalline by x-ray examination, increased with increasing monomer concentration. The degree of the polymerization may be expressed in the following equations:

$$\overline{DP} = \frac{k_p[\text{CM}^-][\text{M}]}{k_{\text{trm}}[\text{CM}^-][\text{M}] + k_{\text{trs}}[\text{CM}^-][\text{S}] + k_{\text{tr}}[\text{CM}^-] + k_{\text{tri}}[\text{CM}^-][\text{Init}]} \quad (1)$$

$$\frac{1}{\overline{DP}} = \frac{k_{\text{trm}}}{k_p} + \frac{k_{\text{trs}}}{k_p} \frac{[\text{S}]}{[\text{M}]} + \frac{k_{\text{tr}}}{k_p} \frac{1}{[\text{M}]} + \frac{k_{\text{tri}}}{k_p} \frac{[\text{Init}]}{[\text{M}]} \quad (2)$$

where k_p is a rate constant for propagation; k_{trm} , k_{trs} , and k_{tri} are chain transfer constants to the monomer, solvent, and initiator, respectively; k_{tr} is a rate constant of the monomolecular termination^{7,9}; and $[\text{CM}^-]$, $[\text{M}]$,

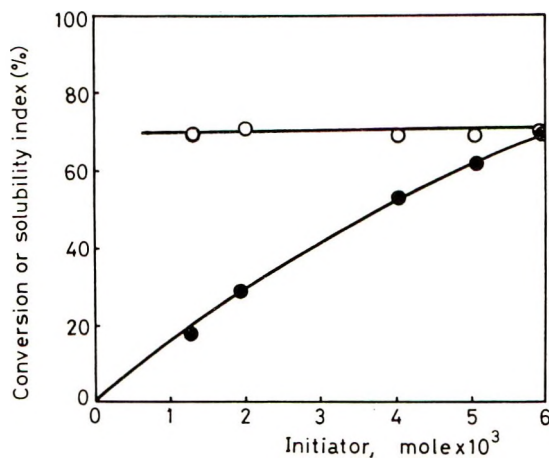


Fig. 4. Effect of 1:3 MgEt_2 -dioxane initiator on polymerization. Polymerization conditions: solvent, toluene 180 ml; monomer, 20 ml; polymerization temperature, 70°C; polymerization time, 4 hr: (●) conversion; (○) solubility index for acetone.

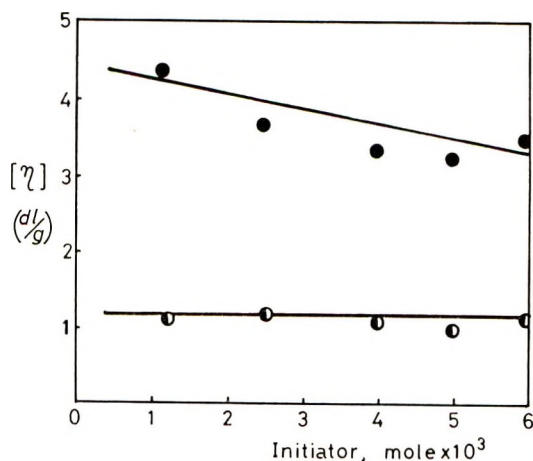


Fig. 5. Effect of 1:3 MgEt_2 -dioxane initiator on polymerization. Polymerization conditions are those given in Figure 4: (●) intrinsic viscosity of acetone-insoluble fraction; (○) intrinsic viscosity of acetone-soluble fraction.

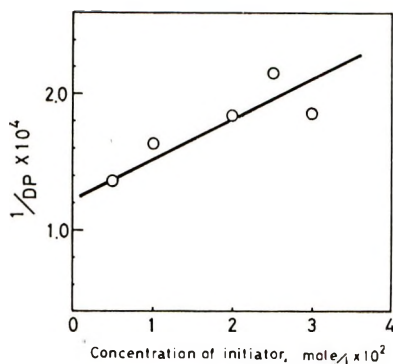


Fig. 6. Relation of $1/\overline{DP}$ versus initiator concentration. Polymerization conditions are those given in Figure 4.

[S], and [Init] are the propagating chain concentration, monomer concentration, solvent concentration, and the concentration of the initiator, respectively.

As speculated in the previous papers,^{3,4} the catalyst may have at least two kinds of species, one being the species that induces the stereospecific polymerization by a coordinated anionic mechanism, and another being the one from which amorphous polymer is formed, probably by a conventional anionic mechanism. In the conventional anionic polymerization, the chain transfer would occur predominantly.⁸ The fact that the molecular weight of the acetone-soluble fractions is independent of the monomer and catalyst concentration indicates that the chain transfer to monomer is so large that the molecular weight of the polymer remains almost constant. On the other hand, the chain transfer to monomer in the coordinated anionic polymerization is rather small; therefore, the molecular weight increases with increasing monomer concentration according to eq. (2). This is substantiated by the fact that the plot of $1/\overline{DP}$ versus $1/[M]$ shows a linear relation, as shown in Figure 3.

Effect of the Catalyst Concentration

Using the $MgEt_2$ -dioxane complex (1:3), the effect of catalyst concentration upon the polymerization was examined. Figure 4 shows that the total conversion increased with increasing catalyst concentration, while the solubility index for acetone was approximately constant. This is explained in terms of an increase in catalytic sites. Figure 5 shows that the viscosity of the acetone-insoluble fraction decreased with increasing initiator concentration. This is explained in terms of the chain transfer to the initiator in the coordinated anionic polymerization, since the relation between $1/\overline{DP}$ and the concentration of the initiator shows a straight line, as shown in Figure 6.

The authors are indebted to Mr. N. Kurashige for his valuable assistance in the course of this work. Grateful acknowledgement is extended to the Mitsubishi Rayon Co., Ltd. for permission to publish this paper.

References

1. G. Natta, G. Mazzanti, and G. Dall'Asta, Italian Pat. 643,282 (1960); G. Natta, G. Dall'Asta, and G. Mazzanti, Italian Pat. 648,564 (1961).
2. G. Natta and G. Dall'Asta, *Chem. Ind. Milan*, **46**, 1429 (1964).
3. Y. Joh, Y. Kotake, T. Yoshihara, F. Ide, and K. Nakatsuka, *J. Polym. Sci. A-1*, **5**, 605 (1967).
4. Y. Joh, T. Yoshihara, Y. Kotake, Y. Imai, and S. Kurihara, *J. Polym. Sci. A-1*, **5**, 2503 (1967).
5. Y. Joh, T. Yoshihara, S. Kurihara, I. Tsukuma, and Y. Imai, *Makromol. Chem.*, **119**, 239 (1968).
6. Y. Joh, S. Kurihara, T. Sakurai, Y. Imai, T. Yoshihara, and T. Tomita, *J. Polym. Sci. A-1*, **8**, 377 (1970).
7. Y. Joh, T. Yoshihara, S. Kurihara, T. Sakurai, and T. Tomita, *J. Polym. Sci.*, in press.
8. A. S. Matlack and D. S. Breslow, *J. Polym. Sci. A*, **3**, 2853 (1965).
9. Y. Joh, Y. Kotake, T. Yoshihara, F. Ide, and K. Nakatsuka, *J. Polym. Sci. A-1*, **5**, 593 (1967).

Received December 24, 1969

Electron Spin Resonance Study on Polymerization of Conjugated Dienes by Homogeneous Catalyst Derived from *n*-Butyl Titanate and Triethylaluminum.

HIDEFUMI HIRAI, KATSUMA HIRAKI, ISAMU NOGUCHI, TAKEO INOUE, and SHOJI MAKISHIMA, *Department of Industrial Chemistry, Faculty of Engineering, University of Tokyo, Bunkyo-ku, Tokyo, Japan*

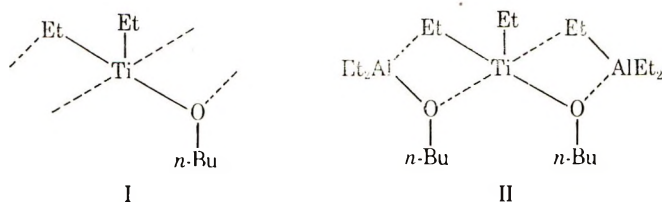
Synopsis

Polymerizations of butadiene, penta-1,3-diene, and isoprene with *n*-butyl titanate-triethylaluminum catalyst are examined by ESR measurements on the polymerization state. At Al/Ti molar ratios greater than 2.9 where the conjugated dienes are polymerized, the polymerization system of butadiene always gives an ESR signal with a *g* value of 1.983 and with a hyperfine structure of about 19 components. This signal does not appear at all, even in the presence of the monomer, at Al/Ti molar ratios smaller than two where butadiene is not polymerized. The absorption intensity of the signal coincides fairly well with the concentration of polymer chain calculated from polymer yield and the molecular weight. On the basis of these facts, the signal is assigned to the growing end of polybutadiene with this catalyst. The structure of the growing end is proposed to have both two substituted π -allyl groups and an alkoxy group in coordination to titanium(III), by analysis of the hyperfine structure. The polymerization system of penta-1,3-diene and that of isoprene respectively, give a new signal with a *g* value of 1.983, although the signal for the former monomer has a hyperfine structure of 11 components and that for the latter monomer has no hyperfine structure. A structure for the growing end in the polymerization of each of these two monomers analogous to that of the growing end of polybutadiene is proposed.

INTRODUCTION

It was reported that conjugated dienes were polymerized by the homogeneous catalyst derived from alkyl titanate and trialkylaluminum at molar ratios of aluminum to titanium (Al/Ti ratio) larger than four.¹⁻³ This catalyst converted butadiene and isoprene into the polymers having high 1,2-unit and the high 3,4-unit contents, respectively, whereas penta-1,3-diene was converted to polymer having predominantly isotactic *cis*-1,4-units.⁴ Natta *et al.*⁵ also succeeded in preparing an optically active poly-penta-1,3-diene by use of *L*-menthyl titanate-triethylaluminum catalyst. Dawes and Winkler⁶ studied the kinetics of polymerization of butadiene with *n*-butyl titanate-triethylaluminum catalyst and proposed a mechanism for the polymerization.

In our previous paper,⁷ the *n*-butyl titanate-triethylaluminum catalyst solution at a room temperature was reported to give two series of electron spin resonance (ESR) signals ascribed to titanium(III) species. One series of seven kinds of signals was detectable at Al/Ti ratios less than two, where no polymerization of the conjugated dienes took place. The other series of four signals with *g* values of 1.934, 1.966, 1.952, and 1.979 was detectable at Al/Ti ratios larger than 2.9, where the conjugated dienes were polymerized. The signals in the latter series were ascribed to the active species for polymerization of the conjugated dienes, and these structures were proposed to have at least two active titanium-ethyl bonds and one alkoxy group as shown by structure I. For example, the structure II was proposed for



the species responsible for the signal with *g* value of 1.952 and with a hyperfine structure of 11 components.⁷

The present study was undertaken in order to elucidate the structure of the growing end of the chains of the conjugated dienes by means of ESR measurements in the polymerization state.

EXPERIMENTAL

Materials

Butadiene (Tokyo Kasei Kogyo Co.) was dried through Molecular Sieve 5A. Penta-1,3-diene and isoprene were refluxed over calcium hydride, distilled under a slight positive nitrogen pressure, and passed through Molecular Sieve 5A immediately before use. Toluene and *n*-butyl titanate were purified according to the methods reported in the previous paper.⁷ Triethylaluminum (a commercial grade, Ethyl Corporation) was used without further purification.

Procedure

The polymerization system was prepared in a 25-ml glass ampoule connected both to an ESR sample tube and a side-arm tube capped with a silicone rubber stopper. A 10-ml portion of toluene solution containing 0.05–1.0 mmole of *n*-butyl titanate was injected with a syringe through the silicone rubber stopper into the ampoule, which had previously been connected to a vacuum line for degassing. A 3-ml portion of monomer was introduced into the ampoule and the resulting mixed solution was degassed twice at -196°C . A toluene solution containing a predetermined amount of triethylaluminum was added to this mixed solution held at -78°C

through the silicone rubber stopper. The catalyst-monomer mixture thus prepared was shaken in a Dry Ice-ethanol bath, and then about 0.7 ml of this mixture was transferred rapidly into an ESR sample tube cooled with Dry Ice-ethanol. The ESR sample tube containing a small part of the mixture and an ampoule containing the remainder of the mixture were sealed off separately. The ampoule was set in a water bath maintained at 25°C for 3 hr.

Both the yield and the intrinsic viscosity of the resulting polymer were determined according to the procedures of Dawes and Winkler.⁶ The viscosity-average molecular weight of the polymer was calculated from the Mark-Houwink relation, $[\eta] = 2.71 \times 10^{-4} [\bar{M}_v]^{0.73}$.

ESR measurements for the sample prepared as stated above were carried out in the X-band with 100-kcps modulation on a Japan Electron Optics Laboratory Model JES-3BS spectrometer equipped with a variable-temperature attachment and an integrator for intensity measurements. Both the differential and integrated curve of the spectrum were recorded simultaneously, at various temperatures from -78°C to +25°C. The absorption intensity of an ESR signal, i.e., the concentration of a titanium(III) species in moles/liter, was evaluated by comparison of the area of the integrated curve of the signal with the corresponding value for the toluene solution of a known concentration of tris(acetylacetonato)titanium(III) as a reference. The hyperfine structure of the signal was simulated by use of a Japan Electron Optics Laboratory JR-5 spectrum computer.

Gas-Chromatographic Analysis of the Liquid Phase of the Butadiene Polymerization System

Ethanol in sufficient amount to deactivate the catalyst was added to the liquid phase of the polymerization system after reaction for 40 min. This sample was analyzed on a gas chromatograph with a 7-m oxydipropionitrile column at 40°C. Each fraction corresponding to a new peak was trapped and analyzed by mass spectroscopy. The fraction was assigned by comparison of the retention time and of the mass spectrograph with the corresponding data for the authentic compound. The amount of each fraction was measured by use of cyclohexane as an internal reference.

RESULTS AND DISCUSSION

Polymerization of Butadiene

The ESR spectra of the homogeneous catalyst derived from *n*-butyl titanate and triethylaluminum at Al/Ti ratios ranging from one to ten had been previously examined at several temperatures from -78°C to +25°C.⁷ The catalyst solution held at a temperature below -70°C yielded a single signal with a *g* value of 1.951 at all Al/Ti ratios.⁷ So long as the polymerization system consisting of the catalyst solution and butadiene was held at temperatures lower than -70°C, the polymerization system yielded

the same signal as the catalyst solution did at -78°C . This indicates that the same kind of first reaction intermediate was produced in both the polymerization system and the catalyst solution.

Above 0°C , three kinds of signals with the g values of 1.934, 1.966, and 1.952, respectively, appeared in the catalyst solution at an Al/Ti ratio of

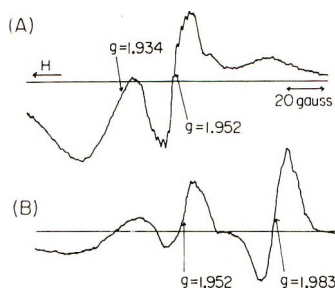


Fig. 1. ESR spectra of *n*-butyl titanate-triethylaluminum catalyst, before and after addition of butadiene: (A) before addition of butadiene, 15 hr after the preparation. (B) 30 min after the addition of butadiene. Conditions: Al/Ti ratio, 6.0; initial *n*-butyl titanate concentration, 0.020 mole/l.; temperature, 24°C ; modulation width, 4 gauss.

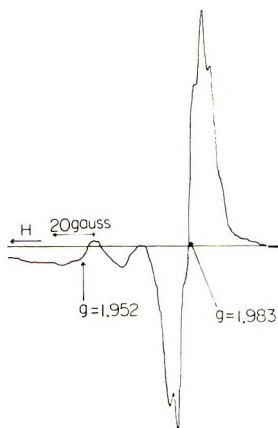


Fig. 2. ESR spectrum of polymerization system of butadiene with *n*-butyl titanate-triethylaluminum catalyst. Conditions: Al/Ti ratio, 6.0; initial *n*-butyl titanate concentration, 0.025 mole/l.; temperature, 21.5°C ; 70 min after the mixing of the catalyst components and butadiene at -78°C ; modulation width, 4 gauss.

six, while the signal with the g value of 1.951 decreased rapidly⁷ (see Fig. 1A). On addition of a toluene solution of butadiene to the catalyst solution, a new signal with a g value of 1.983 appeared immediately (see Fig. 1B). On the other hand, the polymerization system prepared in the presence of butadiene at the same Al/Ti ratio, yielded a strong signal with a g value of 1.983 and very weak signals with the g values of 1.934 and 1.952 at a room temperature (see Fig. 2). At Al/Ti ratios less than two where this

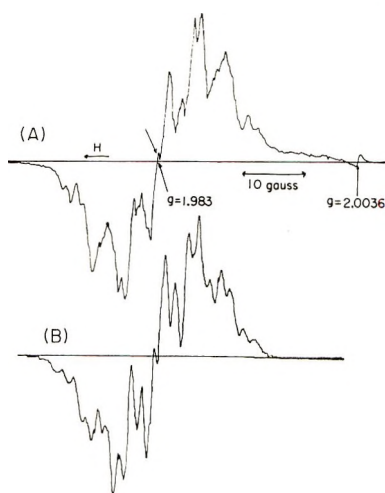


Fig. 3. Hyperfine structure of the ESR signal for the polymerization of butadiene: (A) observed signal and (B) simulation curve. Conditions: Al/Ti ratio, 6.0; temperature 21.5°C; initial *n*-butyl titanate concentration, 0.025 mole/l.; modulation width, 0.25 gauss. Simulation curve $A_3B_3X_2$ type; coupling constants, $a_A = 5.0$ gauss, $a_B = 3.8$ gauss, and $a_x = 1.8$ gauss; half-width, 2.7 gauss.

catalyst did not polymerize butadiene at all, the signal with the g value of 1.983 was never detectable, even in the presence of butadiene (see Table I).

Table I shows the absorption intensity of the signal, together with the concentration of the polymer chain in the polymerization system. The concentration of the polymer chain could be calculated from the ratio of the weight of the polymer in the polymerization system to the molecular weight of polymer determined by viscosity measurement, because it had been confirmed for this polymerization system that the viscosity-average molecular weight was approximately equal to the number-average molecular weight at low conversions.⁶ The absorption intensity of the signal coincides fairly well with the concentration of the polymer chain. These data indicate that the signal with the g value of 1.983 corresponds to a growing end of polybutadiene formed by this catalyst.

The signal with the g value of 1.983 appeared not only for butadiene, but also for penta-1,3-diene and isoprene as shown later; this signal can be reasonably ascribed to a titanium(III) species according to the previous discussion.⁷ The signal for butadiene had a hyperfine structure which consisted of seven well resolved components together with about 12 more finely split ones, while the latter components were observed only by measurements under optimal conditions with the modulation width of 0.25–1.0 gauss (see Fig. 3A). This hyperfine structure can be attributed to A_6X_2 , $A_1B_2X_2$, or $A_3B_3X_2$, and the selection of these types was carried out by means of spectrum simulation. In consideration of the presence of one small splitting line at the center of the signal (arrow in Fig. 3A), the hyperfine structure type responsible for this signal was eventually determined to be an $A_3B_3X_2$

type, which had three kinds of coupling constants of 5.0, 3.8, and 1.8 gauss, corresponding to A, B, and X groups, respectively, and had a half-width of 2.7 gauss (Fig. 3B). The hyperfine structure depended on monomer used, as described later. These facts indicate that the hyperfine structure must be formed by an interaction of the unpaired spin neither with an ^{27}Al nucleus (spin = 5/2, natural abundance = 100%), nor with a ^{47}Ti nucleus (spin = 5/2, natural abundance = 7.32%), nor with a ^{49}Ti nucleus (spin = 7/2, natural abundance = 5.46%), but with the protons of ligands coordinated to the titanium(III). Another example of a hyperfine structure due to an interaction between a transition metal and protons of the ligands was reported⁸ on bis(benzene)chromium(I) cation, $[\text{Cr}(\text{C}_6\text{H}_6)_2]^+$.

TABLE I
Concentration of Growing End in Polymerization of Butadiene^a

Al/Ti ratio	Titanate concn $\times 10^2$, mole/l.	Yield of polymer, %	$\bar{M}_v \times 10^{-5}$ ^b	Polymer concn $\times 10^5$, mole/l. ^c	Ti(III) concn $\times 10^5$, mole/l. ^d
1.9	2.7	0		0	0
2.9	2.7	1.8			0.92
3.4	2.7	5.2	2.8	2.6	3.8
3.9	2.7	20.3	6.5	4.5	4.5
4.8	2.7	22	4.6	6.9	9.2
6.0	0.5	20.7	2.8	4.0	
6.0	1.3				4.0

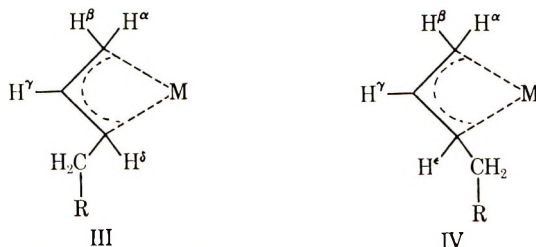
^a Conditions; butadiene, 2.7 mole/l.; temperature, 25.0°C; reaction time, 3.0 hr.

^b Calculated from the viscosity by using $[\eta] = 2.71 \times 10^{-4} \bar{M}_v^{0.73}$.

^c Calculated from the polymer yield and \bar{M}_v .

^d Calculated from the absorption intensity of the signal with the g value of 1.983, by use of a toluene solution of tris(acetylacetonato)titanium(III) of 1.02×10^{-3} mole/l. as a reference standard.

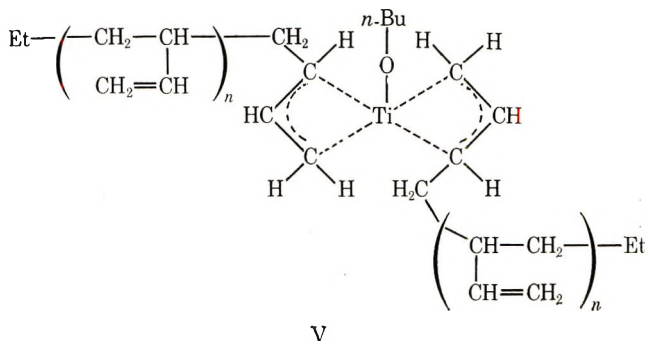
By analysis of the hyperfine structure, the growing end in this polymerization was assigned to the titanium(III) species coordinated with two 1-substituted π -allyl groups. The coupling constants of 5.0, 3.8, and 1.8 gauss can be associated with *anti* protons α and δ , *syn* protons β and ϵ , and a middle proton γ , respectively (III and IV). The numerical values of the



coupling constants of protons α , β , and γ corresponded well to the order of τ values of respective protons in the NMR spectrum of a π -allylic com-

plex.^{9,10} The coupling constants of the protons δ and ϵ were considered to be approximately equal to those of the protons α and β , respectively, while the τ value of the proton δ or ϵ in a 1-methyl- π -allyl complex was a little different from that of the proton α or β , respectively.^{9,11} The $A_3B_3X_2$ type for the hyperfine structure excluded both the possibilities that the growing end had two *syn*-1-substituted or two *anti*-1-substituted π -allyl groups, and that these two kinds of growing ends coexisted, because these kinds of the growing ends could not yield the small splitting line at the center of the signal (see Fig. 3B). Accordingly, the growing end had both a *syn*-1-substituted and an *anti*-1-substituted π -allyl group. However, the possibility that a type with two *syn* forms may exist, in addition to this type of growing end can not be excluded in consideration of the accuracy of the signal intensity in the ESR spectrum.

In addition, an alkoxy group must be coordinated to the titanium(III) in the growing end, because the titanium(III) in the growing end should combine with one more negative ligand. This is supported by the evidence that in the preparation of the optically active polybutadiene with *L*-menthyl titanate-triethylaluminum catalyst, at least one *L*-menthoxy group should act on stereoregulation.⁵ On the basis of these discussions, the growing end of polybutadiene with the *n*-butyl titanate-triethylaluminum catalyst was assigned to the structure V. This structure is formally



analogous to iododi- π -allylcobalt(III) and di- μ -iodotetra- π -allyldichromium(III), which yield *cis*-1,4-polybutadiene and cyclododeca-1,5,9-trienes, respectively, from butadiene.¹²

The growing end V is reasonably formed by a successive insertion reaction of butadiene monomers into the titanium-ethyl bonds in the active intermediate, which may be produced transiently in the polymerization systems at Al/Ti ratios larger than 2.9. Analogously, V also can be derived from I or II via the same active intermediate which may be formed with the liberation of the organoaluminum component by reaction between butadiene and I or II. These propositions are also supported by the fact that polyisoprene obtained with *n*-propyl titanate-¹⁴C-labeled triethylaluminum catalyst contained radioactive carbon.³ The structures of I, II, and V are associated with the high activity of the catalyst at Al/Ti ratios larger than

2.9, where the titanium(III) might be alkylated at least by two sites with triethylaluminum,⁷ and with the absence of the activity at Al/Ti ratios less than two, where the titanium(III) was alkylated at most only by one site.¹³

The concentration of the active species decreased to about 0.03 of the initial concentration of *n*-butyl titanate, as seen in Table I and reference 6. Dawes and Winkler⁶ interpreted this small concentration of the active species by use of an equilibrium between the active species and various reaction products. In the polymerization system prepared in the presence of butadiene, however, this kind of equilibrium can not be dominant and the absolute number of active species was actually small, since titanium(III) species other than the growing end were hardly detectable in the spectrum of the polymerization system (see Fig. 2). This interpretation is also supported both by the sharp distribution of the molecular weight of the resulting polymer⁶ and by the very small concentration of the polymer chain relative to the amount of the initial titanate (see Table I).

Polymerization of Penta-1,3-diene

The polymerization system derived from the *n*-butyl titanate-triethylaluminum catalyst and penta-1,3-diene gave also a new kind of ESR signal with a *g* value of 1.983 and with a hyperfine structure of 11 components (shown by arrows in Fig. 4A). This signal was slightly asymmetric owing to an overlap with the signal with a *g* value of 1.966 in the higher field. The hyperfine structure of the signal was simulated with the spectrum computer and determined to be of type A_4X_2 , with two coupling constants of 5.5 and 2.7 gauss and with a half-width of 5.3 gauss. The coupling constant of 5.5 gauss is nearly equal to that of the protons α and δ in structure V, and is attributable to four *anti* protons in two 1,3-disubstituted π -allyl groups. The constant of 2.7 gauss can be associated with two protons on carbon 2 in the

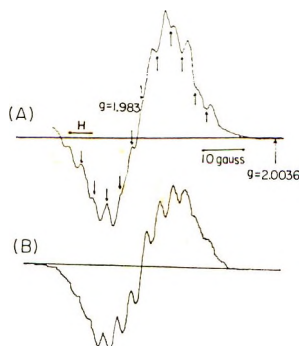
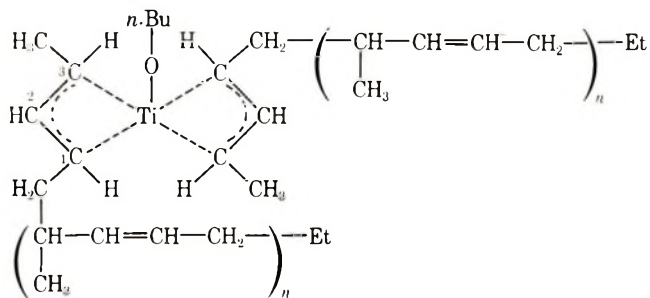


Fig. 4. Hyperfine structure of the ESR signal for the polymerization of penta-1,3-diene: (A) observed signal and (B) simulation curve. Conditions: Al/Ti ratio, 6.0; temperature, 22°C; initial *n*-butyl titanate concentration, 0.025 mole/l.; modulation width, 0.50 gauss. Simulation curve for A_4X_2 type; coupling constants, $a_A = 5.5$ gauss and $a_X = 2.7$ gauss; half-width, 5.3 gauss.

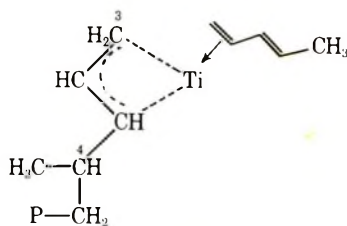
two 1,3-disubstituted π -allyl groups. This signal was considered to result surely from the growing end of poly(penta-1,3-diene), because both the g value and the hyperfine structure of the signal were not only similar to those for the case of butadiene, respectively, but also were characteristic of the polymerization of penta-1,3-diene.

On the basis of analysis of the hyperfine structure for penta-1,3-diene and in view of the discussions in the previous section, the structure VI was proposed for the growing end of poly(penta-1,3-diene). In this structure, a methyl group in the growing end is situated on carbon 3, which is bonded directly to the titanium(III). For a model of the growing end of poly-



VI

penta-1,3-diene, Natta et al.^{3,4} proposed the structure VII, in which the methyl group is bonded to carbon 4. A 1,3-disubstituted π -allyl group in



VII

VI has greater symmetry than a 1-monosubstituted allyl group in VII. If the species corresponding to VII were produced in this polymerization system, it would show the same hyperfine structure as V, since the allylic skeleton in VII was identical with that for V. The hyperfine structure actually observed for penta-1,3-diene, however, was different from that observed for butadiene. Treatment of dichlorodicyclopentadienyltitanium(IV) with penta-1,3-diene and isopropylmagnesium bromide gave *syn* 1,3-dimethyl- π -allyldicyclopentadienyltitanium(III),¹⁴⁻¹⁶ in which the structure of the allylic group was very similar to that of the 1,3-disubstituted π -allyl group in VI.

In the polymerization of penta-1,3-diene with *L*-methyl titanate-triethylaluminum catalyst, the growing end must hold one *L*-menthoxy group in place of the *n*-butoxy group in VI. This growing end explains better

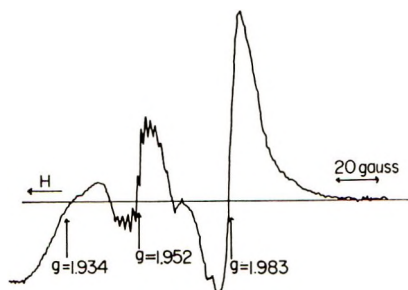


Fig. 5. ESR spectrum of the polymerization system of isoprene with *n*-butyl titanate-triethylaluminum catalyst. Conditions: Al/Ti ratio, 6.0; initial *n*-butyl titanate concentration, 0.025 mole/l.; temperature, 22°C; modulation width, 2 gauss.

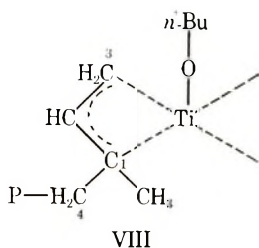
the asymmetric induction polymerization of this monomer⁵ than the model of VII, since the carbon atom to become asymmetric in the polymer chain must be situated nearer to the titanium atom bonded to an optically active *L*-menthoxy group in the former growing end than in the latter model. This explanation is supported by the success of the optical resolution of the chloro(1-acetyl-2-methylallyl)(*S*- α -phenethylamine)palladium complex.¹⁷

Structures V and VI for the growing ends of polybutadiene and of poly-penta-1,3-diene, are similar, as discussed above, in spite of the difference of the substituent. The microstructures of the respective polymers, however, were quite different.³ This suggests that the microstructure of poly-penta-1,3-diene was influenced markedly by the methyl groups in the growing end and probably also by that in the monomer.

Polymerization of Isoprene

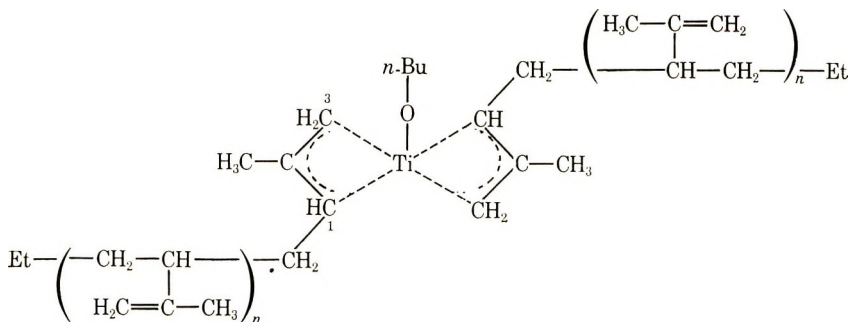
The polymerization system for isoprene and catalyst yielded two signals with *g* values of 1.934 and 1.952, which were the same as observed in the catalyst solution, and in addition a new signal with a *g* value of 1.983 and with an apparent maximum slope width of about 13 gauss (see Fig. 5). This signal can be associated with the growing end of polyisoprene analogously to the cases of butadiene and penta-1,3-diene, because the signal was characteristic of the polymerization of isoprene, but also had almost same *g* value as those in the polymerizations of butadiene and penta-1,3-diene. This was supported by the fact that the kinetic behavior of polymerization of isoprene was very similar to that for butadiene.^{3,6}

The signal with a *g* value of 1.983 for isoprene had no clear hyperfine structure, in contrast with those observed for butadiene and penta-1,3-diene, but had a slightly asymmetric form with a small trough. Accordingly, it is difficult to assign the signal directly to a structure of the growing end of polyisoprene. The structure was assumed to be analogous to structure V, since the microstructure of the resulting polymer was quite analogous to that of the polybutadiene obtained by this catalyst, in spite of difference of the side group in the polymer chain. The structure VIII may be excluded from the growing end of polyisoprene, since the structure



may be unfavorable owing to steric hindrance between the 1-methyl group and 4-methylene one, and since the polyisoprene prepared with this catalyst contained no 1,2-unit,³ which might result from the growing end of structure VIII.

These considerations lead to the proposition that the growing end of polyisoprene with this catalyst has the structure IX. This structure is also analogous to that of 1,2-dimethyl- π -allyldicyclopentadienyltitanium-

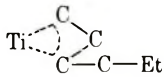
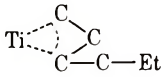
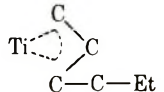


(III), which was prepared by reaction of isoprene, dichlorodicyclopentadienyltitanium(IV), and isopropylmagnesium bromide.¹⁶ Although IX was expected to give a signal with a hyperfine structure of seven components owing to six protons of two 1-substituted methallyl groups, the signal observed actually showed no hyperfine structure. The absence of the hyperfine structure is believed to be due to either the superposition of two signals responsible for two forms of 1-substituted methallyl groups, i.e., a *syn* form and an *anti* form, or the broadening of the signal owing to a rapid exchange between these two forms.

Analysis of Liquid Phase of the Polymerization System

Gas chromatographic analysis of the liquid phase of the polymerization system of butadiene exhibited three peaks, which were assigned to 3-methylpent-1-ene, a mixture of hex-1-ene and *cis*-hex-2-ene, and *trans*-hex-2-ene, respectively. The amount of these components and these assumed sources are listed in Table II. Table II indicates that the total number of moles of butadiene combined with the ethyl group is about 1.4 times that of the initial *n*-butyl titanate.

TABLE II
Analysis of Liquid Phase of Polymerization System^a

GLC peak ^b	Component	Amount of component ^c	Assumed source of the component
1	3-Methylpent-1-ene	0.60	$\begin{array}{c} \text{Ti}-\text{C}-\text{C}-\text{C}=\text{C} \\ \\ \text{Et} \end{array}$
2	Hex-1-ene } <i>cis</i> -Hex-2-ene }	0.56	$\begin{array}{c} \text{Ti}-\text{C}-\text{C}=\text{C} \\ \\ \text{C}-\text{Et} \end{array}$ 
			$\begin{array}{c} \text{Ti}-\text{C}-\text{C} \\ \\ \text{Et}-\text{C}-\text{C}, \end{array}$ 
3	<i>trans</i> -Hex-2-ene	0.23	$\begin{array}{c} \text{Ti}-\text{C}-\text{C}=\text{C} \\ \\ \text{C}-\text{Et}, \end{array}$ 

^a Conditions: Al/Ti ratio, 6; reaction time, 40 minutes; at 25.0°C.

^b With a 7-m oxydipropionitrile column, 40°C.

^c Molar ratio to *n*-butyl titanate.

The amount of these C₆ olefins was almost 200–500 times that of the titanium(III) species detected by the ESR measurements, and also as that of the polymer chain, as seen in Tables I and II. Accordingly, these olefins may be derived from the titanium species which neither showed ESR signal nor yielded polymer. These species may be stabilized by an insertion of only one mole of butadiene into a titanium–ethyl bond¹⁶ which had initially been formed by the reaction between *n*-butyl titanate and triethylaluminum. It can be concluded from these considerations that a large portion of the initial titanate was converted by reaction with triethylaluminum into a titanium species with a more covalent bonding or with a more reduced oxidation state of the titanium than those in structures I, II, and V, and with no activity for polymerization of butadiene. On the other hand, only a very small portion of the initial titanate was converted into active species I or II in the absence of butadiene or into the growing end of polybutadiene, V, in the presence of the monomer.

The authors wish to thank Mrs. Yaeko Goto for her cooperation in the ESR simulation.

References

1. G. Wilke, *Angew. Chem.*, **68**, 306 (1956).
2. G. Natta, *J. Polym. Sci.*, **48**, 219 (1960).
3. G. Natta, L. Porri, and A. Carbonaro, *Makromol. Chem.*, **77**, 216 (1964).
4. G. Natta and L. Porri, paper presented at Chicago Meeting, Division of Polymer Chemistry, American Chemical Society, September 1964; *Polymer. Preprints*, **5**, No. 2, 1163 (1964).

5. G. Natta, L. Porri, and S. Valenti, *Makromol. Chem.*, **67**, 225 (1963).
6. D. H. Dawes and C. A. Winkler, *J. Polym. Sci. A*, **2**, 3029 (1964).
7. H. Hirai, K. Hiraki, I. Noguchi, and S. Makishima, *J. Polym. Sci. A-1*, **8**, 147 (1970).
8. R. D. Feltham, P. Sogo, and M. Calvin, *J. Chem. Phys.*, **26**, 1354 (1957).
9. W. R. McClellan, H. H. Hoehn, H. N. Cripps, E. L. Muettterties, and B. W. Hawk, *J. Amer. Chem. Soc.*, **83**, 1601 (1961).
10. J. Powell and B. L. Shaw, *J. Chem. Soc. A*, **1968**, 597.
11. B. L. Shaw and E. Singleton, *J. Chem. Soc. A*, **1967**, 1972.
12. G. Wilke, B. Bogdanovic, P. Hardt, P. Heimbach, W. Keim, M. Kröner, W. Oberkirch, K. Tanaka, E. Steinrücke, D. Walter, and H. Zimmermann, *Angew. Chem.*, **78**, 157 (1966).
13. T. S. Djabiev, R. D. Sabirova, and A. E. Shilov, *Kinetika Kataliz*, **5**, 441 (1964).
14. H. A. Martin and F. Jellinek, *J. Organometal. Chem.*, **6**, 293 (1966).
15. H. A. Martin and F. Jellinek, *J. Organometal. Chem.*, **8**, 115 (1967).
16. H. A. Martin and F. Jellinek, *J. Organometal. Chem.*, **12**, 149 (1968).
17. P. Corradini, G. Maglio, A. Musco, and G. Paiaro, *Chem. Commun.*, **1966**, 618.

Received September 16, 1969

Revised December 31, 1969

Polymerization of Coordinated Monomers. V. Polymerization of Methyl Methacrylate-Lewis Acid Complexes

HIDEFUMI HIRAI and TADASHI IKEGAMI, *Department of Industrial Chemistry, Faculty of Engineering, University of Tokyo, Hongo, Bunkyo-ku, Tokyo, Japan*

Synopsis

The polymerization of the complex of methyl methacrylate with stannic chloride, aluminum trichloride, or boron trifluoride was carried out in toluene solution at several temperatures in the range of 60° to -78°C by initiation of α, α' -azobisisobutyronitrile or by irradiation with ultraviolet rays. The tacticities of the resulting polymers were determined by NMR spectroscopy. Both the 1:1 and the 2:1 methyl methacrylate-SnCl₄ complexes gave polymers with similar tacticities at the polymerization temperatures above -60°C. With decreasing temperature below -60°C, the isotacticity was more favored for the 2:1 complex, whereas the tacticities did not change for the 1:1 complex. On the ESR spectroscopy of the polymerization solution under the irradiation of ultraviolet rays at -120°C, the 1:1 SnCl₄ complex gave a quintet, while the 2:1 SnCl₄ complex gave both a quintet and a sextet. The sextet became weaker with increasing temperature and disappeared at -60°C. This behavior of the sextet corresponds to the change of the tacticities of polymer for the 2:1 SnCl₄ complex. An intra-intercomplex addition was suggested for the polymerization of the 2:1 complex, which took a *cis*-configuration on the basis of its infrared spectra. The sextet can be ascribed to the radical formed by the intracomplex addition reaction, while the quintet can correspond to that formed by the intercomplex addition reaction. The proportion of the intracomplex reaction was estimated to be about 0.25 at -75°C, and the calculated value of the probability of isotactic diad addition of the intracomplex reaction was found to be almost unity.

INTRODUCTION

It was reported that the complexes of methyl methacrylate (MMA) with zinc chloride and with stannic chloride mainly in bulk polymerization gave polymers whose tacticities took characteristic values depending upon the complex species, i.e., the kind of metal chloride and the stoichiometry.¹ The effects of complex formation on the tacticity were suggested to be mainly two types, i.e., a preorientation of monomers and an intra-intercomplex reaction. In our previous paper,² the proportion of the intracomplex reaction could be estimated by ESR spectroscopy for the polymerization of methacrylonitrile (MAN) complex. The probability of isotactic diad addition of the intracomplex reaction was found to be larger than that of the intercomplex one.

Solution polymerization is preferable for examination of the effects of complex formation on tacticity, since the probability of an intracomplex reaction can increase with decreasing concentration of the complex. The 2:1 MMA-SnCl₄ complex, however, is not too stable so that a stronger dilution and a higher temperature are not preferred for this complex. In the previous study¹ the polymerizations were carried out mainly by using complexes alone without solvent.

In the present study, the complexes of methyl methacrylate with stannic chloride, aluminum trichloride, or boron trifluoride in toluene solution were polymerized at temperatures from -78° to 60°C by irradiation with a high-pressure mercury lamp or by initiation of α, α' -azobisisobutyronitrile. The proportion of the intracomplex reaction was estimated by ESR spectroscopy and the probability of isotactic diad addition was calculated on the basis of the tacticity of the polymer and the proportion of the intracomplex reaction.

EXPERIMENTAL

Materials

Methyl methacrylate and solvents were purified by the accepted procedures. Stannic chloride and aluminum trichloride were purified by distillation in the presence of phosphorous pentoxide and sublimation, respectively. Boron trifluoride was prepared according to the literature.³

Polymerization

Both methyl methacrylate and Lewis acid were mixed in toluene in a quartz ampoule in nitrogen atmosphere. The ampoule was degassed to remove oxygen and sealed in the atmosphere of nitrogen. The ampoule was maintained at several constant temperatures by an electric heater (30° to 60°C), by ice-water mixture (0°C), by the flow of cooled nitrogen gas (-20° to -50°C), by Dry Ice-chloroform coolant (-60°C), or by Dry Ice-methanol coolant (-78°C). Polymerization was effected by irradiation with ultraviolet rays from an Ushio Denki high-pressure mercury lamp Model HB500/B or by using α, α' -azobisisobutyronitrile. The Lewis acid included in the polymer was removed by repeating the dissolution with chloroform and the precipitation with methanol containing hydrochloric acid. The resulting poly(methyl methacrylate) was dried at 60°C *in vacuo*.

Spectral Measurement

Infrared spectra of the complex in solution of toluene were measured on a Beckman Model IR-2 spectrometer. NMR spectra of the polymer were run at 60°C on a Japan Electron Optics Laboratory Model C-60 high-resolution spectrometer at 60 Mc in chloroform solution. The tacticities of polymer were determined according to the method of Bovey and Tiers.⁴

ESR spectra of the polymerization systems were recorded on a Japan Electron Optics Laboratory Model JES-3BSX spectrometer at -120° to -60°C under or after irradiation with ultraviolet rays.

RESULTS AND DISCUSSION

Infrared Spectra of Complexes

Figure 1 shows the infrared spectra of the complexes of methyl methacrylate with stannic chloride in toluene solution. The 2:1 MMA-SnCl₄ complex at concentration of 50 mole-% in toluene gave three absorption bands at 395, 345, and 317 cm⁻¹, while the 1:1 MMA-SnCl₄ complex showed two bands at 398 and 355 cm⁻¹. Dilution with toluene reduced the intensity of the band at 317 cm⁻¹ of the 2:1 complex. The absorption bands of methyl methacrylate and stannic chloride appeared at 360 and 402 cm⁻¹, respectively.

A methyl methacrylate molecule forms complexes with Lewis acids through the coordination of a lone electron pair of a carbonyl group, as previously discussed on infrared and NMR spectra.^{1,5} The structures of the complexes of stannic chloride with esters, nitriles, and ketones, etc., can be determined on the basis of the absorption bands of Sn-Cl in the range of 200 to 500 cm⁻¹, since a *cis*-configuration has three stretching bands and the *trans*-counterpart has only one band, theoretically.^{6,7} The

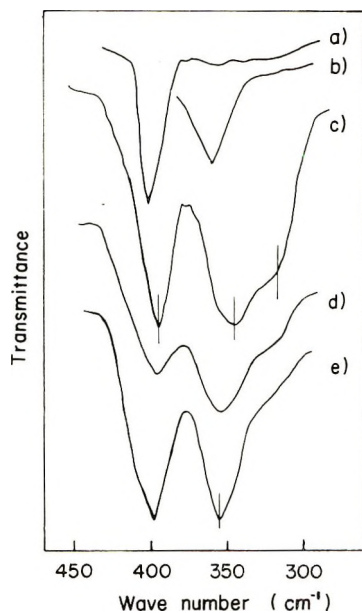


Fig. 1. Infrared spectra of the MMA-SnCl₄ complexes: (a) SnCl₄ in toluene; (b) pure MMA; (c) 2:1 MMA-SnCl₄ complex, 50-mole-% in toluene; (d) 2:1 MMA-SnCl₄, 33 mole-% in toluene; (e) 1:1 MMA-SnCl₄ complex in toluene.

presence of three absorption bands as stated above indicates that the configuration of the 2:1 complex is *cis*. This assumption is supported also by the fact that the acetone forms a complex of *cis*-configuration with stannic chloride.⁸ An isomerization would occur to a certain extent between the *cis*- and *trans*-configurations,⁹ so that the existence of the *trans*-isomer in the solution cannot be excluded.

Result of Polymerization

Tables I and II show the results for polymerization of the complexes with Lewis acids. The values of the conversion contained small deviations arising from unavoidable variations in the absorption conditions of the irradiated specimen with ultraviolet rays. A comparison of the conversion among the species of the complexes is impossible because of differences of the polymerization conditions, but it can be safely said that the boron trifluoride complex gave a higher conversion than the aluminum trichloride complex did. The viscosity-average degree of polymerization was found to be in the range of 1000 to 2000.

TABLE I
Polymerization of Methyl Methacrylate Stannic Chloride Complexes

Initiator ^a	Concn, ^b mole-%	Temp, °C	Time, hr	Conver- sion, %	Tacticity			<i>P</i> (I) ^c	ρ^d
					I%	H%	S%		
1:1 MMA-SnCl ₄ Complex									
γ -Ray	50	-78	14	4.0	10	21	69	0.20	1.52
UV	50	-75	10	3.0	10	18	72	0.19	1.70
UV	50	-50	4.3	13.9	8	25	67	0.21	1.33
UV	50	-40	2.5	1.4	12	22	66	0.23	1.61
2:1 MMA-SnCl ₄ Complex									
γ -Ray	50	-78	14	53.4	18	44	38	0.40	1.09
UV	50	-75	5	3.6	12	40	48	0.32	1.09
UV	50	-63	2	3.4	8	29	63	0.23	1.22
UV	50	-50	4.3	13.9	7	27	64	0.21	1.22
UV	50	-40	1	3.5	8	24	68	0.20	1.33
UV	70	-75	6	2.7	12	36	52	0.30	1.17
UV	33	-75	7	1.0	11	21	68	0.22	1.64
UV	25	-75	8	4.0	9	18	73	0.18	1.64

^a γ -Ray, dose rate 2.7×10^5 r/hr; UV, irradiation with high-pressure mercury lamp.

^b Concentration of complex in toluene solution.

^c Probability of isotactic diad addition.

^d Persistence ratio.

Tacticity of Polymer

The tacticities of poly(methyl methacrylate) obtained from the methyl methacrylate complexes are shown in Tables I and II. The isotacticity of the polymer for the stannic chloride complexes is larger than that for pure

TABLE II
 Polymerization of Methyl Methacrylate-Aluminum Trichloride and
 Methyl Methacrylate-Boron Trifluoride Complexes

Initiator ^a	Temp, °C	Time, hr	Conversion, %	Tacticity			<i>P</i> (I) ^b	ρ^c
				I%	H%	S%		
MMA-AlCl ₃ Complex ^d								
AIBN and UV	0	7	7.5	8	30	62	0.23	1.17
AIBN	60	5	5.0	9	38	53	0.28	1.06
MMA-BF ₃ Complex ^d								
UV	0	7	2.0	3	24	74	0.15	1.06
AIBN	30	8	7.0	4	30	66	0.19	1.03
AIBN	60	5	21.8	5	36	59	0.23	0.98

^a AIBN, 0.42 mole-% to the complex; UV, irradiation with high-pressure mercury lamp.

^b Probability of isotactic diad addition.

^c Persistence ratio.

^d Complex concentration 25 mole-% in toluene.

methyl methacrylate (I% = 0.4, H% = 14, and S% = 86 at -46°C; I% = 2, H% = 23, and S% = 75 at -20°C; and I% = 5, H% = 37, and S% = 58 at 60°C^{1,10}).

The aluminum trichloride complex gave almost the same tacticities as those obtained from pure monomer in the temperature range from 0° to 60°C. On the other hand, the tacticities of polymers obtained from the boron trifluoride complex were not significantly different from those of polymers of pure monomer.

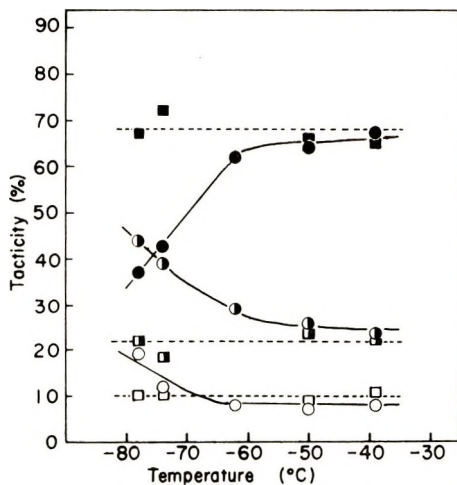


Fig. 2. Dependence of tacticities (I, H, and S) on the polymerization temperature for MMA-SnCl₄ complexes. 2:1 Complex: (○) I; (◐) H; (●) S. 1:1 Complex: (□) I; (◑) H; (■) S.

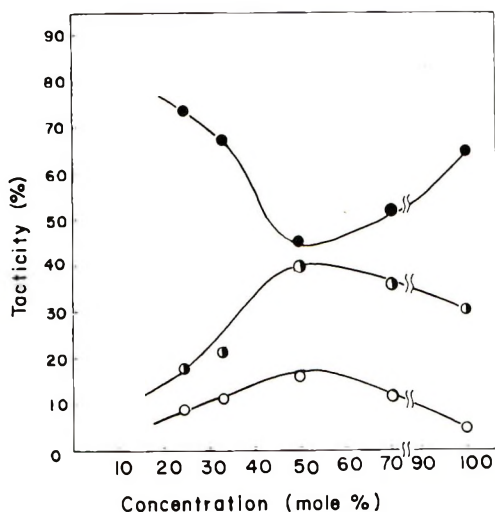


Fig. 3. Effect of concentration of the 2:1 MMA-SnCl₄ complex on tacticities: (○)I; (○)H; (●)S.

The dependence of tacticity on the polymerization temperature for the stannic chloride complexes is depicted in Figure 2. The tacticity for the 1:1 complex was little affected by the temperature, while that for the 2:1 complex varied with temperature. Below -60°C , the heterotacticity increased and the syndiotacticity decreased greatly. This behavior could be due to the configuration of the 2:1 complex and the mode of reaction. The 2:1 complex would isomerize from *cis*- to *trans*-configuration with increasing temperature. Similar behavior of tacticity was observed in the polymerization of methyl methacrylate in the presence of montmorillonite,¹¹ in which the monomer adsorbed on the surface of the additive was supposed to polymerize in a kind of intracomplex addition reaction.

The calculated values of the probability of the isotactic diad addition, $P(I)$, are also listed in Tables I and II. The values for the 2:1 SnCl₄ complex increased with decreasing temperature, while those for the 1:1 complex remained constant. The values for free methyl methacrylate decreased when the polymerization temperature became lower.¹ From this result, a specific polymerization mechanism is anticipated for the 2:1 complex.

Figure 3 shows the effect of concentration of the complex on the tacticity. The minimum point in the syndiotacticity and the maximum point in the isotacticity appeared at a complex concentration of 50 mole-%. At the lower concentration, the tacticity approached that of the polymer for the 1:1 complex.

ESR Spectra of Polymerization System

The ESR spectra of the 1:1 and the 2:1 SnCl₄ complex irradiated with ultraviolet rays at -120°C are shown in Figures 4 and 5. The 1:1 complex

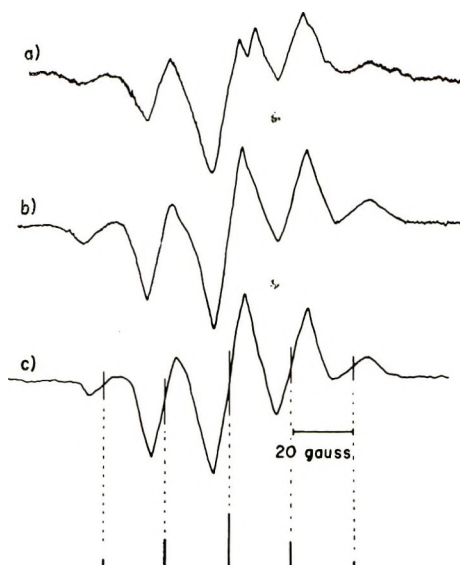


Fig. 4. ESR spectra, observed at -120°C , of 1:1 MMA- SnCl_4 complex in toluene (50 mole-%) after irradiation with ultraviolet rays at -120°C : (a) for 5 min; (b) for 30 min; (c) for 90 min.

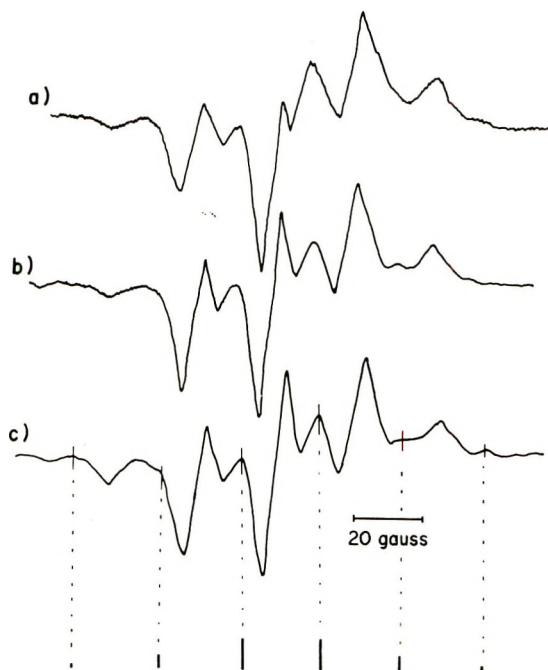


Fig. 5. ESR spectra, observed at -120°C , of the 2:1 MMA- SnCl_4 complex in toluene (50 mole-%) after irradiation with ultraviolet rays at -120°C : (a) for 2 min; (b) for 10 min; (c) for 30 min.

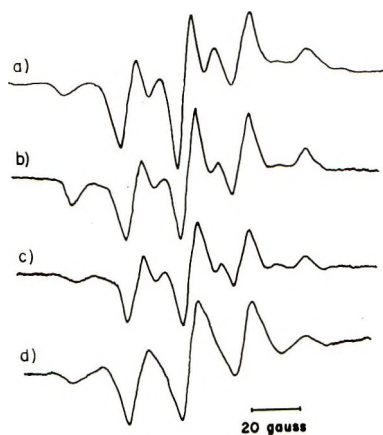


Fig. 6. Effect of temperature on the ESR spectra of the 2:1 MMA-SnCl₄ complex in toluene (50 mole-%). Irradiation with ultraviolet rays: (a) at -120°C; (b) at -100°C; (c) at -75°C, (d) at -60°C.

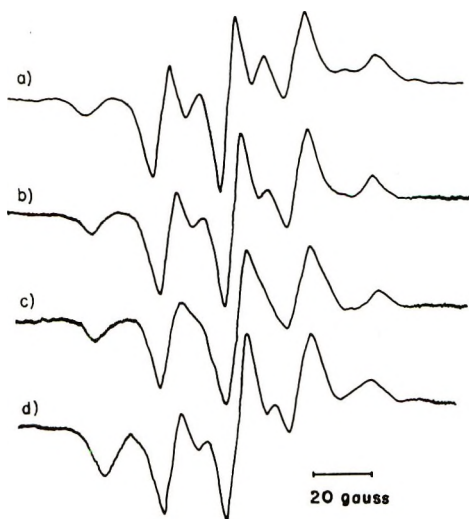


Fig. 7. Effect of concentration on ESR spectra of the 2:1 MMA-SnCl₄ complex irradiated with ultraviolet rays at -120°C and measured at -120°C: (a) 50 mole-% in toluene; (b) 33 mole-%; (c) 14 mole-%; (d) complex bulk.

gave a quintet with a splitting width of 22.2 gauss, while the 2:1 complex gave a spectrum consisting of a quintet with a splitting width of 22.2 gauss and a sextet with a splitting width of 24.0 gauss.

Figure 6 shows the temperature dependence of the spectrum for the 2:1 complex. The intensity of the sextet decreased with increasing temperature and faded out at -60°C. This change corresponds to the change of the tacticities of the polymer. The effect of concentration of the complex on the ESR spectrum is indicated in Figure 7. The sextet is most intense

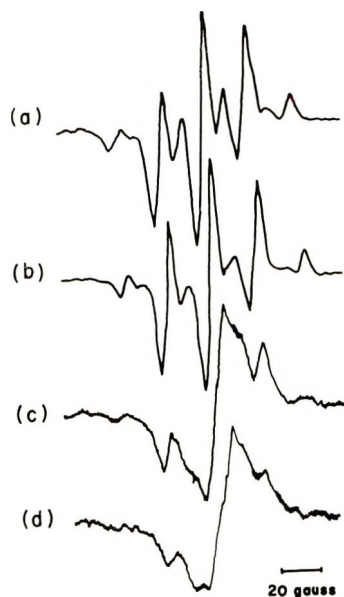


Fig. 8. ESR spectra: (a) of the MMA- AlCl_3 complex in toluene (50 mole-%), irradiated with ultraviolet rays at -75°C for 20 min and measured at -75°C ; (b) of methacrylic anhydride, irradiated at -120°C for 120 min and measured at -120°C ; (c) of the MMA- BF_3 complex in toluene (25 mole-%), irradiated at -120°C for 120 min and measured at -120°C ; (d) of methacrylic anhydride, irradiated at 17°C for 10 min and measured at -120°C .

at a concentration of 50 mole-%. Either the complex bulk or the more diluted solution gave a very weak sextet spectrum. The sextet disappeared at a concentration of 14 mole-%, where the 2:1 complex was considered to be dissociated into the 1:1 complex. The concentration effect on the intensity of the sextet was found to correspond to that on the tacticities of polymer. These results indicate that the sextet originated from the 2:1 complex. This characteristic spectrum was common to both the 2:1 MMA- SnCl_4 and the 2:1 MAN- SnCl_4 complexes.² The relative ratio of the peak height of the sextet to that of the quintet varied with temperature; 0.40 (-120°C), 0.39 (-100°C), 0.33 (-75°C), and 0.0 (-60°C).

Figure 8 shows the ESR spectra of the irradiated MMA- AlCl_3 and the irradiated MMA- BF_3 complex and that of irradiated methacrylic anhydride. The aluminum trichloride complex produced a nine-line spectrum at -75°C . The splitting width was 22.5 gauss. This spectrum is very similar to that of the pure monomer.¹² The spectrum of the irradiated boron trifluoride complex was different from those of other complexes. The spectrum consists of an intense singlet and a triplet with a splitting width of 23.1 gauss. The spectrum observed after irradiation at 17°C gave a similar spectrum as that observed under irradiation at -120°C . The spectrum of the irradiated methacrylic anhydride was similar to that of pure methyl methacrylate, but the quartet in it was weaker.

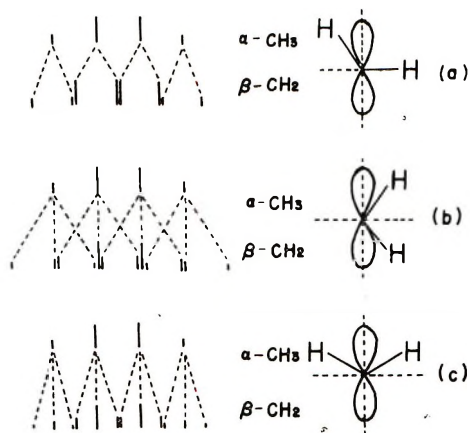


Fig. 9. Conformation of β -methylene protons of the radicals of growing ends and expected hyperfine splittings of their ESR spectra: (a) quintet; (b) sextet; (c) nine-line spectrum.

The conformation of the radicals is proposed in Figure 9. The quintet would be produced by the coupling of α -methyl protons and one of two β -methylene protons. A similar conformation was proposed for pure methyl methacrylate.^{13,14} The sextet can be explained by Figure 9b. In this conformation, methyl and methylene protons interact with the radical. The radicals produced from the MMA- AlCl_3 complex and methacrylic anhydride are explained by the superposition of a quintet signal (Fig. 9a) and a nine-line signal (Fig. 9c) as applied for pure methyl methacrylate.¹⁴ The triplet observed in the case of the BF_3 complex was plausibly due to a methylene radical. The splitting width of 23.1 gauss is similar to that of the methyl radical of 23.0 gauss.¹⁵

Polymerization Mechanism

Infrared spectra of the complex suggest the formation of *cis*-2:1 MMA- SnCl_4 complex in the polymerization solution. As discussed in the previous paper,² the *cis*-complex can undergo intracomplex reaction. The effects of temperature and concentration at polymerization on the tacticity correspond to those on the intensity of the sextet in the ESR spectra on the polymerization system. The sextet would strongly correlate with the regulation of tacticity in the polymerization of the 2:1 complex. The conformation of the radical end formed by the intercomplex reaction of the 2:1 complex is supposedly similar to that of the radical end formed in the polymerization of the 1:1 complex, which can be associated with the quintet. Therefore the sextet can be ascribed to the radical characteristic of the 2:1 complex, i.e., the radical formed by the intracomplex reaction. The dilution of the polymerization solution accelerates the dissociation of the 2:1 complex and the elevation of the temperature is plausibly responsible for the *cis-trans* isomerization and the dissociation of the complex. Conse-

quently, it is reasonable that the sextet becomes weak in these conditions. At higher concentration of the complex in the polymerization solution, the intercomplex reaction will be predominant.

The rate constant of the intracomplex reaction and those of the intercomplex reactions for the growing radical end with and without a coordinated monomer will be referred to as k_a , k_r , and k_r' , respectively, as shown in

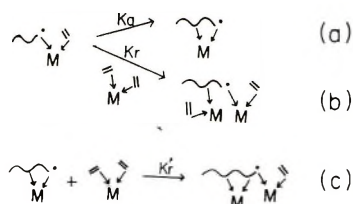


Fig. 10. Reaction scheme for the 2:1 MMA-SnCl₄ complex: (a) intracomplex addition; (b) and (c) intercomplex additions.

Figure 10. The probability of the presence of the growing end formed by intracomplex addition and that of the growing end formed by intercomplex addition are represented by R_a and R_r , respectively; the concentration of the monomer complex is expressed by $[M]$. Then the following equation holds true under a stationary state assumption:

$$\begin{aligned} \frac{dR_a}{dt} &= R_r k_a - R_a [M] k_r' \\ &= 0 \end{aligned} \quad (1)$$

Consequently,

$$\frac{R_a}{R_r} = \frac{k_a}{k_r' [M]} \quad (2)$$

$$R_a = \frac{k_a}{k_a + k_r' [M]} \quad (3)$$

$$R_r = \frac{k_r'}{k_a + k_r' [M]} \quad (4)$$

Provided that the rate constants in the intercomplex reaction, k_r and k_r' , are approximately equal, i.e., $k_r = k_r'$, the probability of the intracomplex reaction, P_c , can be expressed by

$$\begin{aligned} P_c &= \frac{k_a}{k_a + k_r' [M]} \\ &= \frac{k_a}{k_a + k_r [M]} \\ &= R_a. \end{aligned} \quad (5)$$

When the propagation step of the polymerization was analyzed according to the method reported in the previous paper,² the relationship between the probability of isotactic diad addition of intracomplex reaction σ_1 and that of intercomplex reaction σ_2 , was expressed by

$$\sigma_1 = \frac{1}{P_c} \left[\frac{(2I + H)(1 + P_c)}{200} - \sigma_2 \right]$$

The value of σ_2 is estimated to be equal to the probability of isotactic diad addition, $P(I)$, for the 1:1 complex. The values of P_c , σ_1 , and σ_2 are summarized in Table III. The value of σ_1 is very large and approximately 1.0, i.e., the polymer tacticity is regulated isotactically in the intracomplex reaction. A high probability of isotactic diad addition of intracomplex reaction was also observed in the case of the 2:1 methacrylonitrile-SnCl₄ complex² and methacrylic anhydride.^{16,17} In the polymerization of methacrylic anhydride, the ring formed by the cyclic intramolecular addition reaction is assumed to be fairly rigid compared with that formed by the reaction of the complex, and the intramolecular addition reaction seems to proceed very rapidly. Therefore, the ESR spectrum observed on the methacrylic anhydride showed a dominant radical which probably corresponds to the radical formed by the intramolecular addition reaction. Being different from the case of the SnCl₄ complex, the radical end formed by the cyclic

TABLE III

Estimation of Probabilities of Intracomplex Isotactic Diad Addition in the Polymerization of the 2:1 MMA-SnCl₄ Complex and of Intramolecular Isotactic Diad Addition in the Polymerization of Methacrylic Anhydride

Monomer	Solvent ^a	Temp, °C	P_c^b	$P(I)^c$	σ_2^d	σ_1^e
2:1 MMA-SnCl ₄ complex	tol	-78	0.28	0.40	0.20	1.10
	tol	-75	0.25	0.32	0.19	0.84
	—	-78	0.11	0.19	0.13	0.73
	—	-18	(1.0)	0.29	0.13	0.38
	—	15	(1.0)	0.20	0.14	0.36
Methacrylic anhydride ^f	tol	-50	(1.0)	0.33	0.13	0.87
	bz	20	(1.0)	0.56	0.21	0.79
	bz	60	(1.0)	0.66	0.24	0.92

^a tol, Toluene; bz, benzene.

^b Probability of intracomplex reaction.

^c Probability of isotactic diad addition.

^d Value of $P(I)$ for the corresponding 1:1 complex.

^e Probability of intracomplex isotactic diad addition, calculated from the equation

$$\sigma_1 = \frac{1}{P_c} \left\{ \frac{(2I + H)(1 + P_c)}{200} - \sigma_2 \right\}$$

^f Values calculated from the results of the intra-intercyclic polymerization of methacrylic anhydride reported by Miller et al.^{16,17}

intramolecular addition reaction shows a quintet because of the difference of the conformation of the ring.

The persistence ratio ρ of the resulting polymers calculated according to the equation of Coleman and Fox¹⁸ is listed in the last columns of Tables I and II. The SnCl_4 complexes gave larger values than unity. Especially, the values for the 1:1 complex are larger than those for the 2:1 complex. This means that the polymerization of these complexes at temperatures of -40° to -78°C obeys Markoffian statistics, that is, the penultimate effect exists in this system. When the intracomplex addition reaction contributed to polymer tacticity, the persistence ratio became smaller, as in the polymerization of the 2:1 SnCl_4 complex, below -50°C . It seems reasonable that the persistence ratio value is small at lower temperatures if the intracomplex reaction is Bernoullian, since the persistence ratio value is 1.0 for the Bernoullian stereoaddition and the observed value in the polymerization of the 2:1 SnCl_4 complex below -50°C is between 1.0 and the value corresponding to the 1:1 complex. A similar tendency was obtained in the polymerization of methacrylic anhydride at lower temperatures.¹⁹

Boron trifluoride has a different effect on the polymerization. The triplet observed on ESR spectroscopy indicates that the growing end is the β -carbon. Some specific interaction is anticipated between boron trifluoride and the growing radical, as in the case of the polymerization of MMA with alkylboron-oxygen of alkylboron-peroxide systems.²⁰

References

1. S. Okuzawa, H. Hirai, and S. Makishima, *J. Polym. Sci. A-1*, **7**, 1039 (1969).
2. H. Hirai, T. Ikegami, and S. Makishima, *J. Polym. Sci. A-1*, **7**, 2059 (1969).
3. H. S. Booth and K. S. Willson, *Inorg. Syn.*, **1**, 21 (1939).
4. F. A. Bovey and G. V. D. Tiers, *J. Polym. Sci.*, **44**, 173 (1960).
5. T. Ikegami and H. Hirai, *J. Polym. Sci. A-1*, **8**, 463 (1970).
6. J. R. Beattie, *J. Chem. Soc.*, **38**, 1514 (1963).
7. I. Nakagawa and T. Shimanouchi, *Spectrochim. Acta*, **23A**, 2099 (1967).
8. J. R. Beattie, *J. Chem. Soc.*, 3267 (1967).
9. R. A. Walton, *Quart. Rev.*, **19**, 126 (1965).
10. H. Watanabe and S. Sono, *Kogyo Kagaku Zasshi*, **65**, 273 (1962).
11. A. Bumistein and A. Watterson, *J. Polym. Sci. B*, **6**, 69 (1968).
12. R. Marx and M. R. Bensasson, *J. Chim. Phys.*, **57**, 674 (1960).
13. J. Sohma and T. Komatsu, *J. Polym. Sci. A*, **3**, 287 (1965).
14. D. J. Ingram, M. C. R. Symons, and M. G. Townsend, *Trans. Faraday Soc.*, **54**, 409 (1958).
15. R. W. Fessenden and R. H. Schuler, *J. Chem. Phys.*, **39**, 2147 (1963).
16. W. L. Miller, W. S. Brey, and C. B. Butler, *J. Polym. Sci.* **54**, 329 (1961).
17. J. C. H. Hwa, W. A. Fleming, and W. L. Miller, *J. Polym. Sci. A*, **2**, 2385 (1964).
18. R. K. Coleman and T. G. Fox, *J. Polym. Sci. A*, **1**, 3183 (1963).
19. M. Reinmoeller and T. G. Fox, *Polymer Preprints*, **7**, 999 and 1005 (1966).
20. F. S. Arimoto, *J. Polym. Sci. A-1*, **4**, 275 (1966).

Received December 31, 1969

Cyclocopolymerization of *p*-Chlorostyrene with 4-Vinylcyclohexene

WASABURO KAWAI and SHIGERU KATSUTA, *Government Industrial
Research Institute, Osaka, Japan*

Synopsis

4-Vinylcyclohexene was polymerized by triethyl-aluminum-titanium tetrachloride catalyst (mole ratio 5.4:1). Copolymerization of 4-vinylcyclohexene with *p*-chlorostyrene by the same catalyst was also carried out. For these polymerization results, the Roovers-Smets equation was applied and the reactivity ratio parameters, K_c , K_c' , r_2 , and r_3 were determined as follows: $K_c = K_c/k_{11} = 9.1$; $K_c' = k_c/k_{12} \sim \infty$; $r_2 = k_{22}/k_{21} = 1.45$; $r_3 = k_{31}/k_{32} \sim 0$, where subscripts 1, 2 and 3 indicate 4-vinylcyclohexene, *p*-chlorostyrene, and cyclized polymer anion, respectively.

INTRODUCTION

4-Vinylcyclohexene is a bifunctional monomer that has external(vinyl) and internal double bonds. This monomer had been polymerized with Ziegler catalyst ($\text{AlEt}_3\text{-TiCl}_4$, 1:1 mole ratio) by Butler,¹ and it was ascertained by NMR spectroscopy that the polymer had a cyclic structure. In the present work, 4-vinylcyclohexene was polymerized with $\text{AlEt}_3\text{-TiCl}_4$ (5.4:1 mole ratio) catalyst in *n*-hexane, and it was shown by infrared spectroscopy and double bond analysis that the polymer has still residual unsaturation.

Cyclocopolymerization of 4-vinylcyclohexene with *p*-chlorostyrene was also carried out with the Ziegler catalyst, and it was evident that the copolymer involved 4-vinylcyclohexene units having both cyclic and pendent unsaturated structure. For the cyclocopolymerization system for which the scheme shown in the Discussion was assumed, the copolymer composition equations for radical copolymerization of Roovers and Smets² were applied, and the rate constant ratios were determined.

EXPERIMENTAL

Polymerization Procedure

Solvent (*n*-hexane) was charged in the polymerization tube at ice temperature, and then titanium tetrachloride and triethylaluminum were added by means of a semimicro syringe. After aging for 10 min, 4-vinyl-

cyclohexene or a 4-vinyl-cyclohexene-*p*-chlorostyrene mixture was charged, and the tube was sealed in a nitrogen stream. The polymerizations were carried out with shaking in thermostat.

The polymerization products were poured into a methanol-hydrochloric acid mixture, and the polymers were collected by filtration. The polymers were subsequently boiled in *n*-butanol and after cooling, white polymers were obtained by pouring into methanol. The polymers were again collected by filtration and dried in vacuum oven.

Analysis of Polymer

The chlorine content of copolymer of 4-vinylcyclohexene with *p*-chlorostyrene was determined by a combustion method.^{3,4} Determination of double bonds in the polymer was carried out by the hydrogen perbromide method.⁵

RESULTS AND DISCUSSION

Homopolymerization of 4-Vinylcyclohexene

The results of homopolymerization of 4-vinylcyclohexene with Ziegler catalyst are tabulated in Table I. Roovers and Smets² obtained the equation (1) for cyclopolymerization of vinyl *trans*-cinnamate:

$$1/f_c = 1 + K[M] \quad (1)$$

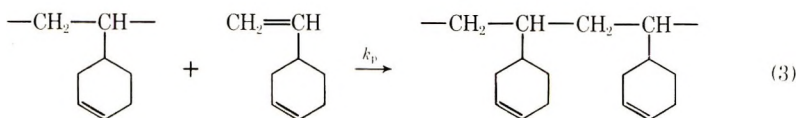
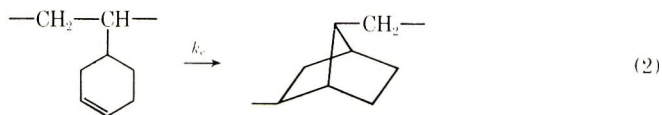
TABLE I
Polymerization of 4-Vinylcyclohexene by $\text{AlEt}_3\text{-TiCl}_4$ Catalyst^a

Expt. no.	4-Vinyl-cyclohexene (VC) mole/l.	N-Hexane, cc	Polymerization time, hr	Polymer yield, g	Content of VC unit having double bonds, wt-%	f_c	$1/f_c$
A-1	4.84	2	24	0.0685	36.7	0.633	1.58
A-2	6.45	2	18	0.0260	41.3	0.587	1.70
A-3	1.61	4	18	0.0206	17.4	0.826	1.21
A-4	2.69	4	18	0.0354	20.7	0.793	1.26

^a AlEt_3 0.0048, mole; TiCl_4 0.00091 mole; $\text{AlEt}_3/\text{TiCl}_4 = 5.4$ (mole ratio); polymerization temperature, 50°C.

where f_c is the fraction of cyclized units in the polymer and $K = k_p/k_c$ (where k_p is the rate of vinyl propagation and k_c is the rate of cyclization), and $[M]$ denotes monomer concentration.

In cyclopolymerization of 4-vinylcyclohexene, the polymerization scheme of eqs. (2) and (3) is confirmed by the presence of cyclized¹ structures and structures showing pendent unsaturation and so for



determination of $K = k_p/k_c$, the use of eq. (1) is possible. A plot of $1/f_c$ versus $[M]$ is shown in Figure 1, and from the slope of straight line, k_p/k_c was determined to be 9.1.

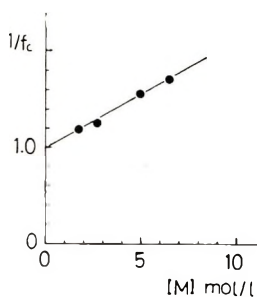


Fig. 1. Plot of $1/f_c$ vs. $[M]$ in cyclocopolymerization of 4-vinylcyclohexene.

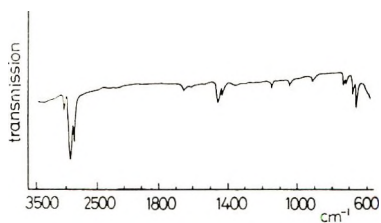


Fig. 2. Infrared spectrum of poly-4-vinylcyclohexene (KBr disk).

The infrared spectrum of poly-4-vinylcyclohexene is shown in Figure 2, and at 3050 cm^{-1} a sharp absorption due to the alicyclic double bond⁶ is observed.

Cyclocopolymerization of 4-Vinylcyclohexene with *p*-Chlorostyrene

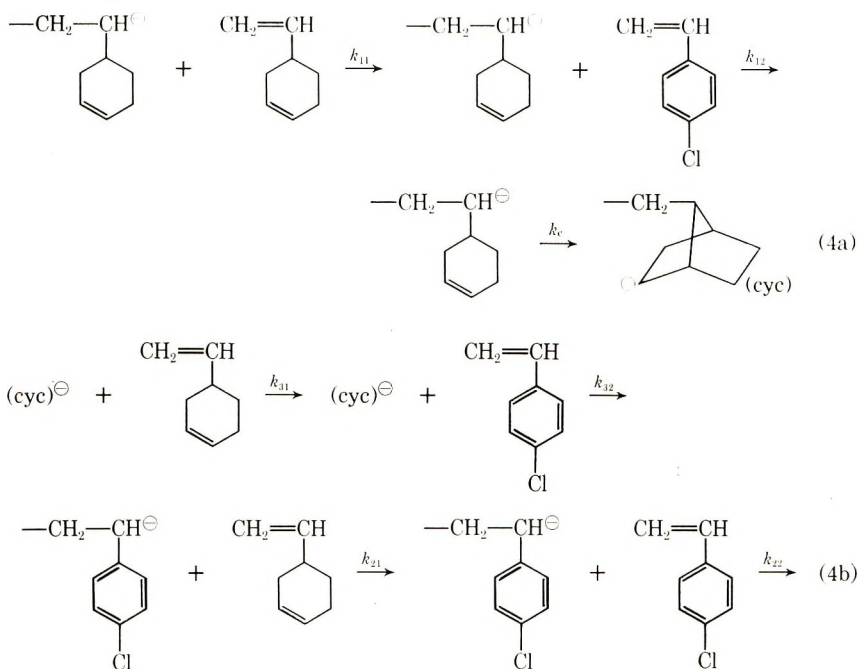
Results of copolymerization of 4-vinylcyclohexene with *p*-chlorostyrene are tabulated in Table II. The relation between mole fraction of *p*-chlorostyrene in copolymer and that in monomer mixture is shown in Figure 3.

TABLE II
 Copolymerization of 4-Vinylcyclohexene and *p*-Chlorostyrene by $\text{AlEt}_3\text{-TiCl}_4$ Catalyst^a

Expt. no.	4-Vinylcyclohexene		<i>p</i> -Chloro styrene		Conversion, %	Cl content, wt-%	In copolymer			
	[M ₁] mole/l.	[M ₂] mole/l.	[M ₁] mole/l.	[M ₂] mole/l.			<i>p</i> -Cl-St dm ₂ , mole-%	VC dm ₁ , mole-%	VC having double bond, wt-%	Cyclic VC, wt-%
AB-5	1.14	4.62	4.62	4.62	28.1	21.7	82.0	18.0	2.96	12.14
AB-6	1.72	4.03	4.03	4.03	26.4	20.8	77.4	22.6	2.95	15.65
AB-7	2.29	3.45	3.45	3.45	21.7	20.5	75.7	24.3	2.41	17.59
AB-8	2.87	2.90	2.90	2.90	12.6	20.4	75.1	24.9	4.02	16.32
AB-9	3.46	2.30	2.30	2.30	4.7	20.2	74.5	25.5	11.3	9.80
AB-10	4.61	1.16	1.16	1.16	3.3	16.9	58.3	41.7	21.2	12.80

^a Reaction conditions: AlEt_3 , 0.00488 mole; TiCl_4 , 0.00091 mole, $\text{AlEt}_3/\text{TiCl}_4 = 5.4$ (mole ratio) polymerization temperature, 50°C; polymerization time, 3 hr; *n*-hexane; 2 cc.

The copolymerization scheme of 4-vinylcyclohexene with *p*-chlorostyrene was assumed to be as shown in eqs. (4).



The scheme is similar to that of cyclopolymerization of vinyl *trans*-cinnamate, and if in cyclopolymerization by coordinated anionic catalyst, the scheme would be accepted in analogy with the radical scheme, we could use Roovers' equation and determine K'_c from eq. (5).

$$d[M_1]/dm - ([M_1]/K_c) = 1 + ([M_2]/K'_c) \quad (5)$$

where $d[M_1]$ is the total 4-vinylcyclohexene unit content in copolymer, dm represents cyclized 4-vinylcyclohexene unit content in copolymer, $[M_1]$ is the concentration of 4-vinylcyclohexene in the feed monomer mixture, and $[M_2]$ is the concentration of *p*-chlorostyrene in the feed monomer mixture.

From the plot by eq. (5) shown in Figure 4, it was found that $1/K'_c$ was near zero and $K'_c (= k_c/k_{12})$ was very high (approaching infinity). Moreover, determination of $r_2 (= k_{22}/k_{21})$ and $r_3 (= k_{31}/k_{32})$ was carried out by using eq. (6); a plot is shown in Figure 5.

$$\frac{1}{R} \left(\frac{\rho}{1 + [M_1]K_c} - 1 \right) = r_3 - r_2 \left\{ \frac{\rho}{R(1 + [M_1]/K_c)} \right\} \quad (6)$$

where

$$\rho = d[M_1]/d[M_2]$$

$$R = [M_1]/[M_2]$$

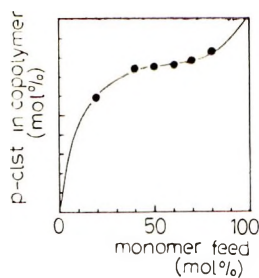


Fig. 3. Composition curve of copolymer of 4-vinylcyclohexene with *p*-chlorostyrene.

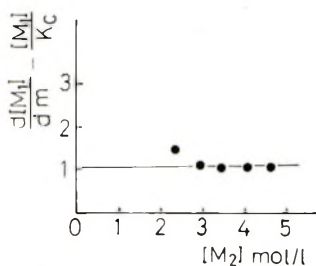


Fig. 4. Plot of $d[M_1]/dm - [M_1]/K_c$ vs. $[M_2]$ according to eq. (5).

TABLE III
Results for Copolymerization 4-Vinylcyclohexene (M_1) and *p*-Chlorostyrene (M_2)

Expt. no.	$d[M_1]$, mole-%	dm , mole-%	$d[M_1]$ dm	$[M_1]$ mole/l.	$[M_1]$ K_c	$[M_2]$ mole/l.	$\frac{d[M_1]}{dm} - \frac{[M_1]}{K_c}$
AB-5	18.0	14.8	1.22	1.14	0.126	4.62	1.09
AB-6	22.6	19.0	1.19	1.72	0.190	4.03	1.00
AB-7	24.3	20.0	1.22	2.29	0.253	3.45	0.967
AB-8	24.9	19.3	1.36	2.87	0.316	2.90	1.04
AB-9	25.5	12.6	2.11	3.46	0.381	2.30	1.73
AB-10	41.7	16.2	2.57	4.61	0.507	1.16	2.06

TABLE IV
Results for Copolymerization of 4-Vinylcyclohexene (M_1) and *p*-Chlorostyrene (M_2)

Expt. no.	R	$1/R^2$	ρ	$A (= 1 + \frac{\rho}{[M_1]/K_c})$	$\frac{\rho}{A R^2}$	$\frac{1}{R} \left(\frac{\rho}{A} - 1 \right)$
AB-5	0.247	1.54	0.212	1.126	2.895	-3.28
AB-6	0.426	5.50	0.292	1.149	1.397	-1.75
AB-7	0.663	2.28	0.321	1.252	0.584	-1.12
AB-8	0.988	1.15	0.332	1.316	0.289	-0.76
AB-9	1.50	0.44	0.342	1.380	0.110	-0.50
AB-10	3.97	0.06	0.715	1.506	0.030	-0.13

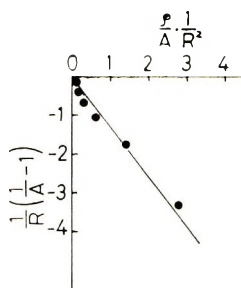


Fig. 5. Plot of $(1/R[1/A] - 1)$ vs. ρ/AR^2 according to eq. (6), where $A = 1 + [M_1]/K_c$.

Thus, reactivity ratio parameters, K_c , K'_c , r_2 and r_3 were estimated (Tables III and IV); the values may be summarized as follows:

$$K_c = k_c/k_{11} = 9.1$$

$$K'_c = k_c/k_{12} \sim \infty$$

$$r_2 = k_{22}/k_{21} = 1.45$$

$$r_3 = k_{31}/k_{32} \sim 0$$

The determination of r_1 and r_2 by the Fineman-Ross method was carried out as shown in Figure 6. If the reactivities of end anions from cyclized and uncyclized polymer are equal, $r_1 (= k_{11}/k_{12})$ will be near $r_3 (= k_{31}/k_{32})$. In fact, r_1 by the Fineman-Ross method was near zero and r_3 by Roovers' method was also near zero. Moreover, $r_2 (= k_{22}/k_{21})$ by the Fineman-Ross

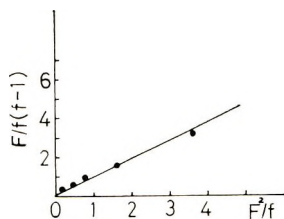


Fig. 6. Fineman-Ross plot for the copolymerization of 4-vinylcyclohexene with *p*-chlorostyrene.

method was 1.03; and r_2 by Roovers' method was 1.45. These agreements are fairly good.

K_c of vinyl *trans*-cinnamate in radical cyclopolymerization was reported to be 11, and so 4-vinylcyclohexene may be a cyclizable monomer comparable to vinyl *trans*-cinnamate.

References

1. G. B. Butler and M. L. Mills, *J. Polym. Sci. A*, **3**, 1609 (1965).
2. J. Roovers and G. Smets, *Makromol. Chem.*, **60**, 89 (1963).
3. W. Schöniger, *Mikrochim. Acta*, **1955**, 123.
4. D. C. White, *Mikrochim. Acta*, **1961**, 449.
5. J. Mitchell, Jr., I. M. Kolthoff, E. S. Proskauer, and A. Weissberger, *Organic Analysis*, Vol. III, Interscience, New York, 1956, p. 243.
6. R. J. De Kock and A. Veermans, *Makromol. Chem.*, **95**, 179 (1966).

Received January 9, 1970

Polyhydrazides. IV. Preparation and Properties of Poly-*N*-Ethyl- and Isopropylhydrazide Oxadiazoles

YOSHIO IWAKURA, KEIKICHI UNO, and SHIGERU KUROSAWA,
*Department of Synthetic Chemistry, Faculty of Engineering, University of
Tokyo, Tokyo, Japan*

Synopsis

High molecular weight poly-*N*-alkylhydrazide-oxadiazoles have been prepared in polyphosphoric acid by alkylation of poly-1,3,4-oxadiazole which was synthesized from terephthalic acid and hydrazine sulfate. Various kinds of reagents having an alkoxy group were used as alkylating agent, and *N*-ethylated and *N*-propylated polyhydrazides containing oxadiazole units were obtained. The thermal properties of the polymers obtained were investigated by using infrared spectroscopy, viscometry, differential thermometric and thermogravimetric techniques. Soluble poly-*N*-alkylhydrazide-oxadiazole are thermally cyclized to poly-1,3,4-oxadiazole with elimination of olefins and water at 226-330°C for propylated polyhydrazide and at 240-360°C for ethylated polyhydrazide. For both, weight loss in polyhydrazides occurs in two distinct stages corresponding, respectively, to cyclization and decomposition of the poly-1,3,4-oxadiazole formed *in situ*.

INTRODUCTION

The preparation of poly-*N*-methylhydrazide (PMe) in fuming sulfuric acid (oleum) and polyphosphoric acid (PPA) was reported recently.^{1,2} In one of these reports, it was indicated that poly-*p*-phenylene-1,3,4-oxadiazole (POx) easily reacted with various kinds of methylating reagent, such as dimethyl sulfate and methanol, to give PMe containing 1,3,4-oxadiazole units. The hydrazide formation was thought to be brought about through initial alkylation and subsequent hydroxylation of 1,3,4-oxadiazole rings.

In the continuation of the previous study, the ring-opening reactions of POx by use of ethylating and propylating reagents were extensively studied in PPA. In addition to the preparation of the poly-*N*-alkylhydrazide-oxadiazoles, the thermal behavior of the polymer obtained was investigated.

Polyhydrazide-oxadiazole contains various amounts of 1,3,4-oxadiazole units, but it will be termed polyhydrazide for simplicity in the following discussion.

EXPERIMENTAL

The reactions of poly-1,3,4-oxadiazole with alkylating reagents were undertaken following the previously reported method³ in 116% polyphos-

phoric acid which was available commercially and used without further purification. Thermoanalytical data were obtained by use of the Rigaku Denki thermogravimetric and differential thermal analyzers.

RESULTS AND DISCUSSION

The reactions of POx with various kinds of alkylating reagent were carried out in PPA. In these reactions triethyl phosphate, diethyl sulfate, ethyl benzoate, ethyl benzenesulfonate, diethyl ether, and ethanol were used as ethylating reagent, and *n*- and isopropanol as propylating reagent. POx used in the present study was prepared by a method reported previously⁴ from terephthalic acid and an excess of hydrazine sulfate in PPA and was used for the next reaction without isolation from the PPA solution.

The results of preparation of *N*-alkylated polyhydrazides are summarized in Tables I and II. Table I lists the results of preparation of poly-*N*-ethyl-terephthalylhydrazide (PEt).

TABLE I
Preparation of Poly-*N*-ethylhydrazide from Poly-*p*-phenylene-1,3,4-oxadiazole (POx) and Various Ethylating Reagents in PPA^a

No.	Ethylating reagent			Reaction condition		Polymer	
	Type	Amt, g	(mole)	Temp, °C	Time, hr	PMT, °C ^b	η_{inh}^c
I-1	(C ₂ H ₅ O) ₃ PO	3.7	(0.02)	140	4	284-286	0.71
I-2	C ₆ H ₅ CO ₂ C ₂ H ₅	9.0	(0.06)	135	4	285-292	0.63
I-3	C ₆ H ₅ SO ₃ C ₂ H ₅	12.0	(0.06)	150	6.5	286-291	0.70
I-4	C ₂ H ₅ OC ₂ H ₅	7.4	(0.10)	130	4	284-290	0.50
I-5	(C ₂ H ₅ O) ₂ SO ₂	4.6	(0.03)	140	5	284-290	0.87
I-6	C ₂ H ₅ OH	3.0	(0.06)	130	4	Inf. ^d	1.15

^a POx was prepared preliminarily from terephthalic acid (1.66 g, 0.01 mole) and hydrazine sulfate (2.0 g, 0.015 mole) in PPA (50 g) at 150°C, and the PPA solution was used in this experiment.

^b Measured on the hot plate.

^c Measured in dichloroacetic acid at 30°C, *c* = 0.2 g/dl.

^d Inf: Infusible.

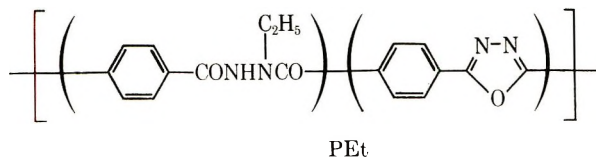
TABLE II
Preparation of Poly-*N*-isopropylhydrazide from POx and *n*- or Isopropanol in PPA^a

No.	Propylating reagent			Polymer
	Type	Amt, g	(mole)	η_{inh}^b
II-1	<i>n</i> -C ₃ H ₇ OH	5.0	(0.08)	0.75
II-2	<i>i</i> -C ₃ H ₇ OH	5.0	(0.08)	0.89

^a POx prepared as in Table I; preparation of hydrazide at 150°C/5 hr

^b Measured in dichloroacetic acid at 30°C, *c* = 0.2 g/dl.

These polyhydrazides were white to yellowish-white flakes. All except that from ethanol gave melting temperatures in the range 284–292°C, and inherent viscosities between 0.50 and 0.87 (0.2 g/dl in dichloroacetic acid at 30°C). On the other hand, a polymer obtained by use of ethanol gave no apparent melting temperature below 400°C and a high inherent viscosity value of 1.15 in dichloroacetic acid. The infrared spectra of these polymers gave absorptions due to a hydrazide linkage, —CONHN(C₂H₅)CO—, at 3300–3240 cm⁻¹ (ν_{NH}), 3000–2950 cm⁻¹ (ν_{CH}) and 1690–1640 cm⁻¹ (broad; two kinds of ν_{CO}), and those characteristic of the 1,3,4-oxadiazole ring around 1570, 1486, and 965 cm⁻¹. These infrared observations indicate the presence of a considerable amount of 1,3,4-oxadiazole in all of the resulting polymers, which are assumed to have the structure I as



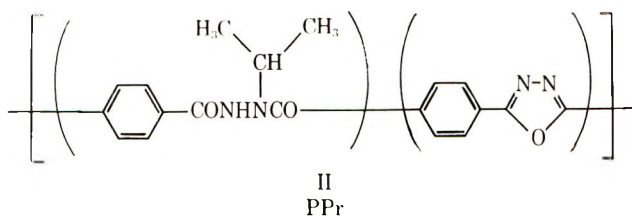
Furthermore, the absorptions of the 1,3,4-oxadiazole rings were found to be much stronger in the infrared spectrum of the infusible polymer (I-6) than in those of the other polymers.

In Table II are summarized the results of the reactions of POx with *n*- and isopropanol as propylating reagent. In these reactions, the reaction temperature was kept at 140°C. When the reaction was carried out above 160°C, the alkylation reaction did not take place and the mother polymer POx was recovered. In this case, propanol appeared to be consumed as propylene formed by dehydration of propanol in PPA.

The polyhydrazides obtained were yellowish-brown powders and did not melt below 400°C. In the infrared spectra of these polymers absorptions attributable to 1,3,4-oxadiazole were observed around 1573, 1485, and 965 cm⁻¹ in addition to the strong absorptions of a hydrazide linkage, —CONHN(C₃H₇)CO—, at 3300–3260 cm⁻¹ (ν_{NH}), 2985–2950 cm⁻¹ (ν_{CH}), and 1690–1640 cm⁻¹ (two kinds of ν_{CO}). Polyhydrazides II-1 and II-2 both showed almost the same infrared spectra except for difference in intensity of the oxadiazole absorptions. This fact suggests the identity of the structure of the *N*-substituent of both polyhydrazides II-1 and II-2, and the *N*-substituent was found to be an isopropyl group through model reactions of 2,5-diphenyl-1,3,4-oxadiazole (Di) with the propanols as described below.

The reactions of Di with *n*- and isopropanols were carried out in PPA in the presence of an equimolar amount of sulfuric acid at 120°C for 5 hr. The only product obtained in both reactions was *N,N'*-dibenzoyl-*N*-isopropylhydrazine, which was identified with an authentic sample by comparing their melting temperatures, infrared spectra and elemental analyses.

Accordingly, the structure of polymers II-1 and II-2 can be designated as II:



Oleum was superior to PPA as reaction medium for preparing PME from POx and methylating reagents, as reported in the preceding paper.³ In the present study, however, use of oleum gave no ethylated or propylated polyhydrazides, but POx was recovered. This may be interpreted on the basis of olefin formation of the ethylating and propylating reagents in oleum.

The elemental analyses of polymers give unsatisfactory results for characterization, probably because of the phosphoryl residues.

Thermal Behavior of Polyhydrazides

The PEt polymers, which melted in the range 284–292°C, foamed and then solidified gradually to give yellowish products above their melting temperatures. Similar behavior was reported on the melting of PME, and this reaction was considered to be the thermal cyclization of hydrazide to 1,3,4-oxadiazole.¹ In case of PEt, too, the behavior above its melting temperature was confirmed to be the oxadiazole formation on the basis of the observations described below.

Since the PPr polymers did not melt below 400°C, there was apparently no clear change. Oxadiazole formation by heat treatment, however, was suggested on the basis of the change of solubility and confirmed by several methods such as infrared spectroscopy, viscosity measurement, gas chromatography and thermoanalytical methods.

Infrared Spectra

For this study, films of PEt and PPr were fabricated from their *m*-cresol solutions and heated at 100°C for 5 hr *in vacuo* to remove the solvent completely. Figures 1a and 1b show the infrared spectra of the PEt film before and after the heat treatment, respectively. After heating the film at 300°C for 0.5 hr, the hydrazide absorptions almost disappeared and absorptions of 1,3,4-oxadiazole at 1570, 1486, and 965 cm^{-1} increased in intensity only slightly (Fig. 1b).

In Figure 2, the change of characteristic absorptions was more clearly seen. The film of PPr showed strong absorptions characteristic of two kinds of amide bond of the hydrazide before heating, whereas after heat treatment at 220–260°C/1 hr the amide absorptions became weaker, and absorptions of 1,3,4-oxadiazole increased in intensity. In the spectrum of

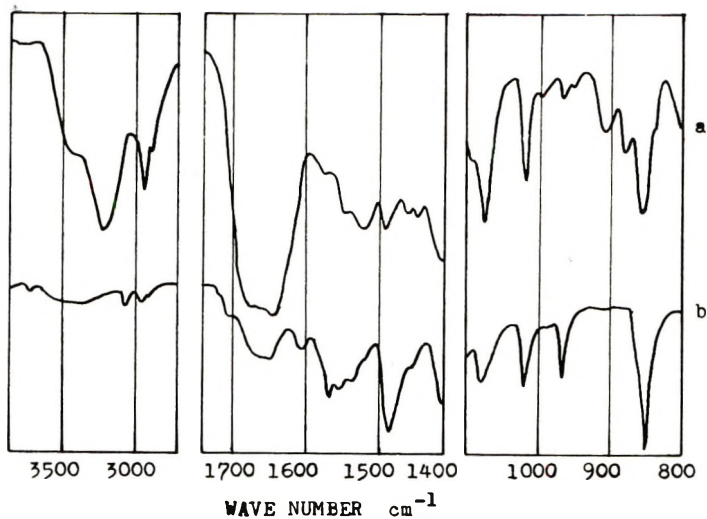


Fig. 1. Infrared spectra of PET: (a) before heat treatment; (b) after heat treatment at 300°C/0.5 hr.

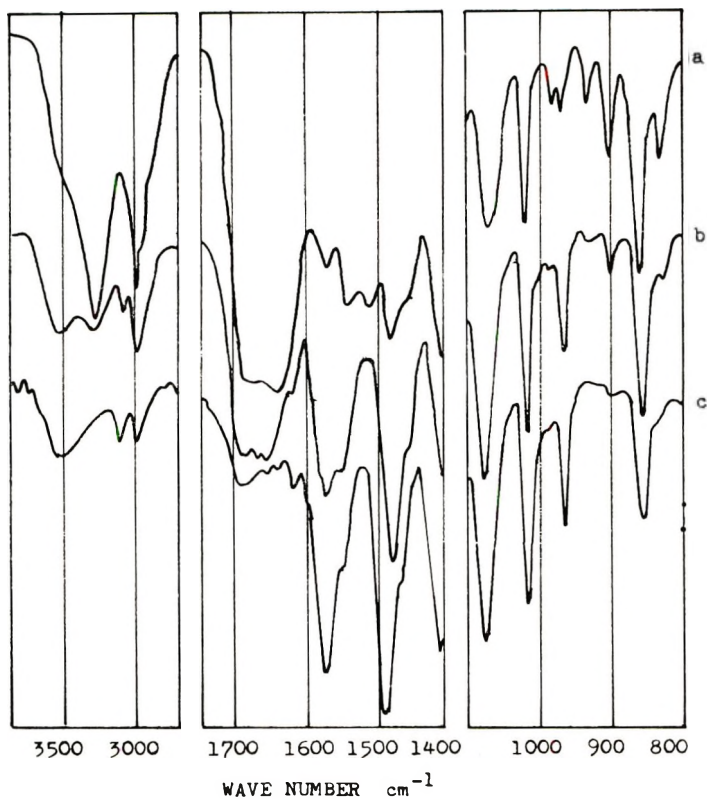


Fig. 2. Infrared spectra of PPr: (a) before heat treatment; (b) after heat treatment at 220°C/1 hr; (c) after heat treatment at 220°C/1 hr and 300°C/0.5 hr.

the film further heated at 300°C/0.5 hr, only a trace of amide absorptions could be seen around 1680 cm^{-1} , and the characteristic absorptions of 1,3,4-oxadiazole became much stronger.

Though the increase in the oxadiazole absorptions after the heat treatment was observed in both of PEt and PPr, it was more notable for PPr. This seems to mean the higher conversion of hydrazide to 1,3,4-oxadiazole for the linkage $-\text{CONHN}(\text{C}_3\text{H}_7)\text{CO}-$ rather than for the linkage $-\text{CONHN}(\text{C}_2\text{H}_5)\text{CO}-$.

Viscosity Changes on Heat Treatment

As reported in the preceding paper,³ the ratio of oxadiazole units to the hydrazide units is reflected in the change of solubility in organic polar solvents. In the present study, however, measurement of the inherent viscosity in 98% sulfuric acid of the heated sample was examined and it seemed to give a better method for getting quantitative information on the thermal conversion of hydrazide to 1,3,4-oxadiazole. In 98% sulfuric acid, *N*-alkylated hydrazide linkages were found to be hydrolyzed with ease to the corresponding carboxylic acid and alkylhydrazine salt, whereas the 1,3,4-oxadiazole unit was not changed. Hence in 98% sulfuric acid, the existence of the hydrazide linkage not changed thermally to 1,3,4-oxadiazole will cause a decrease in the inherent viscosity of the thermally treated polymer.

TABLE III
Inherent Viscosity before and after Heat Treatment

Polymer type	Inherent viscosity ^a		
	Before heat treatment		After heat treatment
	DCA ^b	H ₂ SO ₄ ^c	(H ₂ SO ₄) ^c
PEt (I-5)	0.87	0.04	0.15
PPr (II-2)	0.89	0.08	0.35

^a $c = 0.02$ g/dl, 30°C.

^b DCA: Dichloroacetic acid.

^c H₂SO₄: 98% Sulfuric acid.

Table III lists inherent viscosities of PEt and PPr measured before and after the heat treatment. The inherent viscosity of PEt which gave a value of 0.87 in dichloroacetic acid was 0.04 in 98% sulfuric acid before heating but 0.15 in the same solvent after heat treatment at 330°C/5 hr. The increase in viscosity clearly shows the conversion of PEt to POx, whereas the thermal cyclization reaction is considered to be incomplete from the rather low value of the heated sample.

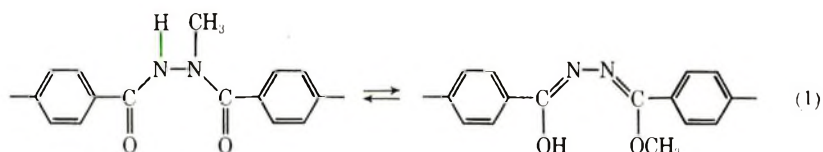
On the other hand, the PPr polymer which gave inherent viscosities of 0.89 in dichloroacetic acid and 0.08 in 98% sulfuric acid exhibited an inherent viscosity of 0.35 in 98% sulfuric acid after heating at 300°C for 5 hr.

This big change in inherent viscosity in sulfuric acid on heat treatment is believed to be due to the almost complete conversion of the hydrazide linkage to the 1,3,4-oxadiazole ring for the PPr polymer.

Gas Chromatography

It was of a particular interest to know what was eliminated in the thermal cyclization reaction of poly-*N*-alkylhydrazide in order to study its mechanism.

In case of PME the hydrazide groups, which are adjacent to aromatic rings on either side, may be capable of partaking in extended conjugation at a high temperature [eq. (1)].



We have suggested that the enol form can be thermally cyclized to 1,3,4-oxadiazole by eliminating methanol. Sekiguchi and Sadamitsu⁵ supported this by gas-chromatographic analysis of volatilized products from the thermal degradation of the PME polymer. In the present study, it was of interest to know whether PEt and PPr were transformed to POx through a similar mechanism. If PEt and PPr are transformed to POx through the same mechanism as that for PME, ethanol and isopropanol will be expected to be eliminated from PEt and PPr, respectively, when they change to POx.

Gas chromatography showed that the eliminated products were not alcohols but olefins; ethylene was eliminated from PEt and propylene from PPr. This fact seems to suggest that PEt and PPr are transformed to POx via a mechanism different from that for PME. The study of the mechanism of cyclization will be described in the latter part of this paper.

Thermogravimetric and Differential Thermal Analysis (TGA and DTA)

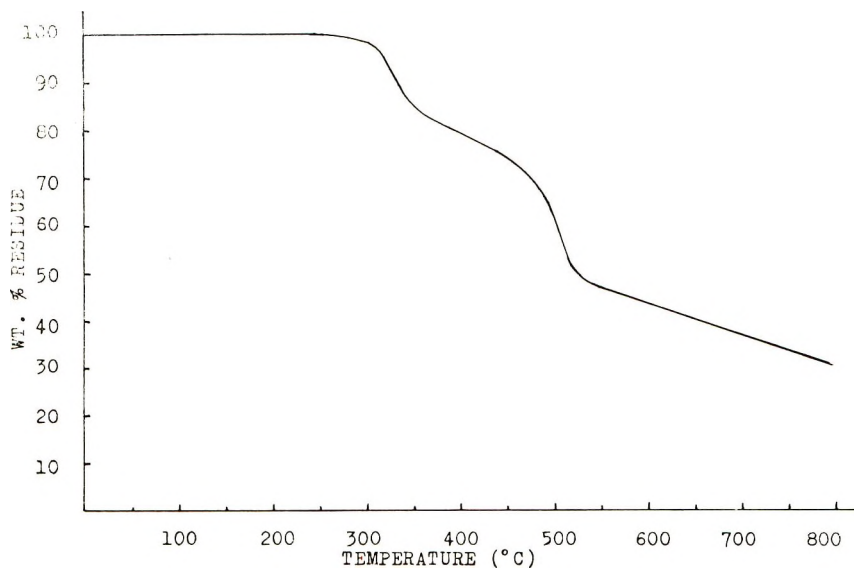
Figures 3a and 3b show typical thermogravimetric curves for representative samples of PEt (I-5) and PPr (II-1). For the study approximately 100 mg of the dried sample was heated in a stream of nitrogen at a programmed rate of 5°C/min.

For the fusible PEt polymer, the first rapid loss in weight occurs at 240°C but for the infusible one (I-6) at 306°C; the weight loss for both continues up to approximately 360°C. Then the residue loses weight slowly and at an almost constant rate up to 445°C.

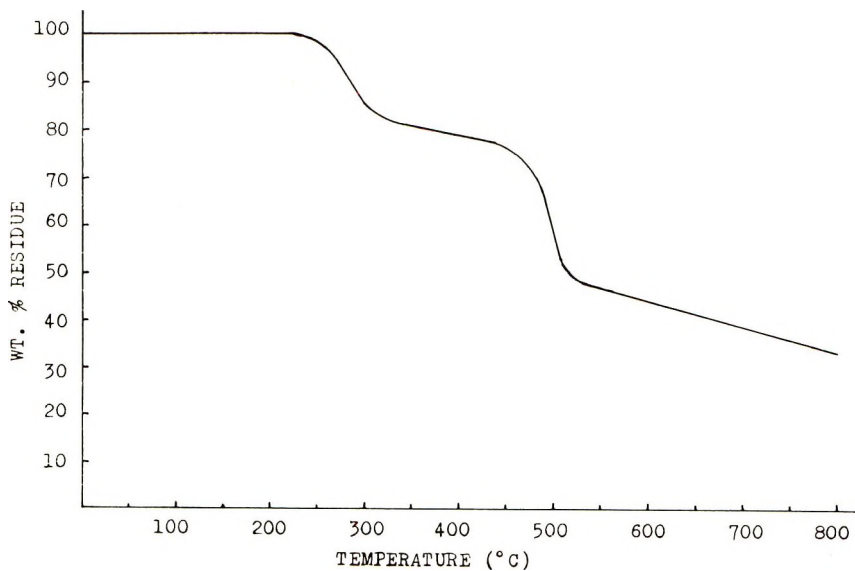
For PPr the first significant break in the curve occurs at a temperature lower than that for PEt (i.e., at 226°C) and continues up to approximately 330°C, followed by a slow loss of weight ranging from 330°C to 445°C. The weight loss in the last stage is very small (i.e., approximately 4.5% of the original weight).

Both polymers exhibit large weight losses from 445°C to about 530°C, and at higher temperature the residues slowly lose weight at a constant rate.

As mentioned above, the two thermogravimetry curves have similar trends and can be divided into four distinct stages; the first rapid loss in weight (A), a subsequent slow and constant-rate weight loss (B), a large, rapid weight loss in the range from 445°C to 530°C (C), and a final slow



(a)



(b)

Fig. 3. Thermogravimetric analysis of polymers under nitrogen: (a) PEt; (b) PPr.

weight loss above 530°C (D). Each stage will be discussed in detail below.

Stage A. In case of the PEt polymer, this stage ranges from 240°C to 360°C for the fusible polymer, and from 306°C to 360°C for infusible PEt. For the PPr polymer, this stage begins at 226°C and terminates at 330°C.

As was described in the infrared study of the heated samples, the PEt film heated at 330°C and the PPr film heated at 300°C showed stronger oxadiazole absorptions than the nonheated films. Hence it is reasonable to consider that the thermal conversion of hydrazide to 1,3,4-oxadiazole with elimination of olefins and dehydration occurs in stage A, and that the weight loss observed corresponds to a loss of the eliminated olefin and water.

For the fusible PEt polymer, initiation of weight loss occurs 60°C lower than for the infusible polymer. This difference can be explained by the difference in mobility of main chains of the polymer. The former, as described in the infrared study, contains a few unreacted 1,3,4-oxadiazole units. The existence of a large amount of hydrazide linkage makes the main chain flexible, and so would favor the intermediate configuration through which the cyclization reaction of hydrazide to 1,3,4-oxadiazole appears to proceed. Furthermore, in this point of view the fusible property of the former would be more favorable for cyclization at a high temperature.

As reported in the previous paper,³ PMe degrades above 320°C. In this case, the thermal fission of the hydrazide linkage and the thermal conversion of hydrazide to 1,3,4-oxadiazole are likely to be competing reactions above 320°C.

For PPr, since this stage ends at 330°C, it is reasonable to think that the cyclization is almost completed before initiation of the thermal fission of the hydrazide main chain. For PEt, however, this stage continues up to 360°C, so that in the latter part of this stage the cyclization reaction and the thermal fission of the hydrazide linkage are likely to compete with each other.

Stage B. The degree of completeness of the cyclization reaction, or on the contrary the content of the residual hydrazide linkage, will have much influence on the weight loss observed in this stage. This stage is believed to correspond also to the competitive reactions of cyclization of the residual hydrazide linkages to oxadiazole and of degradation of the thermally unstable parts, such as the residual hydrazide linkages and end groups. However, the slope of this stage is more gentle than that of the preceding stage. This is attributable to retardation of the rate of cyclization, which is caused by the chain stiffness of the oxadiazole-rich polymer formed *in situ*. The PPr polymer, which is almost completely converted to POx, shows only a small weight loss in this stage (i.e., approximately 4.5% of the original weight). The PEt polymer, whose hydrazide linkages are considered to be partially degraded and partially remain unchanged in the previous stage, would have more thermally unstable parts within its chains and on its polymer ends than the PPr polymer, so that a bigger weight loss

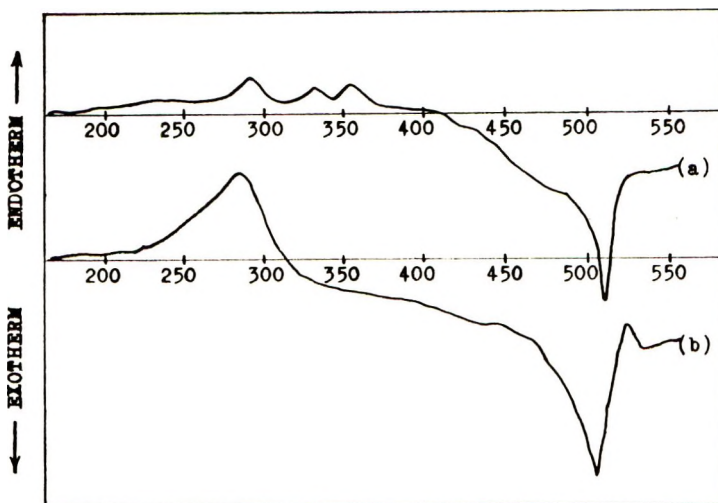


Fig. 4. Differential thermograms of polymers under nitrogen: (a) PEt; (b) PPr. Numbers are temperature (Centigrade).

would result in stage B (approximately 8.5% of the original weight for the fusible PEt and approximately 11.0% for the infusible polymer).

Stages C and D. In both of PEt and PPr, stage C ranges from 445°C to 530°C and the stage D begins at 530°C. Both stages correspond to decomposition of POx formed *in situ*.

As described above, poly-*N*-ethyl- and isopropylterephthalyldiazides can be converted to poly-*p*-phenylene-1,3,4-oxadiazole at a lower temperature and with a higher conversion than the high crystalline poly-*p*-phenylenediazide which was reported by Frazer and Wallenberger.⁶ This is associated with the difference in the reaction mechanism of cyclization and also with a difference in crystallinity. Some investigations of this problem will be described below, and further investigations will be reported in a future communication.

Figure 4 shows typical DTA thermograms for representative samples of PEt (I-5) and PPr (II-1). For the purpose of this study, approximately 100 mg of the dried sample was heated in a nitrogen atmosphere at a programmed heating rate of 5°C/min.

In the differential thermometry curve for PEt, small endothermic peaks are observed at 295, 336, and 356°C, and a strong exothermic peak appears at 509°C. Since the fusible PEt polymer has a polymer melt temperature in the range 284–292°C, the small endothermic peak at 295°C corresponds to polymer melting. This endotherm was also observed in the differential thermometry curve of the infusible PEt polymer without a corresponding weight loss and an apparent phase change. In this case this endotherm appeared to be associated with some chain transition (i.e., crystalline phase change). Above 300°C, the thermal behavior of PEt is complicated, as was described in the TGA study. To judge from the differential thermometry

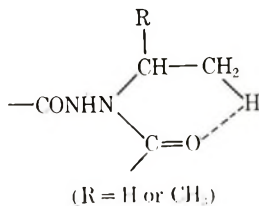
curve of PPr (described below), a peak corresponding to cyclization of PEt is expected to be strongly endothermic. However an exotherm due to decomposition of the thermally unstable parts is also expected in this range. Hence, it might be considered that a slight endotherm resulted apparently by overlapping of two peaks. The second endotherm at 336°C corresponds to the first break in the thermogravimetric curve, but does not coincide well with the maximum rate of the first weight loss. Consequently it will be concluded that this endotherm is attributed to the cyclization reaction. The fusible PEt polymer solidified as the cyclization reaction proceeded. This phase change after melting is attributable to the formation of polyoxadiazole. The third endotherm might indicate a first-order transition (crystalline phase change or melting) of the polyoxadiazole formed *in situ*. Further communications will clarify this problem in comparison with the thermal behavior of nonalkylated polyhydrazides and polyoxadiazoles.

The differential thermometry curve for PPr is much less complex than that for PEt. Two strong peaks are exhibited at 290°C (endotherm) and 503°C (exotherm). These peaks do coincide well with the maximum rate of weight losses of the stages A and C, respectively, in the corresponding thermogravimetric curve. Then the endothermic peak at 290°C is attributable to the oxadiazole formation reaction involving volatilization of propylene and water, and the exothermic peak at 503°C to the decomposition of POx formed *in situ*.

The PPr polymer is transformed to POx without melting. The oxadiazole percentage of the PPr polymers, which were determined from the weight loss of the first step of the thermogravimetric curve, were 57% and 52% for polymers II-1 and II-2, respectively. It has been found that the PMe polymer with oxadiazole content higher than approximately 30% showed no melting temperature. Hence the infusibility of the PPr polymers may be attributed to the high oxadiazole content. For the PPr polymer, however, the conversion of hydrazide to 1,3,4-oxadiazole begins at a low temperature (226°C), so that it is also probable that polymer melting cannot be observed because the cyclization reaction precedes polymer melting. The cause of infusibility of the PPr polymer is a question which cannot yet be resolved, because PPr polymer with oxadiazole content lower than 52% has not yet been synthesized by this method.

Mechanism of Thermal Conversion of Polyhydrazides to Polyoxadiazole

The oxadiazole formation reaction from the *N*-alkylhydrazide linkage appears to involve a new kind of *cis*-elimination reaction which proceeds via a transition state as



As described in the previous section, the initial part of the first break in the thermogravimetric curve for either PEt and PPr is believed to correspond almost purely to the cyclization reaction. Hence the evaluation of the activation energy of cyclization was attempted by use of this part of the curve. For this study approximately 100 mg of the dried sample was heated in a stream of nitrogen at programmed rates of 1, 2.5, 5, and 10°C/min. The temperature of a 2% weight loss was determined, and the value of the activation energy was evaluated from the relation of the heating rate and the temperature of the 2% weight loss according to the method of Ozawa.⁷ The values thus determined were 43.1 and 43.0 kcal/mole for PEt and PPr, respectively. These values differed by less than the experimental error. The explanation of these results may be related to the similarity of the mechanism of the cyclization reaction.

The activation energy value of about 43 kcal/mole is reasonable for a *cis*-elimination reaction. A more detailed study is in progress for many simpler compounds in order to clarify the mechanism of the cyclization reaction of *N*-alkylhydrazide to 1,3,4-oxadiazole by accumulating kinetic data of the similar reactions.

References

1. Y. Iwakura, K. Uno, S. Hara, and S. Kurosawa, *J. Polym. Sci. A-1*, **6**, 3357 (1968).
2. Y. Iwakura, K. Uno, S. Hara, and S. Kurosawa, *J. Polym. Sci. A-1*, **6**, 3371 (1968).
3. Y. Iwakura, K. Uno, S. Hara, and S. Kurosawa, *J. Polym. Sci. A-1*, **6**, 3381 (1968).
4. Y. Iwakura, K. Uno, and S. Hara, *J. Polym. Sci. A*, **3**, 45 (1965).
5. H. Sekiguchi and K. Sadamitsu, paper presented at the 16th Symposium of Polymer Science, Japan, November 1967.
6. A. H. Frazer and F. T. Wallenberger, *J. Polym. Sci. A*, **2**, 1117 (1964).
7. T. Ozawa, *Bull. Chem. Soc. Japan*, **38**, 1881 (1965).

Received December 2, 1969

Revised January 16, 1970

Radiation-Induced Copolymerization of Tetrafluoroethylene and 3,3,4,4,5,5,5- Heptafluoropentene-1 Under Pressure

DANIEL W. BROWN, ROBERT E. LOWRY, and LEO A. WALL,
National Bureau of Standards, Washington, D. C. 20234

Synopsis

An investigation was made of the γ -ray-induced copolymerization of tetrafluoroethylene and 3,3,4,4,5,5,5-heptafluoropentene-1. At 22°C at 5000 and 10 000 atm the polymerization rate changes little between 0 and 75 mole-% tetrafluoroethylene. Above 90 mole-% the rate increases greatly. Molecular weights vary with composition in a fashion similar to the variation of the rates. Crystallization occurs in the bulk pentene at 13 500 atm at 24°C. The polymerization rate is very low in the solid state. Under some conditions polymerization continues long after irradiation is ended. Both reactivity ratios favor the pentene. Several copolymer properties were studied. The polymers are amorphous and soluble in perfluoro ethers, perfluoro alkanes, and perfluoroaromatics if they contain less than 80% tetrafluoroethylene. The glass temperatures of the amorphous polymers decrease and the thermal and radiation stability increases as the tetrafluoroethylene content increases.

INTRODUCTION

This paper describes the copolymerization of tetrafluoroethylene and 3,3,4,4,5,5,5-heptafluoropentene-1 and some properties of their copolymers. Previously a similar study was made with 3,3,3-trifluoropropene as the second comonomer.¹ The results found in the two studies are compared in order to show the different effects of the *n*-perfluoropropyl and trifluoromethyl groups on polymerization characteristics and copolymer properties.

EXPERIMENTAL

Both monomers were purchased from Peninsular ChemResearch, Gainesville, Florida. The tetrafluoroethylene (TFE) was freed from inhibitor as before.¹ Chromatographic analysis revealed only traces ($\sim 0.1\%$) of impurities in four separate purchases of the heptafluoropentene which were used without special purification. Both monomers were passed over Ascarite, dried on phosphorus pentoxide, and thoroughly degassed before use.

The amount of TFE charged in each run was calculated from manometric measurements by use of the perfect gas laws. The fluoropentene was

weighed into the bombs. Polymerization at high pressure and polymer isolation were accomplished as before.¹ Radiation was from an external ⁶⁰Co source. The final monomer composition was calculated from the initial composition, the polymer composition, and the conversion.

Elemental analyses were performed with a Sargent carbon and hydrogen combustion apparatus. Copolymer compositions were calculated from the carbon contents or by an infrared technique described below. The spectrophotometer used was a Perkin-Elmer 221.

Intrinsic viscosities in hexafluorobenzene, glass transition temperatures T_g , and thermogravimetric analyses were obtained as before.^{1,2}

RESULTS

Copolymer Analyses

Carbon contents of the TFE and the pentene are 24.02 and 30.63 wt-%, respectively. The difference between these values is small so that the uncertainty in the copolymer composition ordinarily would be quite large. To decrease the uncertainty, the number of analyses was increased. Five of the copolymers were analyzed ten times each. The uncertainty in their mole fractions of TFE was about 0.02. Ten analyses on every sample would have been prohibitively expensive so the samples above were used as calibrants for infrared analysis of other samples.

Studies were made of the intensity-composition dependence of several infrared bands. All calibrations examined were nonlinear, resulting in sensitivity variations with composition. The method finally chosen involved use of spectra of solutions of 4-7 wt-% polymer in FC-75 (a mixture of perfluoroethers available from Minnesota Mining and Mfg. Co.) at 2990 cm^{-1} . Here more than 90% of the incident light is transmitted by the solvent in cells 0.1 mm thick. By placing solvent in the reference beam the transmission scale could be expanded 10-fold. Ratios of polymer absorp-

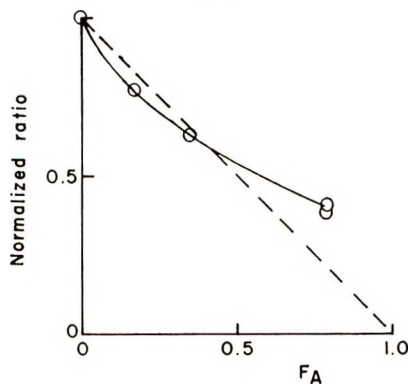


Fig. 1. Ratio of polymer absorbance at 2990 cm^{-1} to the weight fraction of polymer in FC-75 divided by the corresponding ratio for poly-3,3,3,4,4,5,5-heptafluoropentene-1 as a function of the mole fraction of the tetrafluoroethylene in the polymer.

ance in solution at 2990 cm^{-1} to the weight fraction of polymer were divided by the corresponding ratio for the homopolymer of the heptafluoropentene-1. Figure 1 is a plot of these normalized ratios versus F_A , the mole fraction of TFE, in the polymer. Uncertainties in F_A associated with the use of Figure 1 as a calibration curve are about 0.03 and 0.06 at F_A 's of 0.17 and 0.79, respectively.

The absorption maximum shifts from 2955 to 3000 cm^{-1} and a new band appears at 3040 cm^{-1} as F_A increases. Presumably the latter is due to the presence of CH_2 adjacent to CF_2 in the copolymers.³ This combination is not present in the homopolymer of the fluoropentene. Overlap of old and new bands at 2990 cm^{-1} probably causes the curve in Figure 1 to rise above the diagonal. Although a region of overlapping bands is objectionable for analysis use of other bands gave less linear curves.

Polymerization

Results of polymerizations at low radiation intensity are listed in Table I. The headings of the first six columns require no explanation. The next columns give, respectively, the mole percentage of monomer charged converted to polymer; the rate of polymerization R_p , assuming a first-order polymerization rate constant; R_p/R_B , the copolymerization rate relative to the pentene homopolymerization rate; and the intrinsic viscosity of the polymers $[\eta]$ in hexafluorobenzene at 29.7°C .

A year and a half subsequent to the bulk of the work, additional experiments were performed to characterize the reproducibility of the system. These results are included at the bottom of Table I, where they are given the same number as the comparable original experiment followed by an identifying letter. In these lettered experiments, F_A is calculated from the carbon content as determined by duplicate elemental analyses. The dose rate is 20% less than originally used because of the time lapse; this difference would be expected to decrease rates and raise values of $[\eta]$ by about 10%. Experiments 3A, 3B, and 3C are essentially identical. The greatest deviation of the results in these three experiments from one another occurs in the rates where that rate found in experiment 3B is 15% below the average value (0.45%/hr). This average agrees well with the rate in experiment 3 (0.49%/hr). Polymer intrinsic viscosities in experiments 3A, 3B, and 3C agree well but they are about 30% higher than in experiment 3. Values of F_A differ by a 0.04 or less in the old and new work; this is within the uncertainty (0.05 for two determinations) of the analysis. Experiment 13A was performed to check the behavior of the fluoropentene alone. Rates and intrinsic viscosities are slightly higher than in experiment 13. Experiment 10 appeared to have a suspiciously low rate, so 10A was performed. The rate and polymer intrinsic viscosity are 2.4 and 2.8 times the respective values in experiment 10. An additional experiment (10A') used the same pressure and starting monomer composition but the radiation time was increased in order to find out if the rate changed much with conversion at this composition. Apparently this is not the case, since the rate is

TABLE I
Copolymerization of Tetrafluoroethylene and 3,3,4,4,5,5,5-Heptafluoropentene-1^a

Expt.	Pressure atm	Mole fraction C ₂ F ₆			Time, hr	Polymer, mole-%	R _p , %/hr	R _p /R _B	[η], dl/g
		Initial	Final	Polymer					
1	5000	0.97	0.97	0.89 ^b	2.0	2.5	1.25	30.5	insol
2	5000	0.94	0.94	0.79 ^b	7.0	2.24	3.32	7.8	1.0
3	5000	0.93	0.95	0.79 ^b	23.2	10.8	0.49	11.9	0.97
4	5000	0.94	0.94	0.94	46.2	100	>4.5	>100	insol
5	5000	0.53	0.53	0.35	27	1.65	0.061	1.49	0.12
6	5000	0.43	0.44	0.26	89	5.6	0.064	1.76	0.11
7	5000	0.21	0.22	0.08	141	6.6	0.048	1.17	0.07
8	5000	0	0	0	282	10.9	0.041	1	0.10
9	10000	0.90	0.93	0.75	9.3	15.2	1.78	4.8	1.62
10	10000	0.77	0.77	0.48	3.4	1.44	0.42	1.1	0.56
11	10000	0.65	0.69	0.35 ^b	17.7	12.0	0.72	1.9	0.74
12	10000	0.54	0.51	0.21	16	9.5	0.63	1.6	0.74
13	10000	0	0	0	24	8.63	0.38	1	0.32
14	10000	0	0	0	48	16.3	0.37	1	0.33
15	14200	0.41	0.44	0.17 ^b	0.5	10.1	21.3	19.2	0.51
16	14200	0.24	0.29	0.05	2.4	19.2	8.8	7.9	0.30
17	14200	0	0	0	5.25	5.7	1.11	1	0.42
18 ^c	5000	0.53	0.39	0.35	5.25	8.6 ^d	~1.8	4	0.13
19 ^c	5000	0	0	0	21.0	9.1	0.45	1	0.03
3A ^e	5000	0.92	0.94	0.76	23.8	11.0	0.49	12.0	1.36
3B ^e	5000	0.92	0.94	0.75	23.8	8.9	0.39	9.5	1.30
3C ^e	5000	0.92	0.94	0.76	23.8	10.7	0.47	11.5	1.42
13A ^e	10000	0	0	0	24	8.91	0.39	1	0.37
10A ^e	10000	0.79	0.81	0.47	3.8	3.81	1.02	2.6	1.54
10A ^e	10000	0.80	0.84	0.48	15.2	12.8	0.91	2.3	1.63

^a Dose rate 2000 rad/hr, 22°C except as indicated.

^b By elemental analysis.

^c At 100°C.

^d About 10% of charge went to nonpolymeric products.

^e Dose rate 1700 rad/hr.

about 10% lower than in experiment 10A. The low rate and intrinsic viscosity listed for experiment 10 are thought to result from oxygen contamination, since the fluoropentene alone has shown (in other experiments) about half the normal rate and intrinsic viscosity if it is not degassed or if dry oxygen is added to degassed monomer before polymerization.

It appears that careful attempts to reproduce these experiments are likely to give rates and intrinsic viscosities within about 10% of those anticipated. However, two- to threefold discrepancies might result if the degassing were inadequate. Composition data appear reproducible to within the uncertainties indicated under "Copolymer Analysis."

Results of experiments which involved no radiation are in Table II. These indicate that at 22°C thermal rates are much smaller than those at 2000 rad/hr, except at pressures well above 10,000 atm when A is present. At 100°C and 5000 atm a relatively small thermal polymerization rate was obtained when 72% A was present. The yield of nonpolymeric products in experiment 24 much exceeded that of the polymer. One product, also found in experiment 18, is perfluorocyclobutane. Two others were detected by chromatographic analysis but not identified. Their volatility suggests they may be cross dimers, i.e., a combination of the two different monomers.

TABLE II

Thermal Polymerization of Tetrafluoroethylene and 3,3,4,4,5,5,5-Heptafluoropentene-1^a

Expt	Pressure, atm	C ₂ F ₄ charged, mole fr.	Time, hr	Polymer, mole-%	R _p , %/hr	[η], dl/g
20	10000	0	18	0	0	—
21	10000	0.91	16	1.6	0.10	3.20
22	15500	0	18	0	0	—
23	15500	0.26	2	16.5	9.0	1.13
24 ^b	5000	0.72	3.3	2.4 ^c	~0.9	0.39

^a At 22°C except as noted.

^b At 100°C.

^c About 30% of charge went to nonpolymeric products.

Polymerization after removal from the source occurs under some conditions. A detailed study of the dark polymerization is in progress. Data in Table III indicate the pressure region where this and an additional effect become important. Experiments 25, 26, 29, and 30 show that when there is no storage conversions are nearly proportional to radiation time at 5000 and 10 000 atm. Therefore, experiment 27 and 28 indicate that there is no dark effect at 5000 atm. Comparison of experiments 29 and 31 shows that conversion more than doubled on 24 hr storage at 1000 atm. Experiments 32 and 33 suggest that the dark rate is less important if TFE is present. At 14 000 atm more than seven times as much polymer was obtained after storage. Thus in absolute amount the dark effect depends strongly on pressure, being undetected at 5000 atm and large at 14 000 atm.

TABLE III
 After Effects in the Polymerization of 3,3,4,4,5,5,5-Heptafluoropentene-1^a

Expt	Pressure, ^b atm	In source, hr	Stored, hr	Polymer, %	Rate, %/hr	$[\eta]$, dl/g
25	5000	38.3	0	8.3	0.23	0.063
26	5000	75.0	0	13.7	0.20	0.064
27	5000	36.4	50	8.7		0.065
28	5000	43.8	120	9.0		0.065
29	10000	3.5	0	7.2	2.1	0.25
30	10000	6.0	0	12.6	2.3	0.25
31	10000	3.5	17	17.0		0.29
32 ^c	10000	3.0	0	9.9	3.5	0.55
33 ^c	10000	3.0	24	14.8		0.77
34	14000	1.0	0	3.6	3.7	0.40
35	14000	1.0	3	25.8		0.57
36	15500	1.0	0	0.09	0.09	
37 ^d	15500	2.0	0	62	~50	0.92

^a Tetrafluoroethylene present as noted; 22°C, 38000 rad/hr.

^b Before polymerization.

^c 61 mole-% C₂F₄ charged.

^d 26 mole-% C₂F₄ charged.

A sluggish crystallization can occur at 13 400 atm at 22°C, but without preformed crystals the pentene remains liquid at 14 000 atm for times longer than the duration of these experiments. Crystallization actually occurred only in experiment 36; a low rate resulted. Addition of 26% TFE prevents crystallization even at 15 500 atm, so the rate remained high.

DISCUSSION

Mechanism

At 5000 and 10 000 atm most of the results are characteristic of long-chain free-radical reactions in which the steady-state assumption is approximately valid. Rates were found to be independent of conversion, to increase with temperature and to vary approximately as the square root of the radiation intensity. Comparison of rates in Table I with those at corresponding pressures and no storage in Table III demonstrates the latter point. Intrinsic viscosities of these polymers decrease as radiation intensity increases. G values (yield/100 eV absorbed) for monomer consumption may be calculated from the data in Tables I and III by assuming a G value for initiation. If the latter is low, these exceed 250 showing that the kinetic chain is quite long.

The greater conversion found at 10 000 atm after storage seems inconsistent with the invariance of rate with time shown by experiments 29 and 30, which involved no storage. If growing species exist long after the radiation exposure ends their number should increase during irradiation; consequently, the polymerization rate should increase with dose. Work

still in progress has elucidated this apparent paradox. Radiation forms a catalyst in the pentene which decomposes thermally at such a slow rate that its effect on the rate in the source is very slight. The subsequent dark polymerization is initiated by this catalyst. It was initially presumed that pressure-induced viscosity increases caused the dark effect.⁴

Composition Diagram

When the chain is long, the copolymer composition depends on the monomer composition and four propagation constants. These constants are denoted k_{AA} , k_{AB} , k_{BB} , and k_{BA} , where A refers to TFE and B refers to the second monomer, the pentene. In each constant the first subscript indicates the kind of radical end and the second indicates the monomer that is added. An equation relating the instantaneous polymer and monomer compositions is⁵ eq. (1):

$$F_A = (r_1 f_A^2 + f_A f_B) / (r_1 f_A^2 + 2f_A f_B + r_2 f_B^2) \quad (1)$$

F_A is as defined previously; f_A and f_B are the monomer mole fractions of TFE and the pentene, respectively, and r_1 and r_2 are the rate constant ratios k_{AA}/k_{AB} and k_{BB}/k_{BA} , respectively.

Figure 2 is a plot of F_A versus f_A . Symbols represent experimental values taken from Table I, by using the arithmetic mean of the initial and final monomer compositions for f_A . The lines were calculated by using eq. (1) and the indicated values of r_1 and r_2 . For the middle line these were chosen by applying the Fineman-Ross method⁶ to data from the experiments at 5000 atm and 22°C. The upper and lower lines were calculated by using

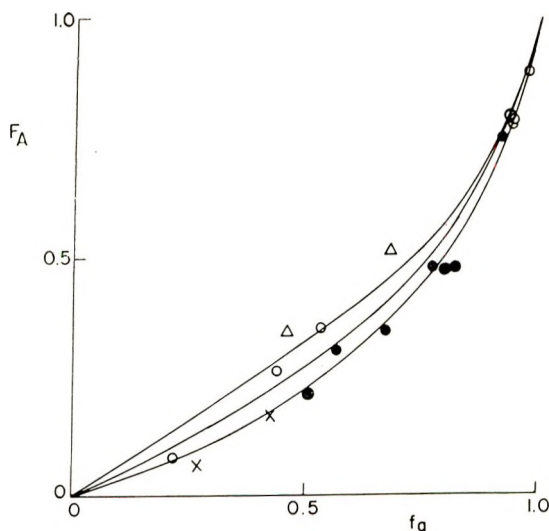


Fig. 2. Mole fraction of tetrafluoroethylene in polymer as a function of that in monomer for copolymers with 3,3,4,4,5,5,5-heptafluoropentene-1: (O) 22°C, 5000 atm; (●) 22°C, 10,000 atm; (X) 22°C, 14,000 atm; (Δ) 100°C, 5000 atm. Curves are theoretical for (upper) $r_1 = 0.21$, $r_2 = 1.5$; (middle) $r_1 = 0.21$, $r_2 = 2.3$; (lower) $r_1 = 0.21$, $r_2 = 3.2$.

the same r_1 as the middle line and r_2 's chosen to span most of the values plotted. It is believed that r_1 and r_2 probably do not change significantly with pressure or temperature in our experimental range. The composition data scatter and more than a twofold change would be required to be significant.

The values of r_1 and r_2 indicate that both radicals add pentene in preference to TFE. A similar situation exists in the TFE-3,3,3-trifluoropropene system, where r_1 and r_2 were found to be 0.12 and 5.0, respectively.¹ The ratio of r_1 in the TFE-pentene system to r_1 in the latter system is the ratio of rate constants for addition of 3,3,3-trifluoropropene and 3,3,4,4,5,5,5-heptafluoropentene-1 to a radical with a TFE end. This ratio is about equal to 2. Thus addition of a vinyl monomer with a perfluoroalkyl group to a radical with a CF_2 end appears little different for monomers with one and three carbon perfluoroalkyl groups.

Copolymerization Rate

The copolymer rate equation [eq. (2), ref. 1] can be used to calculate R_p/R_B if values are assumed for R_A/R_B , the ratio of the polymerization rate of TFE to that of the pentene. Two lines calculated from this equation are shown in Figure 3. When f_A is zero the theoretical and experimental rate ratio equals one. In the experimental range of compositions the position and shape of the theoretical curves are not much affected by variations in the cross-termination parameter ϕ and the assumed value of R_A/R_B , so long

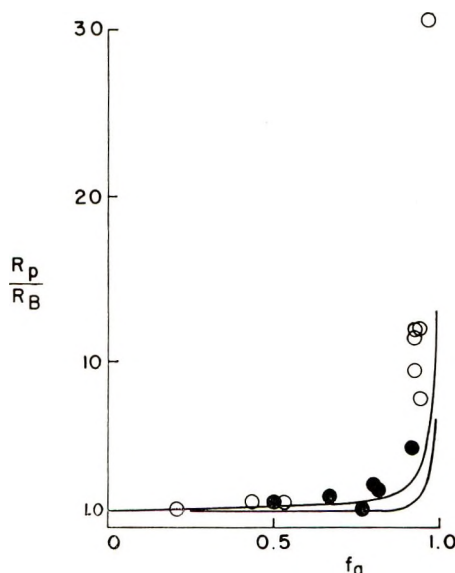


Fig. 3. Variation in the copolymerization rate with the fraction of tetrafluoroethylene, comonomer 3,3,4,4,5,5,5-heptafluoropentene-1. Curves: calculated according to eq. (2) of ref. 1; for $r_1 = 0.21$, cross termination parameter = 1-10, $R_A/R_B = 10^2-10^3$: (upper) $r_2 = 1.5$; (lower) $r_2 = 3.2$. Experimental results: (O) 5000 atm; (●) 10000 atm.

as the latter exceeds 100. Experimental rates are represented by the symbols on the figure. Behavior qualitatively like that of the theoretical curves is found at 5000 and 10 000 atm, in that the observed rate ratios change only slightly over much of the composition range and then increase greatly at high values of f_A . However, almost all the experimental values of R_p/R_B are somewhat above either line. This may indicate that the termination rate constants or the G value for initiation depend on f_A .

At 14 000 atm, R_p/R_B increases greatly at even moderate f_A . Presumably, this is due to increases in the rate of thermal initiation with f_A at this pressure (Table II). A similar observation and explanation apply at 100°C. Variations in the initiation rate with f_A violate an assumption used in deriving the rate equation, so it is not applied to these data.

Activation enthalpies and volumes are about 30 kJ/mole (7 kcal/mol) and $-10 \text{ cm}^3/\text{mole}$, respectively.

Variations in Intrinsic Viscosity

Quantitative relationships between $[\eta]$ and molecular weight for these materials are unknown so discussion must be of a qualitative nature. Polymers formed at pressures of 5000 and 10 000 atm at 22°C have intrinsic viscosities that vary with composition much as do the rates. This implies that the rate controls $[\eta]$ and that transfer is not important. For an R_p of 1%/hr the degree of polymerization is about 10^4 at 2000 rad/hr if transfer is nil. The polymer of the fluoropentene formed at 100°C and 5000 atm has a smaller intrinsic viscosity than that formed at 22°C, implying that transfer becomes important at high temperature. Copolymers formed at 100°C have intrinsic viscosities which increase markedly at moderate contents of TFE. Presumably TFE is less prone to undergo transfer than the pentene so that addition of TFE decreases transfer. This will increase the molecular weight if transfer is important in the homopolymerization.

Copolymer Properties

The copolymers were found to be dissolved on opening the pressure vessels at -80°C if the initial TFE fraction content was 0.80 or less. Polymer from experiment 3 did not dissolve in mixed monomer (93% TFE) at 23°C in a sealed tube. Therefore, unless application of pressure increases the solubility, polymer formed in mixtures of this or higher TFE content precipitates during formation.

Polymers from all runs except 1 and 4 are soluble in hexafluorobenzene, FC-75, and perfluorohexane at room temperature. In hexafluorobenzene, sample 1 swells to about three times its dry volume; sample 4 swells very slightly.

The solubility of the homopolymer of the pentene in nonaromatic perfluorosolvents is surprising when one considers that it has a hydrocarbon backbone. Intrinsic viscosities of one sample in FC-75 and hexafluorobenzene were the same, 0.42 dl/g, indicating no great difference in the dimensions of the polymer molecule in the two solvents. Neither the poly-

mer of trifluoropropene nor its amorphous copolymers with TFE is soluble in FC-75 or perfluorohexane although they dissolve readily in hexafluorobenzene.

One of the more interesting observations is the contrasting solubility behavior of the amorphous copolymers of TFE with the heptafluoropentene and the trifluoropropene in fully fluorinated nonaromatic solvents. The copolymer with the trifluoropropene containing 70% TFE has more CF_2 groups than the homopolymer of the fluoropentene. Yet the former polymer is insoluble and the latter is soluble in these solvents. Thus a structure consisting of a hydrocarbon backbone with three carbon perfluoroalkyl side chains on alternate carbons is more compatible with fluorocarbon solvents than a structure containing many CF_2 groups located in the backbone, and in which each CH_2CH unit of the backbone has only one perfluoromethyl branch.

The glass transition temperatures of the copolymers were measured by the differential scanning calorimetric technique described previously.² The values obtained were in the range 23–58°C, the latter value being that for the homopolymer of the heptafluoropentene-1. The minimum T_g (23°C) occurs between 75 and 89 mole-% TFE.

At the same composition, ~84% TFE, the copolymers become insoluble at room temperature, which can be the result of incipient crystallinity. However, x-ray diffraction patterns which were obtained on samples 1, 3, 4, and 17 indicated definite crystallinity only in sample 4, which contains 94% TFE. In the earlier work with TFE-trifluoropropene copolymer 1, in-

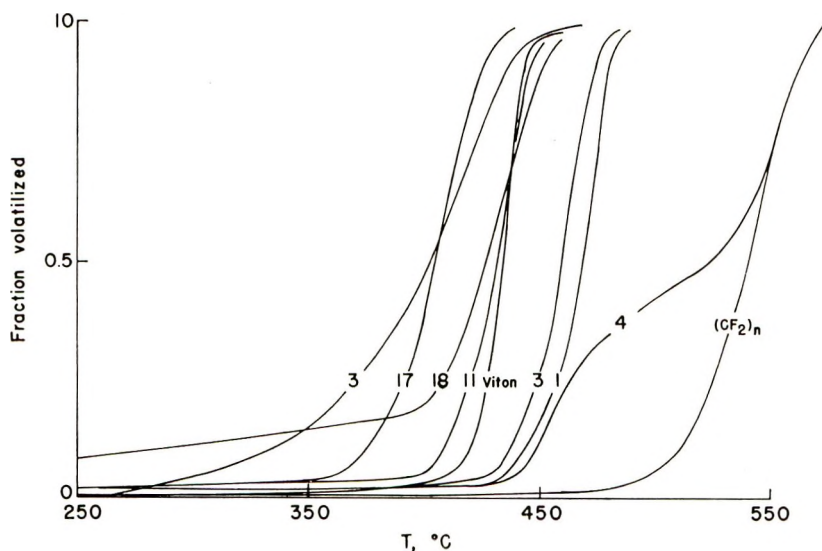


Fig. 4. Thermogravimetric analyses of copolymers of tetrafluoroethylene and 3,3,4,4,5,5,5-heptafluoropentene-1. 1.5°C/min. The number on each curve indicates use of polymer formed in the experiments of the same number in Table I. Curve 3 on left is for a polymer sample that had received 29 Mrad in vacuum before pyrolysis.

solubility occurred at 85% TFE content, while x-ray measurements indicated that crystallinity appeared at 90% TFE content.

Thermogravimetric Analyses

Figure 4 shows results of thermogravimetric analyses performed *in vacuo*. There is a progressive increase in stability as the fraction of TFE increases. In sample 4 the very high conversion in the polymerization presumably is associated with the decrease in slope at 30% weight loss. High polymerization temperature or prior exposure of the polymer to γ -radiation lowers the thermal stability. Reference curves are shown for polytetrafluoroethylene and Viton (the commercial copolymer of vinylidene fluoride and tetrafluoroethylene).

The stability of pentene-TFE and propene-TFE copolymers is the same provided the concentration of tetrafluoroethylene is the same.

Effect of γ -Radiation

Polymers of several compositions were irradiated in vacuum and immersed in hexafluorobenzene. If completely soluble their intrinsic viscosities were determined; otherwise their gel fractions were measured. Results are in Table IV. The homopolymers dissolved completely, whether irradiated above or below T_g . They also became extremely brittle. The copolymers were at or above T_g when irradiated. Those having TFE contents of 75% or more gelled on exposure to γ -radiation. Those containing 51% or less of TFE remained soluble.

Acrid gases were present when the tubes of homopolymer were opened, indicating that hydrogen fluoride forms. Such gases were less noticeable above the copolymers.

TABLE IV
Effect of γ -Radiation in Vacuum on Copolymers of Tetrafluoroethylene and 3,3,4,4,5,5,5-Heptafluoropentene-1^a

F_A , mol fr.	Dose, Mrad	[η], dl/g		W_g gel fr.
		Before	After	
0	7.2	0.49	0.15	0
0	26	0.49	0.07	0
0	14	0.49	0.06	0
0	24 ^b	0.49	0.06	0
0.35	26	0.50	0.12	0
0.51	26	0.39	0.15	0
0.75	26	1.62	gel	0.80
0.79	7.2	0.97	gel	0.80 ^c
0.79	26	0.97	gel	0.88 ^c
0.79	44	0.97	gel	0.90 ^c

^a 45°C, dose rate = 3.6 Mrad/hr except as noted.

^b Irradiated at 3.2 Mrad/hr, 70°C.

^c The ratio of scissions to crosslinked units is estimated to be 0.4 from the variation in gel content with dose.

The homopolymer of 3,3,3-trifluoropropene and its copolymers with TFE crosslinked when irradiated.¹

This paper is based on research supported by the U.S. Army Research Office, Durham, North Carolina.

Certain commercial materials are identified in this paper in order to adequately specify the experimental procedure. In no case does such identification imply recommendation or endorsement by the National Bureau of Standards, nor does it imply that the material or equipment identified is necessarily the best available for the purpose.

References

1. D. W. Brown and L. A. Wall, *J. Polym. Sci. A-1*, **6**, 1367 (1968).
2. D. W. Brown and L. A. Wall, *J. Polym. Sci. A-2*, **7**, 601 (1969).
3. T. Wentink, L. J. Willwerth, and J. P. Phaneuf, *J. Polym. Sci.*, **55**, 551 (1961).
4. D. W. Brown, R. E. Lowry, and L. A. Wall, paper presented at American Chemical Society Meeting, New York, September 1969; *Polymer Preprints*, **10**, 1395 (1969).
5. P. J. Flory, *Principles of Polymer Chemistry*, Cornell Univ. Press, Ithaca, N. Y., 1953, p. 178.
6. M. Fineman and S. D. Ross, *J. Polym. Sci.*, **5**, 259 (1950).

Received July 21, 1969

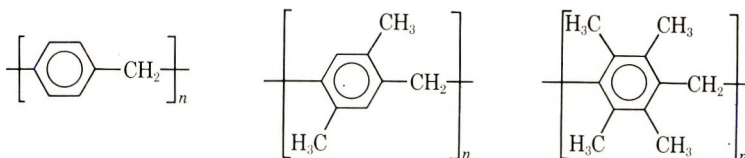
Revised January 16, 1970

Synthesis and Properties of Some Linear Oligobenzyls and Polybenzyls

G. MONTAUDO, F. BOTTINO, S. CACCAMESE, P. FINOCCHIARO, and G. BRUNO, *Institutes of Industrial, Organic and General Chemistry, University of Catania, Italy*

Synopsis

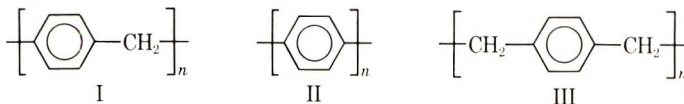
Properties of some linear oligobenzyls corresponding to polybenzyl, poly (2,5-dimethylbenzyl), and poly (2,3,5,6-tetramethylbenzyl) systems are correlated to those of relative polymers. From infrared and x-ray diffraction data, evidence is found that



oligomers tend to assume the same crystal structure of the polymer as early as the tetramer or pentamer stage. Syntheses of oligomers are described. Linear, crystalline polymers, necessary for comparison with oligomers, have been prepared and characterized. Polymerization conditions have been explored to some extent; relevant data are tabulated and discussed.

INTRODUCTION

Recently, interest in polybenzyl polymers (I) has developed from the analogies with *p*-polyphenylenes (II) and *p*-polyxylylenes (III) which are well known polyaromatic systems.^{1,2}



Polycondensation of benzylchloride at room temperature gives a highly branched, amorphous, low melting polymer, which has found little use so far.¹

On the contrary, a linear, crystalline, barely soluble and intractable material is formed in the polycondensation of chloromethylidurene, where all the positions in the benzene ring are blocked by methyls except the position *para* to the chloromethyl group.^{3,4}

Between these two extremes, some authors⁵ have tried to find systems where the substitution is sufficient to prevent branching, but not enough to

inhibit solubility and chain growth. Others⁶ have obtained improvement in the properties of polybenzyls by using very low temperatures of polymerization.

In our approach,^{7,8} we have focused attention on the synthesis of appropriate low molecular weight model compounds and on the study of their solid-state and solution properties.

It is within the scope of our program to investigate syntheses and physical properties of polybenzyls containing differently substituted rings (alternating copolymers).

Syntheses of oligomers may provide information about synthetic routes that could be followed for the synthesis of copolymers.

In this paper, as a first step in the project, we describe some new oligobenzyls and some structure-properties correlations involving oligomers and polymers.

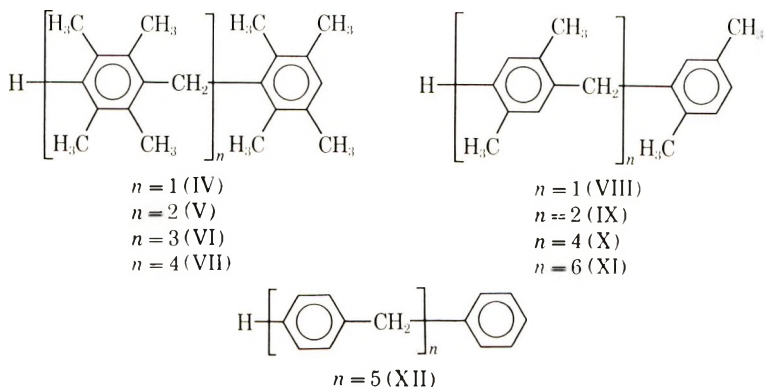
Higher oligomers show melting points, infrared spectra and x-ray patterns similar to those of the related polymers.

This suggests that the formers assume the same conformational structure as the polymers.

RESULTS AND DISCUSSION

Oligomers

Compounds IV–XII were prepared. Their structures have been checked by elemental analysis, molecular weight determination, NMR and infrared spectra, and x-ray powder analysis.



Syntheses were performed in two steps: an aromatic hydrocarbon was chloromethylated and subsequently condensed by Friedel-Crafts reaction with the appropriate hydrocarbon to yield the desired oligomer.

According to this scheme one might choose several routes to prepare a definite oligomer. However, the selection of compounds in the condensation step was often found crucial in order to avoid side reactions (i.e., branching, isomerization and polymerization).

In Figure 1 are plotted melting points versus molecular weights for the three oligobenzyl series investigated, together with the melting points of related polymers.

The durene and *p*-xylene series show higher melting points than the benzene series.

Such behavior is contrary to that observed in the *p*-oligophenylenes⁹ and in *p*-polyphenylenes.¹⁰ In fact, unsubstituted *p*-oligophenylenes show higher melting points with respect to *p*-2,5 dimethylphenylene.⁹

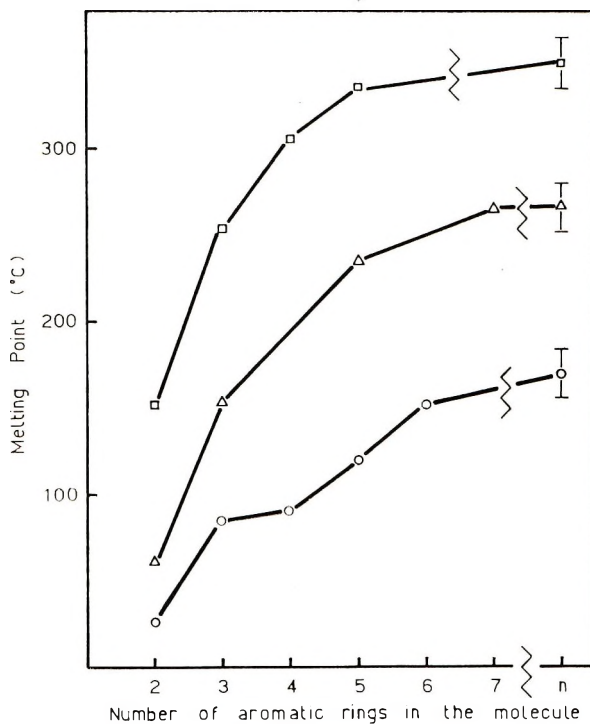


Fig. 1. Melting temperatures versus molecular weight for oligobenzyls: (□) IV-VII; (Δ) VIII-XI; (○) XII.

It may be that in the *p*-oligophenylenes the *ortho* substitution disturbs benzene rings from quasi coplanarity (in solid state), and prevents compact crystal packing of these molecules. The situation is different in polybenzyls because there is a methylene group between adjacent benzene rings.

Curves in Figure 1 rapidly approach asymptotic values, and higher oligomers show melting points in the same range as the related polymers. This might suggest that these oligomers tend to assume the same crystalline structure presented by polymers.

This interpretation has been substantiated by infrared and x-ray data (Figs. 2-4).

In the *p*-xylene series (Fig. 2) the pentamer appears to have virtually identical infrared and x-ray patterns as the heptamer and the polymer.

In the durene series (Fig. 3) the pattern becomes nearly constant already at the tetramer stage.

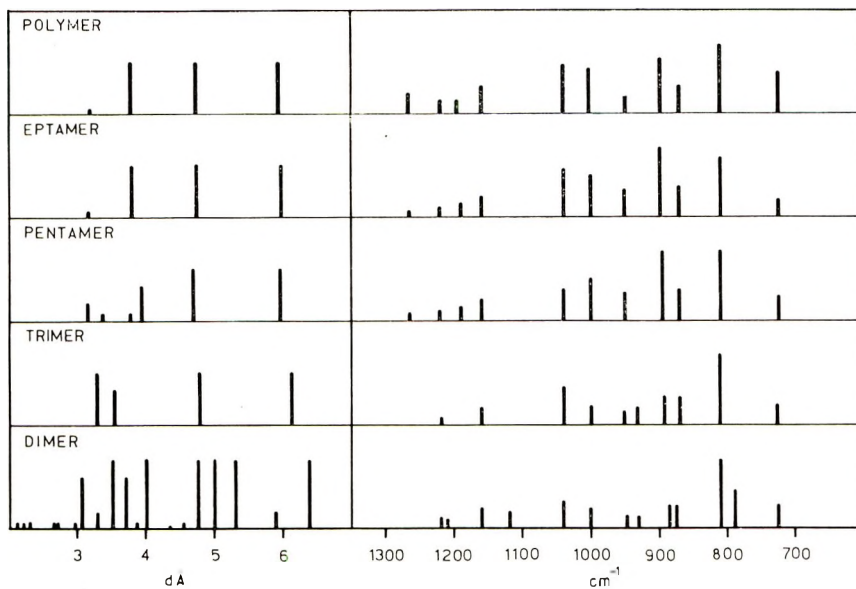


Fig. 2. X-Ray powder diffraction patterns (left) and infrared spectra (right) of oligo (2,5-dimethylbenzyl) and related polymer.

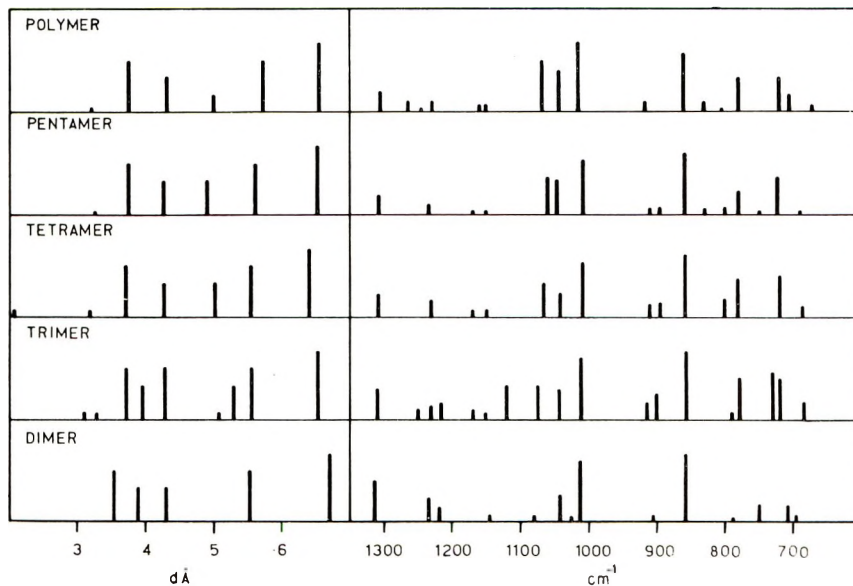


Fig. 3. X-ray powder diffraction patterns (left) and infrared spectra (right) of oligo (2,3,5,6-tetramethylbenzyl) and related polymer.

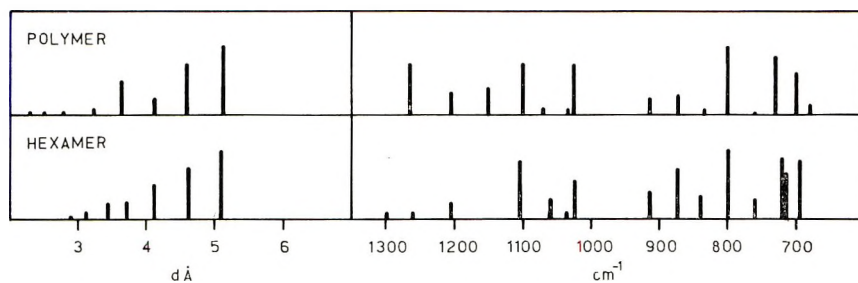


Fig. 4. X-ray powder diffraction patterns (left) and infrared spectra (right) of polybenzyl polymer and oligomer (hexamer).

In the unsubstituted (benzene) series (Fig. 4) the infrared spectrum of the hexamer matches that of the polymer less well, although x-ray features are in fair agreement.

In the three homologous series, the solubility decreases sharply as molecular weight increases. Compounds of the durene series are the least soluble, even in high-boiling aromatic solvents. This is probably due to the shielding effect of methyl groups on the aromatic rings, which restricts the possibility of interaction with the aromatic solvent of the inside of the molecular envelope.

Polymers

Linear, crystalline polymers, necessary for comparison with oligomers have been prepared and characterized. Polymerization conditions were explored to some extent. Relevant data are summarized in Table I.

Poly-2,3,5,6-tetramethylbenzyls are high-melting, sparingly soluble or insoluble materials. Data on these polymers have been reported also by other workers,³⁻⁵ but details on polymerization conditions and/or polymers characteristics are often missing so that useful comparison with our data is not always possible.

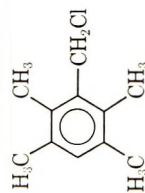
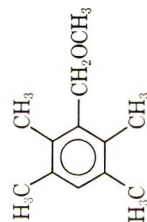
Poly-2,5-dimethylbenzyls appear to be crystalline even when prepared at room temperature (Table I). They are soluble in xylene and *o*-dichlorobenzene above 100°C. Melting points range around 235–270°C for higher molecular weights.

Kennedy and Isaacson⁶ report two crystalline polymers of this formula, prepared at low temperature, having very different melting points [148–165°C and 300(190)°C, respectively]. The low melting sample is probably a mixture of oligomers (Fig. 1). The x-ray diffraction patterns of the higher melting sample coincide fairly well with ours.

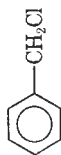
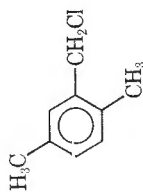
Crystalline, linear polybenzyls were described recently by Kennedy and Isaacson⁶ by polycondensation of benzyl chloride at very low temperatures (–135°C).

However, our attempts to duplicate the experiments of Kennedy and Isaacson failed to give, directly, crystalline polymers. High conversion

TABLE I
Synthesis and Characteristics of Polybenzyls

Monomer	No.	Solvent	Catalyst	[C]/[M], $\times 10^2$, mole/- mole	Temp, °C	Time min	Conver- sion, %	M_n^a	Mp, °C	Crystallinity <i>d</i> spacings, Å ^b
	1	C ₆ H ₅ NO ₂	SnCl ₄	4.1	20	1,200	93.5	940	302	
	2	C ₆ H ₅ NO ₂	SnCl ₄	1.6	50	1,560	75.0	743	310	
	3	C ₆ H ₅ NO ₂	SnCl ₄	64.0	50	1,680	75.0	1,800	320	
	4	C ₆ H ₅ NO ₂	SnCl ₄	8.0	100	600	31.2	1,950	320	
	5	C ₆ H ₅ NO ₂	SnCl ₄	3.2	100	600	32.5	2,380	370	
	6	C ₆ H ₅ NO ₂	SnCl ₄	20.0	50	350	70.0	Insoluble	350	{ 6.54 (s); 5.72 (s); 5.00(m); [4.32 (m); 3.76 (s); 3.20 (w),

7	EtNO ₂	SnCl ₄	S.S	67	20	52.0	1,260	270	6.03 (s); 4.73 (s); 3.83 (s); 3.23 (s).
8	EtNO ₂	SnCl ₄	7.0	-20	300	66.0	680	184	5.93 (s); 4.73 (s); 3.82 (s); 3.23 (w).
9	EtNO ₂	AlCl ₃	3.0	22	10	11.0	1,260	235	
10 ^c	EtCl	AlCl ₃	9.1	-80	10	98.0	2,500	250	6.03 (s); 4.74 (s); 3.86 (s)
F1 ^d							2,300	260	Amorphous
F2 ^d							5,400	276	
								dec.	
11	EtCl	AlCl ₃	9.1	-131	10	11	800	205	6.03 (s); 4.69 (s); 3.82 (s); 3.23 (w).
12 ^c	EtCl	AlCl ₃	3.0	-135	15	10	1,560	115	Amorphous
F3 ^d								165	{5.17 (s); 4.61 (s); 4.12 (m); 3.68 (m); 3.24 (m)
F4 ^e								185	{5.12 (s); 4.56 (s); 4.14 (m); 3.64 (m); 3.17 (w); 2.82 (w); 2.50 (w); 2.28 (w).
F5 ^e							2,000	155	{5.13 (s); 4.57 (s); 4.34 (m); 3.64 (m); 3.31 (w)



^a Determined by vapor-pressure osmometry at 130°C in *o*-dichlorobenzene.

^b s = strong; m = medium; w = weak.

^c whole polymer.

^d Fractionated by xylene/methanol.

^e Extracted by MEK.

samples yielded amorphous polymers even when fractionated. Fractionation of low conversion samples (10%), combined with selective extraction with the appropriate solvents yielded crystalline polymers (Table I).

EXPERIMENTAL

Analytical Procedures

Infrared spectra were recorded on a Perkin-Elmer 237 infrared spectrophotometer.

NMR spectra were obtained on a Varian A 60 analytical spectrometer, equipped for variable temperature work.

The *d* spacing of crystalline polymers and of oligomers were calculated from powder diffraction photographs taken with Ni-filtered $\text{CuK}\alpha$ radiation (camera 57.3 mm.).

Molecular weights determinations were obtained by vapor-pressure osmometry by use of a Mechrolab 302 Thermoelectric Osmometer which could be operated in the temperature range 25–130°C in xylene or *o*-dichlorobenzene solutions.

Melting points were obtained in glass capillary tubes sealed under vacuum and checked with a Kofler hot-stage microscope.

Elemental analyses were obtained commercially.

Materials

Nitroethane and nitrobenzene were purified by following standard procedures.¹¹

Ethyl chloride of high purity ($\geq 99.8\%$) was purified by passage of the gas over BaO.

Aluminum chloride was sublimed before use, and ethyl chloride solutions were obtained and titrated by the method of Kennedy and Thomas.¹²

Stannic chloride was vacuum-distilled before use.

Diphenylmethane, *p*-xylene, and durene were commercial products (Fluka) of highest available purity.

Benzyl chloride and 2,5-dimethylbenzylchloride were freshly vacuum-distilled before use.

1,4-Bis(chloromethyl)-2,5-dimethylbenzene was a commercial product (Fluka) used without further purification.

2,3,5,6-Tetramethylbenzyl chloride, 2,3,5,6-tetramethylmethoxymethylbenzene, and 1,4-bis(chloromethyl)-2,3,5,6-tetramethylbenzene were obtained according to literature procedures.^{13,14}

Polycondensation Procedure

All experiments were carried out in thermostated Pyrex reactors under a stream of nitrogen. Polymerization reactions developed a deep red color which disappeared when the reaction was terminated by addition of methanol (1:20). Methanol addition caused polymer precipitation; the precipitate was washed with HCl, methanol, and dried under vacuum.

The same general procedure was employed when chloromethyl or methoxymethyl derivatives were used.

In the reactions carried out with methoxymethyl derivatives, methanol was removed as formed by applying gentle vacuum. The amount of catalyst necessary was generally greater than for reactions in which chloromethyl derivatives were used.

Oligomer Synthesis

Bis(2,3,5,6-tetramethylphenyl)methane (IV). To a stirred solution of chloromethyldurene (0.01 mole) and durene (0.07 mole) in nitroethane at 50°C was added SnCl₄ (0.005 mole). The reaction (as well as all the other reactions described below) was carried out under nitrogen. Stirring was continued for 1 hr at 50°C, the solution poured into ice, and the crude product obtained was treated with HCl, hot methanol and dried under vacuum (yield 45%).

Recrystallization from ethanol afforded a white solid, mp 152–153°C (lit.¹⁵ mp 155–156°C).

NMR (CHCl₃) data gave 5.53 (1), 7.63 (6), 7.85 (6) τ , where τ values are against TMS as internal standard and the number in parentheses refers to relative intensities (for all other NMR data as well).

The x-ray *d* spacings were 6.70 (s), 5.58 (s), 4.30 (m), 3.89 (m), and 3.54 (s) Å.

The calculated molecular weight for C₂₁H₂₈ was 280.5, found 280 (*o*-dichlorobenzene, 130°C).

3,6-Bis(2,3,5,6-tetramethylbenzyl)-1,2,4,5-tetramethylbenzene (V). Bis-chloromethyldurene (0.01 mole) and durene (0.08 mole) were melted under vacuum in a flask, and Zn powder (0.1 g) added. The temperature was kept at 120°C for 20 min and HCl evolved was removed by aspiration. The excess of durene was removed by extracting the reaction mixture with *n*-hexane; the residue (yield 50%) was crystallized from dioxane, mp 263–264°C (lit.¹⁶ mp 263°C).

NMR (CHCl₃) gave τ values of 5.55 (1), 7.65 (3), 7.83 (3), 7.87 (3) τ .

The x-ray *d* spacings were 6.52 (s), 5.63 (s), 5.30 (m), 5.07 (w), 4.27 (s), 3.96 (m), 3.72 (s), 3.27 (w), and 3.10 (w) Å.

The molecular weight calculated for C₃₂H₄₂ is 426.7; the value found was 427 (*o*-dichlorobenzene, 130°C).

Bis[2,3,5,6-tetramethyl-4(2,3,5,6-tetramethylbenzyl)phenyl]-methane (VI). The chloromethyl derivative (XIII) (0.01 mole) and IV (0.05 mole) were reacted as described in the preceding paragraph. The crude product obtained was treated with hot xylene and dried. The residue (yield 35%) was crystallized from *o*-dichlorobenzene, mp 305–307°C (under vacuum).

NMR (*o*-dichlorobenzene, 150°C) gave τ values of 5.57 (1), 5.60 (2), 7.75 (12), 7.85 (6), 7.88 (6) τ . The x-ray *d* spacings were at 6.40 (s), 5.52 (s), 5.02 (m), 4.27 (m), 3.73 (s), 3.17 (w), and 2.08 (w) Å. The molecular weight calculated for C₄₃H₅₆ was 572.9; the found value was 571.5 (*o*-dichlorobenzene, 130°C).

3,6-Bis[2,3,5,6-tetramethyl-4-(2,3,5,6-tetramethylbenzyl)benzyl]-1,2,4,5-tetramethylbenzene (VII). Bischloromethyldurene (0.01 mole) and IV (0.08 mole) were reacted as above. The crude product was treated with hot xylene and dried. The residue (yield 40%) was crystallized from *o*-dichlorobenzene, mp 335–337°C (under vacuum).

NMR (*o*-dichlorobenzene, 150°C) showed τ values of 5.67 (1), 5.74 (1), 7.75 (3), 7.88 (9), 7.92 (3) τ . The x-ray *d* spacings were at 6.51 (s), 5.63 (s), 4.91 (m), 4.27 (m), 3.76 (s), and 3.26 (w) Å. The calculated molecular weight for C₅₄H₇₀ was 719.1; the found value was 721 (*o*-dichlorobenzene, 130°C).

Chloromethylation of bis(2,3,5,6-tetramethylphenyl)methane(IV). Chloromethylation of (IV) was carried out according to general literature methods¹³ by using equimolecular amounts of hydrocarbon and formaldehyde in acetic acid at 60–80°C for 4 hr. A product melting at about 240°C was obtained in 80% yield. Extraction of this crude product by *n*-hexane gave (30% yield) crystalline [4-(chloromethyl)-2,3,5,6-tetramethylphenyl] (2,3,5,6-tetramethylphenyl) methane (XIII), mp 130–132°C. The infrared spectrum showed $\nu_{\text{CH}_2\text{Cl}}$ 1266 cm⁻¹. The molecular weight calculated for C₂₂H₂₉Cl was 328.9; found, 330 (*o*-dichlorobenzene, 130°C).

The residue from *n*-hexane extraction, crystallized from dioxane, afforded (20% yield) crystalline bis[4-(chloromethyl)-2,3,5,6-tetramethylphenyl] methane (XIV), mp 211–213°C.

The infrared spectrum showed $\nu_{\text{CH}_2\text{Cl}}$ 1266 cm⁻¹.

The molecular weight calculated for C₂₃H₃₀Cl₂ was 377.3; found, 378 (*o*-dichlorobenzene, 130°C).

Bis(2,5-dimethylphenyl)methane (VIII). To a stirred solution of 2,5-dimethylbenzylchloride (0.071 mole) and *p*-xylene (0.65 mole) in nitroethane (100 ml) at 25°C, was added SnCl₄ (0.01 mole). Stirring was continued for 30 min at 25°C, the solution was poured into ice, extracted with chloroform, dried over CaCl₂, and distilled under reduced pressure. The crude product (yield 85%), crystallized from ethanol, melted at 60–61°C (lit.¹⁷ mp 60–60.5°C).

NMR (CHCl₃) gave 5.95 (1), 7.67 (6) τ .

The x-ray *d* spacings were 6.38 (s), 5.89 (m), 5.31 (s), 5.00 (s), 4.76 (s), 4.55 (w), 4.37 (w), 3.99 (s), 3.86 (w), 3.71 (s), 3.51 (s), 3.29 (m), 3.08 (s), 2.97 (w), 2.68 (w), 2.64 (w), 2.30 (w), 2.21 (w), 2.12 (m), 1.92 (w), 1.84 (w), and 1.77 (w) Å.

1,4-Bis(2,5-dimethylbenzyl)-2,5-dimethylbenzene (IX). To a stirred solution of 1,4-bis(chloromethyl)-2,5-dimethylbenzene (0.05 mole) and *p*-xylene (0.81 mole) in nitroethane (100 ml) was added SnCl₄ (0.01 mole) at 25°C. During the reaction a white product precipitated. After 1 hr the mixture was poured into ice and the white solid filtered, washed with ethanol, and dried (yield 85%).

Recrystallization from an ethanol–dioxane mixture yielded a white solid melting at 153–154°C.

NMR (CHCl_3) τ values were 5.94 (2), 7.63 (6), 7.73 (3) τ , NMR (*o*-dichlorobenzene, 150°C) showed 5.94 (2), 7.70 (6), 7.78 (3) τ .

The x-ray *d* spacings were at 6.13 (s), 4.79 (s), 3.55 (m), and 3.30 (s) Å.

Anal. Calcd for $\text{C}_{26}\text{H}_{20}$: C, 91.17%; H, 8.83%; molecular weight, 342.5. Found: C, 90.80%; H, 8.90%; molecular weight *o*-dichlorobenzene, 130°C, 341.

1,4-Bis[2,5-dimethyl-4-(2,5-dimethylbenzyl)benzyl]-2,5-dimethylbenzene (X). To a stirred solution of 1,4-bis(chloromethyl)-2,5-dimethylbenzene (0.0065 mole) and VIII (0.031 mole) in nitroethane (50 ml) at 25°C was added ZnCl_2 (0.002 mole). After 10 min the mixture was poured into methanol, and the precipitate which separated was filtered, washed with HCl, and dried (yield 35%). Crystallization from dioxane yielded a white solid melting at 234–236°C.

NMR (CHCl_3) showed τ values of 5.94 (4), 7.65 (6), 7.73 (9) τ ; NMR (*o*-dichlorobenzene, 150°C) was 5.94 (4), 7.70 (6), 7.75 (9) τ .

The x-ray *d* spacings were at 5.97 (s), 4.70 (s), 3.96 (m), 3.76 (w), 3.34 (w), and 3.17 (w) Å.

Anal. Calcd. for $\text{C}_{44}\text{H}_{30}$: C, 91.29%; H, 8.71%; molecular weight, 578.8. Found: C, 90.96%; H, 8.86%; molecular weight (*o*-dichlorobenzene, 130°C), 588.

1,4-Bis(2,5-dimethyl-4-[2,5-dimethyl-4-(2,5-dimethylbenzyl)benzyl]benzyl)-2,5-dimethylbenzene (XI). To a stirred solution of 1,4-bis(chloromethyl)-2,5-dimethylbenzene (0.0033 mole) and IX (0.012 mole) in nitroethane (100 ml), was added ZnCl_2 (0.001 mole) at 80°C.

After 30 min the mixture was poured into methanol, and the precipitate which separated was filtered, washed with HCl, and dried (yield 70%). Crystallization from xylene afforded a white solid which melted at 262–266°C.

NMR (*o*-dichlorobenzene, 150°C) showed τ values of 5.95 (2), 7.68 (2), 7.75 (5) τ . The x-ray *d* spacings were at 5.88 (s), 4.75 (s), 3.82 (s), and 3.18 (w) Å.

Anal. Calcd for $\text{C}_{62}\text{H}_{40}$: C, 91.34%; H, 8.66%; molecular weight 815.1. Found: C, 91.60%; H, 8.36%; molecular weight (*o*-dichlorobenzene, 130°C), 830.

4,4' - Bis[benzyl - 4(benzyl)]diphenylmethane (XII). To an ethyl chloride (200 ml) stirred solution of 4,4'-bis(chloromethyl)diphenylmethane, XV (0.02 mole) and diphenylmethane (0.30 mole) was added a solution of AlCl_3 (0.5 g) in ethyl chloride (20 ml) at -10°C. After 20 min the mixture was poured in methanol, the white solid precipitate was filtered, washed with HCl, and dried (yield 40%).

Recrystallization from ligroin (120–150°C) gave a white crystalline product which melted at 130–140°C and had molecular weight of 610.

The product, thought contaminated by trace of polymer, was slowly sublimed (200°C 0.05 mm Hg) to yield a white microcrystalline powder melting at 153–156°C.

The infrared spectra showed an aromatic *para* substitution band at 800 cm^{-1} .

The NMR (CCl_4) τ values were 5.94 (3), 5.87 (2), 2.65 (8), 2.41 (5) τ .

The x-ray *d* spacings were at 5.09 (s), 4.60 (s), 4.12 (m), 3.71 (m), 3.44 (m), 3.12 (m), and 2.87 (w) Å.

Anal. Calcd. for $\text{C}_{41}\text{H}_{36}$: C, 93.14%; H, 6.86%; molecular weight, 528.7. Found: C, 93.24%, H, 6.72%; molecular weight (*o*-dichlorobenzene, 130°C), 535.

To a stirred solution of diphenylmethane (0.20 mole) in anhydrous CS_2 (200 ml) at -20°C was added SnCl_4 (0.125 mole) and chloromethyl ether (0.675 mole). After 1 hr the mixture was poured into ice, and the crude product was extracted with CS_2 and distilled under reduced pressure. The white solid obtained (XV, yield 50%) was crystallized from ligroin (120–150°C); mp, 106–108°C (lit.¹⁸ mp, 108°C).

References

1. H. Lee, D. Stoffey, and K. Neville, *New Linear Polymers*, McGraw-Hill, New York, 1967, pp. 83, 307.
2. R. W. Lenz, *Organic Chemistry of Synthetic Polymers*, Interscience, New York, 1967, p. 228.
3. H. C. Haas, D. L. Livingston, and M. Saunders, *J. Polym. Sci.*, **15**, 503 (1955).
4. A. A. Vansheidt, E. P. Melnikova, and G. A. Gladkowskii, *Vysokomol. Soedin.*, **4**, 1178 (1962); *ibid.*, **4**, 1303 (1963).
5. W. C. Overhults and D. A. Ketley, *Makromol. Chem.*, **95**, 143 (1966).
6. J. P. Kennedy and R. B. Isaacson, *J. Macromol. Chem.*, **1**, 541 (1966).
7. F. Bottino, G. Montaudo, P. Maravigna, *Ann. Chim. (Rome)*, **57**, 972 (1967).
8. G. Montaudo, F. Bottino, and S. Caccamese, *Ann. Chim. (Rome)*, **57**, 992 (1967).
9. H. O. Wirth, F. W. Herrmann, and W. Kern, *Makromol. Chem.*, **80**, 120 (1964).
10. J. K. Stille, private communication.
11. A. I. Vogel, *Elementary Practical Organic Chemistry*, Part 1, 2nd ed., Longmans, London, 1966, p. 250.
12. J. P. Kennedy and R. M. Thomas, *J. Polym. Sci.*, **46**, 481 (1960).
13. R. R. Aitken, G. M. Badger, and J. W. Cook, *J. Chem. Soc.*, **1950**, 331.
14. Bergwerkverband, Neth. Appl. 6,401,266; *Chem. Abstr.*, **62**, 7695 (1964).
15. C. M. Welch and H. A. Smith, *J. Amer. Chem. Soc.*, **73**, 4391 (1951).
16. H. Kaemmerer and M. Harris, *Makromol. Chem.*, **66**, 215 (1963).
17. R. C. Huston and D. T. Ewing, *J. Amer. Chem. Soc.*, **37**, 2394 (1915).
18. C. Maquin and H. Gault, *C. R. Acad. Sci. (Paris)*, **234**, 629 (1952).

Received December 1, 1969

Revised January 23, 1970

The Role of Solvent Polarity and Cocatalyst Structure in the Cationic Polymerization of 3,3-Bis(chloromethyl)oxetane*

I. PENCZEK and ST. PENCZEK, † *Research Institute of Plastics,
Department of Polymerization, Warsaw, Poland*

Synopsis

In the cationic polymerization of 3,3-bis(chloromethyl)oxetane induced by BF_3 the solvent polarity (toluene, methylene chloride, ethylene chloride, nitrobenzene, and nitromethane) does not influence the k_{tr}/k_p ratio, where k_{tr} stands for the rate constant of chain transfer to polymer. Increase of the overall polymerization rate is due mainly to the increase of k_i . The application of the steady-state conditions in which the slow formation of the active centers is compensated by the unimolecular chain transfer to polymer allowed the determination of k_{tr}/k_p ratios for several chain-transfer agents of low molecular weight. Alcohols and ethers of different basicities were used. It was established that the k_{tr}/k_p ratio is a linear function of $-pK_a$ of the chain-transfer agents.

It was previously stated¹ that the reactivity of oxetanes in cationic polymerization is greatly affected by the structure and position of substituents in the oxetane ring. It was shown that oxetane, 3,3-dimethyloxetane, 3,3-dimethyleneoxetane, and 3,3-pentamethyleneoxetane polymerize under the standard conditions one to two hundred times faster than 3,3-bis(chloromethyl)oxetane. It was also stressed in the cited paper that the basicity of the investigated monomers should be related with these observed differences.¹ On the other hand, as we were able to demonstrate previously, the mechanism of the cationic polymerization of oxetane elaborated by Rose² can be extended with some additional assumptions for the case of 3,3-bis(chloromethyl)oxetane polymerization, in spite of the heterogeneous character of the last process.³ By using the $[\eta]-\overline{DP}$ relation determined in this Institute by Brzeziński⁴ it was also found that the modified Mayo plot can be used in the 3,3-bis(chloromethyl)oxetane polymerization and, therefore, the determination of the k_{tr}/k_p and $k_{tr(a)}/k_p$ ratios as well as k_{tr} became possible³; here k_{tr} stands for the rate constant of the chain transfer to polymer and $k_{tr(a)}$ for the rate constant of the chosen chain-transfer agent. The comparison of these ratios for several oxetanes could provide valuable information concerning the observed differences of the overall reactivities of oxetanes.

* Presented in Part at the IUPAC Macromolecular Symposium, Prague, 1965.

† Present address: Polymer Institute, Ministry of Education and Polish Academy of Sciences, Łódź 40, Poland.

However, this comparison can be used if the investigated systems are homophasic (i.e., if all the elementary reactions take place in the same phase) and if the slight differences in the dielectric constant of the monomer-solvent mixtures do not influence the reaction rates ratios markedly. For the investigated group of monomers a knowledge of the dependence between elementary reaction rates and the monomer structure is also very important factor in the proper formulation of the new copolymers.

As a measure of reactivity of the growing ion-pair the reaction with transfer agents can be used. This method was successfully applied, for instance, in the case of styrene derivatives.⁵ The use of the appropriate chain-transfer agent for a series of oxetanes should give the necessary information concerning the comparative reactivities of the growing ions.

Thus, in the present work the influence of solvent polarity and structure of chain-transfer agent on the polymerization of 3,3-bis(chloromethyl)oxetane catalyzed by gaseous boron fluoride was investigated.

EXPERIMENTAL

Monomer

3,3-Bis(chloromethyl)oxetane (BCMO) was prepared and purified according to our previous publication.³ The product with $n_D^{20} = 1.48582-1.48586$ was collected and stored at low temperature in the dark under purified argon. Before every kinetic run the necessary quantity of monomer was freshly distilled as previously described.³ The absolute purity of the monomer according to several tests made in this Institute (cryometry, GLC and refractometry) was better than 99.9 mole-%. The water content varied from run to run; the sum of H₂O present in the system was determined from the kinetic data.

Solvents

n-Heptane, cyclohexane, toluene, carbon tetrachloride, methylene and ethylene chlorides, nitrobenzene, and nitromethane were purified according to the published procedures.⁶

Cocatalysts

Methyl and butyl alcohols, butyl and β -chloroethyl ethers, dioxane and anisole were used after careful purification according to the published methods.⁶

Catalyst

Gaseous BF₃ in this work was used directly from the cylinder (BF₃ purum > 99.5%, Fluka).

Polymer Precipitant

Methyl alcohol was used as received. To stop polymerization, methyl alcohol containing enough NH₃ to neutralize all the BF₃ used was added.

Polymerization Apparatus and Procedure

Essentially the same methods as these described earlier³ were used; instead of the BF_3 -anisole decomposition unit a gas buret was employed, mercury being used as the closing liquid and CaH_2 as the desiccant for the gas. All the manipulations with monomer, solvents, and cocatalysts were performed with the use of Hamilton-type or high-precision syringes.

Intrinsic Viscosity and DP

The viscosities were measured at 40°C in cyclohexanone solution³ and the DP values were calculated according to the relation determined with the fractionated samples:⁵ $\overline{\text{DP}} = 1230 [\eta]^{1.195}$ which was used instead of the equation: $\overline{\text{DP}} = 1503 [\eta]^{0.91}$ obtained for the unfractionated samples.³

Experimental Conditions

All the investigations were carried out at $[\text{M}] = 1.0$ mole/l. and $[\text{BF}_3] = 0.10$ mole/l. at 0°C. Cocatalysts and chain transfer agents were used in varied concentrations.

RESULTS

The effect of solvent structure on the cationic polymerization of BCMO was qualitatively studied by Kambara and Hatano.⁷ In this work, to obtain the quantitative dependences the polymerization rates R_p were measured in every solvent at different H_2O (cocatalyst and chain transfer agent) concentrations. This problem was studied in the same manner as previously reported.³ For a given H_2O concentration, the rate was determined from the slopes of conversion curves. As the time for the catalyst addition was 10–20 sec, the conversion-time curves were linear up to ~10% and passed through the origin. Similar plots were obtained for polymerizations in toluene, CCl_4 , chlorobenzene, CH_2Cl_2 , $(\text{CH}_2\text{Cl})_2$, nitrobenzene, CH_2Cl_2 - CH_3NO_2 mixtures and pure CH_3NO_2 . The results (except those for CCl_4 and the nitro solvents) are given in Figure 1. To obtain the quantitative dependence, the comparison of the rates was made at the same cocatalyst concentration. It was also verified that on passing from CH_2Cl_2 solution (polar solvent) to toluene (nonpolar solvent) the order of reaction in monomer did not change, but still remains somewhat higher than first order.³ No additional measurements of the reaction orders were made for the other solvents.

The polymerization in *n*-heptane and cyclohexane solutions cannot be conducted at 0°C as the monomer crystallizes out of solution. At 10°C, however, solutions in cyclohexane are perfectly stable, although immediately after the catalyst addition (10–15 sec) sudden precipitation takes place, and the rate measured is abnormally high. The $\overline{\text{DP}}$'s of polymers obtained in cyclohexane were also considerably higher, indicating the separation of monomer or a monomer/catalyst complex. For the CCl_4

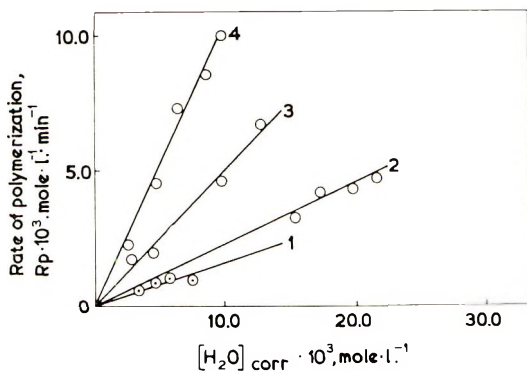


Fig. 1. Dependence of the polymerization rate R_p on $[H_2O]$ in (1) toluene, (2) chlorobenzene, (3) methylene chloride, and (4) 1,2-dichloroethane solution.

solution the rate was as high as that for CH_2Cl_2 solutions, the \overline{DP} being "normal," however.

Different behavior was observed for nitro solvents, the rate of polymerization in CH_3NO_2 being, at comparable conditions, about ten times higher than that for the pure methylene chloride. The polymerization rate depends almost linearly on the CH_3NO_2/CH_2Cl_2 volume ratio but the molecular weight decreases rapidly with increasing CH_3NO_2 content. The \overline{DP} of polymer obtained in the pure CH_3NO_2 is only 80 as compared to \overline{DP} of 600 for polymer formed in pure CH_2Cl_2 at the same conditions. In nitrobenzene solution the \overline{DP} is also very low and equal to 120.

The dependence of the polymerization rate and polymerization degree on the composition of the CH_3NO_2/CH_2Cl_2 mixture is given in Figure 2. The general dependence of the polymerization rate on the dielectric constant (d.c.) of the solvent used is given in Figure 3 (the dielectric constant of BCMO at $25^\circ C$ and 1–100 kHz is 4.46 ± 0.02 and as the $[M]$ is low it was not taken into consideration).

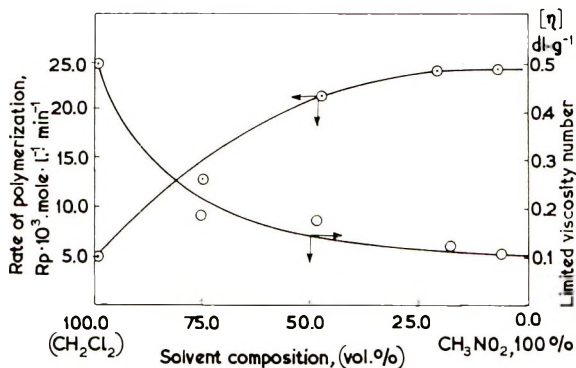


Fig. 2. Variation of the polymerization rate R_p and limited viscosity number on the composition of $CH_3NO_2-CH_2Cl_2$ mixture.

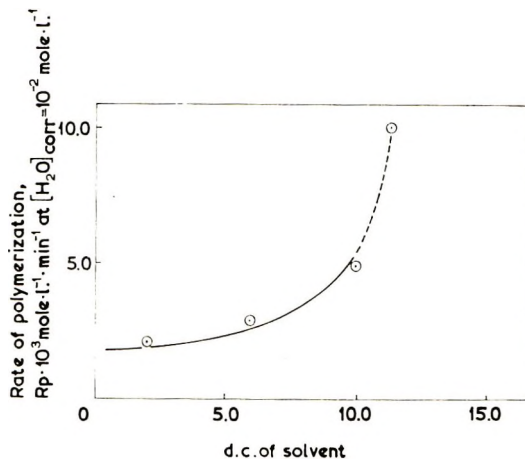


Fig. 3. Polymerization rate vs. dielectric constant of solvent used; conditions same as for Fig. 1.

To obtain further information concerning the dependence of the elementary reaction rates on the solvent polarity the linear plot $[M]/\overline{DP} = k_{tr}/k_p + k_{tr(a)}[H_2O]_{corr}/k_p$ was used. It was demonstrated in our previous work that this relation is valid in the case of BF_3 -catalyzed BCMO polymerization.³ This relation, obtained for low $[H_2O]_{corr}$ (0.0025–0.012 mole/l.) in toluene, CH_2Cl_2 and $(CH_2Cl)_2$ solutions, is plotted in Figure 4. The intersection of the plot with ordinate gives the value of k_{tr}/k_p ; the values of $k_{tr(n)}/k_p$ can be calculated from the slopes of the straight lines according to the equation used. The calculated ratios are: $k_{tr}/k_p = 1.0 \times 10^{-3}$ mole/l. and $k_{tr(H_2O)}/k_p = 0.19$ (in both CH_2Cl_2 and $(CH_2Cl)_2$ solutions) and 0.35 in toluene solution. Thus, in both cases the ratios k_{tr}/k_p are less than unity. These results indicated (see also discussion), that in comparison with trioxane polymerization⁸ the k_{tr}/k_p values are rather low. Therefore it was of interest to compare the action of substances other than H_2O

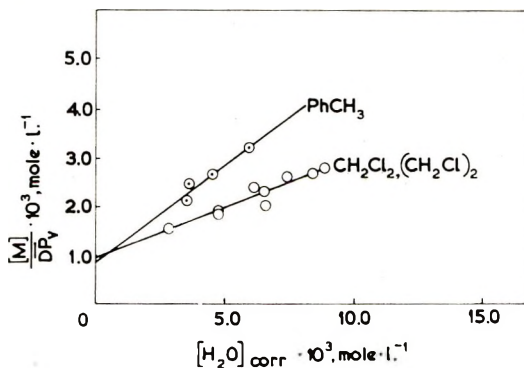


Fig. 4. Dependence of the $[M]/\overline{DP}$ ratio on $[H_2O]_{corr}$ for CH_2Cl_2 solution.

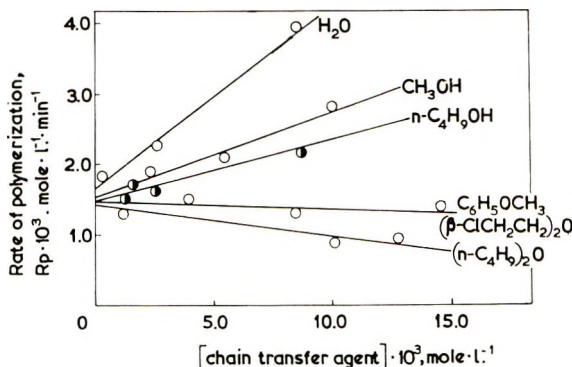


Fig. 5. Dependence of the polymerization rate R_p on the additive concentration for CH_2Cl_2 solution.

to determine the influence of the chain transfer agent structure on its reactivity with a growing ion-pair. For this investigation methanol, butanol, butyl ether, 2-chloroethyl ether and anisole were chosen. They represent two different classes of compounds for which the basicities are fairly well established.⁹

The dependence of the polymerization rate on the concentration of additive used is given in Figure 5. The plot of $\overline{\text{DP}}$ versus additive concentration is given in Figure 6. In this case the equation

$$[\text{M}]/\overline{\text{DP}} = k_{tr(\text{H}_2\text{O})}/k_p + k_{tr}[\text{H}_2\text{O}]_0/k_p + k_{tr(a)}[\text{Add}]/k_p$$

can be used for low conversions. As the first two terms of the right-hand side were constant through the investigation of the every additive but differ slightly from series to series (since monomer source changes), the intercept should give the sum of k_{tr}/k_p and $k_{tr}[\text{H}_2\text{O}]_0/k_p$; these sums will be different and will depend on the level of adventitious impurities. The slopes, however, can be used as a measure of the reactivity of a given addi-

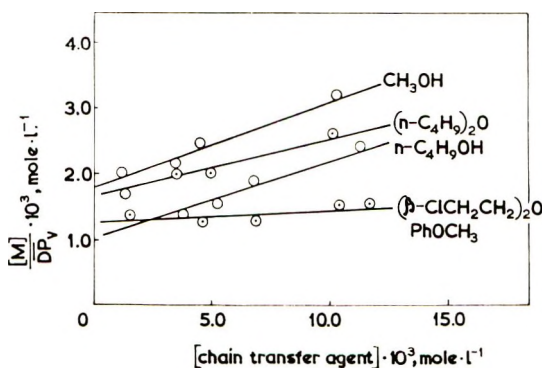


Fig. 6. Determination of the transfer coefficients $[\text{M}]/\overline{\text{DP}}$ vs. concentration of transfer agent for CH_2Cl_2 solution.

tive in the chain transfer. The calculated values for the k_{tr}/k_p ratios for these compounds are given in Table I together with the values of their basicities taken from Arnett.⁹

TABLE I
Chain-Transfer Coefficients ($C_{tr} = k_{tr}/k_p$) as Determined from the Mayo Plot in the BCMO Polymerization at 0°C^a

Chain-transfer agent	Concentration range $\times 10^3$, mole/l.	pK_a^b	C_{tr}^c
H ₂ O	3-9	-1.8 ^d	0.19 ^e
MeOH	1-10	-2.2	0.125
<i>n</i> -BuOH	1-10	-4.1	0.10
<i>n</i> -Bu ₂ O	2-10	-5.4	0.07
C ₆ H ₅ OMe	5-20	-6.5	<0.005
(ClCH ₂ CH ₂) ₂ O	4-11		<0.005

^a Conditions: [M] = 1.0 mole/l., [BF₃] = 0.109 mole/l., [H₂O] < 50 ppm and constant through all series of runs for a given chain-transfer agent.

^b For comparison all the tabulated data were taken for the same method of pK_a determination (the IR shift of CH₃OD⁹).

^c In CH₂Cl₂ solutions.

^d Dispersed values

^e 0.35 in toluene.

DISCUSSION

The results in many instances supplement the investigation of the kinetics and mechanism of BCMO polymerization described in our previous publication.³

Previously, on the basis of the kinetic data, it had been concluded that all the elementary reactions proceed in the liquid phase in spite of phase separation and therefore the full process can be treated as monophasic one. The present data give the further confirmation of this hypothesis. The two-phase propagation should be very sensitive to the changes in the solvation power of the solvent used. One could assume that for such a case the k_t/k_p ratio should be dependent on the type of solvent. In our investigation, however, the k_{tr}/k_p values for all the three solvents, including two of higher solvation power [CH₂Cl₂ and (CH₂Cl)₂] and one in which polymer does not swell (toluene), are similar. These findings can be also complemented by our earlier study of the polymerization in liquid SO₂.¹⁰ Although polymer does not swell in SO₂ at all, the molecular weights obtained in SO₂ and CH₂Cl₂ were very similar. These data verify our previous treatment of the process under study as homophase one in spite of the heterogeneous character of reaction. The recent data of fractionation⁶ giving (even for polymer obtained at higher conversions) the unimodal molecular weight distributions and rather low \bar{M}_w/\bar{M}_n ratio—generally below 1.55—also confirm this hypothesis.

However, the problem of whether the polymeric precipitation is only simple secondary aggregation of dead macromolecules remains still to be solved. Accordingly it would be of interest to compare the results of BCMO polymerization with that in other ionic systems in which polymerization with precipitation occurs (e.g., polymerization of trioxane); however, these data are not available.

The second effect of the use of different solvents is connected with the change of dielectric constant of the reaction milieu. Several different effects of dielectric constant and structure of solvents were observed in the cationic polymerization of vinyl compounds. In our case the overall polymerization rate increases with the dielectric constant; the most significant increase, somewhat surprisingly, was observed on passing from methylene chloride to 1,2-ethylene dichloride. Since the polymerization in CCl_4 also gives higher rates than expected from dielectric constant values it is possible that there are some additional effects not simply related to the dielectric constant of the solvent.

The data of Figure 4 indicate that the k_{tr}/k_p ratios are not altered by changes in solvent dielectric constant and, therefore, as the $R_p \propto k_i k_p / k_{tr}$ in our case³ the observed increase of R_p in more polar solvents should be due to the increase of k_i . This is the generally noted effect in the systems where the production of the ionized species is the rate-determining step in the initiation reaction. In both propagation and termination reactions, according to the previously proposed mechanisms, the effect of the dielectric constant of the solvent should be small.

Chain transfer to water is pronounced in toluene. The data given in Table I indicate that in toluene solution C_{tr} is almost twice as high as the C_{tr} measured in methylene and ethylene chlorides.

It was stressed by Szwarc¹¹ that the average concentrations of catalyst, monomer, and other additives participating in the polymerization process could differ at the proximity of an ion pair from these taken for the kinetic treatment. The concentrations of monomer chain-transfer agent as well as the chain-transfer coefficients should be therefore treated as the "apparent" ones, since preferential solvation can not be ruled out. Thus, the increase of C_{tr} in the toluene solution can be simply related to the changes in the H_2O concentration at the proximity of the ion pairs, due to the presence of less polar solvent.

The observed differences between $C_{tr}(\text{H}_2\text{O})$ in trioxane polymerization and in this study can be the result of the differences between basicities of trioxane and BCMO. According to the published data, basicity increases in the order: $\text{H}_2\text{O} > \text{BCMO} > \text{trioxane}$.^{9,12}

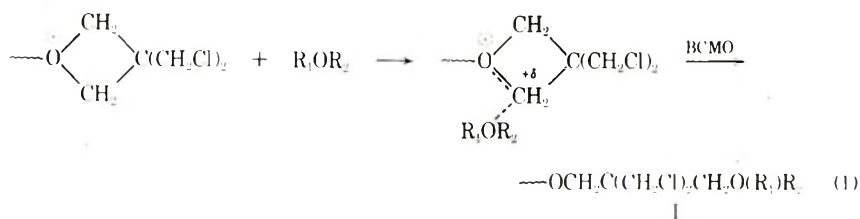
Recently new data concerning the cationic polymerization of trioxane in methylene chloride solution at 25°C were published.¹³ The value for C_{tr} obtained in the cited work (2.6 at 25°C) is comparable with our data ($C_{tr} = 0.19$ at 0°C) if the mentioned differences in basicities are taken into account.

The observed lowering of molecular weight in the presence of both nitromethane and nitrobenzene seems to be the result of an effective chain-transfer process. Chain transfer by nitro compounds was observed also in cationic polymerization of vinyl compounds.¹⁴ In such media a chain transfer to monomer becomes also probable but these problems were not further studied. It should be stressed, however, that in trioxane polymerization catalyzed by BF_3 complexes nitrobenzene does not lower the molecular weight.¹⁵

To compare the role of basicity in chain transfer, the action of MeOH , BuOH , $n\text{-Bu}_2\text{O}$, $\beta\text{-ClEt}_2\text{O}$, $\text{C}_6\text{H}_5\text{OMe}$ and dioxane was investigated, and the obtained data tabulated together with the C_{tr} results discussed above for H_2O .

Dioxane is omitted, since copolymer formation was reported;¹⁶ recently the reactivity ratio for the *p*-dioxane-BCMO pair in the presence of $\text{BF}_3\text{-OEt}_2$ was determined.¹⁷ The increase of reaction rate in the presence of additives (Fig. 5) is consistent with the probabilities of ionic species formation from corresponding BF_3 complexes ($\text{H}_2\text{O} > \text{MeOH} > \text{ethers}$). It is of interest to note that no increase of the rate was observed in the presence of butyl ether and rather slight decrease could be noted. This observation together with the data of Table I suggests that, contrary to water and alcohols, butyl ether acts as a degradative chain-transfer agent and that the produced nonstrained tertiary oxonium ion is probably not capable of reinitiation. The simple complexing action of ether toward catalyst proposed earlier^{7,18} as an explanation of the lowering of the reaction rate, seems to be less important than the above described degradative chain transfer.

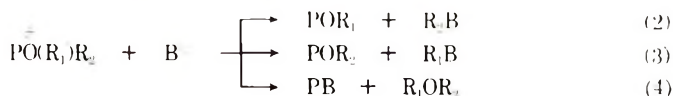
According to our previous work,³ the chain-transfer reaction could be treated as a bimolecular reaction in which the formation of carbonium ion is avoided and the chain-transfer agent is incorporated into the transition state [eq. (1)].



In the mechanism (1), treated as a so-called borderline S_N2 mechanism,¹⁹ the bond breaking is more important than bond formation.

In spite of the inability of the ion I to reinitiate the chain, the R_1 or R_2 could be incorporated into the backbone, since during the polymer isolation three different possibilities of the ion neutralization exist. If R_1 , R_2 and the macromolecule are of equal value in this process, R_1 or R_2 should be

incorporated through reactions (2) and (3) (two counterions of both macroion and deactivating agent B^{\ominus} are omitted).



References

1. S. Penczek and A. A. Vanscheidt, *Vysokomol. Soedin.*, **2**, 296 (1963).
2. J. B. Rose, *J. Chem. Soc.*, **1956**, 242.
3. I. Penczek and S. Penczek, *Makromol. Chem.*, **67**, 203 (1963).
4. J. Brzeziński, *Polimery*, **9**, 367 (1964).
5. I. Imanishi, A. Mizote, T. Higashimura, and S. Okamura, *Kobunshi Kagaku*, **20**, 49 (1963).
6. Houben-Weyl, *Methoden der Organischen Chemie*, Vol. I/2, Thieme Verlag, Stuttgart, 1959, pp. 775-846.
7. S. Kambara and M. Hatano, *Kogyo Kagaku Zasshi*, **60**, 1585 (1957).
8. M. Kučera and E. Spousta, *Makromol. Chem.*, **76**, 183, 190 (1964).
9. E. M. Arnett, in *Progress in Physical Organic Chemistry*, Vol. 1, S. G. Cohen, A. Streitwieser, Jr., and R. W. Taft, Eds., Interscience, New York-London, 1963.
10. M. Legocki, M. Markowicz, I. Penczek, and S. Penczek, *J. Appl. Chem. USSR*, **34**, 640 (1961).
11. M. Szwarc, *Adv. Chem. Phys.*, **2**, 147 (1959).
12. S. Iwatsuki, N. Takikawa, M. Okada, Y. Yamashita, and Y. Yoshii, *Kogyo Kagaku Zasshi*, **67**, 1236 (1964).
13. H. Baader, V. Jaacks, and W. Kern, *Makromol. Chem.*, **82**, 213 (1965).
14. A. R. Mathieson, in *The Chemistry of Cationic Polymerization*, P. H. Plesch, Ed., Pergamon Press, London-New York, 1963, pp. 244, 259, 295.
15. S. Okamura, T. Higashimura, and M. Tomikawa, *Kogyo Kagaku Zasshi*, **65**, 717 (1962).
16. J. Furukawa, *Polymer*, **3**, 487 (1962).
17. S. Aoki, T. Otsu, and M. Imoto, *Kogyo Kagaku Zasshi*, **67**, 1958 (1964).
18. J. Furukawa and T. Saegusa, *Polymerization of Aldehydes and Oxides*, Interscience, New York-London, 1963, p. 215.
19. R. E. Parker and N. S. Isaacs, *Chem. Rev.*, **59**, 737 (1959).

Received January 26, 1970

Polycondensation of Benzyl Chloride and its Derivatives: A Study of the Reaction at Different Temperatures

G. MONTAUDO, P. FINOCCHIARO, S. CACCAMESE, and F. BOTTINO, *Institute of Industrial Chemistry, University of Catania, Italy*

Synopsis

The polycondensation reactions of benzyl chloride, α -chloroethylbenzene, and benzhydryl chloride in the presence of SnCl_4 or AlCl_3 as catalysts have been investigated in the temperature range between $+80^\circ$ and -135°C . Polycondensations of benzyl chloride and α -chloroethylbenzene are quite similar in the reaction kinetics and are thought to occur by the same displacement mechanism. Polycondensation of benzhydryl chloride, however, seems to involve the formation of benzhydryl carbonium ions. At low temperatures linear polymers tend to be formed, in contrast with branched polymers produced at room temperature. Steric effects are found to play a major role in protecting polymers from branching at lower temperatures.

Polybenzyl polymers are found to be less linear than poly ($-\alpha$ -methylbenzyl), even when prepared at -135°C .

INTRODUCTION

Benzyl chloride, in the presence of Lewis acids at room temperature, undergoes a rapid self-condensation reaction during which hydrogen chloride is evolved and highly branched polymer is produced.¹ Linear polybenzyls, however, were obtained recently by polycondensation of benzyl chloride at very low temperatures.²

As already realized by earlier workers,^{3,4} benzyl chloride at room temperature reacts slowly with itself to form the dimer. The latter is more activated toward substitution and it is rapidly benzylated by the monomer, yielding a highly branched polymer.³⁻⁶ Very low temperatures, apparently, block the branching reaction and the polymer becomes linear.^{2,7}

This paper is concerned with the investigation of the polycondensation of benzyl chloride, α -chloroethylbenzene, and benzhydrylchloride in presence of SnCl_4 or AlCl_3 as catalysts, in the temperature range between $+80^\circ$ and -135°C .

We undertook this work for the purpose of investigating the mechanism of room temperature reactions and to determine how the formation of linear polymers at low temperatures occurs. A detailed knowledge of room temperature reaction seemed necessary to understand properly the

origin of branching. Low-temperature studies were directed to get insight on factors involved in the suppression of branching.

How steric effects play a major role in determining linearity of these polymers is demonstrated. In fact, polymers from substituted monomers achieve a higher linearity relative to those from benzyl chloride.

KINETICS

Benzyl Chloride

Kinetic studies were possible only at the higher temperatures. At low temperatures, reactions were exceedingly fast, being complete in few seconds.

In Figure 1 is shown a set of typical kinetic curves for the polycondensation of benzyl chloride in nitrobenzene at 12°C with SnCl_4 as catalyst. After an induction period, the rate of HCl evolution remains constant until the reaction is about two-thirds complete.

Although the induction period is inversely proportional to the monomer and catalyst concentrations,^{4,5} the addition of benzyl chloride dimer is much more effective in reducing it, as shown in Figure 2. Figure 3 shows the initial part of a kinetic curve, together with the amount of dimer accumulated in early stages of the reaction. Kinetic orders with respect to monomer and catalyst were obtained from experiments where the concentration of only one reactant at time was gradually varied.

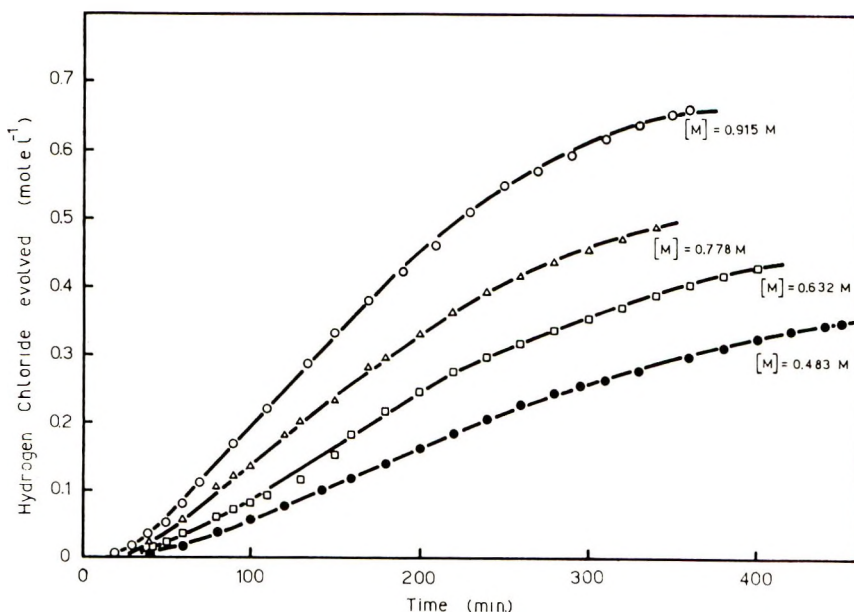


Fig. 1. Evolution of HCl vs. time for the system $\text{C}_6\text{H}_5\text{CH}_2\text{Cl}-\text{C}_6\text{H}_5\text{NO}_2-\text{SnCl}_4$. $T = 12^\circ\text{C}$; $[\text{SnCl}_4] = 0.160M$.

The reaction is second-order with respect to the monomer and first-order with respect to the catalyst, as indicated by rate versus concentration plots in Figures 4 and 5, respectively. Analogous reaction orders were obtained in experiments where SnCl_4 was replaced by AlCl_3 as a catalyst,

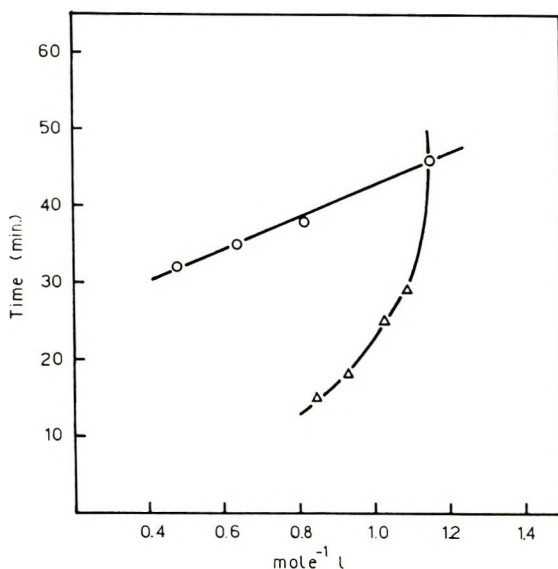


Fig. 2. Effect of dimer addition on the induction period for the system $\text{C}_6\text{H}_5\text{CH}_2\text{Cl}-\text{C}_6\text{H}_5\text{NO}_2-\text{SnCl}_4$: (O) monomer; (Δ) monomer (0.87M) + dimer. $T = 12^\circ\text{C}$; $[\text{SnCl}_4] = 0.173M$.

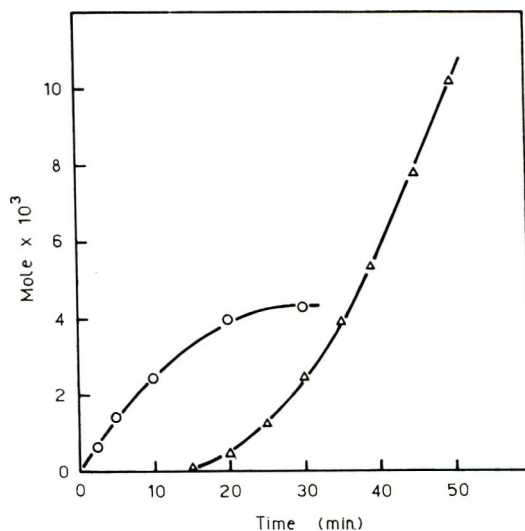


Fig. 3. Amount of dimer formed during the induction period (by VPC) for system $\text{C}_6\text{H}_5\text{CH}_2\text{Cl}-\text{SnCl}_4$: (O) dimer; (Δ) HCl. $T = 20^\circ\text{C}$; $[\text{SnCl}_4] = 0.170M$.

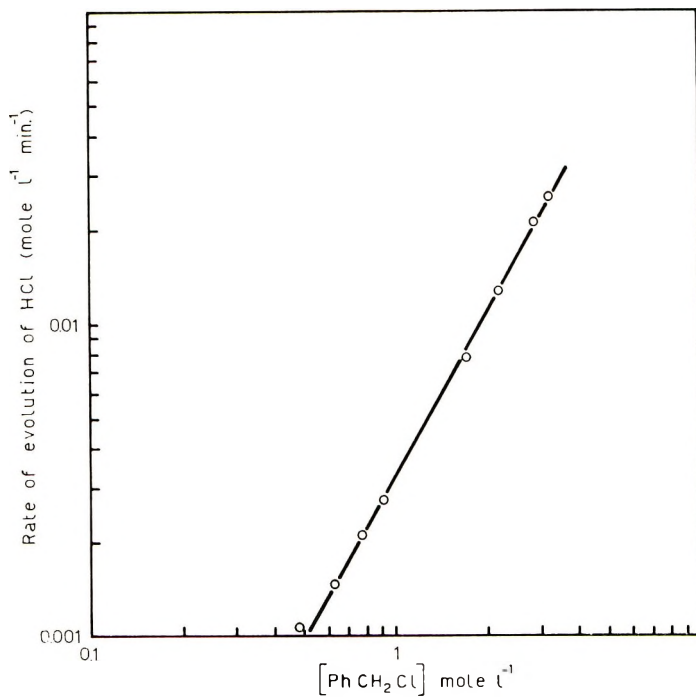


Fig. 4. Variation of reaction rate with monomer concentration for system $C_6H_5CH_2Cl-C_6H_5NO_2-SnCl_4$. $T = 12^\circ C$; $[SnCl_4] = 0.160M$.

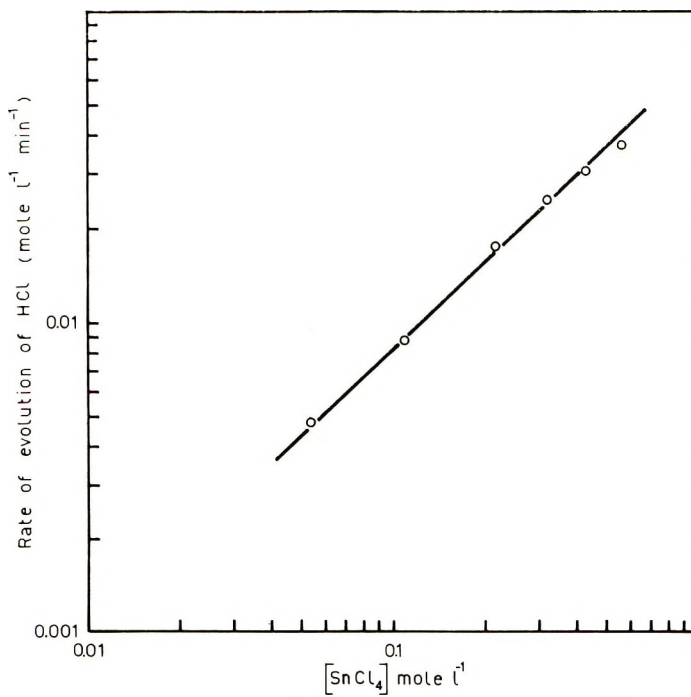


Fig. 5. Variation of reaction rate with catalyst concentration for system $C_6H_5CH_2Cl-C_6H_5NO_2-SnCl_4$. $T = 12^\circ C$; $[M] = 2.150M$.

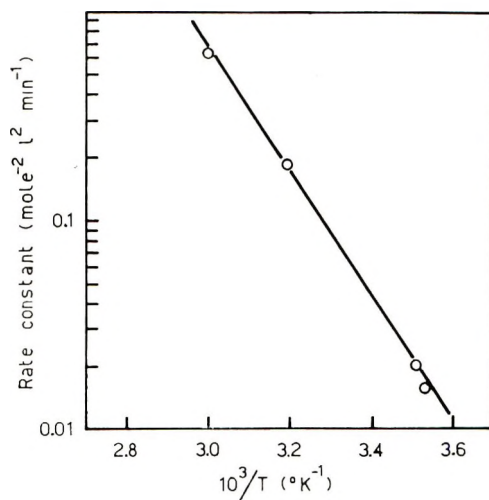


Fig. 6. Activation energy for the polycondensation of benzyl chloride, in $\text{C}_6\text{H}_5\text{NO}_2$, with SnCl_4 as a catalyst.

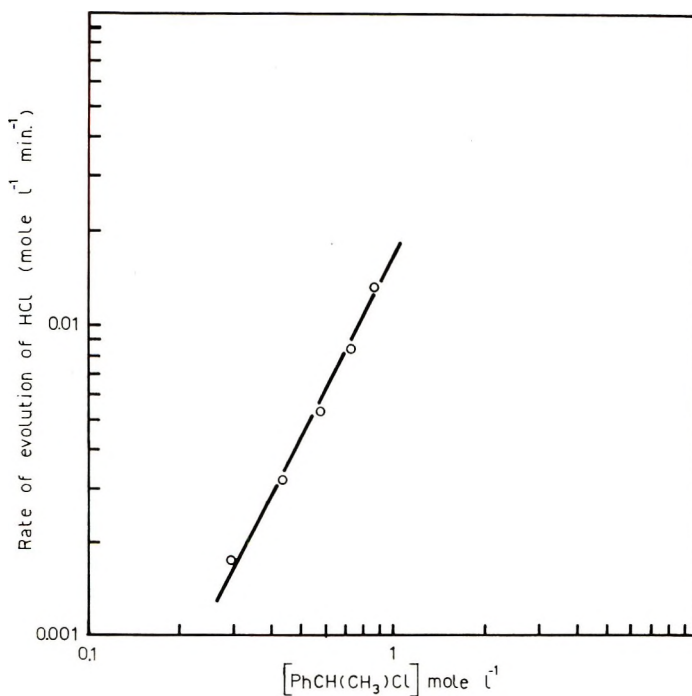


Fig. 7. Variation of reaction rate with monomer concentration for system $\text{C}_6\text{H}_5\text{CH}(\text{CH}_3)\text{Cl}-\text{C}_6\text{H}_5\text{NO}_2-\text{SnCl}_4$. $T = 10^{\circ}\text{C}$, $[\text{SnCl}_4] = 0.160M$.

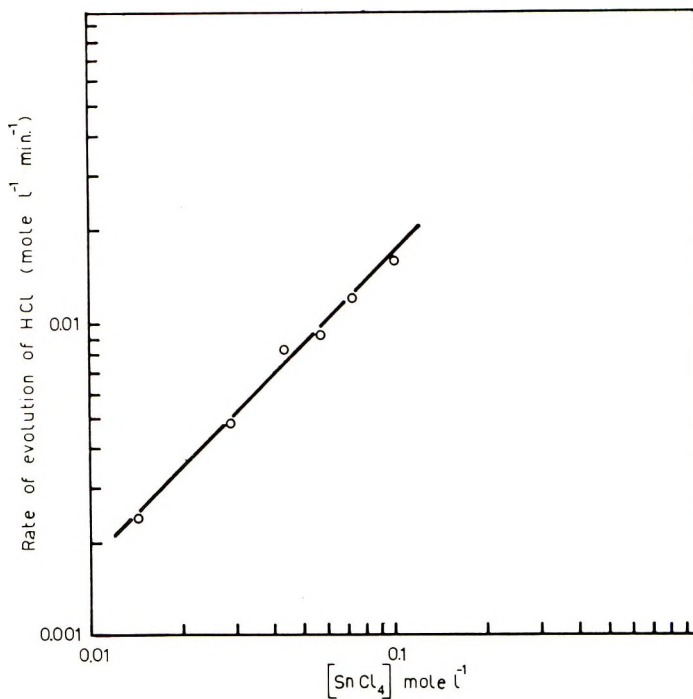


Fig. 8. Variation of reaction rate with catalyst concentration for system $C_6H_5CH-(CH_3)Cl-C_6H_5NO_2-SnCl_4$. $T = 10^\circ C$; $[M] = 1.260M$.

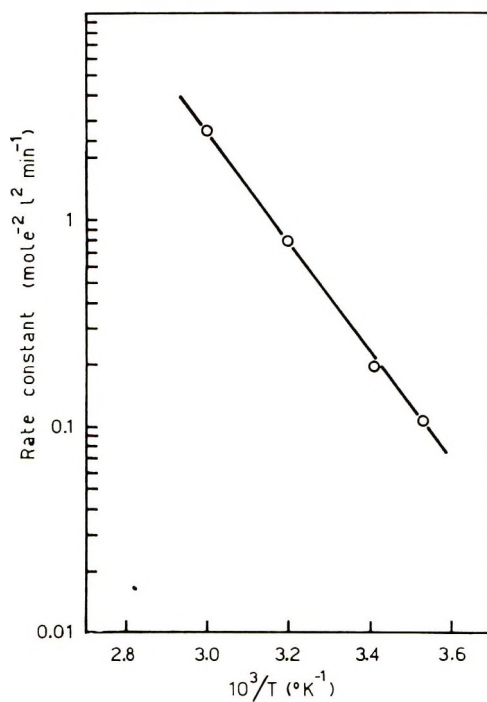


Fig. 9. Activation energy for the polycondensation of α -chloroethylbenzene in $C_6H_5NO_2$ with $SnCl_4$ as a catalyst.

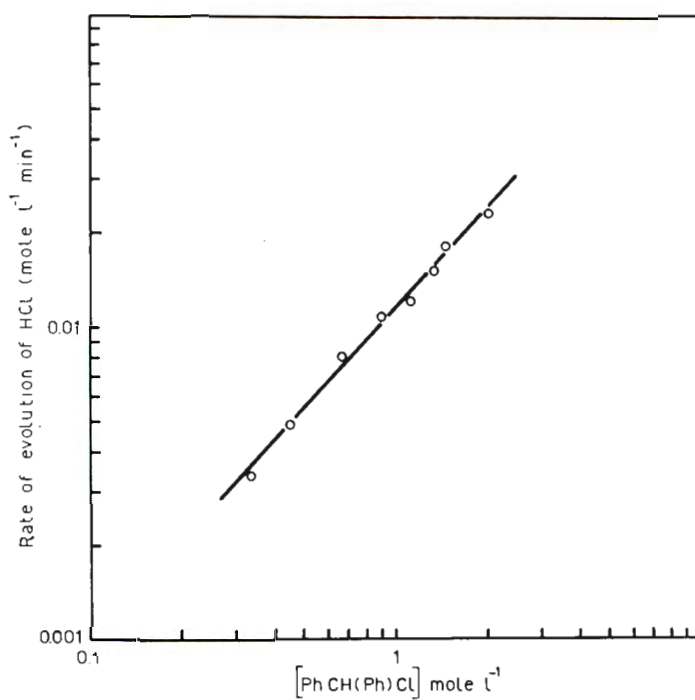


Fig. 10. Variation of reaction rate with monomer concentration for system $(C_6H_5)_2CHCl-C_6H_5NO_2-SnCl_4$. $T = 50^\circ C$; $[SnCl_4] = 0.087M$.

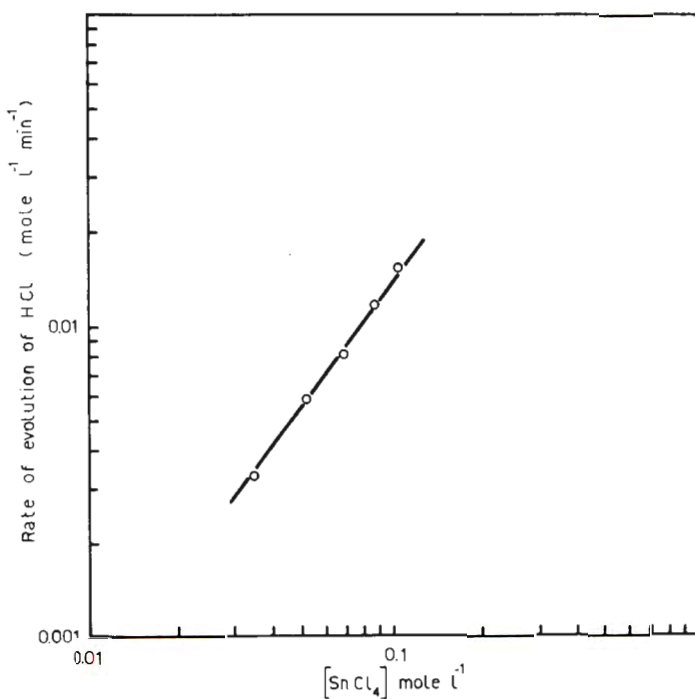


Fig. 11. Variation of reaction rate with catalyst concentration for system $(C_6H_5)_2CHCl-C_6H_5NO_2-SnCl_4$. $T = 50^\circ C$; $[M] = 1.13M$.

although in the latter case overall reaction rates are about twenty fold higher.

For the reaction catalyzed by SnCl_4 , in nitrobenzene, in a temperature range between $+10^\circ$ and $+80^\circ\text{C}$, the activation energy was found to be 13.6 kcal/mole (Fig. 6).

α -Chloroethylbenzene

α -Chloroethylbenzene is polymerized by Lewis acid catalysts at room and very low temperatures, analogous to benzyl chloride.^{2,8}

Kinetic features of the room temperature reaction are the same as those for the benzyl chloride polycondensation. The overall reaction rate is about ten times higher in this case. The reaction is second-order with respect to the monomer and first-order to the catalyst, as indicated by rate versus concentration plots in Figures 7 and 8, respectively. The activation energy of this reaction is found to be of 12.0 kcal/mole (Fig. 9).

Benzhydryl Chloride

The kinetic exploration of benzhydryl chloride polycondensation has shown relevant differences from the pattern common to the other two monomers investigated.

The reaction is first-order both with respect to monomer and catalyst, as indicated by the rate versus concentration plots in Figures 10 and 11, respectively.

The activation energy is 7.1 kcal/mole (Fig. 12), nearly one half of the value obtained for benzyl chloride and α -chloroethylbenzene.

Benzhydryl chloride does not undergo self-condensation at temperatures below -50°C in ethyl chloride.

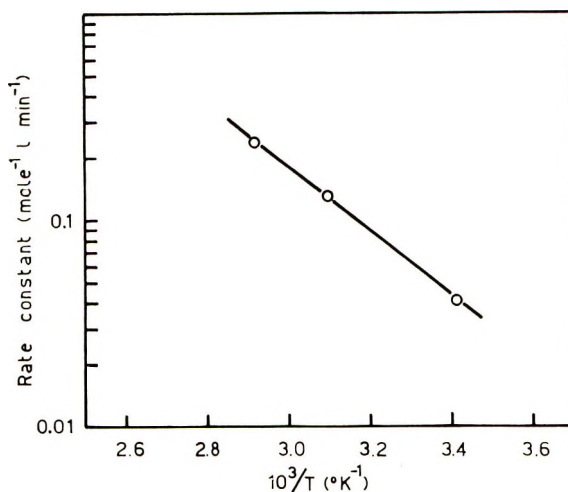


Fig. 12. Activation energy for the polycondensation of benzhydryl chloride in $\text{C}_6\text{H}_5\text{NO}_2$ with SnCl_4 as a catalyst.

Polymers obtained at higher temperatures have low molecular weights ($\bar{X}_n = 8-9$) and are amorphous.

MOLECULAR WEIGHTS

Curves of molecular weights versus the extent of reaction for room and low temperature polycondensations of benzyl chloride are reported in Figure 13.

At room temperature, the polymer formed has nearly constant molecular weight up to about 80% conversion. At higher extent of reaction molecular weights increase sharply because of the end-group reaction of one polymer molecule with the backbone of another. The low-temperature curve, however, does not show a similar increase in the last portion, probably because polymer molecules precipitate as formed, preventing further benzylation in the late stages of reaction.

Curves of molecular weights versus the extent of reaction for α -chloroethylbenzene polycondensation are closely similar to those for benzyl chloride.

Constant molecular weights result from the peculiar features of the reaction. In fact, during the induction period, dimer is slowly formed and its concentration tends to become constant (Fig. 3) because it is benzylated by the monomer.

Steady-state conditions are, therefore, reached, and molecular weights of the polymer formed are relatively high even in the early stages of the reaction and stay constant until the monomer concentration is appreciable.

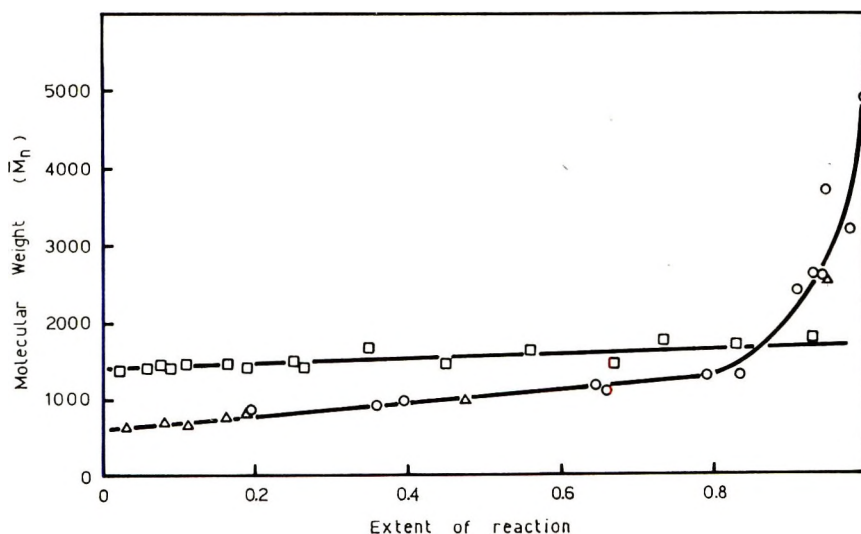


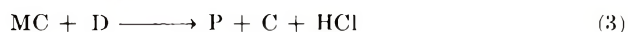
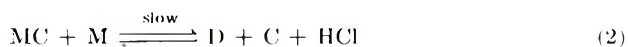
Fig. 13. Variation of molecular weight with extent of polymerization: (O) system $C_6H_5CH_2Cl-SnCl_4$, $T = 50^\circ C$; (Δ) system $C_6H_5CH_2Cl-SnCl_4$, $T = 0^\circ C$; (\square) system $C_6H_5CH_2Cl-C_2H_5Cl-AlCl_3$, $T = -135^\circ C$.

At high conversion, the reaction among polymer molecules takes place and molecular weights increase rapidly (Fig. 13).

The difference in reactivity of functional groups belonging to monomer and dimer molecules is responsible for the preferential reaction of the monomer with the dimer rather than with itself and accounts for the linear decrease of the residual monomer with extent of reaction, as experimentally found.⁵

REACTION MECHANISM

A simplified reaction scheme may be deduced from data collected for the polycondensation of benzyl chloride at room temperature.

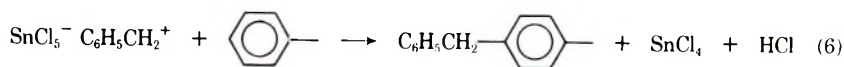


The first step consists of a rapid and reversible formation of a strongly polarized complex (MC) between benzyl chloride (M) and the Lewis acid (C), as was proposed by Brown for the benzylation of aromatic hydrocarbons.⁹

This complex undergoes the nucleophilic attack of the monomer, yielding the dimer (D), through the formation of intermediate σ complexes. Further alkylation of the dimer leads to polymer (P) formation.

This scheme accounts for the following experimental features of the reaction: (a) the accumulation of dimer during the induction period until nearly stationary conditions and constant reaction rate are reached; (b) the experimental finding that the reaction is second-order with respect to the monomer; (c) the dependence of the overall rate from the concentration of the complex MC which, in turn, depends on the relative basicity and acidity of monomer and catalyst.⁹

Recently, Parker, Davies, and South⁶ proposed, for the room-temperature reaction, a scheme where fairly stable benzyl carbonium ion is formed in the first step. This ion attacks the phenyl group of a benzyl chloride molecule leading to alkylation through the formation of σ and/or π complexes.⁶



The major objections to this scheme come from the use of benzyl carbonium ion as a reaction intermediate.

The presence of stable benzyl carbonium ion at room temperature in solution of Lewis acids has been ruled out by the work of Olah¹⁰ and by other workers.¹¹

Besides, it seems difficult to see how the above scheme accounts for the second-order dependence with respect to the monomer in the rate expression and for the different rate of formation of dimer and polymer.

α -Chloroethylbenzene polycondensation may be accounted for by the same reaction scheme as proposed for benzyl chloride, as can be inferred from the similarity of the experimental features in the two systems.

In the case of benzhydryl chloride, however, the reaction seems better interpreted by a mechanism involving benzhydryl carbonium ions, $(C_6H_5)_2CH^+$. The formation of this ion would account for the first-order relation with respect to the monomer, for the low activation energy, and for the fact that the reaction stops at low temperature. In fact, the benzhydryl carbonium ion^{10,11} is known to be more stable than $C_6H_5CH_2^+$ and $C_6H_5-CHCH_3$, and some of its salts have been isolated.¹²

It should be noted that, even if kinetic results for benzyl chloride and α -chloroethylbenzene at room temperature do not favor a mechanism involving carbonium ions as intermediates, very low temperatures tend to increase the stability of carbonium ions,¹⁰ and such mechanism cannot be ruled out in the case of low-temperature polycondensations of these monomers.

LOW-TEMPERATURE REACTIONS

Below $-120^\circ C$, polymerization of benzyl chloride in C_2H_5Cl occurs almost instantaneously without an induction period. The monomer is not

TABLE I
Polymers from Benzyl Chloride

No.	Temperature, $^\circ C$	Solvent	[C]/[M] mole/mole	Conversion %	Linearity % ^a	\bar{M}_n ^b
1	+10	$C_6H_5NO_2$	0.018	88.0	0	3400
2	-90	C_2H_5Cl	0.035	100.0	0	5200
3	-100	C_2H_5Cl	0.035	89.0	0	4000
4	-120	Freon 12 + C_2H_5Cl (1:1)	0.021	8.5	0	1100
5	-149	Freon 12 + C_2H_5Cl (1:1)	0.021	4.0	16.1	1100
6	-135	C_2H_5Cl	0.006	0.10	100.0	
7	-135	C_2H_5Cl	0.008	0.25	53.3	1500
8	-135	C_2H_5Cl	0.009	0.43	49.0	1500
9	-135	C_2H_5Cl	0.010	0.83	38.6	1500
10	-135	C_2H_5Cl	0.013	3.7	14.7	1480
11	-135	C_2H_5Cl	0.021	7.6	8.6	1500
12	-135	C_2H_5Cl	0.030	16.0	6.7	1500
13	-135	C_2H_5Cl	0.100	45.0	5.7	1450

^a Determined by infrared through the ratio of intensities of bands at 800 and 1605 cm^{-1} and assuming sample 6 100% linear.

^b Determined by VPO in xylene at $65^\circ C$.

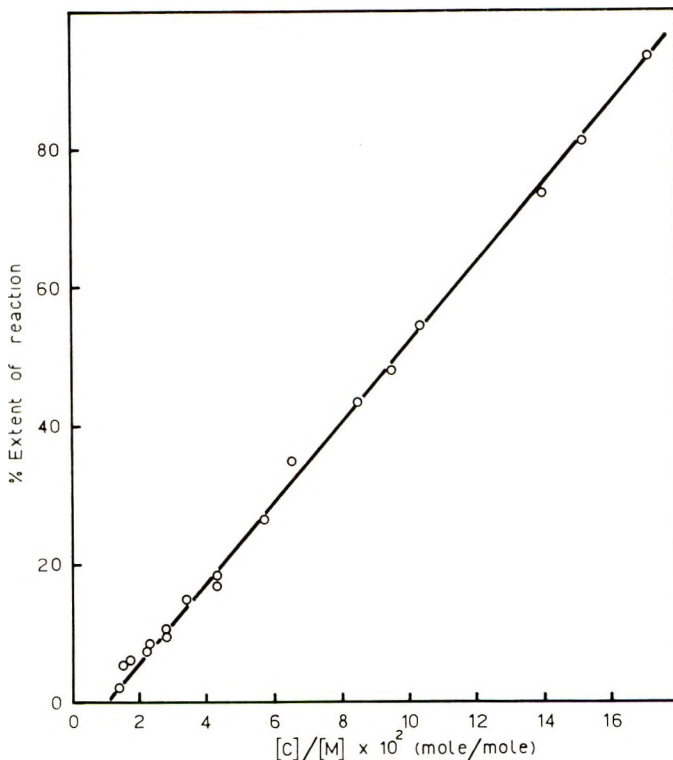


Fig. 14. Extent of reaction vs. catalyst concentration for system $C_6H_5CH_2Cl-C_2H_5Cl-AlCl_3$. $T = -135^\circ C$.

always completely converted, but the conversion is proportional to the catalyst concentration (Fig. 14).

Some data on polymers of benzyl chloride obtained at different temperatures are reported in Table I.

At $-135^\circ C$ the polycondensation of α -chloroethylbenzene is very fast, proceeds without induction period, and the monomer conversion is proportional to the catalyst concentration.

Some data on polymers from α -chloroethylbenzene at different temperatures are reported in Table II.

The most relevant change observed with the temperature is the tendency toward linearity of low-temperature polymers (Tables I and II).

Branching in our polymers is caused mainly by polysubstitution reactions subsequent to *meta* and *ortho* benzylation of the aromatic ring, while *para* benzylation of the aromatic ring is more likely to yield linear polymers.

In Table III are reported isomer distribution (*ortho*, *meta*, *para*) for two model reactions at different temperatures.¹³ There are no drastic changes in these distributions over the temperature range investigated, although *para* substitution is favored at lower temperatures.

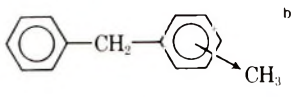
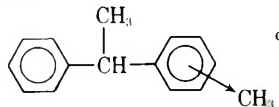
TABLE II
 Polymers from α -Chloroethylbenzene

No.	Temperature, °C	Catalyst	Solvent	[C]/[M] mole/mole	Conversion, %	\bar{M}_n^a	Melting (softening) point, °C	Crystallinity ^b
1	-10	SnCl ₄	Bulk	0.17	25.0	1970	(70-87)	-
2	-10	SnCl ₄	Bulk	0.17	36.0	2050	(70-88)	-
3	-10	SnCl ₄	Bulk	0.17	47.0	2400	(70-88)	-
4	-10	SnCl ₄	Bulk	0.17	65.0	2650		-
5	-10	SnCl ₄	Bulk	0.17	88.0	3200		-
6	-135	AlCl ₃	C ₂ H ₅ Cl	0.0099	7.9	3300	195	+
7	-135	AlCl ₃	C ₂ H ₅ Cl	0.029	25.2	3700		+
8	-135	AlCl ₃	C ₂ H ₅ Cl	0.049	34.1	3700		+
9	-135	AlCl ₃	C ₂ H ₅ Cl	0.058	43.5	3800		+
10	-135	AlCl ₃	C ₂ H ₅ Cl	0.079	61.4	3700	192	+
11	-135	AlCl ₃	C ₂ H ₅ Cl	0.097	90.0	3600		+
12	-135	AlCl ₃	C ₂ H ₅ Cl	0.110	91.0	3800		+

^a Determined by VPO in α -dichlorobenzene at 130°C.

^b Crystallinity determined by x-ray. Plus sign denotes crystallite; minus denotes amorphous sample.

TABLE III
Isomer Distribution at Different Temperatures^a

Temperature, °C	 b		 c	
	<i>para</i> , %	<i>ortho</i> + <i>meta</i> , %	<i>para</i> , %	<i>ortho</i> + <i>meta</i> , %
-21	53	47		
-90	60	40		
-131	66	34		
-12			90	10
-95			98	2
-125			≥99	

^a Isomer distribution determined by VPC.

^b System toluene-benzyl chloride-AlCl₃-C₂H₅Cl.

^c System toluene- α -chloroethylbenzene-AlCl₃-C₂H₅Cl.

However, in the benzylation of toluene, the *para* substitution is only 66%, even at -131°C. Therefore, one might expect only a moderate increase of linearity in polybenzyls prepared at very low temperatures.

In fact, as shown in Table I, the branching reaction is not completely suppressed at these temperatures, and a certain amount of linearity in polybenzyls is achieved only at very low conversions and temperatures. Only fractionation of low conversion samples, combined with selective extraction with opportune solvents yielded crystalline polymers.¹⁴

Instead, low temperature poly- α -methylbenzyls in Table II are crystalline even at high conversion. The *ortho* and *meta* substitutions appear to be absent in this system, in agreement with data in Table III. Plausibly, the steric hindrance of the α -methyl group plays a key role in directing the substitution to the *para* position, and also in protecting the polymer molecule from branching. The importance of steric effects in this connection is also demonstrated by the fact that poly-2,5-dimethylbenzyls are crystalline even when prepared at room temperature.¹⁴

These facts point out that use of low temperatures is a less strict requirement than originally implied.²

Finally, it is interesting to mention that for α -chloroethylbenzene (racemic) the polymerization reaction does not provide a mechanism of steric control for the growing chain, and methyl groups are expected to lie in disordered sequences along the polymer chain.

We have analyzed the NMR spectra of some amorphous (branched) and crystalline (linear) poly- α -methylbenzyl and have found that each peak of the methyl doublet (8.34; 8.47 τ) appears to consist of three peaks, when expanded. Assigning the central peak to the heterotactic sequences, the upfield (+1.0 cps) peak to isotactic, and the downfield (-2.1 cps) one to syndiotactic sequences, a value of the replication parameter σ ,¹⁵ $\sigma =$

0.55 has been calculated. As a consequence, the crystalline polymer does not have ordered sequences of α -methyl groups.

EXPERIMENTAL

Purification of materials, methods, and apparatus used for kinetic experiments were described earlier.⁵

Analytical Procedures

Infrared spectra were recorded on a Perkin-Elmer 237 infrared spectrophotometer. NMR spectra were obtained on a Varian A60 analytical spectrometer.

Crystallinity of polymers was determined by x-ray powder diffraction photographs. Molecular weights determinations were obtained by vapor-pressure osmometry with a Mechrolab 302 thermoelectric osmometer which could be operated in the temperature range between 25 and 130°C, in xylene or *o*-dichlorobenzene solutions.

VPC determinations were obtained with a C. Erba Fractovap C instrument with the use of a 220-cm column packed with 25% methylsilicone polymer on Celite at 210°C.

Polycondensation Procedure

All experiments were carried out in 150-ml thermostated Pyrex reactors under a nitrogen stream. Polymerization reactions produced a deep red color which disappeared when the reaction was terminated by addition of methanol (1:20). Methanol addition caused polymer precipitation; the precipitate was washed with HCl, water, methanol, and dried under vacuum.⁵

The same general procedure was employed when ethyl chloride was used as a solvent in low-temperature reactions. A cold solution of AlCl_3 in ethyl chloride was added dropwise to the monomer solution (0.8M). Cold methanol was added to the flask to terminate the reaction.

In all cases, where the extent of reaction had to be calculated (from the knowledge of the yield and of molecular weight), it was controlled that no polymer precipitated from the mixture methanol-solvent reduced to small volume under vacuum.

Benzyl Chloride Dimer

An authentic sample of α -chloro(*p*-tolyl)phenylmethane was prepared according to the literature.¹⁶ VPC analysis showed that the sample had 90% *para* and 10% *ortho* isomer.

This sample was used in the experiment described in Figure 2 and also to calibrate a VPC curve for the determination of the amount of benzyl chloride dimer in early stages of polycondensation (Fig. 3).

For this purpose, the reaction mixture was poured into a 5% HCl-water solution and the products were extracted with carbon tetrachloride, dried

(Na_2SO_4), and analyzed by VPC. The amount of dimer was estimated as sum of *ortho*, *meta*, and *para* isomers. Isomer distribution in the dimer was: 50% *para*; 20% *meta*; 30% *ortho*.

Model Reactions

Isomer distributions in Table III were determined by VPC by using calibration curves obtained by injecting authentic samples of each isomer produced in the reaction.

Full details, together with the synthesis of model compounds necessary, will be reported later.¹³

References

1. R. W. Lenz, *Organic Chemistry of Synthetic Polymers*, Interscience, New York, 1967, p. 228.
2. J. P. Kennedy and R. B. Isaacson, *J. Macromol. Chem.*, **1**, 541 (1966).
3. H. C. Haas, D. I. Livingston, and M. Saunders, *J. Polym. Sci.*, **15**, 503 (1955).
4. L. Valentine and R. W. Winter, *J. Chem. Soc.*, **1956**, 4768.
5. G. Montaudo, R. Passerini, F. Bottino, S. Caccamese, and P. Finocchiaro, *Ann. Chim. (Rome)*, **57**, 879, 905 (1967).
6. D. B. V. Parker, W. G. Davies, and K. D. South, *J. Chem. Soc., B*, **1967**, 471.
7. P. Finocchiaro and R. Passerini, *Ann. Chim. (Rome)*, **58**, 418 (1968).
8. P. Finocchiaro and R. Passerini, *Boll. Sci. Fac. Chim. Ind. Bologna*, **26**, 245 (1968).
9. H. C. Brown and M. Grayson, *J. Amer. Chem. Soc.*, **75**, 6285 (1953).
10. G. A. Olah, C. V. Pittmann, R. Waak, and M. Doran, *J. Amer. Chem. Soc.*, **88**, 1488 (1966).
11. I. Hanazaki and S. Nagakura, *Tetrahedron*, **21**, 2441 (1965).
12. H. Volz and H. W. Schnell, *Angew. Chem. Internat. Ed.*, **4**, 873 (1965).
13. G. Montaudo et al., to be published.
14. G. Montaudo, F. Bottino, S. Caccamese, P. Finocchiaro, and G. Bruno, *J. Polym. Sci., A-1*, this issue.
15. F. A. Bovey and G. V. D. Tiers, *J. Polym. Sci.*, **43**, 373 (1960).
16. C. Maquin and H. Gault, *C. R. Acad. Sci. (Paris)*, **234**, 629 (1952); *ibid.*, **236**, 383 (1953).

Received December 15, 1969

Revised January 26, 1970

Use of Carbon Suboxide to Obtain Block and Graft Copolymers. I. Grafting of Carbon Suboxide on Polyamide 6

ANDRZEJ BUKOWSKI and STANISLAW POREJKO, *Department of the Technology of Polymers, Polytechnic Institute of Warsaw, Poland*

Synopsis

Polyamide 6 in the form of film was grafted by gaseous carbon suboxide in the form of toluene solutions. The influence of temperature on the extent of grafting was studied. It was concluded that in a sufficiently high temperature a copolymer of high structure appears. The influence of substances that initiate homopolymerization of suboxide upon the course of grafting reaction was studied. It was found that the substances do not increase the effectiveness of grafting. However a significant increase of effectiveness of grafting is produced by introducing into the reaction environment some small quantities of methanol. By the addition of methanol a graft copolymer of a maximum effectiveness of 43.1% was obtained. The copolymer was subjected to further tests and appeared to be c.l. poly(amide-6-*g*-carbon suboxide). Additional tests indicated that the polyamide film graft with carbon suboxide shows some interesting properties.

INTRODUCTION

Carbon suboxide (dioxopropadiene)¹⁻³ is the simplest biketene and as a highly unsaturated compound is an interesting subject of study in polymer chemistry. The carbon suboxide reacts very readily, especially with compounds of mobile hydrogen atoms.

Under certain conditions it polymerizes quite easily, although neither both reaction mechanism and suboxide structure has so far been studied in full. The polymer is not highly thermally stable. Carbon suboxide, $O=C=C=C=O$, is a pale liquid boiling at $+7^{\circ}C$, having a very strong odor and high toxic and lachrymatory properties. As a liquid or in highly concentrated solutions it explodes spontaneously for reasons still not fully investigated. Such a complex of properties hinders work with carbon suboxide and limits the method of conducting the reaction.

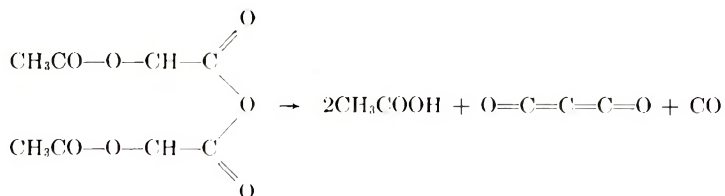
Publications concerning the utilization of carbon suboxide in the chemistry of polymers are relatively rare. The available literature gives no hints concerning production of block copolymers and the grafting by carbon suboxide. Our work is thus based, to some extent on the results of experiments made in our institute.⁴⁻¹⁰ The theoretical possibility of obtaining block and graft copolymers with carbon suboxide might be predicted for two reasons: the ready reaction of carbon suboxide with amino groups

and amide groups, and also the positive results mentioned in literature of grafting of other monomers on polyamide. For as the case of polyamide-carbon suboxide, the following reactions may be theoretically predicted: (1) formation of graft copolymer (c.l.), poly(amide-*g*-carbon suboxide);* (2) formation of block copolymer, poly(amide-*b*-carbon suboxide); (3) formation of graft copolymer (c.l.), poly(amide-*g*-carbon suboxide); (4) crosslinking of polyamide chains by single molecules of carbon suboxide; (5) addition of single molecules of carbon suboxide to NH polyamide groups; (6) addition of single molecules of carbon suboxide to NH₂ end-groups of the polyamide; (7) copolymerization of carbon suboxide.

EXPERIMENTAL

Preparation of Carbon Suboxide

Carbon suboxide was obtained by the Ott method relying on pyrolysis of diacetyltartaric anhydride:



The reaction was conducted at 625°C in a copper tube and the efficiency reached 45%. The crude carbon suboxide was distilled and then collected at solid carbon dioxide temperature in a hermetic glass flask.

Preparation of Polyamide

In all the experiments polyamide 6 (polycaprolactan) was used, in the form of transparent, unplasticized industrially produced film (Pergol), 0.04 mm thick. Its molecular weight was established by viscometry to be about 15,500. In order to avoid both the influence of external factors upon the course of reaction and any possible change of mass during copolymer formation, the film was subjected to some initial preparation before the experiment. The initial preparation consisted of washing the film at 50°C for 1 hr successively in toluene, acetone, and methanol and then drying for 2 hr at 50°C. After drying, the film was aged at room temperature for a minimum of 12 hr.

Experimental Procedure

Because of the explosiveness, toxicity, and low boiling point of carbon suboxide, it was used as a solution in nearly all the experiments. The solvent used was toluene, which mixes with carbon suboxide in every propor-

* Terminology after Ceresa.¹¹

tion, does not hydrolyze the carbon suboxide, does not react with the polyamide, and has a low fusion point and relatively high boiling point. The initial concentrations of the solutions, as obtained by anilide precipitation, were 5–15 wt-%. No higher concentrations were used because of the explosive properties of carbon suboxide. The polyamide film used in the experiment was in the form of rectangular samples weighing about 0.1 g.

Each experiment was carried out on three to six samples of the film inserted simultaneously in the reaction environment. Conical flasks of 50 ml capacity were generally used as the reaction vessel. The flasks were filled with carbon suboxide solution, into which all the remaining components of reaction were introduced. During the experiments at room temperature, the flasks were closed with ground glass stoppers while at higher temperature they were provided with reflux condensers. The final concentrations of carbon suboxide in the reaction mixture were determined by means of anilide precipitation.

A large number of experiments were carried out in a special apparatus providing a constant concentration of carbon suboxide in the solution and enabling the simultaneous grafting of gaseous suboxide. The apparatus consisted essentially of a thermostatted reaction vessel filled with toluene, through which a stream of gaseous carbon suboxide was bubbled at a constant rate. Due to the solubility of carbon suboxide in toluene the solution concentration was remained essentially constant at the given temperature. The film undergoing reaction was submerged in the carbon suboxide solution. Unreacted carbon suboxide gas passed from this reaction vessel, another flask vessel where gaseous-phase grafting was carried out.

Separation of the Product

After the reaction, the grafted films were washed in order to remove the carbon suboxide homopolymer and other side products. In most cases the washing off consisted of mechanical cleaning and immersing in acetone for about $\frac{1}{2}$ hr. The films were dried at 50°C for 2 hr and aged at ambient conditions for at least 12 hr.

Characterization of Product

Considering the simplicity and speed of measurement, the three basic characterization procedures study were used: (1) establishment of weight changes on an analytic balance of 0.0001 g accuracy; (2) determination of solubility in 85% formic acid; (3) assessment of external appearance (laboratory microscope, magnification 1500 \times). If the results of this preliminary study were interesting, further detailed study was carried out, including elementary analysis, infrared analysis, (Unicam Sp 200 and Hilger H 800 instruments) as well as viscometry.

RESULTS AND DISCUSSION

Effect of Temperature

At room temperature, despite the use of long reaction times and maximum solution concentrations of carbon suboxide, the extent of reaction, measured as the increase of weight did not exceed of 7%. The product was most likely a grafted poly(amide 6-*g*-carbon suboxide) copolymer.

The solubility in HCOOH of film grafted at room temperature was slightly poorer than that of the original film. The film was yellowish, but its translucency and elasticity were fully retained. Attempts to graft the suboxide at elevated temperatures were carried out in above described equipment with a constant concentration of carbon suboxide. The reaction was carried out for 2 hr for three samples. The concentrations of carbon suboxide were established by means of anilide precipitation. The experimental results are summarized in Table I.

Films insoluble in boiling formic acid were subjected to a thorough detailed study. It was shown that even further intensive film washing in the solvents of poly(carbon suboxide) does not cause a loss of weight nor a change of their yellowish colour. The grafted films were completely insoluble in concentrated sulfuric acid and *m*-cresol. Infrared analysis

TABLE I
Effect of Temperature upon Grafting of Carbon Suboxide on Polyamide 6

Reaction temperature, °C	Extent of grafting from average increase of mass, film, wt-%	Color of film after reaction	Film solubility in 85% HCOOH	Concentration of carbon suboxide solution in toluene, wt-%
40	2.5	Yellowish	Soluble after about 30 min at room temperature	—
50	3.1	Pale yellow	Insoluble at room temperature; soluble when heated	7.3
60	4.0	Yellowish	"	6.7
65	5.1	Yellowish	Insoluble at room temperature; soluble when hot after several hours	—
70	7.2	Yellow	Insoluble in boiling acid; swells	5.7
75	6.7	Yellow	"	—
80	7.3	Dark yellow	"	4.5
90	7.4	Dark yellow	"	—
95	7.5	Orange	"	3.4
100	7.2	Orange	"	—

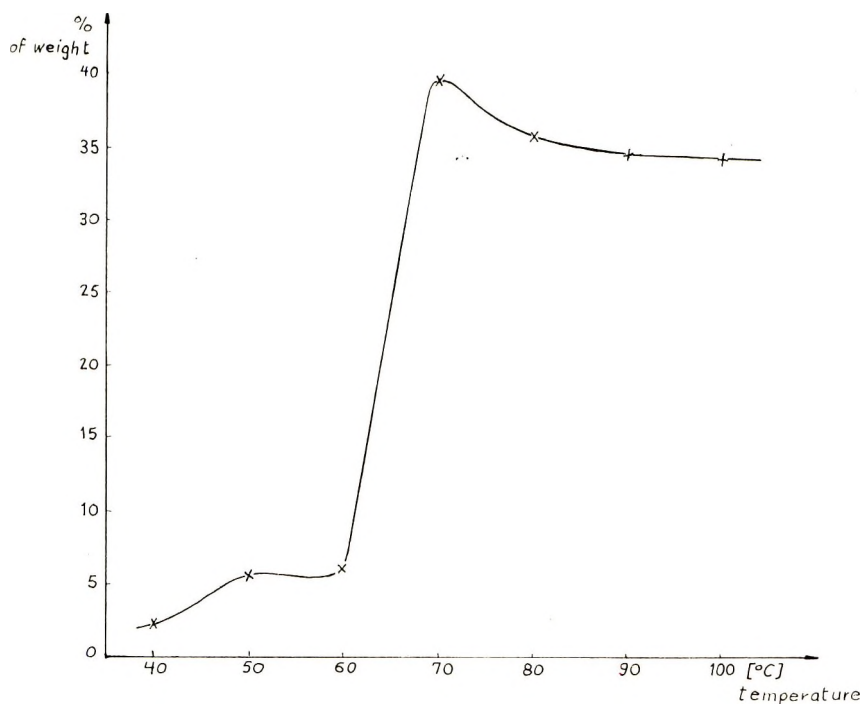


Fig. 1. Effect of temperature on the grafting yield.

showed the presence of a strong band at about 1720 cm^{-1} characteristic of poly(carbon suboxide). These results excluded any chance of external contamination or swelling of the film by the poly(carbon suboxide); they showed, moreover the formation of a cross-linked grafted copolymer.

The results (Table I) show a positive correlation of the increase in temperature with the course of the reaction. At elevated temperature, a crosslinked copolymer forms which is insoluble in acid. The grafting effectiveness, as estimated by the weight increase of the film reaches its maximum at about 75°C and then diminishes slightly, which is probably due to the fall in concentration of carbon suboxide in the solution at elevated temperature. The rise in the film's resistance to formic acid with increasing temperature proves the increasing crosslinking of the product. The swelling of the film in acid and its retention of elasticity indicate that even at 100°C the crosslinking of polyamide is not too high. The effect of temperature upon the extent of grafting is shown in Figure 1.

Influence of Substances That Initiate the Polymerization of Carbon Suboxide

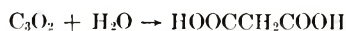
The first series of experiments was carried out at $18 \pm 2^{\circ}\text{C}$ for about 170 hr. In each experiment 0.3 g polyamide and 30 g of 10% carbon suboxide solution in toluene were used in the presence of small amounts of initiators. At the same time comparative runs were carried out without carbon sub-

oxide, thus allowing the effect of swelling of the initiators on polyamide to be established. The initiating substances were acetic acid, sulfuric acid, malonic acid, and water. No satisfactory results were obtained. No high effectiveness was reached and no products insoluble in acid were obtained. The experiment usually resulted in formation of large quantities of poly-(carbon suboxide), swelling, or polyamide destruction. For instance, the experiment at room temperature with the use of increasing quantities of water showed that formation of malonic acid and homopolymerization of carbon suboxide took precedence over grafting. The experiments at an elevated temperature (75°C) in the constant carbon suboxide series gave similar results. The added substances caused destruction or swelling of film or else formation of a large quantity of homopolymer; grafting under these conditions did not produce any large weight increase or properties more interesting than in the films grafted without additions. Only with water was there a large increase in weight. The experiment was carried out at +75°C, for 2 hr with the use of about 0.3 g polyamide and a constant concentration of carbon suboxide in the solution. Water was mixed with toluene before diluting. The results are shown in Table II.

TABLE II
Effect of Water upon Carbon Suboxide Grafting on Polyamide 6

Quantity of water added, g	Increase of mass of film, wt-%	Appearance of film	Solubility in 85% HCOOH
0.05	12.6	Dark orange	Insoluble in boiling acid; swelled
0.1	15.2	Red	Insoluble in boiling acid; very distinct swelling
0.15	19.1	Red	"
0.25	22.0	Red-brownish	Soluble in hot acid
0.35	27.1	Red; soluble in places (holes)	Soluble in cold acid
0.45	8.0	Orange; partly soluble	"
0.70	—	Completely destroyed; sticky mud at the bottom of flask	"

The results of a preliminary experiment on films insoluble in formic acid have shown that the reaction gave crosslinked graft copolymer. A detailed study of the products of this series proved that with the increase in the amount of water, swelling begins to prevail over grafting and malonic acid forms:



When a large amount of acid is formed, the film is finally destroyed.

A comparison of the results of experiments with 0.05; 0.1, and 0.15 g H₂O with the corresponding experiment without water (Table I) indicates

the following: (1) the larger weight increase may be due to the effect of water on the growth of suboxide chains, film swelling by malonic acid, or by homopolymerization of suboxide within the swelled films; (2) the darker color of the films is due to a larger percentage of carbon suboxide chains in the structure of the copolymer; (3) the very distinct swelling of films in boiling acid shows a decreasing copolymer crosslinking with increasing water content.

Effect of Methanol

The literature mentions some positive methanol effect upon grafting effectiveness of polyamide. This was confirmed in the case of grafting of polyamide with carbon suboxide. Because of the possibility of the reaction,



some experiments without methanol were carried out, with addition of methyl malonate alone.

No satisfactory results were obtained. Similarly, a study of the effects of other aliphatic alcohols has proved that they do not give rise to an increase in grafting effectiveness. A study of the effect of the quantity of methanol added was carried out in the set of apparatus with a constant concentration of carbon suboxide in solution. The experiment was carried out for 2 hr at 60°C, with the use of about 0.3 g polyamide in each run. Methanol was carefully mixed with toluene before diluting. The experimental results are summarized in Table III, and the relation between grafting effectiveness and the amount of methanol added is shown in Figure 2.

TABLE III
Effect of Methanol on the Extent of Grafting
on Polyamide 6 with Carbon Suboxide

Amount of methanol, g	Extent of grafting, % of weight	Color of film	Solubility of film in 85% HCOOH
0.02	4.1	Yellow	Insoluble in boiling acid; distinct swelling
0.06	6.3	Yellow	"
0.10	14.8	Dark orange	Insoluble in boiling acid; swelled
0.14	15.5	Red	"
0.20	15.8	Red	"
0.30	16.7	Red	"
0.40	18.1	Dark red, less plastic	Insoluble in hot acid; slightly swelled
0.50	18.3	Dark red	"
0.60	16.5	Red	"
1.00	7.2	Yellow	Insoluble in boiling acid; distinct swelling

The initial increase in yield may be explained by the quantitative increase of the proportion of methanol in the process. The decline in yield is likely to be the result of the reaction of the formation of methyl malonate prevailing over grafting of polyamide. Increasing coloration of the film points to an increasing proportion of polycarbon suboxide chains in the structure of grafted copolymer. The proof of a high degree of crosslinking of the film showing the largest mass increase is its limited solubility and lack of swelling in acid.

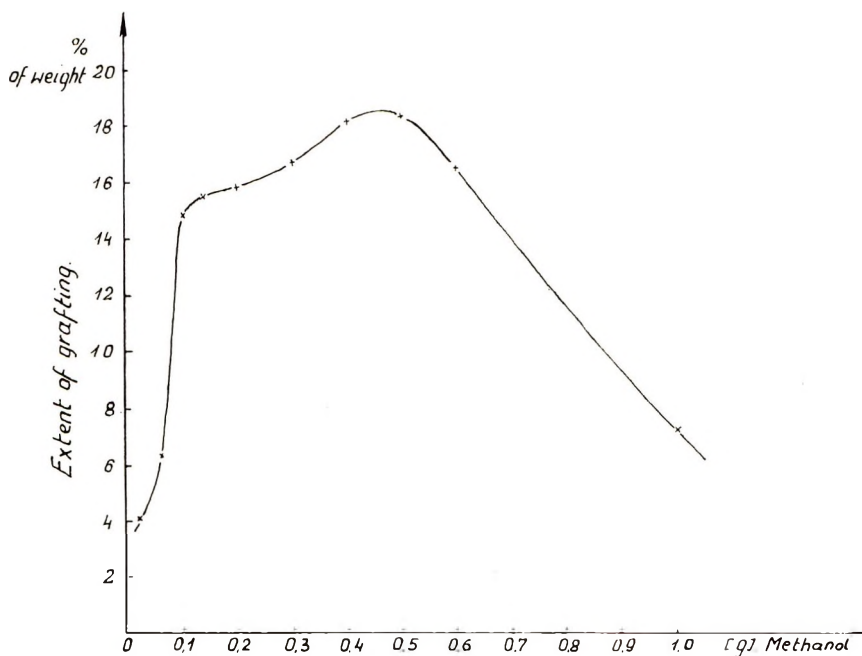


Fig. 2. Effect of methanol on the extent of grafting (increase of film mass) at 60°C.

The next series of experiments was designed to obtain a larger increase of film weight. The experiments were carried out in conical flasks provided with a strong reflux. The solutions of suboxide were of an initial 10% concentration. The reactions were carried out at 50–90°C for 1–10 hr, with the use of 0.3–0.6 g of polyamide, 3–5 g of carbon suboxide, and 0.1–0.5 g methanol. The largest increase in mass was obtained on reaction at 80°C for 6 hr with a reaction mixture composed of 30 g of 10% solution of carbon suboxide in toluene, 0.3 g of polyamide, and 0.3 g of methanol. The reaction carried out in these conditions reached the yield of 32.1%. The grafted films were dark red and were completely insoluble; they did not swell in boiling acid, but became stiff and fragile. Infrared analysis showed a band at 1720 cm^{-1} , characteristic of poly(carbon suboxide). Attempts to wash off homopolymer from the film gave no mass decrease.

Among films grafted with methanol, a special study was made of films having a mass increase of about 15%. The film completely resistant to acids retained translucency and elasticity, which suggests their large practical value. A study of this film has shown: (1) complete resistance to boiling concentrated, formic, acetic, and sulfuric acids (result of crosslinking); (2) the elemental composition fully in accordance with that calculated for copolymer consisting of polyamide chains and poly(carbon suboxide) chains; (3) existence in the infrared spectrum of an absorption band characteristic of poly(carbon suboxide) at 1720 cm^{-1} ; (4) negligible loss of weight from long-term action of solvents of poly(carbon suboxide) (good washing off of homopolymer); (5) carbonation of film at elevated temperature without prior fusion process (structure crosslinked); (6) isolation of CO_2 during the thermal destruction in nitrogen, which is characteristic of the destruction of poly(carbon suboxide chains); (7) visual uniformity of film.

In addition, a study of the physical and mechanical properties of grafted polyamide films was carried out.

The study has shown among other things that grafted films showed about 40% less gas permeability, about 20% higher tensile strength, and about 10 times less elongation at break than the ungrafted films.

Estimating the described results on polyamide films grafted with carbon suboxide it has been stated that the main product of grafting was the cross-linked copolymer (c.l.) poly(amide 6-*g*-carbon suboxide).

Other Experiments to Graft Polyamide with Carbon Suboxide

Experiments to graft liquid and gaseous carbon suboxide with polyamide gave no results of interest. When the reaction was carried out in liquid carbon suboxide at -2°C for 12 hours, no change of film properties was noted. Reaction of film with gaseous suboxide gave visible grafting finally at 90°C . The increase of film mass, however, was insignificant and reached only 3.8% by weight.

Interesting results were obtained in this series when different solvents of carbon suboxide were used. With nitromethane as solvent, the largest mass increase of film, 43.1% by weight, was reached. The examination of the product showed it to be strongly crosslinked copolymer. In addition to these experiments, experiments to graft carbon suboxide on preactivated polyamide films were carried out. The film was activated by ultraviolet irradiation in the air (UV lamp, S-300 burner, 300 W at 30°C for 18 hr at a distance of about 30 cm), irradiation with γ -rays in the air (intensity 170 R/sec, dose 30 rad, at 30°C) or ozonization (mixture of oxygen and about 4% ozone at $18 \pm 2^\circ\text{C}$ for 4 hr). In all grafting experiments on activated films the initial yields were smaller than or close to those reached in corresponding experiments on unactivated films. This indicates that grafting occurs at the nitrogen atoms in the polyamide and not at peroxide groups formed in the activation process.

CONCLUSIONS

At certain high temperatures the carbon suboxide and polyamide give highly crosslinked copolymer poly(amide-6-*g*-carbon suboxide).

At some less elevated temperatures a noncrosslinked grafted copolymer of poly(amide-6-*g*-carbon suboxide) forms.

The presence of small quantities of methyl alcohol shows a positive effect on the yield of copolymers grafted on carbon suboxide with polyamide.

References

1. M. V. Volkenshtein, *Usp. Khim.*, **4**, 610 (1935).
2. I. B. Daszkiewicz and V. G. Beilin, *Usp. Khim.*, **36**, 947 (1967).
3. A. Bukowski and S. Porejko, *Wiadomości Chem.*, in press.
4. S. Porejko, L. Makaruk, I. Glogowska, and M. Hienias, *Polimery*, **7**, 58 (1964).
5. S. Porejko, L. Makaruk, and K. Dobrosz, *Polimery*, **8**, 19 (1963).
6. S. Porejko, L. Makaruk, and W. Gabara, *Polimery*, **8**, 293 (1963).
7. S. Porejko and W. Gabara, *Polimery*, **10**, 107 (1965).
8. S. Porejko and W. Gabara, *Polimery*, **10**, 197 (1965).
9. M. Maciejewski and S. Porejko, *Polimery*, **11**, 157 (1966).
10. M. Maciejewski and S. Porejko, *Polimery*, **11**, 205 (1966).
11. R. I. Ceresa, *Block and Graft Copolymers*, Butterworths, London, 1962.

Received May 22, 1969

Revised February 4, 1970

Use of Carbon Suboxide To Obtain Block and Graft Copolymers. II. Grafting of Carbon Suboxide on Polyethylene

ANDRZEJ BUKOWSKI and STANSISLAW POREJKO, *Department of the Technology of Polymers, Polytechnic Institute of Warsaw, Poland*

Synopsis

Experiments have been carried out on grafting of carbon suboxide on nonactivated polyethylene films and on films previously activated by ultraviolet irradiation and by γ -irradiation. The experiments gave a grafted copolymer. A grafted copolymer was also obtained on grafting carbon suboxide in solution on polyethylene films preactivated by means of ozonization at 70°C. Examination of the copolymer indicated its structure to be cross linked. It has been proved that below 50°C single molecules of carbon suboxide react with polyethylene. The polyethylene thus modified is then easily surface-dyed.

INTRODUCTION

No reference has been found in literature concerning block and graft copolymers of carbon suboxide and polyethylene. The possibility of obtaining such compositions was indicated by the high reactivity of carbon suboxide¹⁻³ and ease of grafting of polyethylene.⁴ In the first stage of the experiment a series of experiments of grafting of carbon suboxide as solutions as well of liquid and gaseous carbon suboxide on polyethylene were carried out; however they gave no satisfactory results. Then experiments on grafting on polyethylene previously activated in air by use of a laboratory UV lamp with the ASH burner emitting ultraviolet radiation in the wavelength range 2800-3200 Å were carried out. Polyethylene in the form of film was irradiated at 30°C at a distance of 15 cm for 1-30 hr. Despite the use of various methods and reaction conditions, no interesting results were reached. Another method of preactivation of polyethylene films was γ -irradiation from a ⁶⁰Co source at a dose rate of 20 r/sec to a final dose of 0.65 Mrad. Irradiation was carried out at 20°C in air. Nevertheless, this procedure did not yield block or graft copolymers. The only effective method of preactivation turned out to be ozonization. Carbon suboxide was finally grafted successfully on polyethylene film preactivated with ozone.

EXPERIMENTAL

Materials

Carbon suboxide was obtained by means of a modified Ott method⁴ (see part I⁶). Polyethylene (Alkathene XLF-28, I.C.I.) was almost exclusively used in the form of a colorless film, 0.03 mm thick. The number-average molecular weight of the polyethylene was determined by a viscometric method to be about 17,700. The preparation of film consisted of thoroughly washing the film in methanol and then in acetone (1 hr each at 50°C) to remove impurities, then drying for 1 hr at 50°C, and aging for 12 hr at ambient conditions. The preactivation of the films involved ozonization with a mixture of 4% ozone and oxygen. Ozone was produced in a Siemens apparatus by means of silent electric discharge in oxygen, and activation was carried out at room temperature for 1–12 hr. Examination of the ozonized films has shown an increase of mass on the average, of 2.2% by weight; in addition, the films became less soluble. The ozonized films were dissolved in tetralin at 174–180°C. The decrease in solubility indicates crosslinking of polyethylene chains, most likely through peroxide linkages, $-O-O-$. The possibility of creating such "super oxygen" groups was confirmed by the results of infrared analysis as well as elementary analysis.

Procedure

The experiments were carried out on rectangular pieces of film weighing 0.1 g. In a few experiments polyethylene in grained form or in already finished products was used. Carbon suboxide was used in the form of gas, liquid, and in solutions. Most experiments were carried out with the use of carbon suboxide in toluene. Toluene was chosen as solvent due to its low freezing point, which permits storage of solutions in solid carbon oxide, its relatively high boiling point, as well as due to the fact that it may be mixed with carbon suboxide in any proportion without simultaneous dissolving poly(carbon suboxide). The drawback to using toluene as solvent is its ability to swell polyethylene at room temperature and to dissolve it at temperatures exceeding 80°C. In order to avoid errors in measuring mass, some preliminary experiments were carried out on the effect of toluene on the ozonized polyethylene film. In addition, with every grafting experiment a run was carried out with toluene only (without carbon suboxide). This enabled us to make the necessary corrections concerning mass measurement. The apparatus and experimental procedure were the same as with grafting of polyamide (see Part I).⁵

Isolation of the Product

After the reactions were carried out, the films were carefully cleaned mechanically with cotton wool moistened in acetone and left ever in the solvent for half an hour. After the poly(carbon suboxide) was washed off as well as other pollutions, the films were dried during 1 hour at 50°C and

then seasoned at room temperature for at least 12 hr. The most frequent way of product isolating will be described below. In some cases some additional washing of the product from both copolymers was carried out.

Characterization of Product

The following examination of grafted products were carried out: determination of mass changes on an analytic balance with an accuracy of 0.0001 g; determination of the solubility of the film in toluene and tetralin, determination of film uniformity by microscopy; infrared spectrophotometric analysis, and additional special examination where warranted.

RESULTS AND DISCUSSION

Effect of Temperature

On the basis of the results of a series of preliminary experiments the following conditions for the grafting reaction were chosen: time of film ozonization, 4 hr; reaction time, 3 hr. In every experiment 30 g of 10% solution of carbon suboxide in toluene was used, as well as about 0.3 g of polyethylene in the form of three film samples. Experiments were carried out in 50-ml conical flasks provided with condenser, placed in an oil bath

TABLE I
Grafting of Carbon Suboxide on Ozonized Polyethylene Film at 70°C

	Initial film weight, g	Final film weight, g	Weight change		Grafting yield (relative increase of weight), %
			g	%	
Ozonization time 4 hr, reaction time 3 hr; 27 g toluene, 3 g carbon suboxide	0.1185	0.1091	0.0094	-9.2	+39.7
	0.1068	0.0974	0.0094		
	0.1012	0.0920	0.0092		
Ozonization time 4 hr, reaction time 3 hr; 27 g toluene, without carbon suboxide	0.1081	0.0566	0.0515	-48.9	
	0.1052	0.0583	0.0469		
	0.1010	0.0505	0.0505		

controlled to $\pm 1^\circ\text{C}$. Simultaneously, runs were carried out under the same conditions but without carbon suboxide. The results of these runs allowed corrections to be made for the effect of toluene on polyethylene film. The percentage increase of film weight was taken as a measure of the extent of grafting. An example of computing reaction yield is presented in Table I for the results of an experiment carried out at 70°C. The results of a series of experiments at various temperatures are presented in Table II.

TABLE II
Effect of Temperature upon the Yield and Form of Product of
Grafting of Carbon Suboxide onto Ozonized Film

Reaction temperature, °C	Grafting yield (relative weight increase), %	Appearance of film after grafting
40	+2.2	Pale yellow, transparent, shape unchanged
50	+5.6	Yellow, transparent, shape unchanged
60	+5.8	Dark orange, shape unchanged
70	+39.7	Brownish red, less transparent, low elasticity, wrinkled
80	+35.9	Brownish-red, translucent, non-elastic, wrinkled
90	+34.5	Brownish-red, almost opaque wrinkled, stiff
100	+34.3	Brownish-red, opaque, wrinkled, fragile

A detailed study of products proved that the temperature has a significant effect upon the course of reaction between ozonized polyethylene and carbon suboxide. At temperatures lower than 50°C, single molecules of carbon suboxide may be joined with the activated groups of ozonized polyethylene film. The attached molecules of carbon suboxide form side chain groups, which easily react with water to form carboxyl groups. After addition of water, the side chain groups of polyethylene may have the structures I or II.



The suggested structure of reaction product is supported by the results of a series of experiments: solution point in tetralin is lower in grafted than in the nongrafted films (result of lower crosslinking of the product due to the loss of a significant proportion of peroxy crosslinkages); there is an increase of film weight in the grafted film on washing in aqueous NaOH solution (result of the reaction with carboxylic groups), the decoloration by grafted films of slightly alkaline phenolphthalein solutions was lower than in the case of nongrafted film; the content of oxygen (result of absorption of carbon suboxide), absolute increase of film weight (addition of carbon suboxide), and infrared analysis [lack of bands characteristic of poly(carbon suboxide)] also support structures I and II.

As is apparent from the results of experiments at below 50°C, no grafted copolymer was obtained, but rather a modified polyethylene. This modi-

fied polyethylene showed good absorption of aqueous solutions of alkaline dyes. This method of dyeing polyethylene was detailed in a patent.⁶

The result of experiments at temperatures exceeding 70°C indicate formation of grafted copolymer (c.l.) poly(ethylene-*g*-carbon suboxide). Such a structure for the product is supported by: insolubility of the film in hot boiling tetralin and hot boiling toluene (result of crosslinking); minimum weight loss under the influence of solvents for poly(carbon suboxide), which indicates the product is not a mixture of homopolymer and copolymer, higher oxygen content than in ozonized polyethylene [the possibility of single molecular linking is excluded, which supports the existence of poly(carbon suboxide) chains], evolution of CO₂ gas during the terminal

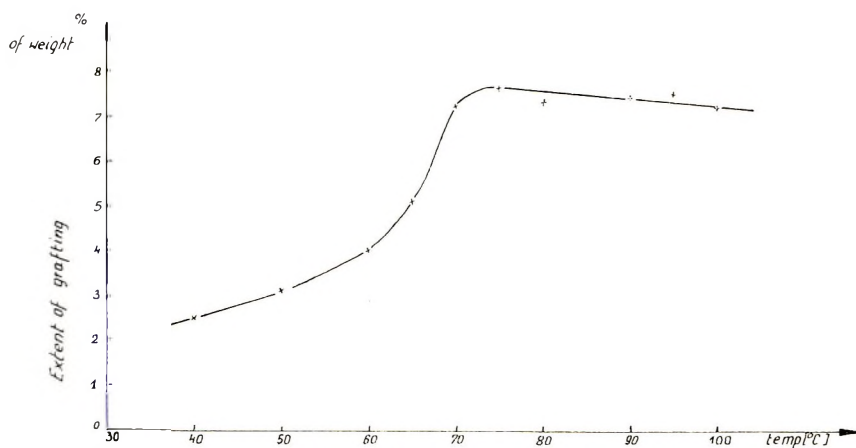


Fig. 1. Effect of temperature on the extent of grafting (increase of film mass).

decomposition of the product, indicating the presence of poly(carbon suboxide) chains, the presence of bands characteristic of poly(carbon suboxide) in the infrared spectrum, the red-brownish color and lack of translucency, high relative weight increase (as high as 40%).

Experiments carried out in the range 50–70°C indicate that this is an intermediate stage where gradual transition from modified polyethylene to grafted crosslinked copolymer occurs. The change is gradual and low crosslinking of the product may be found already about 60°C. The effect of temperature upon the reaction yield (measured by relative weight increase is shown by the curve in Figure 1. The increase of yield in the range of 50°C may be explained by the positive influence of temperature upon the increase in the number of single carbon suboxide molecules absorbed by polyethylene. A further rapid increase of yield between 60 and 70°C is due to increasing predominance of grafting over the reaction of modifying polyethylene. In this range increasing amounts of carbon suboxide are absorbed by polyethylene and the structure of the product becomes more and more crosslinked. Once the maximum is reached at about 70°C, a small but constant decrease of the yield occurs. This may be explained

by the fact that the increase in rate of reaction of grafting is less than the increase in the rate of solution toluene of still ungrafted polyethylene.

Influence of Ozonization Time

The experiments of this series were carried out at 80°C, in exactly the same way as above. The experimental results are presented in Table III.

TABLE III
Effect of Ozonization Time of Polyethylene upon the Grafting Yield of Carbon Suboxide and Appearance of the Product

Ozonization time, hr	Grafting yield (relative weight increase), %	Appearance of film after grafting
1	20.2	Brownish-orange, lower elasticity, transparent, wrinkled.
2	31.3	Brownish-orange, low elasticity, poor transparency, wrinkled
3	34.2	Brownish-red, nonelastic, poorly transparent, wrinkled
4	35.1	"
8	40.6	Brownish-red, nonelastic, almost opaque, wrinkled
12	41.1	"

With increasing ozonization time, the grafting yield increases, which is due to the increase of the number of active groups in polyethylene. The rate of increase of yield is slower, however, because at higher stages of cross-

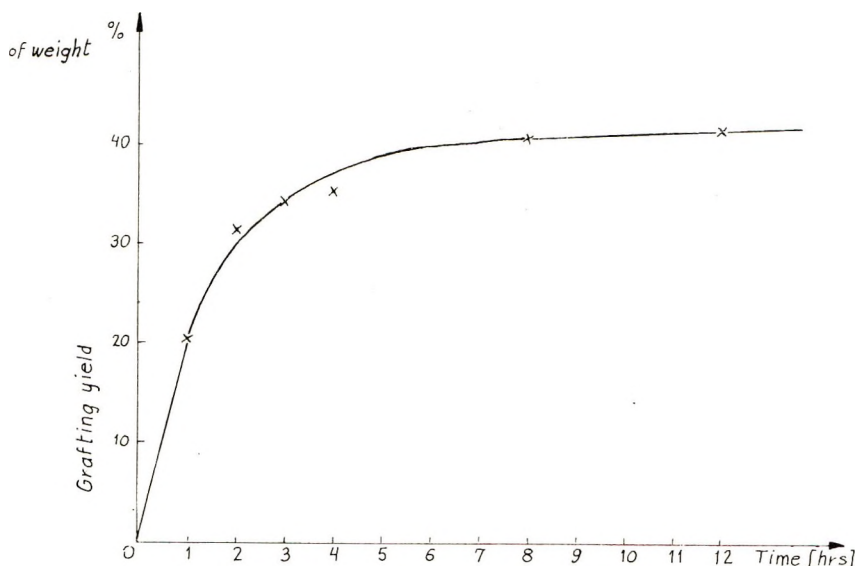


Fig. 2. Effect of the time ozonization of polyethylene film on the grafting yield.

linking of the product the possibility of diffusion of monomer molecules in the toluene solution drops to still unreacted active groups of polyethylene. In this way, with the increase of ozonization time, in spite of larger number of possible grafting places (peroxygen groups), the grafting is slowed down by impedance of diffusion due to the increased crosslinking. The effect of ozonization time upon grafting yield (measured by relative weight increase) is illustrated by the curve in Figure 2.

Effect of Other Factors

In order to carry out detailed research upon the effect of diffusion upon grafting, experiments were carried out with the use of solvents other than toluene, which can swell polyethylene. Ability to swell ozonized polyethylene film was verified by appropriate experiments without carbon suboxide. The effect of the solvent of carbon suboxide on the course of the grafting reaction is summarized in Table IV. The higher reaction yield reached with the use of solvents which are better swelling agents for polyethylene confirms the role of diffusion in the grafting reaction.

TABLE IV
Effect of Solvent on the Yield in Grafting of Carbon Suboxide
on Ozonized Polyethylene Film^a

Solvent	Swelling of ozonized film	Grafting yield (relative weight increase), %	Product properties
Toluene	High	+36.5	Insoluble, red brown
Chlorobenzene	Relatively high	+32.7	"
Nitrobenzene	Small	+3.5	Soluble, yellow

^a Conditions: ozonization time, 4 hr; reaction time, 3 hr; reaction temperature, 80°C; 30 g of 10% solution of C₃O₂, about 0.3 g polyethylene.

Also, grafting experiments on films of different thicknesses confirmed the role of diffusion in the reaction. Experiments were carried out at 80°C for 3 hours with the use of 30 g of 10% solution of carbon suboxide in toluene. Films of 0.03 and 0.06 mm thickness were grafted with polyethylene in grain form. The higher grafting yield was reached with film 0.03 mm thick.

CONCLUSIONS

Polyethylene ozonized at room temperature with a 4% mixture of ozone and oxygen reacts with carbon suboxide in solution. The course of the reaction depends on reaction temperature.

Reactions at temperatures at 70°C or above with the use of carbon suboxide in toluene or other hydrocarbons swelling polyethylene give a cross-

linked copolymer (c.l.), poly(ethylene-*g*-carbon suboxide). The reactions are to a large extent controlled by diffusion.

Reactions carried out at below 50°C cause the modification of polyethylene. The modification is a joining of active groups formed on polyethylene by means of ozonization with single molecules of carbon suboxide. The side groups so formed in polyethylene chains react rapidly with water to form carboxylic groups.

References

1. M. V. Volkenshtein, *Usp. Khim.*, **4**, 610 (1935).
2. L. B. Daszkiewicz and V. G. Beilen, *Usp. Khim.*, **36**, 497 (1967).
3. A. Bukowski and S. Porejko, *Wiadomości Chem.*, in press.
4. R. J. Ceresa, *Block and Graft Copolymers*, Butterworths, London, 1962.
5. A. Bukowski and S. Porejko, *J. Polym. Sci. A-1*, this issue. *
6. A. Bukowski and S. Porejko, Polish Pat. 55062, 1968.

Received May 22, 1969

Revised February 4, 1970

Chain Transfer with Siloxanes During Free-Radical Polymerization

JOHN C. SAAM and DAVID J. GORDON, *Dow Corning Corporation, Midland, Michigan 48640*

Synopsis

Chain transfer constants (C_s) for a number of substrates containing the silicon-oxygen bond are measured in polymerizing methyl methacrylate. Additionally, a few measurements are run in styrene in order to estimate the influence of polar factors on chain transfer. The methylsiloxanes studied all show very low values of C_s (10^{-5} to 10^{-6}). The chain transfer constants of a number of propylsiloxane derivatives are negligibly influenced by the presence of silicon. Thus, $(\text{Me}_3\text{SiO})_2\text{MeSiCH}_2\text{MeCH}(\text{C}_6\text{H}_5)$ shows a value of C_s nearly that reported for cumene, and $(\text{MeO})_3\text{SiCH}_2\text{CH}_2\text{CH}_2\text{SH}$ shows values of C_s close to those reported for alkyl mercaptans.

INTRODUCTION

The degree of interaction of polymeric free radicals with organosiloxanes is unknown. Measurements of chain transfer in free-radical polymerization for some alkyl,¹ aryl,² and chlorosilanes^{3,4} are reported but, with a single exception,⁵ data on substrates containing the silicon-oxygen bond are nonexistent. Inferences based on present literature generally lead to contradiction and confusion. Thus, oxygen in the vicinity of metal-carbon bonds is reported to drastically reduce chain transfer in certain organometallic substrates,¹ whereas the methyl radical is reported to be more reactive with aromatic siloxanes than with benzene or toluene.⁶

Emphasis in the present study is therefore on measurements of chain transfer of various siloxanes with polymerizing methyl methacrylate. Chain transfer constants are measured for methylsiloxanes, alkoxy silanes, and aliphatic as well as aromatic siloxanes and siloxanes containing silicon-hydrogen bonds. The aim is to discover the influence of the silicon-oxygen bond and the importance of polar effects which may arise because of its presence. Certain functional siloxanes are also investigated.

EXPERIMENTAL

Reagents

The siloxanes listed in Table I were prepared by cohydrolysis of the appropriate chlorosilanes or alkoxy silanes. All materials were carefully distilled and pure according to gas-liquid chromatography. Structures

were confirmed by their NMR and infrared spectra. Hexamethyldisiloxane, octamethyltrisiloxane, dodecamethylpentasiloxane, octamethylcyclotetrasiloxane, and tetramethylcyclotetrasiloxane were commercially available and sufficiently pure as received. The alkoxysilanes were also available from commercial sources but some required distillation prior to use. Methyl methacrylate was washed with dilute alkali and then with water, dried, and distilled at reduced pressure just prior to polymerization. Styrene was purified in a similar manner.

TABLE I
Properties of Siloxanes Prepared for Chain Transfer Study

Compound	bp, °C/mm Hg	d_D^{25}	n_D^{25}	R_D found	R_D calcd
(Me ₃ SiO) ₂ SiφMe	121/23	0.908	1.4439	0.2944	0.2937
(Me ₃ SiO) ₂ SiPrMe	117/100	0.828	1.3957	0.2900	0.2912
(Me ₃ SiO) ₂ SiφH	105/10	0.909	1.4433	0.2923	0.2918
(Me ₃ SiO) ₂ SiMeCH ₂ CH ₂ CH ₃	125/5	0.904	1.4493	0.2975	0.3020
(Me ₃ SiO) ₂ SiMeCH ₂ CH ₂ CH ₂ SH	102–103/9	0.899	1.4265	0.2852	0.2858
(Me ₃ SiO) ₂ SiMeH	84/120	0.823	1.3805	0.2846 ^a	0.2846
(Me ₃ SiO) ₂ Siφ(OMe)	115/10	0.948	1.4419	0.2790	0.2812
(Me ₃ SiO) ₂ MeSiCH ₂ CH ₂ CF ₃		0.949	1.3726		

^a From Okawaru and Sakiama.¹²

Measurement of Chain Transfer Constants C_s .

Appropriate mixtures of the monomer M and the silicone substrate S with 10^{-5} moles of azobisisobutyronitrile per mole of monomer were charged into ampoules which were then connected to a vacuum line. The contents were repeatedly frozen with liquid nitrogen, thawed, and re-frozen until a vacuum of at least 10^{-6} mm Hg was attained. The ampoules were sealed and placed in a bath at $79.5 \pm 0.2^\circ\text{C}$ for a period sufficient to give less than 10% polymerization. The tubes were then opened and the contents were transferred to a large excess of ethanol or methanol. The polymer was taken up in benzene, reprecipitated twice, and residual solvents were removed at 60°C at less than 1.0 mm.

Degree of Polymerization

The degree of polymerization was estimated from the intrinsic viscosities measured at 25°C or 35°C using the expressions

$$\log p = 3.43314 + 1.35 \log [\eta]$$

$$\log p = 3.44871 + 1.32 \log [\eta]$$

for polystyrene and poly(methyl methacrylate), respectively.⁷ The chain transfer constants were then calculated using Mayo's equation⁸

$$\frac{1}{P} = C_s \frac{[S]^2}{[M]} + \frac{1}{\bar{P}_0} \quad (1)$$

where $C_s = k_{tr}/k_p$; $[S]$ and $[M]$ are the initial concentrations of substrate and monomer, respectively; and \bar{P}_0 is the degree of polymerization in the absence of a substrate.

RESULTS

The various alkylsiloxanes, when present in the polymerization of methyl methacrylate, decrease molecular weight in a manner predictable from the Mayo equation. Some examples are shown in Figure 1, where the data are fit to eq. (1). The intercept $1/\bar{P}_0$, where no siloxane is present, should be common to all determinations if the rate of propagation is not altered by the substrates studied. Figure 1 shows data for several siloxanes with differing values of C_s converging very close to this experimentally measured point. Validity is further established by determining C_s for cumene in the presence of sufficient octamethyltrisiloxane to approximate conditions under which C_s is determined for the various siloxanes in this study. Octamethyltrisiloxane, having a very low C_s compared with cumene, should not influence the result, unless effects arising from the presence of the siloxane, such as the heterogeneity which occasionally appears during

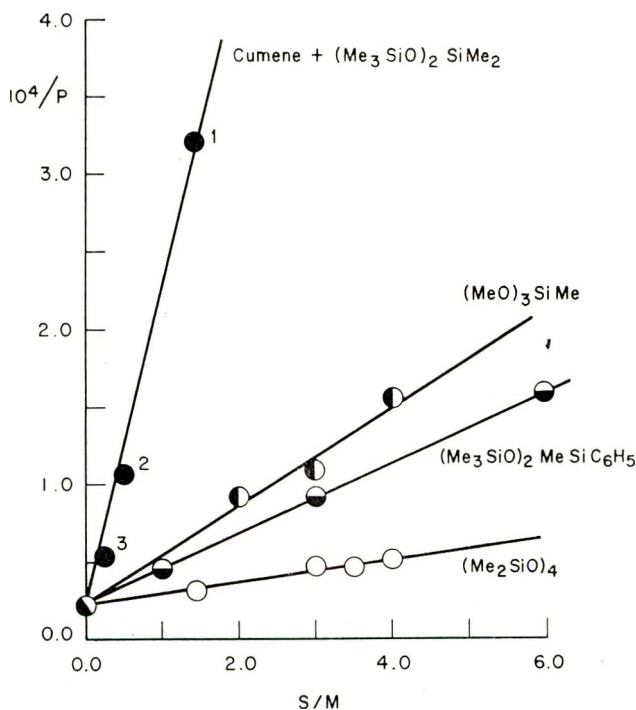


Fig. 1. Plot of S/M vs. $1/P$ for the polymerization of methyl methacrylate at 80°C in the presence of various siloxanes. The y -intercept (\odot) is an average of three determinations run in the absence of a substrate. For cumene + $(\text{Me}_3\text{SiO})_2\text{SiMe}_2$ (\bullet), 37 mole-% siloxane is present in point 1, 40 mole-% in point 2, and 27 mole-% in point 3.

TABLE II
 Chain Transfer of Siloxane Substrates with Methyl Methacrylate at 79.5°C

Substrate	$[S]/[M]$	$P \times 10^{-3}$	$C_n \times 10^6$
None	0.00	43.4	
	0.00	45.3	
	0.00	43.9	
1. $(\text{Me}_3\text{Si})_2\text{O}$	0.645	35.0	1.04
	2.00	29.1	
	3.00	18.3	
	4.00	15.8	
	1.00	43.7	
2. $\text{Me}_3\text{SiO}(\text{Me}_2\text{SiO})_2\text{SiMe}_3$	2.83	36.7	0.316
	4.00	33.9	
	6.00	25.7	
	0.500	48.5	
3. $\text{Me}_3\text{SiO}(\text{Me}_2\text{SiO})_3\text{SiMe}_3$	1.00	41.2	1.45
	2.00	21.3	
	1.44	32.04	
4. $(\text{Me}_2\text{SiO})_4$	3.00	21.25	0.80
	3.50	21.07	
	4.00	19.39	
	1.00	21.7	
5. $(\text{Me}_3\text{SiO})_2\text{Si}\phi$ Me	3.01	10.9	2.32
	6.01	6.2	
	2.00	17.81	
6. $\text{C}_6\text{H}_5\text{Si}(\text{OMe})_2$ Me	3.00	15.24	2.0
	4.00	8.97	
	1.00	35.4	
7. $\text{C}_6\text{H}_5\text{Si}(\text{OMe})_3$	2.00	30.6	0.53
	3.00	25.9	
	2.50	36.0	
8. $(\text{Me}_3\text{SiO})(\text{C}_6\text{H}_5)\text{Si}(\text{OMe})_2$	4.00	28.5	0.32
	2.00	10.90	
9. $\text{MeSi}(\text{OMe})_3$	3.00	9.27	3.31
	4.00	6.42	
	1.00	13.92	
10. $\text{MeSi}(\text{OiPr})_3$	2.00	8.79	6.97
	3.50	3.26	
	0.252	43.0	
11. $(\text{Me}_3\text{SiO})_2\text{SiH}$ Me	0.523	32.2	2.84
	1.00	21.5	
	0.250	12.8	
12. $(\text{Me}_3\text{SiO})_2\text{SiH}$ ϕ	0.500	6.69	18.4
	1.00	4.93	
	0.066	6.11	
13. MeHSiCl_2 Me	0.231	2.74	152.0
	0.377	5.90	

TABLE II (continued)

Substrate	[S]/[M]	$P \times 10^{-3}$	$C_s \times 10^5$
14. $(\text{Me}_3\text{SiO})_2\text{SiCH}_2\text{CH}(\text{C}_6\text{H}_5)\text{CH}_3$	0.131	15.9	20.8
	0.786	4.42	
	1.57	2.88	
15. $(\text{Me}_3\text{SiO})_2\text{SiCH}_2\text{CH}_2\text{CH}_3$ Me	0.25	35.1	1.89
	1.25	23.7	
	2.00	16.8	
16. $(\text{Me}_3\text{SiO})_2\text{SiCH}_2\text{CH}_2\text{CF}_3$ Me	0.252	45.7	2.05
	0.500	41.2	
	1.00	25.6	
17. $(\text{MeO})_3\text{SiCH}_2\text{CH}_2\text{CH}_2\text{SH}$	2.12×10^{-1}	5.36	69,300
	4.24×10^{-4}	3.07	
	6.36×10^{-4}	2.22	
18. $(\text{Me}_3\text{SiO})_2\text{SiCH}_2\text{CH}_2\text{CH}_2\text{SH}$ Me	6.11×10^{-4}	9.27	12,845
	8.15×10^{-4}	8.44	
19. $[(\text{MeO})_3\text{SiCH}_2\text{CH}_2\text{CH}_2\text{S}]_2$	0.03	8.24	258
	0.06	5.44	
	0.15	2.45	
20. $(\text{MeO})_3\text{SiC}_6\text{H}_4\text{CH}_2\text{Br}$	0.03	23.3	298
	0.06	6.33	
	0.25	1.22	

TABLE III

Chain Transfer Constants of Siloxane Substrates with Styrene at 79.5°C

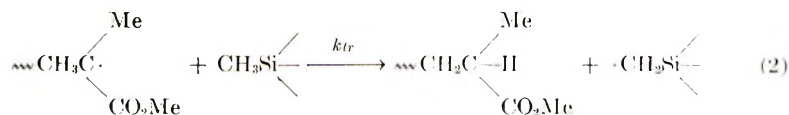
Substrate	[S]/[M]	$P \times 10^{-3}$	$C_s \times 10^5$
None		10.1	
		6.29 ^a	
1. $(\text{Me}_3\text{Si})_2\text{O}^b$	1.41	3.56	3.87
	3.56	2.97	
	2.00	8.40	
2. $\text{Me}_3\text{SiO}(\text{Me}_3\text{SiO})\text{SiMe}_3$	2.96	8.30	0.69
	4.00	8.25	
	1.00	8.59	
	2.50	6.36	
3. $\text{Me}_3\text{SiO}(\text{Me}_3\text{SiO})_3\text{SiMe}_3$	3.00	5.68	2.85
	0.84	7.24	
	1.68	6.22	
	3.0	5.33	
9. $\text{MeSi}(\text{OMe})_3$	4.0	4.73	2.30
	1.57 $\times 10^{-5}$	4.23	
	2.48 $\times 10^{-5}$	3.70	
17. $(\text{MeO})_3\text{SiCH}_2\text{CH}_2\text{CH}_2\text{SH}$	4.96 $\times 10^{-5}$	2.62	590,000
	0.0156	3.01	
	0.0314	2.18	
19. $[(\text{MeO})_3\text{SiCH}_2\text{CH}_2\text{CH}_2\text{S}]_2$	0.058	1.30	1,180

^a Value of P_0 obtained when run with 10^{-5} moles of azo-bis-isobutyronitrile.^b Use $P_0 = 6.29 \times 10^3$.

polymerization, alter C_s . These data are also shown in Figure 1, and the value so obtained, 22.4×10^{-6} at 80°C , agrees well with that reported for cumene.^{9,10} The results are given in Table II for methyl methacrylate and in Table III for styrene.

The results show generally that the methylsiloxanes are unreactive toward both polymerizing styrene and methyl methacrylate and that the values of C_s for the various methylsiloxanes are smaller by at least one power of 10 than C_s reported for tetramethylsilane⁴ or tetraethylsilane.¹ The reduction in C_s due to the presence of the SiO bond is particularly apparent with the substrates numbered 1, 2, 3, and 4.

Polar factors in the attacking free radical play a role in altering the reactivities of the methylsiloxanes 1, 2, and 3, as evidenced by the consistently larger values of C_s measured in the less polar styrene (Table III). This is expressed semiquantitatively in Table IV in terms of the linear free energy relationship described by Bamford et al.¹¹ Here, the values of α and β are given for siloxanes run with both styrene and methyl methacrylate. The magnitude of α indicates the susceptibility of the substrate toward polar factors in the free radical which presumably attacks by reaction (2). A negative value implies a tendency of the substrate to accept electrons in the transition state:



The inherent reactivity of the substrate in the absence of polar factors in the attacking radical is given by β . Here, a low or negative value implies a low activity with nonpolar free radicals relative to a reference material, toluene, where by definition $\beta = 0.00$. The values for α shown in Table

TABLE IV
Substrate Polarity from C_s Measurements

Substrate	α	β
Cyclohexane ^a	-0.2	-0.6
Et ₄ Si ^b	-1.3	1.7
Me ₄ Si ^c	-1.0	1.5
1. (Me ₃ Si) ₂ O	-2.7	0.1
2. Me ₃ SiO(Me ₂ SiO) ₃ SiMe ₃	-1.9	-0.6
3. Me ₃ SiO(Me ₂ SiO) ₃ SiMe ₃	-1.8	-0.1
9. MeSi(OMe) ₃	-0.2	-0.1
17. (MeO) ₃ SiCH ₂ CH ₂ CH ₂ SH	-4.0	5.2
18. [(MeO) ₃ SiCH ₂ CH ₂ CH ₂ S] ₂	-3.0	2.6
<i>n</i> -C ₄ H ₉ SH ^d	-4.8	6.0

^a Based on data from Basu et al.⁹ and Young et al.¹⁰

^b Based on data from Huff and Perry.¹

^c Based on data from Minoura and Enomoto.⁴

^d Based on data from Bamford et al.¹¹

IV indicate a somewhat increased tendency of the siloxanes 1, 2, and 3 relative to Me_4Si or Et_4Si to behave as electron acceptors in the transition state associated with free-radical chain transfer. On the other hand, methyltrimethoxysilane, 9, where increased electrophilic character might be expected, shows a value of α approaching zero. The values of β for the siloxanes 1, 2, 3, and 9 are considerably less than those for Me_4Si and Et_4Si and indicate inherent reactivities more similar to those of hydrocarbons.

Measurements in methyl methacrylate for the siloxanes and alkoxy-silanes numbered 5 through 9 show generally small chain transfer constants and indicate that $-\text{OMe}$ may be replaced with $-\text{OSiMe}_3$ with little effect. In view of the values of C_s approaching zero for substrates 7 and 8, transfer with aromatic and peripheral $-\text{OSiMe}_3$ or $-\text{OMe}$ must be negligible in 5 and 6, and in 9 as well. The methyl groups on the central silicon in substrates 5 and 6 must therefore play a dominant role in determining C_s . Comparison with substrate 2 also indicates an enhancement of reactivity when the central SiMe is adjacent to the aromatic nucleus.

The reactivity of the silicon hydrides 11 and 12 in Table II resembles more that of branched aliphatic or aromatic hydrocarbons rather than that of the highly reactive triphenylsilane² where siloxane bonds are absent. For example, C_s for substrate 12 is very close to that reported for cumene.^{9,10} In view of these observations, the C_s previously reported for $(\text{MeHSiO})_x$ of 183×10^{-5} seems excessively high.⁵ No effort was made to purify this substrate, and chain transfer with impurities instead of SiH may have occurred in this ill-defined material. The greatly increased value of C_s of MeHSiCl_2 over the other silicone hydrides in Table II suggests that the presence of $\text{Si}-\text{Cl}$ activates hydrogen atom abstraction from the silicon hydride bond.

The substrates 14, 15, 17, and 18 show chain transfer constants expected of the related species with no silyl substituent. Thus, in substrate 14 the value of C_s is very close to that reported for cumene, and substrates 17 and 18 show values very close to those reported for alkyl mercaptans.^{9,10} Furthermore, Table IV shows that the values of α and β for the mercaptan, 17, approach those observed for butyl mercaptan. No data are available for similar comparisons of substrates 16, 19, and 20. It is presumed, however, that the silyl group in these species also plays a minor role in determining C_s .

The mercaptan, 17, and the disulfide, 19, show high chain transfer associated with the SH and SS groups and can provide convenient synthesis of interesting alkoxy-silyl-terminated polymers via free-radical polymerization. With the disulfide, the macromolecules will be predominantly terminated at both ends with reactive $(\text{MeO})_3\text{Si}$ groups to give a system capable of forming crosslinked networks upon exposure to moisture. Both the mercaptan and the disulfide should be effective with nonpolar monomers such as styrene and butadiene; and, based on the foregoing results, extraneous transfer in these substrates with SiOMe or SiCH_2 should be negligible compared with SH or SS .

References

1. T. Huff and E. Perry, *J. Polym. Sci. A*, **1**, 1553 (1963).
2. J. Curtice, H. Gilman, and G. S. Hammond, *J. Amer. Chem. Soc.*, **79**, 4754 (1957).
3. G. Hardy, K. Nitrai, G. Kovacs, and V. P. Li, *IUPAC International Symposium on Macromolecular Chemistry*, 1960, Moscow, Papers and Summaries, Sect. II, p. 103.
4. Y. Minoura and Y. Eaomoto, *J. Polym. Sci. A-1*, **6**, 13 (1968).
5. K. Kojima, *Skika Zairyo Kenkyusho Hokoku*, **2**, 220 (1967).
6. S. I. Beilin, N. A. Pokatilo, and B. A. Dolgoplosk, *Vysokomol. Soedin.*, **1** (6), 1085 (1965).
7. J. H. Baxendale, S. Bywater, and M. G. Evans, *J. Polym. Sci.*, **1**, 237 (1946).
8. R. A. Gregg and F. R. Mayo, *J. Amer. Chem. Soc.*, **70**, 2373 (1948); *ibid.*, **75**, 3530 (1953).
9. S. Basu, J. N. Sen, and S. R. Palit, *Proc. Roy. Soc., Series A*, **202**, 485 (1950).
10. L. J. Young, G. Brandrup, and J. Brandrup, in *Polymer Handbook*, J. Brandrup and E. H. Immergut, Eds., Wiley, New York, 1966, p. II-103.
11. C. H. Bamford, A. D. Jenkins, and R. Johnston, *Trans. Faraday Soc.*, **55**, 418 (1959).
12. R. Okawaru and M. Sakama, *Bull. Chem. Soc. Japan*, **29** (5), 547 (1956).

Received February 6, 1970

The Vacuum and Oxidative Pyrolysis of Poly-*p*-xylylene

H. H. G. JELLINEK and S. N. LIPOVAC, *Department of Chemistry
Clarkson College of Technology, Potsdam, New York 13676*

Synopsis

Poly-*p*-xylylene prepared by pyrolysis of di-*p*-xylylene has been degraded under vacuum and in the presence of oxygen as a function of temperature and oxygen pressure. The vacuum pyrolysis is mainly due to "abnormal" structures. Volatiles are initially produced quite slowly, but the reaction accelerates subsequently. Arrhenius equations were derived for various ranges of volatile formation. A mechanism has been formulated consisting of random chain scission followed by depropagation (dimers to pentamers); simultaneously another zip reaction produces hydrogen. The thermal, oxidative degradation has been studied above and below the softening point of the polymer as a function of oxygen pressure. A first-order reaction of volatile formation due to "abnormal" chain scission is followed by normal chain scission, which is also first order. The postulated mechanism leads initially to hydroperoxide formation. Arrhenius equations for volatile formation are different below and above the softening point. Oxygen consumption also follows a first-order reaction with an energy of activation of 31.5 kcal/mole.

INTRODUCTION

The vacuum pyrolysis of poly-*p*-xylylene has been studied from the standpoint of the rate of volatile production and by mass-spectrometric analysis of the reaction products by Madorsky and Straus.¹ Viscometric measurements were performed by Schaeffgen² and chromatography and infrared analysis, by Kalashnik et al.³ In addition, there are a number of observations in the literature concerning the thermal stability of this polymer.⁴⁻⁸ The work was carried out by the above-mentioned authors with polymers prepared according to a method by Swarcz⁵ or by the Wurtz reaction. The general consensus is that such polymers are crosslinked to a certain extent. This conclusion is based on the solubility behavior of the polymer.

More recently, Gorham⁹ published a new method of preparation of poly-*p*-xylylene based on pyrolysis of di-*p*-xylylene under vacuum at about 600°C. This author claims that the polymer obtained by this method is linear and not contaminated by low molecular weight material. The present work deals with the vacuum and oxidative pyrolysis of poly-*p*-xylylene prepared according to Gorham's method.

There is very little information available on the oxidative degradation of poly-*p*-xylylene. Lancaster and Wright¹⁰ compared the thermal stabilities

of various polymers having aromatic rings in the chain. They found that poly-*p*-xylylene prepared by the lithium route is more stable than that obtained by the pyrolysis method. An overall energy of activation for the lithium-prepared polymer of 53 kcal/m was found for oxidative pyrolysis. This result was obtained from first-order plots. These authors¹⁰ found the very high value of 93 kcal/m for vacuum pyrolysis. There may be some difference in the energies of activation for polymers prepared by different methods.

Polybenzyl, a polymer expected to show similarities to poly-*p*-xylylene on oxidative pyrolysis, was investigated by Lady et al.¹¹ and Conley.¹² These authors followed the process by infrared spectra. Conley found an energy of activation of 14.5 ± 3.5 kcal/mole. A reaction scheme was formulated which leads via hydroperoxides to carbonyl and hydroxyl groups and to some chain scission. Appreciable amounts of water were assumed to be formed during the oxidation process.

The present work on vacuum pyrolysis of polymer film samples prepared by Gorham's method leads to the conclusion that the polymer prepared from di-*p*-xylylene contains a small percentage (ca. 1% to 2%) of low molecular weight material. In addition, there are some abnormal structures ("weak links") in the polymer chain where chain scission takes place, followed by depolymerization, producing very low molecular weight material (dimers to pentamers). Hydrogen gas is also evolved, leaving conjugated double bond structures behind. Once these abnormal structures are consumed, pyrolysis practically ceases. These abnormalities in the polymer chain may be due to some branch points.

The oxidative pyrolysis also leads to chain scission due to abnormal structures. In addition, a pyrolysis of normal structures takes place. Again dimers to pentamers are assumed to be produced by unzipping and hydrogen is also evolved leading to conjugated unsaturated polymer structures. Oxidation of hydrogen atoms is believed to lead to appreciable amounts of water.

EXPERIMENTAL

Apparatus

The degradation apparatus was repeatedly described before.¹³ It consists essentially of a quartz-spoon-gauge reaction vessel in conjunction with a Statham gauge and a Sanborn recorder. The polymer is deposited at the inside wall of the calibrated spoon reaction vessel; the sealed and evacuated vessel is plunged into a hot thermostated metal bath. The reaction temperature is reached in about 20 sec and pressure changes are recorded as a function of time.

Viscosities were measured with an Ubbelohde semimicroviscometer, suspended in the vapor of boiling ethylphthalate (298°C). The polymer was dissolved in boiling benzyl benzoate (316.8°C). This took several minutes.

The polymer was prepared according to Gorham's method and was directly deposited as a film on the inside of the spoon reaction vessel. Figure 1 shows the arrangement. The polymerization procedure was as follows: A quartz tube (length 60 cm, i.d. 1.8 cm) contains a boat, M, with 10 to 20 mg of di-*p*-xylylene (K & K Laboratories, Inc.). The furnace, F (Lindberg, Heavi Duty Type 54031A), is heated to 650°C while the tube is evacuated. The part of the tubing outside the furnace at M is heated rapidly with a heating tape to 240°C, and parts a to b and c to d are heated

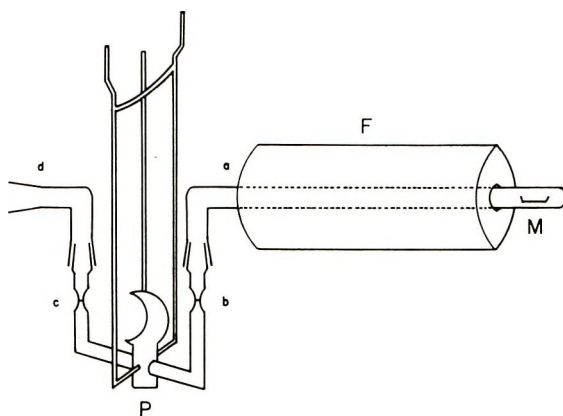


Fig. 1. Apparatus for polymer preparation: (F) furnace (650°C); (M) boat containing di-*p*-xylylene heated to 240°C; (a) to (b) and (c) to (d) heated to 180°C, respectively; (P) spoon reaction vessel cooled by ice-water mixture; (d) leads to high vacuum system.

to 180°C. An even and smooth polymer film is formed at the inside wall of the reaction vessel P (see Jellinek and Clark¹³ for description of reaction vessel), which is cooled by an ice-water mixture. The film thus formed is ca. 60 μ to 100 μ thick. Part d leads to a high vacuum system. After evacuation (10^{-5} mm Hg) for 24 hr, the spoon is sealed off, connected to the degradation apparatus, and plunged into the hot metal bath.

Volatilization in Vacuum

Some typical volatilization curves for various temperatures are shown in Figure 2. The ordinate is given in moles of volatiles produced. The initial amount of polymer was ca. 2×10^{-4} monomeric unit moles. The very initial parts of the curves show a rapid evolution of volatiles, which is typical of polymer films containing low molecular weight material. The curves pass first over into a slowly rising, approximately straight line before increasing more rapidly. The reaction eventually slows down again during its later stages. The logarithms of the reciprocal "slowing down" periods ($1/I = K_I$) are depicted in Figure 3 as function of reciprocal absolute temperature. The Arrhenius equation is

$$\log K_I = 3.98 \times 10^{16} e^{-58100/RT} \text{ min}^{-1}. \quad (1)$$

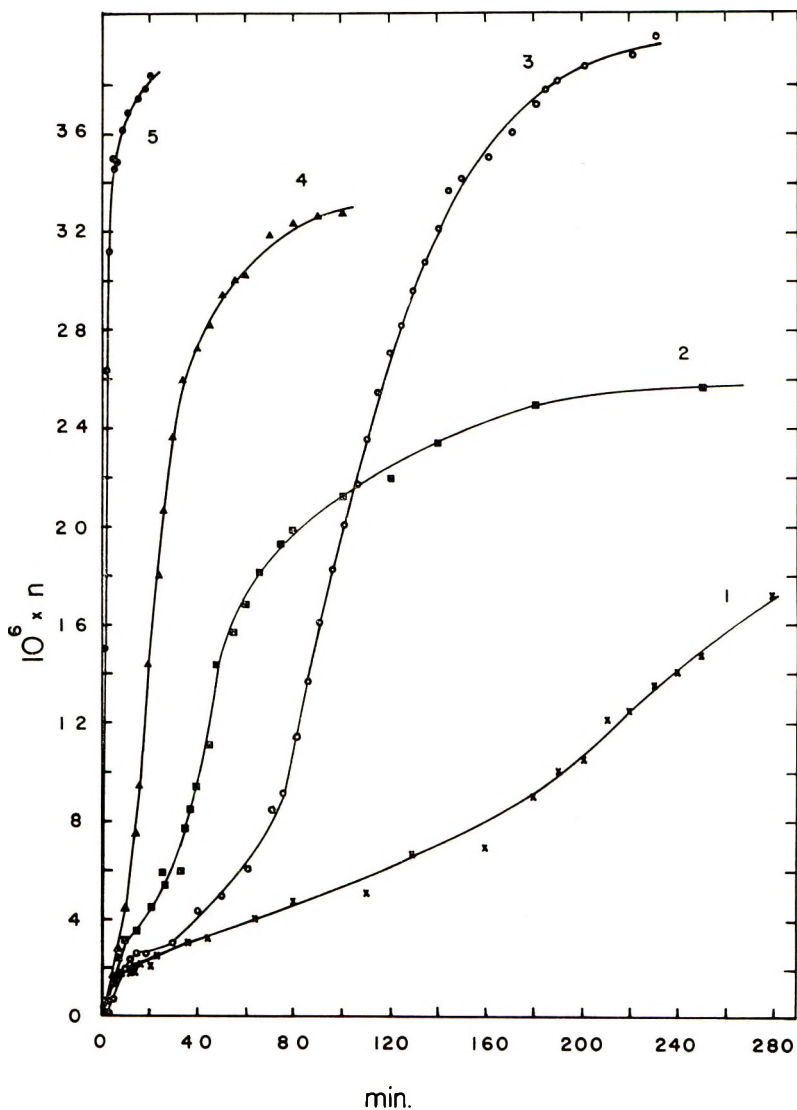


Fig. 2. Typical vacuum-volatilization curves ($m_0 = 2.0 \times 10^{-4}$ monomeric unit moles): (1) 408°C; (2) 436°C; (3) 424°C; (4) 450°C; (5) 515°C.

The straight line does not fit the experimental points too well. These points rather follow two straight lines of different slopes. (see Fig. 3). The energy of activation in the temperature range from 408° to about 450°C is 74.0 kcal/mole and that for 475° to 515°C is 46.5 kcal/mole.

A few viscosity measurements were carried out in order to ascertain whether random chain scission takes place. The polymer was dissolved in boiling benzyl benzoate (bp 316.8°C) which took about 3 min. Viscosities were measured at 298°C under nitrogen.

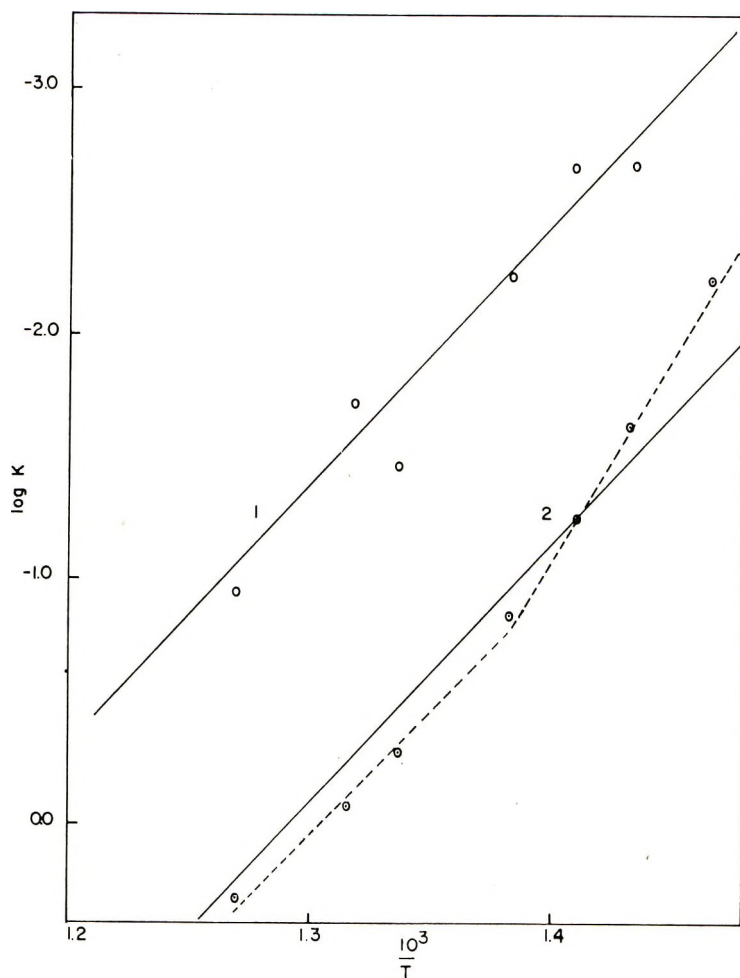


Fig. 3. Arrhenius plots of rate constants for vacuum volatilization eq. (10) and for reciprocal "slow periods," eq. (1), respectively: (1) $2.303 + \log K_v$ vs. $1/T$; (2) $\log K_1$ vs. $1/T$ ($K_1 = 1$).

The viscosity measurements gave the following results: The original sample had a reduced viscosity $\eta_{red} = 1.30$ for $c = 0.065$ g/dl at 25°C . After heating a polymer film for 2 min under vacuum at 424°C , the reduced viscosity decreased to $\eta_{red} = 0.39$ for $c = 0.041$ g/dl. This result clearly indicates that a random chain scission takes place.

Oxidative Degradation: Pressure Changes as a Function of Time

The chart reading was adjusted to zero for $t = 0$ for all experiments. Pressure increases were recorded, which represent the volatiles produced minus the oxygen consumed (excess pressure). Thus, the amounts of volatiles produced were always larger than the amounts of oxygen consumed.

Samples of 10 mg were taken for each experiment. The films were approximately 60μ thick. Oxygen consumption was also measured directly at a few temperatures according to a modified method by Sweetser.^{14,15}

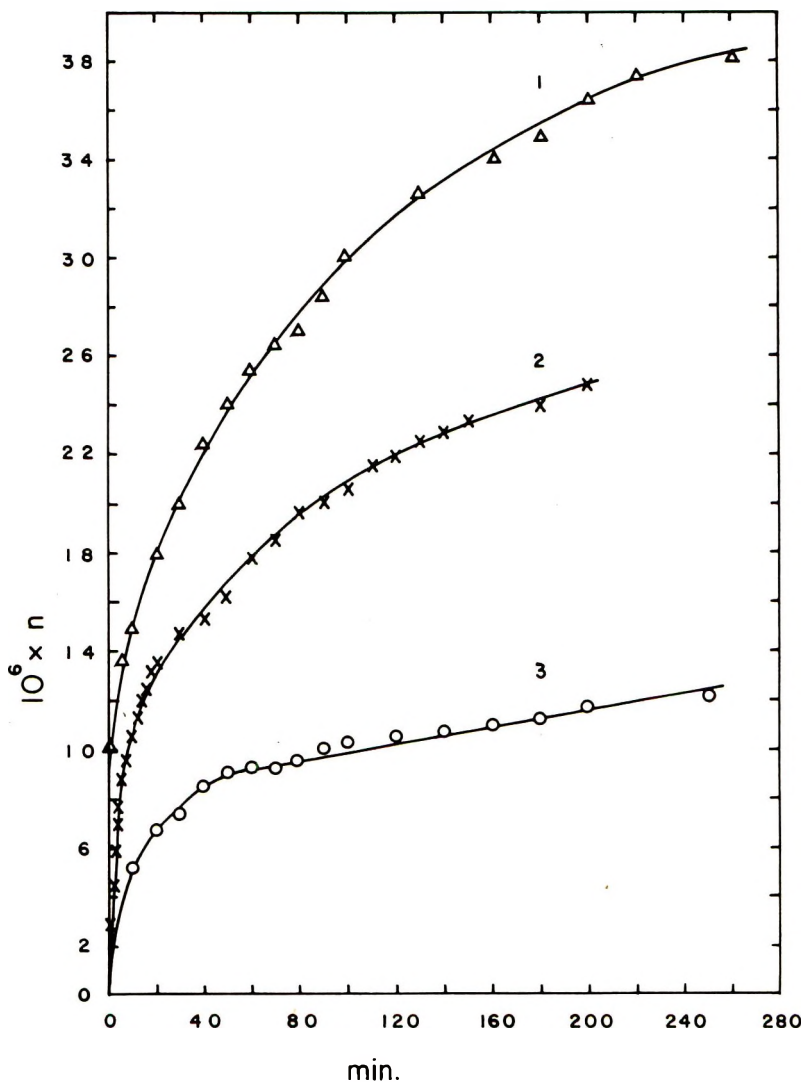


Fig. 4. Typical oxidative volatilization curves below the softening point (ca. 400°C): (1) 361°C , $P_{\text{O}_2,i} = 177 \text{ mm Hg}$; (2) 324°C , $P_{\text{O}_2,i} = 275 \text{ mm Hg}$; (3) 341°C , $P_{\text{O}_2} = 177 \text{ mm Hg}$. ($P_{\text{O}_2,i}$ measured at 25°C .)

Some typical oxidation curves below and above the softening point (somewhat below 400°C) of the polymer are shown in Figures 4 and 5, respectively.

The consumption of oxygen follows satisfactorily a first-order law.

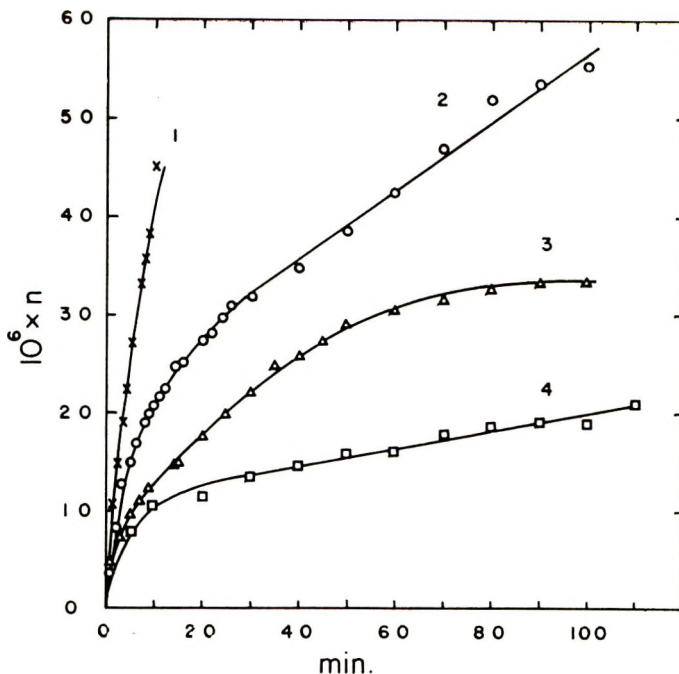


Fig. 5. Typical oxidative volatilization curve above the softening point (ca. 400°C): (1) 463°C, 40 mm Hg; (2) 420°C, 119 mm Hg; (3) 436°C, 51 mm Hg; (4) 436°C, 101 mm Hg.

The rate constants, k_{O_2} , are given below (see Figure 6),

temp, °C:	423	436	463
$10^2 k_{O_2}$, min ⁻¹ :	2.3	4.7	7.0

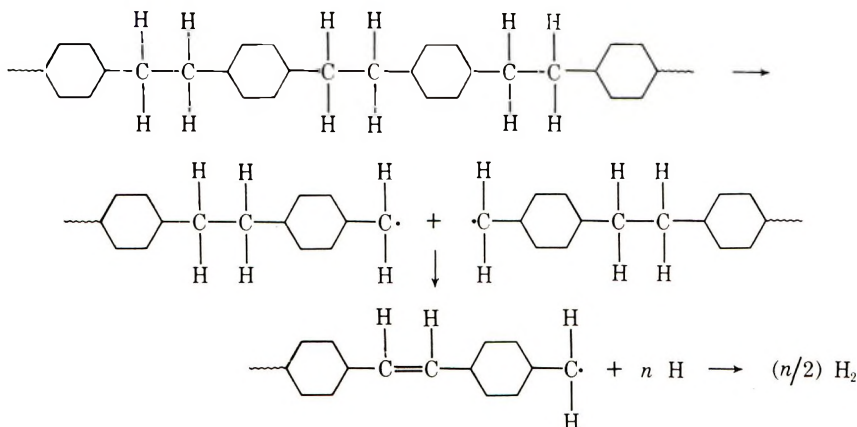
The relevant energy of activation is 31.5 kcal/mole.

DISCUSSION

Vacuum Pyrolysis

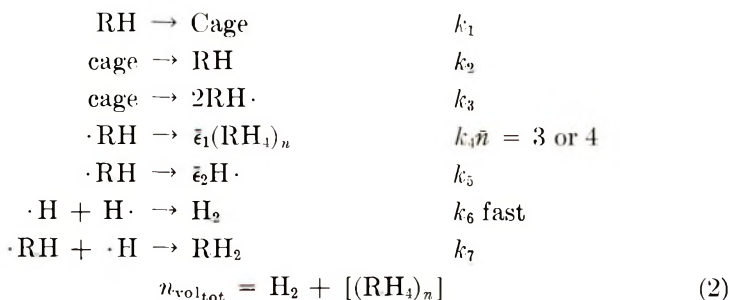
The curves in Figure 2 are similar to those obtained by Madorsky and Straus,¹ except that the reaction in the present case appears to stop when 10% to 15% of the possible monomeric unit moles have volatilized in the form of monomer. If the volatiles were to consist on the average of tetramers or pentamers, 30% to 40% of the polymer would have volatilized under the experimental conditions. The latter assumption agrees with the findings of Madorsky and Straus¹ and Kalashnik et al.³ These workers found very little monomer in the reaction products, but appreciable amounts of dimer, trimer, tetramer, and pentamer. Madorsky and Straus¹ deduced an energy of activation of 76 kcal/mole from the initial rate of volatilization. Schaeffgen² from viscosity measurements found 55 to 58 kcal/mole. The decomposition of gaseous dibenzyl gives 48 kcal/mole.

A tentative mechanism can be formulated which is in agreement with the experimental facts, Kalashnik et al.³ have shown that, in addition to low molecular weight poly-*p*-xylylenes and some other aromatic compounds, appreciable amounts of hydrogen gas are produced, which was also found by Swarcz.^{4,5} The fact that the reaction stops before the polymer is completely volatilized indicates that some abnormal structures (e.g., branch points) are present in the polymer chain. Further, the viscosity measurements show that random chain scission takes place. The mechanism can thus be assumed to consist of random chain scission of abnormal structures in the chain, followed by a depropagation reaction resulting in low molecular weight polymer but very little monomer. In addition, each chain scission is followed by a zip reaction forming hydrogen, leaving a conjugated double-bond structure behind:



The polymer radicals can be terminated by $H\cdot$ radicals or by other polymer radicals after unzipping of a few dimers, trimers, tetramers, and pentamers from the newly formed chain radicals.

The whole mechanism can then be formulated as follows:



Here, $n_{\text{vol}_{\text{tot}}}$ is the total amount in moles of volatiles in the reaction vessel of volume V_R ; H_2 and $[(RH_1)_n]$ are the moles of hydrogen and volatile low molecular weight polymer in the vessel. Further,

$$2 \times n_{w,0} \alpha_t' \bar{\epsilon}_1 = (RH_1)_n \quad (3)$$

and

$$2 \times n_{w,0} \alpha_t' \frac{\bar{\epsilon}_2}{2} = H_2 \quad (4)$$

where $\bar{\epsilon}_1$ and $\bar{\epsilon}_2$ are number-average kinetic chain lengths; $n_{w,0}$ is the total number of moles of weak links in the polymer film at $t = 0$; and α_t' the degree of degradation with respect to weak links at time t , i.e., $\alpha_t' = 1 - n_{w,t}/n_{w,0}$.

Reaction (4) gives the rate of breaking "abnormal" links,

$$-\frac{dn_{w,t}}{dt} = k_3 \text{ cage} = \frac{dRH}{2dt} \quad (5)$$

or, if termination is by small molecular weight radicals or spontaneously only (zero or pseudo-first order) and the cage concentration is obtained by the steady state method, eq. (5) gives

$$-\frac{dn_{w,t}}{dt} = k_3 \frac{k_1}{k_2} n_{w,t} = K_{\text{exp},v} n_{w,t} \quad (6)$$

(during reduction of film volume $[n_w]_t \equiv [n_w]_0 = \text{constant}$ for the major part of the process¹⁶).

Equation (6) represents the rate of breaking "abnormal" links for a polymer sample containing initially $n_{w,0}$ moles of "abnormal" links. $K_{\text{exp},v}$ refers, then, to a polymer sample having one mole of "abnormal" links. If this amount of polymer were to consist of $m_0/n_{w,0}$ monomeric unit moles, then for one monomeric unit mole of polymer the rate constant becomes

$$K'_{v} = \frac{K_{\text{exp},v} n_{w,0}}{m_0 (= 2 \times 10^{-4})} = \frac{K''_{\text{exp},v}}{m_0} \text{ min}^{-1}. \quad (7)$$

It should be remembered that $K_{\text{exp},v} = -dn_{w,0}/n_{w,0}dt$. The rate of breaking "abnormal" links is then given by

$$-\frac{n_{w,0} dn_{w,t}}{(m_0 - n_{v01,t}) dt} = K'_{v} n_{w,t} \text{ min}^{-1}. \quad (8)$$

The experimental curves (Fig. 2) indicate an initially slow volatile formation, probably due to relatively slow attainment of the steady state. The subsequent rise in rate follows a zero-order reaction as the percentage of "abnormal" links ruptured in this range of the reaction is quite small (i.e., $n_{w,t} \cong n_{w,0}$ and $m_0 - n_{v01,t} \cong m_0$; maximum of 20% by weight of the original sample has vaporized at the end of the zero-order period). The zero-order reaction goes then over to a first-order process. The rate constants $K_{\text{exp},v}$ were evaluated from this zero-order range ($n_{v01,\infty} \cong \text{constant}$):

$$-\frac{(\bar{\epsilon}_1 + 2\bar{\epsilon}_2) dn_{w,t}}{dt} = \frac{dn_{v01,t}}{dt} = K_{\text{exp},v} n_{v01,\infty}. \quad (9)$$

Here,

$$K_p = K_{\text{exp},p} \frac{n_{\text{vol},\infty}}{m_0} = K'_{\text{exp},p} \quad (10)$$

where $n_{\text{vol},\infty}$ is the amount of volatiles in moles when all "abnormal" links have been severed. The rate constants, transformed to values referring to one monomeric unit mole of initial polymer, eq. (7), are comprised in Table I. The relevant Arrhenius equation is (see Fig. 3):

$$K_p = 2.95 \times 10^{10} e^{-48500/RT} \text{min}^{-1}.$$

TABLE I
Rate Constants K_p for One Monomeric Unit Mole of Polymer^a for Volatile Formation during Vacuum Pyrolysis of Poly-*p*-xylylene (Eqs. (9) and (10))

	408°C	424°C	436°C	450°C	475°C	487°C	515°C
K_p, min^{-1}	3.5×10^{-6}	1.0×10^{-5}	1.08×10^{-5}	3.0×10^{-5}	0.9×10^{-4}	0.95×10^{-4}	0.57×10^{-3}

^a $m_0 = 2 \times 10^{-4}$ monomeric unit moles of polymer.

The experimental results indicate that the value for $n_{\text{vol},\infty}$ varies from sample to sample in spite of supposedly similar conditions of preparation. This shows that the number of "weak links" is very susceptible to slight variations in the preparation of the polymer film or to some type of side reaction.

Oxidative Degradation

As the energies of activation found are large (see below), it is very unlikely that diffusion is the rate-determining step. Experiments have shown that the oxidation is independent of diffusion up to a film thickness of 120μ at 341°C (softening point ca. 400°C).¹⁷

The pyrolysis can be tentatively assumed to consist of an initial reaction with oxygen leading to random chain scission, followed by unzipping of small polymer fragments of an average chain length of 3 to 4. At the same time, a side reaction takes place, similar to the one postulated for the vacuum pyrolysis, stripping hydrogen atoms from the polymer and leaving unsaturated conjugated polymer structures behind. Hydrogen gas and water are known to be formed as reaction products.

The initial fast rate of volatilization is due to scission of abnormal structures ("weak" links). After consumption of all "abnormal links," the scission of normal links is left, leading to a straight line part for excess volatiles. The amount of oxygen consumed during the initial part is quite small, as only very short durations are considered. The amounts of oxygen used up during the straight line part are even smaller. Hence the assumption that the oxygen pressure is constant during this period is a good approximation. At temperatures below the softening point, the rate con-

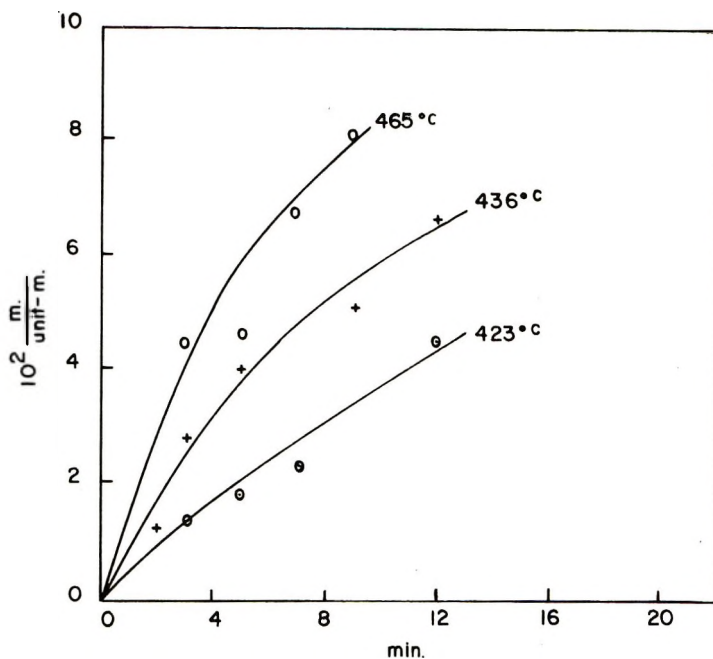
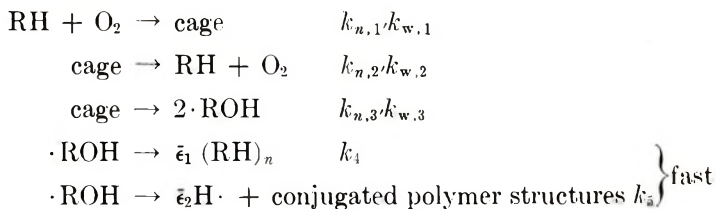


Fig. 6. Oxygen consumption as a function of temperature: $P_{O_2,t} = 50$ mm Hg at 25°C ; oxygen in reaction vessel at $t = 0$, 3.45×10^{-5} mole.

stants change but little with oxygen pressure, indicating that the saturation of the film by oxygen does not change appreciably with increasing pressure. A mechanism for the oxidative pyrolysis is tentatively suggested as follows (w and n refer to "weak" and normal links, respectively):



Several fast reactions may follow involving $2 \cdot \text{RH}$, $\text{H} \cdot + \text{H} \cdot$, $\cdot \text{H} + \text{O}$, $\text{O} + \text{O}$, $\cdot \text{OH} + \cdot \text{OH}$; $\text{H}_2\text{O}_2 \rightarrow \text{H}_2\text{O} + \text{O}$; and $\cdot \text{OH} + \text{H} \rightarrow \text{H}_2\text{O}$.

Reactions (1) and (3) can be pictured as follows:

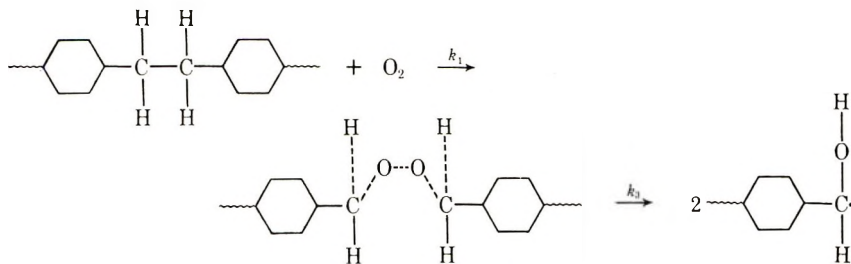


TABLE II
 Rate Constants $K_{\text{exp},n}$ and $K_{\text{exp},w}$ for One Monomeric Unit Mole of Polymer^a for Rupture of Normal and Weak Links, Respectively,
 during Oxidative Pyrolysis of Poly-*p*-xylylene as a Function of Initial Oxygen Pressure [$P_{\text{O}_2,i}$ at 25°C) and Temperature^b

Temp, °C	$10^2 P_{\text{O}_2,i}$, mm Hg	$10^2 K_{\text{exp},n}$ ^c $P_{\text{O}_2,i}$, min ⁻¹	$10^2 K_{\text{exp},n}$, min ⁻¹ mm Hg ⁻¹	$10^6 n_{\text{vol},\text{exp}}$ moles	$10^2 K_{\text{exp},w}$ ^d $P_{\text{O}_2,i}$, min ⁻¹	$10^2 K_{\text{exp},w}$ min ⁻¹ mm Hg ⁻¹
324	1.88	0.03		10.2	2.04	
	1.98	0.19		10.0	1.80	
	1.98	0.14		—	—	
	2.75	0.42	4.6×10^{-4}	7.2	3.17	7.2×10^{-3}
	3.28	0.12	$S.D.(S) = +3.9 \times 10^{-4}$	—	—	$S.D.(S) = \pm 5.8 \times 10^{-3}$
	3.65	0.24	$(I = +0.41; S.D.(I) = +0.12)$	5.2	1.82	$(I = +7.4; S.D.(I) = \pm 1.8)$
	3.92	0.08		19.0	2.28	
	4.90	0.28		14.2	4.54	
341	1.10	0.12		7.9	5.40	
	1.56	0.94		8.8	4.49	
	1.77	0.10	1.6×10^{-3}	9.1	4.60	3.15×10^{-2}
	2.01	—	$S.D.(S) = \pm 5.6 \times 10^{-4}$	8.0	3.44	$S.D.(S) = \pm 1.6 \times 10^{-3}$
	2.54	0.18	$(I = 0.17; S.D.(I) = \pm 0.1)$	22.0	10.34	$(I = 1.3 \times 10^{-3}; S.D.(I) = 0.28)$

361	0.48	0.02	—	—	—
	0.72	0.09	7.8	2.26	—
	0.99	0.11	9.0	3.15	8.2×10^{-2}
	1.18	0.03	—	—	S.D.(S) = $\pm 2.5 \times 10^{-2}$ (I = +2.1; S.D.(I) = ± 2.7)
1.77	0.20	13.5	14.59	—	
2.09	0.80	—	—	—	
420	0.52	0.03	—	—	—
	0.70	0.17	8.7	2.70	—
	0.72	0.17	—	—	4.24×10^{-2}
	0.89	0.12	7.7	5.93	S.D.(S) = $\pm 1.8 \times 10^{-2}$ (I = +0.3; S.D.(I) = ± 1.5)
1.19	0.70	21.0	4.20	—	
0.30	0.46	—	—	—	
436	0.43	1.6	9.0	11.25	—
	0.51	0.59	—	—	—
	0.58	0.43	—	—	1.28×10^{-1}
	0.68	1.1	20.0	11.40	S.D.(S) = $\pm 6.8 \times 10^{-2}$ (I = ± 3.8 ; S.D.(I) = ± 5.1)
0.82	1.4	26.0	28.08	—	
1.01	0.83	11.8	10.97	—	
463	1.20	1.2	14.2	13.49	—
	0.27	0.36	11.2	10.53	—
	0.40	3.1	15.0	15.90	3.16×10^{-1}
	0.52	4.0	—	—	S.D.(S) = $\pm 2.7 \times 10^{-2}$ (I = +0.6; S.D.(I) = ± 1.3)
0.65	4.4	12.0	20.88	—	

^a $m_0 = 1 \times 10^{-4}$ monomeric unit moles.

^b The rate constants are also expressed for 1 mm Hg oxygen pressure, eqs (14), (18) and (19); S.D. \sim standard deviation for slope (S) and interface (I), respectively, for rate constants plotted versus oxygen pressure.

The rate of excess volatile formation (for $m_0 = 1 \times 10^{-4}$ monomeric unit moles of polymer) is given by (all amounts are expressed in moles except for oxygen):

$$\frac{dn_{\text{vol},t}}{dt} = \frac{k_{w,3} + k_{n,3}}{k_{w,2} + k_{n,2}} (\bar{\epsilon}_2 + 2\bar{\epsilon}_1) P_{O_2,t} k'_{w,1} (1 - \alpha'_t) n_{w,0} + k'_{n,1} (1 - \alpha_t) n_0 - k_{O_2} (P_{O_2,0} - P_{O_2,t}) \text{ moles} \times \text{min}^{-1} \quad (11)$$

where $k'_{w,1}$ and $k'_{n,1}$ are rate constants in terms of pressure units; α'_t and α_t are the degrees of degradation for "abnormal" and normal main chain links at time t , respectively; and $\bar{\epsilon}_1$ and $2\bar{\epsilon}_2$ are the number-average kinetic chain lengths for $(RH)_n$ and $H\cdot$ formation, respectively. The total rate of breaking links is then given by:

$$-\frac{dn_{\text{tot}}}{dt} = -\left(\frac{dn_w}{dt} + \frac{dn_n}{dt}\right) = \frac{(k_{w,3} + k_{n,3}) P_{O_2,t} (k'_{w,1} n_{w,t} + k'_{n,1} n_{n,t})}{k_{w,2} + k_{n,2}} \times \text{moles} \times \text{min}^{-1} \quad (12)$$

As the percentage of normal links broken is small, $n_t \cong n_0$ and $m_0 - n_{\text{vol},t} \cong m_0$. At a definite time t_1 , all weak links will have been severed and the volatile formation is then solely due to the breaking of normal links. At t_1 , the excess volatile curve passes over into a straight line. Hence, starting at time t_1 , eq. (12) becomes:

$$-\left(\frac{n_0 d(1 - \alpha)}{dt}\right)_{t_1} = -\left(\frac{dn_n}{dt}\right)_{t_1} = \frac{k_{n,3}}{k_{n,2}} k'_{n,1} n_0 P_{O_2,t_1} \text{ moles} \times \text{min}^{-1} \quad (13)$$

The oxygen pressure remains approximately constant as long as the straight line period prevails. The expression for the rate of excess volatile formation for this part of the pyrolysis is then given by:

$$\left(\frac{dn_{\text{vol}}}{n_0 dt}\right)_{t_1} = (\bar{\epsilon}_2 + 2\bar{\epsilon}_1) \frac{d\alpha}{dt} = (\bar{\epsilon}_2 + 2\bar{\epsilon}_1) \frac{k_{n,3}}{k_{n,2}} k'_{n,1} P_{O_2,t_1} = P_{O_2,t_1} K_{\text{exp},n} \text{ min}^{-1} \quad (14)$$

Values for $K_{\text{exp},n}$ are presented in Table II; maximal amounts volatilized are about 5% of the initial amount of polymer.

The relevant Arrhenius equations are (see Fig. 7) as follows:

$$\text{Below softening point: } K_{\text{exp},n} = 1.2 \times 10^{11} e^{-44800/RT} \text{ min}^{-1} (\text{mm Hg})^{-1} \quad (15)$$

$$\text{Above softening point: } K_{\text{exp},n} = 4.4 \times 10^{12} e^{-53800/RT} \text{ min}^{-1} (\text{mm Hg})^{-1} \quad (16)$$

The Arrhenius equations were obtained by plotting the $K_{\text{exp},n}$ values against the initial oxygen pressures $P_{O_2,t}$ (least square), thus obtaining $K_{\text{exp},n} [\text{min}^{-1} (\text{mm Hg})^{-1}]$. These latter values were used to obtain the Arrhenius parameters.

Volatiles due to chain scission of weak links can be obtained, with good approximation, by subtracting the volatiles due to normal chain scission (by extending the straight line back to $t = 0$). The oxygen pressure is assumed to be approximately constant during the short period necessary for

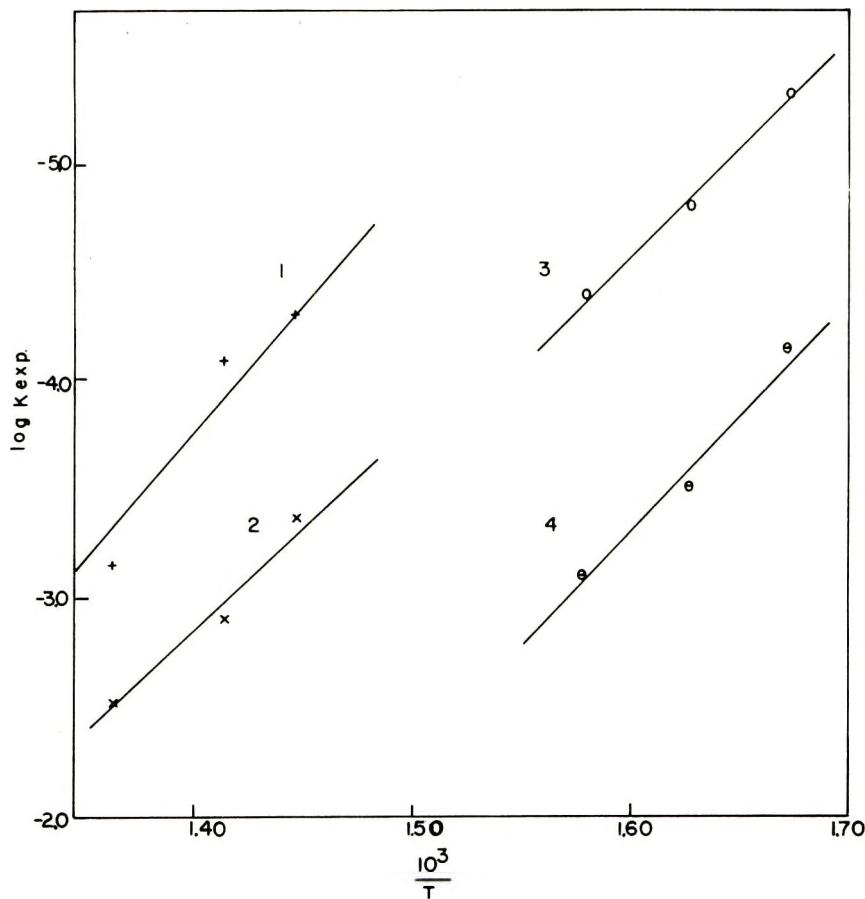


Fig. 7. Arrhenius plots for rupture of normal and "abnormal" links (moles of oxygen per monomeric unit mole of polymer vs. time). Above softening point: (1) normal links ($K_{\text{exp},n}$); (2) "abnormal" links ($K_{\text{exp},w}$). Below softening point: (3) normal links ($K_{\text{exp},m}$); (4) "abnormal" links ($K_{\text{exp},w}$).

all weak links to be severed. Figure 8 shows some typical corrected curves. The rate of excess volume formed after correction is given by ($m_0 - n_{\text{vol},t} \cong m_0$; $m_0 = 1 \times 10^{-4}$ monomeric unit moles of polymer):

$$\frac{dn_{\text{vol},t}}{dt} = \frac{k_w \cdot 3k'_{w,1}}{k_{w,2}} P_{\text{O}_2,0} (n_{\text{vol},\infty} - n_{\text{vol},t}) = P_{\text{O}_2,0} K'_{\text{exp},w} (n_{\text{vol},\infty} - n_{\text{vol},t})$$

× moles min^{-1} . (17)

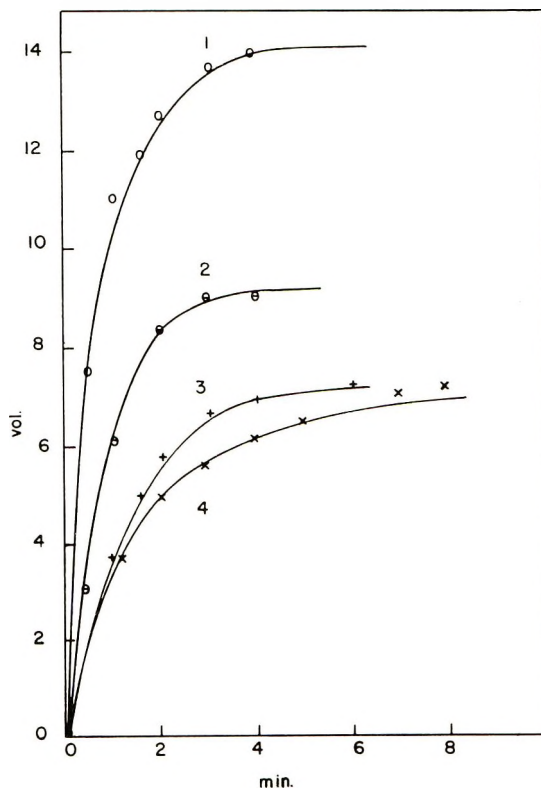


Fig. 8. Typical oxidative volatilization curves for "abnormal" chain scission only, corrected for normal chain rupture: (1) 436°C, 120 mm Hg; (2) 436°C, 43 mm Hg; (3) 341°C, 110 mm Hg; (4) 341°C, 201 mm Hg.

Integration of eq. (17) gives

$$-\ln \left(1 - \frac{n_{\text{vol},t}}{n_{\text{vol},\infty}} \right) = +\ln \left(1 - \frac{n_{\text{w},t}}{n_{\text{w},0}} \right) = +\ln \alpha' = P_{\text{O}_2,0} K'_{\text{exp,w}t}. \quad (18)$$

Figure 9 shows some of the plots according to eq. (18). Table II gives also the relevant rate constants $K'_{\text{exp,w}}/m_0$ multiplied by $n_{\text{vol},\infty}$; hence, for one monomeric unit mole of polymer,

$$K_{\text{exp,w}} = K'_{\text{exp,w}} \frac{n_{\text{vol},\infty}}{m_0} \text{ min}^{-1} (\text{mm Hg})^{-1}. \quad (19)$$

The relevant Arrhenius equations (see Fig. 3) are:

$$\text{Below softening point: } K_{\text{exp,w}} = 1.3 \times 10^{10} e^{-42500/RT} \text{ min}^{-1} (\text{mm Hg})^{-1} \quad (20)$$

$$\text{Above softening point: } K_{\text{exp,w}} = 1.1 \times 10^{13} e^{-46500/RT} \text{ min}^{-1} (\text{mm Hg})^{-1}. \quad (21)$$

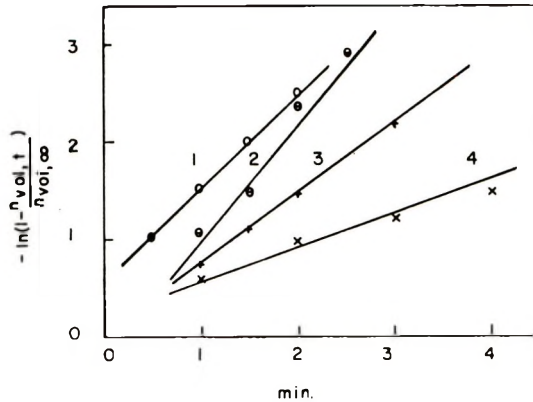


Fig. 9. Curves in Figure 8 plotted according to eq. (18); numbering the same as in Figure 8.

The Arrhenius plots for the abnormal (weak) structures and normal links, respectively, show discontinuities around the softening point of the polymer (ca. 400°C). The values for the energies of activation and pre-exponential factors are somewhat ambiguous, but the grouping of the normal and weak structures, below and above the softening point, respectively, is quite definite.

SUMMARY

Poly-*p*-xylylene prepared by pyrolysis of di-*p*-xylylene has been degraded under vacuum and in the presence of oxygen over appreciable ranges of temperature and pressure. The vacuum pyrolysis is mainly due to abnormal structures which may consist of branch points. The volatiles are initially produced quite slowly. The logarithms of the reciprocal "slow periods" plotted versus reciprocal absolute temperatures give a straight line yielding an energy of activation of 47.9 kcal/mole. Volatile formation accelerates subsequently and follows a pseudo-first-order reaction (i.e., zero order), which eventually goes over into a first-order reaction when the number of "abnormal" links cannot be considered constant any longer. The Arrhenius parameters were derived from the zero-order range of the reaction (48.5 kcal/mole) for experiments carried out above the softening point (ca. 400°C) of the polymer. A mechanism has been formulated that consists of random chain scission initiation followed by depropagation, producing volatiles consisting of short polymer chains (dimers to pentamers); simultaneously a zip reaction occurs producing hydrogen atoms, leaving conjugated polymer structures behind.

The thermal oxidative pyrolysis was carried out over temperature ranges above and below the softening point of the polymer and over a range of oxygen pressures. It follows a first-order reaction for volatile formation due to "abnormal" link scission, provided the volatile formation due to

normal chain scission, which is also first order, is subtracted from that due to "abnormal" chain scission. The postulated reaction scheme leads initially to peroxide formation. Subsequently, chain scission and formation of oxygenated chain ends take place. Small polymer molecules (dimers to pentamers) and hydrogen are produced, similarly as for the vacuum pyrolysis. The Arrhenius plots are different for volatile formation above and below the softening point of the polymer, respectively. The differences for "normal" and "abnormal" volatile formation are marked for similar temperature ranges. Oxygen consumption was investigated in separate experiments; it follows a first-order law with an energy of activation of 31.5 kcal/mole.

The authors are indebted to Dr. S. H. Ronel for assisting with numerical calculations. Thanks are due to the U. S. Army Research Office, Durham, N. C., for financial assistance (Grant No. DA-ARO-D-31-124-G984).

References

1. S. L. Madorsky and S. Straus, *J. Res. Nat. Bur. Stand.*, **55**, 223 (1955).
2. J. R. Schaefgen, *J. Polym. Sci.*, **41**, 133 (1959).
3. A. T. Kalashnik, I. Ye. Kardash, T. S. Shitonova, and A. N. Pravednikov, *Vysokomol. Soedin.*, **8** (No. 3), 526 (1966); *ibid.*, **2B**, 89 (1968).
4. L. A. Errede and M. Swarcz, *Quart. Rev. Chem. Soc.*, **12**, 301 (1958).
5. M. Swarcz, *J. Polym. Sci.*, **6**, 319 (1951).
6. R. S. Corley, H. C. Haas, M. W. Kane, and D. I. Livingston, *J. Polym. Sci.*, **13**, 137 (1954).
7. M. H. Kaufman, H. F. Mark, and R. B. Mesrobian, *J. Polym. Sci.*, **13**, 3 (1954).
8. L. A. Auspos et al., *J. Polym. Sci.*, **15**, 19 (1955).
9. W. F. Gorham, *J. Polym. Sci. A-1*, **4**, 3027 (1966).
10. J. M. Lancaster and W. W. Wright, *J. Appl. Polym. Sci.*, **11**, 1641 (1967).
11. J. H. Lady, I. Kane, and R. E. Adano, *J. Appl. Polym. Sci.*, **3**, 71 (1960).
12. R. T. Conley, *J. Appl. Polym. Sci.*, **9**, 1107 (1965).
13. H. H. G. Jellinek and J. E. Clark, *Can. J. Chem.*, **41**, 355 (1953).
14. P. Sweetser, *Anal. Chem.*, **39**, 979 (1967).
15. H. H. G. Jellinek and S. N. Lipovac, *Macromolecules*, Part I, **3**, 231 (1970); Pt II 237.
16. H. H. G. Jellinek, Degradation, in *Encyclopedia Sci. Techn. Polymers*, Vol. IV, H. Nork et al. (ed). Wiley, New York, 1966, p. 740.
17. H. H. G. Jellinek and H. S. Ronel, unpublished results.

Received December 12, 1969

February 17, 1970

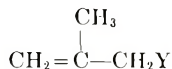
Polymerization Studies on Allylic Compounds. IV. Methallylic Compounds

R. L. HARVILLE and SAMUEL F. REED, JR., *Rohm and Haas Company, Redstone Research Laboratories, Huntsville, Alabama 35807*

Synopsis

The free-radical polymerization of a series of 2-methyl-3-substituted propenes was investigated. These compounds were found to homopolymerize with difficulty to give low molecular weight polymers. Their effect upon the polymerization of methyl methacrylate and styrene was investigated by rate and viscosity measurements. Copolymerizations occurred with a retarding action attributed to pronounced chain transfer reactions.

The free-radical polymerization behavior of 2,3-disubstituted propenes has been extended to include a series of seven 2-methyl-3-substituted propenes of general structure I where Y is represented



by $-\text{Cl}$, $-\text{OH}$, $-\overset{\text{O}}{\parallel}\text{CCH}_3$, $-\text{CH}_3$, $-\overset{\text{O}}{\parallel}\text{CH}_2\text{CCH}_3$, $-\text{C}_6\text{H}_5$ and $-\text{OC}_6\text{H}_5$. Both the homopolymerization of these compounds with the use of 2,2'-azobisisobutyronitrile (AIBN) and benzoyl peroxide initiators in toluene solution, and their copolymerization with methyl methacrylate (MMA) and styrene with the use of AIBN in toluene were investigated. The present data afford a comparison with 2,3-disubstituted propenes where the 2-substituents were carboethoxy and phenyl.¹⁻³ Rates of polymerization were measured by a dilatometric method,¹ and copolymers were characterized by their solution viscosities and in certain instances by elemental analyses. From the results of the study, conclusions may be drawn concerning the relative reactivity of the monomers I.

The propene derivatives examined in the polymerization study were: methallyl chloride (MAC), methallyl cyanide (MACN), methallyl acetate (MAA), methallyl alcohol (MAAL), methallyl benzene (MAB), methallyl acetone (MAAO), and methallyl phenyl ether (MAPE). Each was either purchased from commercial sources or prepared by well-known methods. All were distilled prior to polymerization and their purity checked by gas chromatographic analysis. Each was considered to be of 99.5%+ purity. An Aerograph, Model 100-C, instrument with a 5-ft dinonyl phthalate on

Chromosorb (Johns-Manville Products Corporation) column was employed for the chromatography work. 2,2'-Azobisisobutyronitrile was used as initiator for the copolymerizations; it was recrystallized from absolute methanol (mp 102–103°C, decomposition) and stored at 0°C.

The dilatometric rate measurements were carried out as previously described.¹ Rate measurements were conducted at three different concentrations for the copolymerization of each methallyl compound with MMA and styrene. The copolymerization reactions were allowed to proceed to 10–12% conversion, and the copolymers were isolated and purified by reprecipitation from toluene on the addition of methanol, followed by vacuum drying (1 mm) for a period of 24 hr.

HOMOPOLYMERIZATION

A brief investigation of the polymerization behavior of the methallyl compounds was undertaken. Initial polymerization rate studies on methallyl chloride (MAC), methallyl alcohol (MAAL), and methallyl acetate (MAA) with AIBN as the initiator were unsuccessful because the polymerizations were exceedingly slow and nitrogen formation from the decomposing AIBN created bubbles in the dilatometers forcing termination of the measurements. When benzoyl peroxide (0.05 mole-%) was used, the rate measurements were concluded successfully. The methallyl compounds were found to polymerize at the following rates: 0.0245%/min(MAC), 0.0061%/min(MAAL), and 0.006%/min(MAA). Products of these polymerizations were obtained as low molecular weight liquid polymers which were not characterized. This behavior is typical for allylic compounds,^{4–6} and these three compounds were considered to be representative of the group of compounds under investigation, so that a study of each was not necessary.

COPOLYMERIZATIONS

The effects of the methallyl compounds (I) on the polymerization of MMA and styrene were investigated with emphasis placed on the effect of low, but increasing, concentrations of these compounds. Molar ratios of MMA and styrene to the methallyl compounds were varied from approximately 27:1 to 2:1. Copolymerizations were carried out in toluene, at 60°C, using AIBN as the initiator. The rates of polymerization were observed dilatometrically over the first 8 to 12% conversion. Results are presented in Tables I (MMA) and II (styrene). The R_p values refer to the MMA or styrene polymerization rate in the absence of a comonomer; conditions reproduced those for copolymerizations. Similarly, the $[\eta]_0$ values are the intrinsic viscosity of the MMA and styrene homopolymers.

Attention is directed to the MMA copolymers (Table I). At the lowest concentrations (highest molar ratios of MMA:1), the methallyl compounds exhibited very limited retardation of the polymerization rate as evidenced by the R_p/R_{p_0} values near 1.0. Upon increasing their concentration an almost uniform decrease in the rate was observed. The greatest rate retardation was observed with methallyl acetate (MAA), methallyl phenyl ether

TABLE I
 Experimental Data for MMA Copolymerizations^a

[MMA], mole/l.	Comono- mer	[Comono- mer], mole/l.	Molar ratio MMA/co- monomer	R_p %/ min	R_p/R_{p_0}	$[\eta]$	$[\eta]/[\eta]_0$
4.7	—	—	—	0.215	1.0	0.492	1.0
4.47	MAC	0.255	17.53	0.193	0.90	0.236	0.48
3.96	MAC	0.765	5.18	0.185	0.86	0.135	0.27
3.52	MAC	1.278	2.75	0.174	0.81	0.085	0.17
4.47	MAA	0.203	22.02	0.203	0.94	0.491	1.0
3.96	MAA	0.608	6.51	0.151	0.70	0.426	0.87
3.52	MAA	1.01	3.48	0.127	0.59	0.412	0.84
4.47	MAAL	0.313	14.28	0.232	1.08	0.452	0.92
3.96	MAAL	0.938	4.22	0.196	0.91	0.392	0.80
3.52	MAAL	1.565	2.25	0.187	0.87	0.333	0.68
4.47	MACN	0.25	17.88	0.227	1.05	0.467	0.95
3.96	MACN	0.75	5.28	0.206	0.96	0.439	0.89
3.52	MACN	1.25	2.82	0.177	0.82	0.33	0.67
4.47	MAPE	0.18	24.83	0.23	1.07	0.394	0.80
3.96	MAPE	0.54	7.33	0.20	0.93	0.33	0.67
3.52	MAPE	0.90	3.91	0.115	0.53	0.274	0.56
4.47	MAAO	0.19	23.53	0.218	1.01	0.496	1.00
3.96	MAAO	0.575	6.89	0.192	0.89	0.475	0.97
3.52	MAAO	0.983	3.58	0.171	0.80	0.347	0.71
4.47	MAB	0.165	27.09	0.188	0.87	0.453	0.92
3.96	MAB	0.50	7.92	0.177	0.82	0.409	0.83
3.52	MAB	0.84	4.19	0.125	0.58	0.363	0.74

^a [AIBN] = 0.025 mole/l. (MMA).

(MAPE), and methallyl benzene (MAB); the R_p/R_{p_0} values dropped to 0.5 to 0.6 at the highest concentration of these compounds.

Similar decreases in the $[\eta]$ of the copolymers was noted. Even at the lowest concentration of methallyl chloride (MAC), the lowering of $[\eta]$ was significant; the other compounds displayed less effect at this concentration range. Increasing their concentration resulted in further lowering of $[\eta]$ for the copolymers. Methallyl chloride (MAC) exhibited the most pronounced lowering of $[\eta]$, while methallyl acetate showed the least effect.

Styrene copolymerizations showed similar behavior (Table II). The polymerization rates were affected to a limited extent at the lower concentrations of I; however, a further decrease in rate was observed with increasing concentration. Methallyl alcohol (MAAL) and methallyl phenyl ether (MAPE) gave the greatest rate lowering effect. The $[\eta]$ values for the copolymers were notably affected by the presence of the methallyl monomers at even their lowest concentration.

Analysis of the copolymers containing methallyl chloride (MAC) and methallyl cyanide (MACN) were carried out, and the chlorine and nitrogen contents used to determine the composition of these materials (Table III). The calculated values were obtained based on the composition of the origi-

TABLE II
 Experimental Data for Styrene Copolymerizations^a

[Styrene], mole/l.	Comonomer	[Comonomer], mole/l.	Molar ratio styrene/ comonomer	Rate. %/min	R_p/R_{p0}	$[\eta]$	$[\eta]/[\eta]_0$
4.36	—	—	—	0.063	1.0	0.35	1.0
4.14	MAC	0.255	16.24	0.057	0.90	0.24	0.69
3.71	MAC	0.765	4.85	0.048	0.76	0.195	0.55
3.26	MAC	1.278	2.55	0.043	0.68	0.16	0.46
4.14	MAA	0.203	20.39	0.066	1.05	0.26	0.74
3.71	MAA	0.608	6.10	0.063	1.00	0.21	0.60
3.26	MAA	1.01	3.23	0.055	0.87	0.23	0.65
4.14	MAAL	0.313	13.23	0.052	0.83	0.27	0.77
3.71	MAAL	0.938	3.96	0.047	0.75	0.24	0.69
3.26	MAAL	1.565	2.08	0.026	0.41	0.23	0.65
4.14	MACN	0.25	16.56	0.059	0.94	0.29	0.83
3.71	MACN	0.75	4.95	0.049	0.78	0.23	0.65
3.26	MACN	1.25	2.61	0.036	0.57	0.21	0.60
4.14	MAPE	0.18	23.00	0.061	0.97	0.21	0.60
3.71	MAPE	0.54	6.87	0.055	0.87	0.21	0.60
3.26	MAPE	0.902	3.61	0.022	0.35	0.20	0.57
4.14	MAAO	0.19	21.79	0.065	1.03	0.213	0.61
3.71	MAAO	0.575	6.45	0.063	1.00	0.195	0.55
3.26	MAAO	0.983	3.32	0.057	0.90	0.155	0.44
4.14	MAB	0.165	25.09	0.057	0.90	0.24	0.69
3.71	MAB	0.50	7.42	0.051	0.81	0.215	0.61
3.26	MAB	0.84	3.88	0.048	0.76	0.074	0.21

^a [AIBN] = 0.05 mole/l. (styrene).

nal comonomer charges. Both the chlorine and nitrogen contents of the copolymers were low. It is noted that the chlorine content increased slightly with an increase in the methallyl chloride (MAC) concentration, whereas the nitrogen content of the methallyl cyanide (MACN) copolymers remained constant and independent of concentration. In most copolymers the chlorine or nitrogen content was 10–20% of that present in the original comonomer mixtures and these results are indicative of copolymer compositions low in the methallylic component.

The retarding action of the methallyl monomers (I) on the polymerization of MMA and styrene results from several factors. In assessing the factors on a qualitative basis, a consideration of the nature of the MMA or styrene monomers relative to that of the methallyl compounds is important. Both MMA and styrene are reactive monomers in polymerization reactions; both give stable radicals of low reactivity because of resonance stabilization. In contrast, the methallyl compounds are relatively unreactive in polymerization reactions, but yield unstable and highly reactive radicals. Comonomer combinations involving a reactive monomer (MMA or styrene) with an unreactive monomer (the methallyl compounds) are known⁷ to undergo copolymerization with difficulty, and usually little of the unreactive mono-

TABLE III
Elemental Analysis Data for Copolymers

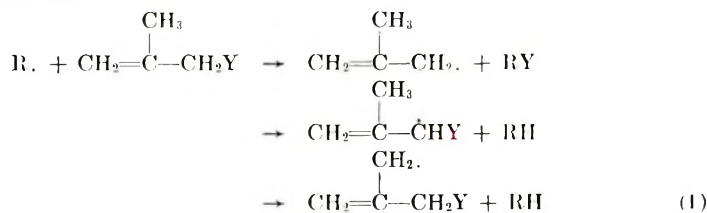
Copolymer	ratio of comono- mers	Elemental Analysis							
		Calculated				Found			
		C, %	H, %	Cl, %	N, %	C, %	H, %	Cl, %	N, %
MMA-MAC	17.53	59.66	7.99	1.93	—	60.2	8.06	0.2	—
	5.18	58.97	7.96	5.81	—	60.9	7.96	0.62	—
	2.75	58.29	7.94	9.67	—	59.7	8.08	0.73	—
MMA-MACN	17.88	60.61	8.03	—	0.75	60.8	8.42	—	0.4
	5.28	61.87	8.09	—	2.29	60.6	8.19	—	0.4
	2.82	63.14	8.14	—	3.86	60.8	8.22	—	0.47
S-MAC	16.24	90.31	7.69	1.99	—	90.6	7.46	0.43	—
	4.85	86.33	7.70	5.97	—	89.6	7.52	0.66	—
	2.55	82.36	7.70	9.94	—	89.0	7.63	1.54	—
S-MACN	16.56	91.49	7.73	—	0.76	91.8	7.98	—	0.41
	4.95	89.82	7.82	—	2.35	91.6	7.98	—	0.34
	2.61	88.12	7.91	—	3.97	91.8	7.87	—	0.43

mer becomes incorporated into the copolymer, i.e., the styrene-vinyl acetate system. This behavior arises because each monomer must compete for the same radicals, and the greater reactivity of the most active monomer becomes very evident. This accounts for the limited quantities of MAC and MACN, and supposedly the other methallyl compounds, found in the copolymers upon analysis.

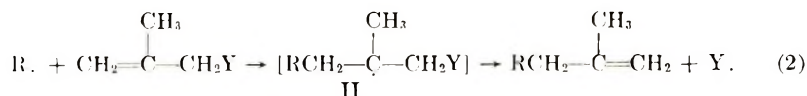
Other factors contributing to the lowering of the rate of polymerization and the $[\eta]$ of the copolymers reflect the distinctive character of the polymerization of allylic compounds. In previous studies involving the polymerization of allyl acetate,⁴ allyl chloride,⁴ and allyl alcohol,⁶ it has been postulated that the reactions involve the formation of polymer radicals of both a vinylic and allylic nature. The vinylic radicals are reactive and are directly responsible for propagation or chain growth. The allylic radicals are stabilized by resonance, have a distinctly lower reactivity, and may or may not be capable of propagating the reaction. It is reasonable to expect methallylic compounds to display similar radical character in their polymerization.

Since the allylic radicals are those responsible for chain-transfer reactions, it is of interest to consider their possible modes of formation in the methallyl systems.

Radical Abstraction:



Allylic Radical Displacements:



Radical abstraction reactions (1) would be affected by the nature of the Y group because steric considerations would be of some concern, and it is reasonable to assume that abstraction of a polyatomic Y substituent would not occur. Reactions involving radical displacements (2) have been predicted⁸ involving large substituent groups. These reactions would be dependent upon the nature of the R. and Y. radicals involved, and their frequency would depend not only upon the lifetime of the intermediate radical II but also on the presence of other monomers such as MMA and styrene.

Both transfer mechanisms lead to the same polymerization kinetics provided the allylic radicals are capable of rapidly initiating new polymer chains. However, it has been demonstrated that degradative chain transfer does occur in the homopolymerization of allylic compounds⁴⁻⁶ and is assumed to occur in the homopolymerizations of methallylic compounds. The phenomenon of degradative chain transfer implies that a situation exists in which a radical of low reactivity is present in a mixture with a monomer of low reactivity; hence the radicals are consumed by the most energetically favorable processes, i. e., dimerization or disproportionation, and do not continue the chain propagation. A somewhat different situation exists in the present copolymerization reactions. Undoubtedly, the overall reaction is very complex; even though the methallylic radicals are of low reactivity, there is present a highly reactive monomer (MMA or styrene) which likely contributes to the continued chain propagation by the allylic radicals and reduces the degree of degradative chain transfer.

This study of the copolymerization of methallyl compounds has indicated that the reactions proceed via chain transfer reactions, as evidenced by the decrease in rate of the reactions and the lower $[\eta]$ of the copolymers. The possibility exists that the MMA-MAC reactions were taking place with more extensive degradative chain transfer than the other methallyl compounds because of the exceedingly low $[\eta]$ values, although the rate measurements did not decrease to the extent expected. This is likely, since allyl chloride is known⁴ to give extensive degradation in its homopolymerizations. From the available data, the exact mechanism cannot be determined, although it is thought that the degradative chain transfer processes are reduced by the presence of the reactive comonomers. It should be stressed that the most important factor controlling the lack of copolymerization between the comonomer pairs is the difference in monomer reactivities.

This work was performed under the sponsorship of the U.S. Army Missile Command, Redstone Arsenal, Alabama, under Contract DAAH01-67-C-0655.

References

1. M. G. Baldwin and S. F. Reed, *J. Polymer Sci.*, **A1**, 1919 (1963).
2. S. F. Reed and M. G. Baldwin, *J. Polym. Sci. A-1*, **2**, 1355 (1964).
3. M. G. Baldwin and S. F. Reed, *J. Polym. Sci. A-1*, **6**, 2627 (1968).
4. P. D. Bartlett and R. Altschul, *J. Amer. Chem. Soc.*, **67**, 812, 816 (1945).
5. P. D. Bartlett and F. A. Tate, *J. Amer. Chem. Soc.*, **75**, 91 (1953).
6. A. C. R. Brown and D. G. L. James, *Can. J. Chem.*, **40**, 796 (1962).
7. F. R. Mayo, C. Walling, F. M. Lewis, and W. F. Hulse, *J. Amer. Chem. Soc.*, **70**, 1523 (1948).
8. N. G. Gaylord, *J. Polym. Sci.*, **22**, 71 (1956).

Received April 29, 1969

Revised February 17, 1970

Electron Spin Resonance Study of Polymerization of Butadiene with Tris(acetylacetonato)titanium and Triethylaluminum

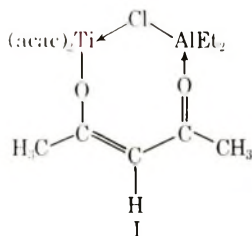
KATSUMA HIRAKI, TAKEO INOUE, and HIDEFUMI HIRAI,
*Department of Industrial Chemistry, Faculty of Engineering, University
of Tokyo, Hongo, Bunkyo-ku, Tokyo, Japan.*

Synopsis

ESR spectra of homogeneous catalyst derived from tris(acetylacetonato)titanium(III) and triethylaluminum were observed at several temperatures from -78°C to $+25^{\circ}\text{C}$, at molar ratios of aluminum to titanium of 1-108. At -78°C , this catalyst yields a violet complex which shows an ESR signal with a g value of 1.959 and is associated with the first intermediate. At -40°C to -30°C , this signal decreases, and two signals with g values of 1.947 and 1.960 are observed. The latter two signals diminish at -5°C to $+10^{\circ}\text{C}$, while two kinds of new signals with g values of 1.965 and 1.969 appear overlapping each other. The structures of the species corresponding to these five signals are discussed on the basis of the ESR spectra, the intensity change, and the unpaired spin distribution. A new signal with a g value of 1.978 is found in the presence of butadiene at 25°C at $\text{Al/Ti} > 8$ and is assigned to a growing end of polybutadiene with this catalyst. The polymer yield increases remarkably at Al/Ti molar ratios greater than 10. The microstructure of the resulting polymer consists almost completely of 1,2 units. The structure of the growing end is proposed to be a titanium(III) species containing two 1-substituted allyl groups, by comparison with the structure ascribed to the growing end of polybutadiene with *n*-butyl titanate-triethylaluminum catalyst.

INTRODUCTION

The system of tris(acetylacetonato)titanium(III) $[\text{Ti}(\text{acac})_3]$ and triethylaluminum has been studied as a homogeneous Ziegler catalyst for polymerization of styrene, and ESR spectra of the system have been examined.¹ A catalyst derived from $\text{Ti}(\text{acac})_3$, aluminum trichloride, and triethylaluminum was reported to polymerize butadiene to a polymer containing *cis*-1,4, *trans*-1,4, and 1,2 linkages in about the ratio 50:30:20.² Ikeda and his co-workers³ obtained some complexes coordinated with an organic solvent by the reaction between $\text{Ti}(\text{acac})_3$ and diethylchloroaluminum in the presence of the solvent. Recently, Watt et al.⁴ studied polymerization of ethylene catalyzed by $\text{Ti}(\text{acac})_3$ -diethylchloroaluminum catalyst and proposed an intermediate in the reaction between the catalyst components, as shown by structure I.



In the present study, $\text{Ti}(\text{acac})_3$ -triethylaluminum catalyst was found to polymerize butadiene to a polymer composed of a high percentage of 1,2 units at molar ratios of aluminum to titanium (Al/Ti ratios) larger than 5. In addition, the catalyst solution and the polymerization system were investigated by means of ESR spectroscopy in order to elucidate the reaction between the catalyst components and the structure of a growing end of polybutadiene, respectively. These results were compared with those obtained with *n*-butyl titanate-triethylaluminum catalyst,^{5,6} which yielded 1,2-polybutadiene having a similar microstructure.

EXPERIMENTAL

Materials

The complex, $\text{Ti}(\text{acac})_3$ was prepared and purified according to the method of Barnum⁷ and stored as a toluene solution in a nitrogen atmosphere. Toluene, triethylaluminum, and butadiene each was treated and used as described in the previous papers.^{5,6}

Procedure

The $\text{Ti}(\text{acac})_3$ -triethylaluminum catalyst for ESR measurement was prepared and treated as described in the previous paper,⁶ where *n*-butyl titanate was used in place of $\text{Ti}(\text{acac})_3$. The polymerization system of butadiene with the $\text{Ti}(\text{acac})_3$ -triethylaluminum catalyst was prepared and separated into two portions; one for an ESR measurement and the other for a polymerization run, similarly to the polymerization system with *n*-butyl titanate-triethylaluminum catalyst.⁶ An ampoule containing a large portion of the polymerization system for the polymerization run was set in a water bath maintained at 25°C for 3 hr. Both the yield and the intrinsic viscosity of the resulting polybutadiene were determined by the procedure of Dawes and Winkler.⁸ The viscosity-average molecular weight of the polymer was calculated from the Mark-Houwink relation,

$$[\eta] = 2.71 \times 10^{-4} [\bar{M}_v]^{0.73}$$

ESR measurements both for the catalyst and for the polymerization system prepared as stated above, were carried out by means of the apparatus and the technique described for *n*-butyl titanate-triethylaluminum catalyst,^{5,6} The absorption intensity of an ESR signal, i.e., the concentration

of the titanium(III) species in mole/l., was evaluated by comparison of the area of the integrated curve of the signal with the corresponding value for a toluene solution of 1.02×10^{-3} mole/l. of $\text{Ti}(\text{acac})_3$ as a reference standard. The hyperfine structure of the signal was confirmed by measurement of the second derivative of the signal.

RESULTS

Electron Spin Resonance Spectra of Tris(acetylacetonato)-titanium-Triethylaluminum Catalyst

A toluene solution of $\text{Ti}(\text{acac})_3$ was indigo-blue and showed an ESR signal with a g value of 1.943 and with a maximum slope width of 88 gauss. ESR spectra of the catalyst solution prepared from $\text{Ti}(\text{acac})_3$ and triethylaluminum at Al/Ti ratios of 1–108 at a temperature below -70°C were examined at several temperatures from -78°C to $+25^\circ\text{C}$. The reaction between $\text{Ti}(\text{acac})_3$ and triethylaluminum yielded six kinds of ESR signals, which will be referred to as the first, second, . . . , sixth signals, in order of appearance. Figures 1 and 2 show the spectra measured at Al/Ti ratios of 10.4 and 5.2, respectively.

By a reaction with triethylaluminum at -78°C , $\text{Ti}(\text{acac})_3$ was converted into a violet complex which showed the first ESR signal with a g value of 1.959 and with a maximum slope width of 16.8 gauss (see Fig. 1A). At -40°C , a second signal with a g value of 1.947 and with a maximum slope width of 13.3 gauss appeared, while the first signal decreased. At -30°C , the third signal with a hyperfine structure of 11 components and with a

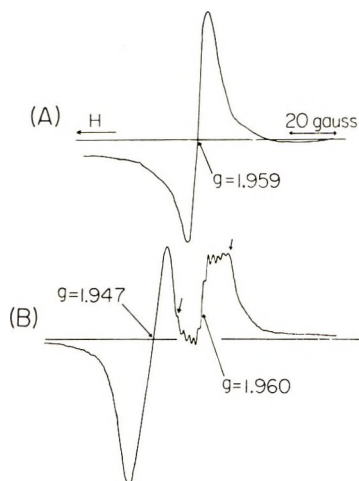


Fig. 1. ESR spectra of $\text{Ti}(\text{acac})_3$ -triethylaluminum catalyst at low temperatures. (A) at -78°C , (B) at -5°C , 70 min. after the temperature began to rise from -78°C . (The two outermost splitting-lines in the signal with g value of 1.960 are shown by the small arrows.) Conditions; Al/Ti ratio, 10.4; initial concentration of $\text{Ti}(\text{acac})_3$, 7.0×10^{-3} mole/l.

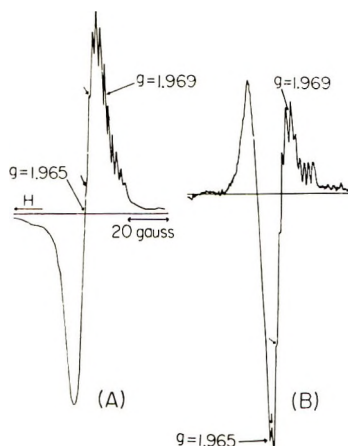


Fig. 2. ESR spectra of $\text{Ti}(\text{acac})_3$ -triethylaluminum catalyst at 25°C : (A) the differential curve, (B) the second derivative, (In both figures, the two splitting-lines in the higher field in the signal with g value of 1.969 are shown by the small arrows.) Conditions: Al/Ti ratio, 5.2; initial concentration of $\text{Ti}(\text{acac})_3$, 7.0×10^{-3} mole/l.; reaction time, 150 min. for (A) and 130 min. for (B), respectively, after the temperature had arrived at 25°C .

coupling constant of 2.2 gauss was observed at a g value of 1.960 overlapping with the second signal, while the first signal had disappeared already (see Fig. 1B). The color of the catalyst solution was then black-brown.

At temperatures ranging from -5°C to $+10^\circ\text{C}$, two kinds of new signal, the fourth and the fifth ones, appeared overlapping each other and accompanying the decrease of the second and the third signals (see Fig. 2A). The fourth signal had a g value of 1.965 and a maximum slope width of 11 gauss, and overlapped with the decreasing third signal. The fifth signal with a g value of 1.969 had a hyperfine structure, which consisted of 11 components with a coupling constant of 2.2 gauss and was confirmed by the second derivative of the signal, shown by Figure 2B. After several days, the fourth signal decreased, and a fifth one became dominant. These five signals were observed at Al/Ti ratios over the range of 5.2–58.

At an Al/Ti ratio of 108, a sixth signal with a g value of 1.997 and with a maximum slope width of 14 gauss appeared at 25°C , in addition to the fourth and the fifth signals (see Fig. 3A). On the other hand, at an Al/Ti ratio of 3, the first, the second, and the fourth signals and the very weak fifth signal were detectable, while neither the third signal nor the signal of $\text{Ti}(\text{acac})_3$ was observed. At an Al/Ti ratio of one, the large signal of $\text{Ti}(\text{acac})_3$ and the weak second and fourth signals were detected.

Figure 4 shows plots of the absorption intensity of each signal, observed at the Al/Ti ratio of 10.4 with the temperature increasing at a rate of about $1.5^\circ\text{C}/\text{min}$ from -78°C to -15°C , and at about $0.33^\circ\text{C}/\text{min}$ from -15°C to $+25^\circ\text{C}$. The sum of the absorption intensity of all signals decreased rapidly in the earlier stage of the reaction from -40°C to 0°C , and grad-

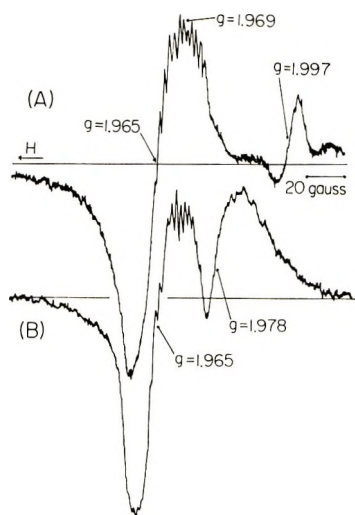


Fig. 3. ESR spectra of $\text{Ti}(\text{acac})_3$ -triethylaluminum catalyst at an Al/Ti ratio of 108: (A), catalyst solution in the absence of butadiene; (B) polymerization system in the presence of butadiene. Conditions: temperature, 25°C ; reaction time, 2.5 hr; initial concentration of $\text{Ti}(\text{acac})_3$, 7.0×10^{-3} mole/l.; initial concentration of butadiene, 2.67 mole/l.

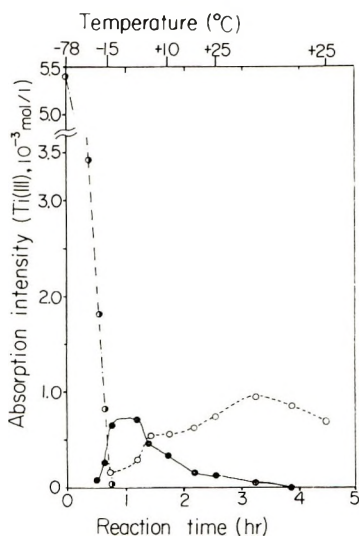


Fig. 4. Plots of absorption intensity of ESR signals against time and temperature: (●) for the first signal ($g = 1.959$); (●), for the second signal ($g = 1.947$); (○), the sum of the absorption intensity of the third signal ($g = 1.960$), of the fourth one ($g = 1.965$), and of the fifth one ($g = 1.969$). Conditions: Al/Ti ratio, 10.4; initial concentration of $\text{Ti}(\text{acac})_3$, 7.0×10^{-3} mole/l.; rate of temperature increase, $1.5^\circ\text{C}/\text{min}$ from -78°C to -15°C and $0.33^\circ\text{C}/\text{min}$ from -15°C to $+25^\circ\text{C}$.

ually in the later stage of the reaction at 25°C. This indicates that in the earlier stage a large part of the initial titanium(III) species was converted into titanium species which showed no ESR signal, probably owing to the formation of an aggregate and to the reduction to the lower valent state. Actually, a small amount of black precipitate was obtained after a few hours in the absence of butadiene. The intensities of the first, second, and third signals depended on an increasing rate of temperature increase, i.e., the faster the rate, the smaller the intensity of the signal.

Electron Spin Resonance Spectra of Polymerization System

ESR spectra of the polymerization system prepared from butadiene, triethylaluminum, and $\text{Ti}(\text{acac})_3$ at a temperature below -70°C were measured at several temperatures from -78°C to $+25^\circ\text{C}$ at Al/Ti ratios of 3–108. The spectra observed at increasing temperatures from -78°C to $+25^\circ\text{C}$ were similar to those of the catalyst solution at the same Al/Ti ratio.

TABLE I
Polymerization of Butadiene with Tris(acetylacetonato)-
titanium-Triethylaluminum Catalyst^a

Al/Ti ratio	Polymer yield, %	\bar{M}_v $\times 10^{-3}$	Concn of polymer chain $\times 10^3$, mole/l. ^b	Concn of Ti(III) $\times 10^3$, mole/l. ^c
3.0	0			0
5.2	1.9			ca. 0
8.0	5.3			0.018
10.4	14.3			
58	50			0.14
108	58	78	1.2	0.17

^a Polymerization conditions: concentration of $\text{Ti}(\text{acac})_3$, 7.0×10^{-3} mole/l.; initial concentration of butadiene, 2.67 mole/l., temperature, 25°C ; reaction time, 3.0 hr.

^b Calculated from the polymer yield and \bar{M}_v .

^c Calculated from the absorption intensity of the signal with the g value of 1.978, for a toluene solution of tris(acetylacetonato)titanium of 1.02×10^{-3} mole/l. as a reference.

A characteristic signal of the polymerization of butadiene was found at a g value of 1.978 at 25°C only at Al/Ti > 8 (see Fig. 3). This signal had a poorly splitted hyperfine structure of several components and an apparent maximum slope width of about 26 gauss. Table I shows the results of the polymerization runs at Al/Ti ratios of 3–108 and the absorption intensity of the ESR signal observed for the sample taken out of the ampoule in each polymerization run. As seen in Table I, this catalyst at Al/Ti < 3 gave no polymer at all. The yield of polybutadiene, however, was considerably high at the Al/Ti > 10 . The microstructure of the resulting polybutadiene was composed of 1,2,*cis*-1,4- and *trans*-1,4 linkages in the ratio 74:23:3, respectively.

DISCUSSION

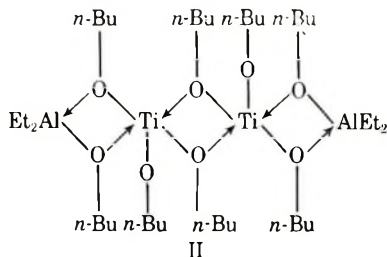
**Electron Spin Resonance Spectra of
Tris(acetylacetonato)titanium-Triethylaluminum Catalyst**

The catalyst solution derived from $\text{Ti}(\text{acac})_3$ and triethylaluminum yielded six distinct titanium(III) species, because the g values and the widths of these six signals observed in this catalyst solution were quite characteristic of titanium(III) species, but not of titanium(II) species, as discussed in the preceding paper.⁵ The titanium(III) species corresponding to the first, second, . . . , sixth signals are referred to as the first, second, . . . , sixth species, respectively, in the order in which they appeared.

The third and the fifth signals each had a hyperfine structure of 11 components with an approximate intensity ratio of 1:2:3:4:5:6:5:4:3:2:1. This hyperfine structure in the present system can be assigned to an interaction between an unpaired d -electron of the titanium(III) atom and two equivalent²⁷Al nuclei (spin = 5/2), as seen in n -butyl titanate-triethylaluminum catalyst.^{5,9,10} Consequently, the third and the fifth species each was coordinated with two equivalent organoaluminum components.

The formation of these titanium(III) species containing two organoaluminum components suggests the existence of a titanium(III) species including only one organoaluminum component as a reaction intermediate or as a component of an equilibrium. However, the catalyst solution gave no signal with a hyperfine structure of six components, which was expected to be produced by an interaction between the unpaired spin of the titanium(III) atom and one ²⁷Al nucleus.^{11,12} The electronic spectrum of $\text{Ti}(\text{acac})_3$ showed a $d_e \rightarrow \pi^*$ transition band, which was associated with a partial donation of the d_e -electron to the conjugated acetylacetonato ligand.⁷ The absence of the hyperfine structure in the first, second, and fourth signals was reasonably attributed to the distribution of the unpaired spin to the chelating acetylacetonato ligands, that is, two or three acetylacetonato ligands chelating the titanium(III) atom may decrease the unpaired spin density on the ²⁷Al nucleus of the organoaluminum coordinated to the same titanium(III) atom. This effect may cancel the hyperfine structure arising from the interaction between the unpaired spin and the ²⁷Al nucleus, since the coupling constant is proportional to the unpaired spin density on the nucleus concerned. The titanium(III) species containing both two organoaluminum components and one acetylacetonato ligand, however, showed the hyperfine structure of 11 components, as mentioned above. This fact indicates that only one acetylacetonato ligand may be insufficient to cancel the hyperfine structure. The ESR spectra of $(\text{C}_5\text{H}_2)_2\text{TiCl}_2\text{AlCl}_2$ and of $(\text{C}_5\text{H}_5)_2\text{TiCl}_2\text{Al}(\text{CH}_3)_2$ represented the effect of the distribution of the unpaired spin on ²⁷Al nucleus on the hyperfine structure distinctly; the former complex with the electron-attracting chlorine ligands had a hyperfine structure of six components, and the latter complex with the electron-releasing methyl ligands showed no hyperfine structure.¹¹

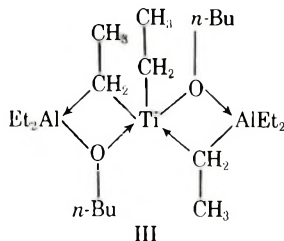
The first signal was observed both in the catalyst solution and in the polymerization system maintained at a temperature below -70°C , and diminished rapidly at temperatures higher than -40°C . Thus, in the reaction between $\text{Ti}(\text{acac})_3$ and triethylaluminum, the first signal corresponded to the first, very unstable intermediate, which was converted easily into the other titanium species at the temperatures above -40°C . Such behavior of this intermediate was consistent with that of a titanium(III) complex, II, which was formed by the reaction between *n*-butyl



titanate and triethylaluminum at -70°C .⁵ As II itself had no titanium(III)-ethyl bond, triethylaluminum probably did not alkylate a titanium(II)-alkoxy bond at this temperature. The titanium(III)-acetylacetonato chelation, which was expected to be stronger than the titanium(III)-alkoxy bond, was not possibly alkylated with triethylaluminum at -70°C . Accordingly, the first intermediate retained three strongly chelating acetylacetonato ligands. In addition, the reaction of $\text{Ti}(\text{acac})_3$ with triethylaluminum at -70°C was accompanied by a simultaneous color change from indigo blue to violet, corresponding to the slight shift of the absorption band to a shorter wavelength. Furthermore, an oxygen atom of the acetylacetonato ligand may be also coordinated to another metal atom,¹³ and monomeric triethylaluminum is very susceptible to accepting an electron pair of a donating oxygen atom. In view of these factors, the first intermediate was probably to a very unstable addition complex of $\text{Ti}(\text{acac})_3$ with triethylaluminum. An addition compound of tris(acetylacetonato)-chromium(III) with triphenylaluminum was reported as a product of the reaction between these two components.¹⁴

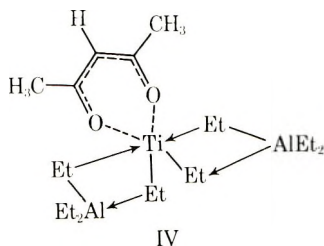
The second signal appeared at -40°C , coincident with the disappearance of the first signal, and diminished at -5°C , with the appearance of the third and the fourth signals. These facts mean that the second species can be regarded as a considerably unstable intermediate in a reaction path from the first intermediate to the third and the fourth species. Accordingly, one acetylacetonato ligand in the second species must have an unstable interaction with triethylaluminum. On the basis of these discussions and of the fact that the second species had no hyperfine structure, this species was ascribed to the titanium(III) species, which presumably contained both two strongly chelating acetylacetonato ligands and an unstably coordinated organoaluminum component.

The third signal with a hyperfine structure of 11 components was observable at -30°C and decreased at the temperatures above 10°C . The coupling constant of 2.2 gauss in this signal suggests a quite strong interaction between the titanium(III) atom and the ^{27}Al nucleus, by comparison with the coupling constant of 2.6 gauss in III, found in *n*-butyl titanate-triethylaluminum catalyst.⁵ This evidence indicates that the third titanium(III) species is coordinated with two equivalent organoaluminum components in an unstable form, in which an enolic acetylacetonato ligand



probably bridges the aluminum atom to the titanium(III), similarly to the alkoxy group in III. It is ambiguous whether the acetyl oxygen in the enolic acetylacetonato ligand is coordinated to the aluminum atom in same form as that in I, or not.

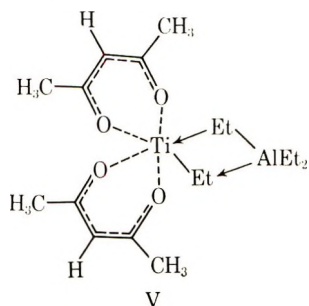
At temperatures higher than 10°C , two other molecules of triethylaluminum must replace easily the unstably coordinated organoaluminum components in the third species, liberating two moles of very stable diethyl-(acetylacetonato)aluminum. The newly incoming triethylaluminum molecules are coordinated to the titanium(III) atom in a more stable bridging form, converting the third species into a new titanium(III) species, as shown in structure IV. The fifth signal was assigned to IV, because Ti-Et-



Al bridges in IV possibly give rise to the interaction between the unpaired spin and two ^{27}Al nuclei. Such a ligand-substitution reaction between $\text{Ti}(\text{acac})_3$ and triethylaluminum is supported both by the decrease in an infrared band at 432 cm^{-1} attributable to a titanium-acetylacetonato chelate structure,¹ and by the increase in the infrared band at $490\text{--}500\text{ cm}^{-1}$ responsible for the aluminum-acetylacetonato chelate structure.¹ The titanium(III)-ethyl bond in IV is stable, presumably owing to the bridge structure with a triethylaluminum molecule, although a titanium-ethyl bond is generally expected to be too unstable to persist at room temperature. In fact, no other

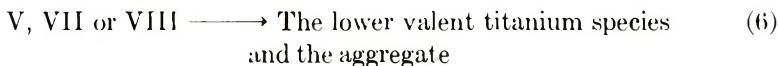
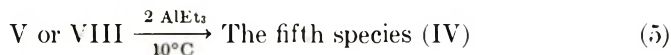
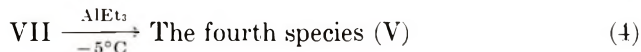
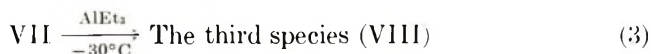
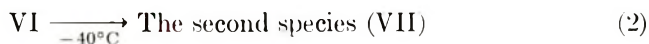
stable interaction between the titanium(III) and the ^{27}Al nucleus than this kind of bridge structure could be expected in the $\text{Ti}(\text{acac})_3$ -triethylaluminum system. Furthermore, this bridge structure is quite analogous to that present in a triethylaluminum dimer.

The behavior of the fourth signal was very similar to that of the fifth one, as shown in Figure 2. Accordingly, the stability of the fourth species and the bonding between the titanium(III) and the organoaluminum component in this species were probably analogous to those found for IV, respectively. On the basis of these considerations and of the fact that the fourth signal



had no hyperfine structure, structure V was proposed as the fourth species. V was possibly derived from the second species by the substitution reaction with other molecules of triethylaluminum, followed by the liberation of one mole of diethyl(acetylacetonato)aluminum.

Thus, careful measurements of the ESR spectra from -78°C to $+25^\circ\text{C}$ disclosed signals corresponding to the unstable intermediates which could not be detected by the measurement only at room temperature. The detection of these intermediates and of the reaction products elucidated the outline of the mechanism of the reaction between $\text{Ti}(\text{acac})_3$ and triethylaluminum, shown in eqs (1)–(6).

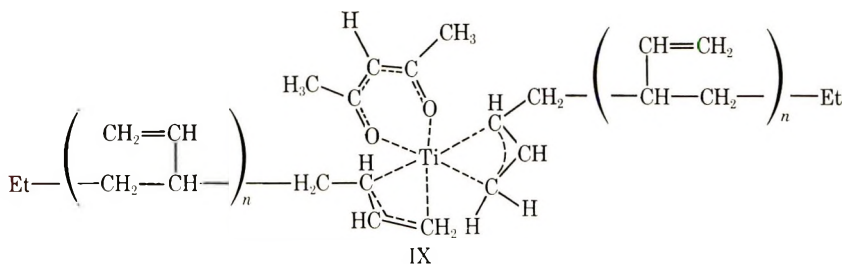


Electron Spin Resonance Spectra of the Polymerization System

The signal with the g value of 1.978 was observed in the presence of butadiene at 25°C only at the Al/Ti ratios larger than eight, where the catalytic

activity was considerably great (see Fig. 3 and Table I). Thus, this signal was distinctly characteristic of the polymerization of butadiene. The absorption intensity of the signal was about one seventh of the concentration of the polymer chain calculated from the polymer yield and the molecular weight, suggesting the occurrence of a chain-transfer reaction by an excess amount of triethylaluminum. The g value of the signal was close to 1.983 i.e., that of the signal responsible for the growing end of polybutadiene with *n*-butyl titanate-triethylaluminum catalyst.⁶ On this evidence, the signal with a g value of 1.978 is associated with a growing end of the polybutadiene with the $\text{Ti}(\text{acac})_3$ -triethylaluminum catalyst.

The hyperfine structure of this signal was too poorly split to be analyzed. This catalyst also gave 1,2-polybutadiene, the microstructure of which was very similar to that of polybutadiene obtained with *n*-butyl titanate-triethylaluminum catalyst.^{6,8,15} In either case, the yield of polybutadiene increased markedly with increasing Al/Ti ratio. The optimum Al/Ti ratios for the yield, however, were about 100 and 5.8 for the $\text{Ti}(\text{acac})_3$ -triethylaluminum catalyst and the *n*-butyl titanate-triethylaluminum one,⁸ respectively. This large difference of the optimum Al/Ti ratio between these two catalysts was due to the difference of susceptibility to the substitution by triethylaluminum between the acetylacetonato ligand and the *n*-butoxy one. These facts suggest an analogy between the structures of the growing ends of polybutadienes with these two catalysts. On the ground of these considerations, structure IX was proposed as the structure of the growing



end of polybutadiene with the $\text{Ti}(\text{acac})_3$ -triethylaluminum catalyst. IX is quite analogous to acetylacetonatodi(π -allyl)rhodium(III).¹⁶

IX can be reasonably derived from the third species, with the liberation of diethyl(acetylacetonato)aluminum and with a successive insertion of butadiene molecules into the titanium-ethyl bonds. The absorption intensity of the third signal, however, was not a good index for the catalytic activity for the polymerization of butadiene, since the signal was transitional and overlapped with the fourth signal. IV also contained formally two ethyl groups and two triethylaluminum components. The fifth signal did not seem to be the index for the catalytic activity, owing to the overlap with the fourth signal.

References

1. M. Takeda, K. Iimura, and Y. Nozawa, paper presented at the 14th Symposium on Polymers, The Society of Polymer Science, Japan, Kyoto, Oct. 1965; *Preprints*, p. 269.
2. K. Matsuzaki and T. Yasukawa, *J. Polym. Sci. A-1*, **5**, 511 (1967).
3. S. Ikeda, A. Yamamoto, M. Murai, and N. Oshima, paper presented at the 16th Annual Meeting on Polymers, The Society of Polymer Science, Japan, Tokyo, May 1967; *Preprints*, p. 45.
4. W. R. Watt, F. H. Fry, and H. Pobnor, *J. Polym. Sci. A-1*, **6**, 2703 (1968).
5. H. Hirai, K. Hiraki, I. Noguchi, and S. Makishima, *J. Polym. Sci. A-1*, **8**, 147 (1970).
6. H. Hirai, K. Hiraki, I. Noguchi, T. Inoue, and S. Makishima, *J. Polym. Sci. A-1*, in press.
7. D. W. Barnum, *J. Inorg. Nucl. Chem.*, **21**, 221 (1961).
8. D. H. Dawes and C. A. Winkler, *J. Polym. Sci. A*, **2**, 3029 (1964).
9. T. S. Djabiev, R. D. Sabirvova, and A. E. Shilov, *Kinetika i Kataliz*, **5**, 441 (1964).
10. E. Angelescu, C. Nicolau, and Z. Simon, *J. Amer. Chem. Soc.*, **88**, 3910 (1966).
11. A. H. Maki and E. W. Randall, *J. Amer. Chem. Soc.*, **82**, 4109 (1960).
12. M. Takeda, K. Iimura, and N. Koide, *Kogyo Kagaku Zasshi*, **71**, 563 (1968).
13. G. J. Bullen, R. Mason, and P. Pauling, *Inorg. Chem.*, **4**, 456 (1965).
14. G. Sartori and G. Costa, *Z. Elektrochem.*, **63**, 105 (1959).
15. G. Wilke, *Angew. Chem.*, **68**, 306 (1956).
16. J. Powell and B. L. Shaw, *J. Chem. Soc. A*, **1968**, 583.

Received October 29, 1969

Revised February 17, 1970

Alkyl Chain Branching in Ethylene-Vinyl Acetate Copolymer

mitsutaka SAITO, HIDEO TADA, and YUJIRO KOSAKA, *Polymer
Laboratory, Nippon Polychemicals Company, Ltd., Nanyo-cho,
Yamaguchi-ken, Japan*

Synopsis

Ethylene-vinyl acetate copolymers contain two kinds of side chains: acetoxy branches originating from incorporated vinyl acetate and alkyl branches. The alkyl branching was determined by infrared analysis after converting the ethylene-vinyl acetate copolymer to a hydrocarbon polymer by three steps: hydrolysis, iodation with hydriodic acid containing red phosphorus, and reductive hydrogenation with lithium aluminum hydride. It was found that physical properties such as stiffness were dependent both on the degree of alkyl chain branching and on vinyl acetate content.

INTRODUCTION

Ethylene-vinyl acetate copolymers have unique physical properties in the flexible, elastomeric thermoplastic field. One of the most important characteristics of ethylene-vinyl acetate copolymers is high flexibility, greater even than that of low-density polyethylene.

Ethylene-vinyl acetate copolymers prepared by a free-radical process are expected to contain both acetoxy groups originating from the vinyl acetate comonomer and alkyl branches as side chains. Both side chains affect the crystallinity of the copolymer and because of this they affect polymer flexibility. Although the effects of vinyl acetate content on the various properties of EVA copolymer have been investigated by many workers,^{1,2} the contribution of alkyl chain branching on those properties has not been reported yet. It is the purpose of this paper to determine accurately the number of alkyl branches and to study the contribution of alkyl branching on the properties of ethylene-vinyl acetate copolymer.

The degree of alkyl short chain branching can be determined if the copolymers are transformed into polyethylene by reductive removal of the acetoxy groups. We have achieved the reduction of ethylene-vinyl acetate copolymers with three steps; hydrolysis, iodation, and hydrogenation. The degree of alkyl chain branching has been determined by infrared analysis of the reduced copolymers.

EXPERIMENTAL

Materials

Ethylene-Vinyl Acetate Copolymers. Samples used in this experiment were commercial ethylene-vinyl acetate copolymers synthesized by a high-pressure process: Nipoflex (Nippon Polychemicals Co.), Evaflex (Mitsui Polychemical Co.), and Evatate (Sumitomo Chemical Co.).

Polyethylenes. Petrothene resins are low-density polyethylenes manufactured by Nippon Polychemicals Co. Hizex resins are Ziegler-type high-density polyethylenes (Mitsui Petrochemical Industries).

Solvents. The solvents used were benzene, xylene, decalin, methanol, ethanol, and tetrahydrofuran. Benzene was washed with concentrated sulfuric acid, aqueous sodium hydroxide, and water, respectively, dehydrated with calcium chloride, and then distilled over metallic sodium. Tetrahydrofuran was refluxed over metallic sodium, then distilled. The other solvents were the purest commercially obtainable and used without further purification.

Reagents. The reagents used were potassium hydroxide, red phosphorous, lithium aluminum hydride, and hydriodic acid. They were the purest commercially obtainable grade and used without further purification.

Hydrolysis

A 10-g portion of an ethylene-vinyl acetate copolymer was dissolved in 500 ml of xylene with warming in a 1-liter flask equipped with a condenser, dropping funnel, and mechanical stirrer. A 2% potassium hydroxide-ethanol solution (100 ml) was added to the polymer solution with stirring, and the solution was refluxed for 1 hr. The reaction mixture was then poured into approximately 2 liters of methanol. The polymer was filtered, then dried.

Iodation

In a 300 ml flask equipped with an efficient reflux condenser was placed 2 g of the hydrolyzed ethylene-vinyl acetate copolymer, 30 ml of decalin, 1 g of red phosphorus, and 20 ml of 57% hydriodic acid. The vessel was maintained at about 250°C for 5 hr. It was stirred occasionally by hand during this time.

After the reaction the mixture was dissolved in 80 ml of xylene and the unreacted phosphorus was precipitated. The clear upper solution was decanted and filtered. The polymer solution was then poured into approximately 600 ml of methanol. The polymer was filtered and dried *in vacuo*.

Reduction

In a 100-ml stainless steel ampoule was charged 1 g of the polymer described above, 20 ml of purified tetrahydrofuran, 1 g of lithium aluminum hydride, and 20 ml of purified benzene under flushing with nitrogen. The

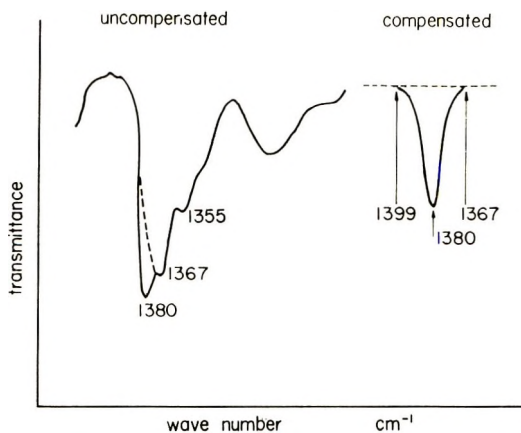


Fig. 1. Resolution of the 1380 cm^{-1} methyl band: compensation for $1367/1355\text{ cm}^{-1}$ methylene doublet.

ampoule was sealed. Reaction was allowed to proceed at 70°C for 24 hr. The polymer was isolated by the addition of water, filtered, washed with dilute hydrochloric acid, water, and methanol, and dried.

Determination of Degree of Chain Branching

The product thus obtained has properties similar to those of low-density polyethylene, so the determination of degree of chain branching was achieved according to a modification of Willbourn's method.³ The method was a double-beam compensation method. The sample being examined and the compensation polymethylene sample are both solid, the latter being wedge-shaped. The aim was to compensate completely the $1367/1355\text{ cm}^{-1}$ methylene doublet. This was achieved by alternately setting the wavelength to 1367 and to 1399 cm^{-1} , where there was no absorption for either material. When the recorder read the same at these two wavelengths, the wedge was correctly situated. The 1380 cm^{-1} band assigned to methyl groups was then scanned and recorded as a symmetrical undistorted band, and its intensity was measured (see Fig. 1).

The degree of chain branching was obtained by eq. (1):

$$A(\text{CH}_3/1000\text{C}) = 1.15 \times 10^3 (E/\sigma) \quad (1)$$

where A is the number of methyl groups per 1000 carbon atoms, E the absorbance, and σ the thickness of the sample in units of mg/cm^2 . The calibration of the molar absorptivity was carried out by using n -alkanes such as tetracosane, dotriacontane, and dopentacontane.

The spectrometer used in this experiment was a Shimadzu Model IR-27G infrared spectrophotometer equipped with a grating, and the measurement conditions were as follows; scanning speed 45 min, gain 4, and slit width $420\text{ m}\mu$ at 1380 cm^{-1} .

RESULTS AND DISCUSSION

Reduction to a Hydrocarbon Polymer

Estimation of branches by infrared techniques on the hydrocarbon polymer could be used as an index of alkyl branching in ethylene-vinyl acetate copolymer if reduction did not involve chain cleavage, molecular rearrangement, or extensive double-bond formation. The reduction of ethylene-vinyl acetate copolymer to a hydrocarbon polymer was achieved by three steps; hydrolysis, iodation, and reductive hydrogenation.

Hydrolysis. Ethylene-vinyl acetate copolymer was hydrolyzed with potassium hydroxide and ethyl alcohol in xylene solution. The infrared spectra of the original ethylene-vinyl acetate copolymer and the hydrolyzed copolymer are shown in Figures 2 and 3. Since absorptions appearing at $1700\text{--}1730\text{ cm}^{-1}$ in Figure 3 are quite weak and not changed by further saponification, the hydrolysis reaction seems to be complete. The weak absorption bands in the $1700\text{--}1730\text{ cm}^{-1}$ region may originate from long-chain branching residues on acetyl side chains, but we have not ascertained this yet.

Iodation. The hydroxy polyethylene was reacted with hydriodic acid containing red phosphorus in decalin at 250°C for 5 hr. Under these conditions, approximately 60% of the hydroxyl groups were replaced by iodine and the rest were hydrogenated. Iodine content in the copolymer was determined by Shöniger's flask combustion method.^{4,5} The infrared spectrum of the product is shown in Figure 4. This spectrum indicates the existence of the C-I bond in the 500 cm^{-1} region, replacement of the alcohol units.

Reductive Hydrogenation. Finally, the polymer obtained in the second step was completely reduced with lithium aluminum hydride in a benzene-

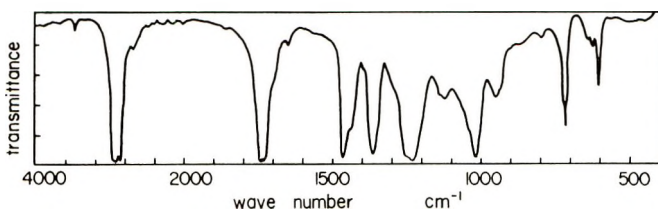


Fig. 2. Infrared spectrum of the original ethylene-vinyl acetate copolymer.

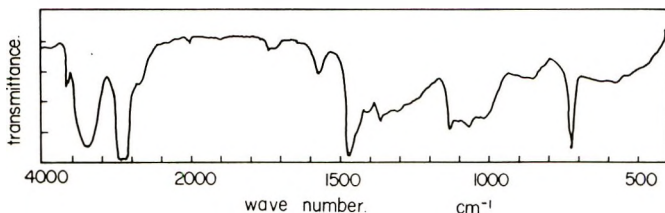


Fig. 3. Infrared spectrum of the hydrolyzed ethylene-vinyl acetate copolymer.

tetrahydrofuran mixture at 70°C for 24 hr according to a modification of Cotman's procedure.⁶

The infrared spectrum of a fully reduced ethylene-vinyl acetate copolymer is shown in Figure 5. The spectrum is similar to that of low-density polyethylene. The absorption at 3600 cm^{-1} is assigned to hydroxyl groups which may originate from both long-chain branching residues of the original ethylene-vinyl acetate copolymer, and trace amounts of aluminum hydroxide contaminant from the reductive hydrogenation process. The

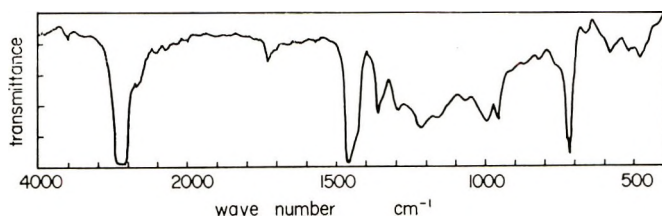


Fig. 4. Infrared spectrum of the product treated with hydriodic acid and red phosphorus.

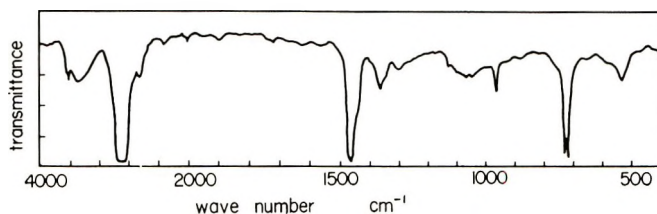


Fig. 5. Infrared spectrum of the completely hydrogenated ethylene-vinyl acetate copolymer.

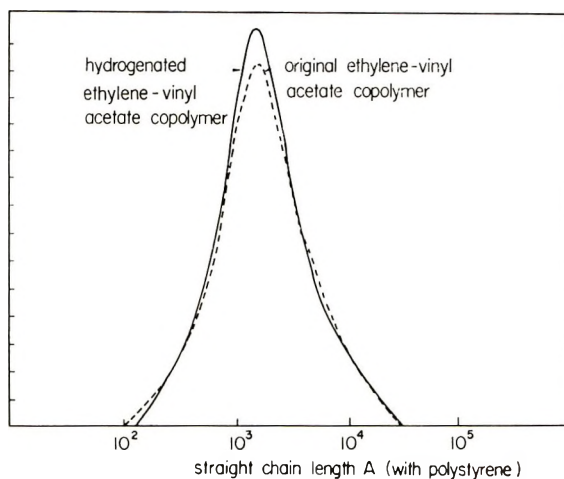


Fig. 6. GPC curves of hydrogenated ethylene-vinyl acetate copolymer and the original: GPC conditions: column, 10^6 , 10^5 , 10^4 , 10^3 Å; temperature, 135°C; eluent, 1,2,4-trichlorobenzene.

absorption at 965 cm^{-1} is assigned to the *trans* double bond produced during the hydrogenation processes. However, since these unexpected absorptions are very weak, they do not affect the determination of alkyl chain branching. The crystalline band appearing at 730 cm^{-1} reveals a high degree of crystallinity of the fully reduced polymer.

The GPC curves of both the original and fully hydrogenated ethylene-vinyl acetate copolymers are shown in Figure 6. Both curves are very similar. This indicates that there was no chain scission during the hydrogenation processes.

Branching and Some Physical Properties

It is well known that there are a few long-chain branches and many short-chain branches in low-density polyethylene prepared by high-pressure processes. Ethylene-vinyl acetate copolymers made by high-pressure processes are expected to contain both short- and long-chain branches on the polymer backbone like low-density polyethylene and acetoxy groups.

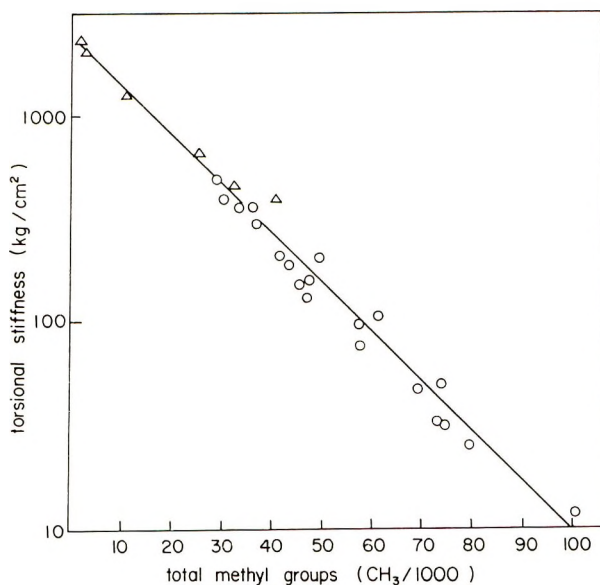


Fig. 7. Plot of torsional stiffness vs. total chain branching number: (O) ethylene-vinyl acetate copolymer; (Δ) polyethylene.

Furthermore ethylene-vinyl acetate copolymers may contain long-chain branches on acetoxy groups, since long-chain branching is caused by intermolecular chain transfer between a polymer radical and a labile site of a completed polymer molecule.

We have focussed on alkyl short-chain branching in ethylene-vinyl acetate copolymers and determined the amount of alkyl branching and its effect on the properties of the copolymers.

TABLE I
Short-Chain Branching and Torsional Stiffness

Sample	Melt index, g/10 min	VAc, wt-%	Torsional stiffness, kg/cm ²	CH ₃ COO/1000C ^a	CH ₂ /1000C	Total branches/1000C
Nipoflex						
634	2.39	24.5	75	47.8	10.2	58.0
750	23.7	31.1	31	64.1	10.5	74.6
630	1.49	15.8	175	29.0	15.0	44.0
633	19.8	17.2	150	31.8	15.8	47.6
631	1.58	18.0	145	33.4	12.3	45.7
Evaflex						
420	141	18.0	102	33.4	28.8	62.2
460	2.65	18.0	125	33.4	14.4	47.8
320	235	24.5	49	47.8	27.4	75.2
360	2.09	23.7	97	45.9	12.0	57.9
250	15.8	27.0	46	53.7	15.5	69.2
220	148	27.9	33	55.9	17.9	73.8
150	28.6	31.1	25	66.2	13.6	79.8
40	60	39.4	10-20	87.3	13.6	100.9
Evatate						
D2021	1.35	9.2	260	16.0	19.7	35.7
K2010	2.46	21.8	94	41.6	20.2	61.8
H4011	17.9	17.7	120	32.7	17.9	49.6
K4010	18.8	30.0	43	61.2	14.3	75.5
Hizex						
1000J	5.82	0	2020	0	3.3	3.3
5000B	0.29	0	2340	0	2.0	2.0
Petrothene						
107	0.4	0	480	0	32.6	32.6
115	5.12	0	670	0	26.4	26.4
202	22.3	0	425	0	42.5	42.5
219	3.03	0	1200	0	12.2	12.2

^a Calculated from vinyl acetate content.

The alkyl short-chain branching determined for copolymers having various acetate contents, melt indexes, and torsional stiffness are listed in Table I. As shown in Table I, the ethylene-vinyl acetate copolymers having the same composition but different amount of alkyl branches differed considerably in flexibility; flexibility increased with the amount of alkyl branches.

Plots of torsional stiffness against the sum of acetoxy groups and alkyl branches for various ethylene-vinyl acetate copolymer, fall on a straight line, as shown in Figure 7. Furthermore, the linear relationship extends to polyethylene, i.e., plots of torsional stiffness against alkyl branching for polyethylene lie on the straight line obtained from ethylene-vinyl acetate copolymers. This shows that the torsional stiffness is noticeably dependent on the degree of total chain branching, which affects the crystallinity.

It should be emphasized that both vinyl acetate content and degree of short alkyl chain branching affects physical properties such as stiffness.

References

1. R. L. Alexander, H. D. Anspou, F. E. Brown, B. H. Clampitt, and R. H. Hughes, *Polymer Eng. Sci.*, **6**, 5 (1966).
2. P. M. Kamath and R. W. Wakefield, *J. Appl. Polym. Sci.*, **9**, 3159 (1965).
3. A. H. Willbourn, *J. Polym. Sci.*, **34**, 569 (1959).
4. W. Shöniger, *Mikrochim. Acta*, **1955**, 123.
5. W. Shöniger, *Mikrochim. Acta*, **1956**, 869.
6. J. D. Cotman, Jr., *J. Amer. Chem. Soc.*, **77**, 2790 (1955).

Received December 8, 1969

Revised February 24, 1970

The Reaction Between Diethyl Succinylsuccinate (1,4-Diethoxycarbonyl-2,5-dihydroxy-1,4-cyclohexadiene) and Amines and Its Application to Polymer Synthesis

FUKUJI HIGASHI, AKIRA TAI, and KAZUO ADACHI, *Research Center, Tekkoshu Co. Ltd., Musashino-shi, Tokyo, Japan*

Synopsis

Polymers having polyamine structures were obtained by the condensation reaction between diethyl succinylsuccinate (1,4-diethoxycarbonyl-2,5-dihydroxy-1,4-cyclohexadiene) and aliphatic diamines. The reactions were carried out in high polar solvents such as N-methylpyrrolidone (NMP) and N,N-dimethylformamide (DMF). The mode of the polymerization reaction and the structure of the polymers were verified by studies of model compounds. The polymers thus obtained were conveniently utilized as coating and adhesive materials and were able to be cast into films.

INTRODUCTION

Diethyl succinylsuccinate (1,4-diethoxycarbonyl-2,5-dihydroxy-1,4-cyclohexadiene) has recently been prepared as an important intermediate for the synthesis of organic pigments and has become easily available commercially. The reactions between diethyl succinylsuccinate (DSS) and aromatic amines have been well studied in the course of investigations on the synthesis of quinacridones.^{1,2}

Not long ago Kimura³ applied this reaction to polymer synthesis and prepared polymers having a quinolone structure. In the case of the reaction with aliphatic amines, several 1,4-diethoxycarbonyl-2,5-dialkylamino-1,4-cyclohexadienes have been made,^{4,5} but no details of the reaction routes or isolation of intermediates have been reported.

The present paper describes the results of further studies of the reactions between DSS and aliphatic amines and their application to polymer synthesis.

RESULTS AND DISCUSSION

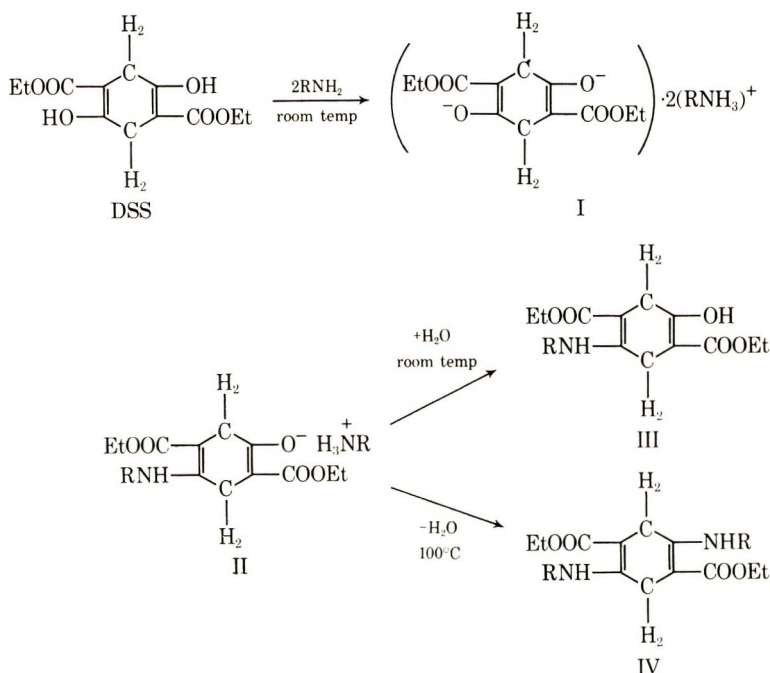
DSS has four functional groups (two enolic hydroxy and two ethoxycarbonyl groups) which could participate in stepwise condensations with diamines. To prepare linear polymers from this compound, it is essential to discover reaction conditions such that only the hydroxy groups should

participate in the polymerization. The reactivity of the hydroxy groups was investigated by model reactions with aliphatic monoamines, i.e., *n*-propyl-, *n*-butyl-, *n*-amyl-, and *n*-hexylamine.

The reactions were carried out in *N*-methylpyrrolidone (NMP), with an excess of the amines, under various conditions. Monoalkylammonium salts of DSS (I), monoalkylammonium salts of III (II), 1,4-diethoxycarbonyl-2-hydroxy-5-alkylamino-1,4-cyclohexadienes (III), and 1,4-diethoxycarbonyl-2,5-dialkylamino-1,4-cyclohexadienes (IV) were synthesized as model compounds. The products with each amine are listed in Table I.

The salt I was formed as a precipitate by the addition of an amine to a solution of DSS in NMP at room temperature. An NMP solution of II was obtained by keeping the slurry of I in NMP at 50–70°C for 3 hr. The salt II was then hydrolyzed quantitatively to III by pouring the above solution into water. The salt II was also isolated as a precipitate from the system at low temperature. Compound IV was obtained by keeping either a slurry of I in NMP or an NMP solution of III and amine for 2 hr at a temperature above 100°C.

The route of the model reaction between DSS and the amines is summarized in Scheme 1:



Scheme 1

Compound I was stable in such solvents as DMF, NMP, and *n*-hexane, but decomposed to starting substances in protonic solvents such as methanol, ethanol, and water. It also decomposed spontaneously to DSS and the amine when exposed to air. The results of an acid–base titration of

TABLE I
Relationship Between Reaction Conditions and Products.

Amine	Reaction conditions		Reaction products		
	Temp, °C	time, hr	product	mp, °C	yield, %
<i>n</i> -Propyl	60	3	IIIa	82-3	84
	120	2	IVa	109-10	93
Isopropyl	50	3	IIIb	145	83
	110	2	IVb	140	95
<i>n</i> -Butyl	65	3	IIIc	77-8	88
	120	2	IVc	97-8	100
<i>n</i> -Amyl	70	3	III d	65-6	90
	120	2	IV d	76-7	100
<i>n</i> -Hexyl	70	3	III e	69-70	93
	120	2	IV e	84-5	100

freshly prepared I indicated that 2 moles of the amine were associated with 1 mole of DSS.

The properties of II were very similar to those of I. In air, II changed into III by releasing the amine spontaneously, and in water it decomposed to III and the amine in equimolar ratio.

The reaction conditions required to produce II in the system were studied indirectly by the determination of III, which was obtained by treating the system with water. A selective formation of II could be achieved by carrying out the reaction at around 60°C. As shown in Table I, the temperature required to produce II increased from 50° to 70°C with increasing chain length of the amines.

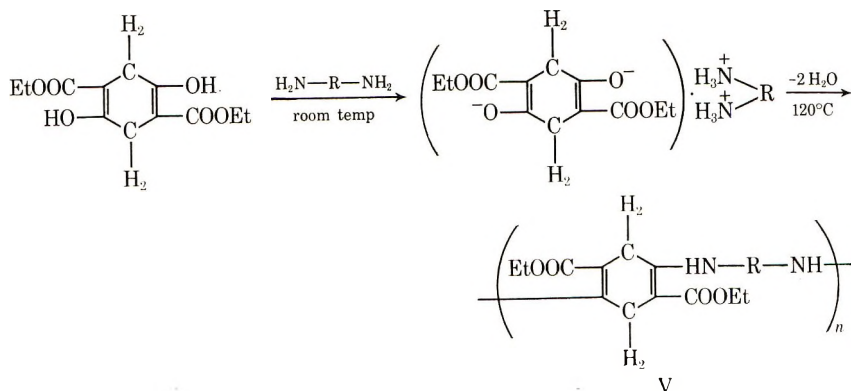
Compound IV was obtained as end product of the reactions, in a yield that was almost quantitative when the reaction temperature was above 100°C.

Exposure of a mixture of IV and an amine to drastic conditions (heating in a sealed tube at 200°C) caused no further reaction such as amidation of ethoxycarbonyl groups. Also, IV did not react with strong nucleophilic reagents such as RNH-MgI in boiling tetrahydrofuran.

The abnormal chemical properties of the ethoxycarbonyl groups in positions 1 and 4 in IV could be explained by the electronic and steric effects of the alkylamino groups in positions 2 and 5. Thus, the electron density on the carbonyl carbons was increased by the electron-donating effect of amino groups exerted through the double bonds, inhibiting strongly the otherwise expected nucleophilic attack of amines.

The results of the work on the model reactions indicated that although the reactivities of the two hydroxy groups in DSS were not equivalent at lower temperatures, at higher temperatures DSS was able to react as a bifunctional compound to produce linear polymers with diamines without any side reactions.

The polymerization should be carried out above 100°C. The proposed route of polymerization is shown in Scheme 2.



Scheme 2

The solvents used as polymerization medium were chosen to satisfy the following requirements: (1) They should be capable of dissolving all substances in the system, so that the polymerization is conducted in a homogeneous solution. (2) They should be inert to all substances in the system. (3) The boiling point should be above 150°C . (4) They should be miscible with water. DMF, DMAc, and NMP were found to be suitable on the basis of these criteria. The best results were obtained in NMP.

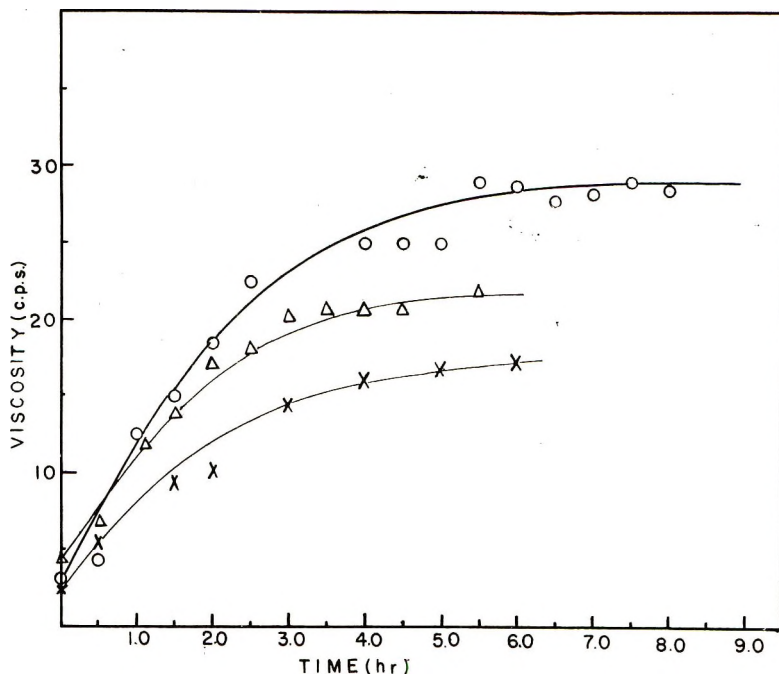


Fig. 1. Viscosity of the polymerization system as a function of reaction time. Initial monomer concn. 34% temp 120°C ; solvent, NMP: (O) hexamethylenediamine; (X) octamethylenediamine; (Δ) ATU.

TABLE II
Physical Properties of the Polymers

Diamine component	P.M.T., °C (decomp.)	η_{inh} , dl/g	M_n^c	Electrical properties ^d	Remarks
Ethylenediamine	250 (decomp.)	0.20 ^a			no films, orange powder
Tetramethylenediamine	260 (decomp.)	0.43 ^b		v.r. = 10^{15} ohm/cm ³ tan δ = $2.0 \times 10^{-3} 10^3$ Hz ϵ = $2.3 \cdot 10^3$ Hz	flexible films, yellow powder
Hexamethylenediamine	155	1.11 ^b	42,100	v.r. = 10^{15} ohm/cm ³ tan δ = $2.3 \times 10^{-3} 10^3$ Hz ϵ = $2.3 \cdot 10^3$ Hz	tough and flexible films, orange powder, excellent adhesion to metals and glass
Octamethylenediamine	115	0.55 ^b	19,700	v.r. = 10^{15} ohm/cm ³ tan δ = $2.5 \times 10^{-3} 10^3$ Hz ϵ = $2.3 \cdot 10^3$ Hz	tough and flexible films, orange powder, excellent adhesion to metals and glass
ATU	110	0.52 ^b		v.r. = 10^{15} ohm/cm ³ tan δ = $2.5 \times 10^{-3} 10^3$ Hz ϵ = $2.3 \cdot 10^3$ Hz	tough and flexible films, orange powder, excellent adhesion to metals and glass
Methanediamine	170	0.14 ^b			no films, yellow powder

^a In *m*-cresol at 30°C, polymer concentration 0.5 g/100 ml.

^b In tetrachloroethane at 30°C, polymer concentration 0.5 g/100 ml.

^c Determined by membrane osmometry in cyclohexanone at 65°C.

^d v.r. = volume resistivity; tan δ = dissipation factor; ϵ = dielectric constant.

The polymerization was usually carried out in NMP at 120°C under nitrogen. The diamines used in this study were ethylenediamine, tetramethylenediamine, hexamethylenediamine, octamethylenediamine, menthanediamine, and 3,9-bis(3-aminopropyl)-2,4,8,10-tetroxaspiro(5.5)-undecane (ATU).

The rate of polymerization was followed by the change in the system's viscosity (see, for example, Fig. 1). Generally speaking, the viscosity reached asymptotic values in 4 hr, and the polymerizations therefore seemed to be completed in 5 hr. Reddish-orange viscous solutions were obtained at this stage.

The polymers, isolated as solids by pouring the solutions into cold water, were yellowish-orange powders soluble in *m*-cresol, chloroform, dichloroethane, and trichloroethane at room temperature. They were also soluble in hot DMAc, DMF, NMP, and cyclohexanone.

The polymerizations could also be carried out in aprotic polar solvents such as DMF and DMAc.

Some physical properties of these polymers are listed in Table II. The polymers were conveniently utilized for coating and adhesive materials and could also be cast into films.

STRUCTURAL ANALYSIS

Compound IIIa

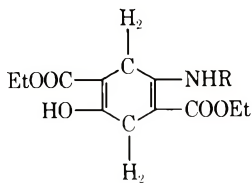
The infrared spectrum (KBr disk) showed characteristic absorptions at 5.95, 6.01, 6.10, and 6.20 μ . The pair of absorptions at 5.95 and 6.10 μ , which was almost identical with that given by 2-ethoxycarbonylcyclohexanone, was attributed to the C=O stretching vibration of the ester carbonyl and the C=C stretching vibration of the enol double bond, respectively. Another pair of absorptions, at 6.01 and 6.20 μ , was attributed to the C=O stretching of the ester and the C=C stretching of the enamine, respectively. The shift of the C=O band to the longer wavelength was explained by the effects of the conjugated double bond and of hydrogen bonding of the NH group with the carbonyl group. These absorptions were in good agreement with those of ethyl β -aminocrotonate which was studied by Witkop.⁶ The presence of an ester was also confirmed by the absorption at 8.20 μ .

The NMR spectrum showed two quartets centered at $\delta = 4.10$ and 4.24, and two triplets centered at $\delta = 1.25$ and 1.33. These resonances indicated the presence of two $-\text{O}-\text{CH}_2-\text{CH}_3$ groups in slightly different environmental conditions, which were caused by deshielding effects of NH and OH groups, respectively. Two downfield signals at $\delta = 8.92$ (one proton) and 12.11 (one proton) were caused by protons bonded with heteroatoms. The two peaks disappeared in deuterated water. The former was closely related to that of OH protons in DSS, and the latter was matched with that

of the NH proton in diethyl (ethylenebis- β -aminocrotonate) studied by Dudek and Holm.⁷

All the above evidence suggested the presence of HO—C=C—COOCH₂CH₃ and RNH—C=C—COOCH₂CH₃, and this was further confirmed by two absorptions, $\lambda_{\max} = 260 \text{ m}\mu$ and $\lambda_{\max} = 309 \text{ m}\mu$, in the ultraviolet spectrum. The characteristic singlet absorption at $\delta = 3.19$ (four protons) in the NMR spectrum indicated the presence of methylene groups between tetrasubstituted ethylene units.

The fundamental structure of compound IIIa is therefore envisaged as:



The spectroscopic data excluded the possibility of alternative structures such as keto or ketimine form. The radical R was also determined to be —CH₂—CH₂—CH₃ by the NMR spectrum, which showed signal at $\delta = 1.00$ (*t*, —CH₂—CH₃, 3H), 3.20 (*q*, —NH—CH₂—CH₂—, 2H), and 1.60 (*m*, —CH₂—CH₂—CH₃, 2H). The final structure of IIIa was thus confirmed as 1,4-diethoxycarbonyl-2-hydroxy-5-*n*-propylamino-1,4-cyclohexadiene. The empirical formula, C₁₅H₂₃O₅N, determined by elemental analysis and molecular weight determination, also supported this structure.

All other compounds (IIIb—IIIe) showed key absorptions identical with those of IIIa discussed in this section, and their structure was determined as 1,4-diethoxycarbonyl-2-hydroxy-5-alkylamino-1,4-cyclohexadiene.

Compound IVa

The infrared spectrum (KBr disk) is shown in Figure 2. The pair of absorptions at 6.01 and 6.20 μ was identical with that of IIIa and was attributed to the C=O stretching of the ester group and the C=C stretching of the enamine, respectively. The presence of an ester was also confirmed by the C—O—C stretching vibration (absorption at 8.20 μ).

The NMR spectrum showed a triplet at $\delta = 1.29$ and a quartet at $\delta = 4.14$, which indicated the —O—CH₂CH₃ group. The downfield signal at $\delta = 8.89$, which disappeared in deuterated water, was attributed to NH protons. It was also matched with that of the NH proton in diethyl (ethylene-bis- β -aminocrotonate). These facts suggested the presence of the RNH—C=C—COOCH₂CH₃ moiety. The absorption $\lambda_{\max} = 293 \text{ m}\mu$ in the ultraviolet spectrum further justified the above assignments. The singlet at $\delta = 3.19$ (four protons) in the NMR spectrum showed methylenes having the structure —C=C—CH₂—C=C—.

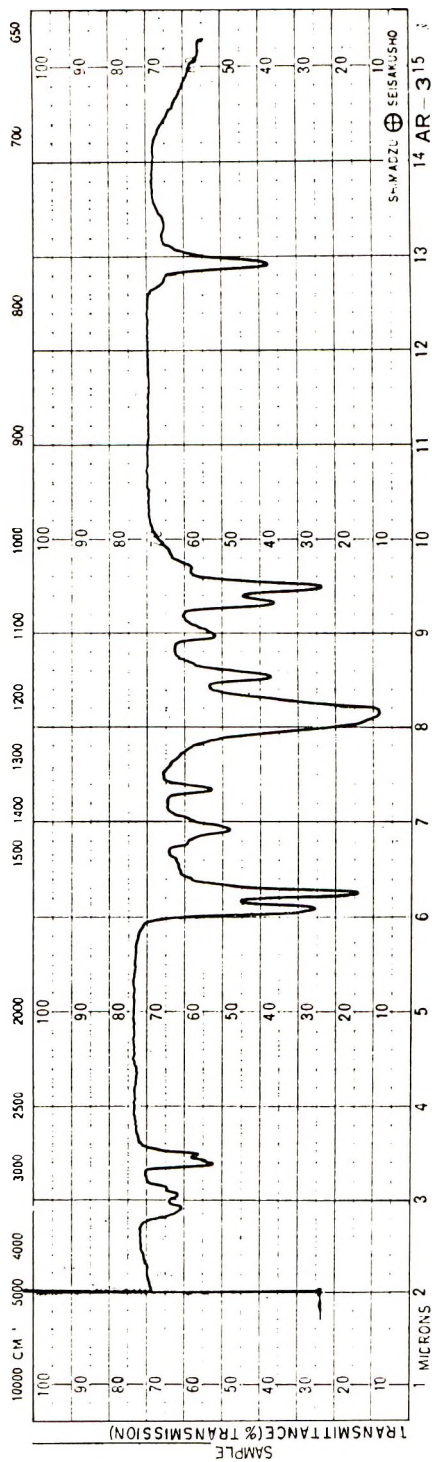


Fig. 2. Infrared spectrum of model compound IVa.

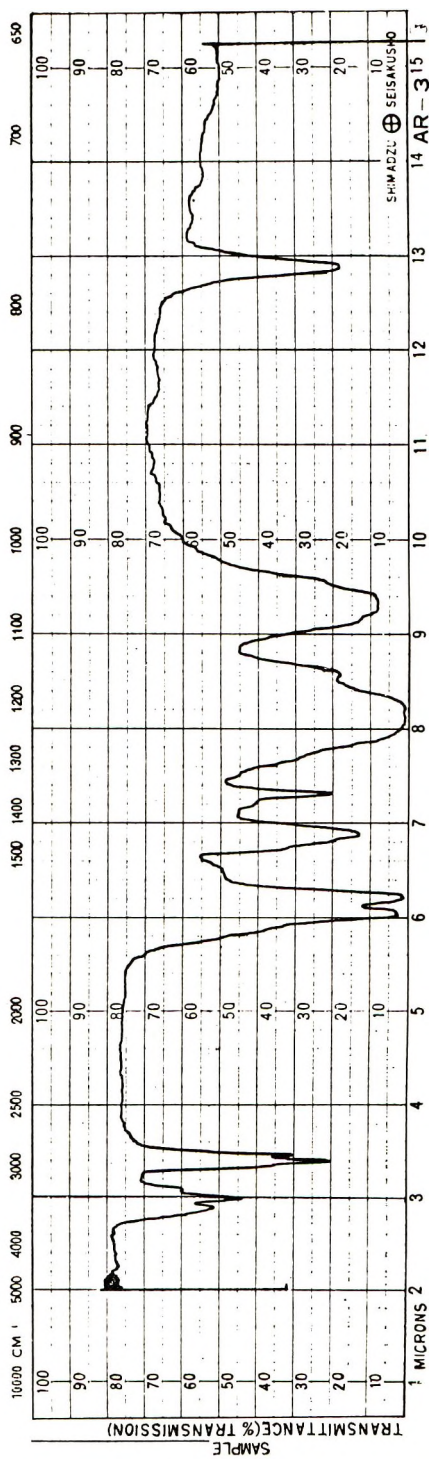
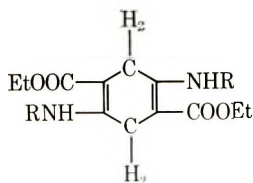


Fig. 3. Infrared spectrum of polymer Va.

The basic structure of IVa was therefore envisaged as:



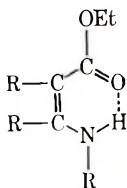
The spectroscopic data excluded the possibility of alternative structures such as the ketimine form. Radical R was also determined as $-\text{CH}_2\text{CH}_2-\text{CH}_3$ by the NMR spectrum, which showed signals at $\delta = 1.00$ (*t*, $-\text{CH}_2-\text{CH}_3$, 6H), 1.60 (*m*, $-\text{CH}_2-\text{CH}_3$, 4H), and 3.20 (*q*, $-\text{NH}-\text{CH}_2-\text{CH}_2-$, 4H).

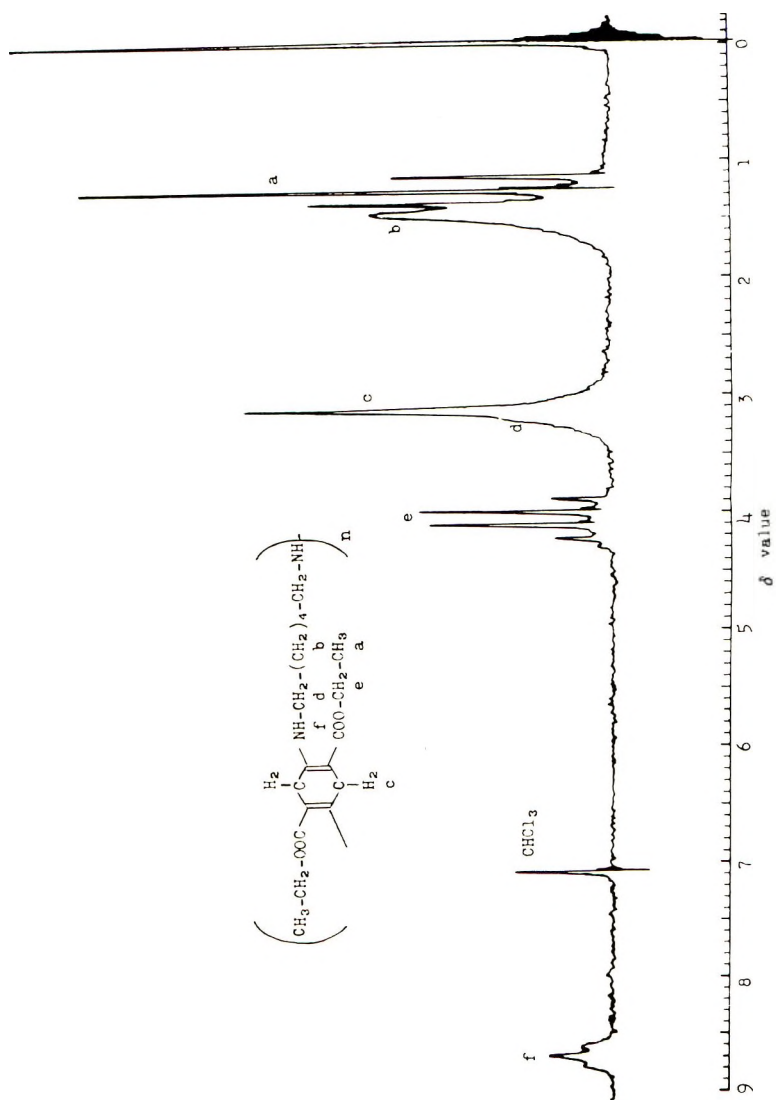
The final structure was then confirmed as 1,4-diethoxycarbonyl-2,5-dipropylamino-1,4-cyclohexadiene. The empirical formula, $\text{C}_{18}\text{H}_{30}\text{N}_2\text{O}_4$, determined by elemental analysis and molecular weight determination, also supported the above structure.

All other compounds (IVb–IVe) showed key absorptions identical with those of IVa discussed in this section, and their structure was established as 1,4-diethoxycarbonyl-2,5-dialkylamino-1,4-cyclohexadiene.

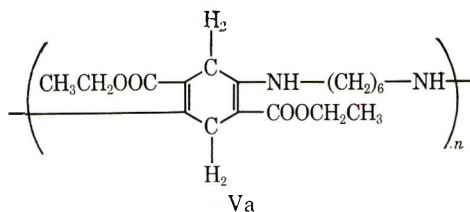
Polymer Between DSS and Hexamethylenediamine (Va)

The infrared spectrum (KBr disk) shown in Figure 3 was quite similar to that of compound IVa. The key absorptions at 6.01, 6.20, and 8.20 μ suggested an ester and an enamine in the molecule. The NMR spectrum taken in CDCl_3 is shown in Figure 4. The resonances at $\delta = 1.23$ (triplet) and 4.15 (quartet) represented the $\text{O}-\text{CH}_2\text{CH}_3$ groups. The peak centered at $\delta = 3.13$ was believed to consist of two overlapping absorptions, a singlet at $\delta = 3.13$ and a distorted quartet at $\delta = 3.14$. The former was caused by methylene protons between tetrasubstituted ethylene groups, and the latter represented methylene protons adjacent to an NH group. The downfield absorption at $\delta = 8.70$ (distorted triplet) was completely matched by that of the NH proton in IVa. The absorption was assigned to the NH proton of an enamine interacting with a carbonyl group, as follows:



Fig. 4. NMR spectrum of polymer Va in CDCl₃.

The results discussed in this section suggested strongly the structure shown below:



The empirical formula of the compound supported this structure.

Polymers synthesized with other diamines showed key absorptions identical with those of Va in spectroscopic analyses.

EXPERIMENTAL

The infrared spectra were recorded on an AR-275 spectrometer using the KBr pellet method. The NMR spectra were taken on a JEOL-JMC-60HL and a JEOL-JNM-4H-100. The sample was dissolved in CCl_4 or CDCl_3 with TMS to lock the signal at $\delta = 0$. The ultraviolet spectra were recorded on a Shimadzu RS-27 spectrometer, with ethanol as the solvent. The Brookfield viscometer (Tokyo Keiki Co., Type BL), built into a reaction vessel, was used to measure the viscosity of the reaction system. The inherent viscosity of the polymers was measured by a Cannon-Fenske viscometer. The molecular weight was determined using a vapor pressure osmometer (Mechrolab, Model 301A) and a membrane osmometer (Hewlett Packard, Model 502, Sartorius Membrane filter 5-10 $\text{m}\mu$).

Salts of amines with DSS (I)

With *n*-Propylamine (Ia). *n*-Propylamine (2.36 g) was added to a solution of DSS (2.56 g) on 50 ml of NMP at 60°C , and the system was cooled in an ice bath with vigorous stirring. The reddish-yellow precipitate of Ia was filtered off and washed with five 50-ml portions of NMP. The composition of Ia was determined as follows:

A 0.3-g portion of Ia was placed in a flask containing 50 ml of 0.5*N* aqueous hydrochloric acid and the flask was shaken vigorously for 30 min at room temperature. Compound Ia decomposed completely to DSS and the amine hydrochloride. The DSS regenerated in this procedure was collected on a sintered glass filter, dried in an oven for 24 hr at 60°C , and weighed. The filtrate was transferred to a 100-ml volumetric flask and made up to the mark with water. A 10-ml portion of the solution was analyzed by acid-base titration to determine the amount of the amine released from Ia. The results of the analysis indicated that Ia was a salt of 1 mole of DSS with 2 moles of the amine.

With Other Amines. The same preparative procedure and analysis were applied to homologs of *n*-alkylamines (*n*-butyl-, *n*-amyl-, and *n*-hexyl-

amine). The same results as those mentioned above were obtained. In the case of isopropylamine, however, isolation of the salt was unsuccessful because of its easy decomposition in the course of filtration.

Salts of Compound III and with Amines

With *n*-Propylamine (IIa). A 2.56-g sample (0.01 mole) of DSS and 2.36 g (0.04 mole) of *n*-propylamine in 50 ml of NMP were heated for 3 hr at 60°C, under a current of nitrogen with stirring, and then cooled below -20°C. The yellowish-pink precipitate (IIa) was filtered off and washed with five 100-ml portions of cold NMP. On homogenization of IIa in water, a pale-yellow solid was obtained. Spectroscopic analysis of the compound indicated that it was identical with IIIa mentioned below. The decomposition of IIa was determined as follows:

A 0.3-g sample of IIa was treated with 50 ml of water with vigorous stirring for 1 hr. The yellow precipitate (IIIa) was filtered off and washed with five 10-ml portions of water. The precipitate, collected on a sintered glass filter, was dried in an oven at 50°C for 24 hr and weighed. The combined filtrate was analyzed by acid-base titration to measure the amount of amine released from IIa.

The results of the analysis indicated that IIa was a salt of 1 mole of the amine with 1 mole of IIIa.

With Other Amines. The same preparative procedure and analysis were applied to homologs of *n*-alkylamines (*n*-butyl-, *n*-amyl-, *n*-hexylamine). The same results as those of IIa were obtained.

1,4-Diethoxycarbonyl-2-hydroxy-5-alkylamino-1,4-cyclohexadiene (III) and 1,4-Diethoxycarbonyl-2,5-dialkylamino-1,4-cyclohexadiene (IV)

With *n*-Propylamine (IIIa). A 5.1-g sample (0.02 mole) of DSS and 2.4 g (4 moles) of *n*-propylamine in 80 ml of *N*-methylpyrrolidone were heated under nitrogen for 3 hr at 60°C, with stirring. The reaction mixture was divided into two portions. One portion was poured into cold water and gave a yellow precipitate. Filtration, washing, and recrystallization from methanol gave 2.4 g of IIIa (yield 81%). The other portion, which was stored in the reaction flask, was heated for another 2 hr at 120°C. Isolation of the product from the system was carried out in the same manner as in the case of IIIa, to yield 3.0 g (93%) of IVa.

IIIa: Yellow crystals, mp 82–83°C. Calcd for $C_{15}H_{23}O_5N$: C, 60.59%; H, 7.80%; N, 4.71%. Found: C, 60.64%; H, 7.58%; N, 4.67%. The spectroscopic data are reported in the text.

IVa: Pink crystals, mp 109–110°C. Calcd for $C_{18}H_{30}O_4N_2$: C, 63.88%; H, 8.94%; N, 8.28%. Found: C, 63.97%; H, 8.81%; N, 8.28%. The spectroscopic data are reported in the text.

With Other Alkylamines. Homologs of III and IV were prepared in the same manner as described above under the conditions outlined in Table I.

The physical, analytical, and spectroscopic data can be summarized as follows;

IIIb: Yellow solid, mp 145°C (sublimed). Calcd for $C_{15}H_{23}O_5N$: C, 60.59%; H, 7.80%; N, 4.71%. Found: C, 60.65%; H, 7.72%; N, 4.73%. IR: 5.95 μ (C=O, ester), 6.01 μ (C=O, ester), 6.10 μ (C=C, enol), 6.20 μ (C=C, enamine), 8.20 μ (C—O—C, ester). NMR ($CDCl_3$): δ = 1.24 (*d*, $-\text{CH} \begin{matrix} \swarrow \text{CH}_3 \\ \searrow \text{CH}_3 \end{matrix}$, 6H), 1.31 (*t*, $-\text{COOCH}_2\text{CH}_3$, 6H), 3.09 (*s*, $=\text{C}-\text{CH}_2-\text{C}=\text{C}$, 4H), 3.65 (*m*, $-\text{NH}-\text{CH} \begin{matrix} \swarrow \\ \searrow \end{matrix}$, 1H), 4.03 (*q*, $-\text{COOCH}_2\text{CH}_3$, 2H), 4.20 (*q*, $-\text{COOCH}_2\text{CH}_3$, 2H), 8.89 ($-\text{NH}-\text{CH} \begin{matrix} \swarrow \\ \searrow \end{matrix}$, 1H), 12.11 (*s*, $-\text{OH}$, 1H).

IIIc: Orange-yellow solid, mp 77–78°C. Calcd for $C_{16}H_{25}O_5N$: C, 61.71%; H, 8.09%; N, 4.50%. Found: C, 62.02%; H, 8.09%; N, 4.67%. IR: 5.95 μ (C=O, ester), 6.01 μ (C=O, ester), 6.10 μ (C=C, enol), 6.20 μ (C=C, enamine), 8.20 μ (C—O—C, ester). NMR ($CDCl_3$): δ = 0.95 (*t*, $-(\text{CH}_2)_3-\text{CH}_3$, 3H), 1.25 (*t*, $-\text{COOCH}_2\text{CH}_3$, 3H), 1.33 (*t*, $-\text{COOCH}_2\text{CH}_3$, 3H), 1.50 (*m*, $-\text{CH}_2-(\text{CH}_2)_2-\text{CH}_3$, 4H), 3.19 (*s*, $=\text{C}-\text{CH}_2-\text{C}=\text{C}$, 4H), 3.21 (*q*, $-\text{NH}-\text{CH}_2-\text{CH}_2-$, 2H), 4.10 (*q*, $-\text{COOCH}_2\text{CH}_3$, 2H), 4.24 (*q*, $-\text{COOCH}_2\text{CH}_3$, 2H), 8.92 ($-\text{NH}-\text{CH}_2-$, 1H), 12.11 (*s*, $-\text{OH}$, 1H).

IIIId: Orange-yellow solid, mp 65–66°C. Calcd for $C_{17}H_{27}O_5N$: C, 62.75%; H, 8.36%; N, 4.30%. Found: C, 63.09%; H, 8.15%; N, 4.40%. IR: 5.95 and 6.01 μ (C=O, ester), 6.10 μ (C=C enol), 6.20 μ (C=C, enamine), 8.20 μ (C—O—C, ester).

IIIe: Orange-yellow solid, mp 69–70°C. Calcd for $C_{18}H_{29}O_5N$: C, 63.69%; H, 8.61%; N, 4.13%. Found: C, 63.88%; H, 8.49%; N, 4.27%. IR: 5.95 and 6.01 μ (C=O, ester), 6.10 μ (C=C, enol), 6.20 μ (C=C, enamine), 8.20 μ (C—O—C, ester). NMR ($CDCl_3$): δ = 0.90 (*t*, $-\text{CH}_2-\text{CH}_3$, 3H), 1.25 (*t*, $-\text{COOCH}_2\text{CH}_3$, 3H), 1.33 (*t*, $-\text{COOCH}_2\text{CH}_3$, 3H), 1.50 (*m*, $-(\text{CH}_2)_4-$, 8H), 3.19 (*s*, $=\text{C}-\text{CH}_2-\text{C}=\text{C}$, 4H), 3.21 (*q*, $-\text{NH}-\text{CH}_2-\text{CH}_2-$, 2H), 4.10 (*q*, $\text{COOCH}_2\text{CH}_3$, 2H), 4.24 (*q*, $-\text{COOCH}_2\text{CH}_3$, 2H), 8.92 ($-\text{NH}-\text{CH}_2-$, 1H), 12.11 (*s*, $-\text{OH}$, 1H).

IVb: Pale pink solid, mp 140°C (sublimed). Calcd for $C_{18}H_{30}O_4N_2$: C, 63.88%; H, 8.94%; N, 8.28%. Found: C, 63.94%; H, 8.81%; N, 8.32%. IR: 6.01 μ (C=O, ester), 6.20 μ (C=C enamine), 8.20 μ (C—O—C, ester). NMR ($CDCl_3$): δ = 1.24 (*d*, $-\text{CH} \begin{matrix} \swarrow \text{CH}_3 \\ \searrow \text{CH}_3 \end{matrix}$, 12H), 1.31 (*t*, $-\text{COOCH}_2\text{CH}_3$, 6H), 3.09 (*s*, $=\text{C}-\text{CH}_2-\text{C}=\text{C}$, 4H), 3.65 (*m*, $-\text{NH}-\text{CH} \begin{matrix} \swarrow \\ \searrow \end{matrix}$, 2H), 4.05 (*q*, $-\text{COOCH}_2\text{CH}_3$, 4H), 8.82 ($-\text{NH}-\text{CH} \begin{matrix} \swarrow \\ \searrow \end{matrix}$, 2H).

IVc: Pink solid, mp 97–98°C. Calcd for $C_{20}H_{34}O_4N_2$: C, 65.54%; H, 9.35%; N, 7.64%. Found: C, 65.43%; H, 9.19%; N, 7.65%. IR: 6.01 μ (C=O, ester), 6.20 μ (C=C, enamine), 8.20 μ (C—O—C, ester). NMR ($CDCl_3$): δ = 0.95 (*t*, $-(\text{CH}_2)_2-\text{CH}_3$, 6H), 1.29 (*t*, $-\text{COOCH}_2\text{CH}_3$, 6H), 1.50 (*m*, $-(\text{CH}_2)_2-\text{CH}_3$, 8H), 3.21 (*s*, $=\text{C}-\text{CH}_2-\text{C}=\text{C}$, 4H), 3.23 (*q*, $-\text{NH}-\text{CH}_2-$, 4H), 4.14 (*q*, $-\text{COOCH}_2\text{CH}_3$, 4H), 8.87 ($-\text{NH}-\text{CH}_2-$, 2H).

IVd: Red solid, mp 76–77°C. Calcd for $C_{22}H_{38}O_4N_2$: C, 66.97%; H, 9.71%; N, 7.10%. Found: C, 67.07%; H, 9.43%; N, 7.20%. IR: 6.01 μ (C=O, ester), 6.20 μ (C=C, enamine), 8.20 μ (C—O—C, ester).

IVe: Reddish-pink solid, mp 84–85°C. Calcd for $C_{24}H_{42}O_4N_2$: C, 68.21%; H, 10.02%; N, 6.63%. Found: C, 68.08%; H, 10.09%; N, 6.70%. IR: 6.01 μ (C=O, ester), 6.20 μ (C=C, enamine), 8.2 μ (C—O—C, ester). NMR ($CDCl_3$): δ = 0.90 (*t*, $-(\text{CH}_2)_6-\text{CH}_3$, 6H), 1.29 (*t*, $-\text{COOCH}_2\text{CH}_3$, 6H), 1.70–1.30 (*m*, $-(\text{CH}_2)_4-\text{CH}_3$, 16H), 3.21 (*s*, $=\text{C}-\text{CH}_2-\text{C}=\text{C}$, 4H), 3.23 (*q*, $-\text{NH}-\text{CH}_2-\text{CH}_2-$, 4H), 4.14 (*q*, $-\text{COOCH}_2\text{CH}_3$, 4H), 8.87 (*t*, $\text{H}-\text{N}-\text{CH}_2-$, 2H).

Polymer of DSS and Hexamethylenediamine (Va)

In a specially designed flask which could be assembled with a Brookfield viscometer, DSS (88.534 g), hexamethylenediamine (40.143 g), and NMP

(270 ml) were placed. The flask was then connected to the viscometer and the system was heated at 120°C in an oil bath, with stirring under nitrogen. The viscosity of the system was measured every 30 min. The reaction was continued for 8 hr. After cooling to 40°C, the reaction mixture was poured into cold water (1.0 liter) with vigorous stirring. The solids were filtered off, washed twice with water (200 ml), crushed in a ball mill, and dried in a vacuum desiccator; 115 g of fine, yellow powder was obtained. The average molecular weight determined by membrane osmometry was 42,100.

Calcd for $(C_{18}H_{28}O_4N_2)_n$: C, 64.26%; H, 8.93%; N, 8.33%. Found: C, 63.58%; H, 8.35%; N, 8.04%. The spectroscopic data are reported in the text.

Polymer of DSS and Octamethylenediamine (Vb)

Similarly to the case of Va, DSS (17.425 g) and octamethylenediamine (9.850 g) were polymerized in NMP (70 ml) to yield 24 g of yellowish-orange powder. The average molecular weight determined by membrane osmometry was 19,700.

Calcd for $(C_{22}H_{36}N_2O_4)_n$: C, 67.31%; H, 9.24%; N, 7.14%. Found: C, 64.98%; H, 8.98%; N, 7.05%. IR (KBr disk): 6.01 μ (C=O ester), 6.20 μ (C=C, enamine), 8.20 μ (C—O—C, ester). NMR (CDCl₃): δ = 1.29(t, —COOCH₂CH₃, 6H), 3.21 (s, =C—CH₂—C=, 4H), 3.23 (q, —NH—CH₂—CH₂—, 4H), 4.14 (q, —COOCH₂CH₃, 4H), 8.87 (t, —NH—CH₂—, 2H).

Polymer of DSS and ATU (Vc)

Similarly to the case of Va, DSS (57.336 g) and ATU (61.379 g) were polymerized in NMP (250 ml) for 6 hr at 120°C to yield 98 g of orange powder.

Calcd for $(C_{25}H_{33}O_8H_2)_n$: C, 60.71%; H, 7.74%; N, 5.66%. Found: C, 60.11%; H, 7.16%; N, 5.35%. IR: 6.01 μ (C=O, ester), 6.20 μ (C=C, enamine).

Polymer of DSS and Other Diamines

The same procedure was applied to ethylenediamine, tetramethylenediamine, and menthenediamine. However, the polymerization could not be followed by the viscometric method, owing to the poor solubility of these polymers. The polymers showed key absorption identical with those of Va in IR spectroscopic analysis.

We are indebted to Prof. Y. Izumi and N. Masuda of the Institute of Protein Research, Osaka University, to Messrs T. Uno and H. Toyama of Japan Electron Optics Lab. Co., for their cooperation in the NMR analyses, and to Mr. O. Shoji of our laboratory for measuring the physical constants of the samples.

References

1. W. S. Struve and N. J. Chathan, U. S. Pat. 2,821,541 (1958).
2. S. S. Labana and L. L. Labana, *Chem. Rev.*, **67**, 1 (1967).
3. S. Kimura, *Makromol. Chem.*, **117**, 203 (1968).
4. H. Liebelmann, *Ann. Chem.*, **404**, 291 (1914).
5. H. Kauffmann, *Chem. Ber.*, **48**, 1268 (1915).
6. B. Witkop, *J. Amer. Chem. Soc.*, **78**, 2873 (1956).
7. G. O. Dudek and R. H. Holm, *J. Amer. Chem. Soc.*, **83**, 2099 (1961).

Received May 22, 1969

Revised Feb. 27, 1970

Polymerization of Unsaturated Episulfides

F. LAUTENSCHLAEGER and H. SCHNECKO,* *Dunlop Research Centre, Sheridan Park, Ontario, Canada*

Synopsis

The polymerization of four unsaturated episulfides, vinylthiirane, endo-2,3-thioepoxy-norbornene, cyclooctadiene-1,5-monoepisulfide and allyloxymethylthiirane can be affected by various ionic catalysts, BuLi, ZnEt₂·H₂O, BF₃·Et₂O, etc. In case of conjugated functional groups, some catalysts afford isomeric structures resulting from participation of both the olefinic and the episulfide group; the latter can also be opened separately, but even for radical initiation of vinylthiirane no 1,2-structure of a pure vinyl polymer was obtained. A rearrangement of 1,3- to 1,5-polymer has been observed in some cases by post treatment.

INTRODUCTION

It is well known that diolefinic hydrocarbons may undergo more than one mode of polymerization leading to different structures of the repeating unit in the polymer. In case of radical polymerization of butadiene, structure variation can only be achieved by temperature variation and is limited by the relatively narrow range (< 150°C) of polymerization temperatures.¹ With ionic catalysts, the range of molecular structures for conjugated dienes is widened and can be predetermined by suitable choice of catalyst, complexing agents, solvents, etc.² Similarly, nonconjugated cyclic or bicyclic olefins can polymerize in various ways which involve more than one double bond. Generally, the resulting polymer structures correspond to addition products to these monomers. For example, in case of bicyclo-[2.2.1]hepta-2,5-diene (norbornadiene), transannular polymerizations were reported for radical³⁻⁵ and ionic initiators.⁶ Nortricyclene repeating units were first observed in the free-radical polymerization of 2-carbethoxybicyclo-[2.2.1]-2,5-heptadiene.⁷ Similarly, for 1,5-cyclooctadiene, two transannular structures of the polymer bicyclo[4.2.0]- and bicyclo[3.3.0]octane units can be visualized, of which only the former has been confirmed⁸ for Ziegler catalysts. Modified, soluble catalysts based on tungsten afford ring-opening polymerization leading to 1,4-polybutadienes.^{9,10} If an olefinic site is formally replaced by a three-membered cyclic structure (I), reactivity



* Present address: Dunlop Forschungslaboratorium, 645 Hanau, Germany.

differences between the two functional groups can be expected. Basically, three modes of addition may be anticipated in case of butadiene derivatives (Fig. 1). In case of vinylcyclopropane, II, the somewhat unexpected formation of crystalline 1,2-polymer with Ziegler-Natta-type catalyst has been reported.^{11,12} Later, this monomer and its alkyl and halogen derivatives were found to give both 1,2-repeating units by cationic initiation and 1,5-repeating units by radical initiation.^{13,14}

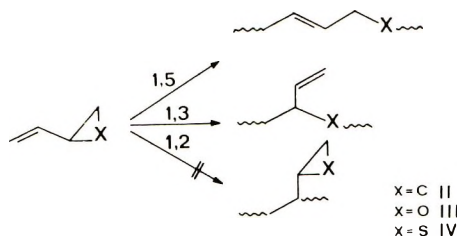


Fig. 1. Modes of opening of unsaturated three-membered ring compounds.

Recently, similar results have been reported for a homolog containing two cyclopropyl groups, 1,1-dicyclopropyl ethylene.¹⁵ However, in the oxygen-containing homolog, III, pure 1,3-polymer has been observed with chelated Al-organic compounds¹⁶ and with $\text{ZnEt}_2 \cdot \text{H}_2\text{O}$ at 30°C , although a small amount of 1,5-polymer (Fig. 1) is observed if the polymerization is carried out at 80°C .¹⁷ The different reactivity between the heterocyclic three-membered ring and the cyclopropyl structure with the vinyl group, which is the prime target for insertion into the polymer chain,¹⁸ is significant. In this paper, results obtained in the polymerization of some difunctional monomers containing sulfur as heteroatom in the three-membered ring (I, $\text{X} = \text{S}$) are reported.

RESULTS

Vinylthiirane

Results of polymerizations of this monomer are compiled in Table I. At temperatures between -20 and $+130^\circ\text{C}$, solid polymers of moderate molecular weight, as evidenced by their intrinsic viscosities, and of varying ratio of 1,3- to 1,5-structure are obtained. The latter consist entirely of *trans*-units as judged from their NMR and infrared spectra. Both cationic and anionic catalysts produce the 1,3-polymer, but higher temperatures give lower proportions of this structure (Fig. 2). A linear decrease of 1,3-polymer with temperature is observed.

It is of interest that in the boron trifluoride etherate-catalyzed polymerization the reaction temperature has a more pronounced influence than the polarity of the solvent. Remarkable is also the low content of 1,5-polymer using tropilium hexachloroantimonate as initiator or if the polymerization is carried out in liquid sulfur dioxide with no added catalyst.

TABLE I
 Polymerization of Vinylthiirane (IV)

Catalyst	Catalyst conc, mole-%	Solvent	Temp, °C	Time, hr	Yield of polymer, % ^a	Conversion, % ^b	Proportion of isomeric structures ^c
ZnEt ₂ ·H ₂ O	5	toluene	-20	24	100 (0.95)	100	100:0
ZnEt ₂ ·H ₂ O	5	benzene	40	2	100 (0.73)	100	100:0
ZnEt ₂ ·H ₂ O	5	toluene	120	0.1	100 (0.60)	100	95:5
BF ₃ ·Et ₂ O·H ₂ O	5	ethyl ether	-20	48	88	90	92:8 ^d 85:15 ^e
BF ₃ ·Et ₂ O·H ₂ O	5	ethyl ether	30	102	95	95	85:15
BF ₃ ·Et ₂ O·H ₂ O	5	CH ₂ Cl ₂	30	0.5	95 (0.14)	98	95:5
BF ₃ ·Et ₂ O·H ₂ O	5	benzene	80	6	95	100	84:16
BF ₃ ·Et ₂ O·H ₂ O	5	xylylene	130	0.2	95 (0.11)	100	70:30
TiCl ₄	2	benzene	40	6	60	90	70:30
70% HClO ₄ /H ₂ O	0.5	benzene	40	4	100 (0.13)	100	60:40
C ₂ H ₇ ⁺ SbCl ₆ ⁻	2	CH ₂ Cl ₂	30	12	94	96	98:2
—	—	SO ₂	-20	240	95 (0.16)	100	90:10
Dabco ^g	0.5	benzene	80	120	(49) ^f	98	5:95
Dabco ^g	2	benzene	60	24	19	42	30:70
Dabco·2H ₂ O	1	benzene	80	120	74	100	35:65
Dabco·5H ₂ O	2	benzene	60	24	80	84	60:40
BuLi	2	benzene	80	120	(48) ^f (0.09)	98	20:80
NaOH/CH ₃ OH	1	CH ₃ OH	68	40	78	97	90:10
AIBN	2	benzene	80	12	(62) ^f	95	37:63

^a Crude reaction product after evaporation of volatiles. Inherent viscosities [η] shown in parentheses.

^b Determined by gas-chromatographic analysis, based on the amount of vinylthiirane remaining.

^c Proportion of 1,3- versus 1,5-repeating units.

^d Ether-soluble fraction.

^e Ether-insoluble fraction.

^f Containing sulfur as impurity.

^g Triethylenediamine.

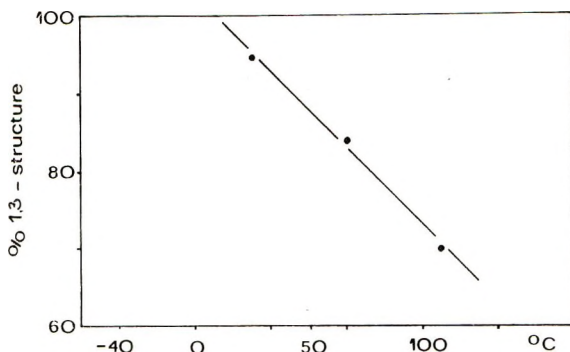
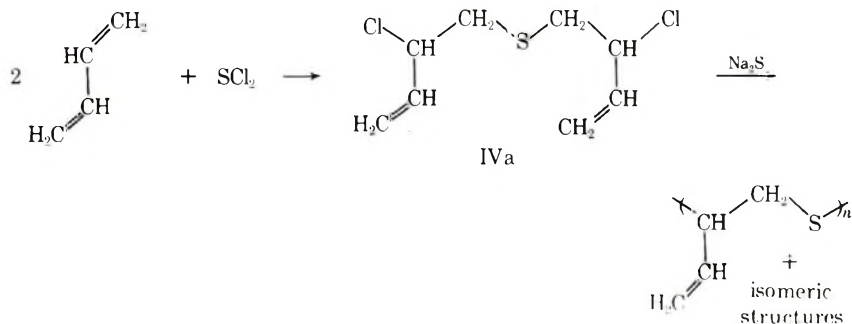


Fig. 2. Temperature dependence of 1,3- vs. 1,5-content in the polymerization of vinylthiirane, initiated by $\text{BF}_3 \cdot \text{Et}_2\text{O}$.

A less efficient catalyst is the tertiary amine triethylenediamine (Dabco); here, the 1,5-polymer is formed almost exclusively in relatively low yield at higher temperature. On shorter reaction times at lower temperatures, a higher amount of 1,3-structure can be detected, the proportion of which increases somewhat if water is present in the reaction medium. There occurs considerable desulfuration, as indicated by the formation of (a) free S_8 in the polymer, and (b) the detection of butadiene by gas-chromatographic analysis of the crude polymer solution.

Traces of dihydrothiophene are also observed. In the case of the polymerization of II, cyclization to cyclopentene is a competing reaction.^{19,20} Applying azo-bis-isobutyronitrile (AIBN) as initiator, polymerization proceeds again with elimination of sulfur and a high proportion of 1,5-polymer is obtained. This polymerization provides the only example where the formation of *cis*-unsaturation was observed, as evidenced by an intense infrared absorption band at 678 cm^{-1} , in addition to the unsaturation bands at 986 and 920 cm^{-1} for vinylic and 960 cm^{-1} for *trans*-unsaturation (Fig. 3). Insufficient separation of $\text{CH}_2=\text{CH}-$ as well as $-\text{CH}=\text{CH}-$ (*cis*-) and $-\text{CH}=\text{CH}-$ (*trans*-) protons in the NMR spectrum prevented a quantitative determination of the proportion of *cis*- and *trans*-unsaturation.

A product of composition identical with that of polymer IV was thought to be available by the treatment of a sulfur dichloride addition product of butadiene-1,3, IVa, with sodium sulfide. Although the structure IVa, re-



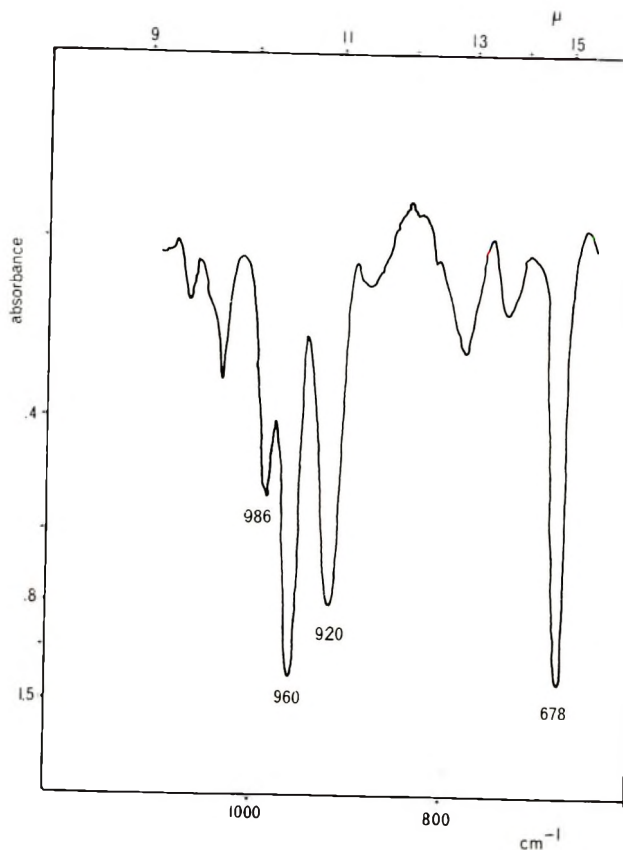


Fig. 3. IR spectrum of polyvinylthiirane, initiated by AIBN.

resulting from an exclusive 1,2-addition, was confirmed,²¹ the polymer resulting on treatment with sodium sulfide shows an infrared absorption nearly identical with that obtained from the monomer IV with AIBN as initiator, particularly with respect to its presence of *cis*-unsaturation.

Endo-2,3-thioepoxynorborn-5-ene, Norbornadiene Episulfide (V)

Results of the polymerization of this novel bicyclic episulfide V are shown in Table II. Isomeric structures result from competing transannular reactions, as evidenced from the NMR and infrared spectra of the resulting polymers.

The presence of olefinic and nortricyclene absorption frequencies suggests the formation of both structural units VII and VIII in varying proportion, although further structural rearrangements cannot be excluded. In the infrared spectrum, intense peaks at 815 and 803 cm^{-1} are attributed to the three-membered ring of structure VIII.⁶ This is further supported by an intense signal in the NMR spectrum at 1.34 ppm (CDCl_3 ; half-width 10 cps) which increases as the signal for the olefinic protons at 6.2 ppm de-

TABLE II
 Polymerization of Bicyclo[2.2.1]heptadiene Monoepisulfide (V)

Catalyst	Solvent	Temp, °C	Time, hr	Conversion, %	Proportion of isomeric structures ^a
ZnEt ₂ ·H ₂ O	toluene	108	21	5	86:14
ZnEt ₂ ·H ₂ O	toluene	-20	168	—	—
ZnCO ₃	ether	+30	168	—	—
BF ₃ ·Et ₂ O·H ₂ O	ether	+30	64	20	66:34
BF ₃ ·Et ₂ O·H ₂ O	xylene	+120	64	40 ^b	23:77

^a 1,3-Structure versus rearranged structure.

^b 33% of additional crosslinked material was obtained.

creases. The latter is assumed to arise from the three-membered ring of the nortricyclene structure. The downfield shift to 1.34 ppm from the position of these protons in the NMR spectrum of polynortricyclene at 0.9 ppm is presumed to be due to the deshielding of these protons by the two sulfur atoms in β -position. The presence of remaining unsaturation is evident from infrared absorptions at 630 and 712 cm^{-1} , the latter indicating the strained *cis*-double bond. It is of interest that these absorption peaks correspond to similar absorptions in the spectrum of S₂Cl₂-addition product to bicycloheptadiene, which exhibits strong infrared absorptions at 820 and 790 cm^{-1} and intense NMR signals at 1.5 ppm (CS₂) for the nortricyclene structure, in combination with a reduced intensity for the NMR signal attributed to unsaturation.²²

Polymerization of V with boron trifluoride at 120°C leads to 33% of a crosslinked material which is insoluble in organic solvents. The infrared spectrum of this material shows no characteristic features. This cross-linking could proceed via the olefinic site of VII or could result from the opening of the strained bicycloheptane ring in analogy to the polymerization of norbornene by noble metal catalysts.²³ The soluble polymeric fraction shows a proportion of 23:77 in favor of the rearranged structure unit.

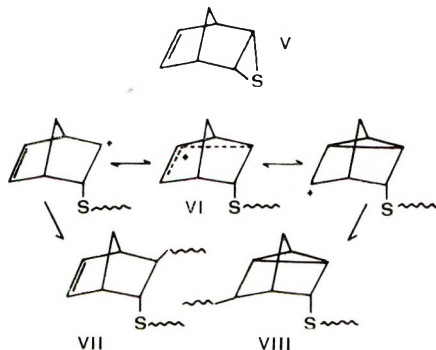


Fig. 4. Bicyclo[2.2.1]heptadiene monoepisulfide.

Polymerization with $\text{ZnEt}_2 \cdot \text{H}_2\text{O}$ leads only to extremely small conversion (Table II) and zinc carbonate fails to polymerize V at all.

Cyclooctadiene-1,5-monoepisulfide (IX)

Polymerization of the unsaturated episulfide IX occurs with greater ease than that of V as evidenced by a comparison of the yields shown in Table III versus those from the polymerization of V shown in Table II. With boron trifluoride etherate in diethyl ether or *p*-xylene, a large extent of isomerized polymer is formed (cf. Fig. 5). For structural assignments, a

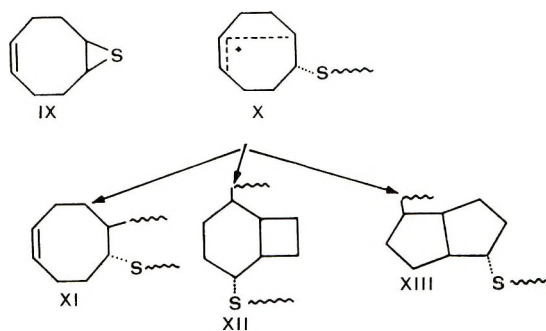


Fig. 5. Cyclooctadiene-1,5-monoepisulfide.

wide signal in the NMR spectrum from 2.9 to 1.4 ppm is attributed to the aliphatic protons, with a signal at 2.76 ppm presumably due to the bridge-head protons of bicyclic structures, XII or XIII. Polymer extraction with pentane leaves 80% of an insoluble product, the NMR spectrum of which (CDCl_3) shows 35% unsaturation as presumed to arise from structure XI.

The temperature effect with respect to the reduction of the 1,3-structure at higher polymerization temperature is quite obvious. In agreement with the polymerization of other olefinic episulfides is the formation of higher 1,3-proportions if $\text{ZnEt}_2 \cdot \text{H}_2\text{O}$ is used as initiator instead of BF_3 etherate.

TABLE III
Polymerization of Cyclooctadiene Monoepisulfide (IX)

Catalyst	Solvent	Temp, °C	Time, hr	Conversion, %	Proportion of isomeric structures ^a
$\text{ZnEt}_2 \cdot \text{H}_2\text{O}$	toluene	30	24	40 ^b	88:12
$\text{BF}_3 \cdot \text{Et}_2\text{O} \cdot \text{H}_2\text{O}$	ether	30	64	75	65:35
$\text{BF}_3 \cdot \text{Et}_2\text{O} \cdot \text{H}_2\text{O}$	xylene	110	1	90	46:54 ^c 35:65 ^d

^a 1,3-Structure versus rearranged structure.

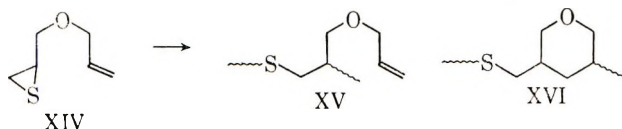
^b Methanol-insoluble products.

^c Soluble in pentane/xylene 1:5 by volume.

^d Insoluble in pentane/xylene.

Allyloxymethylthiirane (XIV)

This monomer forms exclusively the 1,3-polymer XV with boron trifluoride etherate as catalyst. Even if the polymerization is carried out at 160°C in *o*-dichlorobenzene, no evidence for isomeric structures is observed. This is demonstrated by the NMR spectrum of the product, which shows three olefinic protons and the absence of protons nonadjacent to either O or



S which would be expected from a cyclic structure such as XVI or its five- or seven-membered cyclic isomers.

Rearrangement of Polymers

Table IV shows a structural change which occurs with the isolated polymers on subsequent heating with boron trifluoride etherate. A reduction in 1,3-structure in favor of isomeric units is evident.

In case of polyvinylthiirane, this can be verified if $\text{BF}_3 \cdot \text{Et}_2\text{O}$ is added to a 100% 1,3-polymer prepared using $\text{ZnEt}_2 \cdot \text{H}_2\text{O}$ as initiator. Dabco, which also produces a high 1,5-polymer (Table I) is not effective. The rearrangement is drastic in case of the polymer obtained from IX; this polymer had been prepared with $\text{BF}_3 \cdot \text{Et}_2\text{O}$ first and no additional catalyst is required for subsequent rearrangement, which is probably caused by initiator residues. After heating, major spectroscopic changes in the polymer are observed, consisting of a virtual disappearance of infrared bands arising from olefinic unsaturation supported by the detection of only 10% of unsaturation in the NMR spectrum. Secondary rearrangement can also be demonstrated by exposing polymers of V to temperatures above that of their initial preparation, which leads to a decrease of the olefinic content.

The structural changes are accompanied by a decrease in molecular weight, as seen from the inherent viscosity data.

DISCUSSION

It has to be noted that no 1,2-polymer (Fig. 1) is formed; with respect to IV, this is most difficult to rationalize in case of radical initiation since it is well known that episulfides are not amenable to radical opening. The presence of the conjugated vinyl bond in IV must be of paramount importance and in some way permit even the limited formation of 1,3-polymer. The four formal modes of ionic attack on vinylthiirane are summarized in Table V. The last column shows that for both anionic and cationic initiators both 1,3- and 1,5-polymers are possible. This is experimentally confirmed by the results of Table I and is schematically pictured in Figure 6. The abscissa in ionicities^{24,25} is by no means assigned in absolute units and should only be considered approximate. At any rate, on the anionic side, the vari-

TABLE IV
 Partial Conversion of 1,3-Polymers to Rearranged Polymers

Polymer of	Proportion of isomers before	after	Catalyst	Temp, °C ^a	Solvent	η_{sp}/c C-Change
IV	100:0	85:15	BF ₃ ·Et ₂ O	120	xylene	0.73 → 0.20
IV	100:0	100:0	Dabco	80	benzene	0.73 → 0.24
IV	100:0	100:0	— ^b	80	benzene	0.73 → 0.24
V	90:10	70:30	BF ₃ ·Et ₂ O	80	benzene	0.16 → 0.11
IX	65:35	10:90	— ^b	120	xylene	0.30 → 0.12

^a After heating in solution for 72 hr.

^b No additional catalyst added to original polymer.

TABLE V
Vinylthiirane

Nr.	Catalyst	Group attacked	Reaction Scheme	Intermediate	Polymer structure
1	anionic	vinyl			1,5-
2	anionic	thiirane			1,3-
3	cationic	vinyl			(1,2-)
4a	cationic	thiirane			1,3-
4b	cationic	thiirane			1,3- or 1,5-

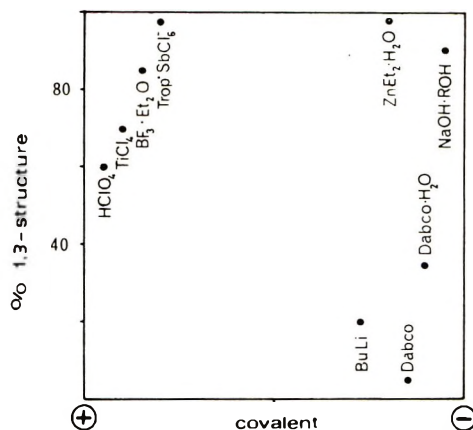


Fig. 6. The 1,3- and 1,5-content of polyvinylthiirane as a function of ionicity of initiators used. Conditions, *cf.*, Table I.

ation in structural extremes is much larger, typical systems like BuLi giving high 1,5-polymer portions whereas systems containing OH⁻ are high in 1,3-content. However, it must be realized that despite high conversion of monomer only low yields of polymers are achieved with these anionic catalysts. This must at least be partially due to the degradation of the polymer by butyl lithium.^{25a} Cationic initiation does in no case give more than 40% 1,5-polymer.

In case of anionic initiation, 1,5-polymer can only be formed via attack on the vinylic double bond; the stability of the intermediate carbanion must be very low to permit rearrangement with participation of the heterocyclic ring similar to radical polymerization. This argumentation is reverse to that used to rationalize products in the polymerization of vinylcyclopropane.¹¹⁻¹⁴ On the other hand, the formation of 1,3-polymer can only be explained on the basis of a primary attack by the initiating nucleophile on the thiirane ring.

The identity of the polymers obtained from the sulfur dichloride addition product IVa and the monomer IV via AIBN initiation with respect to the formation of *cis*-unsaturation and their proportion of *trans*- and vinylic unsaturation is an unexpected result. It may be rationalized that a common feature in both reactions is the involvement of either radical or ionic species. The high proportion of 1,5-polymer with radical initiation was shown in the polymerization of vinylcyclopropane derivatives.^{13,14} The formation of butadiene and 2,5-dihydrothiophene in reactions of IVa has been rationalized before.²⁶

Cationic initiation must also favor the thiirane ring opening; 1,2-structures would be expected if attack occurred at the vinyl group. Depending on whether the primary or the secondary C—S— bond is opened, 1,3- and 1,5-polymer can be expected. (For a discussion of the factors which affect the ring opening of thiirane ring openings, see Schwartz.²⁷) In the latter

case, a π -allylic transition state would be involved which would have two modes of stabilization.

There is some argument as to what affects the mechanism of the initiation by $\text{ZnEt}_2 \cdot \text{H}_2\text{O}$. Generally, coordinated anionic growth is assumed at a proportion of $\text{H}_2\text{O}:\text{ZnEt}_2 = 1:1$ for epoxide polymerizations,^{28, 29} but for tetrahydrofuran, styrene, and oxa-bis-chloromethylcyclobutane, the polymerization rate passes through a maximum at $\text{H}_2\text{O}:\text{ZnEt}_2 < 1$ in a cationic mechanism.³⁰

Our experiment at a ratio of 1:1 does not permit a decision on the mechanism; the exclusive formation of 1,3-polymer might also be possible on the cationic side of Figure 6. There is only a small change as a result of a temperature difference (Table I). It should be reemphasized that the foregoing argument has a formal character; the conclusions on structural attack may be overruled by coordination effects.

In case of the polymer of V, the facile formation of isomeric polymeric products will proceed via the transition state VI; the formation of transannular structures, as, e.g., VIII, is not only known from the polymerization of the parent diene,³⁻⁷ but, in addition, the ultraviolet spectrum of V indicates a degree of conjugation between double bond and thiirane ring by a small bathochromic shift of the absorption maximum to 265 cm^{-1} ($\epsilon = 40$) from the average position of the absorption maximum near 260 cm^{-1} .²⁶ Thirdly, oxidation of V with H_2O or KIO_4 leads to a sulfoxide resulting from transannular rearrangement, demonstrating the facility of transannular reactions on this ring system.²⁶

The polymerization of IX could proceed via 1,3-ring opening to yield polymer of the repeating structure XI, in which case the polymeric chain is assumed to show a *trans*-configuration as a result of *trans*-opening of the intermediate episulfonium ion. Molecular models demonstrate steric interactions in this ring system due to the close proximity of the *endo*-sulfur atom and the olefinic double bond as well as steric interaction between the opposing methylene groups. These factors would provide thermodynamic instability for this ring system. Rearranged structural units could be formed *via* delocalization of the carbonium ion across the ring system as shown in X to give product XII or XIII. Molecular models demonstrate a minimum of intramolecular interactions in XIII, where both chains attached through the sulfur atom are in a quasi-equatorial position. On the other hand, the polymers show a weak signal in its NMR spectrum at 0.83 ppm (CDCl_3), which could arise from a contribution of structure XII.

The fact that XIV was not observed to form isomeric structures could be explained by the absence of allylic or homoallylic intermediate structures. However, monomers of this type could be capable of cyclopolymerization with ionic catalyst systems.³¹

The postulated rearrangement of the above-discussed polymers has an analogy in monomeric 1,2-addition products of butadiene, where isomerization to 1,4-structures are known to proceed at elevated temperature and 1,4-structures are known to make an increased contribution at higher temper-

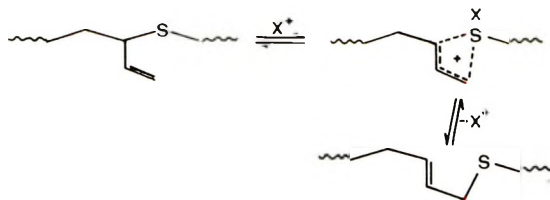


Fig. 7. Rearrangement of 1,3- to 1,5-polyvinylthiirane.

atures, reflecting the fact that 1,4-products are thermodynamically more stable. In case of polymers, however, no such rearrangement has been reported, the only well-known change being *cis-trans* isomerizations of 1,4-polydienes.³²

Rearrangement of polymer chains was also observed in the formation of *o*-hydroxybenzophenone groups from polycarbonates after irradiation,^{33,34} in the formation of amide groups by treatment of polymeric ketones with ammonia or hydroxylamine under the conditions of Schmidt or Beckmann rearrangements,³⁵ during the decarboxylation of polyesters,³⁶ and in the nitrosation of polyamides.³⁷

For the polymers of IV, the change of 1,3- to 1,5-polymer, although resulting in profound alterations of chain dimensions, would be an allylic rearrangement, which would not necessarily require the assumption of an intermediate free carbonium ion; instead, it can satisfactorily be explained by the formation of an ion pair in a concerted reaction (Fig. 7). Rearrangement is only possible if it involves scission of the secondary C—S bond; in a head-to-tail 1,3-polymer of IV, the rearrangement is not conceivable via the primary carbon-sulfur bond. Proximity effects may permit a concerted mechanism for rearrangement of the polymers VII and XI.

It is of interest that extensive heat treatment of the polymers leads to a considerable decrease in $[\eta]$ -values with or without added catalyst (Table IV). However, the formation of rearranged structures is only observed when boron trifluoride etherate was either initially used or is added to the polymer. Rearrangement could, therefore, not be achieved without chain scission. This detracts somewhat from the above mechanism as the only possibility; endgroup effects or unzipping followed by repolymerization to isomerized structures might be alternative possibilities.

EXPERIMENTAL

Materials

The episulfides V (mp 47°C) and IX (bp 44°C, 0.3 mm Hg) were prepared as described in references²⁶ and²². Vinylthiirane, IV (bp 45°C, 9 mm Hg; $n_D^{20} = 1.4975$), and allyloxymethylthiirane, XIV (bp 64°C, 15 mm Hg; $n_D^{20} = 1.4932$), were obtained from the corresponding epoxides.^{38,39} The liquid monomers were distilled and the crystalline monomer V was sublimed prior to use.

Boron trifluoride etherate was distilled before use, tropilium hexachloro-antimonate was prepared according to Bawn et al.,⁴⁰ azo-bis-butyronitrile was recrystallized commercial grade. Zinc diethol/water catalyst was prepared by adding an equimolar amount of water to a benzene solution of the metalorganic compound. Portions of this solution were applied in the reaction.

Polymerization

Polymerizations were carried out in a magnetically stirred three-necked round-bottom flask equipped with condenser, internal thermometer, and rubber cap. An atmosphere of nitrogen was provided by flushing the equipment prior to the addition of the reagents and by maintaining the contents under an overpressure of 5 mm Hg. Solvents were dried with anhydrous magnesium sulfate prior to use. The polymerizations were carried out in 10% solutions of the solvents shown in Tables I to III. The catalysts were dissolved in the solvent prior to the addition of the monomers. Monomers were introduced by means of syringes through the rubber caps.

The polymerization was followed by gas-chromatographic analysis of the reaction mixture. Conversions reported in Tables I to III refer to the decrease of the monomer concentration as observed by that analysis. The crude polymer was obtained by evaporating the solution after decanting from undissolved catalyst.

Satisfactory analyses were obtained for the polymers after one precipitation from benzene solution. Free sulfur, which accompanied several polymerizations, was removed from the polymers by refluxing their solution in acetone for several days until elemental analyses were satisfactory. Structural analysis was carried out prior to this treatment.

Determination of the nature of the olefinic unsaturation in the polymers was carried out either on the basis of integration values of the NMR spectra or the intensity of the olefinic unsaturation bands in the infrared spectra.

For the secondary treatments of the polymers as shown in Table IV, the following procedure was applied. The crude polymers were redissolved in the solvent shown and treated as shown in Table IV in the same equipment that was used for the polymerization studies. After the allotted time, the solvent was evaporated and the crude polymer was again analyzed.

Satisfactory elemental analyses were obtained for the novel polymers:

ANAL. Calcd for IV: C, 55.8%; H, 7.0%; S, 37.2%. Found: 1,5-polymer: C, 54.9%; H, 6.95%; S, 36.5%; 1,3-polymer: C, 55.8%; H, 6.9%; S, 37.0%.

ANAL. Calcd for V: C, 67.7%; H, 6.4%; S, 25.8%. Found: C, 67.4%; H, 6.3%; S, 26.0%.

ANAL. Calcd for IX: C, 68.6%; H, 8.6%; S, 22.9%. Found: C, 68.9%; H, 8.9%; S, 22.4%.

ANAL. Calcd for XIV: C, 55.3%; H, 7.7%; S, 24.6%. Found: C, 55.8%; H, 7.9%; S, 24.3%.

Reaction of a Sulfur Dichloride Addition Product of Butadiene-1,3 with Sodium Sulfide. To a solution of 9.4 g (0.12 mole) of sodium sulfide in a

mixture of 30 ml of water and 30 ml of methanol was added 21.1 g (0.1 mole) of IVa. Stirring of the suspension caused an exothermic reaction and the evolution of gas, which was identified to consist of butadiene-1,3 (by infrared spectroscopy) and hydrogen sulfide. After the reaction had subsided, the mixture was steam distilled, and 2,5-dihydrothiophene was identified by gas-chromatographic analysis among the volatile reaction products. The nonvolatile oily residue was stirred with 100 ml of methanol, which caused the separation of 3 g of polymer shown to be essentially identical by infrared analysis with the product obtained by AIBN-initiated polymerization of IV.

Instrumentation

Viscosity measurements were carried out in toluene solutions (1%) at 35°C in a Ubbelohde viscosimeter. NMR spectra were recorded on a Varian A-60 instrument in deuteriochloroform solution, except for polymer of V, which was recorded in hexachlorobutadiene solution at 90°C. Infrared spectra were obtained on a Perkin-Elmer 521 grating instrument. To obtain the spectra, chloroform solutions of the polymer were added to sodium chloride discs and the solvent was evaporated.

The authors are grateful to Mr. D. MacKillop for spectroscopic identification of the polymers of IV and to the National Research Council of Canada for a grant to one of the authors (F.L.).

References

1. C. A. Uraneck, in *Polymer Chemistry of Synthetic Elastomers*, Vol. I, J. P. Kennedy and E. G. M. Törnqvist, Eds., New York, 1968, p. 176.
2. W. Cooper and G. Vaughan, *Progr. Polym. Sci.*, **1**, 93 (1967).
3. R. H. Wiley, W. H. Rivera, T. H. Crawford, and N. F. Bray, *J. Polym. Sci.*, **61**, S38 (1962).
4. N. L. Zutty, *J. Polym. Sci. A1*, **11**, 2231 (1963).
5. J. Pellon, R. L. Kugel, R. Marcus, and R. Rabinowitz, *J. Polym. Sci. A-2*, **2**, 4105 (1964).
6. J. P. Kennedy and J. A. Hinlicky, *Polymer*, **6**, 133 (1965).
7. M. L. Huggins, *J. Amer. Chem. Soc.*, **66**, 1991 (1944).
8. B. Reichel, C. S. Marvel, and R. Z. Greenley, *J. Polym. Sci. A-1*, **1**, 2935 (1963).
9. N. Calderon, E. A. Ofstead, and W. A. Judy, *J. Polym. Sci. A-1*, **5**, 2209 (1967).
10. P. R. Marshall and B. J. Ridgewell, *Eur. Polym. J.*, **5**, 29 (1969).
11. C. G. Overberger, A. E. Borchert, and A. Katchman, *J. Polym. Sci.*, **44**, 491 (1960).
12. H. D. Noether, C. G. Overberger, and G. Halek, *J. Polym. Sci. A-1*, **7**, 201 (1969).
13. T. Takahashi, *J. Polym. Sci. B*, **3**, 251 (1965).
14. T. Takahashi, *J. Polym. Sci. A-1*, **6**, 403 (1968).
15. J. P. Kennedy, J. J. Elliott, and P. E. Butler, *J. Macromol. Sci.*, **A2**, 1415 (1968).
16. E. J. Vandenberg, *J. Polym. Sci.*, **47**, 486 (1960).
17. T. Tsuruta, S. Inoue, and K. Tsubaki, *Makromolek. Chem.*, **111**, 236 (1968).
18. R. A. Patsiga, *Rev. Macromol. Chem.*, **C1**, 223 (1967).
19. M. C. Flowers, and H. M. Frey, *J. Chem. Soc.*, 3547 (1961).

20. C. A. Wellington and D. E. Hoare, *J. Phys. Chem.*, **66**, 1671 (1962).
21. F. Lautenschlaeger, *J. Org. Chem.*, **33**, 2627 (1968).
22. F. Lautenschlaeger and N. V. Schwartz, *J. Org. Chem.*, **34**, 3991 (1969).
23. R. E. Rinehart and H. P. Smith, *J. Polym. Sci. B-3*, 1049 (1965).
24. C. E. H. Bawn and A. Ledwith, *Quart. Rev. (London)*, **16**, 361 (1962).
25. M. Roha, *Adv. Polym. Sci.*, **4**, 353 (1965).
- 25a. E. J. Vandenberg, Fourth Middle Atlantic Region Conference of the American Chemical Society, held Washington, D.C., Feb. 12-15, 1969.
26. F. Lautenschlaeger, *J. Org. Chem.*, **34**, 3998 (1969).
27. N. V. Schwartz, *J. Org. Chem.*, **33**, 2895 (1968).
28. J. Furukawa and T. Saegusa, *Polymerization of Aldehydes and Oxides*, Interscience, New York, 1963, p. 155.
29. M. Ishimori, O. Nakasugi, N. Takeda, and T. Tsuruta, *Makromolek. Chem.*, **115**, 103 (1968).
30. S. Tsuchiya and T. Tsuruta, *Makromolek. Chem.*, **110**, 123 (1967).
31. R. C. Schulz, *Kolloid-Z.*, **216-217**, 309 (1967).
32. M. A. Golub and C. L. Stephens, *J. Polym. Sci. A-1*, **6**, 763 (1968).
33. D. Bellus, P. Hrdlovic, and Z. Manasek, *J. Polym. Sci. B-4*, **1** (1966).
34. D. Bellus, Z. Manasek, P. Hrdlovic, and P. Slama, *J. Polym. Sci. C*, **16**, 267 (1967).
35. R. H. Michel and W. A. Murphey, *J. Polym. Sci.*, **55**, 741 (1961).
36. K. C. Steuben, *J. Polym. Sci.*, **33**, 447 (1958).
37. M. R. Porter, *J. Polym. Sci.*, **33**, 447 (1958).
38. C. C. J. Culvenor, W. Davis, and N. S. Heath, *J. Chem. Soc.*, 278 (1949).
39. N. Brodoway, U. S. Pat. 3,222,324 (1965).
40. C. E. H. Bawn, C. Fitzsimmons, and A. Ledwith, *Proc. Chem. Soc.*, 391 (1964).

Received January 12, 1970

Revised February 27, 1970

Polymerization and Crosslinking of Epoxides: Base-Catalyzed Polymerization of Phenyl Glycidyl Ether

P. BANKS and R. H. PETERS, *Department of Polymer and Fibre Science,
University of Manchester Institute of Science and Technology,
Manchester, England*

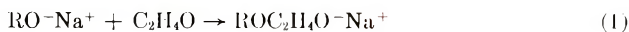
Synopsis

The anionic polymerization of 2,3-epoxypropyl phenyl ether initiated by sodium methoxide and dimethyl sodium in dioxane and in dimethyl sulfoxide has been studied. Kinetic and dielectric constant measurements have been recorded, and a mechanism for the initiation reaction with dimethyl sodium has been put forward. Polymerization initiated with dimethyl sodium revealed almost total absence of sulfur in the polymer by endgroup analysis. The reaction was shown to be inhibited by oxygen. Molecular weight determinations have indicated a reaction involving transfer to give polymers of lower than calculated \bar{M}_n and a ratio of k_p/k_{tr} ratio of approximately 73. Gel-permeation chromatography suggests a narrow molecular weight distribution in the polymers prepared.

INTRODUCTION

The base-catalyzed polymerization of epoxides has been known for a considerable time, the first reports on this subject appearing in the latter part of the last century.^{1,2} More recently however, detailed kinetic studies of the sodium alkoxide-initiated polymerization of ethylene oxide and propylene oxide in alcohol-dioxane mixtures have been reported by Gee³⁻⁵ and co-workers, who have shown that the reaction takes place by the mechanism of eqs. (1) and (2).

Initiation:



Propagation:



In the presence of hydroxylytic solvents, chain transfer can occur by protonation of the growing chain, the new alkoxide ion formed being capable of initiating a new chain [eq. (3)].



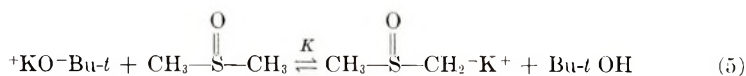
The kinetics of this reaction were shown to be first-order with respect to monomer and to initiation and the rate was found to vary with the dielec-

tric constant of the alcohol employed. In such a system, in the absence of transfer the number-average molecular weight of the polymer formed may be expressed as shown in eq. (4).

$$\bar{M}_n = \frac{[\text{Monomer}]_0 \times \text{Monomer mol. wt.}}{[\text{Alcohol}]_0 + [\text{Initiator}]} + M_{RO^-} \quad (4)$$

where M_{RO^-} is the added weight to account for the end groups. Number-average molecular weights of polyethylene oxides were consistent with this relationship, but this was not the case for poly(propylene oxide), where transfer had taken place during polymerization. In addition, this kind of reaction should yield a product whose molecular weight distribution is narrow: the results of Miller⁶ and Weibull⁷ using anionically polymerized epoxides suggest a Poisson distribution of molecular weights.

The base-catalyzed polymerization of various epoxides and vinyl monomers⁸⁻¹⁰ in dimethyl sulfoxide (DMSO) has achieved considerable interest recently; Bawn¹¹ and co-workers¹²⁻¹⁴ have investigated the polymerization of some epoxides using potassium *tert*-butoxide as the initiator in DMSO. In this system, initiation is considered to occur via the strongly basic sulfinyl carbonion (dimsyl ion) formed from the equilibrium (5):



The reported value for K is very small (1.5×10^{-7}), but the very fast rates of initiation and propagation in DMSO compensate for the low concentration of dimsyl ions present. The high rates are due to the low solvating power of DMSO towards anions and to its relatively high dielectric constant.

If initiation occurs solely by means of the dimsyl anions, elemental analysis should indicate one atom of sulfur for each polymer chain formed. This is apparently the case for poly(ethylene oxide) formed by the above mechanisms.¹² The molecular weights of the polymers should also be in agreement with eq. (4) if no transfer occurs. No transfer reactions have been reported to occur during the polymerization of ethylene oxide, but for propylene oxide abstraction of one of the hydrogen atoms from the methyl group occurs yielding an unsaturated product, the ratio of the reaction constants for the propagation reaction and the transfer reaction (k_p/k_{tr}) has been found to be 20 at room temperature.¹⁵

Because of the interest in DMSO as a solvent of the anionic polymerization of epoxides, the present authors have examined its use for the polymerization of 2,3-epoxypropyl phenyl ether (phenylglycidyl ether or PGE) using anionic initiators. Comparison is made with corresponding reactions with dioxane as a solvent.

EXPERIMENTAL

Materials

Commercial phenyl glycidyl ether was purified by standing over calcium hydride and distilling through a 12-in. column containing glass Lessing rings using a reflux ratio of 15:1. The pure product had a boiling point of 97.5°C/62 mm and a specific gravity of 1.0949 at 22.5°C. Methyl alcohol was purified by reacting over magnesium turnings in the presence of a trace of iodine and then distilling through a column at a 10:1 reflux ratio; the pure product boils at 64.2°C/75.67 cm.

1,4-Dioxane was purified by refluxing 1 liter of the commercial product with 14 ml of concentrated HCl and 100 ml water (for 12 hr) while passing a slow stream of nitrogen through the mixture. The cooled solution was shaken with fresh sodium hydroxide pellets for a further 24 hr and was then refluxed over sodium metal until it remained bright. Finally the dioxane was distilled from sodium and the portion of boiling at 101.5°C/76 cm Hg was collected.

Dimethyl sulfoxide was obtained commercially (BDH) and, in its impure state, had an unpleasant characteristic odor. It was purified by being allowed to stand over anhydrous potassium carbonate followed by distillation under vacuum with the use of a nitrogen bleed, to give a colorless, odorless liquid boiling at 64.0°C/4.0 mm.

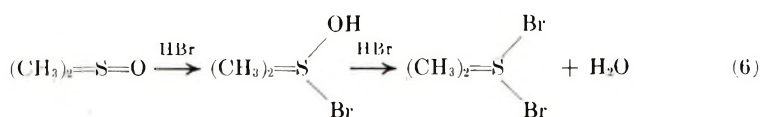
Sodium methoxide was prepared by dissolving sodium metal, cut under liquid paraffin, in pure methanol and was not farther purified. If the preparation is carried out carefully, a clean solution can be obtained having a concentration up to 6-7 N; clouding was generally caused by the formation of sodium hydroxide by exposure to moisture. All cloudy solutions were discarded.

Methyl sulfinyl sodium (dimesyl sodium) was prepared by the method of Corey and Chaykowski,¹⁶ which consists, briefly, of reacting dimethyl sulfoxide with sodium hydride under nitrogen. The product formed reacts rapidly with oxygen, and stringent precautions to avoid contact with air during its preparation and subsequent handling and storage are necessary.

All reagents were stored under nitrogen in glass vessels fitted with a side-arm for the introduction of nitrogen. Dry, oxygen-free nitrogen¹⁷ supply was obtained by passing nitrogen containing <10 ppm oxygen (supplied by British Oxygen Company as "white spot") through two columns, 42 in. long and 1½ in. in diameter, the first of which contained manganous oxide pellets and the other sodium aluminum silicate (Molecular Sieve Type 4A, BDH). The manganous oxide was obtained by the reduction of manganese dioxide pellets, 1/8 × 1/8 in. in size, supplied by Peter Spence Ltd., by passing coal gas through the pellets contained in a glass column at a temperature of ca. 600°C.

Kinetic Measurements

Kinetic runs were carried out by weighing the reagents into a reaction vessel which was fitted with a separate bulb to hold the initiator solution, a nitrogen inlet and a sample withdrawal tube. After stringent degassing at 10^{-3} mm Hg, the reaction vessel was filled with nitrogen and the initiator and monomer solutions were brought to the required reaction temperature prior to mixing. The course of the polymerization was followed by titration of the epoxy group by the Durbetaki¹⁸ method in experiments where dioxane was used as solvent; this method could not be used when DMSO was the solvent, owing to interference from the reaction¹⁹ (6).



The method of analysis therefore used for DMSO was a derivation of the Nicolet and Poulter method.^{20,21} Isolation of the polymer poly(phenyl glycidyl ether) was carried out by first treating the "living" polymer with a small quantity of pyridinium chloride solution in order to protonate the endgroups of the polymer chains. The polymer solution was then slowly added to a rapidly stirred excess of diethyl ether to precipitate the polymer. This was filtered under vacuum and washed thoroughly with more ether and dried in a vacuum oven at 40°C for 2–3 weeks. The number-average molecular weights of the polymers were determined by using a Mechrolab vapor-pressure osmometer with benzene as solvent.

The dielectric constant of reaction mixtures was measured by using a Wayne Kerr B221 capacitance bridge operating at a frequency of 1592 cps and the CD 221 Skydrol capacitance cell. The dielectric constant at various stages of reaction was measured on samples withdrawn from the reaction mixture; these samples were then rejected. These measurements were carried out only on reaction mixtures in which dioxane was the solvent, because the capacitance bridge could not be used to determine accurately dielectric constants of liquids where this value lay above 20. This is due to the fact that these liquids tended to become conductors at the relatively low frequency of the capacitance bridge.

Gel-permeation chromatography (GPC) was carried out by eluting 80 μ l of a 5% solution of poly(phenyl glycidyl ether) in DMSO through a 1 m. \times 1 cm diameter column packed with a Waters' 1000 Å Styrogel cross-linked polystyrene, tetrahydrofuran being used as eluent. The detector was a Unicam SP 500 spectrophotometer operating at 280 m μ and fitted with a 1-mm pathlength flow cell. The results were compared with those obtained by using a sample of monodisperse polystyrene obtained from Pressure Chemical Company (Pittsburgh, Pa.) with a quoted number-average molecular weight of 3690 and $\bar{M}_w/\bar{M}_n = 1.06$.

RESULTS AND DISCUSSION

Effect of Oxygen

It was found that if phenyl glycidyl ether (PGE) is polymerized in dry air with the use of dimethyl sodium as initiator, the reaction mixture quickly becomes colored brown and that the reaction then slows down and eventually stops. An example of this inhibition reaction is shown in

TABLE I

Expt. no.	PGE, eq/l.	CH ₃ ONa, eq/l.	CH ₃ OH, eq/l.	$k_1 \times 10^{-5}$, sec ⁻¹	$k_2 = k_1 / \text{CH}_3\text{ONa} \times 10^{-4}$, l./eq-sec
1	3.021	0.202	0.803	9.22	4.56
2	3.020	0.179	0.803	8.67	4.84
3	3.021	0.144	0.805	7.28	5.05
4	3.031	0.115	0.803	5.44	4.73
5	3.021	0.094	0.804	3.86	4.13
6	3.021	0.072	0.801	3.53	4.92
7	3.042	0.025	0.150	0.815	2.76
8	3.048	0.146	0.579	6.44	4.14
9	3.048	0.146	1.266	7.93	5.43
10	3.918	0.116	0.464	4.62	3.98

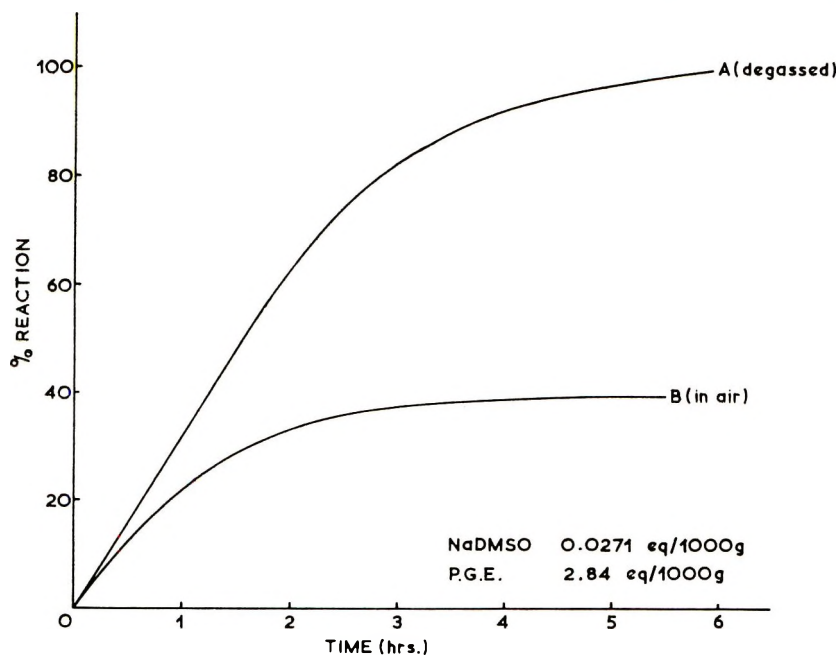
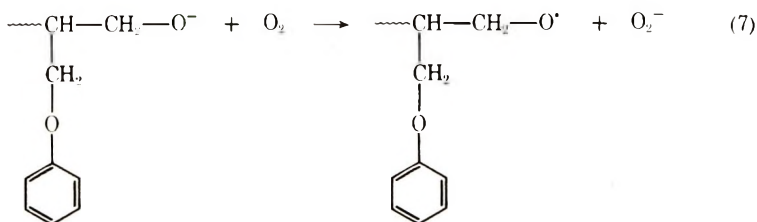


Fig. 1. Effect of oxygen on the polymerization of PGE in DMSO with NaDMSO as initiator: (A) degassed; (B) in air. NaDMSO, 0.0271 meq/g; PGE, 2.84 meq/g.

Figure 1. The precise nature of the inhibition is not fully understood, but could take place by a similar mechanism to that postulated by Szwarc²² when styrene is polymerized with sodium naphthalene [eq. (7)]



However, no oxygen inhibition of this type is observed in the sodium methoxide-initiated polymerization of propylene oxide, and it therefore follows that the reaction is peculiar to aromatic epoxides only; the same effect takes place with resorcinol diglycidyl ether and with the diglycidyl ether of bis-2,2(4-hydroxyphenyl)propane (Bisphenol A diglycidyl ether).

Polymerization with Dioxane as Diluent

The polymerization of PGE in dioxane solution using sodium methoxide (in methanol) as initiator was found to be first order with respect to the

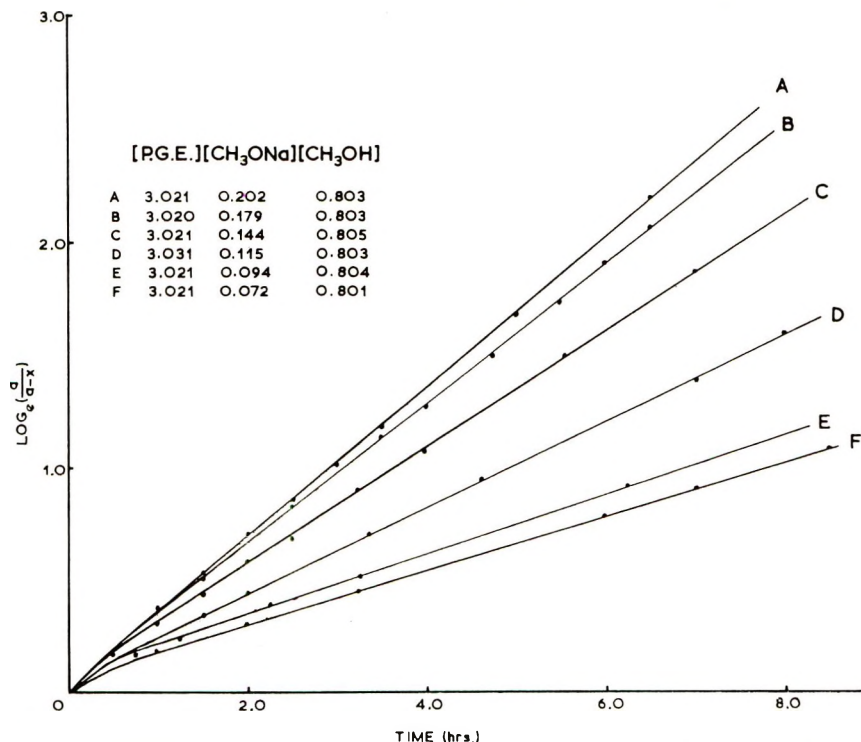


Fig. 2. Influence of CH₃ONa concentration on the rate of polymerization of PGE in dioxane at constant methanol concentration.

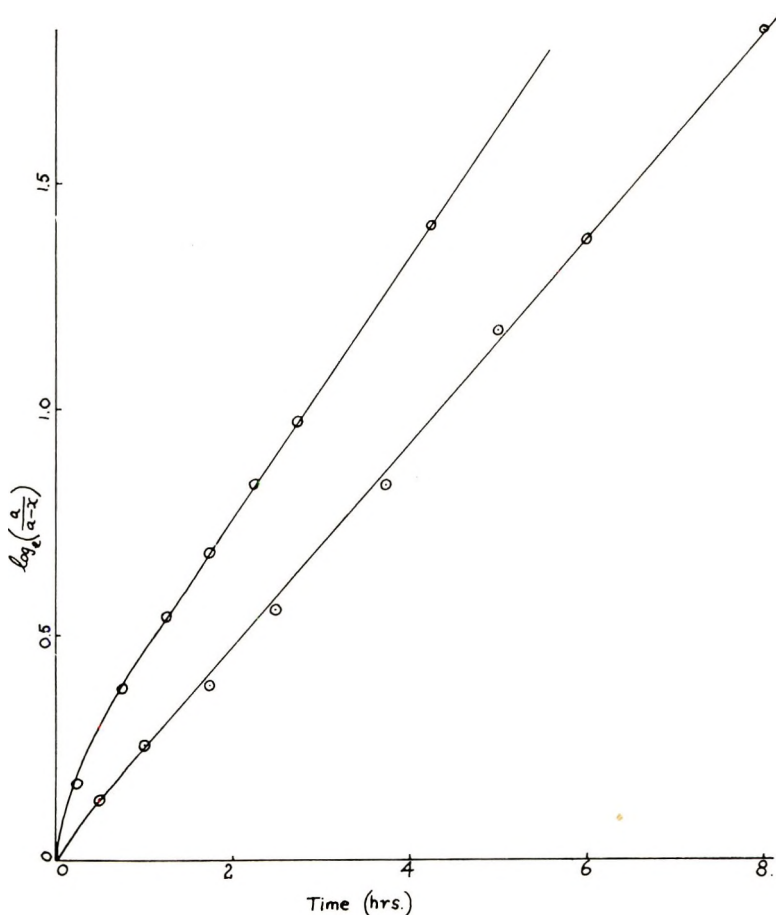


Fig. 3. Influence of methanol concentration on the polymerization of PGE in dioxane: (○) $\text{CH}_3\text{OH} = 0.597$ mole/l.; (○) $\text{CH}_3\text{OH} = 1.266$ mole/l. $[\text{PGE}]$, 3.048 mole/l.; $[\text{CH}_3\text{ONa}]$, 0.146 mole/l.

epoxide. Figure 2 shows a number of first-order rate plots for polymerizations in which the ratio $[\text{PGE}]/[\text{CH}_3\text{ONa}]$ was varied, but where the $[\text{PGE}]/[\text{methanol}]$ ratio was maintained constant; in these plots, a represents the initial epoxide concentration and x that at time t . The variation of the first-order rate constant k_1 with $[\text{initiator}]$ was shown to be constant, indicating that the reaction is also first-order with respect to initiator (see Table I). The reaction mechanisms for the initiation and propagation steps are therefore analogous to those for ethylene and propylene oxide, and the overall rate equation may be represented as

$$-d[\text{PGE}]/dt = k_2[\text{PGE}][\text{CH}_3\text{ONa}] \quad (8)$$

where k_2 is the bimolecular rate constant.

The nonlinear portions during the initial steps of the polymerization shown in Figure 2 are attributed to protonation of the growing anion by

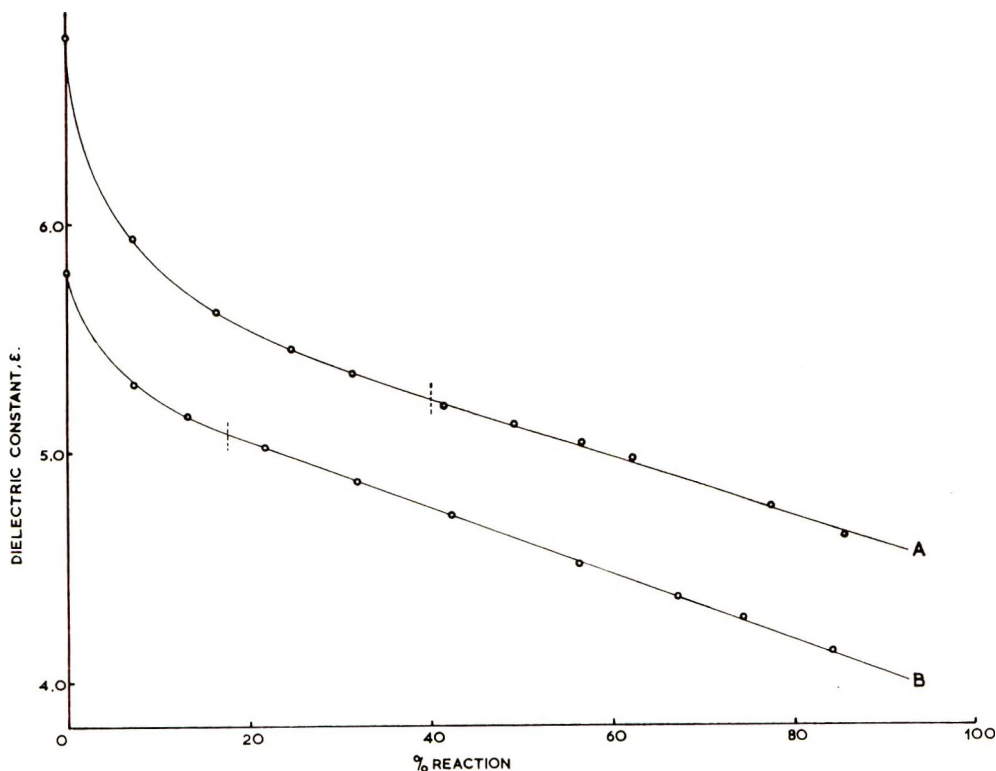
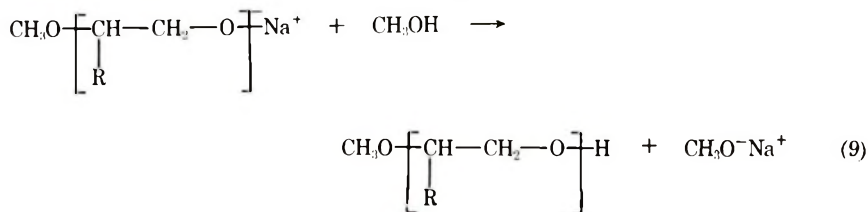


Fig. 4. Influence of methanol concentration on the variation of the dielectric constant with extent of reaction in the polymerization of PGE in dioxane: (A) $[\text{CH}_3\text{OH}] = 1.266$ mole/l.; (B) $[\text{CH}_3\text{OH}] = 0.579$ mole/l. $[\text{PGE}]$, 3.048 mole/l.; $[\text{CH}_3\text{ONa}]$, 0.146 mole/l.

methanol to form "dead" polymer and a new initiator molecule,^{3,4} by the mechanism (9):



where F is $-\text{CH}_2\text{OC}_6\text{H}_5$. This reaction may be expected to cause a change in the dielectric constant of the reaction mixture. Experiments to determine the stage of the polymerization at which this occurs were carried out by following the change in dielectric constant with conversion for reaction mixtures with different methanol concentrations. The results of these experiments are shown in Figures 3 and 4, where the nonlinear portions in the first-order plots and in the dielectric constant-extent of reaction plots occur for about the same extents of reaction for each experi-

ment. The initially high dielectric constant of the reaction mixtures is caused by the presence of methanol (dielectric constant, $\epsilon = 32.6$), only small quantities of which are required to increase significantly the dielectric constant of the PGE reaction mixture ($\epsilon_{\text{dioxane}} = 2.209$, $\epsilon_{\text{PGE}} = 13.4$). The nonlinear portion of the plots for the reaction mixture containing the higher methanol portion corresponds to about the first 40% of reaction, and this in turn corresponds to the initial [methanol]/[PGE] ratio (≈ 0.4); an analogous extent of nonlinearity can be observed from the experiment where a lower [methanol]/[PGE] ratio was used. It therefore follows that protonation by methanol takes place during the early stages of the polymerization and continues until all of the methanol has reacted. There

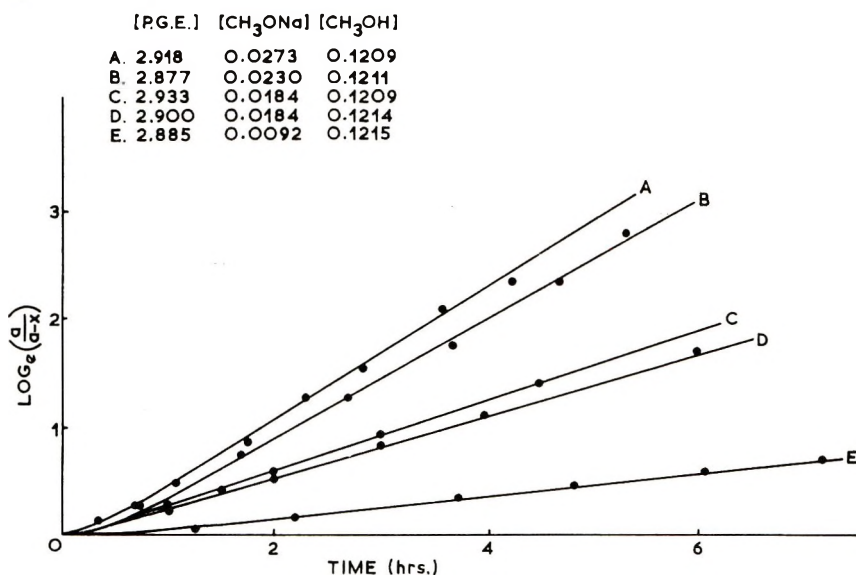


Fig. 5. Variation of rate of polymerization of PGE with CH₃ONa concentration in DMSO in the presence of CH₃OH.

is little difference in the first-order rate constants for these two experiments, although the reaction mixture containing the higher methanol concentration gives a slightly higher rate. This is probably due to higher dissociation of the alkoxide ion pair to form alkoxide ions in the medium of higher dielectric constant; it was shown by Gee^{3,4} that free methoxide ions are more reactive by a factor of about ten than when they are associated with the cation in the form of an ion pair. The molecular weight distribution of the polymers formed can be expected to be narrow, owing to the lack of termination and on the assumption that transfer reactions to monomers do not occur. It will be shown in the following section that transfer resulting in the formation of significantly lower than theoretical molecular weights does in fact occur.

Polymerization with DMSO as Diluent

The use of DMSO as diluent was brought about by the poor solubility of the polymers formed from PGE in dioxane when the theoretical \overline{DP}_n was above 4–6 monomer units.

Figure 5 (see also Table I)²² shows several first-order plots for the polymerization of PGE with sodium methoxide (in methanol) as initiator and DMSO as diluent; the methanol concentration was kept constant for each experiment, and good linear plots possessing small nonlinear portions at the beginning of the reaction were obtained. The variation of the polymerization rate of PGE initiated by dimethyl sodium (in the absence of methanol) is given in Figure 6, and a plot of the first-order rate constant k_1 against initiator concentration for both initiator systems used is shown in Figure 7. This shows that reactions in which dimethyl sodium is the sole initiator gives faster polymerization rates below an initiation concentration of about 2.5×10^{-5} eq/g (when the monomer concentration is 2.9×10^{-3} eq/g). This is attributed to the absence of hydrogen bonding between the anion on the growing chain and the hydroxyl-terminated species present in the runs in methanol; such bonding, which may be caused by methanol or by a protonated chain, with a growing chain

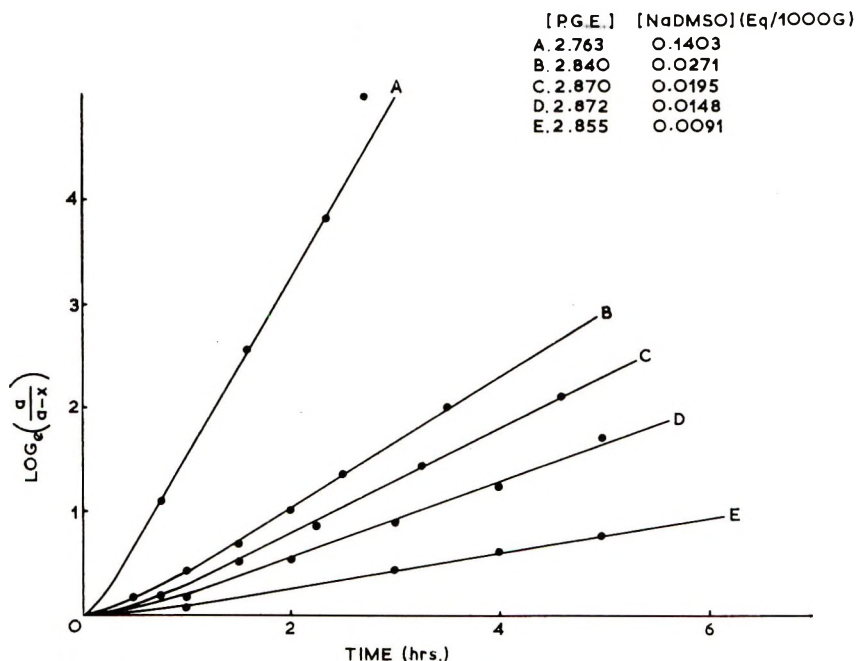
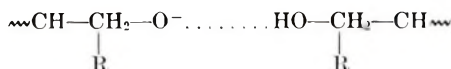


Fig. 6. Variation of rate of polymerization of PGE with NaDMSO concentration in DMSO in the absence of CH_3OH .

TABLE II
 Polymerization Kinetics for PGE in DMSO Solution at 50°C

PGE ₀ meq./g ^a	Catalyst	Cat. meq./g ^a	CH ₃ OH meq./g ^a	M _n		% S		k ₁ × 10 ⁻³ , sec ⁻¹	k ₂ × 10 ^{-4b}
				Calcd	Found	Calcd	Found		
2.763	NaDMSO	0.1403	—	3,030	2,200	1.45	0.05	4.55	3.24
2.864	"	0.0273	0.1204	2,990	1,770	1.82	0.08	16.3	5.97
2.880	"	0.0094	0.119	3,440	—	—	—	2.78	2.96
2.840	"	0.0271	—	15,800	5,700	0.56	0.08	16.3	6.02
2.870	"	0.0195	—	23,080	9,150	0.35	0.08	12.8	6.54
2.855	"	0.0091	—	47,910	8,700	0.37	0.03	4.44	4.88
2.872	"	0.0148	—	29,230	11,970	0.27	0.13	9.68	6.53
2.853	"	0.0148	0.116	3,350	—	—	—	5.20	3.51
2.850	"	0.0272	0.116	3,070	—	—	—	16.30	6.00
2.865	"	0.0147	0.187	2,220	—	—	—	3.47	2.35
2.000	"	0.0530	—	5,670	4,200	—	—	25.35	4.80
1.990	"	0.0890	—	3,360	4,100	—	—	28.8	3.25
1.992	"	0.0260	—	11,570	5,200	0.78	0.06	15.8	6.09
2.918	CH ₃ ON ^a	0.0273	0.121	2,990	1,970	1.62	0.04	16.3	5.97
2.915	"	0.0184	0.082	4,400	2,630	1.22	0.00	10.5	5.71
2.900	"	0.0184	0.121	3,150	1,656	1.94	0.00	7.78	4.23
2.885	"	0.0092	0.122	3,350	2,090	1.53	0.04	2.64	2.87
2.877	"	0.0230	0.121	3,030	1,480	—	—	14.2	6.18
2.933	"	0.0184	0.121	3,240	—	—	—	8.61	4.68
3.042 ^c	"	0.0295	0.150	2,990	3,530	—	—	0.81	2.75

^a Concentration expressed in equivalents/liter = 0.91 × concentration in meq/g.

^b k₂ = k₁/[catalyst].

^c Carried out in dioxan at 79.8°C.

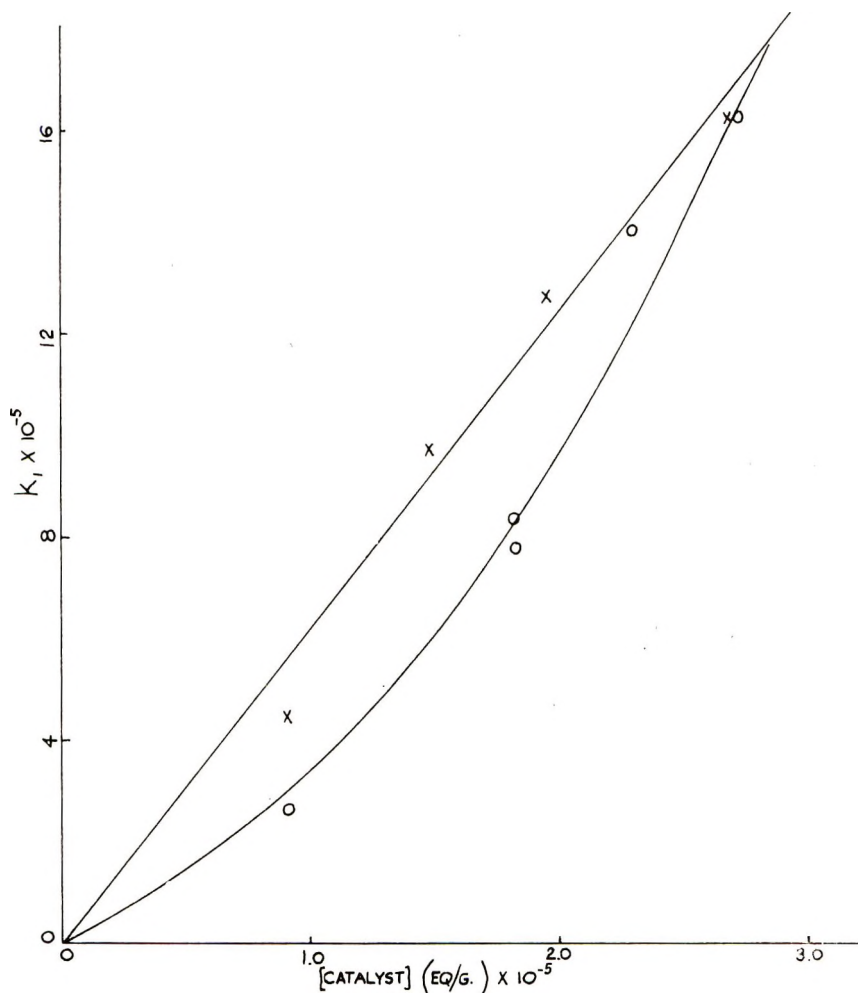


Fig. 7. Variation of first-order rate constant k_1 with catalyst concentration for the polymerization of PGE in DMSO: (x) NaDMSO, CH_3OH absent; (o) CH_3ONa , constant CH_3OH concentration.

where R is $-\text{CH}_2\text{OC}_6\text{H}_5$), would effectively reduce the catalytic reactivity of the growing anion.

One feature of the kinetics must be noted, namely, that in both kinds of systems the reaction in the initial stages is slow and builds up after a short period of time to the first order rate expected. This initial retardation suggests that the first reaction is to form a less reactive species which itself is mainly responsible for the initiation. A second curious feature is shown in the data in Table II, namely, that the polymers did not contain appreciable amounts of sulfur. Such a result is contrary to that found by Bawn¹² for the polymerization of ethylene and propylene oxides. The absence of sulfur in these polymers shows that the dimethyl ion is not, in fact, the

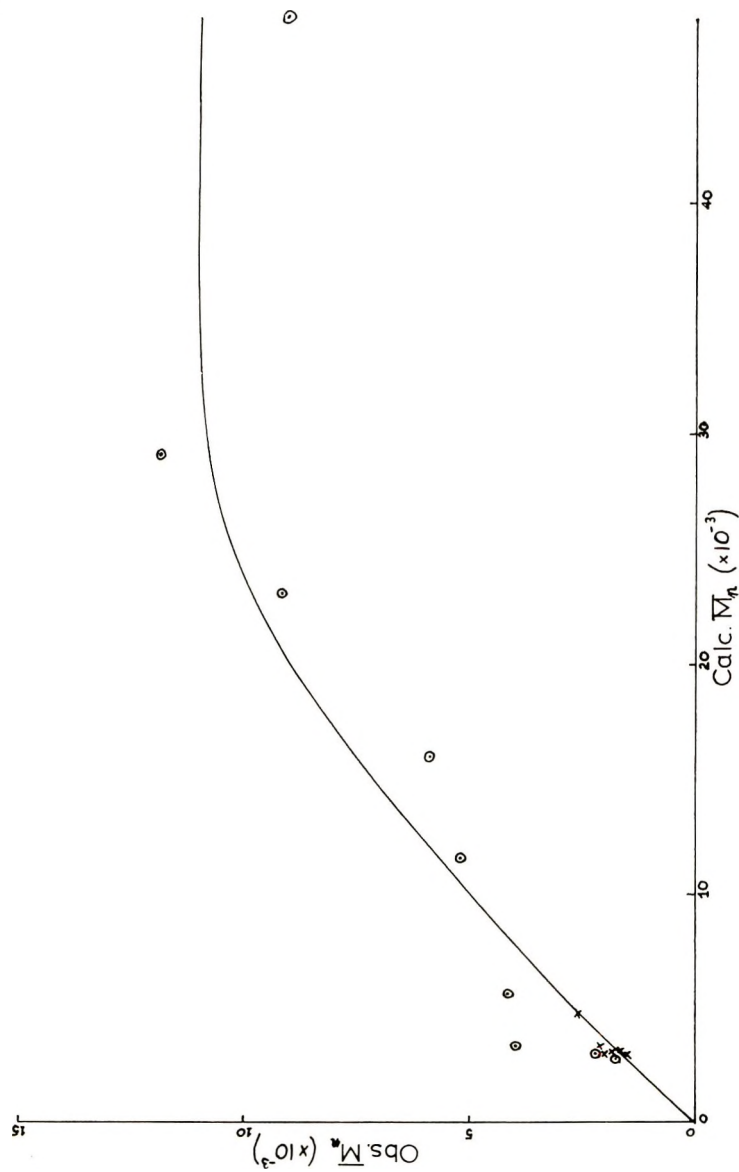


Fig. 8. Observed and calculated \bar{M}_n of poly(PGE): (O) experiments with NaDMSO initiator system; (X) experiments with $\text{CH}_3\text{ONa}-\text{CH}_2\text{OH}$ initiator system.

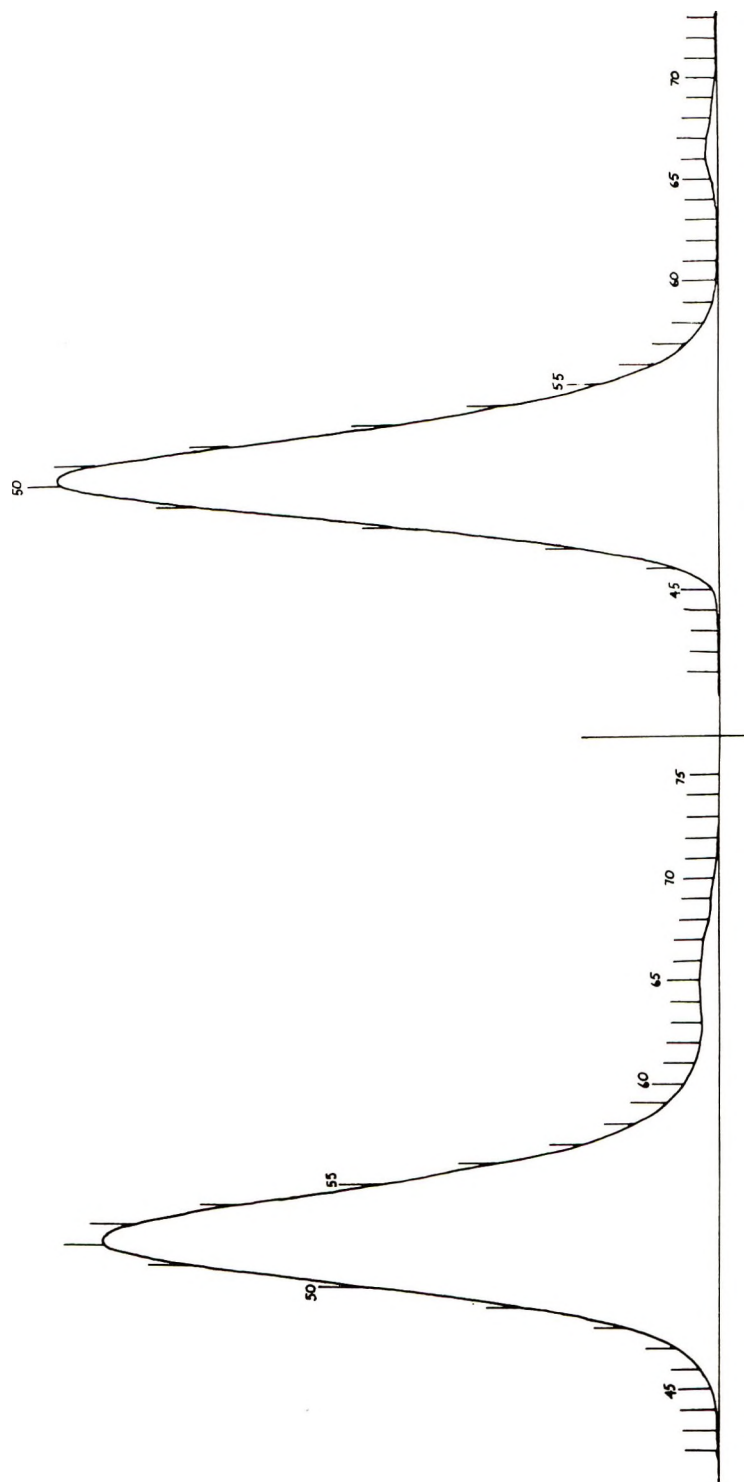


Fig. 9. GPC of (A) poly(phenyl glycidyl ether) and (B) monodisperse polystyrene.

initiating species; it seems likely therefore that in systems in the presence and absence of methanol, the transfer of a proton from the glycidyl ether itself can take place, yielding a less reactive anion. The most likely product of such a transfer is an allylic ion, $C_6H_5OCH = CHO^-$.

Such a transfer is in line with the mechanism put forward by Price,¹⁵ who has examined the possible transfer which occurs when alkoxide ions react with methyl-substituted ethylene oxides. The transfer itself leads to unsaturated products such as have been demonstrated for propylene oxide polymers formed anionically²³ and in PEG by Price et al.,²⁴ who postulated the same mechanism.

This transfer reaction, producing a less active anion which in the main initiates the polymerization, can account for the apparent retardation in the initial stages and the comparatively small contents of sulfur in the final polymer. Moreover, a transfer reaction which apparently occurs quite readily will take place during the main part of the reaction and hence lead to polymers of molecular weights less than the theoretical.

Molecular Weight of Poly(PGE)

Table II shows that there is a considerable discrepancy between the observed number-average molecular weights and those calculated on the basis of eq. (4). A plot of observed versus calculated molecular weight is given in Figure 8, which shows a maximum of about 10,500, indicating a ratio of $k_p/k_{tr} \approx 73$ in DMSO. This is considerably higher than the value $k_p/k_{tr} = 20$ quoted¹⁶ for the anionic polymerization of propylene oxide in DMSO. A much narrower molecular weight distribution may therefore be expected for the poly(PGE). To obtain some idea of the molecular weight distribution, one of our polymers was subjected to gel permeation chromatography and compared with a monodisperse polystyrene of similar molecular weight, in the manner described in the experimental section. The two GPC scans obtained are shown in Figure 9, where the eluent counts (in milliliters of tetrahydrofuran) are marked on each curve. It is evident from the volume counts at the maximum of the two peaks, that the poly-(phenyl glycidyl ether) has a slightly lower molecular weight than the polystyrene. The distribution of the poly(PGE) is slightly wider than that of the polystyrene but is narrow enough to be in agreement with the other results discussed above. The small peaks to the right-hand side of the main peaks are assigned to residual monomers in the polymers.

One of us, (P.B.) wishes to record his thanks to the S.R.C. for financial support during the course of this work.

References

1. A. Wurtz, *Ber.*, **10**, 90 (1877).
2. E. Raithner, *J. Chem. Soc.*, **68**, 319 (1895); *Monatsh.*, **15**, 665 (1894).
3. G. Gee, W. C. E. Higginson, and G. T. Merrall, *J. Chem. Soc.*, **1959**, 1345.
4. G. Gee, W. C. E. Higginson, P. Levesley, and K. J. Taylor, *J. Chem. Soc.*, **1959**, 1338.

5. G. Gee, W. C. E. Higginson, K. J. Taylor, and M. W. Trenholme, *J. Chem. Soc.*, **1961**, 4298.
6. S. A. Miller, B. Bann, and R. D. Thrower, *J. Chem. Soc.*, **1950**, 3623.
7. B. Weibull and B. Nycander, *Acta Chem. Scand.*, **8**, 847 (1954).
8. L. Trossarelli, M. Guaita, and A. Priola, *Atti Acad. Sci. Torino*, **100**, 367 (1966).
9. L. Trossarelli, M. Guaita, S. Priola, and G. Saini, paper presented at International Symposium on Macromolecular Chemistry, Prague, 1965, reprint 578.
10. J. E. Mulvaney and R. L. Markham, *J. Polym. Sci. B*, **4**, 343 (1966).
11. C. E. H. Bawn, *Trans. J. Plast. Inst.*, **34**, No. 109, 1 (1966).
12. C. E. H. Bawn, A. Ledwith, and N. R. McFarlane, *Polymer*, **8**, 484 (1967).
13. A. Ledwith, *J. Appl. Chem.*, **77**, 334 (1967).
14. C. E. H. Bawn, A. Ledwith, and N. McFarlane, *Polymer*, **10**, 653 (1969).
15. C. C. Price and D. D. Carmelite, *J. Amer. Chem. Soc.*, **88**, 4039 (1966).
16. E. J. Corey and M. Chaykowski, *J. Amer. Chem. Soc.*, **87**, 1345 (1965).
17. British Oxygen Co., Brit. Pat. 757,037 (1956).
18. A. J. Durbetaki, *Anal. Chem.*, **28**, 2000 (1956).
19. A. C. Whitley (British Drug Houses Ltd., Liverpool), private communication.
20. B. H. Nicolet and T. C. Poulter, *J. Amer. Chem. Soc.*, **52**, 1186 (1930).
21. W. R. Sorenson and T. W. Campbell, *Preparative Methods of Polymer Chemistry*, Interscience, New York, 1961, p. 310.
22. M. Szwarc, *Nature*, **178**, 1168 (1956).
23. C. C. Price and L. E. St. Pierre, *J. Amer. Chem. Soc.*, **78**, 3432 (1956).
24. C. C. Price, Y. Atarashi, and R. Yamamoto, *J. Polym. Sci. A-1*, **7**, 569 (1969).

Received November 11, 1969

Revised February 27, 1970

A Polyamide from Anthraquinonediketene

PRABIR K. DUTT and C. S. MARVEL,
*Department of Chemistry, University of Arizona,
 Tucson, Arizona 85721*

Synopsis

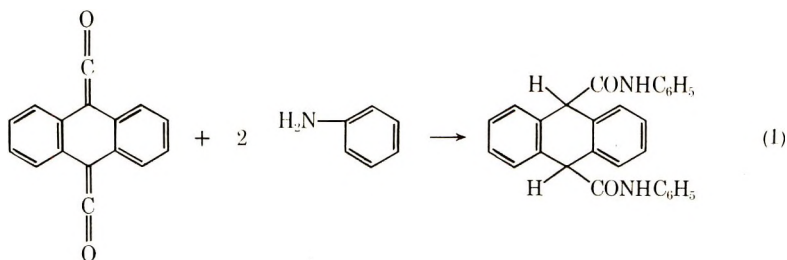
A polyamide has been synthesized by condensing anthraquinonediketene with *m*-phenylenediamine ($\eta = 0.62$; 0.5% concentration in dimethylacetamide, 30°C). The polymer was not thermostable but decomposed rapidly above 275°C.

INTRODUCTION

The condensation of a diketene with a diamine leading to a polyamide seemed to be useful in the field of laminates, since there is no elimination of small molecules during the polycondensation process. The present paper is concerned with the preparation and properties of such a polyamide obtained by the condensation of anthraquinonediketene¹ with *m*-phenylenediamine under suitable conditions.

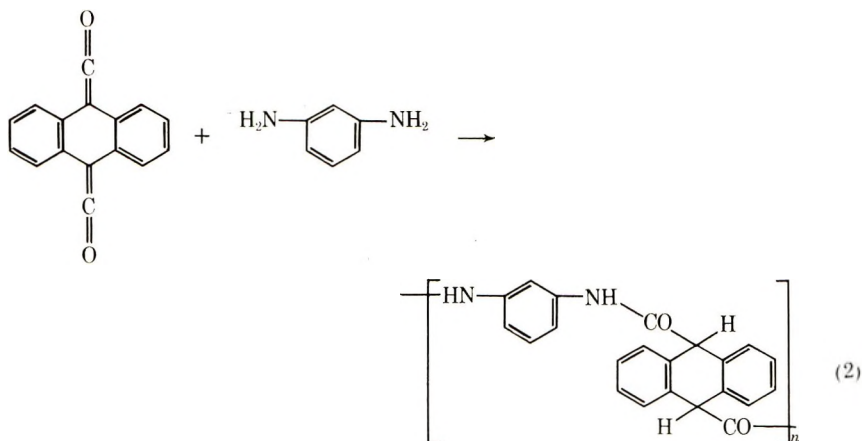
RESULTS AND DISCUSSION

The reaction of anthraquinonediketene in benzene solution with aniline to give a mixture of dianilides has been reported [eq. (1)].



This reaction has been extended to get a polymer by reacting anthraquinonediketene with *m*-phenylenediamine under N₂ atmosphere [eq. (2)].

The polymer obtained in the benzene medium was of very low molecular weight due to the extreme insolubility of the polymer in the reaction mixture. However, the molecular weight was increased by using a mixture of benzene and dimethylacetamide as solvent.



The polymer was a very pale yellow powdery solid having a softening range between 270 and 285°C. It was quite easily soluble in dimethylacetamide but not so soluble in formic acid. The infrared and elemental analysis data indicated it to be a polyamide. (Fig. 1). The thermogravimetric analysis of the polymer under nitrogen atmosphere indicated the polymer to be somewhat stable up to 275°C, after which it broke down completely (Fig. 2).

EXPERIMENTAL

Monomers

Anthraquinonediketene. The preparation of the diketene has been achieved by the dehydrochlorination of 9,10-dihydroanthracene-9,10-dicarbonyl chloride with triethylamine.¹ The dicarbonyl chloride has again been prepared from the corresponding 9,10-dihydroanthracene-9,10-dicarboxylic acid.^{2,3} A 3-g portion of the acid chloride was dissolved in 25 ml of deoxygenated benzene under a stream of dry nitrogen; 2.2 g of triethylamine was added to the solution. The mixture was allowed to stand for 5 hr. The orange-red benzene solution of the anthraquinonediketene was used for further polymerization reaction.

***m*-Phenylenediamine.** Commercial *m*-phenylenediamine was recrystallized several times from water and dried over P₂O₅ under vacuum.

Polymer

Condensation of anthraquinonediketene with *m*-phenylenediamine was carried out in benzene or in benzene-dimethylacetamide.

In Benzene Medium. To the orange-red solution of the diketene in benzene was now added 0.92 g of *m*-phenylenediamine. A precipitate of the product was formed instantaneously. The mixture was kept at 50°C for 0.5 hr and the product filtered, washed with ethyl alcohol, and dried.

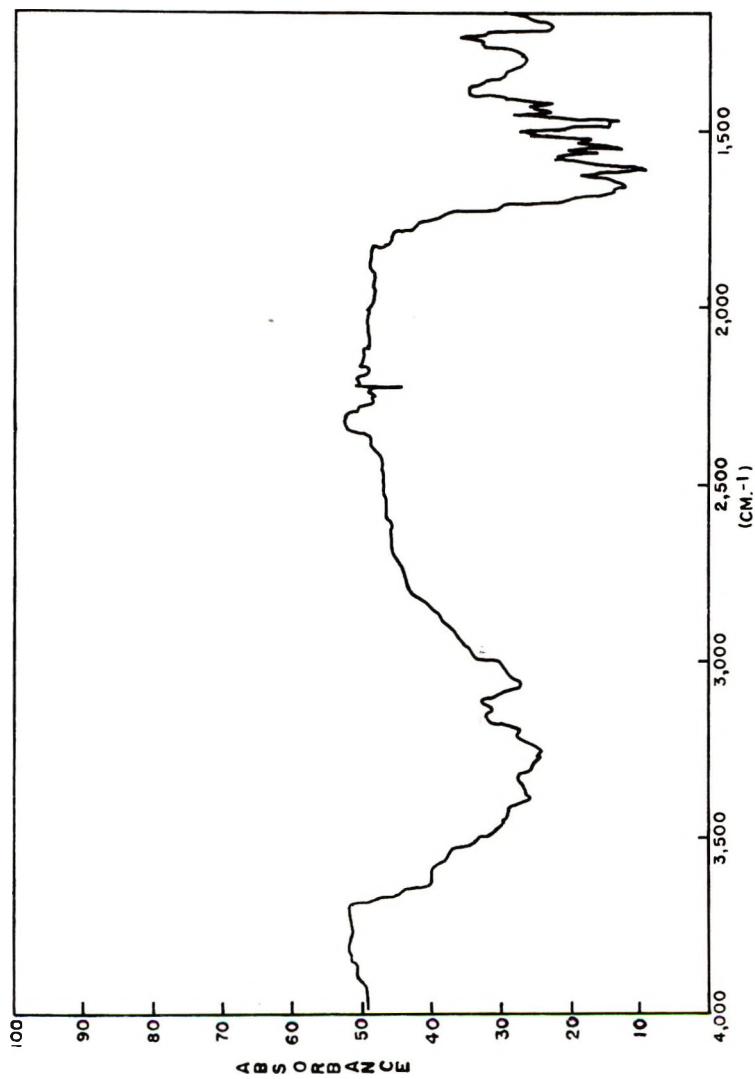


Fig. 1. Infrared spectrum of polyamide.

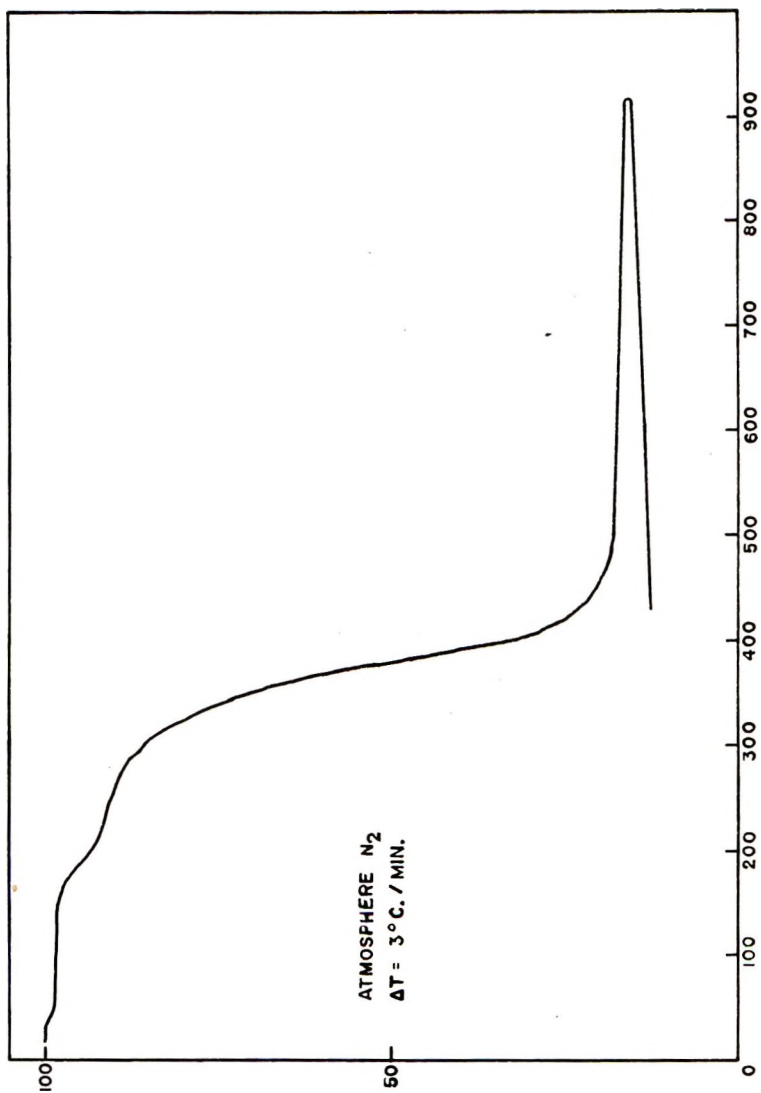


Fig. 2. TGA curve for polyamide in nitrogen; heating rate 3°C./min.

The yield was quantitative and the molecular weight was very low ($\eta = 0.15$; 0.5% concentration in dimethylacetamide, 30°C.).

ANAL. Calcd for $C_{22}H_{16}N_2O_2$: C, 77.6%; H, 4.7%; N, 8.2%. Found: C, 76.7%; H, 4.84%; N, 8.8%

In Benzene-Dimethylacetamide Mixture as Medium. The same polymerization reaction was carried in a mixture of 1:1 benzene and dimethylacetamide. The polymer remained in solution and was precipitated with petroleum ether. The molecular weight was higher ($\eta = 0.62$; 0.5% concentration in dimethylacetamide, 30°C.).

ANAL. Calcd for $C_{22}H_{16}N_2O_2$: C, 77.6%; H, 4.7%; N, 8.2%. Found: C, 76.8%; H, 4.7%; N, 8.72%.

This work was supported by the Air Force Materials Laboratory, Air Force Systems Command, Wright-Patterson Air Force Base, Ohio.

References

1. A. T. Blomquist and Y. C. Meinwald, *J. Amer. Chem. Soc.*, **79**, 2021 (1957).
2. C. S. Rondestredt, Jr., and I. Nicholson, *J. Org. Chem.*, **20**, 348, 1955.
3. X. X. Beckett, *J. Chem. Soc.*, **1959**, 2411.

Received March 2, 1970

The Morphology of the Monomer-Polymer Particle in Styrene Emulsion Polymerization*

M. R. GRANCIO† and D. J. WILLIAMS, *Chemical Engineering
Department, The City College of The City University of New York, New York,
New York 10031*

Synopsis

A heterogeneous model for the monomer-polymer particle in styrene emulsion polymerization is presented. In this model, the growing particle consists of an expanding polymer-rich core surrounded by a monomer-rich shell which serves as the major locus of polymerization. This core-shell model was suggested by kinetic studies with continuously uniform latices which showed that the systems of interest were of the Smith-Ewart case II type but that the dynamic—as opposed to equilibrium swelling—particle monomer concentrations were continuously variable. Supporting evidence for the suggested morphology was obtained by electron microscope observation of ultrathin sections of latex particles.

INTRODUCTION

In both theoretical and experimental kinetic studies of styrene emulsion polymerization, it is generally assumed that the growing monomer-polymer particles are homogeneous in character and that the locus of polymerization may be anywhere within the particle. In this paper we present kinetic evidence that suggests and supports a heterogeneous core-shell model for the growing monomer-polymer particle. In this model, the particle consists of an expanding polymer-rich core surrounded by a monomer-rich shell, and the outer shell serves as the major locus of polymerization. This morphology was suggested by kinetic data obtained in constant rate studies with continuously uniform latices. The data of interest were derived from measurement of the particle monomer concentration during the progress of the run, measurement of rates of polymerization, and initiator perturbation studies. The model, in turn, suggested a confirming physical test, which involved electron microscope observation of the ultrathin sections of latex particles.

After a brief review of the literature pertinent to this study, we discuss our results in three stages: the kinetic studies leading to the proposed

* Presented in part to The Division of Organic Coatings and Plastics Chemistry, The American Chemical Society, Minneapolis, April 1969.

† Present address: Monsanto Company, Hydrocarbon and Polymer Research Department, 730 Worcester St., Indian Orchard, Massachusetts 01051.

model, presentation of the model, and the electron microscope study of the latex particle morphology.

Constant Rate Polymerization

Constant rate emulsion polymerization is often encountered in polydispersed systems in the stage of growth following particle nucleation. As will be shown, the uniform particle-size styrene systems of interest in this study exhibit constant rates from zero to about 60% conversion. Theoretically, the rate of styrene emulsion polymerization is usually explained in terms of the Smith-Ewart theory¹ and various modifications of it.²⁻⁹ Constant rate behavior is described by case II of the Smith-Ewart theory, in which the number of free radicals per monomer-polymer particle approximately equals $1/2$. For this case the overall rate of polymerization, R_p , and the rate of polymerization per particle R_{pp} , are given by

$$R_p = N_p R_{pp} \quad (1)$$

$$R_{pp} = k_p \bar{n} [M] \quad (2)$$

where N_p = number of particles, k_p = rate constant for propagation, \bar{n} = number of free radicals per particle, and $[M]$ = the monomer concentration within the particles. For constant rate growth, eqs. (1) and (2) require that if the number of particles remains constant and if the number of free radicals per particle is $1/2$ and constant, then the particle monomer concentration must also remain constant.

TABLE I^a
Title: Initiator Perturbation Studies in Uniform Constant Rate Styrene Runs.

Sample number	time, min	Particle diameter, Å		
		Control	$2 \times I_0$	$3 \times I_0$
1	20	450	—	—
2	35	785	—	—
3	65	1030	1070	1065
4	180	1350	1380	1425
5	300	1930	1910	1950
6	420	2220	2190	2130
7	540	2400	2370	—
Final	—	2800	2800	2860

^a Data exhibit constant rate behavior in that plots of per cent conversion (calculated as the cube of the ratio of intermediate to final particle diameter) vs. time yield straight lines.

Evidence for $\bar{n} = 1/2$ and constant in styrene polymerization is based on initiator perturbation studies which are rather direct and convincing.^{10,11} In the perturbation technique the initiator concentration of a run in progress is suddenly increased. Invariance in the rate is evidence for $\bar{n} = 1/2$ and constant. Table I shows affirmative results obtained by Williams¹² for uniform constant rate styrene runs (generated by slow addition of

potassium laurate) in which the original initiator concentration was doubled and tripled at 65 min.

These results are in line with those of Smith¹⁰ who worked with seeded styrene latices and doses of $1/4$ and 4 times the original initiator concentration. On the other hand, Gerrens and Kohnlein^{13,14} observed rate increases ranging from 1.3 to 2.14 times the original, but they perturbed their original systems by massive incremental initiator doses ranging from 5 to 34 times. Also, the condition of their formulations was markedly different from those ordinarily encountered in emulsion polymerizations in that a 16:1 water-to-monomer ratio was utilized.

Recent speculations as to the nature of the particle monomer concentration during the course of the polymerization process have been derived from the extrapolation of results from equilibrium swelling measurements^{9,15-18} rather than from direct measurements during the course of a run. Several investigators have found the equilibrium concentration to be only a moderately increasing function of particle size over a substantial range in sizes. However, evidence based on direct measurement of dynamic rather than equilibrium monomer-polymer ratios has long existed in the literature,^{19,20} showing the monomer concentration to be a continuously changing variable. The lack of consistency between the results obtained in equilibrium and dynamic experiments and its implication with regard to eq. (2) prompted us to perform the dynamic measurements subsequently described.

EXPERIMENTAL KINETIC STUDIES

Polymerization

Interest in this study centered on formulations known to generate continuously uniform latices.^{21,22} By continuously uniform latices we mean those in which all particles are of identical size throughout the entire growth process. In these systems dynamic equivalence will exist between all particles, and the particle monomer concentration and particle rate processes will be the same for each and every particle. The consequences of this dynamic equivalence are particularly important in this study in that the particle size dependence of such key parameters as monomer concentration and rates of polymerization per particle, R_{pp} , can be accurately and unambiguously established. That is, particle size dependence will not be obfuscated by measuring the parameters of interest for a range of particle sizes. Furthermore, since particle nucleation is virtually instantaneous, simultaneous particle nucleation and growth never occur, and data analysis is not complicated by the need to separate the effect of these simultaneous events on the mechanism of polymerization at low conversions.

The formulations used were based on 180 g water, 100 g monomer, 0.5 g potassium persulfate, 3.0 g Triton X-100 (a nonionic octylphenoxyethyl surfactant, product of Rohm and Haas Co., Philadelphia, Pa.) 0.075 g KOH, and either 0.15 g or 0.30 g sodium lauryl sulfate. The different

amounts of sodium lauryl sulfate produced final uniform particle diameters of 2300 Å (0.15 g) and 1950 Å (0.30 g) and constant conversion rates up to about 60% of $13 \pm 2\%$ /hr and $21 \pm 2\%$ /hr, respectively. Some scatter was always experienced, about $\pm 2\%$, in measuring the rates of conversion between individual runs for both the 13% /hr and 21% /hr runs. This scatter probably resulted from our inability to accurately reproduce the initial conditions from run to run. This was in turn manifested in a moderate fluctuation in the number of particles formed and thus in the rate of polymerization, R_p . The polymerizations were conducted in a paddle-mixed 1-liter kettle reactor at $60 \pm 1^\circ\text{C}$ with pH = 9.0 (constant). The reactor was fitted with a thermometer, condenser, and a glass tube device for purging and sampling. The entire formulation, except for the initiator solution, was charged initially. After a $1/2$ -hr nitrogen purge at 60°C , the persulfate was added in solution form as 0.5 g/10 ml water.

Dow styrene monomer at inhibitor (*p-tert*-butylcatechol) level 12T was vacuum distilled and caustic washed to remove all traces of inhibitor. The styrene was nitrogen purged for 30 min immediately before use, to remove oxygen. The water was distilled and boiled vigorously immediately before use, to remove oxygen. Triton X-100 was used as obtained from Rohm and Haas, containing 98% active ingredient. All other materials were reagent grade of at least 98% purity.

Conversion and Particle Size

Since the latices were continuously uniform, the extent of reaction could be determined in two ways: (a) by taking the ratio of the cubes of the intermediate to final particle diameters and (b) by gravimetric means. Electron micrographs of the particles were obtained at progressive stages of growth using now standard techniques.²¹ The results of the particle size analysis and per cent conversions for the 13% /hr run are shown in Table II.

TABLE II
Particle Size Analysis for the 13% /hr Run

Sample number	Conversion, % (grav.)	Number of particles counted	Particle diameter, Å	Uniformity ratio ^a	Conversion, % (from D_p)
1	8	14	1025	1.01	8.8
2	22	30	1390	1.01	22.0
3	42	20	1740	1.01	43.2
4	76	40	2100	1.01	76.2
5	100	40	2300	1.001	100.0

^a Ratio of weight-average to number-average particle diameter, D_p .

The same results for the 21% /hr run are published elsewhere.²² These data show that the particles are remarkably uniform throughout the course of the run and that gravimetric and particle size analysis gave the same conversions.

Particle Monomer Concentration

The individual particle monomer concentrations were measured from unaltered samples taken from a run in progress to yield dynamic rather than equilibrium values. Samples were collected from the kettle directly into a centrifuge tube containing the inhibitor paraquinone, which halts further polymerization. The samples were immediately centrifuged. It was found that 1 min of centrifuging time was sufficient to remove all of the monomer present in monomer droplets. Further centrifugation showed no increase in the amount of monomer removed. In a like manner, diluting the latex with an equal volume of water did not alter the total monomer centrifuged at conversions above 5%.

Actual concentrations were determined, via gas chromatography, from peak height ratios of water to styrene and the independently determined conversion. Direct injection of the sample was not found to be possible because the latex coagulated in the syringe needle. Instead, 2–5 ml portions of the centrifuged latex were dissolved in 50 ml of refluxing tetrahydrofuran (THF) and injected (still hot) into the previously calibrated chromatograph. To obtain reproducible results, the samples must remain hot and well stirred before injection. The instrument was calibrated by analyzing prepared standard solutions containing styrene, water, and THF in proportions covering the required range and measuring the resulting water-to-styrene peak height ratios. The calibration varied moderately from day

TABLE III
Rate Data for $13 \pm 2\%$ /hr Runs

Run and sample no.	Time, min	Conversion, %
I—1	80	17.5
2	165	34.1
3	245	50.0
4	340	76.0
II—1	30	8.0
2	95	22.0
3	165	36.0
4	230	54.0
5	320	92.0
III—1	20	6.5
2	40	11.2
3	60	16.0
Add initiator	80	21.0
5	120	31.5
6	150	38.5
7	180	46.5
8	210	54.0
9	240	69.5
10	270	89.0
11	300	90.0

to day, so the instrument was recalibrated prior to each run. A Carbowax and Teflon column was used with an oven temperature of 95°C and a helium gas flow rate of 60 cc/min. The temperatures of the injection port and conducting detector were 185°C and 230°C, respectively.

RESULTS OF KINETIC STUDIES

Smith-Ewart Case II Character of Runs

Shown in Tables III and IV and Figures 1 and 2 are the rate data for the formulations of interest. These data are plotted with an interval time

TABLE IV
Monomer Concentration and Conversion-Time Data

Run and sample no.	Time, min	Conversion, %	Weight fraction monomer
13%/hr Runs			
I—1	40	9.3	0.69
2	82	18.7	0.735
3	123	28.5	0.70
4	173	39.6	0.555
II—1	20	4.2	0.715
2	60	13.4	0.73
3	100	24.7	0.735
4	140	35.3	0.59
5	180	47.6	0.455
III—1	27	4.7	0.715
2	55	9.7	0.72
3	90	17.5	0.725
4	110	21.3	0.735
5	135	27.0	0.69
6	162	32.3	0.635
21%/hr Runs			
IV—1	45	14.6	0.745
2	75	25.4	0.705
3	100	34.8	0.65
4	127	44.8	0.555
5	160	55.3	0.445
6	180	63.5	0.34
7	225	84.0	
8	255	88.0	
9	270	90.0	
V—1	15	6.2	0.785
2	45	17.3	0.765
3	75	28.6	0.70
4	105	38.6	0.65
5	135	49.7	0.54
6	165	61.8	0.40
7	225	91.0	

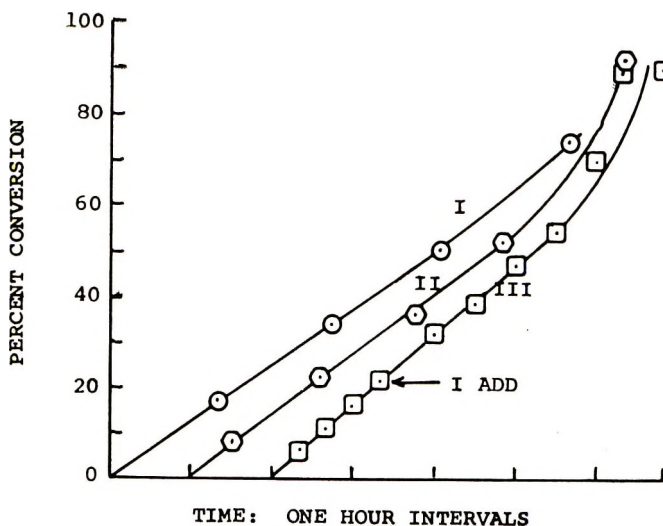


Fig. 1. Conversion time for $13 \pm 2\%$ hr runs. Runs I, II, and III from Table III. I ADD: Add initiator.

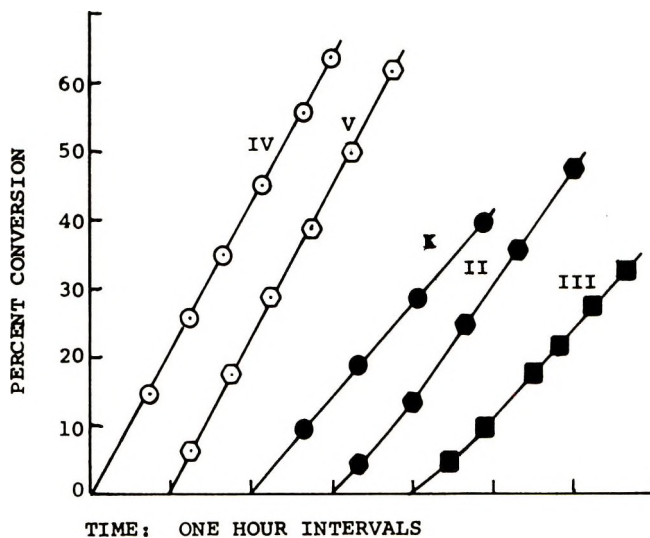


Fig. 2. Rate data for monomer fraction studies of Figure 3. Runs I to V from Table IV.

scale so as to show each curve separately. The data very clearly show the linear conversion character of our runs up to about 60%. Very modest deviations from linearity are observed in two runs at less than 10% conversion, but this is probably due to the presence of trace amounts of impurities which serve to inhibit or retard the initial rate.

Furthermore, the 15%/hr run shown in Figure 1 and Table III was perturbed at 80 min by the addition of 0.5 g potassium persulfate, thereby approximately doubling the initial initiator concentration. In this per-

turbed run there is no deviation from normal behavior up to 60% conversion, which indicates that \bar{n} is indeed $1/2$. Replicate data were obtained but are not shown. Attempts to further increase the perturbation dose resulted in latex instability.

From Table II, since both gravimetric and particle diameter methods yield the same conversion, the number of particles, N_p , must be constant. Finally, with N_p and R_p constant and $\bar{n} = 1/2$ (constant), one must conclude that our runs exhibit Smith-Ewart case II kinetics.

Particle Monomer Concentration

The results for the two formulations of interest and for multiple dynamic measurement of the monomer concentrations are shown in Table IV and Figure 3 as weight fraction monomer versus % conversion. For both the 13%/hr and 21%/hr runs this fraction varies significantly during their periods of constant rate polymerization. For the 13%/hr run the weight fraction monomer rises slightly from about 0.71 at low conversions to about 0.73 at 27% conversion, when the emulsified monomer disappears; it then drops along the overall ratio curve to 0.40 at 60% conversion. For the 21%/hr run, the fraction of monomer drops continuously from 0.8 at low conversions to 0.40 at 60% conversion. Thus, according to these data and eqs. (1) and (2), the rates of conversion should decrease to about one

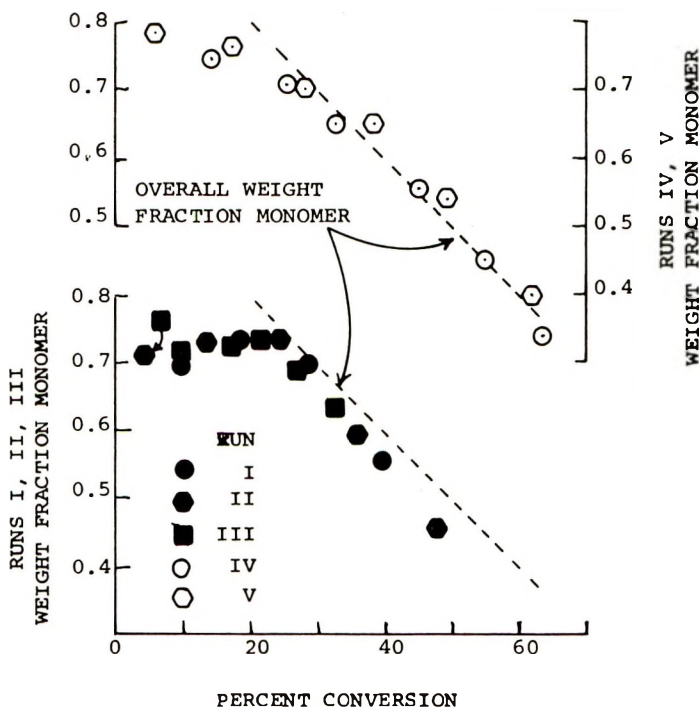


Fig. 3. Particle monomer concentration vs. % conversion. Data from Table IV.

half their early conversion values by the time 60% conversion is reached. The data of Figures 1 and 2 clearly show that this is not the case.

It is also interesting to note that our 21%/hr monomer fraction data, replotted as monomer-polymer ratio versus conversion, exactly matches the behavior of the data obtained by Harkins et al.^{19,20} for similarly executed dynamic measurements. That some dynamic monomer concentration data differ markedly from those obtained in equilibrium swelling measurements is clearly evident. That is, equilibrium swelling measurements for several latex systems show this concentration to be a moderately increasing function of particle size^{9,15-18} while dynamic measurements show that this concentration may actually decrease with particle size in certain systems. Certainly, the practice of assuming a constant particle monomer concentration in analytic treatments of emulsion polymerization ought to be followed with increased caution.

THE MONOMER-POLYMER PARTICLE MORPHOLOGY: A CORE-SHELL MODEL

The foregoing kinetic data coupled with eqs. (1) and (2) suggest a heterogeneous model for the monomer-polymer particle. Such a model must reconcile the results of the kinetic studies which show that, during a period of constant rate polymerization, \bar{n} is constant but the overall particle monomer concentration is continuously variable. From eqs. (1) and (2), since R_{pp} , \bar{n} , and k_p are constant, one can only conclude that $[M]$ must also be constant at the actual site of polymerization. It follows, therefore, that a zone of constant monomer concentration must exist within the particle during constant rate polymerization and that this zone must be the major locus of polymerization. We suggest that the growing particle consists of an expanding polymer-rich (monomer-starved) core surrounded by a monomer-rich (polymer-starved) spherical shell. In this core-shell model the outer shell serves as the major locus of polymerization while virtually none occurs in the core because of its monomer-starved condition. A Smith-Ewart on-off mechanism necessarily prevails within the monomer-rich shell. The core is pictured as growing outward somewhat as a ball of string constructed from many single strands. In such a model a changing overall particle monomer concentration is consistent with constant particle rates because reaction takes place in an essentially pure monomer environment.

The proposed model is further supported by kinetic evidence if we consider eq. (2) and the rates of polymerization per particle. Since the final particle diameter can be measured with a high degree of accuracy, N_p can be readily and accurately evaluated. The results of the calculations of N_p and R_{pp} for both the 13%/hr and 21%/hr runs are shown in Table V. The fact that the R_{pp} values are identical and constant, independent of particle size or overall particle monomer concentration, is consistent with the proposed morphology.

In addition, we can substitute appropriate values for \bar{n} , $[M]$, and k_p into eq. (2): namely, $\bar{n} = (1/2)[1/(6.02 \times 10^{23})]$ moles/particle, $[M] = 905$ g/l. (the density for pure styrene), and $k_p = 282$ l/mole sec (a value calculated from bulk experiments²³). We are thus calculating the rate of polymerization for a single active species growing one half the time in pure monomer just as the model suggests. We calculate $R_{pp} = 2.12 \times 10^{-19}$ g/particle-sec for rather good agreement with the experimental value of 2.40×10^{-19} shown in Table V.

TABLE V
 N_p and R_{pp} for 13%/hr and 21%/hr Runs

Overall rate, %/hr	Final $D_p, \text{Å}$	N_p^a	R_{pp} , g/particle-sec
13	2300	1.49×10^{16}	2.38×10^{-19}
21	1950	2.46×10^{16}	2.42×10^{-19}

^a Basis: 100 g monomer converted to polymer.

ELECTRON MICROSCOPE STUDY

The following experiment was proposed to provide additional corroborating evidence for the core-shell morphology: To a run in its early stages of growth, charge a portion of butadiene. Copolymerization should result and, if the model is correct, the final latex particle should consist of a pure polystyrene core—corresponding to the core which existed when the butadiene was charged—surrounded by a spherical styrene-butadiene copolymer shell. Since the unsaturated butadiene repeat unit can be stained with osmium tetroxide, an ultrathin section taken through the center of the particle should appear as a doughnut shape under electron microscope observation.

To ascertain how the inherent incompatibility of the styrene homopolymer and butadiene-styrene copolymer molecules might affect any conclusions we intended to draw from the proposed study, we also prepared for electron microscope observation thin films of the latex polymer formed by casting from an initially homogeneous solution. As will be shown for the latex particles constituted for this study, the structures which result from actual phase separation because of the inherent incompatibility of the component molecules are orders of magnitude smaller than the expected characteristic structure of the latex particle. This result indicates that compatibility considerations should not interfere with the objectives of the proposed study.

Sample Preparation

Since butadiene is a gaseous monomer at 60°C, polymerization in this study was conducted in a bottle polymerizer using standard procedures.¹² Butadiene was liquified by passing the gas through chilled coils. Five to ten ml of the collected butadiene was charged to a 13%/hr standard formu-

lation with 0.1 ml of dodecyl mercaptan at 20% conversion, and the reaction was carried to completion. The resultant latex was frozen at -10°C to destabilize it and then dried in air. The particles were washed several times with methanol to remove soap and again dried in air.

The particles were embedded in Epon resin, and oven cured at 45°C for 48 hr. The embedded sample was then sectioned with a microtome. The slices were picked up on grids, exposed to osmium tetroxide, and then viewed in the electron microscope.

Thin films were prepared for observation by first casting films of the latex polymer over water from a 1% amyl acetate solution. Grids were placed on the floating film and then picked up in such a way as to carry off the cast film. These specimens were dried, exposed to osmium tetroxide, and then viewed in the electron microscope.

Results

Figure 4 is an electron micrograph of a sectioned particle obtained in the manner just described. It clearly shows the expected unstained core and the stained ring. The very thin, light outer ring could have arisen from one of two sources: interaction of the embedding material with the particle surface; or, since butadiene polymerizes at a faster rate than styrene, all the butadiene may have been consumed before the styrene and the outer ring may consist of pure polystyrene.

Figure 5 shows an electron micrograph, at two times the magnification of Figure 4, of a typical area of the thin films prepared from a homogeneous solution of the latex polymer. The structures in this micrograph are clearly orders of magnitude smaller than the characteristic features of the core-shell particle. If the growing particles were homogeneous when the butadiene was introduced, eventual phase separation would be expected to result in a particle morphology similar to that of Figure 5 and not that of Figure 4.

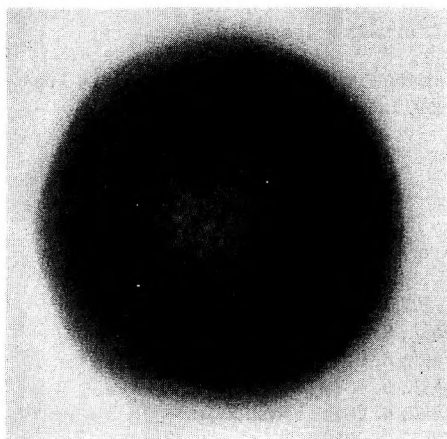


Fig. 4. Ultrathin section of composite butadiene-styrene particle, 250,000X.

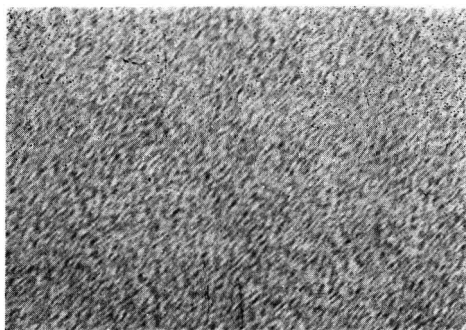


Fig. 5. Thin film cast from homogeneous solution of butadiene-styrene latex, 500,000X.

These results supply convincing physical evidence, to support the proposed core-shell morphology.

CONCLUSION

We present substantial evidence to suggest and support a core-shell model for the growing monomer-polymer particle in styrene emulsion polymerization. This evidence was drawn from experiments with Smith-Ewart case II emulsion polymerizations in a single type of uniform system formulation. The results should be valid, however, for a considerable variety of systems. It has been shown²¹ that the styrene systems of the type of interest in this study are kinetically equivalent to their polydispersed counterparts, and several monomers in emulsion polymerization exhibit characteristics similar to those of styrene. The evidence is certainly strong enough to support the need for analogous studies in other systems.

The major portion of this work was supported by a grant from the National Science Foundation—NSF GK-1375. We acknowledge with thanks the assistance of Mr. Mark Roller in the measurement of the monomer concentrations and Mr. John Bodnaruk in the preparation of the electron micrographs.

This paper is based on the Ph.D. Thesis of M. R. Grancio, The City College of The City University of New York, 1969.

References

1. W. V. Smith and R. H. Ewart, *J. Chem. Phys.*, **16**, 592 (1948).
2. W. H. Stockmayer, *J. Polym. Sci.*, **24**, 314 (1957).
3. J. T. O'Toole, *J. Appl. Polym. Sci.*, **9**, 1291 (1965).
4. J. L. Gardon, *J. Polym. Sci. A-1*, **6**, 623 (1968).
5. J. L. Gardon, *ibid.*, **6**, 643 (1968).
6. J. L. Gardon, *ibid.*, **6**, 665 (1968).
7. J. L. Gardon, *ibid.*, **6**, 687 (1968).
8. J. L. Gardon, *ibid.*, **6**, 2853 (1968).
9. J. L. Gardon, *ibid.*, **6**, 2859 (1968).
10. W. V. Smith, *J. Amer. Chem. Soc.*, **70**, 3695 (1948).

11. B. M. E. van der Hoff, *Polymerization and Polycondensation Processes*, Advances in Chem. Series, No. 34, American Chem. Soc., Washington, D. C., 1962.
12. D. J. Williams, Ph.D. Thesis, Case Institute of Technology, 1964, Cleveland, Ohio.
13. H. Gerrens, *Angew. Chem.*, **71** (No. 19), 608 (1959).
14. H. Gerrens and E. Kohleln, *Z. Elektrochem.*, **64**, 1199 (1960).
15. W. V. Smith, *J. Amer. Chem. Soc.*, **71**, 4077 (1949).
16. M. Morton, S. Kaizerman, and M. W. Altier, *J. Colloid Sci.*, **9**, 300 (1954).
17. E. J. Meehan, *J. Amer. Chem. Soc.*, **71**, 628 (1949).
18. E. Vanzo, R. H. Marchessault, and V. Stanett, *J. Colloid Sci.*, **20**, 62 (1965).
19. W. D. Harkins, *J. Amer. Chem. Soc.*, **69**, 1428 (1947).
20. S. H. Herzfeld, A. Roginsky, M. L. Corrin, and W. D. Harkins, *J. Polym. Sci.*, **5**, 207 (1950).
21. D. J. Williams and E. G. Bobalek, *J. Polym. Sci. A-1*, **4**, 3065 (1966).
22. D. J. Williams and M. R. Grancio, *J. Polym. Sci. C*, **27**, 139 (1969).
23. G. Olive-Henrici and S. Olivé, *Makromol. Chem.*, **37**, 71 (1960).

Received August 15, 1968

Revised March 3, 1969

A Study on the Mechanism of Polyvinyl Chloride Stabilization by Lead Salts

E. N. ZILBERMAN, A. E. KULIKOVA, S. B. MEIMAN,
N. A. OKLADNOV, and V. P. LEBEDEV, *Research Institute of
Organochlorine Compounds and Acrylics, Dzerzhinsk, U.S.S.R.*

Synopsis

Infrared spectroscopic and DTA measurements and chemical analysis have shown that during stabilization of PVC with organic and inorganic basic lead salts various reactions occur: (a) binding of the evolved HCl by these salts with the formation of lead chloride and complexes, including HCl, which catalyze the PVC degradation; (b) complex-forming reaction with the reactive PVC groups, which decreases the intensity of color of the polymer. In addition, with weak-organic-acid basic lead salts, exchange of labile Cl atoms for acid residues in PVC occurs, which results in an increase in inherent polymer stability.

INTRODUCTION

In our previous study of the PVC interaction with basic sulfate lead salts¹ it was shown that the HCl evolved during PVC dehydrochlorination is bound by basic lead sulfates with the formation of lead chloride as well as complexes $x\text{PbCl}_2 \cdot y\text{PbSO}_4 \cdot z\text{HCl}$. These complexes are rather stable and practically do not lose HCl after heating for 1 hour at 170°C under nitrogen. They appeared to be degradation catalysts for PVC, probably because of their acidic nature. These compounds markedly increase the rate of dehydrochlorination of PVC in the presence of tribasic lead sulfate (TLS). In spite of the more extensive PVC dehydrochlorination in the presence of some basic lead salts than in the presence of sodium carbonate, the polymer, after being heated with these salts, and the related rolled films were less colored than identical samples obtained in the presence of sodium carbonate. Infrared-spectroscopic, DTA, and TGA measurements showed that the favorable effect of the basic sulfate lead salts on the color of PVC was due to the complex formation between the basic sulfate salts and reactive PVC groups (conjugated double bonds, labile Cl atoms, oxygen-containing groups, etc.). It must be pointed out that the assumption of the direct stabilizer interaction with the polyenes has already been proposed by Wartman.² Completed experimental studies, however, convinced him to prefer another hypothesis, according to which one of the factors that influence the color stability is the efficiency of the hydrogen chloride pickup by the stabilizer.

Besides the basic lead salts of sulfuric acid organic-acid basic lead salts are widely used as PVC stabilizers. Therefore it was interesting to estimate to what extent the laws established by us for the interaction of PVC with the sulfate salts were valid for the reaction of this polymer with other basic lead salts.

The mechanism of PVC stabilization by the monobasic lead salts of stearic (MLS), phthalic (MLP), and caprylic (MLC) acids and by dibasic lead phosphite was studied in this work.

EXPERIMENTAL

PVC (*K*-value 65) was obtained by suspension polymerization with azo-isobutyronitrile as an initiator and with the partly neutralized styrene and maleic acid copolymer as a protective colloid. For the experiments chemical-grade yellow lead oxide, lead sulfate, and lead chloride were used.

Partly dehydrochlorinated PVC (DPVC) was prepared by treatment with sodium alcoholates.³ Monobasic lead sulfate, dibasic lead phosphite, and monobasic lead phthalate, stearate, and caprylate were synthesized from lead oxide and the corresponding acids. The results of lead analysis of the synthesized materials correlate well with the calculated lead content on the basis of their formulas.

The amount of gaseous HCl evolved in the reaction of PVC with basic salts (175°C under air) was determined by the procedure described by Wartman.² In order to estimate the amount of HCl bound by lead salts, the reaction products were extracted with water at 80–90°C and the water extracts were potentiometrically titrated with silver nitrate.

Infrared spectra were measured using a double-beam spectrophotometer UR-10. Thermograms were measured as before.¹

RESULTS AND DISCUSSION

The curves for the dehydrochlorination rate of PVC in the presence of different salts are given in Figure 1. Curve 5 represents the rate of binding of HCl by MLP. The position of this curve shows the high ability of PVC to accept HCl; but at the same time the whole amount of HCl, evolved on heating of PVC in the presence of MLP (curve 6), slightly exceeds the amount of HCl evolved in the absence of MLP (curve 7). Curves 1 and 3, which represent the rate of HCl binding by basic lead stearate (MLS) and caprylate (MLC), respectively, are positioned much lower than curve 5. Both salts are claimed poor acceptors of HCl, as compared to MLP, but they retard the degradation of PVC appreciably (curves 2 and 4). The high ability of MLP to accept HCl seems to be owing to the planar structure of phthalic acid lead oxide and lead cation of MLP, making them easily accessible to HCl.

The decreased HCl acceptability of MLS and MLC may be explained in terms of a screening effect of the long-chain acid residues that arises from their coiled conformation.⁴ As for the ability of these salts to retard de-

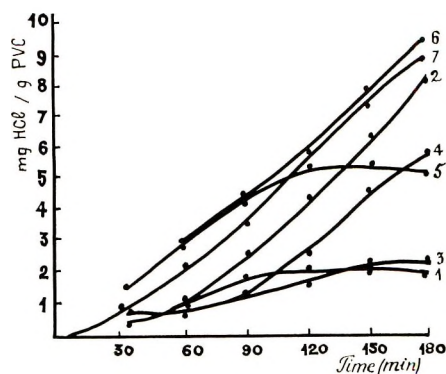


Fig. 1. Hydrogen chloride evolution from PVC in the presence and in the absence of additives (1.5% by weight of Pb): bound (1) and total (2) HCl in the presence of MLS; bound (3) and total (4) HCl in the presence of MLC; bound (5) and total (6) HCl in the presence of MLP; (7) PVC dehydrochlorination without additives.

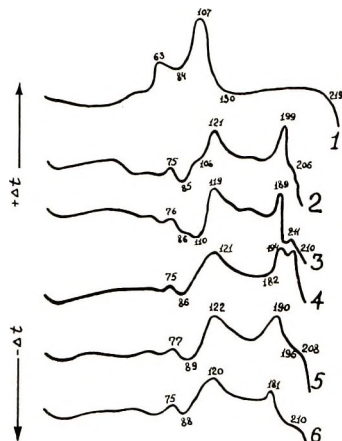


Fig. 2. Thermograms: (1) DPVC; (2) mixture of DPVC with 5% of: (2) monobasic lead sulfate; (3) MLS; (4) MLP; (5) dibasic lead phosphite; (6) tetrabasic lead sulfate.

hydrochlorination of PVC, it is believed that basic lead salts of stearic and caprylic acids, as well as the organic acids salts^{5,6} of Ba, Cd, and Zn, interact with labile Cl atoms in PVC with the formation of more thermostable ester groups. In the infrared spectrum of polymers, obtained by heating of PVC with MLS and MLC at 175°C for 90 min, there actually appeared an intensive absorption band at 1740 cm^{-1} , which corresponded to the ester group. In addition, the initial degradation temperature of the polymer obtained, after removal of the stabilizer, is much higher (171°C) than that of the original PVC (141°C).

In order to gain additional information concerning the stabilizing action of the organic-acid basic lead salts, the DTA method was used. The interaction of partly dehydrochlorinated PVC (DPVC), obtained by the reaction

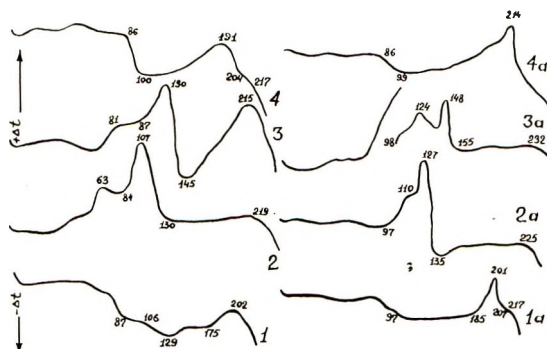


Fig. 3. Thermograms of DPVC, obtained by dehydrochlorination of PVC in the presence of: (1) sodium methylate; (2) sodium ethylate; (3) sodium butylate; (4) by thermal degradation in the presence of $ZnCl_2$; (1a), (2a), (3a), (4a) same as (1), (2), (3), (4), but with 5% TLS.

of PVC with sodium ethylate and containing 48% chlorine, with MLP, MLS, and other basic lead salts was studied. From the data obtained (Fig. 2) it appears that the DPVC thermogram up to $\sim 100^\circ C$ has a character similar to that of PVC.⁷ The observed endothermal effect in both polymers at $70\text{--}100^\circ C$ may be connected with the intensification of the chemical processes during the transition from glassy to the rubber-like state, i.e., when sufficient segmental mobility of macromolecules is realized. Above $100^\circ C$, DPVC differs from PVC in that it gives a single exothermal effect, with maximum position at $105\text{--}130^\circ C$, which may be connected with the transformation of the oxidized groups of this polymer.¹ The addition of 5% by weight of basic lead salts to DPVC cause additional exothermal effects with maxima at $180\text{--}210^\circ C$. In accordance with the previous findings¹ it can be concluded that these exothermal effects were in line with the formation of complex compounds between the basic salts and DPVC. Normal lead salts did not display such effects during the reaction with DPVC. Different values of the exothermal effects with various lead salts may be explained by the influence of the anions structure upon the reactivity of the salts. It is worth notice that the exothermal effect caused by DPVC interaction with the basic lead salts often appears not as a single peak but as a double one or as a peak with a shoulder. This phenomenon may be explained in terms of the structure heterogeneity of the DPVC macromolecules. Owing to this heterogeneity, the various groups in DPVC that react with the basic lead salts differ in their reactivity.

In addition, the interaction of tribasic lead sulfate with DPVC samples obtained by dehydrochlorination of PVC in the presence of sodium methylate, ethylate, and butylate, and also by the thermal dehydrochlorination of PVC in the presence of zinc chloride, was studied by the DTA method. These samples contained 54%, 48%, 35%, and 40% chlorine, respectively. On heating DPVC samples without a stabilizer, one exothermal effect was observed; the position of its maximum changed (Fig. 3), depending on

the conditions of PVC treatment. In the study of mixtures of the above-mentioned DPVC samples with tribasic lead sulfate (TLS), the additional exothermal effects were always observed, which indicated DPVC interaction with basic lead salts regardless of the method of DPVC preparation.

The possibility of complex formation between basic lead salts and the reactive PVC groups was checked on a model compound, 1,3-pentadiene. This compound, together with MLC, was stirred in an open vessel (in the presence of air) at room temperature for 10 hr. The residue was removed from the reaction mixture by freezing out (-25°C) with further filtration, and then the volatile products were distilled off under vacuum at room temperature. After washing with benzene, a tough, bright-yellow product containing 30–34% lead was obtained, which fused at $115\text{--}130^{\circ}\text{C}$ with flashing. The infrared spectrum of this product differed from that of the starting compounds: 1,3-pentadiene gives intensive absorption bands at 1660 cm^{-1} and 1610 cm^{-1} , and MLC gives a strong absorption band at $1530\text{--}1560\text{ cm}^{-1}$. With their interaction product, the absorption band at 1610 cm^{-1} was not observed and at 1660 cm^{-1} was weak, but a strong position at $1530\text{--}1560\text{ cm}^{-1}$ was maintained. In the course of treating the mixture of 1,3-pentadiene and a normal caprylic acid salt under identical conditions, no colored interaction products were obtained.

Thus, from the foregoing it is apparent that, under the conditions of the PVC processing, the basic lead salts accept the HCl evolved during the degradation of macromolecules; this is well in accordance with prior data. However, it may be considered that color stability depends mainly on the complex-forming reaction between stabilizer and the partly decomposed polymer and not on HCl acceptance.

References

1. E. N. Zilberman, A. E. Kulikova, S. B. Meiman, N. A. Okladnov, V. P. Lebedev, *High Molec. Comp. USSR*, **11A**, 1512 (1969).
2. L. H. Wartman, *Ind. Eng. Chem.*, **47**, 1013 (1955).
3. M. Tokarzewska and L. Tokarzewski, *Plaste Kautschuk*, **9**, 230 (1962).
4. M. S. Newman, Ed., *Steric Effects in Organic Chemistry*, New York, 1960.
5. A. H. Frye and R. Horst, *J. Polym. Sci.*, **45**, 1 (1960).
6. W. I. Bengough and M. Onozuka, *Polymer*, **6**, 625 (1965).
7. V. P. Lebedev, N. A. Okladnov, and M. N. Shlikova, *Plastics USSR*, **N4**, 8 (1968).

Received November 26, 1969

Revised March 3, 1970

Ethylene Polymerization Catalysis over Chromium Oxide

J. P. HOGAN, *Research and Development Department, Phillips Petroleum Company, Bartlesville, Oklahoma 74003*

Synopsis

A study of the nature of polymerization catalysis over CrO_3 -silica and of the nature of the polyethylene obtained is presented. A fixed surface chromate (or possibly dichromate) species was shown to be activated for polymerization by an oxidation-reduction reaction with the monomer or with other reactive compounds such as CO. A change in catalyst color from orange to blue occurred simultaneously, and an indigo-blue color was present only during ethylene addition, indicating involvement of Cr d orbitals. A spectacular chemiluminescence, due to excitation of oxygen, occurred when CO-treated catalyst was exposed to air. Active site population and the rate at which each site produced polymer molecules were calculated. A reaction mechanism compatible with the experimental data is depicted.

INTRODUCTION

The chromium oxide polymerization catalysts of Phillips Petroleum Company¹⁻⁴ have been the object of an almost world-wide investigation during recent years, as evidenced by published literature. Conflicting views of the nature of the catalytic site have come out of research approaches ranging from wet chemistry to electron spin resonance. The chemistry of chromium was occasionally neglected and sometimes almost repealed. The present paper presents some studies which we have made over a number of years of the nature of the catalysis and the polyethylene obtained. Emphasis is to be placed first on the chemical nature and reactivity of the chromium(VI) compound which is an essential part of the activated catalyst.¹

RESULTS AND DISCUSSION

Catalyst Composition

The high-temperature chemistry of chromic anhydride (CrO_3) which has a melting point of only 196°C , should be considered first. Figure 1 presents the results of a thermogravimetric analysis run on bulk CrO_3 in a dry air atmosphere, the temperature being increased at a rate of $10^\circ\text{C}/\text{min}$. It is seen that oxygen loss begins at about 255°C and occurs in three definite stages. Calculations from weight losses give empirical formulas

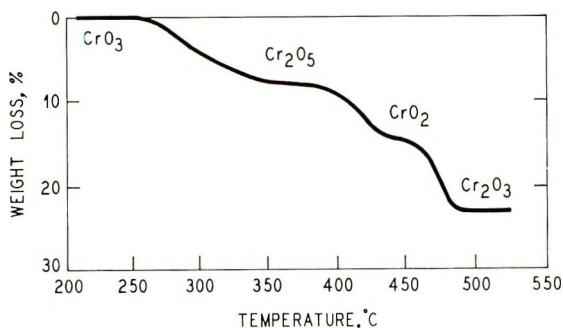


Fig. 1. Thermogravimetric analysis of CrO_3 . Dry air atmosphere; rate of temperature increase, $10^\circ\text{C}/\text{min}$.

corresponding fairly well to Cr_2O_5 , CrO_2 , and Cr_2O_3 for these three stages. It is noted that pure CrO_3 is unstable at high temperature even in air and is converted to Cr_2O_3 at a temperature well below 500°C .⁵

Chromium oxide polymerization catalysts can be prepared by dry mixing or nonaqueous impregnation but are readily made by impregnation of silica-alumina or silica with an aqueous solution of a soluble chromium compound such as CrO_3 . Following drying, the finely divided catalyst is normally activated by fluidizing in air at 500 – 1000°C for several hours. It is then stored in dry air or nitrogen.

Some catalysts which were prepared by a standard aqueous impregnation and then activated in air are shown in Tables I and II.

From Table I it can be seen that at a loading of 1–5% Cr on silica, the CrO_3 is well stabilized at Cr(VI). However, at higher loadings, a large percentage of the CrO_3 is converted to Cr_2O_3 at 540°C . In the presence of wet air, there is a sharp increase in conversion to Cr_2O_3 , even at the lower

TABLE I
Chromium Oxide-Silica Catalysts

Activation conditions ^a		Catalyst after activation	
Temp, $^\circ\text{C}$	Air	Total Cr, wt %	Cr(VI), % of total Cr ^b
540	Dry	0.96	93
540	Dry	2.46	94
540	Dry	4.91	94
540	Dry	11.8	57
540	Wet ^c	2.46	81
540	Wet ^c	4.91	33
800	Dry	0.99	85
800	Dry	2.45	87
800	Dry	5.03	65

^a Silica catalysts activated 5 hr at temperature in air as shown.

^b Determined independently by solubility and by reaction with Fe^{++} .

^c Saturated with water vapor at 38°C .

TABLE II
Chromium Oxide-Silica-Alumina Catalysts

Activation conditions ^a		Catalyst after activation	
Temp, °C	Air	Total Cr, wt-%	Cr(VI), % of total Cr
540	Dry	0.94	93
540	Dry	2.49	90
540	Dry	4.99	81
540	Dry	10.1	55
540	Wet	0.99	80
540	Wet	2.39	21

^a Silica-alumina (88/12) catalysts activated 5 hr in air as shown.

loadings. At 800°C in dry air, an appreciably higher conversion to Cr₂O₃ occurs at 5% Cr loading than at 540°C.

From Table II it can be seen that the same principles apply when silica-alumina is the support, although stabilization of CrO₃ at Cr(VI) appears to be less efficient on silica-alumina. As Cr loading is increased from 1 to 5% the increase in percentage of Cr₂O₃ is apparent from a change in color of the catalyst from orange to green. Catalysts activated in wet air also tend to be green, illustrating the high percentage of Cr₂O₃ in these catalysts.

These data suggest several important points: (1) high Cr loading causes conversion of CrO₃ to Cr₂O₃ because a larger fraction of the CrO₃ can act as bulk CrO₃ does; (2) high activation temperature increases mobility of CrO₃, increasing the reaction: $2\text{CrO}_3 \rightarrow \text{Cr}_2\text{O}_3 + 1\frac{1}{2}\text{O}_2$; (3) CrO₃ reacts with the silica to become a fixed surface compound. This accounts for the ability of silica to stabilize Cr(VI) at temperatures far above its normal decomposition temperature. It further explains the adverse effect of

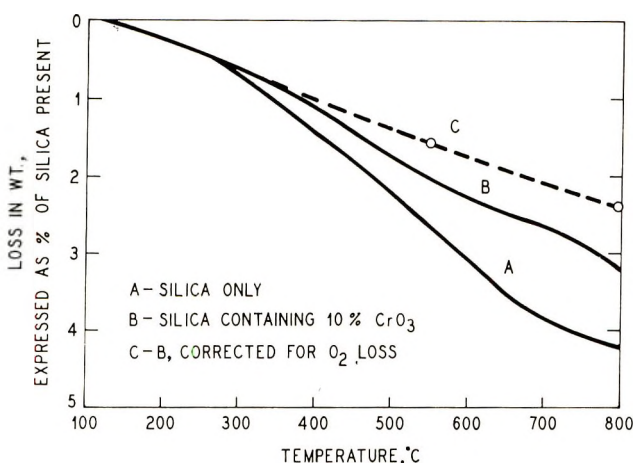
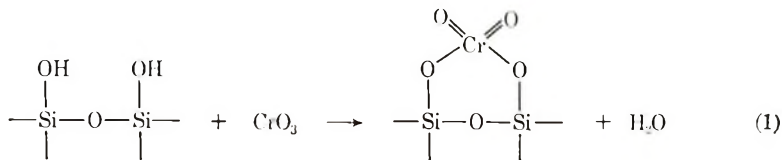


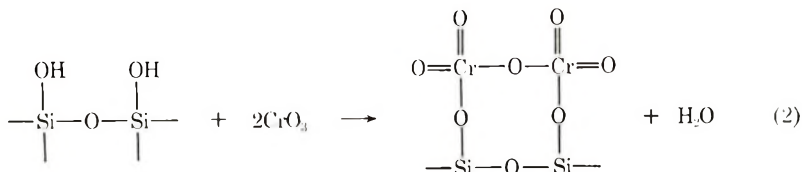
Fig. 2. Thermogravimetric analysis of silica and catalyst: (A) silica alone; (B) silica containing 10% CrO₃; and (C) curve B corrected for loss of oxygen from CrO₃.

moisture which prevents the formation of a fixed surface compound. This reaction is limited to certain definite sites, since a limited amount of CrO_3 can be stabilized.

At $600 \text{ m}^2/\text{g}$ surface area and about 5% Cr stabilized as Cr(VI) (Table I), we have an average distance between adjacent Cr(VI) atoms of 10 \AA . This turns out to be about the accepted population of silanol groups on a typical silica surface after calcination at 500°C . The formation of a surface chromate by reaction between CrO_3 and silanol is thus reasonable.



Formation of dichromate is also to be considered [eq. (2)].



To shift the equilibrium of eq. (1) or (2) to the right, all one has to do is raise the temperature and remove the water with dry air as it is formed. The reaction may be shifted to the left at any temperature by an excess of water. This occurred in the experiments in which wet air was used (Tables I and II); the reaction could not go completely to the right, so bulk (unreacted) CrO_3 on the surface decomposed to Cr_2O_3 and oxygen as in Figure 1. The water did not act as a reducing agent. Another example of shifting the reaction to the left is the easy removal of the Cr(VI) from an activated catalyst by washing with water.

If surface chromate or dichromate forms as indicated above, it should be possible to verify this reaction, and also to determine whether chromate or dichromate formation is favored, by measuring water that may be given off when CrO_3 reacts with silica. If chromate is formed, one mole of water should be released per mole of CrO_3 present; dichromate formation should result in $1/2$ mole of water per mole CrO_3 . Two different experiments were designed, and both studies showed quite clearly that surface chromate is formed at first, although conversion of chromate to dichromate at higher temperatures is not necessarily excluded.

In one experiment, silica was wetted with water and then dried at 150°C to constant weight. It was then wetted with a solution containing a known amount of CrO_3 and again dried to constant weight. Repeated experiments, with appropriate controls, were made which showed that for each mole of CrO_3 present, slightly more than one extra mole of water was released from the silica.

In the other experiment, samples of silica and of identical silica containing 10% CrO_3 were examined by thermogravimetric analysis. The samples were held at 120°C until a constant weight was obtained with dry air flush. Then the temperature was increased $2.5^\circ\text{C}/\text{min}$ until a temperature of 800°C was reached, air flush being continued. Figure 2 presents the results of this experiment. Weight loss is expressed as per cent of the weight of silica present in the sample. The sample containing CrO_3 (curve *B*) lost less weight than the pure silica sample (curve *A*), even though CrO_3 certainly gave up some oxygen as temperature was increased. By correcting for the expected loss of oxygen by the CrO_3 present (data on 5% Cr catalysts, Table I), curve *C* was obtained. The difference between curves *A* and *C* can be accounted for only by a difference in bound water content at 120°C . This difference is about constant above 700°C and amounts to approximately 1.8%. The calculated difference expected, based on eq. (1), is 2%. [It cannot be argued that the CrO_3 displaced free water instead of bound (silanol) water, since curves *A* and *B* moved apart only at a temperature well above that at which free water remains.]

We thus have a Cr—O—Si bond in surface chromate (and possibly dichromate) structure which accounts on the one hand for the stability, at temperatures well above 800°C , of Cr(VI) which is normally unstable at 450°C . On the other hand, it accounts for the easy recovery of CrO_3 from the catalyst with water leaching at room temperature. Both these phenomena are compatible with the chemistry of known chromates and dichromates.

The weight loss of 2.4% shown by curve *C* of Figure 2 was water, coming largely from silanol groups which were not involved in a reaction between CrO_3 and silica. Removal of silanols increases polymerization activity.

Chemical Reactivity of Cr(VI) on a Silica Surface

The well known ability of CrO_3 to act as a strong oxidizing agent in inorganic and organic reactions was observed to carry over into its chemistry as a surface species on the polymerization catalyst very early in our work. Contact with hydrocarbons at 100°C resulted in development of a green color in the catalyst, a decrease in average Cr oxidation state, and the formation of oxygenated organic compounds.

Some studies of chromium oxide-silica-alumina catalysts were performed in an apparatus depicted in Figure 3. The general procedure, which involves circulating a gas over a heated catalyst bed in a closed system and observing pressure changes in the system, was first reported by Hill and Selwood⁶ and later by Holm, Bailey, and Clark.^{7,8} For the apparatus shown here, a simple but powerful pump was designed, and the system was provided with a continuous pressure recorder, actuated by an aneroid bellows, which was capable of recording a 0.1% change in system pressure. The system was enclosed in a thermostated cabinet to avoid pressure changes from slight changes in room temperature.

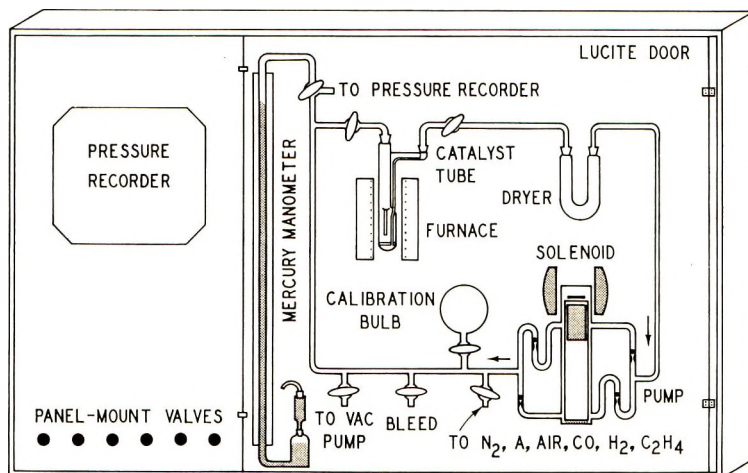


Fig. 3. Pyrex circulating system with magnetic pump.

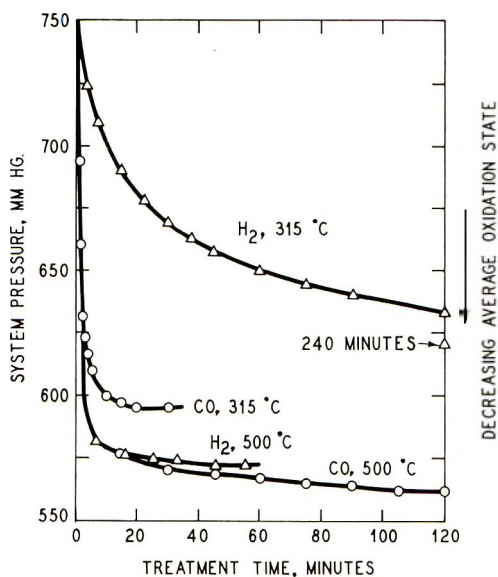


Fig. 4. Consumption of reducing gas vs. time at constant temperature with H_2 and CO treatments of 2.5% Cr. Silica-alumina catalyst activated at $540^\circ C$.

The temperature of the activated catalyst bed was slowly increased to determine onset of reaction, shown by a decrease in system pressure, when either hydrogen or CO was circulated through the catalyst and then passed through an adsorbent to remove water in the case of H_2 or CO_2 in the case of CO .

Surprisingly, CO began to be converted to CO_2 at a much lower temperature than H_2 began to react to produce water ($150^\circ C$ compared to $205^\circ C$). Having determined minimum temperature for reaction, studies

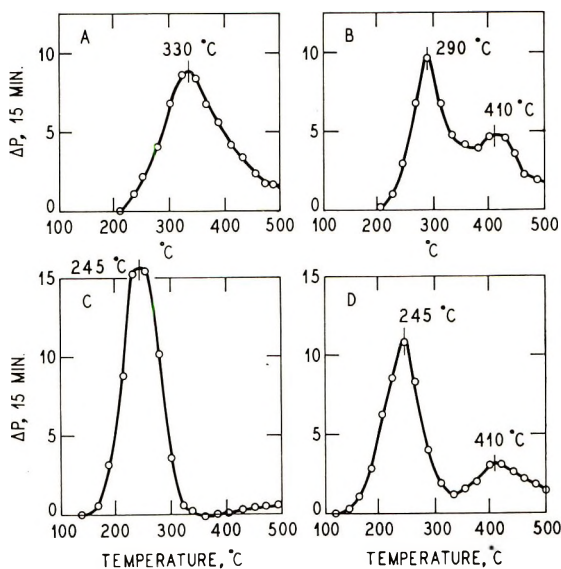


Fig. 5. Reduction profiles of $\text{CrO}_3\text{-SiO}_2\text{-Al}_2\text{O}_3$. Rate of gas consumption vs. temperature when temperature is increased at rate of $1.5^{\circ}\text{C}/\text{min}$: (A) H_2 gas, dry catalyst; (B) H_2 gas, catalyst containing 5% H_2O ; (C) CO gas, dry catalyst; and (D) CO gas, catalyst containing 5% H_2O . 2.5% Cr catalyst activated at 540°C .

were then made at higher, constant temperatures. Following control runs to establish that quantitative data on extent of reaction of metal oxides could be relied on and other experiments to determine reaction of CO and H_2 with unpromoted silica-alumina, data were obtained on CrO_3 -silica-alumina. (Decrease in system pressure was converted to volume of gas consumed, the system volume with catalyst in place at temperature having been previously calibrated.) Results are shown in Figure 4.

As shown in Figure 4, the rate of reaction at 315°C is much faster with CO than with H_2 , and final extent of reaction with CO is greater. At 500°C , rates of reaction are similar, although final extent remains greater with CO . The colors of H_2 -treated and CO -treated catalysts after cooling to room temperature in nitrogen were found to be quite different, being gray-green and blue, respectively.

What accounts for the difference in treatment with CO and H_2 ? In hydrogen treatment, water is formed. We have already shown that moisture causes hydrolysis of the Cr-O-Si bond; thus, treatment with hydrogen is accompanied by hydrolysis and formation of Cr_2O_3 , which is difficult to reduce. Treatment with CO produces only CO_2 , which does not cause decomposition of the Cr-O-Si surface species. The effect of the presence of excessive moisture during treatment is illustrated by Figure 5. The catalyst used in this study was activated at 540°C . Treatment was done in the apparatus shown in Figure 3 by increasing the temperature continuously at a rate of $1.5^{\circ}\text{C}/\text{min}$. The rate of decrease in system

pressure due to reaction was plotted against catalyst temperature. Shown in curve *A* is the treatment of a sample of the dry catalyst with H_2 ; curve *C* is for treatment of dry catalyst with CO ; in curves *B* and *D*, catalyst samples which were first exposed to moist air to add 5% moisture were treated with H_2 and CO , respectively. These curves show that the presence of an excess of moisture causes a two-stage reaction to occur, even with CO . That is, part of the $Cr(VI)$ is converted to Cr_2O_3 in the presence of moisture.

A blue color develops upon CO treatment followed by stripping with N_2 and cooling in N_2 . If the blue catalyst is evacuated at moderate vacuum and room temperature, the color changes immediately to light green. If nitrogen is readmitted, the color returns immediately to blue. However, if CO is admitted, the color is purple. Pumping with a good vacuum does not remove the CO as it does the N_2 , and the color remains purple. If the blue material is exposed to air at room temperature, a brilliant orange light emission occurs. This is demonstrated by permitting air to pass through a glass tube containing the blue catalyst. The color returns to the color of the catalyst before CO treatment. The warming is slight, so that this phenomenon is chemiluminescence of a rather spectacular sort. The emission produces a very sharp peak at about 6158 \AA on a monochromator. Emission spectra tables show that, of the elements present (Cr , Si , Al , N , O), only oxygen produces a significant line (at 6158.2 \AA) of major intensity in this region.

Detailed Studies of CO -Treated Catalyst

Silica catalyst containing 1% Cr was activated at $800^\circ C$, CO -treated at $425^\circ C$, and flushed with N_2 at $425^\circ C$ until all CO was removed. It was then cooled to room temperature in N_2 . The color was blue, as stated earlier. It was then divided into two portions in a nitrogen atmosphere in stopcock-equipped Pyrex flasks. Each flask was evacuated to constant weight, being heated to complete the removal of N_2 . The color was light green, as stated earlier. CO was then admitted at room temperature to one of the flasks. An immediate color change to purple occurred. Upon re-evacuation to constant weight, the catalyst remained purple. The weight gain was determined and was found to amount to 0.0408 g, or 1.45 mmole CO . The sample of catalyst weighed 7.475 g and contained, by analysis on the catalyst before CO -treatment, 1.08% total Cr . Thus, the quantity of $Cr = 7.475 \times 1.08/52 = 1.55$ mmole. The ratio of CO adsorbed to Cr is thus approximately 1/1. This much CO is complexed tightly enough to be stable under vacuum at room temperature (Experiments have shown that a significant amount of CO is not held on the catalyst at $425^\circ C$.)

Ethylene gas was now admitted, at room temperature, to the evacuated flask containing the purple, CO -complexed catalyst. An immediate change in color to indigo-blue occurred. After several minutes contact with ethylene at 1 atm in the flask, the flask was again evacuated to constant

weight. Some fading in color occurred, but the catalyst remained blue. A weight gain of only 0.006 g had occurred. Thus, no polymerization had occurred, the slight gain in weight probably being accounted for by the incomplete evacuation of ethylene adsorbed on the silica surface. Ethylene was now readmitted, and polymerization was now rapid, as evidenced by the large amount of heat liberated. The color was a deeper indigo during polymerization but faded again when the flask was evacuated to remove all gaseous ethylene. Weighing showed that 0.4 g of polymer had been produced in a very short time. A drop or two of water was then slowly admitted to the evacuated flask, where it quickly flashed and caused a change in color from indigo-blue to pink. Addition of more water changed the color to light blue, which remained even in the presence of liquid water as long as air was excluded. The vapor phase above the catalyst, after addition of water, was analyzed and was found to contain a small amount of ethylene and higher olefins.

The second sample of CO-treated, evacuated catalyst was exposed to ethylene at room temperature without first being exposed to CO. In this case, an indigo-blue color developed immediately and polymerization was rapid. Still another example was exposed to a mixture of 75% ethylene and 25% CO. In this case, the indigo-blue color developed, but polymerization did not occur until the flask was re-evacuated and refilled with pure ethylene. If, instead, of readmitting ethylene, water vapor was added, then ethylene corresponding approximately to 1 mole per mole Cr was found in the gas phase in the flask. These experiments have indicated the following. (1) Addition of C_2H_4 to CO-complexed catalyst replaces CO at the primary coordination position, but CO in a secondary position blocks polymerization. (2) Re-evacuation readily removes this CO occupying a secondary position; one molecule of C_2H_4 remains complexed to each Cr atom. (3) Following re-evacuation, the catalyst will then polymerize ethylene if it is readmitted; the CO has been removed from the secondary position, and ethylene can add to the growing chain from this position. (4) When polymerization is stopped by pumping out the gaseous ethylene, the active sites remain. Addition of water vapor destroys the active sites and liberates ethylene or growing chains.

Reaction of Cr(VI) on Silica with Ethylene

Catalyst was activated in dry air at 800°C and degassed at 500°C and 1 μ pressure in the apparatus shown in Figure 3. After cooling, the catalyst tube was surrounded by a small water bath at 95°C in such a manner that it could be observed. Ethylene gas was then admitted to the catalyst. The orange color of the catalyst changed to indigo-blue, and polymerization as evidenced by rapid drop in system pressure and whitening of the catalyst by polymer occurred. The bed soon plugged.

If the degassed catalyst (at 95°C) was first exposed to CO, degassed, and then exposed to ethylene, the orange color remained and no polymer formed. But if it was heated to 300°C while being degassed, the ethylene

would then react at 95°C to change the color, and polymerization would occur.

Oxygenated compounds of the type formed by reaction of hydrocarbon with Cr(VI) are temporary catalyst poisons if added to the reactor at concentrations calculated to be present at initiation, and cause perhaps a 50% reduction in reaction rate for a few minutes. Thus, oxygenated compounds formed during initial reduction of Cr(VI) may help to account for the lower starting polymerization rate that is sometimes observed. Pretreatment of the catalyst with CO reduces formation of oxygenated compounds and permits much faster initiation.

Reaction Mechanism

A description of what the catalyst appears to be like when polymerization starts has already been presented. Other information which is quite pertinent to the question of polymerization mechanism is as follows.

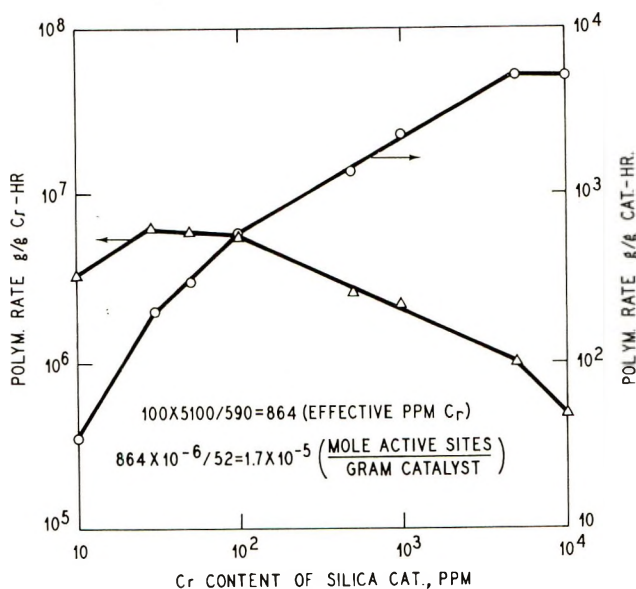


Fig. 6. Effect of Cr concentration on polymerization rate.

The polyethylene produced has a vinyl group at one end and a methyl group at the other end of a long, unbranched chain of methylene groups: $\text{CH}_2=\text{CH}-(\text{CH}_2-\text{CH}_2)_n-\text{CH}_2-\text{CH}_3$.

Chain termination, re-initiation, and growth is rapid, and molecular weight is primarily a function of reaction temperature.

Polymer molecular weight is decreased by addition of hydrogen⁹ or addition of α -olefin, which produces short branches and some branched-vinyl unsaturation.⁴

Acetylene is converted cleanly to benzene at high rates over this same catalyst.¹⁰ This indicates space for simultaneous coordination of three acetylene molecules around a single Cr site.

Molecular configuration was determined by infrared analyses. The information on chain growth and termination was obtained by the following methods. To calculate termination frequency, it is necessary to know the number of active sites and the number of polymer molecules produced in a given time.

Two independent methods were used to arrive at the number of active sites. By varying the Cr concentration on silica and using the resulting catalysts for polymerization, the results shown in Figure 6 were obtained. It is seen that, at 30–100 ppm Cr loading, Cr efficiency was at a maximum, and it was assumed that each Cr atom was an active site. However, total catalyst efficiency improved up to about 0.5% Cr loading with this particular silica. To estimate the concentration of active sites on a 1% Cr catalyst the ratio of polymerization rates obtained with 1% Cr and 100 ppm Cr catalysts ($5100/590 = 8.64$) was multiplied by 100 ppm Cr: $8.64 \times 100 = 864$ ppm effective Cr. This gives $864 \times 10^{-6}/52 = 1.7 \times 10^{-5}$ mole/g active Cr sites. This value should be conservative, since diffusion rate and other factors may begin to limit polymerization rate rather than number of active sites at high Cr loading. (The apparent decrease in Cr efficiency with increase in concentration may also be due in part to chromium oxide clumping on the surface.)

TABLE III

Catalyst present in reactor, g	Triethylamine added, mole	Decrease in C ₂ H ₄ flow rate, %	Active Sites, mole/g
0.0707	7.7×10^{-7}	32	3.4×10^{-5}
0.0745	1.5×10^{-6}	63	3.2×10^{-5}

The second method of estimating number of active sites was to inject a measured amount of catalyst poison into a polymerization reactor going at maximum rate (with 1% Cr catalyst) and accurately to determine the per cent decrease in reaction rate by means of the ethylene rotameter (pressure and temperature being held constant). A strongly polar, hydrocarbon-soluble, monofunctional molecule must be used to ensure some degree of poisoning permanence and to prevent poisoning more than one site per molecule of poison. Triethylamine proved to be the best of several compounds tested. It was assumed that one active site was poisoned per molecule of triethylamine added and that the percentage of catalyst sites poisoned was proportional to the decrease in ethylene flow rate. An average value of 3.3×10^{-5} mole of active sites per gram of catalyst was obtained as shown in Table III.

This method might be expected to give values which are slightly high because of the possibility of some triethylamine being adsorbed at non-active sites.

The relatively good agreement (1.7×10^{-5} and 3.3×10^{-5} mole/g) between these two independent methods was surprising. An average value of 2.5×10^{-5} mole/g will be assumed, being in excellent agreement with the value of 2.7×10^{-5} mole/g obtained by Clark et al. using a different method¹¹ and 3×10^{-5} mole/g obtained by Eden et al. with the use of a site-poisoning method only.¹²

Chain termination frequency was now calculated as follows:

$$\begin{array}{rcl} \text{Wt. polymer, g/hr/g catalyst (from Fig. 6)} & = & 5,100 \\ \text{Number-average molecular weight } (\bar{M}_n) & = & 20,000 \\ \text{Polymer, mole/hr/g catalyst} & = & \frac{5,100}{20,000} = 0.25 \end{array}$$

$$\text{Polymer molecules produced/sec/active site} = 0.25 / (3600 \times 2.5 \times 10^{-5}) = 2.8$$

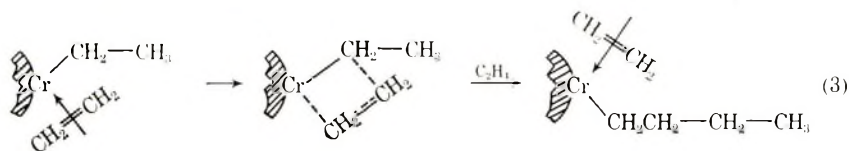
$$\text{Monomer addition rate} = 2.8 \times 20,000 / 28 = 2,000 \text{ molecules/sec}$$

It is obvious that the time required for termination of a growing chain and initiation of a new one is of necessity quite small.

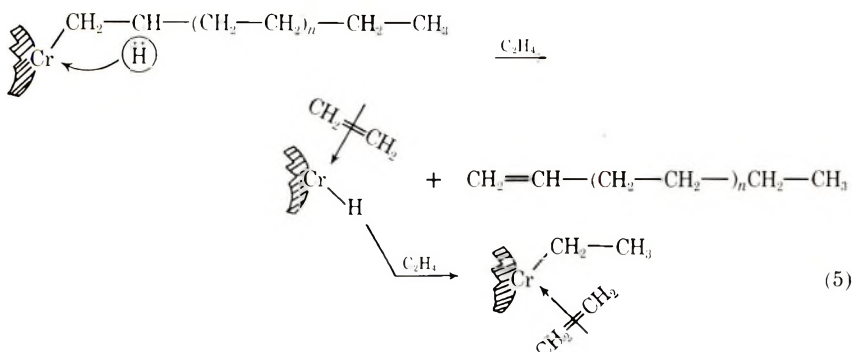
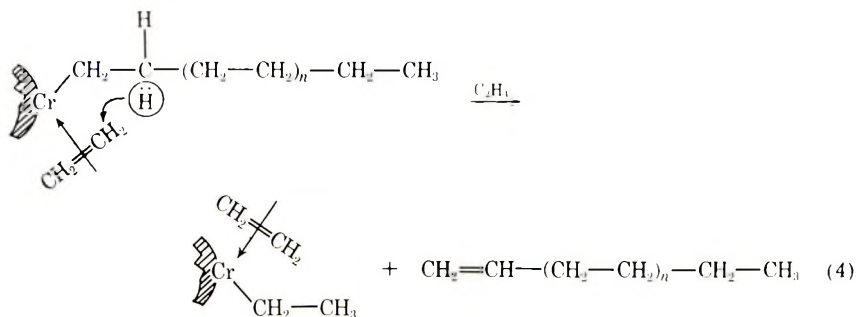
An ethylene polymerization mechanism, compatible with the foregoing facts, is now proposed. The catalyst, after activation, contains a Cr(VI) oxide species which can be represented as a silyl chromate surface compound having Cr-O-Si bonds which fix the Cr atom on the surface. Upon contact with ethylene, the inevitable oxidation-reduction reaction, characteristic of Cr(VI), occurs. The resulting oxygenated organic compounds are readily displaced from the Cr by the preponderance of ethylene, and a Cr-ethylene complex forms. In the presence of excess ethylene, a deep indigo-blue complex, indicating the presence of at least two ethylenes, forms, and ethylene polymerization proceeds. The color changes are an indication of the involvement of Cr *d* orbitals with ethylenic π orbitals.

Initiation of polymerization must be accompanied with the gain of a hydride ion to account for the methyl group at one end of each polymer molecule. It will be shown later that the vinyl group probably results from termination, not initiation as has been proposed elsewhere.¹³ To say that the first hydride ions comes from the "refuse" of the oxidation-reduction step would be convenient if one forgets that CO-treated catalyst is even faster in initiation. It has been customary in the past to obtain the first required hydrogen ion in similar situations by various contortions, or to ignore the problem completely. The latter course is selected as preferable for the time being; it is entirely conceivable that the first polymer molecule produced at a site does not have a methyl group at one end. Several thousand more molecules produced at the same site in a typical run would so dilute the initial, nontypical molecule that it can be ignored.

Polymer growth can be pictured in eq. (3) (the source of the methyl group being shown later):



Termination of the growing chain may occur by hydride-ion transfer [eq. (4) or (5)].



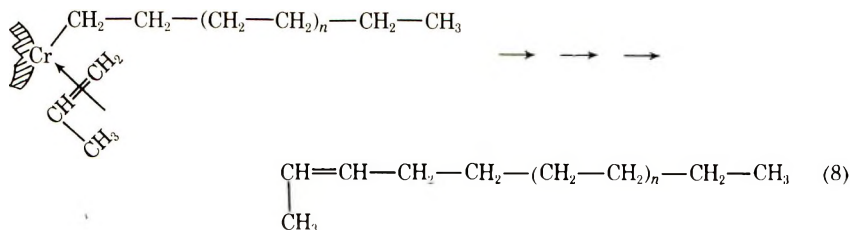
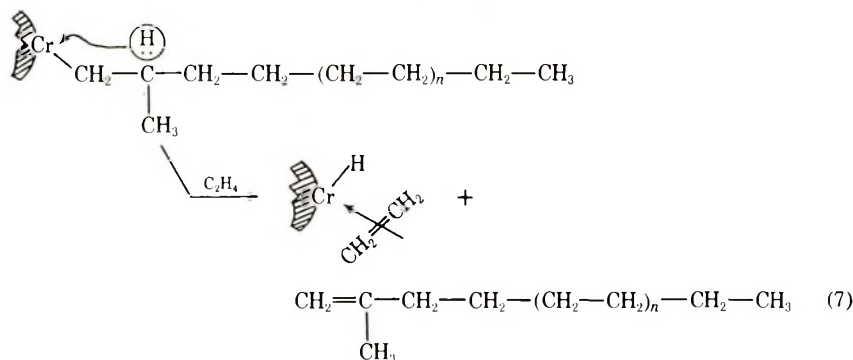
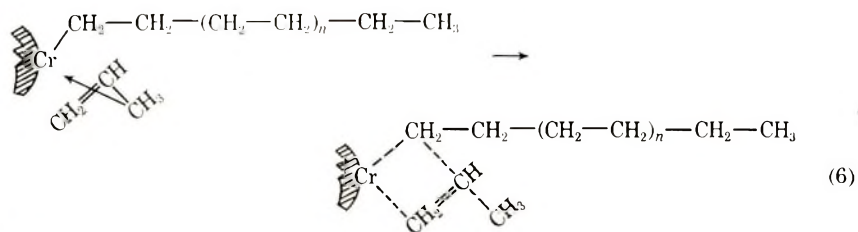
Transfer of hydride to the active site instead of to the monomer [eq. (5)] is a possibility. In either case, the methyl group on the starting end and the vinyl group on the terminating end are being accounted for.

As stated earlier, hydrogen added to the system results in a lowering of molecular weight. Vinyl unsaturation is not significantly decreased, so it must be assumed that hydrogen acts in some way other than hydrogenation to shorten chain length. Deuterium was used in place of hydrogen to modify molecular weight, and it was found that deuterium appeared in the polymer. Differential infrared spectra showed definite absorptions at 2173 and 2138 cm^{-1} , assigned to $-\text{CH}_2\text{D}$ and $-\text{CHD}-$ stretching, respectively. Since the vinyl group remained, these groups did not come from deuteration of the double bond. The $-\text{CHD}-$ could be accounted for by H-D exchange, since some HD could be found in the effluent, but H-D exchange could not very well account for the prominent $-\text{CH}_2\text{D}$;

there is only one methyl group per 1000 $-\text{CH}_2-$ groups. From this experiment, it is indicated that addition to monomer of hydride ion from the catalyst site [eq. (5)] instead of directly from the terminating chain is dominant. In the presence of deuterium, exchange between the $\text{Cr}-\text{H}$ and D_2 can result in $\text{Cr}-\text{D}$ and subsequent formation of $\text{Cr}-\text{CH}_2\text{CH}_2\text{D}$ when ethylene adds.

If an α -olefin is mixed with the ethylene feed, short branches are formed in the growing chain and branched vinyl unsaturation now appears, at a concentration high enough to indicate that α -olefin acts as a mild terminating agent.⁴ Lowered molecular weight is confirming evidence.

The addition of α -olefin to the growing chain and the formation of branched vinyl unsaturation is pictured as shown in eqs. (6) and (7) but not as in eq. (8).



The transfer of tertiary hydride (compared to transfer of secondary hydride where only ethylene is in the chain) can account for the increased termination rate (lowered molecular weight) brought about by the presence of α -olefin.

Finally, there is apparently some polarity in the Cr—R bond during polymerization, with the Cr positive with respect to the growing chain. In the addition of propylene, if the propylene is so oriented that the methyl group is attached to the carbon atom adjacent to the Cr site [eq. (8)], then termination after addition of propylene will give internal unsaturation, which is not found. Since the double bond carbon to which the methyl is attached is the more positive due to the electron-releasing effect of a methyl group,^{14,15} the orientation required to account for branched vinyl unsaturation indicates that Cr is more positive than the growing chain.⁴

EXPERIMENTAL

Materials

Silica and silica-alumina used in catalyst preparation were finely divided materials obtained from commercial suppliers. These catalyst supports were impregnated with an aqueous solution of CrO₃, the quantity and concentration of the solution being just sufficient to convert the dry powder to a free-flowing slurry containing the desired amount of CrO₃. Following drying of this slurry to a free-flowing powder in an evaporating dish, the catalysts were calcined in air in a fluidized bed at the desired temperature and time.

Ethylene and hydrocarbon diluents used in polymerization studies were dried over activated alumina. Nitrogen used to blanket catalysts and polymerization equipment contained less than 10 ppm oxygen and was also dried over activated alumina.

Equipment

Thermogravimetric studies were done with a du Pont Model 900 differential thermal analyzer fitted with a disk cell.

Polymerization studies were made in a 2-liter stainless steel autoclave having a marine-type three-bladed stirrer turning at 350 rpm. Polymerization was done by suspending the catalyst in a paraffin hydrocarbon diluent and maintaining a constant pressure of ethylene on the reactor. Ethylene flowed automatically on demand to maintain a constant pressure. Ethylene concentration in the diluent was about 6 wt-%. The rate of ethylene flow was determined at all times by means of a calibrated rotameter and was confirmed at the end of the run by weighing the polymer. Operating temperature was in the vicinity of 100°C and the polymer was formed in granules in the reactor.

Data on polymerization rate and concentration of active sites were taken after polymerization rate had reached a plateau, usually about one hour after start. Injection of triethylamine into the reactor to obtain a partial kill of the reaction was done by sweeping a measured amount of very dilute triethylamine-hydrocarbon solution into the reactor with pure hydrocarbon and ethylene.

The writer is indebted to A. O. Frenzel for infrared work on identification of C-D bonds and to D. R. Witt and B. E. Nasser for assistance in several areas.

References

1. J. P. Hogan and R. L. Bank (Phillips Petroleum Co.), Belg. Pat. 530,617, January 24, 1955; U. S. Pat. 2,825,721, (March 4, 1958).
2. A. Clark, J. P. Hogan, R. L. Banks, and W. C. Lanning, *Ind. Eng. Chem.*, **48**, 1152 (1956).
3. A. Clark and J. P. Hogan, in *Polyethylene*, 2nd ed., A. Renfrew and P. Morgan, Eds., Interscience, New York, 1960, p. 29.
4. J. P. Hogan, in *Copolymerization* (High Polymers, Vol. XVIII), G. E. Ham, Ed., Interscience, New York, 1964, Chap. 3.
5. J. W. Mellor, *A Comprehensive Treatise on Inorganic Theoretical Chemistry*, Vol. XI, Longmans, Green, New York, 1931, p. 206.
6. F. N. Hill and P. W. Selwood, *J. Amer. Chem. Soc.*, **71**, 2522 (1949).
7. V. C. F. Holm, G. C. Bailey, and A. Clark, *Ind. Eng. Chem.*, **49**, 250 (1957).
8. V. C. F. Holm and A. Clark, *J. Catal.*, **11**, 305 (1968).
9. Solvay et Cie, Belg. Pat. 570,981, September 5, 1958.
10. A. Clark, J. P. Hogan, D. R. Witt, and W. C. Lanning, paper presented at Fifth World Petroleum Congress, 1959, Section IV, paper 26.
11. A. Clark, J. N. Finch, and B. H. Ashe, *Third Congress on Catalysis (Amsterdam, 1964)*, Vol. II, North-Holland Publishing Company, Amsterdam, 1965, p. 1010.
12. C. Eden, H. Feilchenfeld, and Y. Haas, *J. Catal.*, **11**, 263 (1968).
13. L. L. van Reijen and P. Cossee, *Discussions Faraday Soc.*, **41**, 277 (1966).
14. T. Alfrey, Jr., J. J. Bohrer, and H. Mark, *Copolymerization* (High Polymers, Vol. VIII), Interscience, New York, 1952, p. 224.
15. C. C. Price, *Discussions Faraday Soc.*, **2**, 304 (1947).

Received December 31, 1969

Revised March 3, 1970

Thermal Degradation of Copolymers of Styrene and Acrylonitrile. I. Preliminary Investigation of Changes in Molecular Weight and the Formation of Volatile Products

N. GRASSIE and D. R. BAIN,* *Chemistry Department, The University of Glasgow, Glasgow, W. 2, Scotland*

Synopsis

By the use of thermal volatilization analysis (TVA), 292°C was chosen as a suitable temperature for a preliminary experimental survey of the thermal degradation of styrene-acrylonitrile copolymers. TVA also indicated that there is no fundamental change in reaction mechanism as the acrylonitrile content of the polymer is increased from zero to 33.4% although there is a progressive increase in the rate of volatilization. The increase in the rate of volatilization over that of polystyrene is directly proportional to the acrylonitrile content of the copolymer. From the changes in molecular weight which occur during the reaction it is clear that the primary effect of the acrylonitrile units on stability is to cause an increased rate of chain scission, but there is a small proportion of "weak links" which are associated with the styrene units and which are broken instantaneously at 292°C. The number of monomer molecules liberated per chain scission, the zip length, is about 40 for polystyrene in the initial stages of degradation and decreases only to the order of 20 even in copolymer containing 24.9% acrylonitrile. Thus the unzipping process is not severely affected by the acrylonitrile units; this is borne out by the fact that acrylonitrile appears among the products in very much greater concentrations than from pure polyacrylonitrile. The proportion of larger chain fragments (dimer, trimer, etc.) also increases with acrylonitrile content.

INTRODUCTION

Copolymers are becoming increasingly important commercially. Sometimes it has been possible to exploit new or improved physical properties compared with those of the corresponding homopolymers. In these cases the monomers are usually both present in significant amounts as, for example, in styrene-butadiene, ethylene-propylene and vinyl acetate-vinyl chloride copolymers. On the other hand, trace concentrations of a second monomer are often used to confer enhanced stability on a commercial homopolymer.

It has become clear that the stability of copolymers can seldom be predicted accurately from the stabilities of the corresponding homopolymers,

* Present address: Air Force Materials Laboratory, Wright-Patterson Air Force Base, Dayton, Ohio, U. S. A.

and a recent series of papers¹⁻⁴ has demonstrated some of the ways in which comonomers may influence the stability of homopolymers either favorably or adversely. The work described in the present paper represents a continuation of this systematic study of copolymer stability. Styrene-acrylonitrile copolymers are themselves of commercial interest, but they also represent one of the major structures present in some of the acrylonitrile-butadiene-styrene (ABS) materials which are currently being exploited. It was formerly demonstrated how traces of styrene can influence the thermal degradation reaction which occurs in polyacrylonitrile.⁵ This and subsequent papers are concerned with the other end of the composition scale and deal principally with the influence of acrylonitrile on the depolymerization process which occurs in polystyrene.

EXPERIMENTAL

Preparation of Copolymers

Styrene (Forth Chemicals Limited) and acrylonitrile (Hopkins and Williams Limited) were purified by the standard method of washing with sodium hydroxide (5*M*) to remove inhibitor and with distilled water to remove alkali and dried successively over calcium chloride and calcium hydride. They were then degassed by the freezing and thawing technique under vacuum and twice distilled, the first time into a calibrated reservoir and the second time into the dilatometer in which the polymerization was to be carried out, which was then sealed off under vacuum. The purity of both monomers was checked by gas chromatographic methods, only single products being detected in each case.

The initiator, 2,2'-azobisisobutyronitrile (Kodak Limited), was purified by recrystallization from methanol.

Polymerizations were carried out at $60 \pm 0.1^\circ\text{C}$ to a maximum of 10% conversion. Sufficiently accurate estimates of conversion were obtained from the volume contraction in the dilatometer assuming that the values of 26.7% and 15.0% for the volume contractions for complete polymerization of acrylonitrile⁶ and styrene⁷ were additive in the copolymerizing mixture.

All copolymers (0.25-50% acrylonitrile) were soluble in the monomer mixture. All except the 50/50 copolymer (SA 9) were purified by precipitating three times, twice by methanol (Analar) from toluene (Analar) solution and finally by methanol from dioxane solution, the latter giving a polymer which is more readily ground to a fine powder. SA 9, which, like polyacrylonitrile, is insoluble in toluene, was similarly precipitated by methanol from acetone (Analar) solution. Polymers were finally ground, passed through a 40-60 mesh sieve, and heated to 50°C in a vacuum oven for 48 hr to remove last traces of solvent. For the calculation of the molar ratio of monomers necessary to produce a copolymer of the required composition the following reactivity ratios were used:⁸ $r_{\text{styrene}} = 0.41$, $r_{\text{acrylonitrile}} = 0.04$.

TABLE I
Copolymer Data

Copolymer	Composition		Molecular weight	Initiator, % (w/v)
	Styrene, mole-%	Acrylonitrile, mole-%		
PS 3	100	0	470 000	0.03
SA 4	99.75	0.25	347 000	0.03
SA 2	99.0	1.0	370 000	0.03
SA 7	95.3	4.7	857 000	0.03
SA 8	95.3	4.7	331 000	0.06
SA 3	91.7	8.3	411 000	0.03
SA 6	84.5	15.5	470 000	0.03
SA 5	75.1	24.9	650 000	0.03
SA10	66.6	33.4	366 000	0.06
SA 9	50	50	—	0.06

Initiator concentrations were chosen in order to give a series of copolymers within as narrow a molecular weight range as possible in order to ensure that any effect of molecular weight was minimized on comparing the degradation behavior of the various copolymers. Composition and molecular weight data for materials mentioned in this and the following two papers^{9,10} are presented in Table I.

Degradation Experiments: The Molecular Still Technique

A modified form of the Grassie and Melville¹¹ molecular still was used for measuring rates of volatilization and for studying changes in molecular weight under isothermal conditions. The principal modification compared with previous forms of the apparatus concerned the use of an improved proportional temperature controller which minimized the "heating up" and "cooling down" times and allowed the temperature of the degrading polymer to be maintained within $\pm 1^\circ\text{C}$ for long periods without attention.

The principal weakness of this form of degradation apparatus is revealed when a detailed product analysis is to be carried out as described in the following paper, since products volatile at the degradation temperature but involatile at ambient temperature become coated on the inside surfaces of the molecular still and are thus impossible to estimate quantitatively. This feature is particularly valuable, on the other hand, when, as in the present work, it is desirable to make a rapid estimate of the ratio of chain fragments to monomeric products. The monomer fragments are collected in a liquid nitrogen trap and estimated while the weight of chain fragments is given by the difference between the weight of monomers and the total loss in weight of the polymer.

Thermal Volatilization Analysis (TVA)

The technique of TVA, which is really an automated and temperature programmed form of the above molecular still, has been described by Mc-

Neill.^{12,13} Essentially the pressure which exists between the hot decomposing sample and a cold trap in a continuously pumped system is continuously monitored as the temperature is raised linearly (10°C/min). This pressure is a nonlinear measure of the rate of volatilization of the polymer.

Measurement of Molecular Weight

Molecular weights were measured at 25°C by using a Mechrolab 501 high-speed membrane osmometer with Cellophane 300 membranes and toluene as solvent. Typical osmotic plots are presented in Figure 1, from which it is clear that there is a constant slope for each polymer during degradation but the osmotic slope decreases as expected with increase in acrylonitrile content, since the solvent is becoming less "good." Since the 50/50 copolymer is insoluble in toluene, it is not surprising that the osmotic slope for SA 10 (33.4% acrylonitrile) is close to zero.

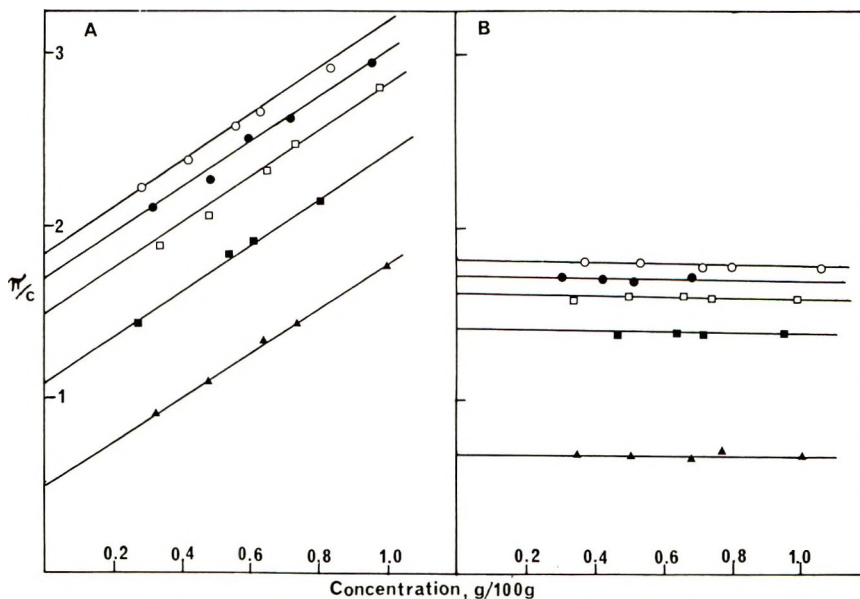


Fig. 1. Osmotic plots for (A) SA 6 and (B) SA 10, undegraded and degraded for various times, at 25°C: (▲) undegraded; (■) 3 hr; (□) 6 hr; (●) 8 hr; (○) 10 hr.

RESULTS

Preliminary TVA Studies

It has been found particularly useful in previous studies of this kind¹⁻⁴ to examine changes in molecular weight during reaction, rates of volatilization, and the chemical nature of the volatile products. Usually it has been appropriate to study the first two of these just below the threshold temperature for rapid volatilization so that changes in molecular weight may be studied uncomplicated, as far as possible, by volatilization and so that

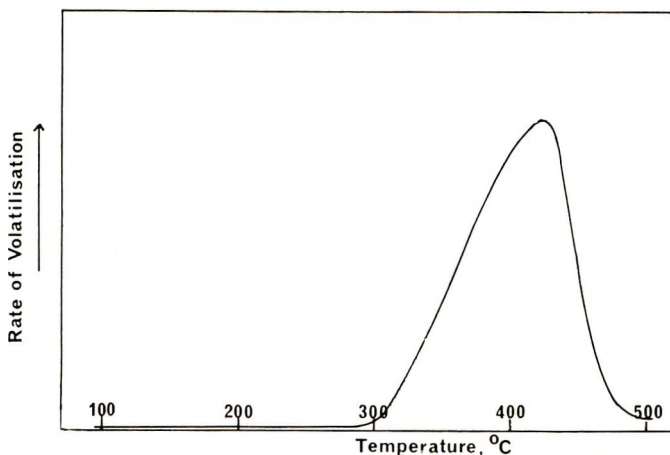


Fig. 2. TVA thermogram of SA 2.

initial rates of volatilization may be measured with high precision. TVA is particularly useful for making a rapid assessment of appropriate degradation temperatures.

A typical TVA thermogram is illustrated in Figure 2, from which a temperature of 292°C was chosen as appropriate at which to make a preliminary survey. It was also interesting to note at this stage that although the rate of volatilization appears to increase somewhat with the acrylonitrile content of the copolymer throughout the composition range from 0 to 33% acrylonitrile, the thermogram always consists of a single peak having, within experimental error, an invariant maximum at $426 \pm 3^\circ\text{C}$. Thus, although the slightly increased rate of volatilization suggests that acrylonitrile units introduce a degree of instability into polystyrene, the essential similarity of the shapes of the thermogram and the invariant maximum suggests that there is no fundamental change in reaction mechanism. The maximum for a 50% copolymer is considerably lower (405°C), but it is clear that this material, which must contain some acrylonitrile sequences of considerable length, exhibits both physical and chemical properties rather more akin to polyacrylonitrile than to polystyrene.

Volatilization-Time-Chain Length Relationships at 292°C

The results of degradations carried out at 292°C are presented in Table II. A plot of volatilization versus time is shown in Figure 3. The slopes of the straight lines represent the rates of volatilization, and Figure 4 demonstrates that the increase in the rate of volatilization over that of polystyrene is directly proportional to the acrylonitrile content of the copolymer.

Changes in average chain length with time are illustrated in Figure 5, from which it would appear that acrylonitrile units are causing an increased rate of chain scission in the copolymer. On the other hand, the chain

TABLE II
Degradation of Copolymers at 292°C

Copolymer	Time, hr	Volatilization, %	M_n $\times 10^{-5}$	CL $\times 10^{-3}$	CL , % of original	n $\times 10^3$	Average zip length	
PS 3 (0% AN)	0	0	4.70	4.50	100	0	—	
	1	2.2	1.49	1.43	31.8	0.46	48	
	3	3.3	1.22	1.18	26.2	0.60	55	
	4	4.5	1.02	0.98	21.8	0.75	60	
	6	7.6	0.86	0.83	18.4	0.91	84	
	10	13.8	0.57	0.55	12.2	1.35	102	
	12	15.3	0.62	0.60	13.3	1.19	129	
SA 4 (0.25% AN)	0	0	3.47	3.35	100	0	—	
	1	1.9	1.49	1.43	43.7	0.39	49	
	3	4.2	1.09	1.05	31.3	0.61	69	
	4	4.7	0.95	0.91	27.1	0.75	63	
	6	8.0	0.70	0.69	20.6	1.03	78	
	10	13.9	0.55	0.53	15.8	1.32	105	
	12	18.1	0.52	0.50	14.9	1.34	135	
SA 2 (1% AN)	0	0	3.70	3.58	100	0	—	
	1	1.9	1.39	1.34	37.4	0.45	42	
	3	3.8	0.88	0.85	23.7	0.85	45	
	4	5.7	0.88	0.85	23.7	0.83	69	
	6	6.7	0.76	0.74	20.7	0.98	68	
	10	11.8	0.61	0.59	16.5	1.22	97	
	12	18.9	0.51	0.49	13.7	1.37	138	
SA 8 (4.7% AN)	0	0	3.31	3.26	100	0	—	
	2	3.9	0.92	0.91	27.9	0.75	52	
	4	7.5	0.64	0.63	19.3	1.16	65	
	6	10.1	0.52	0.51	15.6	1.45	70	
	8	16.2	0.38	0.37	11.3	1.95	83	
	SA 3 (8.4% AN)	0	0	4.11	4.11	100	0	—
		1	3.1	1.02	1.02	24.9	0.71	44
3		7.1	0.53	0.53	12.9	1.51	47	
4		11.2	0.51	0.51	12.4	1.50	75	
6		16.7	0.38	0.38	9.3	1.95	86	
10.25		29.0	0.33	0.33	7.8	1.91	150	
SA 6 (15.5% AN)		0	0	4.70	4.89	100	0	—
	1	6.6	0.92	0.96	19.7	0.77	86	
	2	8.2	0.44	0.46	9.4	1.80	46	
	3	13.9	0.36	0.37	7.6	2.18	64	
	4	17.0	0.30	0.31	6.4	2.48	69	
	6	24.5	0.25	0.26	5.3	2.70	91	
	7	34.7	0.20	0.21	4.3	2.91	119	
	9.5	45.0	0.17	0.18	3.7	2.85	158	
	12	53.0	0.18	0.19	3.9	2.27	234	
	SA 5 (24.9% AN)	0	0	6.50	7.12	100	0	—
1		7.3	0.64	0.70	9.8	1.18	62	
3		20.3	0.33	0.36	5.1	2.07	98	
4		25.8	0.33	0.36	5.1	1.92	134	
6		43.2	0.21	0.23	3.2	2.33	185	
10		69.4	0.16	0.18	2.5	1.56	445	

length/volatilization relationships illustrated in Figure 6 are less dependent upon copolymer composition, although there is obviously a tendency for the amount of volatilization, for a given decrease in molecular weight, to decrease slightly with increasing acrylonitrile content of the copolymer.

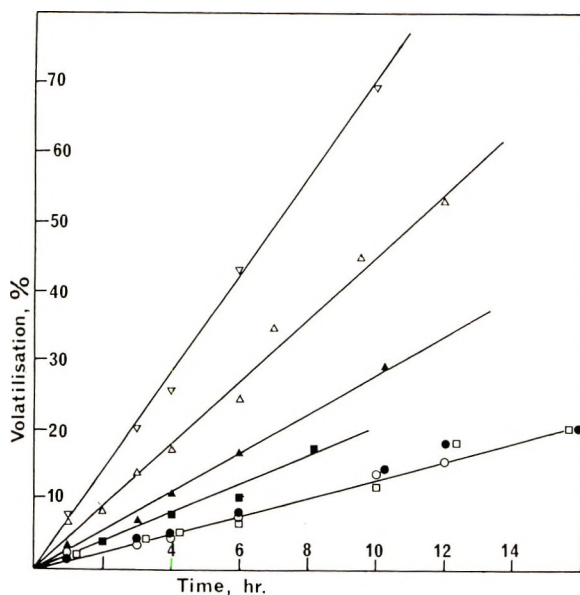


Fig. 3. Volatilization of copolymers of styrene and acrylonitrile at 292°C: (○) PS 3; (●) SA 4; (□) SA 2; (■) SA 8; (▲) SA 3; (△) SA 6; (▽) SA 5.

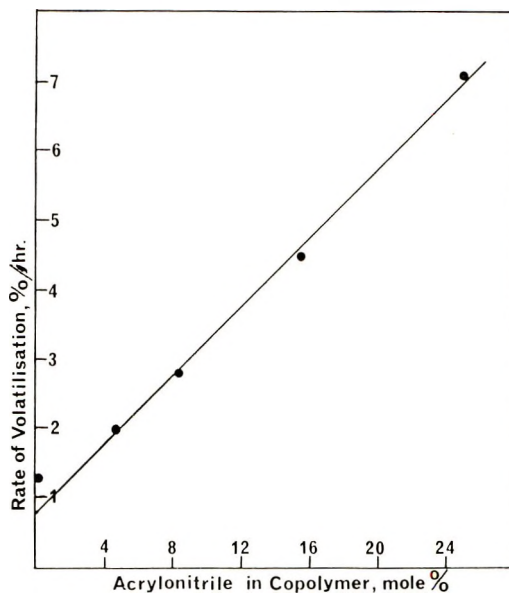


Fig. 4. Dependence of rate of volatilization at 292°C on the acrylonitrile content of copolymers of styrene and acrylonitrile.

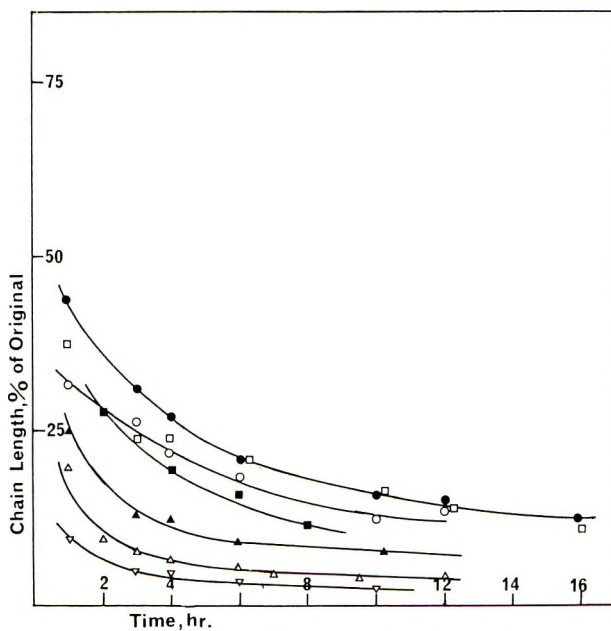


Fig. 5. Changes in molecular weight with time of degradation at 292°C of copolymers of styrene and acrylonitrile: (○) PS 3; (●) SA 4; (□) SA 2; (■) SA 8; (▲) SA 3; (△) SA 6; (▽) SA 5.

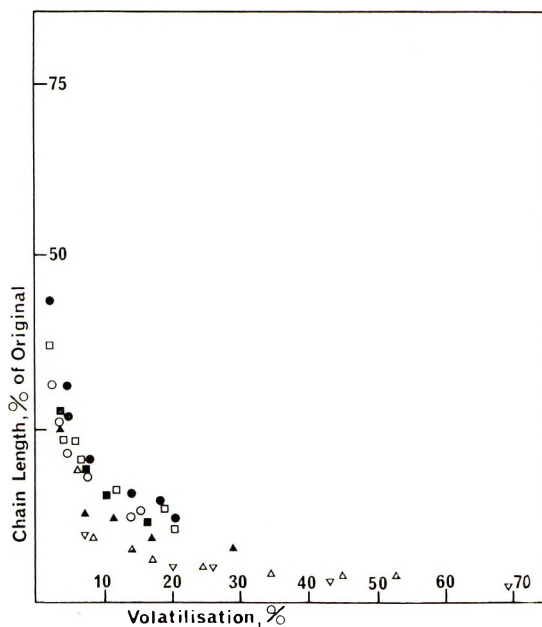


Fig. 6. Changes in molecular weight with volatilization of copolymers of styrene and acrylonitrile at 292°C: (○) PS 3; (●) SA 4; (□) SA 2; (■) SA 8; (▲) SA 3; (△) SA 6; (▽) SA 5.

Chain Scission-Volatilization Relationships

It has been shown previously⁴ that the number of chain scissions per unit length of chain (monomer unit) n is given by,

$$n = \frac{1 - x}{CL} - \frac{1}{CL_0} \quad (1)$$

in which CL_0 is the original chain length of the polymer and CL is the chain length when a fraction x has been volatilized. By using this equation, polymers of different initial molecular weights may be directly compared but the equation is only valid if polymer molecules are not being lost to the system by complete unzipping. Values of n obtained in this way are presented in the seventh column of Table II, and the time dependence of n is illustrated in Figure 7. The data for polystyrene and copolymers SA 4,

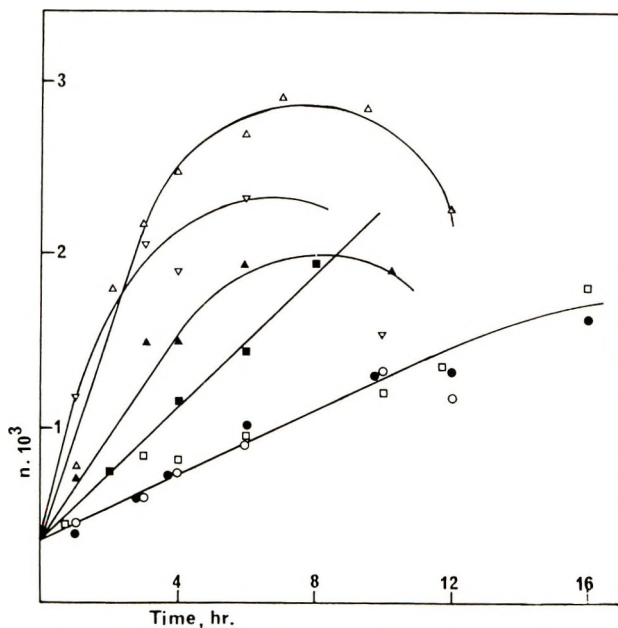


Fig. 7. Chain scissions per unit of chain length in copolymers of styrene and acrylonitrile at 292°C: (O) PS 3; (●) SA 4; (□) SA 2; (■) SA 8; (▲) SA 3; (△) SA 6; (▽) SA 5.

SA 2, SA 8, and SA 3 may reasonably be represented by straight lines, but the curvature, which becomes progressively more severe as the copolymers become richer in acrylonitrile, is undoubtedly due to the fact that molecules are being lost by complete unzipping. Two important features are revealed in Figure 7, however. Firstly, it is confirmed that the rate of chain scission increases with acrylonitrile content. Secondly, there is an intercept on the chain scissions axis which, at least for polystyrene, SA 4, SA 2, SA 8, and SA 3, is constant within experimental error. It suggests that a

proportion of weak links are present which are associated with the styrene units.

From the volatilization and chain scissions data in columns 3 and 7 in Table II, the average number of monomer units liberated per chain scission (the zip length) may easily be calculated. These are presented in the last column of Table II, and the relationship between average zip length and volatilization is illustrated in Figure 8. The tendency for zip length to

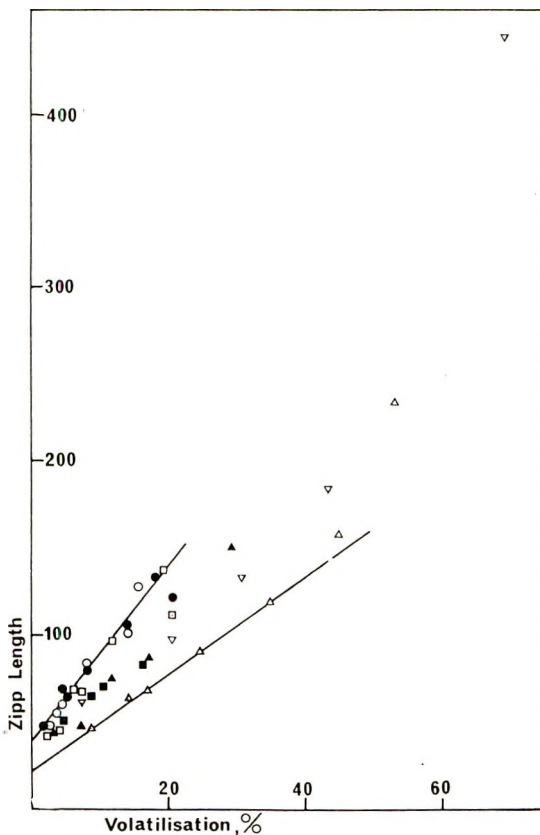


Fig. 8. Relationship between zip length and volatilization in co-polymers of styrene and acrylonitrile degrading at 292°C: (○) PS 3; (●) SA 4; (□) SA 2; (■) SA 8; (▲) SA 3; (△) SA 6; (▽) SA 5.

increase with volatilization is clearly a measure of the increasing probability, as the reaction proceeds, that complete unzipping will occur so that equation 1 does not give a true measure of chain scissions in the later stages of reaction. However, Figure 8 demonstrates that, for comparable extents of reaction, there is no well marked change in zip length with the introduction of acrylonitrile units into polystyrene molecules, although there is a small tendency to lower zip lengths at high acrylonitrile contents. Thus the tendency for a greater decrease in molecular weight to occur in acrylo-

TABLE III
Chain Fragment/Monomer Ratios

Copolymer	Ratio
PS 3	1.0
SA 4	1.0
SA 2	1.0
SA 3	1.5
SA 6	2.0
SA 5	2.5

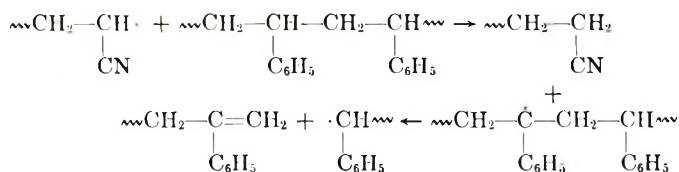
nitrile-rich copolymers, as in Figure 6, can be explained in terms of a decrease in zip lengths.

From Figure 8 it is clear that the zip length is approximately 40 for the polystyrene and the copolymers containing up to 1% acrylonitrile. A slight decrease can be discerned for the 4.7% acrylonitrile copolymer, and the value decreases further as the acrylonitrile content is increased. Since the zip length for polystyrene is 40 and the acrylonitrile units in the 1% and 4.7% copolymers are, on average, approximately 100 and 20 styrene units apart, it is not surprising that the zip length begins to be affected significantly in this acrylonitrile content range. However, that the zip length is over 20 even when the acrylonitrile units are, on average, approximately 4 units apart is a clear indication that the depropagation processes are not severely held up by the acrylonitrile units. Although the detailed analysis of reaction products will be described in the following paper,⁹ it is relevant to the qualitative understanding of the influence of acrylonitrile units to record at this point the changes which occur in the ratio of chain fragments to monomer with change in copolymer composition. The depropagation processes which occur during thermal degradation of polystyrene are reverse polymerization, which produces monomer, and intramolecular transfer which produces chain fragments (mainly dimer, trimer, and tetramer).¹⁴ The relative rates of these reactions are such that the weight ratio, chain fragments/monomer, is approximately unity. The ratios for the series of copolymers are recorded in Table III, from which it is clear that the tendency for intramolecular transfer to occur is greater at acrylonitrile-terminated than at styrene-terminated degrading radicals.

DISCUSSION

A qualitative picture of the influence of copolymerized acrylonitrile on the thermal degradation of polystyrene emerges from these observations. Thus the invariant position of the maximum and shape of the TGA curves suggests that the presence of acrylonitrile does not alter the reaction mechanism in any profound way and this is confirmed by the negligible influence of up to 4.7% acrylonitrile on both rates of volatilization and changes in molecular weight. With higher acrylonitrile content there is an increase in rate of volatilization which is closely proportional to the acrylonitrile content and which, in terms of the radical chain nature of the reaction, must

be due either to an increased rate of initiation or to an increase in the zip length. Rates of chain scission calculated from molecular weight measurements demonstrate quite clearly that the primary influence of the acrylonitrile is to increase the rate of chain scission to produce depropagating radicals. The zip length is relatively unaffected, showing that the depropagation can pass relatively easily through acrylonitrile units in the polymer chains although an increasing ratio of chain fragments to monomer among the products, as the acrylonitrile content is increased, demonstrates that acrylonitrile-terminated radicals show a greater tendency than styrene-terminated radicals to liberate larger chain fragments in intramolecular transfer processes rather than monomer. Since the amount of intramolecular transfer thus clearly increases with acrylonitrile content it seems possible that the acrylonitrile-terminated degrading radical may also show a greater tendency to take part in intermolecular transfer processes



than the styrene-terminated radical. Since the zip length is calculated on the assumption that all scission is direct, a small amount of intermolecular transfer could account for the decrease in the calculated zip length with increasing acrylonitrile content.

For a more complete understanding of this reaction it should be profitable firstly, to make a detailed analysis of the products of the reaction with particular reference to any changes in the pattern of products with copolymer composition and, secondly, to make a more detailed study of the chain scission reaction. These subjects are dealt with in subsequent papers.^{9,10}

One of the authors (D. R. B.) is grateful to the Science Research Council for the award of a Research Studentship during the tenure of which this work was carried out.

References

1. N. Grassie and B. J. D. Torrance, *J. Polym. Sci. A-1*, **6**, 3303, 3315 (1968).
2. N. Grassie and E. Farish, *Europ. Polym. J.*, **3**, 619, 627 (1967).
3. N. Grassie and E. Farish, *Europ. Polym. J.*, **3**, 305 (1967).
4. N. Grassie and E. M. Grant, *Europ. Polym. J.*, **2**, 255 (1966).
5. N. Grassie and J. N. Hay, *J. Polym. Sci.*, **56**, 189 (1962).
6. C. H. Bamford and A. D. Jenkins, *Proc. Roy. Soc. (London)*, **A210**, 315 (1953).
7. H. W. Melville and L. Valentine, *Trans. Faraday Soc.*, **46**, 210 (1950).
8. F. M. Lewis, F. R. Mayo, and W. F. Hulse, *J. Amer. Chem. Soc.*, **67**, 1701 (1945).
9. N. Grassie and D. R. Bain, *J. Polym. Sci. A-1*, **8**, 2663 (1970).
10. N. Grassie and D. R. Bain, *J. Polym. Sci. A-1*, **8**, 2677 (1970).
11. N. Grassie and H. W. Melville, *Proc. Roy. Soc. (London)*, **A199**, 1 (1949).
12. I. C. McNeill, *J. Polym. Sci. A-1*, **4**, 2479 (1966).
13. I. C. McNeill, *Europ. Polym. J.*, **3**, 409 (1967).
14. S. L. Madorsky and S. Straus, *J. Res. Nat. Bur. Stand.*, **40**, 417 (1948).

Received September 17, 1969

Thermal Degradation of Copolymers of Styrene and Acrylonitrile. II. Reaction Products

N. GRASSIE and D. R. BAIN,* *Chemistry Department, The University of
Glasgow, Glasgow, W. 2, Scotland*

Synopsis

Hydrogen cyanide is a minor product of degradation of copolymers of styrene and acrylonitrile. The liquid products have been separated and identified by combined gas chromatography and mass spectrometry (GC-MS), as styrene, acrylonitrile, toluene, and benzene. The ratio of styrene to acrylonitrile monomers in the products is approximately twice that of the monomer units in the copolymers, and the ratios of styrene to toluene and benzene are the same as are obtained from pure polystyrene. These ratios were determined by using infrared spectral methods. The fraction of products volatile at the temperature of degradation but involatile at ambient temperature was also analyzed by using GC-MS. A series of four dimers and four trimers were fairly reliably identified. The residual material from copolymers containing up to 33.4% acrylonitrile is always soluble in toluene. The 50/50 copolymer and its residues are insoluble in toluene. Yellow coloration develops in the residues from high acrylonitrile copolymers at advanced stages of degradation. Infrared and ultraviolet spectra suggest that this is due to conjugated unsaturation in the polymer chain backbone which may be associated with the liberation of hydrogen cyanide from the acrylonitrile units.

INTRODUCTION

The previous paper¹ has shown that changes in the characteristics of the degradation of polystyrene brought about by the presence of acrylonitrile units in the polymer chains are associated with chain scission at acrylonitrile units and the ability of the depropagation reaction, which is typical of polystyrene, to pass through acrylonitrile units. As a further step to the clarification of the degradation reactions involved it is therefore obviously of interest to make a detailed study of the reaction products and the influence on them of copolymer composition. The present paper is devoted to this aspect.

EXPERIMENTAL

Preparation of Copolymers

The copolymers referred to in this paper are those described previously.¹

* Present address: Air Force Materials Laboratory, Wright-Patterson Air Force Base, Dayton, Ohio, U. S. A.

Degradation Experiments: Sealed-Tube Technique

To facilitate the total analysis of products, degradations were carried out in the apparatus illustrated in Figure 1. The polymer (approximately 200 mg) was introduced into the tube in powder form through the B 14 standard cone. The tube was then evacuated for several hours to 10^{-6} torr and sealed off. The end of the tube containing the polymer was inserted in a

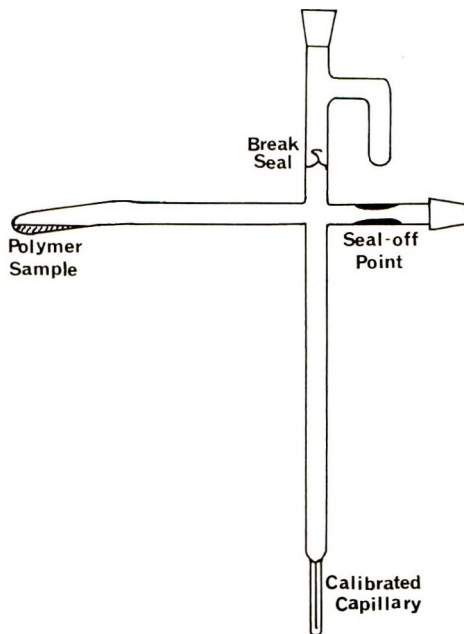


Fig. 1. The Sealed-Tube degradation apparatus.

furnace, controlled to $330 \pm 1^\circ\text{C}$, and the capillary end cooled in liquid nitrogen. Chain fragments, involatile at ambient temperature, accumulated on the walls of the tube just outside the furnace and more volatile products in the capillary. At a predetermined time the tube was withdrawn from the furnace and cooled rapidly.

Analysis of the gaseous products was carried out by attaching the tube directly to the inlet of a mass spectrometer (MS 10, A.E.I. Limited) and breaking the breakseal. Where necessary, the mass spectrum was scanned with cold traps at various temperatures (-178°C to 0°C) around the capillary. This considerably reduced the complexity of the spectrum by reducing the number of components volatile at any one time. Separation of three main products, namely, residue, chain fragments, and liquid products, was effected by cutting the tube at appropriate points. The products were then analyzed by appropriate techniques.

Thermal Volatilization Analysis (TVA)

This technique, which was referred to briefly in the previous paper, has recently been further developed by McNeill² to incorporate differential condensation. Thus, four cold traps at temperatures of -100 , -75 , -45 and 0°C are mounted in parallel between the reaction vessel and the trap at -196°C . The pressure in the vicinity of each cold trap is continuously monitored and automatically recorded so that a simultaneous series of four thermograms is obtained which provides information about the distribution of the volatilities of the products being evolved from the degrading polymer. Samples used for each analysis were 50 mg.

Gas-Liquid Chromatography (GLC)

A Microtek 2000 R gas chromatograph equipped with dual columns, a flame ionization detector, and a linear temperature programmer was used. The efficient fractionation which occurred in the sealed tube obviated the need for further fractionation of the volatile products and chain fragments. A 10% dinonyl phthalate column with an operating limit of 120°C gave good separation of the volatile products. A 1% SE 30 column, which could be used to 300°C , was suitable for separation of chain fragments.

Attempts to measure the styrene/acrylonitrile ratio by using GLC were abandoned in favor of the more favorable infrared technique described below. The high styrene/acrylonitrile ratio coupled with the unfavorable response of the flame ionization detector to acrylonitrile made the method inaccurate. For example, a 1/1 molar mixture of styrene and acrylonitrile gave a peak area ratio of 4/1.

Combined Gas Chromatography-Mass Spectrometry (GC-MS)

An LKB 9000 (LKB - Produkter, Stockholm) instrument was used. Chromatographic columns as described in the previous section were used as appropriate. The instrument allows the mass spectrum of each component to be obtained as it emerges from the chromatographic column.

Quantitative Infrared Analysis

Because of the inaccuracy, referred to above, of the estimation of acrylonitrile in the volatiles by GLC, other methods were sought, and the linearity of the optical density of the nitrile peak at 2230 cm^{-1} with concentration was made use of in the following way.

With the use of a microcell with 0.1 mm path length, 10 μl volume (R.I.I.C. Ltd.), the spectra of standard styrene-acrylonitrile mixtures were recorded on a Unicam SP 100 double-beam infrared spectrometer. A plot of optical density against the molar percentage of acrylonitrile as in Figure 2 was thus obtained, and from it the composition of an unknown mixture can obviously be readily obtained. Toluene and benzene were estimated by using similar methods.

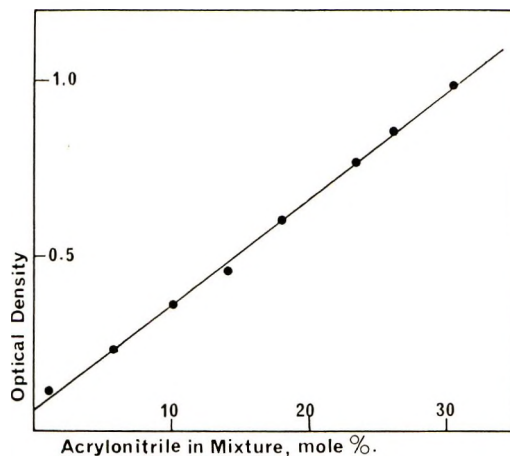


Fig. 2. Calibration curve for infrared analysis of the acrylonitrile content of the liquid fraction.

Infrared spectra of parent copolymers and residues were obtained by using Perkin-Elmer 225 and 257 spectrometers. Films deposited on sodium chloride disks from chloroform solution were used.

Ultraviolet Spectra

Ultraviolet spectra were obtained in chloroform (Analar) solution using a Unicam SP 800 instrument with 2-mm quartz cells and at a concentration of approximately 1 mg/ml.

RESULTS

Thermal Volatilization Analysis

The use of TVA to provide information about the temperature at which degradation occurs in styrene-acrylonitrile copolymers was described in the previous paper.¹ It has been shown that by incorporating differential condensation into this technique additional information may be obtained quite rapidly about the distribution of products over the range of volatility.²

TVA thermograms for two copolymers are illustrated in Figure 3; from them a number of qualitative conclusions may be arrived at about the nature of the volatile products. Curves 1 and 2, which are coincident, record all material volatile at 0°C and -45°C. Since there is a greater area under these curves in A than B, it is obvious that more chain fragments larger than monomer (dimer, trimer, etc.), which are involatile at this temperature, are produced from the copolymer richer in acrylonitrile, and this is borne out by the greater "cold ring fraction" observed from SA 10. On the other hand, curve 3 demonstrates a larger amount of material volatile at -75°C in B than in A. Since acrylonitrile, but not styrene, is volatile at this temperature, it is possible that not all the acrylonitrile is

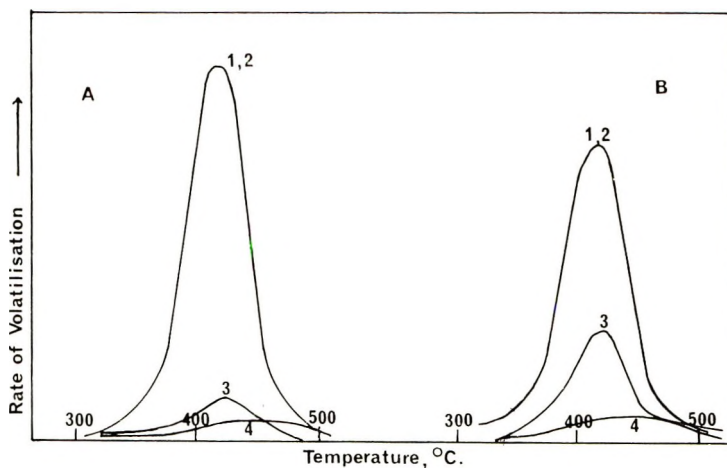


Fig. 3. Differential condensation TVA thermograms of copolymers of styrene and acrylonitrile, (A) SA 7, (B) SA 10 at various trap temperatures, (1) 0°C; (2) -45°C; (3) -75°C; (4) -100°C.

liberated in larger chain fragments but that a good deal of it appears as monomer, in spite of the fact that from pure polyacrylonitrile, monomer is a very minor product. Finally curves 4 show that small but definite amounts of very volatile products are evolved. This could be hydrogen cyanide or ammonia, products which have been reported to occur in the degradation of polyacrylonitrile.

Volatile Products

Products volatile at -100°C were identified as hydrogen cyanide and acrylonitrile by the parent peaks in the mass spectra.

The products liquid at ordinary temperatures were reported and identified by using the LKB gas chromatograph-mass spectrometer. They are acrylonitrile, benzene, toluene, and styrene; the last three are typical of the degradation of pure polystyrene.

Styrene/Acrylonitrile Ratio

The ratios of monomers in the degradation products were measured by using the infrared technique described above. For each copolymer, the ratio did not change significantly with extent of reaction, and results for the series of copolymers are illustrated in Figure 4 which demonstrates that the probability that monomeric acrylonitrile will be liberated from an acrylonitrile-terminated degrading radical is approximately half the probability that styrene will be liberated from a styrene-terminated radical. Thus the acrylonitrile terminated radical must show a greater tendency to undergo transfer than the styrene terminated radical which accounts for the higher proportion of chain fragments as the copolymer becomes richer in acrylonitrile.¹ In a study of the sequence distribution of monomer units

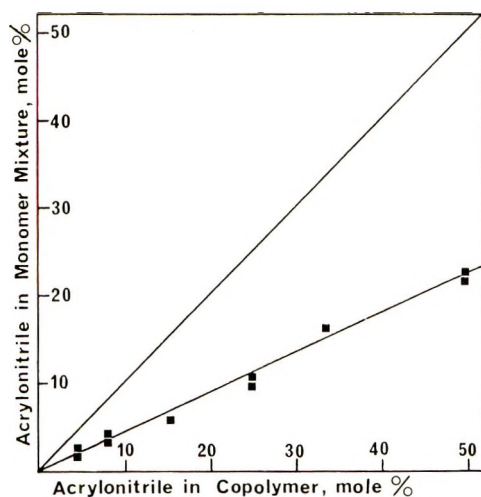


Fig. 4. Relationship between the copolymer composition and the proportion of acrylonitrile in the monomer mixture obtained on degrading copolymers of styrene and acrylonitrile at 330°C.

in copolymers, Harwood³ has developed a method whereby the amount of each type of linkage in the copolymer may be calculated. The data in Table I were obtained in this way. The occurrence of two adjacent acry-

TABLE I
Sequence Distribution in Copolymers
(A = Acrylonitrile, S = Styrene)

Copolymer	A, mole-%	Intermonomer linkages, %		
		S-A	S-S	A-A
SA 2	1	1.92	98.08	0
SA 8	4.7	9.48	90.52	0
SA 3	8.3	16.54	83.45	0.01
SA 6	15.5	30.90	69.05	0.05
SA 5	24.9	49.53	50.29	0.18
SA 10	33.4	65.72	33.76	0.52
SA 9	50	88.69	5.65	5.65

lonitrile units is almost negligible in copolymers containing less than 33.3% acrylonitrile, so the increased probability of transfer must be associated only with single acrylonitrile units.

Toluene and Benzene

An estimate of the amount of toluene in the volatile products was obtained by the use of the band at 738 cm^{-1} in the infrared spectrum of toluene. This band is unaffected by the presence of styrene, acrylonitrile,

and benzene. Comparison of the optical density of this peak with a calibration graph obtained by use of toluene-styrene mixtures indicated that the toluene/styrene ratio is of the order of 0.03. By similar methods the benzene/styrene ratio was found to be less than 0.01. Since these are approximately the proportions of toluene and benzene obtained by thermal degradation of pure polystyrene, further investigation was not considered necessary.⁴

Chain Fragments

In his early work on polystyrene, Staudinger,⁵ using classical methods of analysis, was able to identify dimer, trimer, and tetramer among the products of degradation.

In the present investigations the chain fragment fraction was found to be separable on a 1% SE 30 GLC column (10 ft) temperature programmed to 250°C. Once separation conditions had been established, it was possible to examine the chain fragments by using GC-MS.

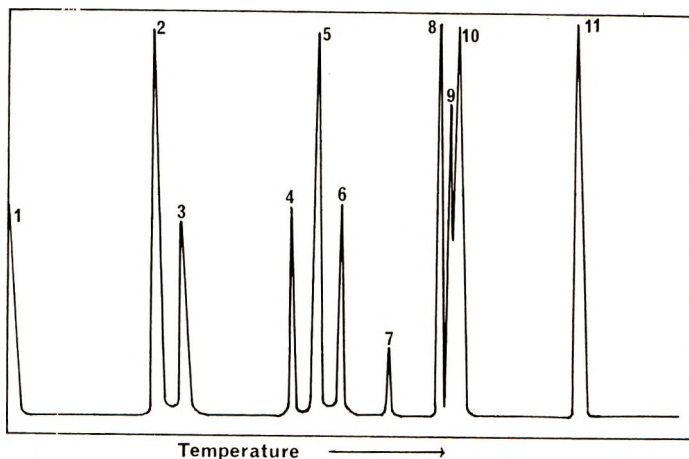


Fig. 5. GLC of chain fragment fraction from SA 5 degraded at 330°C.

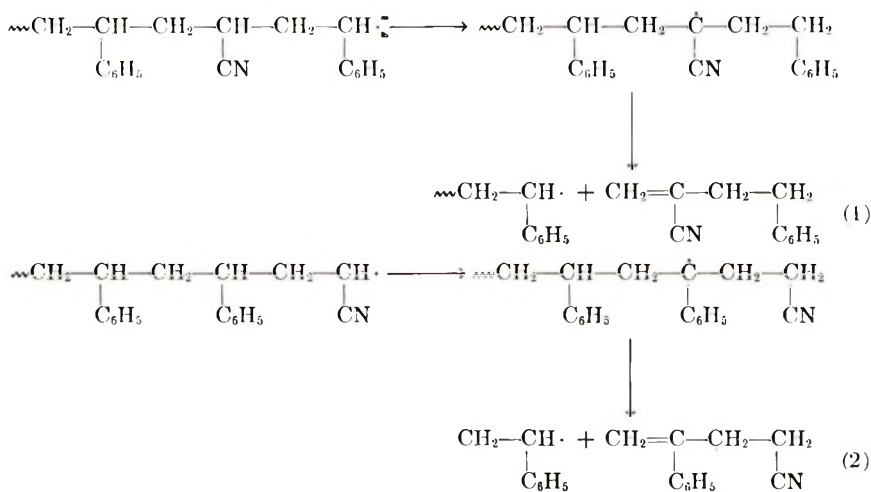
The chromatogram obtained from a solution of chain fragments from SA 5 is shown in Figure 5. A mass spectrum was obtained for each constituent at 70 eV in order to obtain the full cracking pattern necessary for identification. Parent peaks at m/e values of 157, 208, 261, and 312, indicate that not only are styrene dimer and trimer formed but also chain fragments containing acrylonitrile units. Molecular weights deduced from parent peaks are presented in the second column of Table II, from which it is clear that isomeric species may also be present. Methods of identification may be illustrated by considering the two styrene-acrylonitrile dimers (molecular weight = 157). It is reasonable to assume that the dimers are

TABLE II
Chain Fragments from a 3/1 Styrene/Acrylonitrile Copolymer

Peak no. ^a	Molecular weight	Structure
1	—	Tail of solvent peak (chloroform)
2	157	$\text{CH}=\underset{\text{CN}}{\text{C}}-\text{CH}_2-\underset{\text{C}_6\text{H}_5}{\text{CH}_2}$
3	157	$\text{CH}_2=\underset{\text{C}_6\text{H}_5}{\text{C}}-\text{CH}_2-\underset{\text{CN}}{\text{CH}_2}$
4	196	$\text{CH}_2-\underset{\text{C}_6\text{H}_5}{\text{CH}}-\underset{\text{C}_6\text{H}_5}{\text{CH}_2}-\text{CH}_2$
5	208	$\text{CH}_2-\underset{\text{C}_6\text{H}_5}{\text{CH}}-\text{CH}_2-\underset{\text{C}_6\text{H}_5}{\text{C}}-\text{CH}_3$
6	208	$\text{CH}_2=\underset{\text{C}_6\text{H}_5}{\text{C}}-\text{CH}_2-\underset{\text{C}_6\text{H}_5}{\text{CH}_2}$
7	239	Unknown
8	261	$\text{CH}_2=\underset{\text{CN}}{\text{C}}-\text{CH}_2-\underset{\text{C}_6\text{H}_5}{\text{CH}}-\underset{\text{C}_6\text{H}_5}{\text{CH}_2}-\underset{\text{C}_6\text{H}_5}{\text{CH}_2}$
9	261	$\text{CH}_2=\underset{\text{C}_6\text{H}_5}{\text{C}}-\text{CH}_2-\underset{\text{C}_6\text{H}_5}{\text{CH}}-\underset{\text{C}_6\text{H}_5}{\text{CH}_2}-\underset{\text{CN}}{\text{CH}_2}$
10	261	$\text{CH}_2=\underset{\text{C}_6\text{H}_5}{\text{C}}-\text{CH}_2-\underset{\text{CN}}{\text{CH}}-\underset{\text{C}_6\text{H}_5}{\text{CH}_2}-\underset{\text{C}_6\text{H}_5}{\text{CH}_2}$
11	312	$\text{CH}_2=\underset{\text{C}_6\text{H}_5}{\text{C}}-\text{CH}_2-\underset{\text{C}_6\text{H}_5}{\text{CH}}-\underset{\text{C}_6\text{H}_5}{\text{CH}_2}-\underset{\text{C}_6\text{H}_5}{\text{CH}_2}$

^a Peak numbers refer to the chromatogram in Fig. 5.

formed by intramolecular transfer at styrene- and acrylonitrile terminated radicals as shown in eqs. (1) and (2).



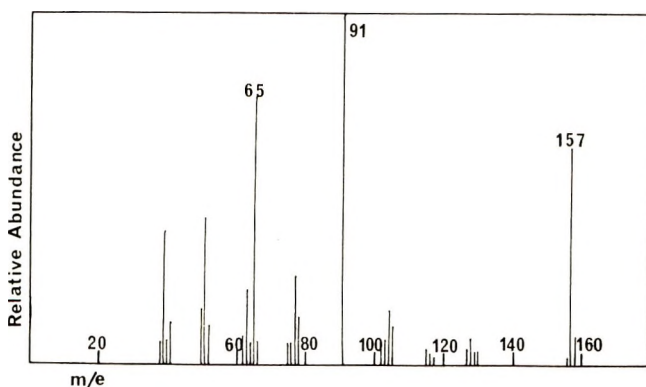
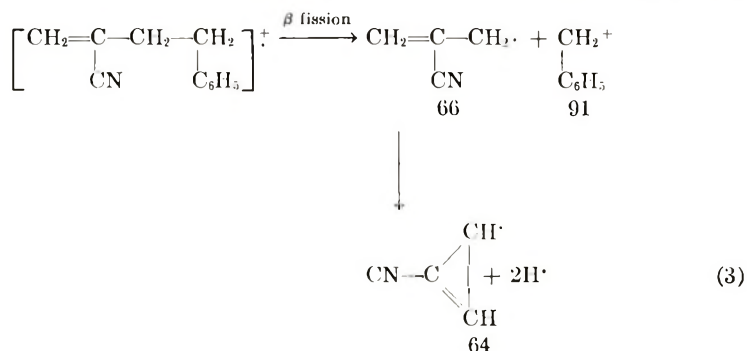
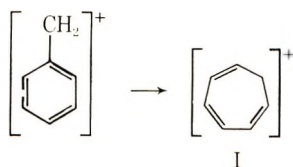


Fig. 6. Mass spectrum of the styrene/acrylonitrile dimer appearing as peak 2 in Fig. 5 (from GC-MS).

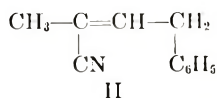
The fragmentation patterns which might reasonably be expected from these structures can be formulated and compared with the mass spectra [eq. (3)].



This fragmentation is in agreement with the line diagram in Figure 6 obtained from peak 2 in Figure 5. The base peak at $m/e = 91$ is due to the stable tropylium ion (I) formed by rearrangement of $\text{C}_6\text{H}_5\text{—CH}_2^+$,

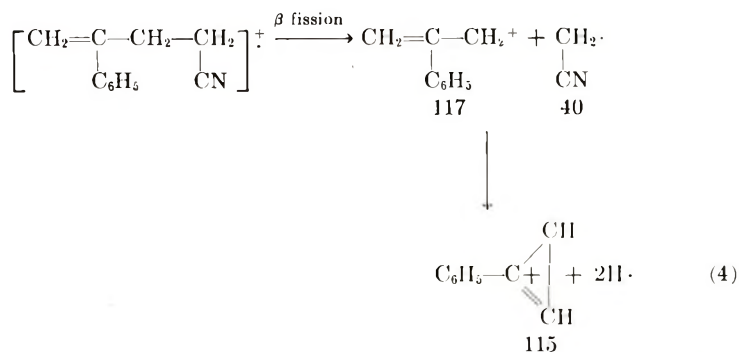


which arises as a result of fission β to the double bond which would be particularly favored. This is confirmed by the peaks at 66 and at 64 corresponding to the formation of the more stable cyclic radical. Peaks at $m/e = 39, 50, 51, 52,$ and 65 are the result of fragmentation of the benzene ring. The structure II



would also give the $m/e = 91$ peak, but the absence of a peak at $m/e = 142$ corresponding to loss of a methyl group suggests that the structure is not formed either during degradation or by isomerization in the electron beam.

The fragmentation of the dimer obtained from the second reaction above should be expected to occur as shown in eq. (4).



On comparing this with the line diagram in Figure 7, several points of similarity are observed. As in the previous case, initial scission is assumed to be β to the double bond. This results in the ion at $m/e = 117$. This, however, rearranges to the more stable substituted cyclopropenyl ion ($m/e = 115$), and the rearrangement is supported by evidence for a "metastable" ion at $m/e = 113$ and a peak at $m/2e = 57.5$, both indicative of the high stability of the cyclopropenyl ion. The peak at $m/e = 91$ is small compared with that of the parent ion, indicating that it is not formed at a point

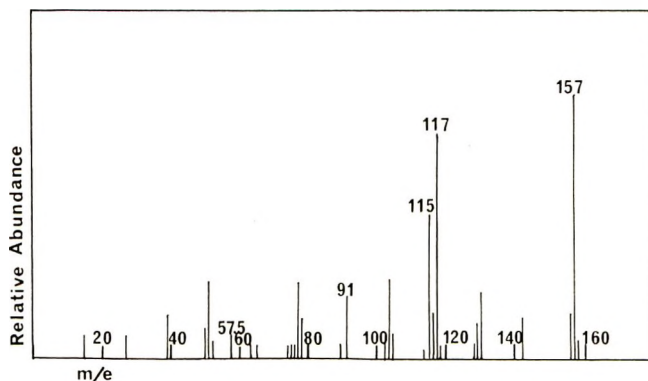
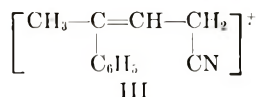


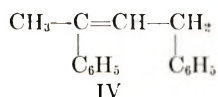
Fig. 7. Mass spectrum of the styrene/acrylonitrile dimer appearing as peak 3 in Fig. 5 (from GC-MS).

in the molecule where fission is highly favorable. The appearance of an ion at $m/e = 142$ suggests the loss of a methyl group from the ion III,



but the structure is thought to arise from isomerization in the electron beam rather than as a product of degradation. The fact that in Figure 7, $m/e = 157$ is the base peak suggests that the isomer formed in the second reaction above is more stable than that formed in the first reaction, which would favor some isomerization before fragmentation.

From a study of the cracking patterns of all the products revealed by Figure 5 the structures in Table II are suggested. The mass spectra of the trimers with molecular weights of 261 agree well with the structures predictable from reaction of the various chain terminal radicals. The styrene dimer (208) structures are less satisfactory in this respect, the material of the largest peak in the chromatogram having the structure IV



which is unlikely in terms of transfer processes. The shape of the chromatographic peak does not indicate isomerization on the column. Although the data in Table II are believed to be fairly reliable, it would obviously be necessary to make an extensive study of deuterated materials in order to assign all these structures with absolute certainty. The compound associated with peak 7 was not identified but may be associated with fragments of the polystyrene molecule from which benzene or toluene has been evolved.

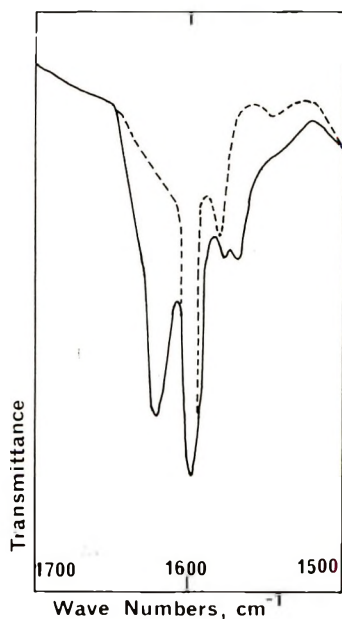


Fig. 8. Infrared spectrum of (---) SA 9 and (—) the chain fragments from SA 9 degraded at 330°C.

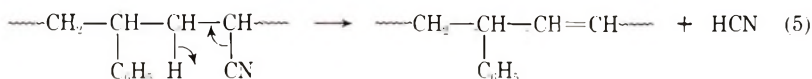
Infrared Spectra of Chain Fragments

The chain fragment fraction discussed above was always colorless. The 1500–1700 cm^{-1} region of its infrared spectrum is compared in Figure 8 with that of the parent copolymer. The additional absorption at 1625 cm^{-1} confirms the present of ethylenic structures⁶ in accordance with the structures in Table II.

Residual Polymer

Molecular weight changes in the residue after degradation were discussed in the previous paper¹ and will be referred to again in the following paper.⁷ All the degradation residues except these from the 50/50 copolymer (SA 9) were completely soluble in toluene. Indeed the solution properties of all the copolymers containing up to 33.4 mole-% of acrylonitrile are similar to these of polystyrene. SA 9 and its residues are, like polyacrylonitrile, insoluble in toluene.

The residues from the high acrylonitrile copolymers, particularly SA 9, are slightly yellow, and both infrared and ultraviolet spectra indicate main-chain unsaturation. For example the ethylenic absorption at 1625 cm^{-1} present in the infrared spectra of chain fragments is also observed in the residue. Only the residue from SA 9 shows significant absorption in the 275–400 $\text{m}\mu$ region of the ultraviolet spectrum indicative of conjugated unsaturation suggesting that the unsaturation is associated with acrylonitrile units which, only in this polymer, exist in appreciable amounts in adjacent sequences. The presence of hydrogen cyanide among the reaction products suggests that this unsaturation may be due to the reaction (5)



as in the photolysis of polyacrylonitrile.⁸ The cyclization of the nitrile units, which is typical of polyacrylonitrile, is inhibited by the blocking effect of the styrene units as previously discussed by Grassie and Hay.⁹

DISCUSSION

The principal products of the degradation of styrene-acrylonitrile copolymers containing up to 33% acrylonitrile can be explained in terms of the same kind of depolymerization mechanism as occurs in polystyrene and which involves depropagation to produce monomer and intramolecular transfer to give chain fragments, principally dimer and trimer. In spite of the fact that acrylonitrile is not a significant product of degradation of polyacrylonitrile, depropagation can readily pass through isolated acrylonitrile units in polystyrene rich copolymers, liberating monomer. As the proportion of acrylonitrile in the copolymer is increased, however, the chain fragment/monomer ratio increases, and the acrylonitrile/styrene monomer ratio indicates that the probability that an acryloni-

trile-terminated macroradical will liberate an acrylonitrile monomer molecule rather than undergo intramolecular transfer is approximately half the probability that a styrene-terminated radical will liberate styrene rather than a larger chain fragment. The structures of the chain fragments containing acrylonitrile, which all incorporate terminal double bonds, are consistent with the intramolecular transfer processes to be expected. It is rather surprising, however, that the principal styrene-styrene dimer has an internal double bond.

The appearance of hydrogen cyanide as a minor product is associated with the development of ethylenic unsaturation in the residual polymer. Although the amounts of hydrogen cyanide have not been accurately measured, it is clear that they are proportionately greater than are obtained from pure polyacrylonitrile. This may be associated with the fact that separation of acrylonitrile units by styrene in the copolymers inhibits the nitrile condensation reaction which occurs so readily in polyacrylonitrile⁹ at much lower temperatures. The intact acrylonitrile units are thus still free to decompose to acid and olefin at the higher temperatures at which the present investigations were carried out.

The minor products, toluene and benzene, are produced in about the same proportions, relative to styrene, as from polystyrene but, as in previous polystyrene degradation studies, their precise mode of formation has not been investigated. The unidentified product which has a molecular weight of 239 (Fig. 5, peak 7) may be associated with the formation of benzene and/or toluene, however, and in this connection it could be profitable to apply the GC-MS method to the study of the chain fragment fraction obtained from pure polystyrene.

In the previous paper it was shown that both chain scission and volatilization are progressively accelerated by increasing concentrations of acrylonitrile units in polystyrene. The overall degradation process is therefore initiated by chain scission at acrylonitrile units. The following paper⁷ is devoted to a more detailed study of the effect of acrylonitrile units on chain scission.

One of the authors (D. R. B.) is grateful to the Science Research Council for the award of a Research Studentship during the tenure of which this work was carried out.

References

1. N. Grassie and D. R. Bain, *J. Polym. Sci. A-1*, **8**, 2651 (1970).
2. I. C. McNeill, *Europ. Polym. J.*, **6**, 373 (1970).
3. H. J. Harwood, *Angew. Chem. Int. Ed.*, **4**, 483 (1965).
4. S. L. Madorsky and S. Straus, *J. Res. Nat. Bur. Stand.*, **40**, 417 (1948).
5. H. Staudinger and A. Steinhöfer, *Ann.*, **517**, 35 (1935).
6. L. J. Bellamy, *The Infra-Red Spectra of Complex Molecules*, 2nd Ed, Methuen, London, 1958.
7. N. Grassie and D. R. Bain, *J. Polym. Sci. A-1*, **8**, 2677 (1970).
8. H. H. G. Jellinek and I. J. Bastian, *Can. J. Chem.*, **29**, 2056 (1961).
9. N. Grassie and J. N. Hay, *J. Polym. Sci.*, **56**, 189 (1962).

Received September 17, 1969

Thermal Degradation of Copolymers of Styrene and Acrylonitrile. III. Chain-Scission Reaction

N. GRASSIE and D. R. BAIN,* *Chemistry Department, The University of Glasgow, Glasgow, W. 2, Scotland*

Synopsis

The chain-scission reaction which occurs in copolymers of styrene and acrylonitrile has been studied at temperatures of 262, 252, and 240°C. Under these conditions volatilization is negligible, and chain scission can be studied in virtual isolation. At 262°C three kinds of chain scission are discernible, namely, at weak links which are associated with styrene units, "normal" scission in styrene segments of the chain and scission associated with the acrylonitrile units. The rate constants for normal scission and scission associated with acrylonitrile units are in the ratio of approximately 1 to 30. The molecular weight of the copolymer has no effect on the rates of scission. At 252°C the same general behavior is observed for the copolymers containing up to 24.9% acrylonitrile. The 33.4% acrylonitrile copolymer is anomalous, however. At 240°C the trends observed at 262°C appear to break down completely although individual experiments are quite reproducible. This behavior at the lower temperatures is believed to be associated with the fact that the melting points of the various copolymers are in this temperature range. Thus the viscosity of the medium, which should be expected to have a strong influence on the chain scission reaction, will be changing rapidly with temperature, copolymer composition, and molecular weight in this temperature range.

INTRODUCTION

The first paper in this series¹ demonstrated that chain scission is a vital factor in the overall thermal degradation process which occurs in styrene-acrylonitrile copolymers. In the second paper² a detailed analysis of the products of reaction was described. The experiments described in the first paper show that the interpretation, in terms of chain scission, of the changes in molecular weight which occur at 292°C are considerably complicated by the production of volatile material. Thus chain scission may be studied quantitatively only at very early stages of reaction when volatilization is negligible, and the experiments described in the present paper show how this was achieved by studying the reaction at lower temperatures than formerly.

* Present address: Air Force Materials Laboratory, Wright-Patterson Air Force Base, Dayton, Ohio, U. S. A.

EXPERIMENTAL

The copolymers used in this work, the degradation techniques, and the method of molecular weight measurement are all as described in the two previous papers.^{1,2}

RESULTS

Random Scission with Negligible Volatilization

When chain scission occurs in absence of volatilization, the relationship between the average number of chain scissions per molecule (N) and the average chain length (CL) is given by

$$N = (CL_0/CL) - 1$$

in which CL_0 is the initial chain length. The fraction of bonds ruptured n is given by

$$n = N/(CL_0 - 1)$$

Since CL_0 is large, this is approximately equivalent to

$$\begin{aligned} n &= N/CL_0 \\ &= (1/CL) - (1/CL_0) \end{aligned}$$

If k is a first-order rate constant for bond scission, then, in the early stages of reaction when n is small,

$$n = kt$$

In their work on polystyrene, Cameron and Kerr³ found that whereas anionically prepared polystyrene obeys this relationship, a positive intercept is obtained on the n axis for thermally initiated polystyrene. This was taken as evidence that "weak links" are present in polystyrene prepared by free radical mechanisms but not in anionic polystyrene. Nakajima and his colleagues⁴ have also concluded that isotactic polystyrene has no weak links. It is interesting in this connection that Grassie and Cameron,⁵ on the basis of ozonization experiments, associated the weak links in polystyrene with unsaturated structures and McNeill and his co-workers^{6,7} have recently shown that radical-initiated polystyrene incorporates main-chain unsaturation while anionic polystyrene does not. It is clear from the work of Cameron and Kerr³ that evaluation of the intercept on the n axis is a very much more satisfactory method of measuring the weak-link concentration in polystyrene than the method used by Grassie and Kerr,⁸ which involves extrapolating the later stages of the molecular weight-extent of volatilization relationship to zero volatilization.

Preliminary experiments demonstrated that in the temperature range 240–265°C measurable chain scission occurs in reasonable times (up to 10 hr) without too much volatilization.

Reaction at 262°C

Results of a series of experiments carried out at 262°C are presented in Table I. The rapid decrease in molecular weight, which is associated with weak-link scission in polystyrene, is obviously also occurring in the copolymers and the time dependence of chain scission is illustrated in Figure 1. The concentration of weak links, measured by the intercept on the n axis, is seen from Figure 1 to be independent, within experimental error, of the acrylonitrile content of the copolymer, at least for low acrylonitrile concentrations, but there is a clear tendency for the intercept to decrease in the higher acrylonitrile copolymers which supports the association of these

TABLE I
Degradation of Copolymers at 262°C

Copolymer	Time, hr	Vola-tilization, %	$\bar{M}_n \times 10^{-5}$	$CL \times 10^{-3}$	$CL, \% \text{ of original}$	$n \times 10^3$
PS 3 (polystyrene)	0	0	4.70	4.50	100	0
	3	0.3	2.14	2.06	45.7	0.27
	6	0.1	1.92	1.85	41.1	0.32
	8	0.5	1.85	1.78	39.5	0.34
	10	0.4	1.81	1.74	38.6	0.36
SA 8 (4.7% AN)	0	0	3.31	3.26	100	0
	3	0.7	1.63	1.61	49.4	0.32
	6	1.7	1.35	1.33	40.8	0.44
	8	2.0	1.31	1.29	39.6	0.47
	10	1.4	1.20	1.18	36.2	0.54
SA 3 (8.4% AN)	0	0	4.11	4.11	100	0
	3	0.8	1.68	1.68	40.9	0.36
	6	1.2	1.56	1.56	38.0	0.40
	8	1.6	1.21	1.21	29.4	0.59
	10	1.3	1.11	1.11	27.0	0.66
SA 6 (15.5% AN)	0	0	4.70	4.89	100	0
	1	1.8	1.73	1.80	36.8	0.36
	3	2.1	1.48	1.54	31.5	0.45
	6	3.0	1.10	1.15	23.5	0.67
	8	3.9	0.94	0.97	19.8	0.80
SA 5 (24.9% AN)	0	0	6.50	7.12	100	0
	3	1.4	1.42	1.55	21.8	0.50
	6	2.0	1.04	1.13	15.9	0.74
	8	3.0	0.80	0.87	12.2	1.00
	10	3.5	0.68	0.74	10.4	1.21
SA 10 (33.4% AN)	0	0	3.66	4.21	100	0
	1	1.25	1.45	1.67	39.6	0.36
	2	1.7	1.18	1.36	32.2	0.50
	3	2.1	1.22	1.40	33.2	0.48
	6	3.15	0.77	0.89	21.2	0.89
	8	7.1	0.51	0.59	14.0	1.46

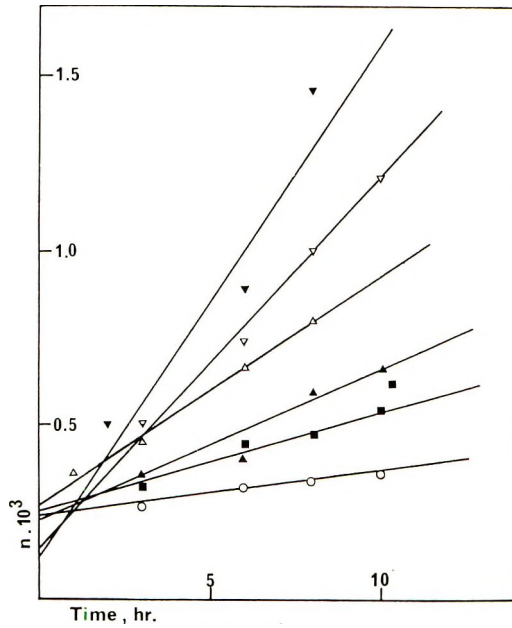


Fig. 1. Fraction of bonds broken as a function of time during degradation of copolymers of styrene and acrylonitrile at 262°C: (○) PS 3; (■) SA 8; (▲) SA 3; (△) SA 6; (▽) SA 5; (▼) SA 10.

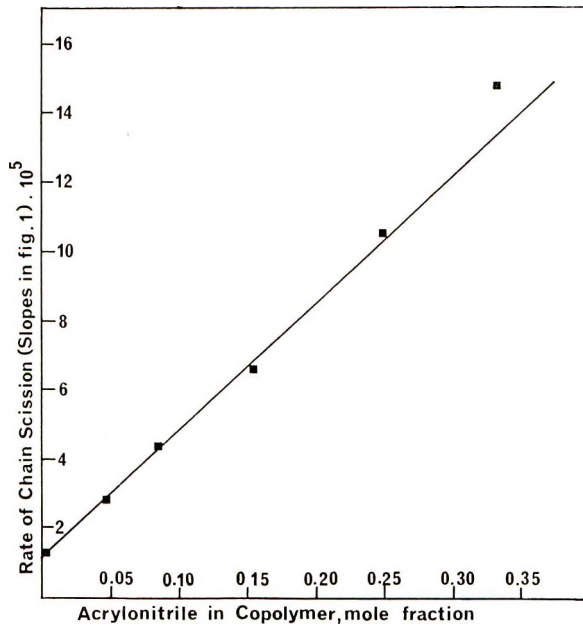


Fig. 2. Rate of chain scission at 262°C as a function of the acrylonitrile content of copolymers of styrene and acrylonitrile.

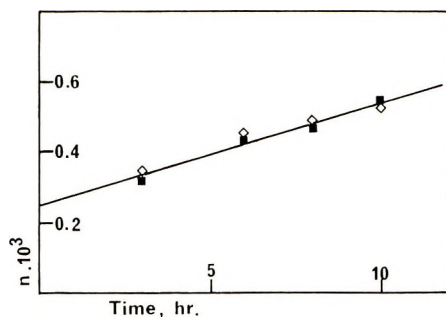


Fig. 3. Comparison of rates of bond scission at 262°C; (\diamond) in SA 7; (\blacksquare) in SA 8.

weak links with styrene units. The slopes of the lines in Figure 1, which measure the rates of "normal" scission, are related in Figure 2 to the acrylonitrile content of the copolymers, from which it is seen that the increase in rate of chain scission over that of polystyrene is strictly proportional to the acrylonitrile content of the copolymer.

The relative rate constants for chain scission associated with styrene and acrylonitrile units can be deduced from the data in Figure 2 by using the following simple kinetic treatment.

The total rate of chain scission, R_{cs} , in any copolymer will be given by,

$$R_{cs} = k_s S + k_n A$$

in which S and A are the mole fractions of styrene and acrylonitrile in the copolymer and k_s and k_n are rate constants for the scissions associated with styrene and acrylonitrile units respectively. But,

$$S = 1 - A$$

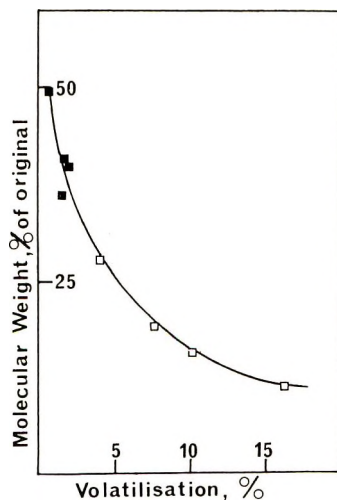


Fig. 4. Changes in molecular weight with volatilization of SA 8; (\blacksquare) at 262°C; (\square) at 292°C.

Therefore

$$\begin{aligned} R_{cs} &= k_s(1 - A) - k_a A \\ &= k_s + A(k_a - k_s) \end{aligned}$$

Thus values of k_s and $k_a - k_s$ may be obtained from the intercept and slope of the straight line in Figure 2, and individual values of k_s and k_a may be calculated as follows,

$$k_s = 1.2 \times 10^{-5} \text{ hr}^{-1}$$

$$k_a = 36.3 \times 10^{-5} \text{ hr}^{-1}$$

The polymers used in this work were so prepared that their molecular weights fell in a fairly narrow molecular weight range. While the above results give no evidence of any effect of molecular weight on weak-link concentration, in order to be certain it is necessary to compare the behaviors of two copolymers of the same composition but different molecular weights. Data for SA 7 and SA 8, which both incorporate 4.7% acrylonitrile but have molecular weights of 8.57×10^5 and 3.3×10^5 , respectively, are presented in Figure 3 and are obviously identical within experimental error.

TABLE II
Degradation of Copolymers at 252°C

Copolymer	Time, hr	Vola-tilization, %	$\bar{M}_n \times 10^{-5}$	$CL \times 10^{-3}$	$n \times 10^3$
SA 3	0	0	4.11	4.11	0
	3	1.3	2.46	2.46	0.163
	6	1.65	2.08	2.08	0.237
	8	2.0	1.93	1.93	0.273
	10	1.85	1.78	1.78	0.319
SA 6	0	0	4.70	4.89	0
	3	2.4	2.32	2.41	0.211
	6	2.5	1.85	1.93	0.314
	8	1.9	1.53	1.59	0.424
	10	2.7	1.37	1.42	0.500
SA 5	0	0	6.50	7.12	0
	3	2.7	2.26	2.47	0.265
	6	2.4	1.45	1.59	0.488
	8	3.0	1.27	1.39	0.580
	10	3.4	1.00	1.09	0.776
SA 10	0	0	3.66	4.21	0
	3	1.3	1.58	1.82	0.313
	6	1.3	1.19	1.37	0.493
	8	2.4	1.04	1.20	0.596
	10	2.2	0.92	1.06	0.706

Although conditions were chosen for these experiments such that volatilization is minimized while significant changes in molecular weight are still observed, nevertheless definite amounts of volatilization are still occurring, as shown in Table II. Figure 4 confirms that this volatilization bears the same relationship to chain scission as at 292°C, since the two sets of data are represented by a single curve. In comparing data obtained at the two temperatures in this and the previous papers it may therefore be assumed that there is no significant change in reaction mechanism within this temperature range.

Reaction at 252 and 240°C

In order to obtain further information about the nature of various kinds of structures at which chain scission occurs it would be of interest to make similar investigations to those described above over a range of temperatures. Since volatilization interferes increasingly with the measurement of chain scission at temperatures above 262°C, series of experiments were carried out at 252 and 240°C, and the results are presented in Tables II and III. Chain scission-time relationships are illustrated in Figures 5 and 6 and the relationship between rate of bond scission at 252°C and copolymer composition in Figure 7. At 252°C the behavior of the copolymer with the highest acrylonitrile content is obviously anomalous, although quite reproducible. At 240°C there is no obvious trend in the rate of chain

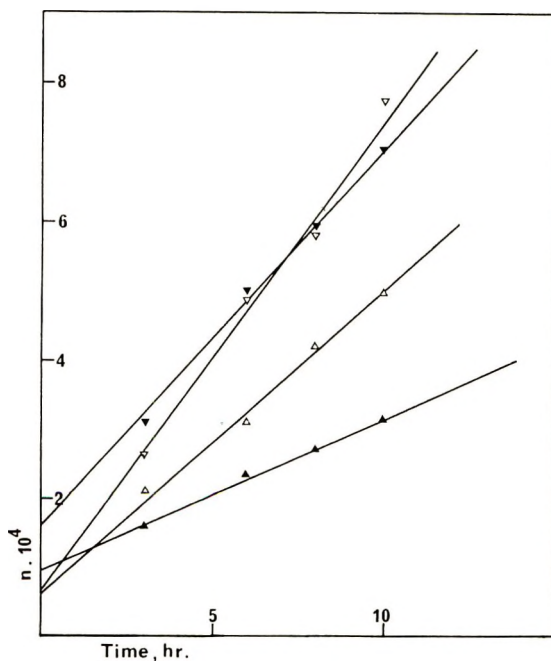


Fig. 5. Fraction of bonds broken as a function of time during degradation of copolymers of styrene and acrylonitrile at 252°C: (▲) SA 3; (△) SA 6; (▽) SA 5; (▼) SA 10.

TABLE III
Degradation of Copolymers at 240°C

Copolymer	Time, hr	Volatilization, %	$\bar{M}_n \times 10^{-5}$	$CL \times 10^{-3}$	$n \times 10^3$
SA 3	0	0	4.11	4.11	0
	3	1.3	2.18	2.18	0.215
	6	1.5	2.22	2.22	0.207
	8	1.4	2.10	2.10	0.232
	10	1.2	1.86	1.86	0.294
SA 6	0	0	4.70	4.89	0
	3	1.6	3.05	3.18	0.110
	6	1.9	2.58	2.68	0.169
	8	2.0	1.99	2.07	0.279
	10	1.6	1.87	1.95	0.308
SA 5	0	0	6.50	7.12	0
	3	1.5	2.36	2.58	0.248
	6	1.4	1.92	2.10	0.336
	8	1.7	1.93	2.11	0.334
	10	2.0	1.54	1.69	0.452
SA 10	0	0	3.66	4.21	0
	3	1.5	1.89	2.19	0.222
	6	1.6	1.63	1.98	0.298
	8	1.2	1.51	1.74	0.341
	10	1.6	1.44	1.66	0.368

scission with copolymer composition, although once again the results obtained are reasonably reproducible. No clear explanation has been discovered for this behavior. However, the melting points of polystyrene and polyacrylonitrile are quoted as 235–250°C and 319°C, respectively,⁹ and it is

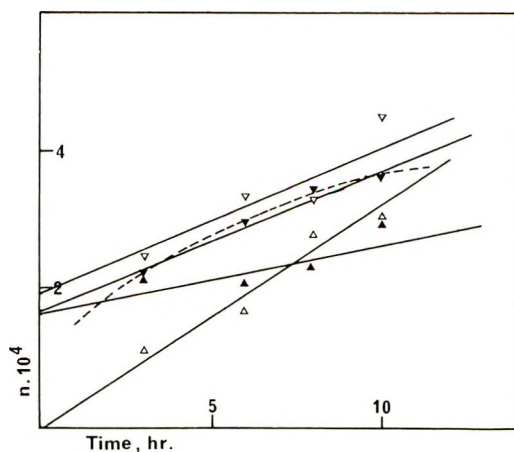


Fig. 6. Fraction of bonds broken as a function of time during degradation of copolymers of styrene and acrylonitrile at 240°C: (▲) SA 3; (△) SA 6; (▽) SA 5; (▼) SA 10.

to be expected that the melting points of the copolymers in question will also be in this region. Thus the reactions are taking place under conditions in which the viscosity of the medium must be changing rapidly with temperature, copolymer composition, and molecular weight, and it is to be expected that the viscosity of the medium will be a strong influence on chain

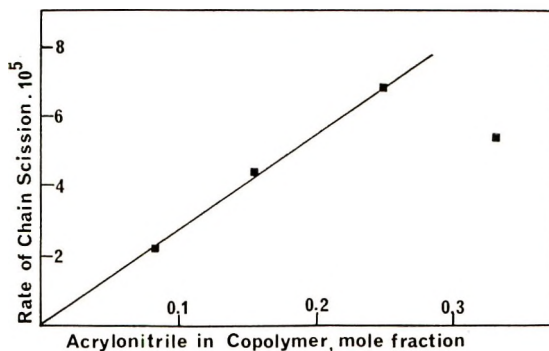


Fig. 7. Rate of chain scission at 252°C as a function of the acrylonitrile content of copolymers of styrene and acrylonitrile.

scission. On this basis, the low value for the rate of scission of SA 10 at 252°C may be due to the fact that its high acrylonitrile content brings the melting point into this temperature range. In addition to these viscosity effects, the rate of weak-link scission may no longer be regarded as “instantaneous” at these temperatures, and the data in Figure 6 may be better represented by curves (dotted line) rather than straight lines.

DISCUSSION

At 262°C, the increase in the rate of chain scission over that in polystyrene is proportional to the concentration of acrylonitrile in the copolymers and independent of molecular weight. The increase in rate is observed as an increase in the rate of “normal” scission. The weak-link concentration decreases as the acrylonitrile content of the copolymer is increased and is thus a property of the styrene units. At 252°C the same general trends are observed, except that the copolymer with the highest acrylonitrile content (33.4%) exhibits anomalous behavior. At 240°C these relationships break down completely, and it is suggested that this, and the anomaly at 252°C, is probably due to the fact that the melting points of the copolymers, which will vary slightly with copolymer composition and molecular weight, lie in this temperature range, so that at either of these temperatures, and especially at 240°C, we may be comparing reactions in materials of widely different viscosities.

One of the authors (D. R. B.) is grateful to the Science Research Council for the award of a Research Studentship during the tenure of which this work was carried out.

References

1. N. Grassie and D. R. Bain, *J. Polym. Sci. A-1*, **8**, 2651 (1970).
2. N. Grassie and D. R. Bain, *J. Polym. Sci. A-1*, **8**, 2663 (1970).
3. G. G. Cameron and G. P. Kerr, *Europ. Polym. J.*, **4**, 709 (1968).
4. A. Nakajima, F. Hamada, and T. Shimizu, *Makromol. Chem.*, **90**, 229 (1966).
5. N. Grassie and G. G. Cameron, *Makromol. Chem.*, **53**, 72 (1962).
6. I. C. McNeill and T. H. Makhdumi, *Europ. Polym. J.*, **3**, 637 (1967).
7. I. C. McNeill and S. A. Haider, *Europ. Polym. J.*, **3**, 551 (1967).
8. N. Grassie and W. W. Kerr, *Trans. Faraday Soc.*, **53**, 234 (1957); *ibid.*, **55**, 1050 (1959).
9. J. Brandrup and E. H. Immergut, Eds., *Polymer Handbook*, Interscience, New York, 1966.

Received September 17, 1969

Double-Bond Isomerization and Hydrogenation in Polyethylene with Soluble Nickel Catalysts

D. R. WITT and J. P. HOGAN, *Phillips Petroleum Company, Research Center, Bartlesville, Oklahoma 74003*

Synopsis

Polyethylene exhibits an increase in melt viscosity (melt index drop-off) when subjected to extreme thermal treatment. Although stabilizers and antioxidants do not prevent this change it has been possible to stabilize high-density polyethylene by isomerization or hydrogenation of the polymer unsaturation. A soluble nickel octoate-triethylaluminum complex was an active catalyst system for these reactions. A triethylaluminum/nickel ratio of three appeared optimum for maximum activity. Of particular interest regarding this catalyst system was the fact that the terminal vinyl unsaturation of the polymer had to be isomerized to some internal position before hydrogenation commenced. However, when this catalyst system was impregnated on a predried silica or when butyllithium was substituted for triethylaluminum, both isomerization and hydrogenation occurred simultaneously. The addition of a light olefin such as ethylene to the reaction mixture slowed the overall reaction until most of the ethylene had been hydrogenated. At this point the isomerization-hydrogenation reaction path previously mentioned commenced.

INTRODUCTION

The melt viscosity of high-density polyethylene increases when the polymer is extruded or injection-molded. This phenomenon has been shown to be caused by long-chain branching and is generally referred to in our laboratory as melt index drop-off. Melt index drop-off is accompanied by losses in processability and by an increase in melt retraction and warpage of injection molded articles. Die-face build-up on extruders and fish eyes in film have sometimes been attributed to this phenomenon. The addition of various stabilizers has not solved this problem of melt viscosity change resulting from thermal treatment of the polymer. This suggested that a different approach be taken to stabilize the polymer.

Phillips-type high-density polyethylene can be considered essentially a polymethylene containing one vinyl group per molecule. A logical point of initiation of the branching reaction would be expected to involve this vinyl group. The vinyl group concentration is approximately one group per thousand carbon atoms, which is not large. However, it has been shown that only a small amount of long-chain branching is required to effect a large change in polymer melt viscosity. Two possibilities exist for the modification of the terminal vinyl unsaturation of the polymer. They are:

(1) saturation of the vinyl group with hydrogen or other groups and (2) isomerization of the vinyl group to some internal position.

Considerable literature¹⁻⁵ relates to the hydrogenation of diene polymers, waxes, and polymeric residues found in hydrocarbon mixtures using various catalysts and at varying conditions. However, little information relates to the hydrogenation of α -olefin polymers such as polyethylene.⁶⁻⁸ Most of the hydrogenation catalysts consist of metals such as nickel, platinum and palladium, either supported or unsupported. More recently, new catalyst systems have been described for the hydrogenation of olefins and aromatics. Sloan⁹ and co-workers reported the hydrogenation of olefins at low temperatures with various soluble organometal-alkylaluminum systems. They proposed the formation of a metal hydride as a step in the hydrogenation reaction. At about the same time Lapporte and Schuett¹⁰ described hydrogenation of benzene by use of the nickel octoate-triethylaluminum system and also proposed the formation of nickel hydride.

In our study it was possible to hydrogenate high-density polyethylene by using various nickel-metal alkyl catalyst systems and to obtain thermally stable polymers. By slight modification of the catalyst system it was possible to obtain this same stability by isomerizing the vinyl unsaturation to some internal position.

EXPERIMENTAL

Materials

The triethylaluminum was purchased from Texas Alkyls and diluted with cyclohexane. *n*-Butyllithium was obtained as 10 wt-% solution in *n*-hexane from Lithium Corporation of America. The compounds of nickel, cobalt, and iron were obtained from Shepherd Chemical Company.

The polyethylene used was a Phillips Petroleum Company product in pelletized form and contained no antioxidants or stabilizers. The cyclohexane, pentene-1 and hexene-1 were also obtained from Phillips Petroleum Company as pure grade materials and were deaerated before drying over Alcoa H151 or F-1 alumina.

Matheson ultrapure hydrogen was used in all of the hydrogenation reactions.

Apparatus and Procedure

Evaluation of the various metal compounds and metal alkyls was done in a 1.3-liter, chrome-plated reactor which was mechanically stirred at 350 rpm. Other isomerization and hydrogenation experiments were conducted in a similar type reactor of 5-gal capacity to allow sampling without depleting the reaction mixture.

Dried polymer pellets were added to a warm reactor and deaerated prior to addition of cyclohexane solvent and metal salt. When the reaction mixture had reached the desired temperature the catalyst was formed in

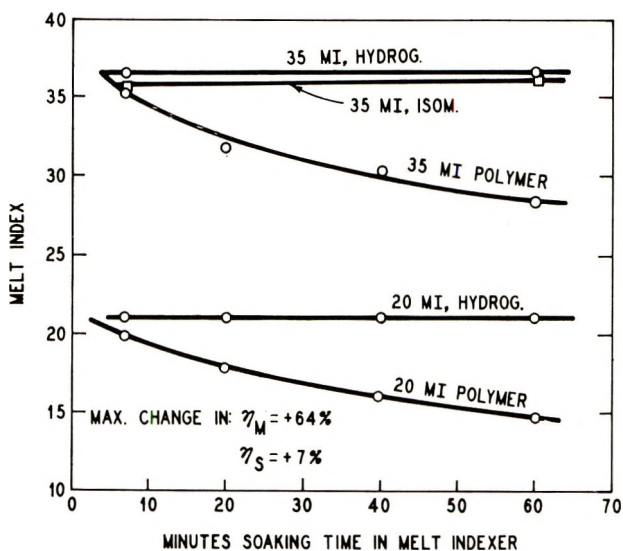


Fig. 1. Effect of hydrogenation on MI drop-off.

the reactor by rapidly adding the metal alkyl to the solvent-polymer-metal carboxylate mixture. This addition was immediately followed by cyclohexane wash and hydrogen in amounts as desired.

Polymer samples were removed from the reactor through the induction tube after flushing before each sample, dried and molded into disks for infrared analysis. Measurement of the double-bond content of each polymer sample was made by using a Perkin-Elmer Model 137B Infracord spectrophotometer. Calculations were made from baseline absorbances of infrared bands near 10.35 and 11.0 μ as indicated in Figure 2 below.

RESULTS

Melt Index Drop-Off

Melt index drop-off can be readily demonstrated in a melt index apparatus. This is done by charging polymer to the melt index barrel and allowing the polymer to heat-soak for various lengths of time before measuring the melt index of the polymer. Figure 1 shows the change in melt index of 20 and 35 melt index polymers which were exposed to heat treatment at 190°C before extrusion and melt index measurement. A sharp decrease in melt index was observed. Heat treatment at 230°C was even more drastic.

To obtain further information on what occurred in the examples shown in Figure 1, the melt and solution viscosities of each heat-soaked sample were determined. As indicated in Figure 1, melt viscosity increased a maximum of 64% while solution viscosity increased 7%. This large increase in melt viscosity with only a slight increase in solution viscosity is indication of long-chain branching. In melt flow, in which polymer

TABLE I
Transition Metal Compounds Used with Triethylaluminum^a

Compounds used	Physical form	Metal used, ppm	TEA/M ^b	Time required to hydrogenate polymer, min
Nickel octoate	Dissolved in mineral spirits	50	3/1	<5
Nickel tallate	" " "	50	3/1	5-10
Nickel stearate	" " "	50	3/1	5-10
Nickel naphthenate	" " "	50	3/1	15-30
Nickel acetate	Ball-milled in mineral oil after drying at 200°F	80	3/1	15-30
Nickel formate	" " "	80	3/1	0.9 <i>trans</i> groups re- maining after 60 min
Iron octoate	Dissolved in mineral spirits	100	4.5/1	30-60, (0.1 <i>trans</i> groups remaining after 30 min)
Cobalt octoate	" " "	30	3/1	<5
Cobalt octoate	" " "	30	3/1	5-10

^a Hydrogenation runs at 150°C with 25-30 psi hydrogen added; 8-10% polymer concentration in cyclohexane.

^b Molar ratio of triethylaluminum to Group VIII metal.

molecules are in close proximity to each other, even a slight amount of branching can cause considerable hindrance to flow. On the other hand, in a dilute solution, the polymer molecules are separated from each other and viscosity is hardly affected by slight branching. As shown additionally in Figure 1, either hydrogenation or isomerization of the unsaturation in these polymers prevented melt index drop-off. Further description or physical properties of these polymers have been reported in another paper.¹¹

Catalyst Compositions

In the preliminary scanning of catalysts for this study a number of Group VIII metal compounds were used with triethylaluminum to form the active catalyst species (Table I). The hydrogenation and isomerization

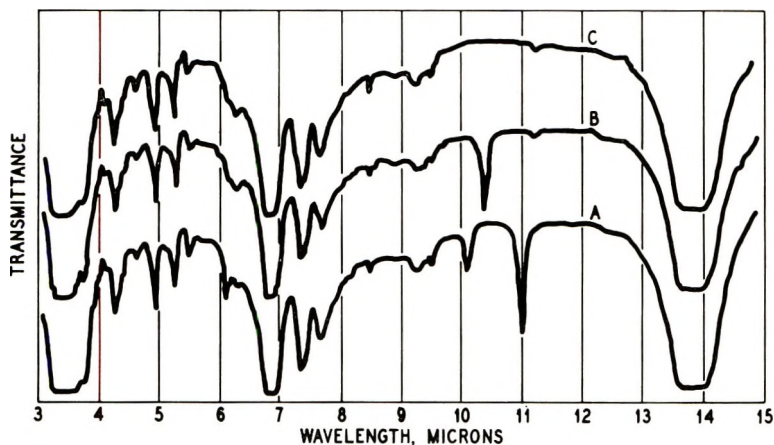


Fig 2. Infrared spectra of Phillips polyethylenes: (A) typical homopolymer; (B) sample A after double-bond isomerization; (C) sample A after double-bond hydrogenation

activity of these catalysts was followed by measuring the changes in vinyl and t-internal unsaturation of the polymer by infrared techniques. The spectral changes¹² which were measured are indicated in Figure 2. Of the various metal compounds tested, nickel and cobalt gave the most active catalysts. Nickel octoate (ethylhexoate) was the most active of the nickel compounds and was chosen for further studies.

The effectiveness of other metal alkyls as cocatalysts with nickel octoate is presented in Table II. These data show that triethylaluminum was the preferred cocatalyst. It was found that a triethylaluminum/nickel ratio larger than one was required to develop the full activity of the catalyst.

Reaction Path

When a low nickel concentration was used it was possible to follow the course of the hydrogenation reaction by frequent sampling of the polymer

TABLE II
Study of Metal Alkyl Cocatalysts^a

Cocatalyst		Time on stream for reaction, min	
Metal alkyl	Molar ratio metal alkyl/Ni	100% Isomerization	100% Hydrogenation
Triethylaluminum	3	5	20
Butyllithium	4	90	90
	8	15	30
Diisobutyl aluminum hydride	3	90	50% in 90 min

^a Nickel octoate (50 ppm Ni, based on polymer) plus metal alkyl as catalyst; 150°C, 25 psi hydrogen pressure, 8-10% polymer concentration in cyclohexane.

solution and analyzing the dried polymer. The general reaction path obtained was that shown in Figure 3.

The first change in unsaturation was found to be only that of isomerization. As the *trans* unsaturation in the polymer increased a similar decrease in the amount of vinyl unsaturation also resulted. During this time the total amount of unsaturation in the polymer was nearly equal to the amount of vinyl unsaturation found in the original polymer. After the vinyl content had reached nearly zero, hydrogenation commenced and continued at a rate somewhat slower than that of isomerization.

The fact that isomerization was essentially complete before hydrogenation began strongly indicates that not only do these reactions occur on the same type sites but that the nickel site is completely shielded from hydrogen as long as vinyl groups remain in the system.

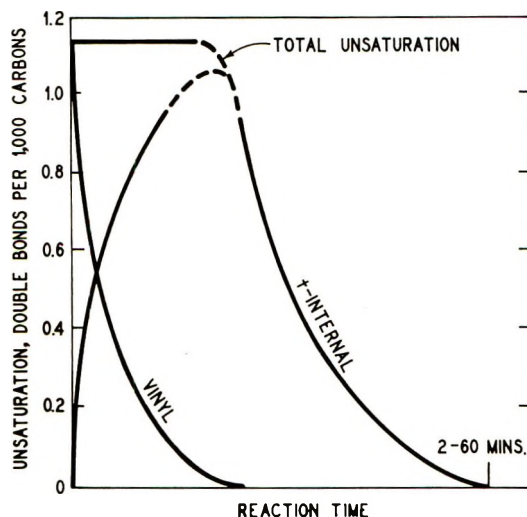


Fig. 3. Hydrogenation of polyethylene with Ni-TEA. Ni/TEA = 3/1; 20-80 ppm Ni; 150°C; 15-30 psi H₂.

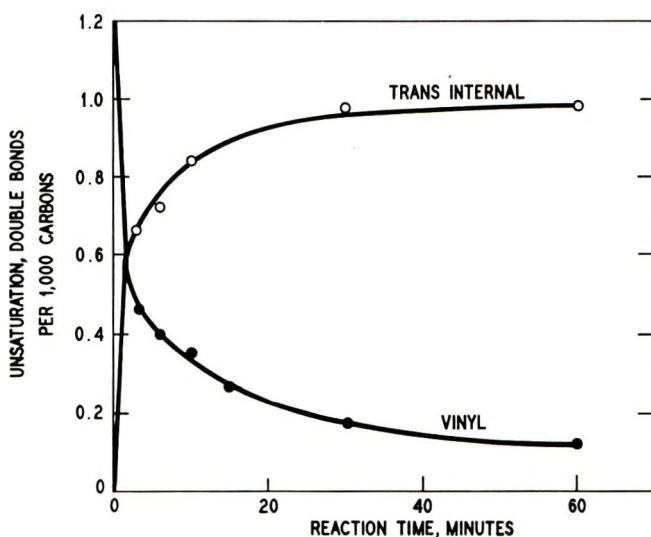


Fig. 4. Isomerization (no H_2 added), Ni-TEA; $150^\circ C$.

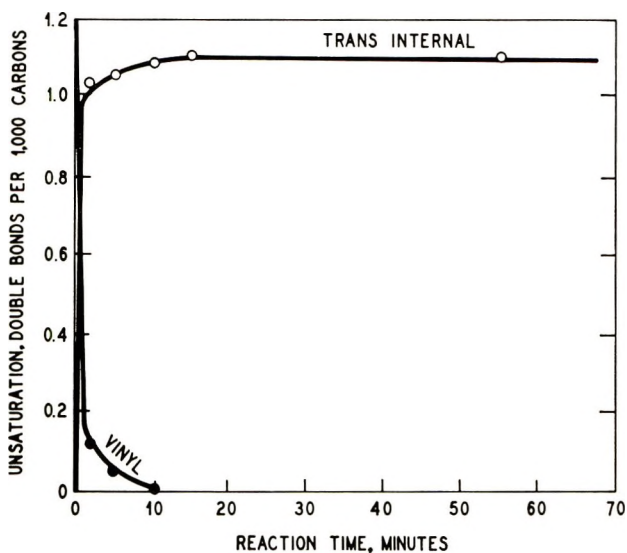


Fig. 5. Isomerization with H_2 added, 5% of stoichiometric.

Further experiments indicated that if hydrogen were omitted, isomerization still occurred, as shown in Figure 4. The isomerization rate was quite rapid initially but decreased with time such that isomerization was not complete in 1 hr. However, when 5% of the amount of hydrogen needed to saturate the double bonds was added the isomerization rate was increased considerably (Fig. 5). In this instance isomerization was complete within 10 min with little or no hydrogenation occurring.

Reaction Path with Other Metal Alkyls

When butyllithium was reacted with nickel octoate at an 8/1 mole ratio a different course of reaction resulted. Both isomerization and hydrogenation reactions occurred concurrently, as is shown in Figure 6.

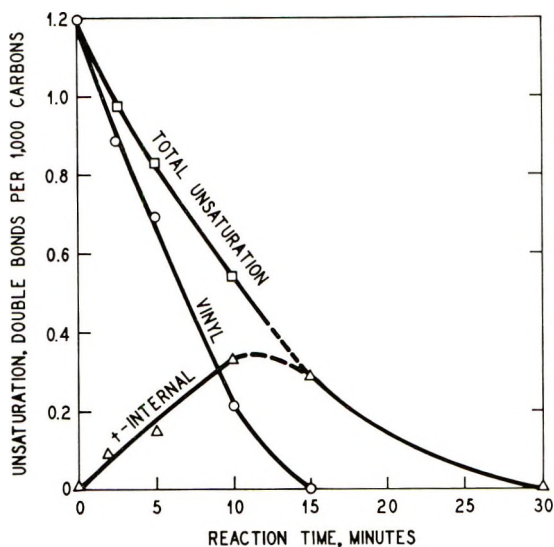


Fig. 6. Hydrogenation of polyethylene with butyllithium-Ni. BuLi/Ni = 8/1; 50 ppm Ni.

Deuteration

A few brief experiments were made in which deuterium was substituted for hydrogen in both the isomerization and hydrogenation steps. The C—D bonding which resulted was followed by using differential infrared techniques. Results are presented in Table III.

In run 4 the nickel-butyllithium catalyst produced considerably more terminal deuterium than did the nickel-triethylaluminum catalyst. This indicated that the nickel-butyllithium catalyst permitted hydrogenation of the vinyl group.

The data indicated appreciable H—D exchange in all cases, and deductions from data of this sort should always be made with a great amount of restraint.

Supported Nickel Octoate

Nickel octoate was readily adsorbed from a hydrocarbon solution onto a predried support material such as silica. Following the adsorption step the nickel octoate was reacted with triethylaluminum to form the hydrogenation catalyst on a solid support.

The course of the isomerization-hydrogenation reaction was changed by the presence of the silica as shown in Figure 7. The conditions chosen

TABLE III
Isomerization, Hydrogenation and Deuteration of 35 MI Polyethylene

Run number	Catalyst	Reaction (to completion)	Samples used in differential spectrum	Dominate position of D ^a	Minor position of D ^a
1	Ni-TEA	Hydrogenation	—	—	—
2	Ni-TEA	Deuteration	2/1	CHD	CH ₂ D, CD ₃
3	Ni-TEA	Isomerization (H ₂) then deuteration	3/1	CHD	CH ₂ D
4	Ni-TEA	Isomerization (D ₂ present)	—	Little if any D	—
5	Ni-BuLi	Deuteration	4/1 4/2	CH ₂ D, CD ₃ , CHD CD ₃	— CH ₂ D

^a Relative to polymer to which sample is compared. HD was found in reactor, indicating that some HD exchange occurred.

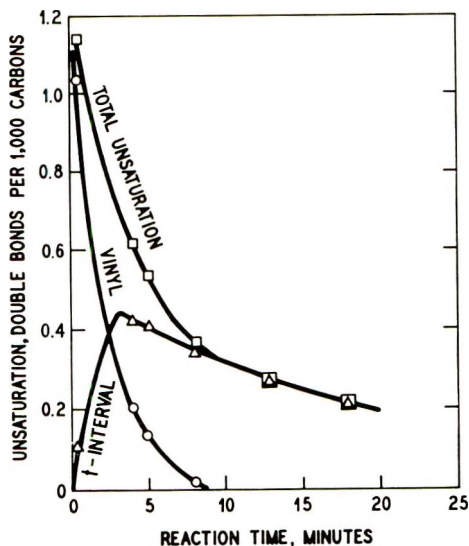


Fig. 7. Hydrogenation of polyethylene with triethylaluminum-nickel octoate-silica. TEA/Ni = 3/1; Syloid 404 silica/Ni = 40/1; 25 psi H₂; 150°C.

for this experiment were such that isomerization and hydrogenation rates were slow enough to be followed. These curves are similar to those obtained with the nickel-butyllithium catalyst system in that both isomerization and hydrogenation occurred simultaneously.

Effect of Light Olefins

One further experiment was made with the supported nickel-triethylaluminum catalyst which involved hydrogenation of polymer in the presence of a small amount of light olefin to determine the effect of unsaturation apart from the polyethylene. An ethylene concentration of 0.1 wt-% of the polymer-cyclohexane solution was used, making the double bond concentration due to ethylene approximately five times as populous as double bonds due to polymer. The results obtained are shown in Figure 8.

The reaction had now become more complex. In this instance isomerization of the vinyl unsaturation to internal unsaturation was the only reaction occurring during the first 10 min. During this time the ethylene was being hydrogenated linearly with time. When the unsaturation due to ethylene has been reduced to about the same level as that present in the liquid phase due to the polymer alone at the beginning, both isomerization and hydrogenation of the polymer unsaturation became quite rapid. From this point on the curves closely resembles those of Figure 7. Isomerization was complete immediately after hydrogenation of all of the ethylene.

The fact that most of the ethylene was hydrogenated before rapid isomerization and hydrogenation of the polymer occurred indicates that the ethylene was adsorbed at the catalyst sites more readily than the polymer.

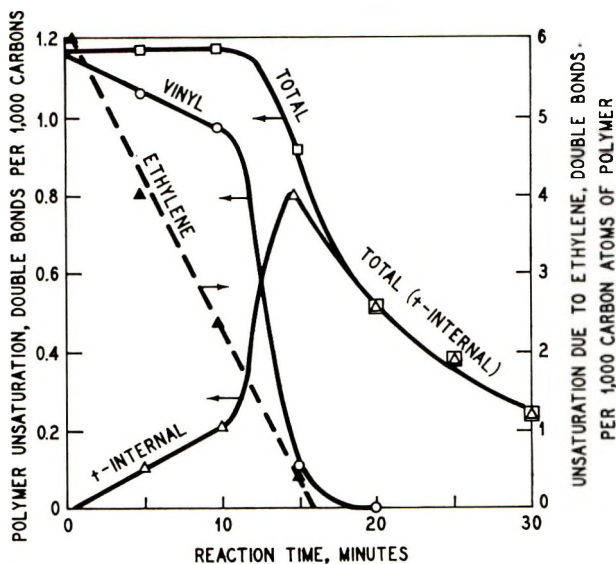


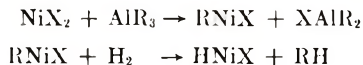
Fig. 8. Hydrogenation of polyethylene with triethylaluminum-nickel octoate-silica in presence of ethylene. TEA/Ni = 3/1; Syloid 404 silica/Ni = 40/1; 25 psi H₂; 0.1 wt-% C₂H₄ in solution; 150°C.

This was probably due to the greater mobility of the ethylene and lack of steric hindrance.

DISCUSSION

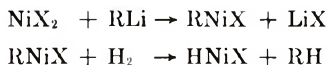
It is always interesting to propose a mechanism for a new reaction. However, the present work does not permit a detailed mechanistic analysis to be made, since it was designed only to explore the general descriptive features of the reaction. Based on the information obtained in this work some consideration of catalyst structure is possible.

At least two catalyst structures can be proposed for this nickel catalyst. One relates to the formation of a metal hydride in the presence of molecular hydrogen as suggested by Sloan et al.⁹ and also Lapporte and Schuett.¹⁰



where X denotes a $\text{R}-\text{C} \begin{array}{l} \text{O} \\ \parallel \\ \text{O} \end{array}$ group.

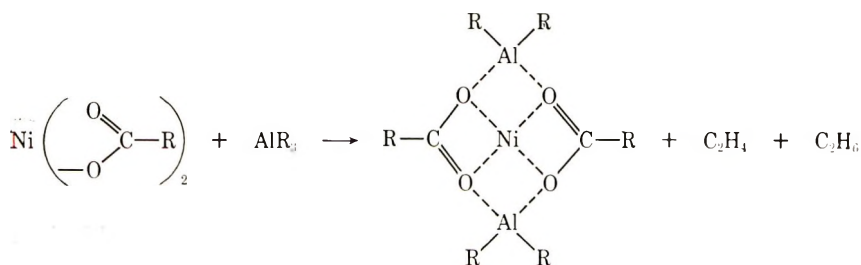
One would also expect the same type of reaction to result with butyllithium.



If such a similar metal hydride catalyst were formed with both catalyst systems one would expect a similar isomerization-hydrogenation reaction path to occur with the polymer. This did not result and suggests that a different catalyst structure may exist.

It was also shown that this catalyst was capable of isomerizing the terminal vinyl unsaturation of the polymer internally in the absence of molecular hydrogen. However, the addition of small amounts of hydrogen increased the isomerization rate considerably. When deuterium was substituted for hydrogen in the isomerization reaction, little if any deuterium was detected in the polymer, indicating that hydrogen (or D_2) did not take a direct role in the isomerization reaction.

Another structure might be a zero-valent nickel complex involving coordination of the nickel and aluminum with oxygen of the carboxy group.



Ethane was observed to have formed during the interaction of the triethylaluminum and nickel(II) 2-ethylhexanoate. Although no ethylene was measured in the reaction it may have formed and remained with the catalyst as an adsorbed species. The fact that the nickel reaction product was not magnetic lends support to the idea of a zero-valent nickel complex.

Because of its different electronegativity butyllithium might be expected to form a related complex which coordinates olefin and hydrogen in such a manner that isomerization and hydrogenation could occur simultaneously. Supporting the nickel on a predried silica before interaction with triethylaluminum might also create catalyst sites whereby both isomerization and hydrogenation could occur at the same time.

A further brief study was made of the isomerization-hydrogenation reaction of pentene-1 and hexene-1 to determine if the reaction path was similar to that observed with the polymer using the nickel-triethylaluminum catalyst system. These experiments indicated that isomerization of the lower molecular weight olefins did not precede the hydrogenation reaction but occurred simultaneously. Both hexene-2 and hexene-3 were formed when hexene-1 was isomerized and hydrogenated, suggesting that the unsaturation in the polymer undoubtedly had been moved internally several carbon atoms from the end before being hydrogenated.

References

1. J. Wicklatz, in *Chemical Reactions of Polymers* (High Polymers Vol. XIX) E. M. Fettes, Ed., Interscience, New York-London-Sydney, 1964.
2. A. I. Yakubchik, B. I. Tikhomirov, and I. A. Klopatoва, USSR Pat. 165,883 (October 26, 1964); *Chem. Abstr.*, **62**, 6589e (1964).
3. A. I. Yakubchik, B. I. Tikhomirov, I. A. Klopatoва and L. N. Mikhailova, *Dokl. Akad. Nauk SSR*, **161**, (1965); *Chem. Abstr.*, **63**, 4412q (1965).
4. Shell Internationale Research Maatschappij N. V., Belg. Pat. 651,281 (October 5, 1964).
5. K. Schmeidl (to Badische Anilin-& Soda-Fabrik Aktiengesellschaft), U. S. Pat. 3,285,902 (Feb. 6, 1962).
6. W. Mechlinski, T. Ziminski, L. Falkowski, and E. Borowski, *Roczniki Chem.*, **39**, 497 (1965); *Chem. Abstr.*, **63**, 16199h (1965).
7. H. S. Hagemeyer, Jr., and R. L. Etter, Jr. (to Eastman Kodak Co.), French Pat. 1,389,768 (Feb. 19, 1965); *Chem. Abstr.*, **63**, 15120a (1965).
8. D. Folzenlogen and M. B. Edwards (to Eastman Kodak Co.), U. S. Pat. 3,313,824; *Chem. Abstr.*, **68**, 22334t (1968).
9. M. F. Sloan, A. S. Matlock, and D. S. Breslow, *J. Amer. Chem. Soc.*, **85**, 4014 (1963).
10. S. J. Lapporte and W. R. Schuett, *J. Org. Chem.*, **28**, 1947 (1963).
11. J. E. Pritchard, J. P. Hogan, and L. R. Kallenbach, *Chim. Ind. Genie Chim.*, **96**, 1631 (1966).
12. J. P. Hogan and R. W. Meyerholtz, in *Encyclopedia of Chemical Technology*, Vol. 14, Kirk and Othmer, Eds., Wiley, New York, 1967, p. 243.

Received November 26, 1969

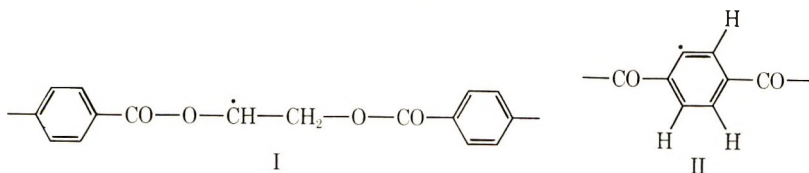
Revised February 2, 1970

Post-Irradiation Free-Radical Reactions in Poly(ethylene Terephthalate)

D. CAMPBELL,* L. K. MONTEITH,† and D. T. TURNER,‡
*Research Triangle Institute, Camille Dreyfus Laboratory,
 Research Triangle Park, North Carolina 27709*

Synopsis

Exposure of poly(ethylene terephthalate) to γ rays results in the formation of radical I, radical II (tentatively), and to an unassigned radical (III) which is responsible for a



central peak in the ESR spectrum. It is believed that completely amorphous samples of polymer contain radicals II and III. On heating, the radicals decay, and the relative proportion of radical III increases. The kinetics of the overall decay process were followed by measuring the decrease in peak height with time. After an initially rapid reaction the decay of the radical population conformed to second order kinetics. An Arrhenius plot of the logarithm of specific rate versus $1/T$ indicated two lines which intersected at 72°C , which is close to the glass transition temperature. The activation energies were 112 kcal/mole above 72° and roughly 25 kcal/mole below 72°C . Reference to reports in the literature suggests that this decay can be explained by long-range movement of the polymer molecules, even in the glassy solid. The decay of radical I in the crystalline regions of an oriented sample was shown to follow first-order kinetics. As the decay occurs at temperatures as low as 100°C (the melting point is about 260°C), it seems that decay by normal physical movement is unlikely. The results might be explained by invoking the hypothesis of chemical migration of free radical sites by hydrogen atom hopping.

INTRODUCTION

The rate at which free radicals disappear during the post-irradiation heating of a polymer depends on their distribution and "movement." Eventually, after the disappearance of closely spaced radicals, the remaining population may be sufficiently random for the subsequent decay to conform to simple second-order kinetics. This poses an interesting ques-

* Present address: The University, Leicester, England.

† Present address: North Carolina State University, Raleigh, N. C.

‡ Present address: Drexel Institute of Technology, Philadelphia, Pa.

tion about the process which permits polymer radicals to come together over an average distance as great as 100 Å, as would be necessary for decay in a sample containing 10^{18} radicals/cm³. In the case of an amorphous sample of poly(methyl methacrylate), Ohnishi and Nitta pointed to the correspondence of their experimental value of 28 kcal/mole for the activation energy of the second-order radical decay with a value of 27 ± 10 kcal/mole obtained from NMR measurements and concluded that both processes were due to motions of segments of the polymer molecules.¹ Notwithstanding, it seems surprising that the decay occurred in the temperature range of 28–55°C which is considerably below the glass transition temperature of about 70°C. This type of difficulty seemed so extreme in the case of similar studies of a partially crystalline sample of nylon 6 that Ballantine and Shinohara invoked the idea that radical sites can move along and between polymer chains by a sequence of hydrogen atom shifts *i.e.*, by repetition of chemical reactions of the kind,² $\text{RH} + \text{R}'\cdot \rightarrow \text{R}\cdot + \text{R}'\text{—H}$. Earlier this idea of radical site migration had been introduced by Dole, Keeling, and Rose^{3,4} to account for certain features of the radiation chemistry of polyethylene and recently a good case has been made by Gehmer and Wagner⁵ that such a process could account quantitatively for the magnitude of the second-order rate constant reported by Charlesby, Libby, and Ormerod for the post-irradiation decay of alkyl radicals in polyethylene.⁶ On the other hand, Auerbach⁷ has presented detailed evidence that the rate of decay of alkyl radicals in polyethylene correlates closely with the temperature range in which the polymer is known to change from a glassy to a viscoelastic material and concluded that the process is controlled by normal diffusion. A puzzling feature of this latter picture is that it seems to account for the whole radical population by reference to the amorphous content which composes only about 20% of the polymer.

At present it does not seem to be possible to decide between physical and chemical processes of radical "movement" in polymers. One long-range approach to the problem is to document radical decay processes further and to urge their continued consideration alongside the development of other diverse methods of assessing "movement" in polymers. Eventually it should then be possible to judge more critically any cases in which physical movement appears to be inadequate. In this further documentation it would seem judicious to make a clear distinction between processes in amorphous and crystalline regions. The present paper describes some current experiments in this direction with poly(ethylene terephthalate), PET. Previously, two brief reports have appeared concerning the formation and decay of radicals on irradiation of partially crystalline samples,^{8,9} but these do not appear to be pertinent to the present work which seeks to differentiate between events in amorphous and crystalline regions.

EXPERIMENTAL

The samples were a biaxially oriented film of thickness 0.0025 cm (Mylar C: Du Pont) of about 50% crystallinity, an amorphous precursor of thick-

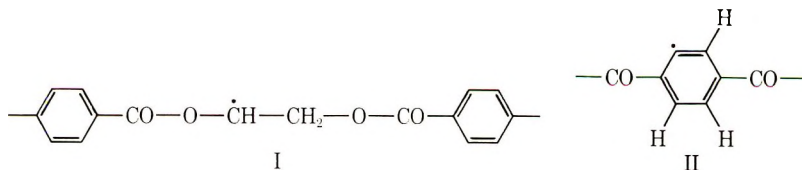
ness 0.03 cm, and a polycrystalline sample of about 70% crystallinity obtained by heating the amorphous sample for 48 hr at 235–240°C in a vacuum.¹⁰ The crystalline content was estimated from x-ray diffraction data.

Samples were thoroughly degassed and sealed in Suprasil quartz tubes at a pressure $<10^{-4}$ mm Hg; sheetlets from the oriented film were packed in stacks of about 30 to a total weight of ca 0.5 g (for other details see Campbell et al.¹¹). After irradiation with γ -rays from a ^{60}Co source at a dose rate of 0.3 to 0.5 Mrad/hr. the quartz was annealed in a flame and first and second derivatives of the absorption curve recorded at room temperature, in every case, with a Varian V4502-10 spectrometer. The number of free radicals in the sample was estimated by double integration of the first derivative spectrum and comparison with α, α' -diphenyl- β -picrylhydrazyl or, relatively, by reference to a peak height. The latter method was especially convenient in following the disappearance of radicals resulting from immersion of the Suprasil tubes in a silicone oil bath maintained at a temperature of $\pm 0.005^\circ\text{C}$. The two methods gave closely similar estimates up to doses of about 80 Mrads but differed somewhat at high doses [cf. peak height (O, ●) and double integration values (●) for the same samples in Figure 1].

RESULTS AND DISCUSSION

Accumulation of Radicals

As in the case of oriented films of PET, both amorphous and polycrystalline samples gave a featureless ESR spectrum when examined at -196°C following irradiation at this temperature. On warming to room temperature the number of spins decreased by about one order of magnitude, presumably due to loss of charged species by recombination. The residual signal from the polycrystalline sample was found to comprise superimposed sets of six and eight lines which could be assigned to different orientations of radical I. The signal from the amorphous sample was poorly resolved but obviously quite different; it has been assigned, tentatively, to radical II. In addition both samples include a central singlet spectral component which has not been assigned.¹¹



Despite the qualitative differences mentioned above the total concentrations of radicals trapped in amorphous and polycrystalline samples of PET at room temperature, following irradiation at -196°C , were closely similar as may be seen by comparison of the blocked circles and squares in

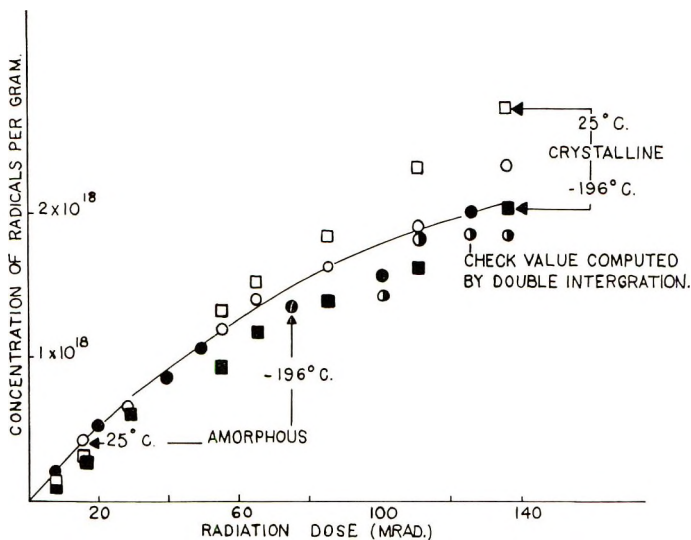


Fig. 1. Accumulation of free radicals with dose in amorphous and polycrystalline samples of poly(ethylene terephthalate).

Figure 1. When comparisons were made following irradiation at room temperature, it was found that after higher doses fewer radicals had accumulated in the amorphous sample presumably because it is a less efficient trapping medium (cf. the open symbols in Fig. 1). On the other hand, after low doses there may be slightly more radicals in the amorphous samples indicating a higher $G(\text{radical})$ value than in the crystalline regions. However, it should be noted that this effect would appear small when contrasted with the claim that in the case of polyethylene radicals are generated much more efficiently in glassy than in crystalline regions.¹²

Decay of Radicals in Amorphous Samples

When a preirradiated amorphous sample is heated above room temperature, while still sealed in the Suprasil tube, the radicals disappear and the singlet component increases relative to the signal assigned to radical II. The overall rate of disappearance was followed by measurement of the peak height of the first derivative spectrum. The data were obtained with samples which had been given the following doses at room temperature, 60°C (300 Mrad); 65, 70, 75, and 77°C (40 Mrad); 80°C (225 Mrad) as shown in Figure 2. As comparisons are being made with samples given varying doses it should be pointed out that this variable was found to be unimportant in these studies. For convenience of presentation, all these results have been normalized to the same initial concentration of radicals.

Following an initially more rapid rate, the disappearance of radicals settles down to a linear relationship between the reciprocal of the concentration of radicals and time, i.e., in conformity with a second-order rate

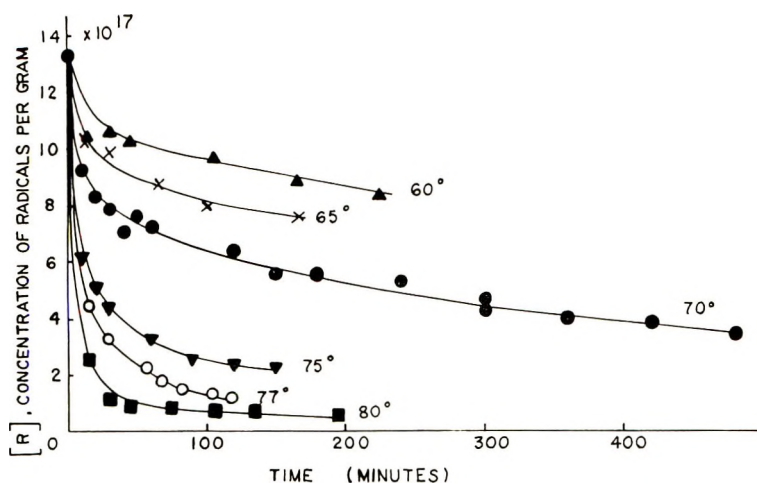


Fig. 2. Decay of free radicals in amorphous poly(ethylene terephthalate). The samples studied at 60° and 80°C actually had a higher concentration of radicals than indicated.

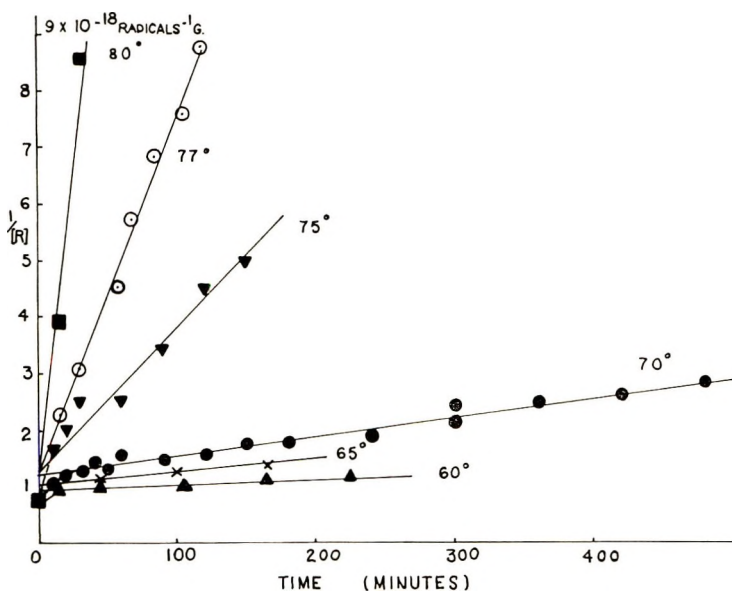


Fig. 3. Second-order plots for decay of free radicals in amorphous poly(ethylene terephthalate).

reaction as required by eq. (1) in which $[R]$ and $[R_0]$ are, respectively, radical concentrations at times t and zero (Figure 3).

$$1/[R] - 1/[R_0] = kt \quad (1)$$

Values of the rate constant k , obtained from the slopes in Figure 3, have been plotted as a function of temperature according to the conventional

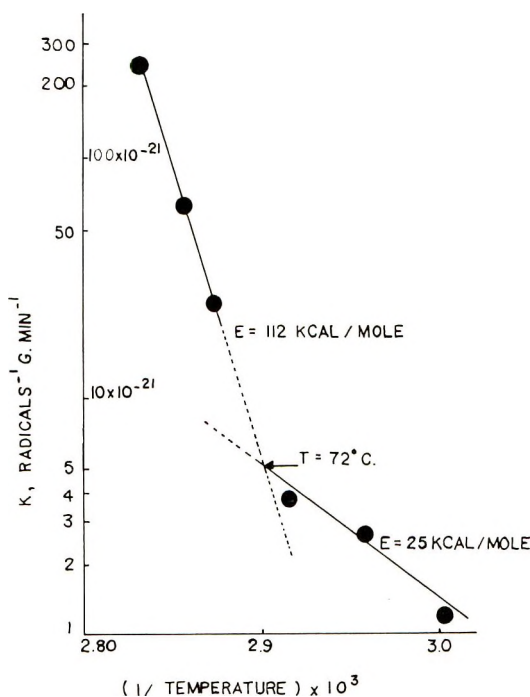


Fig. 4. Arrhenius plot for decay of radicals in amorphous poly(ethyleneterephthalate).

Arrhenius equation, $k = A \exp \{-E/RT\}$, in Figure 4. If the data are taken to define two lines, as shown in Figure 4, these intersect at a point corresponding to a temperature of 72°C and give activation energies E of 112 and roughly 25 kcal/mole. As the glass transition temperature T_g of amorphous PET is about 70°C ,¹³ and as large increases of activation energy for various physical processes are on record in traversing T_g for both low and high molecular weight compounds, these findings appear reasonable.¹⁴ Previously, the post-irradiation decay of free radicals through T_g has been studied in the case of poly(methyl methacrylate) but, apparently, the results did not conform to simple kinetics, and activation energies were not determined.¹⁵

The movement of segments of polymer molecules over distances of about 10^2 \AA is readily acceptable as a plausible mechanism of polymer radical decay above the glass transition temperature. Below T_g it is more difficult to envisage such large-scale movement but, nevertheless, evidence which suggests that this is possible has recently appeared for a number of polymers. In the case of amorphous PET, Yeh and Geil¹⁶ have shown by electron microscopy that small ball-like structures, of diameter 45–100 \AA , are present in the glassy solid and, significantly, that after 6 days at 60°C (5°C below T_g) these had rearranged into larger spherical aggregates of about 5 to 10 balls in diameter. As pointed out by Yeh and Geil, a 75 \AA sphere would correspond to a single molecule with a molecular weight of

about 100,000 and therefore, by comparison with the osmotic molecular weight of 15,000, is expected to comprise a small number of molecules. This suggests that it would be reasonable to adduce from these macroscopic movements evidence for large-scale movements on a molecular scale which could account for the present results. It is to be hoped that further work will permit more quantitative comparisons between the two methods.

Decay of Radicals in Crystalline Samples

The decay of radicals in polycrystalline samples was studied by following the decrease in height of the central peak of the first derivative spectrum with time of heating. At 100°C, about 40% of the radicals survived after 10 hr, and these decayed only slightly on further heating. At 120°C about 30% of the radicals were long-lived (Fig. 5). The decay did not conform to simple kinetics.

In contrast to the above findings, a simple first-order decay of radical I was observed in specially treated samples of oriented crystalline polymer. A linear dependence of the logarithm of radical concentration on time of heating held for the decay of about 80% of the radicals at 100°C and for 95% at 120°C; the respective rate constants were 1.0×10^{-4} and $2.7 \times 10^{-4} \text{ sec}^{-1}$ (Fig. 6). These simple results were obtained only at the price of what, hopefully, may prove to be an unnecessarily complicated sequence of operations which were as follows.

(1) Oriented films of PET were briefly exposed to air, for about 5 min, following γ -irradiation in a vacuum. The films were then thoroughly degassed and resealed in a vacuum. The rationalization of this process is that access of oxygen destroys free radicals in amorphous regions leaving a

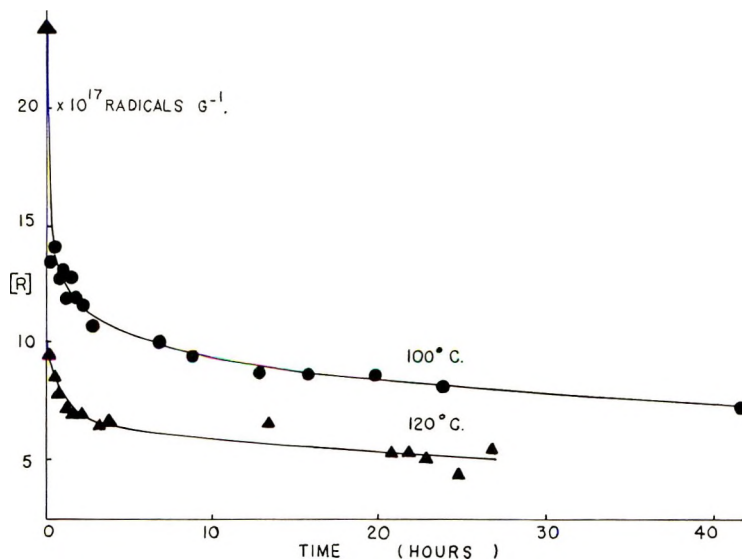


Fig. 5. Decay of radicals in polycrystalline samples of poly(ethylene terephthalate).

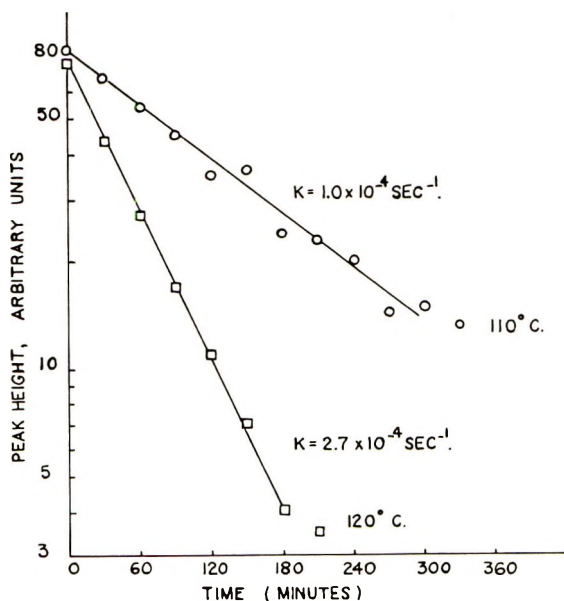


Fig. 6. First-order plots for decay of type I radicals in oriented crystalline poly(ethylene terephthalate).

population predominantly of radical I along with radical II and the species giving the unassigned singlet in the crystallites.¹¹ (2) The sample was heated at 160°C until radical I had decayed, after about 1 hr. (3) The sample was exposed to laboratory fluorescent lighting for several weeks, during which time radical II was replaced by radical I by a photochemical reaction.¹⁷

The population of radical I generated in the above way gave the usual well resolved ESR spectrum, six or eight lines depending on orientation in the magnetic field.¹¹ The decay was followed by reference to the heights of outer peaks which have the advantage of being clearly separated from central components of the spectrum. Similar results were obtained by reference to peaks 1 and 2 of both six- and eight- line spectra.¹¹ During this decay the central portion of the spectrum did not change significantly and it is concluded that radical I disappears largely by bimolecular reactions rather than by conversion into other radical species.

In order to account for first-order kinetics it is suggested that the rate-determining step is the movement of a radical site to the surface of a crystallite. At the surface, the radical is supposed to react rapidly with similarly situated radicals in other crystallites which are moving freely in an amorphous matrix 30°C, or more, above T_g . The smallest dimension of a crystallite in PET is 100–200 Å,^{18,19} and the question remains of how radicals could move over such distances in a crystalline medium. Reference to the high melting point of the polymer, about 260°C, suggests that long-range segmental displacements are unlikely to be important at tempera-

tures as low as 110°C. In these circumstances, it would appear reasonable to adopt the hypothesis of the migration of free radical sites by hydrogen atom hopping.²⁻⁵ Moreover, consideration of atomic arrangement in crystalline PET²⁰ would suggest that such hopping would follow prescribed routes along isolated stacks of $-\text{CH}_2-\text{CH}_2-$ groups which would tend to minimize bimolecular reactions of radicals within the crystallites.

CONCLUSIONS

The disappearance of free radicals in amorphous PET can be accounted for by reference to physical movement, even below the glass transition temperature. The disappearance of radicals in crystalline regions occurs at temperatures so far below the melting point that it seems necessary to invoke some further hypothesis for radical migration; the chemical hypothesis of radical site hopping by hydrogen atom transfer is adopted.

Two of us (L. K. M. and D. T. T.) were supported by the Langley Research Center of the National Aeronautics and Space Administration under contract NAS1-7553. Dr. C. J. Heffelfinger is thanked for providing samples of polymer.

References

1. S. I. Ohnishi and I. Nitta, *J. Polym. Sci.*, **38**, 451 (1959).
2. D. S. Ballantine and Y. Shinohara, paper presented at 5th International Symposium on Free Radicals, Session B3 (No. 5), Uppsala (1961).
3. M. Dole, C. D. Keeling, and D. G. Rose, *J. Amer. Chem. Soc.*, **76**, 4304 (1954).
4. M. Dole in *Crystalline Olefin Polymers* Part 1, R. A. V. Raff, and K. W. Doak, Eds., Interscience New York, 1965.
5. D. O. Yehmer and C. D. Wagner, *Natosc*, **208**, 72 (1965).
6. A. Charlesby, D. Libby, and M. G. Ormerod, *Proc. Roy. Soc. (London)*, **A262**, 207 (1961).
7. I. Auerbach, *Polymer* **7**, 283 (1966).
8. H. Sobue, Y. Tabata, and M. Hiraoka, *Kogyo Kagaku Zasshi*, **64**, 372 (1961).
9. Y. Hama, S. Okamoto, and N. Tamura, *Repts. Prog. Polym. Phys., Japan*, **7**, 351 (1964).
10. D. Campbell and D. T. Turner, *J. Polym. Sci. A-1*, **5**, 2199 (1967).
11. D. Campbell, K. Araki, and D. T. Turner, *J. Polym. Sci. A-1*, **4**, 2597 (1966).
12. B. R. Loy, *J. Polym. Sci.*, **44**, 341 (1960).
13. H. J. Kolb and E. F. Izard, *J. Appl. Phys.*, **20**, 564 (1949).
14. F. Bueche, *Physical Properties of Polymers*, Interscience, New York, 1962.
15. S. Shida, J. Higuchi, R. Kasaka, and T. Miyamae, unpublished.
16. G. S. Y. Yeh and P. H. Geil, *J. Macromol. Sci (Phys.) B*, **1**, 235 (1967).
17. D. Campbell and D. T. Turner, *J. Polym. Sci. B*, in press.
18. W. O. Statton, *J. Polym. Sci.*, **41**, 143 (1959).
19. J. C. Collier and E. Baer, Tech. Rept. No. 20, Cast Institute of Technology, (1966).
20. R. de P. Daubeney, C. W. Bunn, and C. J. Brown, *Proc. Roy. Soc. (London)*, **A-226**, 531 (1954).

Received December 2, 1969

Revised February 4, 1970

A Convenient Technique for Determination of Reactivity Ratios

ELOISA B. MANO and ROBERTO RIVA DE ALMEIDA,
*Instituto de Química da Universidade Federal do Rio de Janeiro,
Rio de Janeiro, Brazil*

Synopsis

A new technique to determine the reactivity ratios for monomers is described. It is based on vapor-phase chromatography and can be used for any volatile monomer. A new simplified equation was deduced which permits the direct use of the retention times to obtain the pair $r_1 r_2$. The method is suggested for use in determination of the molar ratios of the chemical units in the polymer chain, regardless of chemical composition or constitution. The simplicity of this technique allows its use for monomer-polymer systems composed of any number of volatile monomers. The validity of this method was checked by using the pair methyl methacrylate-styrene. This technique is also being applied to the study of kinetics in polymerizations, since it allows the measurements of several samples taken from a single experiment.

INTRODUCTION

Vapor-phase chromatography (VPC) has been used to determine residual monomers in polymers.¹

Harwood and co-workers² used VPC by the direct technique for the determination of the monomer ratios for the pair methyl methacrylate-styrene. Their technique consisted of conducting polymerization reactions for various times and then terminating the polymerization by adding an equal volume of hydroquinone saturated toluene to the polymerization mixtures. Portions of diluted solutions were then analyzed directly for styrene, methyl methacrylate and toluene by vapor-phase chromatography.

Harwood's technique required one polymerization system for each analytical data to be obtained.

In order to reduce the time and reagents required and to minimize the number of variables, we developed an improved technique, to be used in homogeneous systems, that allows the use of a single polymerization flask, during the reaction period, to obtain several kinetic data for each molar ratio of reagents.

New simplified equations were deduced to permit the direct use of the retention times to obtain the pair $r_1 r_2$.

EXPERIMENTAL

Materials

Methyl methacrylate (bp 99–100°C/760 mm), styrene (bp 145°C/760mm), and toluene (bp 110°C/760 mm) were distilled and used immediately. Hydroquinone was used as supplied. AIBN, the initiator, was recrystallized from hot methanol. Nitrogen and helium were used as supplied.

Equipment

A gas chromatograph, model CG-12—IP (made in Brazil), equipped with a thermoconductivity detector and connected to a Sargent model SRG recorder, was used. Peak areas were measured by a Disc Chart Integrator model 204 (Disc Instrument Inc.). In order to separate the polymer and other nonvolatile compounds present in the sample, a 20-cm glass wool-filled precolumn unit was employed. A 4-m column with Apiezon L, supported on Chromosorb-P, was used. Constant temperature ($\pm 0.1^\circ\text{C}$) was maintained with a Labline water bath.

Model Experiment

The stability of the monomers under the chromatography conditions was checked.

The polymerization technique described by Harwood² was used, with the following modifications. A screw-cap, NBR-gasketed flask suitable for syringe in-take of samples was used. The use of a single system to collect several samples requires special care due to the variation of the total mass in the polymerization. The samples weights were obtained by difference, by taking about 0.4 g of polymer-monomer solution and pouring at once into a 0.4 ml solution of hydroquinone in toluene. The reaction flask was immediately returned to the water bath, until the next sample collection.

The polymer conversion for every sample was carefully determined by precipitation in methanol.

The toluene solutions of the samples were then subjected to chromatography.

RESULTS AND DISCUSSION

In the Mayo and Lewis³ and Fineman and Ross⁴ copolymerization equations, the ratios M_1/M_2 , m_2/m_1 or m_1/m_2 are unknown (molar ratio in the charge and in the copolymer respectively). The chromatogram of P_0 grams of monomer sample, and toluene (reference) gave, at zero time of polymerization, the counts $a_{1,0}$, $a_{2,0}$, and $a_{t,0}$ respectively. If the mass $w_{t,0}$ of toluene gave $a_{t,0}$ counts, then $a_{1,0}$ counts of monomer 1 will correspond to mass $w_{1,0}$.

$$w_{t,0}a_{1,0} = w_{1,0}a_{t,0} \quad (1)$$

On using the thermal relative response factor R referred to benzene,⁵ the number of moles in the polymerization system will be:

$$M_1 = (w_{t,0}/P_0)(a_{1,0}/a_{t,0})(R_t/R_1)(P/A_1) \quad (2)$$

$$M_2 = (w_{t,0}/P_0)(a_{2,0}/a_{t,0})(R_t/R_2)(P/A_2) \quad (3)$$

and the ratio M_1/M_2 will be:

$$M_1/M_2 = (a_{1,0}/a_{2,0})(R_2/R_1)(A_2/A_1) \quad (4)$$

where A_1 and A_2 are the molecular weights of monomers 1 and 2, respectively, and P is the total mass of polymerization. R_1 , R_2 and R_t are the thermal relative response factor referred to benzene, of the monomers 1, 2 and toluene respectively.

In an analogous manner, at time t of the polymerization, the molar concentration N_1 and N_2 of each monomer will be:

$$N_1 = w_{t,t}/P_t(a_{1,t}/a_{t,t})(R_t/R_1)(P/A_1) \quad (5)$$

$$N_2 = (w_{t,t}/P_t)(a_{2,t}/a_{t,t})(R_t/R_2)(P/A_2) \quad (6)$$

The number of moles of each monomer incorporated into the polymer chain at time t will be equal to the number of moles of the corresponding monomer charged in the beginning of the reaction, minus the number of moles of each unreacted monomer at time t :

$$m_1 = M_1 - N_1 \quad (7)$$

$$m_2 = M_2 - N_2 \quad (8)$$

By replacing the values obtained in eqs. (2), (3), (5) and (6) in eqs. (7) and (8), we will arrive at the desired equations:

$$\frac{m_1}{m_2} = \frac{(w_{t,0}a_{1,0}P_t a_{t,t} - w_{t,t}a_{1,t}P_0 a_{t,0})R_2 A_2}{(w_{t,0}a_{2,0}P_t a_{t,t} - w_{t,t}a_{2,t}P_0 a_{t,0})R_1 A_1} \quad (9)$$

$$\frac{m_2}{m_1} = \frac{(w_{t,0}a_{2,0}P_t a_{t,t} - w_{t,t}a_{2,t}P_0 a_{t,0})R_1 A_1}{(w_{t,0}a_{1,0}P_t a_{t,t} - w_{t,t}a_{1,t}P_0 a_{t,0})R_2 A_2} \quad (10)$$

The technique as well as the mathematical treatment proposed in this work were successfully tested for the pair methyl methacrylate-styrene, according to the data of Harwood and co-workers,² as shown in Table I.

TABLE I
Copolymerization of Methyl Methacrylate-Styrene

Investigator	r_1 (styrene)	r_2 (methyl methacrylate)
Harwood and co-workers ²	0.51 ± 0.02	0.46 ± 0.02
This paper	0.49 ± 0.02	0.48 ± 0.02

A computerized version (IBM 1130—V.1, Fortran IV) of this method has been developed and will be applied for the calculations of the reactivity ratios of other monomer systems, as well as kinetic studies.

This research was supported by funds provided by Banco Nacional do Desenvolvimento Econômico (BNDE) and Coordenação do Aperfeiçoamento de Pessoal de Nível Superior (CAPES). We wish to thank Dr. Ailton de Souza Gomes and Dr. Remolo Ciola for much helpful discussion, and Mr. Ronald Leal for assistance in computer programming.

References

1. R. Feinland, in *Encyclopedia of Polymer Science and Technology*, Vol. 3, Interscience, New York, 1965, p. 745.
2. H. J. Harwood, H. Baikowitz, and H. F. Trommer, paper presented at American Chemical Society Meeting, 1963; *Polym. Preprints*, **4**, No. 1, 133 (1963).
3. F. R. Mayo and F. M. Lewis, *J. Amer. Chem. Soc.*, **66**, 1594 (1944).
4. M. Fineman and S. D. Ross, *J. Polym. Sci.*, **5**, 259 (1950).
5. R. Ciola *Introdução à Cromatografia em Fase Gasosa*, Assoc. Bras. Química, Reg. Paraná, Curitiba, Brasil, 1969.

Received March 30, 1970.

NOTES

*Abnormal Effect of Hydrogen on Propylene Polymerization
with $TiCl_3-Al(C_2H_5)_2Cl$*

Although many investigations have been made on the effect of hydrogen on the polymerization of olefin with Ziegler-Natta catalysts,¹⁻⁴ the kinetic character of hydrogen has not yet been clarified completely. This note will point out an abnormal effect of hydrogen on the polymerization of propylene with $TiCl_3-Al(C_2H_5)_2Cl$.

The same apparatus and procedures were used as reported in the previous paper.⁵ Propylene (Mitsubishi Petrochemical Co., purity 99.9%) of a constant pressure (40 cm Hg) was polymerized in the presence of various pressures of hydrogen (0-25 cm Hg) with $TiCl_3$ (AA grade, Stauffer Co.), $[Al]/[Ti] = 1$, and *n*-heptane (Enjay Co.) or toluene as a solvent.

The tacticity and the molecular weight of the produced polymer were measured by infrared⁶ and viscometric⁷ methods, respectively.

As reported before,⁸ the polymerization rate with $TiCl_3-Al(C_2H_5)_2Cl$ decreases monotonously with increasing of hydrogen added, and the effect of hydrogen could be explained as a retardation due to an adsorption of hydrogen on the surface of $TiCl_3$.

On the other hand, the dependences of the stationary polymerization rates on the pressure of hydrogen are rather curious in the case with $Al(C_2H_5)_2Cl$, as shown in Figures 1 and 2.

Figure 2 shows that the stationary polymerization rate becomes constant at high levels of hydrogen pressure, passing through a maximum as the hydrogen pressure increases. It should be noted here that the rates at higher pressure of hydrogen recover rapidly from the constant value to the maximum one on pumping out the hydrogen, as marked by upward arrows. Such a recovery was found in the case with $Al(C_2H_5)_2Cl$.

In order to clarify the abnormal effect of hydrogen observed in the case with $Al(C_2H_5)_2Cl$ and toluene, the following experiments were carried out.

When TA- $TiCl_3$ is used in place of AA- $TiCl_3$, no maximum is observed. TA grade $TiCl_3$ is prepared by the reduction of $TiCl_4$ with titanium metal and activated. This suggests that $AlCl_3$ from AA- $TiCl_3$ may be responsible for the abnormal effect.

The total weight of polymer produced under the optimum pressure of hydrogen corresponding to the maximum was the same as that of propylene consumed. This indicates that there exist no other reactions, such as hydrogenation, during the polymerization.

Using AA- $TiCl_3$ washed with toluene prior to polymerization with $Al(C_2H_5)_2Cl$, we obtain the stationary rate of the polymerization shown by Figure 2A. To determine which part of the catalyst mixture, i.e., liquid phase or solid, is responsible for the phenomenon, polymerization with fresh AA- $TiCl_3$ and liquid phase extracted from the system, AA- $TiCl_3-Al(C_2H_5)_2Cl$ -hydrogen-toluene, was carried out. The stationary rate in this case is given in Figure 2B.

Polymerization with various samples of AA- $TiCl_3$ were carried out in the presence of hydrogen; the stationary rates are shown in Figure 1. Figure 1C corresponds to the case of polymerization with AA- $TiCl_3$ washed with toluene, Figure 1D is obtained with AA- $TiCl_3$ washed with toluene- $Al(C_2H_5)_2Cl$, and Figure 1E shows the rate with AA- $TiCl_3$ washed with toluene- $Al(C_2H_5)_2Cl$ -hydrogen. This indicates that the increase in the polymerization rates is due to some effect that comes from the mixture, AA- $TiCl_3-Al(C_2H_5)_2Cl$ -toluene-hydrogen.

Polymerization at 55°C was carried out for 1 hr, and the polymerization temperature was decreased to 45°C. The resultant rate is, as indicated by Figure 2F, lower than

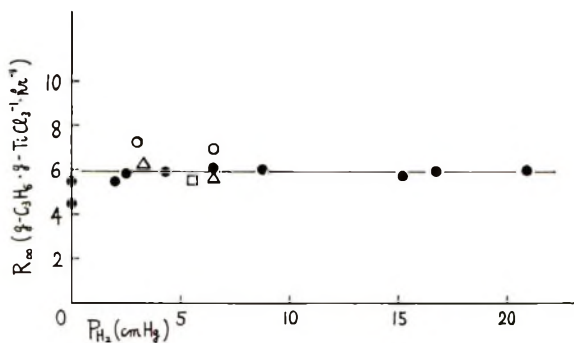


Fig. 1. Stationary polymerization rate at 45°C vs. hydrogen pressure on *n*-heptane solvent: (Δ) C, (\square) D, (\circ) E.

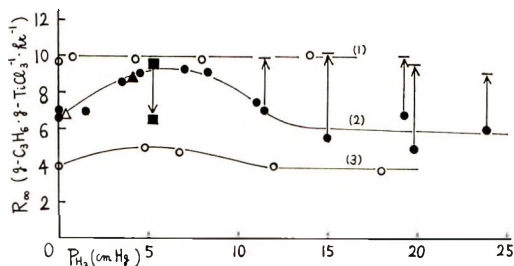


Fig. 2. Stationary polymerization rates vs. hydrogen pressure in the presence of toluene: (1) 55°C, (2) 45°C; (3) 35°C; (\blacktriangle) A (\triangle) B (\blacksquare) F. The arrow indicates the elimination of hydrogen.

that expected at 45°C. This suggests to us that the polymerization centers which are responsible for the increase in the rate are thermally unstable.

It has been confirmed that the tacticity of polymer produced is independent of hydrogen pressure. The molecular weight decreased with the increase of hydrogen pressure, as expected, but it was independent of solvent.

In considering the effect of hydrogen in the case with AA-TiCl₃-Al(C₂H₅)₂Cl-toluene, it is noteworthy that AlCl₃ is involved in AA-TiCl₃ and its solubility for toluene (27×10^{-6} mole/100-g toluene-g TiCl₃) is much larger than that for *n*-heptane ($0 \sim 1.2 \times 10^{-6}$ mole/100 g *n*-heptane-g TiCl₃).⁹

Our experimental results can be explained by formation of new active sites on the surface of AA-TiCl₃ as the result of washing out AlCl₃ and reducing the fresh surface of TiCl₃ by Al(C₂H₅)₂Cl with the aid of hydrogen. The new sites may be supposed to be the same as those formed on the surface with Al(C₂H₅)₃ which is stronger than Al(C₂H₅)₂Cl in reducing power, because there are observed similar recoveries of the rate on removal of hydrogen from the system.

References

1. G. Natta, G. Mazzanti, P. Longi, and F. Bernardini, *Chem. Ind. (Milan)*, **41**, 519 (1959).
2. A. Schindler, *J. Polym. Sci. B*, **3**, 793 (1965).
3. A. S. Hoffman, B. F. Fries, and P. C. Condit, in *Macromolecular Chemistry (J. Polym. Sci. C, 4)*, M. Magat, Ed., Interscience, New York, 1963, p. 109.
4. G. Bourat, J. Ferrier, and A. Perez, in *Macromolecular Chemistry (J. Polym. Sci. C, 4)*, M. Magat, Ed., Interscience, New York, 1963, p. 103.

5. T. Keii, M. Taira, and T. Takagi, *Can. J. Chem.*, **41**, 206 (1963).
6. J. P. Luongo, *J. Appl. Polym. Sci.*, **3**, 302 (1960).
7. J. B. Kinsinger, paper presented at the 132nd Meeting, American Chemical Society, New York, 1957.
8. A. Takahashi and T. Keii, paper presented at the 19th meeting of the Chemical Society of Japan, 1966.
9. Y. Hattori and T. Keii, unpublished data.

ICHIRO OKURA
KAZUO SOGA
AKIRA KOJIMA
TOMINAGA KEII

Department of Chemical Engineering
Tokyo Institute of Technology
Meguro, Tokyo, Japan

Received August 20, 1968

Polymerization of Terminal Acetylenes by the Ferric Naphthenate-Triisobutylaluminum Initiator System

The polymerization of terminal acetylenes can be accomplished with certain coordination-type catalyst systems to produce low molecular weight polymers.¹ Relatively high molecular weight polymers have been prepared by the use of ferric acetylacetonate-organoaluminum. For example, polyphenylacetylene was prepared by using ferric acetylacetonate with triethylaluminum² or with diisobutylaluminum hydride,³ and 4-methyl-1-hexyne was polymerized by ferric acetylacetonate-triisobutylaluminum initiator.⁴

We wish to report on the use of ferric naphthenate, a commercial solution of the iron salt of a highly refined naphthenic acid, and triisobutylaluminum as an initiator for the polymerization of terminal acetylenes. Ferric naphthenate is soluble in toluene and is easily and accurately handled in this manner.

GENERAL POLYMERIZATION PROCEDURE

Polymerizations were conducted in 12-oz-oven-dried beverage bottles with 10-g charges of monomer. The bottles, with or without solvent, were purged with nitrogen at 3 l./min. for 5 min before capping with self-sealing rubber gaskets fastened by crown caps. Ferric naphthenate was charged as a 0.05*M* toluene solution by means of a syringe. Similarly, triisobutylaluminum was charged as a cyclohexane solution. This mixture was allowed to agitate in a 50°C constant temperature bath for 1 hr. The monomer was added subsequently by syringe and the reaction mixture agitated in a constant-temperature bath for the indicated reaction time. Upon completion of the reaction time, the polymers were coagulated in acetone and protected with 2% antioxidant. The polymers were dried at ambient temperature under vacuum.

RESULTS AND DISCUSSION

The results of several experiments are summarized in Table I. Excellent yields of polymer were obtained. Cyclohexane appeared to be the best solvent screened. The optimum molar ratio of $(i\text{-C}_4\text{H}_9)_3\text{Al}$ to ferric naphthenate was found to be 3:1. Polymer yield decreased with decreasing ferric naphthenate level, but 7% poly-1-hexyne was obtained with the lowest level of ferric naphthenate tested, 0.2 mmole. Considerable gel was observed in the polymers prepared at 5°C. The 50°C reaction temperature gave the best overall balance of good conversion and high inherent viscosity.

The polymerization was rapid, with the formation of a very viscous, gelatinous, reaction mixture soon after addition of monomer; however, additional reaction time at 50°C gave a higher molecular weight polymer. Two distinct reactions may have been occurring, propagation and crosslinking. The inherent viscosities of polymers obtained after 24 hr reaction time at 50°C are approximately twice those at 2 hr. Also, the molecular weight distribution as determined by gel-permeation chromatography was broad and contained several peaks (see Fig. 1). The molecular weight distribution of the polymer prepared from ferric acetylacetonate-triisobutylaluminum under identical conditions was similar.

Acetone was used as the coagulation material for ease of removal because of its low boiling point. The polyacetylenes decomposed when heated, even in the vacuum oven. For example, the decomposition temperature of a sample of poly-1-hexyne prepared in the ferric naphthenate-triisobutylaluminum system was 126°C when the temperature was raised 10°C/min in a differential thermal analysis run in air. Similar results were obtained with a polymer prepared in the ferric acetylacetonate-triisobutylaluminum system when run in either air or argon. It was thought that catalyst residues might be contributing to this decomposition and that these residues might be more easily removed when prepared from the toluene soluble ferric naphthenate; however, iron and aluminum residues remained in the polymer after acetone coagulation. Methods of catalyst residue removal need to be developed to establish the reason for polymer instability.

TABLE I
 Polymerization of Terminal Acetylenes with $\text{Fe}(\text{III})\text{Naphthenate-(}i\text{-C}_4\text{H}_9\text{)}_3\text{Al}$

Monomer (10 g)	Fe(III)- Naphthenate, mmole	$(i\text{-C}_4\text{H}_9)_3\text{-}$ Al, mmole	Solvent		Polymerization			Yield, %	Inherent viscosity	Gel, %
			Type	Volume, ml	Tempera- ture, °C	Time, hr				
1-Butyne	1	3	Cyclohexane	100	5	24	100	2.06	39	
1-Hexyne	1	3	None	—	50	2	30	2.33	0	
1-Hexyne	1	3	Cyclohexane	100	50	2	62	2.06	0	
1-Hexyne	1	3	Cyclohexane	100	50	24	89	3.96	0	
1-Hexyne	1	3	Cyclohexane	150	50	24	91	4.23	0	
1-Hexyne	1	3	Cyclohexane	200	50	24	90	4.89	0	
1-Hexyne	0.8	2.4	Toluene	150	5	24	26	5.84	40	
1-Hexyne	0.8	2.4	n-Hexane	150	5	24	55	3.70	0	
1-Hexyne	0.8	2.4	Cyclohexane	150	70	0.5	26	2.95	19	
1-Hexyne	0.8	2.4	Cyclohexane	150	-30	24	62	4.76	31	
1-Dodecyne	1	3	Cyclohexane	100	5	24	94	2.29	19	

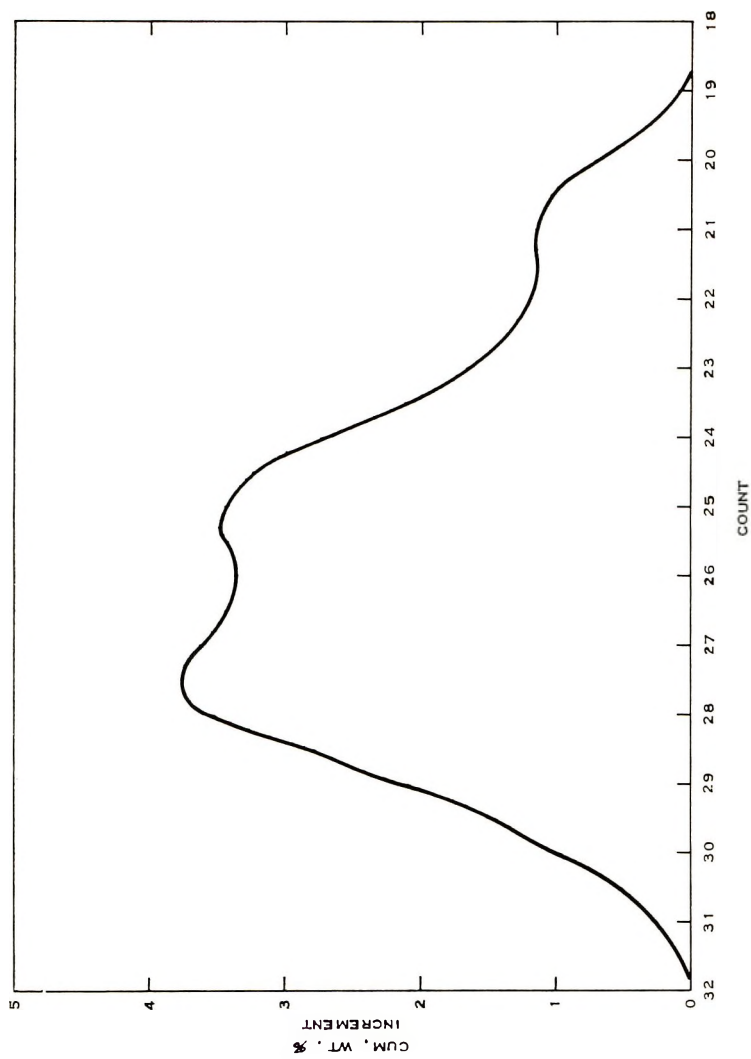


Fig. 1. Molecular weight distribution of poly-1-hexyne by gel-permeation chromatography.

Attempts to prepare copolymers of 1-hexyne and butadiene, isoprene, or styrene, respectively, in the ferric naphthenate-triisobutylaluminum system were unsuccessful. Only poly-1-hexyne homopolymer was obtained. The reaction product of ferrocene and triisobutylaluminum was not active for the polymerization of terminal acetylenes. Traces of polymer were obtained from triisobutylaluminum and cobalt naphthenate, manganese naphthenate and vanadium naphthenate, respectively, with 1-hexyne.

The authors wish to express their thanks to Drs. R. P. Zelinski and C. A. Uranek for helpful discussions and suggestions and to Mr. W. O. Drake for Differential Thermal Analysis determinations.

References

1. G. Natta, G. Mazzanti, and P. Pino, *Angew. Chem.*, **69**, 685 (1957).
2. S. Kambara, N. Yamazaki, and M. Hatano, paper presented to Division of Petroleum Chemistry, American Chemical Society, Meeting, 1964; *Preprints*, **9**, No. 4, A-23 (1964).
3. R. J. Kern, *J. Polym. Sci. A-1*, **7**, 621 (1969).
4. F. Ciardella, E. Benedetti, and O. Pieroni, *Makromol. Chem.*, **103**, 1 (1967).

WILLIAM J. TREPKA
RICHARD J. SONNENFELD

Phillips Petroleum Company
Bartlesville, Oklahoma 74003

Received February 19, 1970

Contents (continued)

F. LAUTENSCHLAEGER and H. SCHNECKO: Polymerization of Unsaturated Episulfides	2579
P. BANKS and R. H. PETERS: Polymerization and Crosslinking of Epoxides: Base-Catalyzed Polymerization of Phenyl Glycidyl Ether	2595
PRABIR K. DUTT and C. S. MARVEL: A Polyamide from Anthraquinonediketene	2611
M. R. GRANCIO and D. J. WILLIAMS: The Morphology of the Monomer-Polymer Particle in Styrene Emulsion Polymerization	2617
E. N. ZILBERMAN, A. E. KULIKOVA, S. B. MEIMAN, N. A. OKLADNOV, and V. P. LEBEDEV: A Study on the Mechanism of Polyvinyl Chloride Stabilization by Lead Salts	2631
J. P. HOGAN: Ethylene Polymerization Catalysis over Chromium Oxide	2637
N. GRASSIE and D. R. BAIN: Thermal Degradation of Copolymers of Styrene and Acrylonitrile. I. Preliminary Investigation of Changes in Molecular Weight and the Formation of Volatile Products	2653
N. GRASSIE and D. R. BAIN: Thermal Degradation of Copolymers of Styrene and Acrylonitrile. II. Reaction Products	2665
N. GRASSIE and D. R. BAIN: Thermal Degradation of Copolymers of Styrene and Acrylonitrile. III. Chain-Scission Reaction	2679
D. R. WITT and J. P. HOGAN: Double-Bond Isomerization and Hydrogenation in Polyethylene with Soluble Nickel Catalysts	2689
D. CAMPBELL, L. K. MONTEITH, and D. T. TURNER: Post-Irradiation Free-Radical Reactions in Poly(ethylene Terephthalate)	2703
E. B. MANO and R. R. DE ALMEIDA: A Convenient Technique for Determination of Reactivity Ratios	2713

NOTES

ICHIRO OKURA, KAZUO SOGA, AKIRA KOJIMA, and TOMINAGA KEII: Abnormal Effect of Hydrogen on Propylene Polymerization with $TiCl_3-Al(C_2H_5)_2 Cl$	2717
WILLIAM J. TREPKA and RICHARD J. SONNENFELD: Polymerization of Terminal Acetylenes by the Ferric Naphthenate-Triisobutylaluminum Initiator System	2721

The *Journal of Polymer Science* publishes results of fundamental research in all areas of high polymer chemistry and physics. The *Journal* is selective in accepting contributions on the basis of merit and originality. It is not intended as a repository for unevaluated data. Preference is given to contributions that offer new or more comprehensive concepts, interpretations, experimental approaches, and results. Part A-1 *Polymer Chemistry* is devoted to studies in general polymer chemistry and physical organic chemistry. Contributions in physics and physical chemistry appear in Part A-2 *Polymer Physics*. Contributions may be submitted as full-length papers or as "Notes." Notes are ordinarily to be considered as complete publications of limited scope.

Three copies of every manuscript are required. They may be submitted directly to the editor: For Part A-1, to C. G. Overberger, Department of Chemistry, University of Michigan, Ann Arbor, Michigan 48104; and for Part A-2, to T. G. Fox, Mellon Institute, Pittsburgh, Pennsylvania 15213. Three copies of a short but comprehensive synopsis are required with every paper; no synopsis is needed for notes. Books for review may also be sent to the appropriate editor. Alternatively, manuscripts may be submitted through the Editorial Office, c/o H. Mark, Polytechnic Institute of Brooklyn, 333 Jay Street, Brooklyn, New York 11201. All other correspondence is to be addressed to Periodicals Division, Interscience Publishers, a Division of John Wiley & Sons, Inc., 605 Third Avenue, New York, New York 10016.

Detailed instructions in preparation of manuscripts are given frequently in Parts A-1 and A-2 and may also be obtained from the publisher.

CARBANIONS, LIVING POLYMERS, AND ELECTRON-TRANSFER PROCESSES

By MICHAEL SZWARC, *New York Polymer Research Center at the College of Forestry, Syracuse, New York*

"...this book will be quickly appreciated as a valuable contribution by a distinguished author." — *Nature*

"In this monograph, Professor Szwarc extensively and critically reviews the mechanistic aspect of the electron transfer reactions and of the additions of carbanions to olefins and other unsaturated substrates. As excellent examples of such reactions are especially found in the field of anionic polymerization, the monograph turns out to be at the same time a review of the kinetic and mechanistic aspects of anionic polymerization processes....The volume is extremely well written in a lively even if rigorous style, and must be warmly recommended to all those investigators interested in the fields of carbanion chemistry and of anionic polymerization."

— *CHIMIA*

1968 695 pages \$29.95

MACROMOLECULAR REVIEWS, Volumes 3 & 4

Edited by A. PETERLIN, *Camille Dreyfus Laboratory, North Carolina*, M. GOODMAN, *Polytechnic Institute of Brooklyn*, S. OKAMURA, *Kyoto University, Japan*, and H. F. MARK, *Polytechnic Institute of Brooklyn*

From reviews of volume three —

"...maintain the tradition of high quality, timeliness and superior technical merit established in the first two volumes of this hard-cover series." — *SPE Journal*

"...certainly belongs in every chemistry library." — *Journal of The Franklin Institute*

It has become more difficult for the polymer scientist at the university and in the industrial research and development laboratory to keep informed on the progress in his field. Even if he restricts his reading to a narrow area, the wealth of new information is so great, and scattered through so many journals, that he still will not be able to read all the articles of interest to him.

The review article, as a consequence of this situation, is becoming the primary source of information to a large majority of scientists, and this series, *Macromolecular Reviews*, exists to aid the entire polymer community in the development and understanding of new polymeric materials.

Volume 3: 1968 437 pages \$17.50

Volume 4: 1970 352 pages In Press

wiley

WILEY-INTERSCIENCE

a division of JOHN WILEY & SONS, Inc., 605 Third Avenue, New York, N.Y. 10016
In Canada: 22 Worcester Road, Rexdale, Ontario